RPT-SLAW-003, Rev 0
PNNL-25577, Rev 0

Pacific Northwest
NATIONAL LABORATORY

Proudly Operated by **Battelle** *Since 1965*

Getter Incorporation into Cast Stone and Solid State Characterizations

September 2016

RM Asmussen
CI Pearce
AR Lawter
JJ Neeway
B Miller
B Lee
N Washton
J Stephenson
RE Clayton
M Bowden
E Buck
E Cordova
BD Williams
NP Qafoku

U.S. DEPARTMENT OF
ENERGY

Prepared for the U.S. Department of Energy
under Contract DE-AC05-76RL01830

PACIFIC NORTHWEST NATIONAL LABORATORY
operated by
BATTELLE
for the
UNITED STATES DEPARTMENT OF ENERGY
under Contract DE-AC05-76RL01830

Printed in the United States of America

Available to DOE and DOE contractors from the
Office of Scientific and Technical Information,
P.O. Box 62, Oak Ridge, TN 37831-0062;
ph: (865) 576-8401
fax: (865) 576-5728
email: reports@adonis.osti.gov

Available to the public from the National Technical Information Service
5301 Shawnee Rd., Alexandria, VA 22312
ph: (800) 553-NTIS (6847)
email: orders@ntis.gov <http://www.ntis.gov/about/form.aspx>
Online ordering: http://www.ntis.gov

RPT-SLAW-003, Rev 0
PNNL-25577, Rev 0

Getter Incorporation into Cast Stone and Solid State Characterizations

RM Asmussen
CI Pearce
AR Lawter
JJ Neeway
B Miller
B Lee
N Washton
J Stephenson
RE Clayton
M Bowden
E Buck
E Cordova
BD Williams
NP Qafoku

September 2016

Prepared for
the U.S. Department of Energy
under Contract DE-AC05-76RL01830

Pacific Northwest National Laboratory
Richland, Washington 99352

Executive Summary

Washington River Protection Solutions (WRPS) is collecting relevant available data on waste forms for use as a supplemental immobilization technology, to provide the additional capacity needed to treat low-activity waste (LAW) in Hanford Site tanks and complete the tank waste cleanup mission in a timely and efficient manner. One candidate supplemental waste form, fabricated using a low-temperature process, is a cementitious grout called Cast Stone. Cast Stone has been under investigation for this application at Pacific Northwest National Laboratory (PNNL) since initial screening tests in FY13. This report is the culmination of work to lower the diffusivities of Tc and I from Cast Stone using getters. Getters are compounds added to a waste form designed to selectively sequester a species of interest to provide increased stability to the species. The work contained within this report is related to waste form development and testing and does not directly support the 2017 integrated disposal facility (IDF) performance assessment. However, this work contains valuable information which may be used in performance assessment maintenance past FY17, and in future waste form development.

This report on performance characterization of Tc and I getters in Cast Stone fabricated with simulated LAW covers several areas of interest and provides major findings to WRPS:

1) *Investigating performance of potassium metal sulfide (KMS-2-SS) and tin (II) apatite (Sn-A) as Tc getters when incorporated into Cast Stone*. It was found that including the KMS-2-SS Tc getter in Cast Stone had the largest effect in lowering Tc observed diffusivities to a minimum of 5.4×10^{-13} cm^2/s in 63 d of EPA Method 1315 leach testing in simulated Hanford vadose zone pore water (VZPW). The Tc observed diffusivity of Cast Stone without getters was measured at 1.2×10^{-11} cm^2/s after 63 d leaching in VZPW. This marked improvement showcases the promise of using sulfide-based Tc getters to lower Tc release from cementitious waste forms and sequestering Tc from LAW. We suggest that the KMS-2 or other sulfide based materials warrant additional investigations as a Tc getter in Cast Stone waste forms.

2) *Investigating performance of silver exchanged zeolite (Ag-Z) and argentite (Arg) as I getters when incorporated into Cast Stone*. Through EPA Method 1315 leach testing, it was found that these two I getters, added at between 0.083 to 0.5 and 0.29 wt% of the Cast Stone dry blend, respectively were ineffective in significantly lowering I observed diffusivities. The amount of these two Ag-based I getters added corresponded to 100 × the molar I content of the LAW simulant, thus we would have expected these two Ag-based getters to have formed low solubility AgI precipitates, which would have reduced iodide diffusivities from the Cast Stone. While the Ag-Z I getter removed > 98 % of the initial iodide from the LAW simulant, it was ineffective in significantly lowering I release when solidified into Cast Stone that contained both a Tc and I getter. A pH effect and competition for Ag from the blast furnace slag's (BFS) and KMS-2-SS's sulfide component of the Cast Stone are postulated as reasons for the instability of the AgI formed by the getters. This is an important finding as relying on the low solubility of the AgI salt may not be a sufficient approach to slowing I release from

cementitious waste forms unless the optimum amount of Ag is determined as previous work (in less harsh simulants) that higher loading of Ag-based getters led to lower I D_{obs}.

3) *Utilizing sequential addition of Tc and I getters to overcome any deleterious interactions between the getters in solution*. It was found that sequential addition can overcome deleterious interactions between Tc and I getters when they are added simultaneously as shown previously (Asmussen et al. 2015). Sn-A and Ag-Z added to LAW simulant sequentially (separated by 24 to 48 hr) led to 65% of Tc removal and > 98 % I removal. Adding KMS-2-SS to the LAW simulant followed by its removal by filtering led to > 95% removal of Tc, however I removal by both Ag-Z and argentite following their addition to the filtered simulant was drastically reduced as residual KMS-2-SS colloid particles or soluble sulfide passed through the filter and remained in the LAW simulant. Adding KMS-2-SS to the LAW and not filtering gave > 98 % Tc removal, and performed similarly to the filtered system in the Cast Stone leach testing, showing that filtering of the KMS-2-SS is not a required unit operation to attain high levels of Tc removal and retention. It was then concluded that deleterious interactions between getters can be limited by using sequential additions of the materials.

4) *Determining, for the first time, Tc distribution within the cured Cast Stone and its evolution during leaching*. Using single particle digital autoradiography, the Tc distribution in Cast Stone cross sections was observed in both pre- and post-EPA Method 1315 leach testing. In Cast Stone without getters added, Tc distribution is rather uniform before leaching but begins to congregate at the monolith outer wall following leaching. Upon adding getters, Sn-A and KMS-2-SS, the Tc in Cast Stone was observed to be present in discrete locations, randomly distributed throughout the monoliths cross section. Modelling of contaminant of concern (COC) release from cementitious waste form assumes a homogenously distributed source. However, these observations show this to be an inaccurate assumption, as getter containing systems created Tc “hot spots”. The Tc must first be released from these sites before leaching out of the Cast Stone monoliths, such knowledge should be included in future performance assessment maintenance.

5) Performing solid state characterization of getters and Cast Stone samples to support leach test findings and develop a mechanistic understanding of the processes that control Tc and I release into solution. A variety of state-of--art techniques were utilized that confirmed i) slower re-oxidation of Tc-sulfides compared with Tc-oxides within the Cast Stone, ii) discrete locations of Tc forming on the Cast Stone outer wall, visible as black spots, iii) isolations of Ag on the Cast Stone outer wall in leaching in deionized water, iv) the presence of Cr(VI) at the monolith outermost surface compared with Cr(III) throughout the interior, v) differences in local Al bonding relative to the outer surface of the monolith and with leaching time and vi) growth of *Proteobacteria* as the dominant biological phylotype present on the Cast Stone surfaces when leached in VZPW These studies show the importance of complementary solid state investigations into waste form behavior are important to fully understand, model and predict radionuclide and COC release over long times.

Based on these findings, additional studies are recommended to address the following issues:

1) Develop getter materials which can sequester both Tc and I from different waste streams.
2) Determine the re-oxidation rate of Tc-S formed within cementitious waste forms containing KMS-2-SS getters.
3) Identify chemical composition and mineral identity of Tc "hot spots" observed in the Cast Stone samples with Tc getters. Single particle digital autoradiography imaging can be used to find Tc hot spots, which can then be effectively interrogated with microscopic and spectroscopic techniques.
4) Perform leaching studies on cementitious waste forms containing reductants in partially saturated conditions, and with wet/dry cycling, in relevant conditions to the IDF.
5) Perform tests with higher Tc getter loading within Cast Stone to determine optimal compositions that may lead to even lower Tc release.
6) Determine the evolution of these Tc "hot spots" during leaching by imaging the unleached monolith surface with iQid, followed by time-dependent leaching to observe if preferential dissolution of Tc occurs from specific locations/Tc bonding environments. This would allow for further waste form tailoring and accurate long-term prediction of Tc release from the waste form.
7) Perform tests with higher I getter loading in Cast Stone, to confirm the hypothesis that I release is controlled by AgI solubility and previous Ag-based getter Cast Stone poor testing results can be improved by using higher I getter loading amounts.
8) Develop non-Ag based I getters to overcome the I release caused by competition for the available Ag by other reactants/soluble species (such as sulfide).
9) Develop a quantitative standard to apply for single particle digital autoradiography imaging to correlate Tc locations with absolute Tc concentrations and follow concentration changes as a function of leaching time.
10) Determine the influence of biological growths on cementitious waste forms on Tc and I releases.
11) Study sulfide-based materials as Tc getters in cementitious waste forms fabricated with other liquid waste streams (e.g., ETF).
12) Measure the influence of pH on reduced Tc(IV) species solubility to determine if this is the factor controlling the higher Tc D_{obs} values measured in DIW compared with VZPW.

Acknowledgments

This work was completed as part of the Supplemental Immobilization of Hanford Low-Activity Waste project. Support for this project came from Washington River Protection Solutions. The authors wish to acknowledge the Kanatzidis group at Northwestern University for providing the KMS-2, RJ Lee Group for providing the Sn-Apatite, and Dave Swanberg (Washington River Protection Solutions, Supplemental Treatment Waste Form Development Project) for programmatic guidance, direction, and support. The authors acknowledge Ian Leavy, Erin McElroy, Steven Baum and Keith Geiszler for analyzing simulants and Cast Stone leachates, along with Micah Miller for his expertise in obtaining µ-XRF data, Wayne Lukens for collection of the Tc K-edge XANES spectra and Nicole Overman for collection of the KMS SEM images. Tc K-edge XANES spectra were obtained at the Stanford Synchrotron Radiation Lightsource, SLAC National Accelerator Laboratory, which is supported by the U.S. Department of Energy, Office of Science, Office of Basic Energy Sciences under Contract No. DE-AC02-76SF00515. Cr L-edge XAS data were collected at the Advanced Light Source (ALS), Berkeley, which is supported by the Director, Office of Science, Office of Basic Energy Sciences (OBES) of the U.S. Department of Energy (DOE) under contract No. DE-AC02-05CH11231. The authors would like to thank Ben Williams for his expertise and assistance in Cast Stone monolith fabrication. The authors wish to thank Jeff Serne for his technical peer review and Guzel Tartakovsky for calculation review. Veronica Perez, Chrissy Charron provided word processing and editorial support prior to publication. The authors also wish to thank Dan Kaplan, Walter Kubilius, Alex Cozzi, and additional staff at Savannah River National Laboratory, Robert Andrews of INTERA, Dave Swanberg, Elvie Brown and Pat Lee from WRPS for their technical review of the report.

Acronyms and Abbreviations

Ag-Z	silver exchanged zeolite
ASTM	American Society for Testing and Materials
BFS	blast furnace slag
BSE	backscattered electrons
CCD	charge coupled device
CMOS	complementary metal oxide semiconductor
C_o	initial concentration
COC	contaminant of concern
DDI	deionized water (18.2 MΩ·cm)
D_{obs}	observed diffusivity
DIW	deionized water (building)
DOE	United States Department of Energy
DP	direct polarization
EC	electrical conductivity
EDS	X-ray energy dispersive spectroscopy
EPA	United States Environmental Protection Agency
ESL	Environmental Sciences Laboratory
ETF	Effluent Treatment Facility
FA	fly ash
FY	fiscal year
GCCS	getter containing Cast Stone
HLW	high level waste
HTWOS	Hanford Tank Waste Operations Simulator
IC	Ion chromatography
ICP-MS	inductively coupled plasma mass spectroscopy
ICP-OES	inductively coupled optical emission spectroscopy
IDF	Integrated Disposal Facility
iQid	ionizing-radiation quantum imaging detector
KMS	potassium metal sulfide
LAW	low activity waste
NIST	National Institute of Standards and Technology

NMR	nuclear magnetic resonance spectroscopy
OPC	ordinary Portland cement
PNNL	Pacific Northwest National Laboratory
QA	quality assurance
QIIME	Quantitative Insights Into Microbial Ecology
R&D	research and development
SEM	scanning electron microscopy
Sn-A	tin(II) apatite
SRIM	stopping and range of ions in matrix
SRNL	Savannah River National Laboratory
TC&WM EIS	Tank Closure and Waste Management Environmental Impact Statement
VZPW	vadose zone pore water
WRPS	Washington River Protection Solutions
WTP	Waste Treatment Plant
WWFTP	WRPS Waste Form Testing Program
XANES	X-ray absorption near edge structure
XAS	X-ray absorption spectroscopy
XRD	X-ray diffraction spectroscopy
µ-XRF	Micro X-ray fluorescence spectroscopy

Contents

Figures

Tables

1.0 Introduction and Background

The Department of Energy (DOE) Hanford Site in Eastern Washington houses approximately 56 million gallons of radioactive wastes stored in 177 underground tanks. (Xu et al. 2016) Prior to final disposal, the liquid tank wastes will be pre-treated and solidified at the Hanford Tank Waste Treatment and Immobilization Plant (WTP) (currently under construction). The wastes will be segregated into two waste streams: 1) small volume high-level waste (HLW) containing most of the radioactivity and 2) a larger volume of less radioactive low-activity waste (LAW). The HLW will be vitrified to a glass waste form and destined for ultimate disposal at a federal repository. At least a portion of the LAW inventory is slated for vitrification and disposal on-site in a near-surface disposal facility, the Integrated Disposal Facility (IDF). As a result of the WTP activities, liquid secondary waste streams from process condensates and LAW melter off-gas scrubbed effluents are generated and solidified in a cementitious grout at the Effluent Treatment Facility (ETF). In addition solid secondary wastes will be generated that will also be encapsulated or shredded and mixed with cementitious grout. Grouts are not limited in potential application to secondary wastes. Recently, a hydrated lime based grout has been shown in relatively short-term leach tests to retain Tc and limit its release. The liquid simulant solidified was based on future secondary waste streams which contain high sulfate concentrations after evaporative concentration and processing at the ETF. This hydrated lime grout formulation is used to induce ettringite formation in the early stages of curing to prevent swelling and volume changes (Um et al. 2016). At the Savannah River Site a grout waste form called saltstone, comprised of three dry blend ingredients (blast furnace slag (BFS), fly ash (FA) and ordinary Portland cement (OPC)), is used to solidify LAW tank wastes (Cantrell et al. 2013). Cast Stone, a grout with similar dry blend composition to saltstone is being evaluated as a possible supplemental immobilization technology to provide the necessary LAW treatment capacity to complete the tank waste cleanup mission at the Hanford site in a timely and efficient manner (Westsik et al. 2013). The hydrated lime grout formulation may not be feasible for LAW immobilization due to the relatively low sulfate content of LAW and its high pH.

The *Tank Closure and Waste Management Environmental Impact Statement for the Hanford Site, Richland, Washington* (TC&WM EIS; DOE 2012)[1] identifies Technetium-99 and Iodine-129 as radioactive tank waste components contributing the most to future groundwater impacts. The TC&WM EIS evaluates a number of alternative waste forms and potential radionuclide release rates from them, including waste treatment options that solidify the liquid secondary waste and supplemental LAW in grout waste forms.

A diffusion-limited release model was used in the TC&WM EIS impact analyses to estimate the release of different contaminants from cementitious waste forms. Effective diffusivities of 5.2×10^{-9} cm^2/s for Tc and 1.0×10^{-10} cm^2/s for I were used in the TC&WM EIS modeling. The Washington State Department of Ecology, in their foreword to the TC&WM EIS, calls for improving the performance of grout waste forms, for example, lowering the diffusivity of I to a performance standard of 1×10^{-12} cm^2/s at a recharge water infiltration rate of 3.5 mm/y. Their desired I diffusion rate would “thus delete this waste from the list of dominant contributors to risk” (DOE 2012).

One possible method to lower the release of radionuclides/contaminants of concern (COC) from grout waste forms is through the addition of materials to selectively sequester radionuclides and/or other COC

---

[1] TC&WM EIS; DOE/EIS-0391, available at http://www.hanford.gov/page.cfm/FinalTCWMEIS.

from the waste stream. Such materials are termed "getters". Several reviews of published literature have been conducted on possible getters for Tc and I. (Mattigod et al. 2003, Pierce et al. 2010a, Mattigod et al. 2011). Though many potential getters have been identified, only a few meet general performance factors including:

- Adequate selectivity and capacity for the COC
- Low rates of release of the COC over long periods of time
- Chemical and physical stability
- Compatibility with the waste form and any other getters

Past work by these authors and the work conducted at Pacific Northwest National Laboratory (PNNL) in fiscal years (FY) 2013- 2015 show that ability of getters to remove Tc and I vary considerably under different experimental conditions. The effects of exposure time, radionuclide concentration and getter:solution ratio on Tc and I removal by getters were studied in a series of batch experiments during FY 2013 and FY 2014 at PNNL. This work was complemented with initial solid-phase characterization (using scanning electron microscopy with energy dispersive x-ray spectroscopy (SEM/EDS) and x-ray adsorption spectroscopy (XAS)). The results have been published in two reports. (Qafoku et al. 2014, Neeway et al. 2015) These studies investigated the effectiveness of different Tc and I getter materials, including the Tc getters blast furnace slag (BFS), Sn(II)-treated apatite (Sn-A), Sn(II) chloride, nanoporous Sn-phosphate, KMS-2 (a potassium-metal-sulfide), and Sn(II) hydroxyapatite. The I getters investigated included layered Bi hydroxide, natural argentite (Ag_2S) mineral, synthetic argentite, Ag-impregnated carbon, and Ag-exchanged zeolite (Ag-Z).

High levels of $Tc(VII)O_4^-$ removal by the getters were measured in experiments conducted in deionized water (18.2 MΩ·cm, DDI) under anoxic (FY2014) (Qafoku et al. 2014) and oxic (FY2015) (Asmussen et al. 2015) conditions. The highest level of Tc(VII) removal in this simple environment was achieved by Sn-A (> 98 % removal), where the final solid phase product was identified as $Tc(IV)O_2{\cdot}xH_2O$. However, the Tc(VII) removal values measured in batch experiments conducted in a highly alkaline, high ionic strength LAW simulant showed very limited Tc removal (<10%) from solution by the Sn-A at a 1 g : 100 mL solid to solution ratio. The high alkalinity of the LAW simulant and the presence of Cr(VI) competing with Tc(VII) for reducing equivalents were suggested as causes of the decrease in getter reactivity toward Tc(VII). Experiments to examine the competing effect of $Cr(VI)_2O_7^{2-}$ on removal of $Tc(VII)O_4^-$ from solution showed that Cr(VI) competes directly with Tc(VII) for the removal capacity of the Tc getters (Asmussen et al. 2016a). To mitigate the effects of the LAW simulant, the getter:solution ratio was increased and this led to an improvement in Tc(VII) removal by Sn-A (> 60%). The only Tc getter capable of removing > 95 % of Tc(VII) from the LAW simulant was KMS-2. (Qafoku et al. 2014, Neeway et al. 2016). KMS-2 has a high reduction capacity (between 7000 – 20000 µeq/g) and removes $Tc(VII)O_4^-$ from solution via a redox mechanism involving the sulfide moiety in the KMS-2 structure(Neeway et al. 2016). The final solid phase product of Tc(VII) removal from solution by KMS-2 has been identified as a $Tc(IV)_2S_7$ species.

For the I getters, Ag-Z and synthetic argentite were the most effective in the LAW simulant (> 99.9 % I removal), with the Ag-Z achieving this level of removal in a shorter time frame than the argentite. The mechanism of I^- removal from solution by both Ag-Z and argentite is precipitation, with AgI as the final solid phase product. The other I getters showed limited effectiveness (< 10%) for removal of I^- from the LAW simulant. All of the successful Tc and I getters tested have shown stability in the presence of O_2, with limited release of Tc and I back into solution over a 15 d time span (Asmussen et al. 2015).

Tc and I getters do not act independently of one another. Batch experiments containing both Tc getters (Sn-A or KMS-2) and an I getter (Ag-Z), showed deleterious effects on the removal of Tc and I, in DDI and in LAW simulant. The presence of both Ag-Z and Sn-A in solution decreased the Tc(VII) removal by Sn-A, likely due to the competitive effect of the Ag(I) present in the Ag-Z for reducing equivalents. In experiments containing both KMS-2 and Ag-Z, Tc(VII) removal from solution was drastically lowered, likely as a result of the combined effects of: (i) the affinity of Ag(I) for the interlayer space of KMS-2, where it binds to S in the structure, potentially limiting its reductive capacity; (Hassanzadeh Fard et al. 2015) and (ii) the competition between Ag(I) and Tc(VII) for reaction with HS(-I) in solution(Asmussen et al. 2015). In addition, the Ag-Z showed much lower I removal (~50% initially), and the I removed was subsequently released back into solution over a period of < 24 h. This was likely a result of KMS-2 extracting Ag(I) directly, or the reaction between Ag(I) and HS(-I) in solution to form Ag_2S, driving the release of Ag(I) from AgI according to Le Chatelier's principle. It was found that sequential addition of the getters can overcome these deleterious interactions and lead to successful Tc and I removal.

The work contained within this report is related to waste form development and testing and does not directly support the 2017 IDF performance assessment. However, some waste streams may eventually include engineered getters and measuring K_d values for getters in LAW environments and D_{obs} for radionuclides and COC's from grout waste forms containing getters will be useful to support future IDF performance assessment iterations.

1.1 Objectives

The overall objectives of the getter testing program were to:

- Determine an acceptable formulation that includes getters for the LAW simulants in cementitious grouts, such as Cast Stone.
- Demonstrate the robustness of the formulations in terms of Tc and I release as quantified using observed diffusivities.
- Provide cementitious grout/Cast Stone contaminant release data for environmental risk assessments such as future IDF performance assessments.

The specific objectives for the research effort presented in this report are to:

1. Investigate the performance of Tc and I getters when included in Cast Stone. This was achieved by fabricating Cast Stone with differing combinations of Tc getters and I getters added in differing sequences and testing using U.S. Environmental Protection Agency (EPA) Methods 1315 and 1313.
2. Evaluate getter interactions with one another, as well as with Cast Stone dry blend components.
3. Investigate the structural evolution of the getter containing Cast Stone (GCCS) throughout leaching by using state-of-the-art solid state analysis techniques to determine changes in chemical composition and COC distribution within GCCS.

1.2 Report Contents and Organization

The ensuing sections of this report describe the technical scope and approach of the testing program, the presentation and discussion of results, conclusions, and the identification of future study needs. The appendices contain information about the LAW simulant preparation (Appendix (A); pH and electrical conductivity measurements from EPA 1315 leaching experiments (Appendix (B); data and calculations used in this report from EPA 1315 testing (Appendix C); a summary of Tc reduction by Sn(II) materials performed at SRNL on liquid secondary waste simulants (Appendix D); the EPA Method 1315 slope checks for all analytes (Appendix E).

2.0 Technical Scope and Approach

2.1 Quality Assurance

This work was conducted with funding from Washington River Protection Solutions (WRPS) under contract 36437-166, Supplemental Immobilization of Hanford Low-Activity Waste. The work was conducted as part of Pacific Northwest National Laboratory (PNNL) Project 66596, Supplemental Immobilization of Hanford Low-Activity Waste.

All research and development (R&D) work at PNNL is performed in accordance with PNNL's laboratory-level Quality Management Program, which is based on a graded application of NQA-1-2000, *Quality Assurance Requirements for Nuclear Facility Applications*, to R&D activities. In addition to the PNNL-wide quality assurance (QA) controls, the QA controls of the WRPS Waste Form Testing Program (WWFTP) QA program were also implemented for the work. The WWFTP QA program consists of the WWFTP Quality Assurance Plan (QA-WWFTP-001) and associated QA-NSLW-numbered procedures that provide detailed instructions for implementing NQA-1 requirements for R&D work. The WWFTP QA program is based on the requirements of NQA-1-2008, *Quality Assurance Requirements for Nuclear Facility Applications*, and NQA-1a-2009, *Addenda to ASME NQA-1-2008 Quality Assurance Requirements for Nuclear Facility Applications*, graded on the approach presented in NQA-1-2008, Part IV, Subpart 4.2, "Guidance on Graded Application of Quality Assurance (QA) for Nuclear-Related Research and Development". Performance of the FY2016 Tc and I getter tests and preparation of this report were assigned the technology level "Applied Research" and were conducted in accordance with procedure QA-NSLW-1102, *Scientific Investigation for Applied Research*. All staff members contributing to the work have technical expertise in the subject matter and received QA training prior to performing quality-affecting work. The "Applied Research" technology level provides adequate controls to ensure that the activities were performed correctly. Use of both the PNNL-wide and WWFTP QA controls ensured that all client QA expectations were addressed in performing the work.

2.2 Simulant

The Cast Stone monoliths fabricated in this report used a 6.5 M LAW simulant (LAW), based on the Hanford Tank Waste Operations Simulator (HTWOS) model which supports the River Protection Project System Plan Revision 6 (Certa et al. 2011). The metal spike levels were determined based on a previous report, in which simulant preparation does not include Hg and Ag as they are known to interact with I. (Russel et al. 2013) The simulant preparation method was based on combined knowledge from Savannah River National Laboratory and previous LAW preparation at PNNL. (Russel et al. 2013) To produce the LAW simulant Millipore water (DDI) (18.2 MΩ·cm) was added to a 4 L glass beaker.

The dry chemical reagents, listed in Table 2-1, were then added one at a time, following the order as listed. The next chemical was not added until the previous chemical had completely dissolved. A visual sequence of the simulant preparation can be found in Appendix A. Following the chemical addition the solution was stirred and heated to ~ 70 °C to achieve full dissolution of the chemical, and continued with these conditions for 16 h, after which the solution was cooled to room temperature for 8 h. At this point, DDI was added to reach the target mass for the simulant. The simulant was transferred to a 10L plastic carboy. The final anion and cation concentrations of this LAW simulant were measured immediately after fabrication; see Table 2-1 (anions measured from ion chromatography (IC) and cations with inductively couple plasma optical emission spectroscopy (ICP-OES)).

It should be noted that the trace amounts of Pb, Ni and Cd added to previous versions of the LAW simulant were not added following discussions with WRPS as they were deemed to have minimal impact on the getter performance. OH^- content was determined using titration with 2 N H_2SO_4 to the first inflection point between pH 11 and pH 8 (pH 9.5). (Bannochie et al. 2005) The LAW simulant had a measured Na concentration of 6.6 M, and the concentration values of the major constituents listed in Table 2-1 are given in terms of mol of the species per mol of Na. The numbers agree well with previous reports of fabrication of HTWOS overall average LAW simulant. (Russel et al. 2013) The density of the LAW simulant was measured to be 1.31 g/mL.

The prepared LAW simulant was separated into 1 L batches for preparation of the Cast Stone monoliths. Each 1 L aliquot was spiked with a 10,000 ppm $NaTcO_4$ and 10,000 ppm NaI stock solution to achieve target concentrations of 16 ppm Tc and 6 ppm I in the LAW simulant. The 16 ppm Tc spike was chosen to be consistent with previous Cast Stone work (Serne et al. 2016). From the HTWOS model for a 6.5 M Na average LAW, the predicted Tc concentration is 4.6 ppm. The 6 ppm I spike was chosen to get detectable iodide concentrations in resultant test leachates.   The 6 ppm I spike level represents 10 × the I concentration expected based on the HTWOS model for a 6.5 M Na average LAW simulant.

Table 2-1-Composition of LAW simulant used in fabrication of GCCS. The recipe for preparation is shown in order of addition for 1 L of simulant, and the measured anion concentrations of the prepared simulant by IC and major cations by ICP-OES.

Compound	Amount for 1 L (g)	Anion/Cation	Measured Concentration (g/L)	Concentration (mol/mol Na)
DDI	200 mL	**Na**	153.33	1.000
KNO_3	4.60	**Al**	11.75	0.065
NaCl	3.04	**Cl**	3.47	0.015
NaF	1.64	**NO_3**	140.00	0.339
Na_2SO_4	15.70	**NO_2**	37.04	0.121
$Al(NO_3)_3$•$9H_2O$	148.74	**SO_4**	11.58	0.018
NaOH (50% soln)	289.12	**K**	2.08	0.008
Na_3PO_4•$12H_2O$	24.71	**PO_4**	1.47	0.002
$NaC_2H_3O_2$	6.64	**Free OH**	35.39	0.312
Na_2CO_3	37.89			
DDI	100 mL			
$Na_2Cr_2O_7$•$2H_2O$	2.31			
DDI	100 mL			
$NaNO_3$	74.03			
$NaNO_2$	50.68			
DDI	100 mL			

2.3 Getter Materials

The getters used in fabrication of the Cast Stone were selected based on previous screening tests . The sequence of getter addition was developed based on the results of scoping tests before the work included in this report started and technical discussions with WRPS and SRNL technical staff.

Sn(II)-treated apatite ($Sn_xCa_y(PO_4)(OH,Cl,F\ )$)*(Sn-A)* – the Sn-A was synthesized by the RJ Lee group using a previously published method (Duncan et al 2012), then stored in a desiccator during transport and until its use in Cast Stone fabrication. The Sn-A reduction capacity was 3469 ± 530 µeq/g based on the Ce(IV) method, see (Asmussen et al. 2016a) for details.

Potassium Metal Sulfide (KMS-2-SS) – Previous work utilized two forms of KMS, KMS-2 which is synthesized via a hydrothermal method and KMS-2-SS which is prepared using solid state synthesis. Details of the synthesis can be found in Neeway et al. (2016). KMS-2-SS has a higher Ce(IV) reduction capacity (21000 µeq/g) than the KMS-2 (7400 µeq/g) (Neeway et al. 2016) and was thus selected for this work. The approximate chemical formula for the KMS-2-SS is $K_{1.3}Mg_{0.95}Sn_{2.1}S_6$.

Silver exchanged zeolite (Ag-Z) – In the previous getters screening tests and work presented in other publications, (Qafoku et al. 2014, Asmussen et al. 2016b), Ag-Z has consistently removed the highest amount of I in the shortest time from LAW environments. The Ag-Z was purchased from Sigma-Aldrich Corporation (St. Louis, MO) and received as > 840 µm pellets. The pellets were crushed with a mortar and pestle to a size < 300 µm to increase the surface area and in hopes of achieving a homogenous distribution of Ag-Z in the Cast Stone mix.

Argentite – Argentite has consistently shown high levels of I removal from LAW simulants. The argentite was synthesized in the Environmental Sciences Lab (ESL) at PNNL via a previously reported method (Kaplan et al. 2000). After synthesis, the argentite was ground with a mortar and pestle to a particle size < 300 µm.

2.4 Cast Stone Monoliths Preparation

Cast Stone monoliths (2-in diameter by 4-in tall right cylinders) were prepared with the LAW simulant described in Section 2.1.2. The Cast Stone dry blend consisted of 47 wt% BFS (northwest source), 45 wt% FA (northwest source), 8 wt% OPC and Tc and I getters included in Table 2-2 below. All mixes were fabricated with a water : dry mix ratio of 0.55 and in an aerobic atmosphere. Small amounts of dry blend mix were removed to compensate for the amount of getter added to keep the water –to-dry blend constant at 0.55. The spikes (Tc, I or AgI) were added to the LAW simulant prior to introduction of the dry blend ingredients. The amount of LAW simulant used was determined to allow for removal of two or three (test dependent) 2 mL aliquots prior to Cast Stone formation while ensuring the 0.55 mix ratio was retained. The tests (T1 through T7) listed in Table 2-2 contain different combinations of Tc and I getters which were added in differing sequences. It should be noted that an apparent evaporation of the LAW simulant occurred between the time of its fabrication and the time of fabrication of the Cast Stone. This led to slightly increased concentrations in the LAW simulant from the aliquots collected prior to fabricating the Cast Stone (see tables in Appendix C) compared with measured values in Table 2-1. The Cast Stone-getter compositions are listed below:

T1 – No getters were added to the control. The dry blend ingredients were added to the LAW simulant in the steps listed in Section 2.4.2. Two aliquots (2 mL) of the simulant were collected for initial analysis.

T2 – An aliquot (2 mL) of the Tc and I spiked LAW simulant (1 L) was collected to determine initial Tc and I concentrations. The Sn-A was first added to the LAW simulant (1 L) and given 24 h to react, after which time an aliquot (2 mL) was collected for analysis. Ag-Z was then added to the LAW simulant (1 L) and given an additional 24 h to react, after which time a final aliquot (2 mL) was collected. The Cast Stone monoliths were then fabricated using the steps listed in Section 2.4.2. Further information on Sn(II) containing materials for Tc removal can be found in Appendix D. This appendix summarizes recent Savannah River National Laboratory (SRNL) studies on simulants of WTP off-gas (secondary wastes) liquid condensates and flush waters that were spiked with $^{99}Tc(VII)O_4$- that were treated with $SnCl_2$ or $SnCl_2$ and hydroxyapatite.

T3/T4 – An aliquot (2 mL) of the Tc and I spiked LAW simulant (1 L) was collected to determine initial Tc and I concentrations. The KMS-2-SS was added to the spiked LAW simulant (1 L) and given 24 h to react, after which time the LAW simulant was filtered using a 0.45 µm Nalgene vacuum filter to collect the KMS-2-SS, and an aliquot (2 mL) of the filtered LAW simulant was collected for analysis. The KMS-2-SS collected from the filter was stored in a sealed container. The I getter (Ag-Z in T3 and argentite in T4) was then added to the filtered LAW simulant and given 48 h to react, after which time an aliquot (2 mL) of the LAW simulant (1 L) was collected for analysis. The KMS-2-SS was then added back into the LAW simulant (1 L) and the sealed container rinsed with LAW simulant several times to ensure all KMS-2-SS was transferred to the LAW batch mixed with dry blend. The Cast Stone monoliths were then fabricated using the steps listed in Section 2.4.2.

T5/T6 - An aliquot (2 mL) of the spiked LAW simulant (1 L) was collected to determine initial Tc and I concentrations. The KMS-2-SS was added to the LAW simulant (1 L) and given 48 h to react, after which time an aliquot (2 mL) of LAW simulant was collected for analysis. The I getter (Ag-Z for T5 and argentite for T6) was fully incorporated directly into the dry blend ingredients. The Cast Stone monoliths were then fabricated using the steps listed in Section 2.4.2.

T7 – This test was performed to investigate the stability of AgI when incorporated into Cast Stone. The preparation was identical to T1, except no Tc or I spike was used. Instead, 0.0198 g of AgI (Sigma-Aldrich), equivalent to 20 ppm I, was added to the LAW simulant before fabrication of the Cast Stone monoliths using 500 mL of LAW simulant. Due to the photosensitivity of AgI, care was taken to keep the AgI in its photo-protective container prior to weighing, which was performed with the room lights off, and then immediately added to the LAW simulant

Table 2-2 – Composition of the Cast Stone batches prepared in this study. All mixes were made at a water : dry mix ratio of 0.55 and in oxic environments. The spikes (Tc, I or AgI) were added to the LAW simulant prior to introduction of the dry blend ingredients.

Batch ID	6.5M Na LAW Ave. Simulant (g)	LAW Simulant Spikes	Total Dry Ingredients & Getters Used (g)	Blast Furnace Slag (g)	Fly Ash (g)	OPC (g)	Type and Mass (g) of Tc Getter	Type and Mass (g) of I Getter or I source
T1	1307.9	none	1750	822.5	787.5	140	none	none
T2	1307.9	Tc & I	1757.25	798.3	764.3	135.9	Sn-A 50.0	Ag-Z 8.75
T3	1307.9	Tc & I	1750	820.7	785.8	139.7	KMS-2-SS 2.35	Ag-Z 1.45
T4	1307.9	Tc & I	1744.95	816.7	781.9	139	KMS-2-SS 2.35	Arg 5.00
T5	1307.9	Tc & I	1750	820.7	785.8	139.7	KMS-2-SS 2.35	Ag-Z 1.45
T6	1307.9	Tc & I	1747.55	818.9	782.3	139	KMS-2-SS 2.35	Arg 5.00
T7	654.0	AgI	875.1	411.3	393.75	70.0	none	AgI 0.0198 g

2.5 Cast Stone Fabrication

In each case, the LAW simulant was placed in a 2 L plastic bucket and then the plastic bucket was placed under the impeller of the mixer (Caframo high torque overhead stirrer) inside a fume hood. In the case of the GCCS (T2-T6) the LAW simulant bottle was rinsed with the LAW simulant several times to ensure all solids had been transferred to the mixing bucket. The impeller shaft was lowered so that the bottom of the impeller was 0.75 in to 1.25 in from the bottom of the bucket and 0.25 in to 0.5 in away from the sides of the bucket. The impeller was placed near the front of the bucket because offsetting the impeller helps to minimize vortexing and prevents the creation of a central vortex, which would entrain unwanted air (see Figure 2.1). The agitator speed started between 180 and 200 RPM. To add the dry ingredients, a corner of the plastic bag was cut off and the mixed dry materials were poured slowly into the bucket. As dry ingredients were added, the agitator speed was slowly increased as needed to promote proper mixing. When needed, the impeller was paused momentarily to release entrained air bubbles that are typically located around the impeller. The impeller was then immediately restarted to continue the mixing process. The dry material was added within five min, but the mixing continued for a total mixing time of 15 min. After the 15 min mixing period, the impeller shaft was raised to allow the 2 L bucket to be removed.

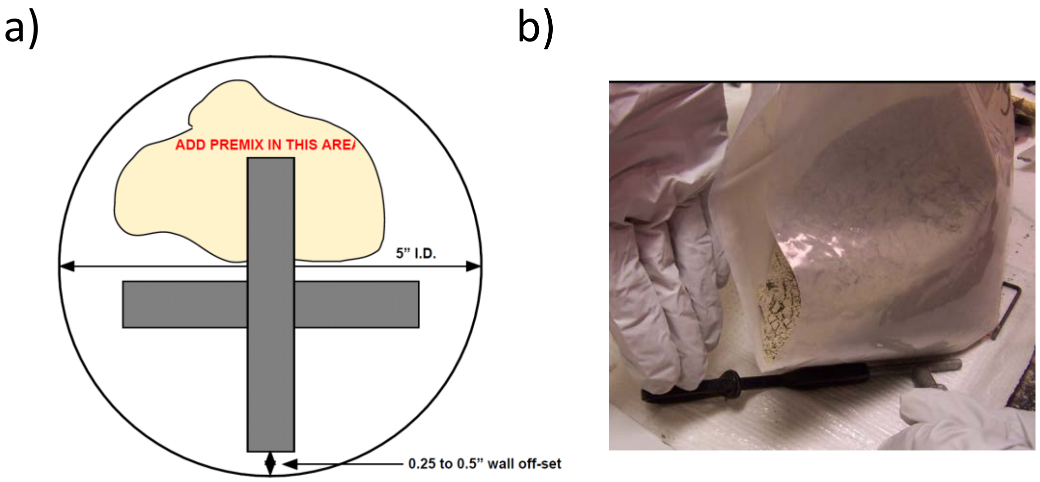

Figure 2-1- Instructions for dry ingredient addition during Cast Stone formation showing (a) location of dry blend introduction to the 2 L bucket containing the simulant and impeller, and (b) cutting of the plastic bag containing the dry blend ingredients.

The grout slurry was then poured into pre-labeled 2 in × 4 in right cylindrical forms. Each batch of Cast Stone produced eight full forms and a ninth partially filled form. Each form was filled approximately 3/4 full with grout first to prevent spillage and then the air was removed by placing the form on a vortexer until air bubbles dissipated. The form was then filled to the top with wet Cast Stone slurry and the air was again carefully released. The form was then gently tapped on the base of the fumehood to ensure no trapped air remained in the grout. The form was then capped with a perforated lid, leaving an air gap between the cap and the wet grout to promote flatness of the cured monolith top. The process was repeated until no mix was remaining in the 2 L bucket. The capped forms were then placed on racks inside 5 gal buckets containing ~1" of DIW on the bottom. The lid of each curing bucket was then closed tightly, providing 100% humidity during the curing, which lasted 28 d at room temperature. The mixer was then thoroughly cleaned before fabricating subsequent batches of grout.

Following the 28 d curing period, the monoliths were removed from their forms, labelled and inspected for defects or damage. Each individual monolith was placed into a separate plastic bag, left open, and the separate plastic bags were placed into a larger plastic bag containing two damp paper towels to maintain humidity until ready to use. Masses and dimensions of each monolith can be found on the second page of Appendix C. A full visualization of the process can be seen in Figure 2.2.

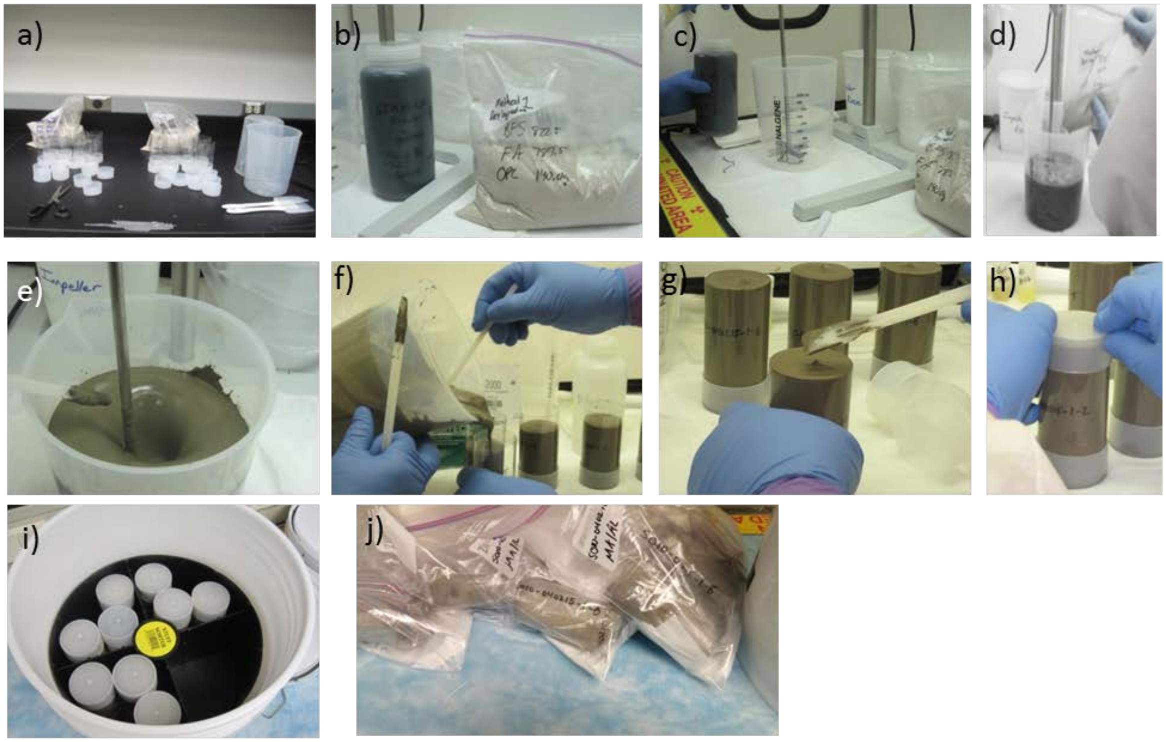

Figure 2-2- Preparation Sequence of Cast Stone Monoliths (a) the Dry Ingredients Used for Fabrication, (b) the LAW Simulant with Getters Added and the Dry Ingredients, c) Placement of the Impeller in the Mixing Bucket, d) Initiation of Dry Ingredient Addition to the LAW Simulant , e) Cast Stone Mixture Following Dry Ingredient Addition, f) Initial Pouring of Individual Monoliths, g) Filling of Monolith Holders and Tapping to Remove Air, h) Capping Monoliths Prior to Curing i) the Cast Stone in molds in the curing bucket and j) Following Curing, Monoliths Placed in Double Zip Bags with Damp Paper Towels.

2.6 EPA Method 1315 Leach Testing

EPA Method 1315 (EPA 2013) was used for leach testing the monoliths using two solutions, building deionized water (DIW) and a synthetic vadose zone pore water (VZPW) (both solutions were open to the atmosphere, and no de-aeration was carried out). The VZPW simulant recipe is shown in Table 2-3. The recipe is based on several direct measurements of actual VZPW removed from Hanford formation sediments from a borehole in the 200 E Area where the IDF is located. Several hundred grams of field moist sediment were removed from core liners drilled into uncontaminated Hanford formation sediments using cable tool drive barreling. The field moist sediments were placed in special holders and ultra-centrifuged for several hours. Small volumes of VZPW passed through the sediment and collected at the bottom of the holders in small sampling cups. When approximately 30 to 50 mL of VZPW was collected from each sediment sample it was immediately filtered through 0.45 µm membrane filters and analyzed for chemical composition. The results from characterizing the pore water from two depths (48.5 and 82.5 ft. bgs) from borehole (C4124; 299-E27-22) (Brown et al. 2006) were averaged and charge balanced. Although Si is present at ~23 ppm in the actual pore waters, it was not added to the simulant recipe. Reagents were added, in the order given in Table 2-4, to the corresponding volume of DIW.

The EPA Method 1315 leach testing involved placing the cured monolith in a holder, not covering more than 2% of the overall monolith surface area, and placed upright in a 2 L bucket. The buckets were filled with DIW or VZPW at a volume determined by a volume to monolith geometric surface area of 9 ± 1 mL/cm^2 creating a saturated environment. It should be noted that partially saturated exposures are expected for waste forms disposed of at the IDF. After placing the monolith in the bucket, a lid was placed on the bucket and then left undisturbed for the duration of the leaching interval. At the conclusion of each leaching interval, the monolith was carefully removed from the bucket and any excess water drained off. The mass of the monolith was then recorded and the monolith returned to a new bucket with fresh solution. During this time, the monolith is exposed to the open atmosphere, and the sampling took ~ 2 min from the time of removal from solution to placing in the fresh leachant. Leaching intervals occurred at 2 h, 1 d, 2 d, 7 d, 14 d, 28 d, 42 d, 49 d, and 63 d. Following the monolith removal from the leaching bucket, the pH and electrical conductivity (EC) of the leachate was measured. A 60 mL aliquot of the leachate was then collected for analyses with ICP-OES, ICP-MS and IC.

Table 2-3 - Vadose Zone Porewater Recipe Listed in Order of Addition of Each Component

	VZPW Recipe			
Order	**Molarity (mol/L)**	**Reagents**	**MW (g/mol)**	**g/L**
1	0.012	$CaSO_4•2H_2O$	172.17	2.07
2	0.0017	NaCl	58.44	0.10
3	0.0004	$NaHCO_3$	84.01	0.03
4	0.0034	$NaNO_3$	84.99	0.29
5	0.0026	$MgSO_4$	120.37	0.31
6	0.0024	$MgCl_2•6H_2O$	203.31	0.49
7	0.0007	KCl	74.55	0.05
Adjust pH to 7.0 (±0.2) with sodium hydroxide or sulfuric acid dependent on initial pH.				

2.7 EPA Method 1313

The second leach test used was EPA Method 1313 (*Liquid-Solid Partitioning as a Function of Extract pH Using a Parallel Batch Extraction Procedure*), (EPA 2012) which is a static test method where a set of extraction experiments are conducted in dilute acid or base at a fixed pH range (from 2 to 13) and fixed liquid-to-solid ratio (10 mL/g). EPA Method 1313 provides the liquid-solid partitioning curve as a function of pH and can be used to determine the solubility and release of key constituents (including technetium and iodine) from Cast Stone monoliths as a function of pH. All stages of the EPA Method 1313 testing were performed in the open atmosphere.

After curing for a minimum of 28 days, the Cast Stone monoliths (T1 – T6) that were used in EPA Method 1313 tests were removed from their form. Prior to initiating the 1313 test, particle size reduction of the Cast Stone monoliths was carried out in a mortar and pestle to achieve particles < 300 µm. The moisture content of the crushed Cast Stone particles was determined using PNNL-MA-567-DI-1 Method which is based on American Society for Testing and Materials (ASTM) procedure D2216-98. (ASTM 2005)

A pre-test titration curve was first prepared using the crushed particles from a T1 monolith. The schedule of acid additions (using 2N nitric acid) followed the list given in EPA Method 1313 for a highly alkaline material (EPA 2012). A 9 point extraction was performed using the formulae present in Table 2-4.

Table 2-4 - Pre-test titration acid equivalent schedule for high alkalinity samples

Bottle #	Equivalents of Acid (meq/g-dry)
1	0
2	0.5
3	1
4	1.5
5	2.5
6	5
7	10
8	15
9	25

The plot of meq of acid vs resulting pH from the pre-test titration was used to determine the volumes of acid to use for the Method 1313extractions for all Cast Stone compositions listed in Table 2-2. An example of the target extractions is shown in Table 2-5, which was used for T1 and T5.

After adding the amounts listed in the schedule of acid additions for the corresponding tests, the reaction bottles were placed on an end over end mixer for 24 h. The bottles were then removed from the mixer and allowed to settle for approximately 15 minutes. The pH, EC and E_h of the supernatant liquid in the reaction bottle was then measured.

Table 2-5 – Example of the schedule of acid additions for EPA Method 1313 testing for the T1 and T5 sets.

Bottle	Target pH	Mass solid dry (g)	Solids Content	Mass to add (g)	meq/g-dry Acid	vol 2N HNO3 (mL)	Moisture in sample (mL)	Volume of reagent water (mL)
1	13	20	0.77	25.97	0	0	5.97	194.03
2	12	20	0.77	25.97	0.8	8	5.97	186.03
3	10.5	20	0.77	25.97	2.8	28	5.97	166.03
4	9	20	0.77	25.97	4.3	43	5.97	151.03
5	8	20	0.77	25.97	5.2	52	5.97	142.03
6	7	20	0.77	25.97	6.3	63	5.97	131.03
7	5.5	20	0.77	25.97	7.9	79	5.97	115.03
8	4	20	0.77	25.97	9.5	95	5.97	99.03
9	2	20	0.77	25.97	17.3	173	5.97	21.03
Blank 1	low acid		0.77	0.00	0.8	8	0.00	192.00
Blank 2	high acid		0.77	0.00	17.3	173	0.00	27.00
Blank 3	water		0.77	0.00	0	0	0.00	200.00

2.8 Solid Phase Characterization

The performance of the GCCS can be investigated using the leaching methods discussed above. However, only the release of COC's can be understood using the leaching tests. In order to correctly predict the long-term behavior of grout waste forms, the waste form itself needs to be characterized before and after leaching. A series of solid phase analyses were performed on the GCCS monoliths in this work using a series of state-of-the-art characterization techniques.

2.8.1 Monolith Preparation

In order to characterize the Cast Stone monoliths they must first be sectioned into smaller pieces. This was done using two methods:

1) Mechanical breaking of the monoliths using a bench top press. This process was used to break the monolith in half either vertically or horizontally. Subsequent sectioning into smaller pieces was then performed and the size and location of the pieces in relation to the monolith outer surface was measured with calipers.

2) A dry circular saw with a diamond blade (~1.58 mm thickness) was used to section monoliths at regularly spaced intervals, creating "pucks" from known positions within the monolith.

For techniques requiring a powder form, the sectioned monolith was ground to a particle size of < 300 µm. For X-ray fluorescence analysis, monolith pieces were fixed in epoxy resin, mounted onto quartz slides, sectioned using a diamond saw and polished to 100 µm thickness.

2.8.2 X-ray Diffraction (XRD)

XRD measurements provide characterization of the mineralogical composition for samples using their diffraction patterns. Powders were loaded into zero-background holders and diffraction data were collected with a Rigaku Miniflex II Bragg-Brentano diffractometer using Cu-Kα radiation (λ = 1.5418 Å) and a graphite post-diffraction monochromator. A known amount of rutile standard was added to each sample for quantitative analysis. Quantitative Rietveld refinements were carried out with the Bruker TOPAS software (v4.2, Bruker AXS) using crystal structures for the relevant phases.

2.8.3 X-ray Photoelectron Spectroscopy (XPS)

XPS measurements provide information about the oxidation state of the elements present in a sample. Powder samples were mounted using carbon tape on a silicon substrate and analyzed using a Kratos Analytical AXIS Ultra X-ray Photoelectron Spectrometer. Survey scans and regional scans for Cr, Tc, Ca, O, C, and Si were collected. Data were analyzed using CasaXPS software.

2.8.4 X-ray Absorption Spectroscopy (XAS)

XAS measurements provide information about the oxidation state of elements present in a sample and information regarding their local chemical environments. Tc K-edge X-ray absorption spectroscopy (XAS) data were obtained at the Stanford Synchrotron Radiation Lightsource Beamline 11-2. The monochromator was detuned 50% to reduce the harmonic content of the beam. Transmission data was obtained using Ar-filled ion chambers. Fluorescence data were obtained using a 100 element Ge detector and data were corrected for detector dead time. Raw XAS data were converted to spectra using SixPack (Webb 2005). Spectra were normalized using Athena. (Ravel et al. 2005). Non-linear least squares fits of the normalized X-ray absorption near edge spectroscopy (XANES) spectra were obtained using standard spectra and the locally-written program, *fites* (http://lise.lbl.gov/RSXAP). XANES standard spectra were carefully energy calibrated using TcO_4^- adsorbed on Reillex-HPQ as the energy reference. The XANES spectral resolution is 7 eV based on the width of the TcO_4^- pre-edge peak. Sample spectra were convolved with a 1.8 eV Gaussian to match the resolution of the TcO_4^- adsorbed on Reillex-HPQ standard spectra. Six standard spectra (TcO_4^-, Tc_2S_7, Tc(V)=O polyoxometallate, Tc(IV) gluconate, $TcO_2 \cdot 2H_2O$ and Tc(IV) EDTA complex) were used in the initial fitting of the sample XANES spectra.

Cr L-edge X-ray absorption spectroscopy (XAS) data were obtained at the Advanced Light Source Beamline 6.3.1. Powdered samples obtained from the interior and exterior of T7 monoliths before and after leaching were pressed into iridium foil attached to a copper measurement probe using silver paint to improve conductivity. The XAS signal was monitored in total electron yield mode.

2.8.5 Scanning Electron Microscopy/Energy Dispersive X-ray Spectroscopy (SEM/EDS)

SEM/EDS allows for imaging of a sample surface and determination of elemental compositions at specific locations. SEM examinations were carried out using an FEI Quanta250 Field Emission Gun equipped with a backscattered electron (BSE) detector and EDAX Genesis x-ray energy dispersive spectrometer (EDS) system. Elemental mapping and line-profiles were performed with the aid of drift-correction software. Semi-quantitative EDS results were obtained using standard ZAF correction conditions and are useful for comparative analysis not quantitative analysis, owing to the uneven surface and variable density and porosity of the materials examined. SEM images were obtained between 10 and

30 keVwith both secondary and backscattered detectors to enable the features of interest to be observed most clearly. The SEM magnification scale was checked against a National Institute of Standards and Technology (NIST) traceable standard, MRS-4. The EDS energy scale was calibrated against the k-lines of a Cu-Al standard

2.8.6 Single Particle Digital Autoradiography (iQid)

Single-particle digital autoradiography was used to assess the spatial distribution of ^{99}Tc within cross sectioned Cast Stone “pucks” with the ionizing-radiation Quantum Imaging Detector (iQID) (Miller et al. 2015). The iQID imager comprises a scintillator in direct contact with a micro-channel plate image intensifier and a lens for imaging the intensifier screen onto a charge coupled device (CCD) or complementary metal oxide semiconductor (CMOS) camera sensor, all within a compact light-tight enclosure. iQID is sensitive to a broad range of radiation including gamma-/X-rays, neutrons, spontaneous fission, conversion electrons, alpha, and beta particles. Individual photons or particles absorbed in a scintillator crystal or phosphor screen produce a flash of light that is amplified via the image intensifier by a factor of 10^4 to10^6 and then imaged onto the camera. Scintillation flashes associated with individual events are captured with high resolution with an array of pixels and referred to as an event cluster. iQID’s ability to localize charged particles, both spatially and temporally, on an event-by-event basis enables radionuclide distributions to be quantified at mBq-levels. Autoradiographs are constructed in real time at high spatial resolutions with an unrestricted dynamic range. The intrinsic spatial resolution of the detector has been measured to resolution levels as high as 20 µm with alpha decays. iQID is a portable, laptop-operated system that requires no cooling and leverages the ever-increasing advances in CCD and CMOS camera sensor technology. For our Cast Stone cross section imaging experiments, a 4-megapixel camera (2048 × 2048 pixels) was used that acquires full-resolution images at approximately 10 frames per second. Disks sectioned from within ~ 0.5” from the center of the Cast Stone monoliths were analyzed using the iQID. The disks, which had a smooth surface, were placed on a scintillation screen for collection times of 45 h. The effective physical size of each pixel during the image acquisition was 55.8 µm with the final images displayed having an effective pixel size of 111.5 µm (2x2 binning). The pixel value corresponds to the number of beta particles detected at that location during the 45 h image run. A test sample with small droplets of pertechnetate enclosed in mylar film was also analyzed to ensure the β-decay signal arises from specific sample areas, with a strong correlation. Further information regarding development and use of the technique can be found in Miller et al. (2015).

2.8.7 Micro X-ray Fluorescence (µXRF)

XRF is utilized to give elemental distribution information within a sample. µ-XRF analysis was performed using an Orbis Micro-XRF Analyzer with a Mo X-ray source and a silicon drift detector. Elemental data were collected under vacuum using a 45 kVp polychromatic beam focused to 30 µm using a poly-capillary optic and displayed as number of counts per element-specific energy levels.

2.8.8 Nuclear Magnetic Resonance Spectroscopy (NMR)

NMR spectroscopy is employed to give information regarding the local chemical bonding of a species within a sample. ^{27}Al direct polarization (DP) experiments were conducted on a 17.6 Tesla wide-bore Bruker Avance III spectrometer, utilizing a 3.2 mm triple resonance probe operating in HX mode tuned to a ^{27}Al frequency of 195.49002 MHz. Spectra were acquired by collecting 16384 transients using calibrated ^{27}Al $\pi/20$ pulses of 0.30 µs, a 500 kHz sweep width, a spinning speed of approximately 18 kHz, and a 1.0 s recycle delay. Time domain free induction decays were apodized with exponential functions corresponding to 150 Hz of Lorentzian broadening prior to Fourier transformation. ^{27}Al resonances were referenced to 0.1 M $AlCl_3$(aq) standard at 0 ppm.

The Cast Stone powders, < 300 µm, were fixed in a solid matrix using Stycast© epoxy in a rod form designed to fit the NMR probe.

2.8.9 Biological Characterization

Apparent biological growths were observed on the many of the monolith surfaces that were leached in VZPW and the identity of the microorganism was investigated as follows. The growths were scraped from the surface of a monolith (T6-5 after immediate removal from solution) and placed into a phosphate buffered saline solution. Samples of the growths were initially stained with DAPI (4,6-diaminophenylindole), which is a fluorescent stain that binds to DNA in cells. These analyses showed the presence of bacteria in the samples. Following identification of microbes in these samples, DNA was extracted from samples using a MoBio Powersoil DNA Isolation Kit, and quantified using a NanoDrop spectrophotometer. DNA barcodes and linkers were added using polymerase chain reaction and the resulting amplicons were sequenced at the Institute for Genomics and Systems Biology Next Generation Sequencing Core Facility at Argonne National Laboratory using an Illumina MiSeq instrument. De-multiplexing, quality filtering, and operational taxonomic unit picking were performed using the Quantitative Insights Into Microbial Ecology (QIIME) toolkit v. 1.8.0) (Caporaso et al. 2010, Kuczynski et al. 2012). Raw sequence reads were processed in silico, and taxonomy was assigned to operational taxonomic units using BLAST alignments compared to the SILVA ribosomal RNA gene database project.

3.0 Results and Discussion

3.1 Cast Stone Fabrication

The GCCS monoliths were fabricated using the procedure described in Section 2.4. Following addition of the getters to the LAW simulant prior to mixing with the dry blend, clear evidence of the radionuclide and contaminant removal from the LAW simulant was observed. The LAW simulant usually has a distinct yellow color, due to its Cr(VI) content prior to any contact with the getters (Figure 3-1a). For the T2 test, the Sn-A was added in excess amount (3.5 × with respect to Cr content and 10 × with respect to Tc content of the LAW simulant) to make sure Tc(VII) was reduced to Tc(IV) after all Cr(VI) in the simulant should be reduced to Cr(III)) based on its reduction capacity of 3469 µeq/g (Asmussen et al. 2016a). This excess Sn-A addition was done because the alkaline nature of the LAW simulant and the high Cr content in this waste stream has been previously shown to hinder Tc removal by Sn-A (Asmussen et al. 2016a). After the addition of excess amounts of Sn-A and prior to the addition of the Ag-Z, it was observed that the yellow color of the LAW simulant had been removed with the LAW simulant turning colorless and a large amount of black colored precipitate appeared, clearly shown in Figure 3-1b). Prior to forming the T2 Cast Stone batch, the bottle was vigorously shaken to ensure the precipitate was transferred to the mixing bucket. Small aliquots of the simulant in the mixing bucket were used to collect any residual precipitate in the LAW simulant bottle.

The KMS-2-SS was added in Cast Stone mixes T3-T6 at a stoichiometric amount to reduce the entire Cr(VI) inventory of the LAW simulant plus 10 × the Tc(VII) content based on its reduction capacity of 20,000 µeq/g (Neeway et al. 2016). In all cases, after addition of KMS-2-SS, the color of the LAW simulant turned from yellow to a dark color, most likely because of the Cr(III) formation, as KMS-2-SS reduced the Cr(VI) in solution, see Figures 3-1c through Figure 3-1f.

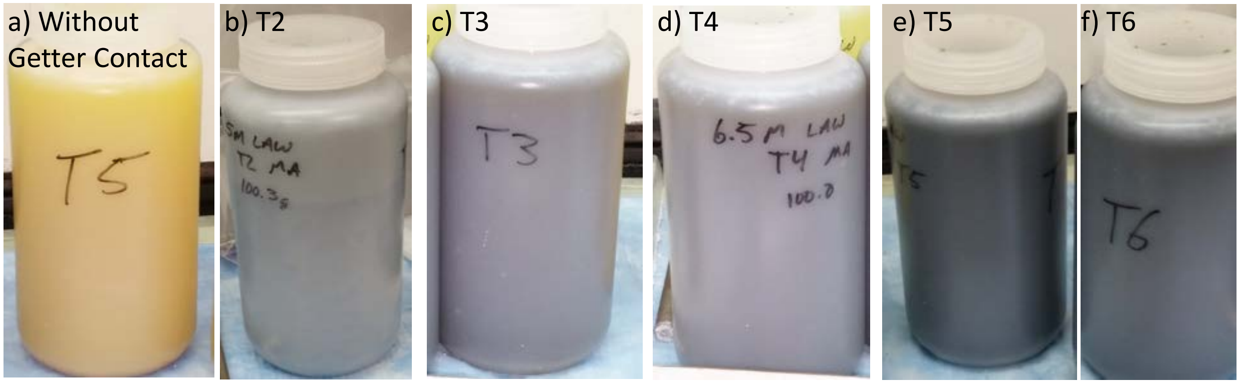

Figure 3-1- The Tc and I spiked LAW simulant used in Cast Stone fabrication with a) no getter contact, and prior to the dry blend addition for the T5 test to b) T2, c) T3, d) T4, e) T5, f) T6

Aliquots of the LAW simulant were collected prior to addition of each getter to determine the amount of Tc or I removed by the getter prior to addition of the dry blend. Figure 3-2 a presents the %Tc removed from the LAW simulant by the Tc getter in each test prior to Cast Stone fabrication. T1 is the experimental control (i.e., no getters were added in the LAW simulant) and therefore no change in Tc concentration occurred from the initial measurement until the dry mix was added to the LAW simulant, as expected. The Sn-A in T2 removed 65 % of the Tc initially present in the LAW simulant. This is similar to the highest level of Tc removal observed in tests conducted with highly caustic, high ionic strength LAW simulants (Asmussen et al. 2016a).

The KMS-2-SS had much greater success in removing Tc from the LAW simulant as shown in Figure 3.2a. In both T3 and T4, 97 % of the initial Tc was removed by the KMS-2-SS. T5 also had 97 % Tc removal, while T6 had a near complete Tc removal at 99.9 % by the KMS-2-SS. This performance by the KMS-2-SS is not surprising as both KMS-2 and KMS-2-SS are the most successful materials tested to date for sequestering Tc from LAW environments. (Neeway et al. 2016).

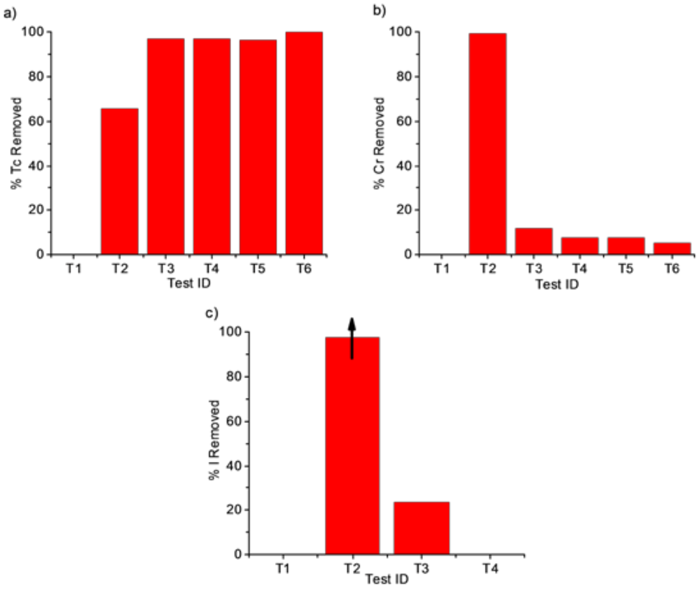

Figure 3-2 – From LAW simulant measurements before and after getter contact, plots showing the amount removed, prior to introduction of the dry blend Cast Stone ingredients, from the six tests for a) Tc, b) Cr, c) I.

As the Tc getters function via a reduction of the Tc(VII) to Tc(IV), they are likely to remove Cr(VI) from solution as well through reduction to Cr(III). Figure 3-2b) shows the %Cr removed by the getters in each test, and a reversed trend was observed. The Sn-A removed 99.6 % of the initial ~880 ppm of Cr present resulting in the loss of color in the simulant. Cr has previously shown a preference for reduction by Sn-A over Tc (Asmussen et al. 2016a). The KMS-2-SS removed < 11% of the Cr in each test, suggesting that KMS-2-SS may preferentially remove Tc irrespective of Cr content. However, the change in simulant color from initially yellow, indicative of the presence of Cr(VI), to dark green, indicative of the presence of Cr(III) was also observed once KMS-2-SS contacted the LAW simulant. It is likely that soluble Cr(III)-bearing species {e.g., $((Cr(III)Cl_2(H_2O)_4]Cl)\cdot 2H_2O)$} might have been formed in this system, which would explain the Cr reduction but not formation of predominately Cr(III) precipitates.

Figure 3-2c) displays the % iodide removed from the tests where the I getter was added to the LAW simulant. T1 is the control monolith batch and again no change in I was expected nor observed. T2 exemplifies the ability of Ag-Z to remove I from LAW simulant in the presence of Sn-A, as > 98 % of the I was removed. (The I measurement was below the detection limit of the ICP-MS for the resultant T2 LAW simulant).

However, in the system where KMS-2-SS contacted the LAW simulant prior to introducing the I getter, the observed I removal was lower. In T3 the KMS-2-SS was filtered out of the LAW simulant prior to the addition of the Ag-Z. Regardless, only 24 % of the I was removed by the Ag-Z, a sharp decrease compared with the > 98% removal by the Ag-Z in T2. T4 showed no measurable change in I after argentite was added to solution as an I getter, indicating that argentite was not removing I from the simulant. It is likely that residual soluble sulfide from the KMS-2-SS, or small particles of the KMS-2-SS, were able to pass through the 0.45 µm filter. If either of these are present in the LAW simulant, the Ag in both the Ag-Z and argentite I getters may preferentially react with the sulfur, and thus will not be available for reaction with I. Due to the high level of sulfate in the LAW simulant, detection of a change in total sulfur content (the species measured by ICP-OES) of the LAW simulant due to the KMS-2-SS is not possible. No attempt was made to measure reduced sulfur species (sulfide or elemental sulfur) in the getter reacted LAW. T5 and T6 were designed to alleviate the interaction between KMS-2-SS and Ag by adding the I getters directly to the dry blend. Thus, no I changes were measured in the LAW for T5 and T6 simulants prior to fabricating the Cast Stone monoliths and curing them.

3.2 EPA Method 1315

EPA Method 1315 leach testing was performed on the GCCS batches in both VZPW and DIW and observed diffusion coefficients (D_{obs}) were determined for contaminants of concern Tc, I and Cr and mobile components Na, NO_3^- and NO_2^-. As stated in EPA Method 1315 “This method is a characterization method and does not provide a solution considered to be representative of eluate under field conditions”. A lower D_{obs} represents a lower release of that species from the monolith. The D_{obs} was determined using the equation for simple radial diffusion from a cylinder into an infinite bath, presented in EPA Method 1315 (EPA 2013). The equation used is based on Fick’s 2nd law and is as follows:

$$D_{obs} = \pi \left[\frac{M_{t_i}}{2\rho C_o(\sqrt{t_i} - \sqrt{t_{i-1}})} \right]^2 \qquad \text{Equation 3.1}$$

where D_{obs}= observed diffusivity of a specific constituent for leaching interval, *i* (m^2/s)

M_{ti} = mass of specific constituent released during leaching interval (mg/m^2)

t_i = cumulative contact time at the end current leach interval, *i* (s)

t_{i-1} = cumulative contact time after previous leaching interval, *i-1* (s)

C_o = initial concentration of constituent in the dry Cast Stone mix (mg/kg_{dry}) calculated using the theoretical initial constituent concentration in the simulant based on additions made in simulant preparation

ρ = Cast Stone dry bulk density (kg_{dry}/m^3).

It should be noted that the common units for effective or observed diffusion coefficients in transport modeling activities is cm^2/s, in which case the value resulting from equation 3.1 is multiplied by 10^4 to convert from m^2/s to cm^2/s. The initial concentration (C_o) of individual species was calculated solely based on their content in the liquid waste simulant and any constituents that were present in the dry blend ingredients were assumed to be in an inert form and not prone to leaching. All D_{obs} values presented herein were calculated using the average D_{obs} based on data collected from leaching two replicate monoliths in each solution (DIW or VZPW), and error bars are the standard deviation of the mean. Further explanation of EPA Method 1315 and its application in Cast Stone leaching can be found elsewhere (Serne et al. 2016). Full data and calculations for the EPA Method 1315 tests can be found in Appendix C.

3.2.1 Technetium

The calculated D_{obs} values for Tc for the GCCS can be seen in Figure 3-3 for the 63 d leaching period. For the GCCS leached in VZPW (Figure 3-3a), the most accurate representation of the conditions of the disposal site of such waste forms at the IDF, an improvement in Tc diffusivity from the presence of getters is definitely observed.

The control T1 monoliths showed a consistent increase in D_{obs} from 1.4×10^{-13} cm^2/s in the first 2 h interval reaching a maximum of 1.2×10^{-11} cm^2/s at 49 d and ending at 4.6×10^{-12} cm^2/s at 63 d. This trend of increasing D_{obs} as cumulative time increases has previously been observed in some Cast Stone mixes in < 100 d leaching in previous testing (Westsik et al. 2013, Serne et al 2016). This trend may result from steady ingress of oxygen into the monoliths assisting in re-oxidation of Tc(IV) species. These Tc D_{obs} values for the control T1 monolith are within the 63 d range of other getter-free Cast Stone mixes leached in DIW, see Table 3.3 in Serne et al. (2016).

In T2 with Sn-A added as a Tc getter, the D_{obs} values were measured at 3.5×10^{-12} cm^2/s for the first 28 d. After this point the D_{obs} decreased, unlike the D_{obs} values for T1, to 1.1×10^{-12} cm^2/s at 63 d. The KMS-2-SS containing monoliths showed further improvement in reducing the Tc D_{obs}.

T3 and T4, which used KMS-2-SS as a Tc getter that was collected via filtration before addition of the I getter to the LAW simulant, with the KMS-2-SS getter then added back into the wet slurry as the dry blend was mixed into the LAW simulant, initially measured D_{obs} values were 3.2×10^{-12} cm^2/s and 2.7×10^{-12} cm^2/s respectively in the first 2 h sampling interval. The D_{obs} values then decreased steadily, at a faster rate than T2, to 5.4×10^{-13} cm^2/s and 6.1×10^{-13} cm^2/s for the T3 and T4 monoliths. This represents a near order of magnitude improvement in the Tc D_{obs} values over the control T1 monolith Tc D_{obs} values.

In the T5 and T6 monoliths, where the KMS-2-SS was not removed from solution and I the getters added to the dry blend, the Tc D_{obs} values show a similar trend to the T3 and T4 Tc D_{obs} values. The T5 and T6 monoliths measured initial Tc D_{obs} values of 7.0×10^{-12} cm^2/s and 5.1×10^{-12} cm^2/s at the 1 d interval and decreased to 8.0×10^{-13} cm^2/s and 6.9×10^{-13} cm^2/s respectively at 63 d leaching. These Tc D_{obs} values are similar to those for the T3 and T4 monoliths, showing that the removal of the KMS-2-SS from solution prior to I getter addition has a minimal effect on Tc retention in the cured Cast Stone monoliths that contained KMS-2-SS.

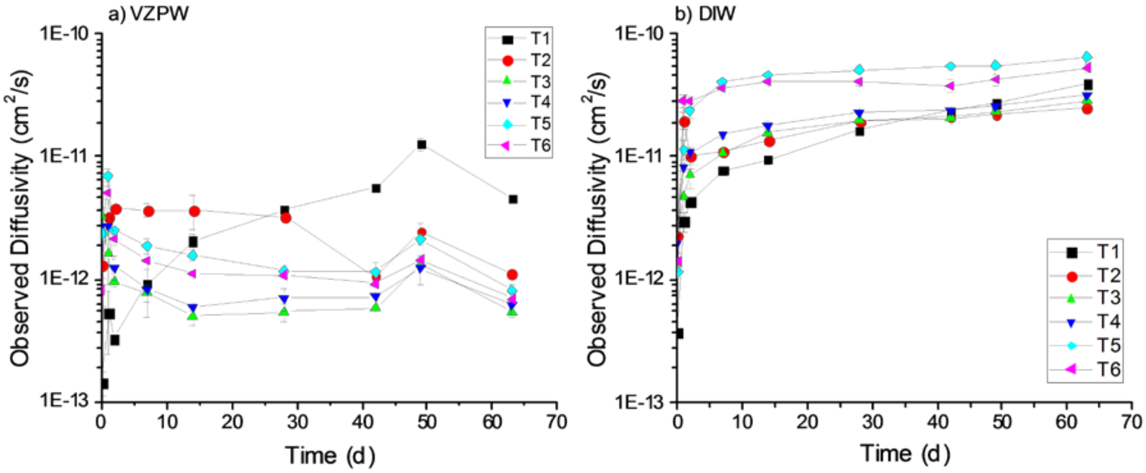

Figure 3-3- Observed diffusivities of Tc in a) VZPW (post leaching pH ~10.7) and b) DIW (post leaching pH of ~12) from EPA Method 1315. The error bars are resulting of the standard deviation of the mean for the two monoliths tested.

A noticeable increase in Tc D_{obs} was observed for all monoliths leached in the VZPW at 49 d, possibly due to the short time interval between placing the monoliths in fresh VZPW after the 42 d interval and conducting the next leach interval at 49 d (only a 7-d long interval compared with 14 d for the preceding and following intervals), which did not allow for the monoliths to equilibrate and for the pH buffering capacity of the VZPW to take effect, resulting in the larger release of contaminants for this sampling interval. Determination of this anomaly was outside of the scope of this work and should be investigated in future studies.

In the tests conducted with DIW, Figure 3-3b), less difference between the Tc D_{obs} values were observed between the Cast Stone compositions. All the monoliths followed a similar trend with a steady increase in Tc D_{obs} over the 63 d leaching period. The T1 monolith began at a Tc D_{obs} value of 3.7×10^{-13} cm^2/s at the 2 h interval and increased to 3.9×10^{-11} cm^2/s at 63 d. This Tc D_{obs} value in DIW for the T1 batch is near the mid-range of previously reported Tc D_{obs} values for an 47/45/8 wt% BFS/FA/OPC Cast Stone fabricated with LAW, see Figure 7-16 in Westsik et al. (2013) and Table 3.3 in Serne et al. (2016). This range of Tc diffusivities was very similar to those measured for the T2, T3 and T4 monoliths. The initial D_{obs} values measured were 2.3×10^{-12} cm^2/s, 1.2×10^{-12} cm^2/s, and 1.9×10^{-12} cm^2/s for the T2, T3 and T4 groups at 2 h, and increased to 2.5×10^{-11} cm^2/s (T2), 2.8×10^{-11} cm^2/s (T3) and 3.2×10^{-11} cm^2/s (T4) at 63 d leaching. The T5 and T6 monoliths showed were slightly different Tc D_{obs} values, starting at 1.1×10^{-12} cm^2/s (T5) and 1.4×10^{-12} cm^2/s (T6) at the 2 h interval and increasing to 6.5×10^{-11} cm^2/s (T5) and 5.3×10^{-11} cm^2/s (T6) at 63 d.

It is not unexpected that lower D_{obs} values for Tc were measured in VZPW compared with DIW due to the buffering effect of the VZPW lowering the pH to near 10.70, as compared to pH ~12 in DIW (see Appendix B), and also due to the formation of the calcium carbonate (calcite/aragonite) layer on the outer monolith surface in VZPW (Serne et al. 2016). However, the reason why the GCCS monoliths do not have an effect on D_{obs} values for Tc in the DIW is unknown. It can be postulated that the mechanism of Tc retention by the getters involves reduction of soluble Tc(VII) to insoluble Tc(IV) and previous studies have shown an increase in Tc(IV) solubility with increasing pH above pH 9.5 (Eriksen et al. 1992, Warwick et al. 2007). Thus, at the higher pH in DIW leachate, the beneficial role of the Tc getters that were studied could be negated. If the pH of the internal Cast Stone pore water (not measured) has similar ranges in the two leachates as the bulk solution, this pH-dependent re-oxidation Tc solubility mechanism may be the process occurring. Also at higher pH, larger amounts of Al and Si are released from the leaching monoliths, as can be seen in Appendix B, and this dissolution of the monolith in DIW may lead to increased loss of Tc from the getters. The pH of the Cast Stone internal porewater was not measured, but a similar process may be occurring within the Cast Stone pores.

As suggested in EPA Method 1315, the release of the chemical species of interest is likely being controlled by a purely diffusive process if a plot of the logarithm of the cumulative release of the species vs. the logarithm of leaching time yields a trend line with a slope of 0.5 ± 0.15. Further information can be found in Section 12.2.4 of EPA Method 1315. Select plots for Tc release from the T1 (control), T2 (Sn-A) and T3 (KMS-2-SS) monoliths in DIW and VZPW are displayed in Figure 3-4 with the equation of the trend line listed in the upper left quadrant of the plots. The slope of the T1 plots in both Figure 3-4a) DIW (0.75) and b) VZPW (0.70) give slopes outside of the 0.5 range. This suggests the release of Tc is not purely diffusion controlled; a redox process involving Tc(IV) may be invoked as well. For the Sn-A system in T2, both DIW (0.61) and VZPW (0.55) plots give a slope within the 0.5± 0.15 range. The KMS-2-SS containing monolith in T3 was calculated to have a slope outside of the range in DIW (0.70) but within range in VZPW (0.40). The variance in the measured slopes throughout all the tests shows that the mechanism of release cannot be described by a purely diffusive process. Thus, the mechanisms controlling the effective diffusivities calculated from leach testing must be further investigated through solid state characterization of the waste form after leaching. A summary of all cumulative release plots for all analytes is given in Appendix E.

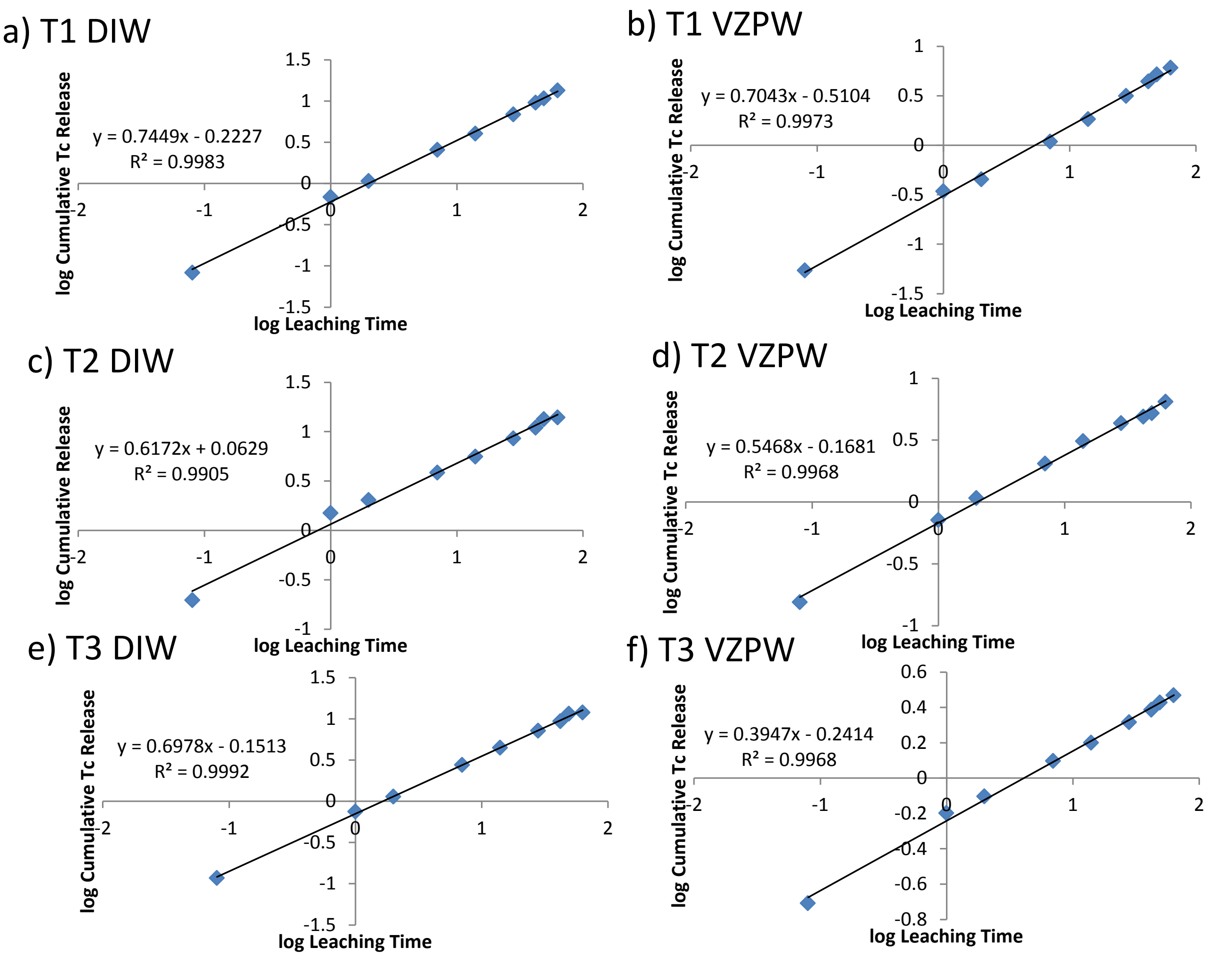

Figure 3-4 -plots of log cumulative Tc release vs log of leaching time for individual monoliths from a) T1 in DIW, b) T1 in VZPW, c) T2 in DIW, d) T2 in VZPW, e) T3 in DIW and f) T3 in VZPW. The equation of the trend line is shown in the upper left quadrant of the plots.

3.2.2 Iodide

The calculated D_{obs} values for I (as iodide, the species spiked into the LAW simulant and likely species in the reducing environment of the Cast Stone) are shown in Figure 3-5 from leaching in (a) VZPW and (b) DIW. Aside from T2, the monoliths in all tests have similar I D_{obs} values over time. In the VZPW, Figure 3-5a), the T1 control monolith with no getter measured an I D_{obs} of 3.5×10^{-8} cm^2/s at the 1 d interval and decreased to 6.6×10^{-9} cm^2/s at 63 d. Adding Ag-Z to the LAW simulant in T2, in which > 98 % of the I was removed from the LAW simulant prior to fabricating the Cast Stone monoliths, the measured I D_{obs} reached a maximum of 6.2×10^{-8} cm^2/s at 2 d and decreased to 5.0×10^{-9} cm^2/s at 63 d. In T3 the Ag-Z removed 23.5% of the I in the LAW simulant prior to fabrication of the Cast Stone. The I D_{obs} values in VZPW for T3 were measured at a maximum of 1.7×10^{-8} cm^2/s at the 2 d interval and decreased to 3.7×10^{-9} cm^2/s at 63 d. Whereas T4, where no measurable I was removed from the LAW simulant by argentite, the measured I D_{obs} was highest (3.4×10^{-8} cm^2/s) at 2 d and decreased to 6.4×10^{-9} cm^2/s at 63 d. T5, with the Ag-Z I getter added directly to the dry blend, the I D_{obs} values measured a maximum D_{obs} at 2 d of 2.9×10^{-8} cm^2/s and decreased to 6.4×10^{-9} cm^2/s at 63 d. T6, argentite as an I getter added to the dry blend, measured a maximum I D_{obs} of 3.1 × 10^{-8} cm^2/s at 2d before decreasing to 6.0 × 10^{-9} cm^2/s at 63 d.

Similar trends were observed in the tests conducted in DIW, Figure 3-5b). The highest measured D_{obs} was found for T2 at 6.6 × 10^{-8} cm^2/s in early leach times and by 63 d leaching the D_{obs} I values for each test were measured at 8.3 × 10^{-9} cm^2/s (T1), 4.4 × 10^{-9} cm^2/s (T2), 4.9 × 10^{-9} cm^2/s (T3), 8.2× 10^{-9} cm^2/s (T4), 7.3 × 10^{-9} cm^2/s (T5), and 8.1 × 10^{-9} cm^2/s (T6). The initial higher I D_{obs} values between 2 h and 2d may be a result of the "wash off" effect observed in previous testing. No uptick in I D_{obs} was observed at 49 d as was observed for the Tc. It should be noted that the D_{obs} values for I are consistently higher for the T2 set in the first 14 d of leaching. It is possible that the higher getter loading in the T2 mix increased porosity in the cured monoliths leading to increased I release.

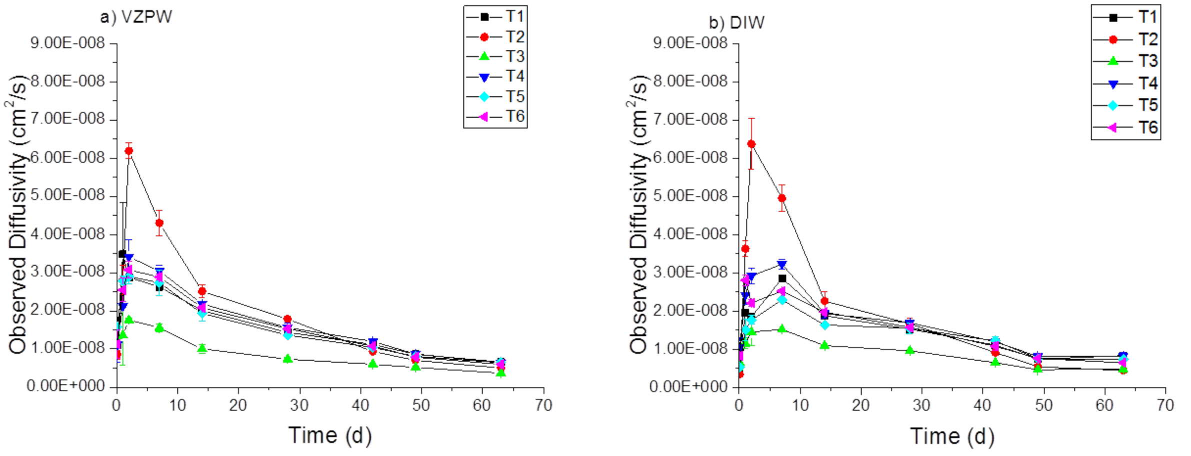

Figure 3-6- Observed effective diffusivities of Iodide in a) VZPW (pH ~10.7) and b) DIW (pH ~12) from EPA Method 1315. The error bars are resulting of the standard deviation of the mean for the two monoliths tested.

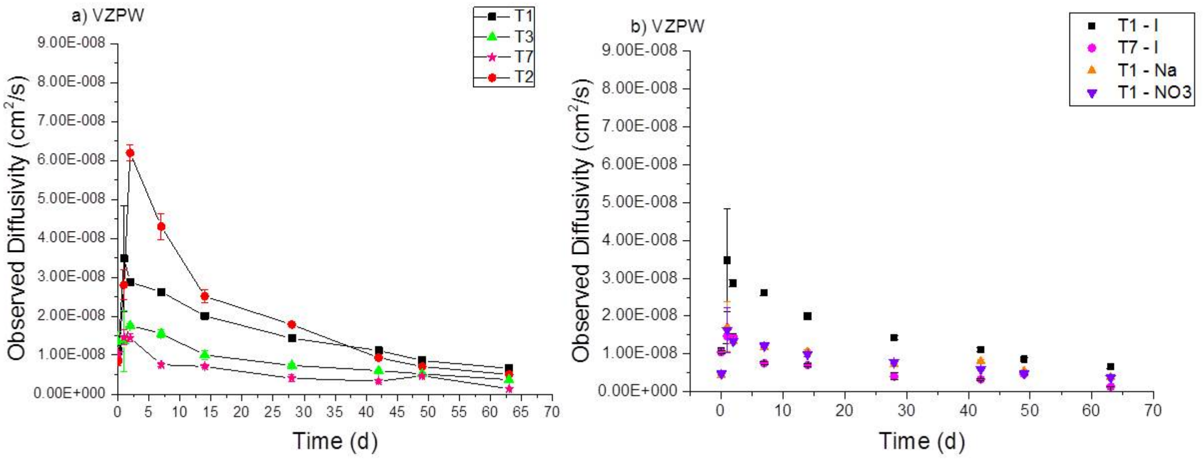

Figure 3-5- Observed diffusivity of Iodide in VZPW from EPA method 1315 testing a) comparing T1 (no getter), T2 (Ag-Z), T3 (Ag-Z) and T7 (AgI added) and b) comparing I D_{obs} to those of Na and NO_3 for T1. The error bars are resulting of the standard deviation of the mean from the two monoliths tested

In VZPW, the T1, T4 (argentite added to LAW simulant), T5 and T6 (I getter added to dry blend) all these monoliths give I D_{obs} values near 6.0×10^{-9} cm^2/s at 63, whereas T2 and T3 with Ag-Z sequestering I from the LAW simulant gave slightly lower I D_{obs} values of 5.0×10^{-9} cm^2/s and 3.7×10^{-9} cm^2/s respectively. A similar trend was observed in DIW with T1, T4, T5 and T6 exhibiting I D_{obs} values near 8.0×10^{-9} cm^2/s while T2 and T3 I D_{obs} values were $< 5.0 \times 10^{-9} cm^2/s$. These differences in I D_{obs} at 63 d are not large, yet could be a result of the Ag-Z addition. However the improvement in Cast Stone performance in terms of I diffusivity is not as significant as the one observed when KMS-2-SS was used as a Tc getter, despite the I getter effectiveness in sequestering I from LAW itself.

The I getters function through precipitation of soluble I^- to form insoluble AgI. Thus all I will be sequestered as AgI within the cured Cast Stone, irrespective of the I getter used, or whether it was added first to the LAW simulant or to the dry blend. The release of I from the cured waste form will therefore be dependent on the release of I from the discrete particles of AgI within the Cast Stone. An additional test was performed (T7) in which AgI was added directly to the LAW simulant at a level corresponding to 20 ppm I, this is similar to a test performed by Atkins et al. (1990) using OPC only and OPC + BFS grouts. Two monoliths from this batch were leached under the EPA 1315 protocol in VZPW. Figure 3-6 a) displays the measured I D_{obs} from the T7 test compared with T1 and T3. The I D_{obs} values for T7 are slightly lower than those for T1 and T3, with a maximum I D_{obs} of 1.5×10^{-8} cm^2/s at 1 d and dropping to 1.3×10^{-9} cm^2/s at 63 d. This result confirms that the release of I from the waste form is controlled only by the solubility of the solid I^--containing phase in the grout. The I D_{obs} are also similar to the D_{obs} measured for the mobile constituents (such as Na, discussed in section 3.2.3), and a comparison is shown in Figure 3-6 b). This similarity suggests that there is no chemical binding of the I within the Cast Stone and it is free to diffuse out of the monolith. Thus, the I retention by the I getters in LAW Cast Stone cannot be improved unless a phase with a solubility product constant lower than AgI ($K_{sp} = 8.5\times10^{-17}$) or a chemical transformation to another iodine species with a lower K_{sp} is formed in the grout.

3.2.3 Mobile Constituents

Na, NO_3, and NO_2 are considered “mobile” constituents within the Cast Stone as they are unlikely to be involved in chemical processes that slow release from the waste form. That is, mobile species release solely via diffusion-based pathways. For the Na and NO_3 D_{obs} measurements in VZPW, the nominal measured concentrations of those species in the VZPW were subtracted from the measured value of the leachates. No NO_2 was added or measured in the VZPW. Figure 3-7a) displays the measured D_{obs} values for Na in VZPW. The T2 monolith gave the highest Na D_{obs} values in the first 49 d intervals, reaching a maximum of 2.7×10^{-8} cm^2/s at 2 d, resulting from the “wash off” effect. At 63 d leaching all six Cast Stone mixes the Na D_{obs} ranged from 5.0×10^{-9} cm^2/s (T2) to 3.5×10^{-9} cm^2/s (T3). In DIW, Figure 3-7b), the T2 monoliths had the highest Na D_{obs} at 2.6×10^{-8} cm^2/s at 7d, with the Na D_{obs} values for all six Cast Stone mixes ranging from 5.3×10^{-9} cm^2/s (T2) to 4.0×10^{-9} cm^2/s (T6) at 63 d. These values are all within previously measured ranges for LAW Cast Stone (see Westsik et al. 2013 and Serne et al. 2016)

The D_{obs} values for NO_3 are displayed in Figure 3-7c) for VZPW and d) in DIW. Many similarities can be seen between the NO_3 and the Na D_{obs} values with a steady decrease in D_{obs} after the initial “wash off” phase. In VZPW the highest NO_3 D_{obs} measured was T2 at 2.7×10^{-8} cm^2/s at 2 d, and after 63 d the Na D_{obs} measured between 4.9×10^{-9} cm^2/s (T2) and 3.4×10^{-9} cm^2/s (T3, T4, T5, and T6). Similar values were observed in DIW with the highest NO_3 D_{obs} measured for T2 of 2.7×10^{-8} cm^2/s at 7d then ranging between 5.3×10^{-9} cm^2/s (T2) and 4.3×10^{-9} cm^2/s (T4). The NO_2 D_{obs} values are also similar to the NO_3 and Na values as shown in Figure 3-7e) VZPW and f) DIW. In the VZPW, the largest NO_2 D_{obs} measured was 3.3×10^{-8} cm^2/s for T2 at 2 d, and the NO_2 D_{obs} values ranged between 5.7×10^{-9} cm^2/s (T2) and 3.8×10^{-9} cm^2/s (T3 and T4) at 63 d. In DIW the NO_2 D_{obs} values ranged between 5.9×10^{-9} cm^2/s (T2) and 4.5×10^{-9} cm^2/s (T4) at 63 with the highest measured NO_2 D_{obs} value being 2.8×10^{-8} cm^2/s (T2) at 7 d.

Again, the D_{obs} values for the mobile constituents are consistently higher for the T2 set in the first 49 d of leaching as was observed for I. The likely cause of the increase in D_{obs} values for the T2 system is alteration of the physical characteristics of the monolith due to the high getter loading.

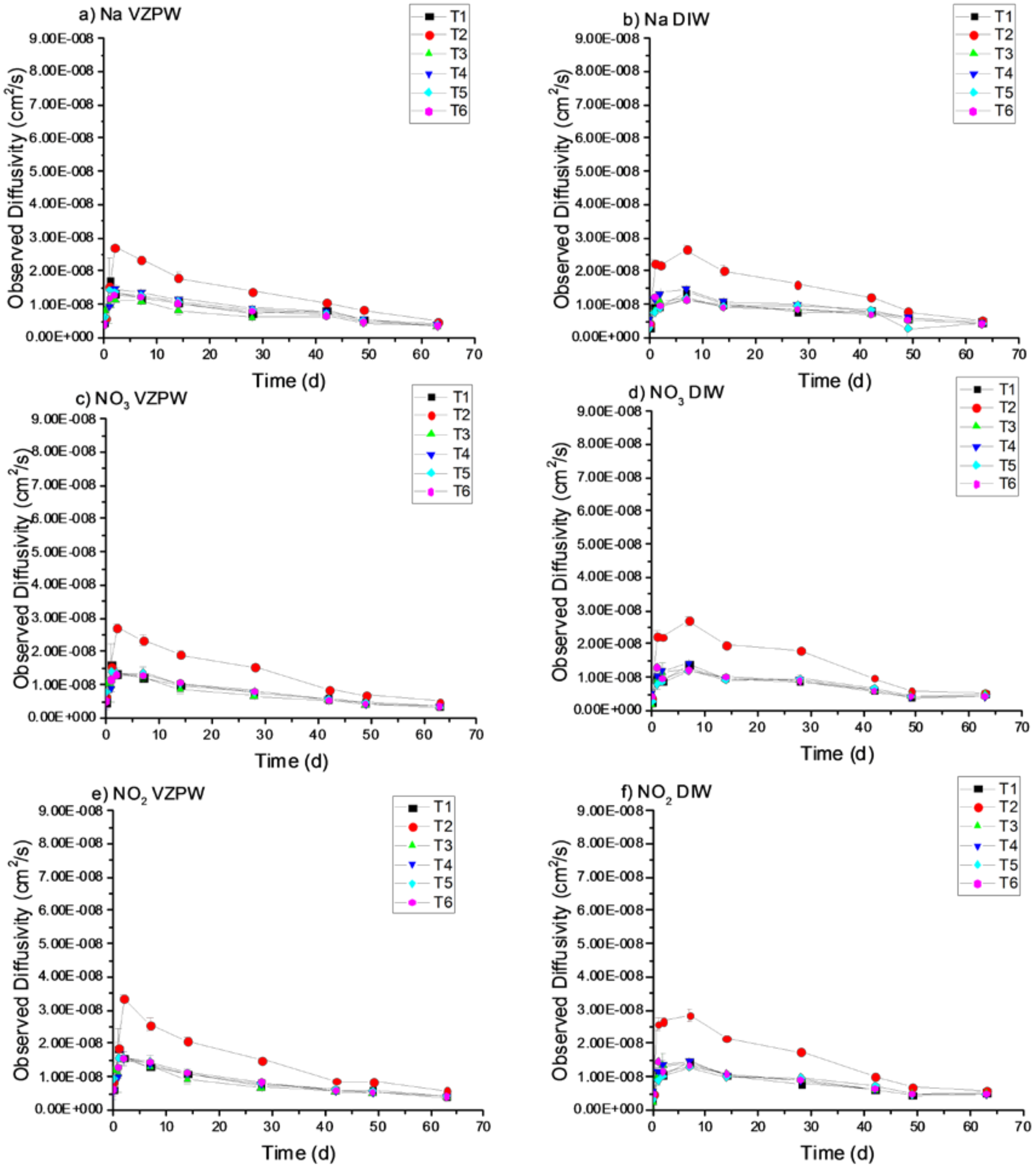

Figure 3-7 - Observed diffusivities of Na in a) VZPW and b) DIW, NO_3 from c) VZPW and d) DIW and NO_2 from e) VZPW and f) DIW from EPA Method 1315. The error bars are resulting of the standard deviation of the mean for the two monoliths tested.

3.2.4 Chromium

Leachate aqueous Cr concentrations were below the matrix determined detection limit (6.95 µg/L) for the ICP-OES for many of the Cast Stone leachates from the EPA-1315 tests. A summary of the resulting D_{obs} values for Cr in both DIW and VZPW is shown in Table 3-1. The italicized values represent Cr D_{obs} calculated using the matrix determined detection limit when the measurement of leachates was below this value. At 63 d the D_{obs} for Cr are below 1.3× 10^{-13} cm^2/s in both DIW and VZPW. No cumulative release plots for Cr were prepared for Appendix E as the concentration of Cr in most leachates was below the matrix determined detection limit.

Table 3-1 – Observed diffusivity values for Cr in VZPW and DIW from EPA Method 1315 testing. Values in *italics* indicate the some leachate measurements were below the matrix determined detection for the ICP-OES, while **bold** D_{obs} values had all leachates above the detection limits.

Days DIW	D_{obs} T1	St.Dev T1	D_{obs} T2	St.Dev T2	D_{obs} T3	St.Dev T3	D_{obs} T4	St.Dev T4	D_{obs} T5	St.Dev T5	D_{obs} T6	St.Dev T6
2	*< 6.0E-13*	*< 2.1E-14*	*< 5.6E-13*	*< 1.4E-14*	*< 5.7E-13*	*< 3.9E-15*	*< 6.3E-13*	*< 6.0E-15*	*< 5.9E-13*	*< 1.2E-14*	*< 5.9E-13*	*< 8.5E-16*
7	**9.2E-14**	**7.7E-15**	**9.4E-14**	**5.7E-15**	**1.0E-13**	**2.2E-15**	**1.0E-13**	**4.2E-15**	**8.0E-14**	**6.7E-15**	**8.6E-14**	**4.3E-15**
14	*< 8.6E-14*	*< 3.0E-15*	*< 8.0E-14*	*< 2.0E-15*	*< 8.1E-14*	*< 5.6E-16*	*< 9.1E-14*	*< 8.5E-16*	*< 8.4E-14*	*< 1.7E-15*	*< 8.4E-14*	*< 1.2E-16*
28	*< 4.3E-14*	*< 1.5E-15*	*< 4.0E-14*	*< 1.0E-15*	**6.1E-14**	**2.4E-15**	**4.9E-14**	**3.9E-15**	**6.5E-14**	**7.3E-15**	**5.1E-14**	**8.9E-15**
42	*< 7.3E-14*	*< 2.5E-15*	*< 6.8E-14*	*< 1.7E-15*	*< 6.9E-14*	*< 4.8E-16*	*< 7.7E-14*	*< 7.2E-16*	*< 7.1E-14*	*< 1.5E-15*	*< 7.1E-14*	*< 1.0E-16*
49	*< 3.8E-13*	*< 1.3E-14*	*< 3.6E-13*	*< 9.1E-15*	*< 3.6E-13*	*< 2.5E-15*	*< 4.0E-13*	*< 3.8E-15*	*< 3.7E-13*	*< 7.6E-15*	*< 3.7E-13*	*< 5.4E-16*
63	*< 1.2E-13*	*< 4.0E-15*	*< 1.1E-13*	*< 2.8E-15*	*< 1.1E-13*	*< 7.7E-16*	*< 1.3E-13*	*< 1.2E-15*	*< 1.1E-13*	*< 2.4E-15*	*< 1.1E-13*	*< 1.7E-16*
VZPW												
2	*< 6.0E-13*	*< 8.9E-15*	*< 5.8E-13*	*< 1.0E-14*	*< 5.7E-13*	*< 1.9E-15*	*< 6.3E-13*	*< 7.6E-15*	*< 5.9E-13*	*< 7.5E-15*	*< 5.8E-13*	*< 9.1E-15*
7	*< 6.8E-14*	*< 1.0E-15*	*< 6.6E-14*	*< 1.2E-15*	*< 6.4E-14*	*< 2.2E-16*	*< 7.2E-14*	*< 8.7E-16*	*< 6.7E-14*	*< 8.5E-16*	*< 6.5E-14*	*< 1.0E-15*
14	*< 8.6E-14*	*< 1.3E-15*	*< 8.3E-14*	*< 1.5E-15*	*< 8.1E-14*	*< 2.8E-16*	*< 9.0E-14*	*< 1.1E-15*	*< 8.5E-14*	*< 1.1E-15*	*< 8.2E-14*	*< 1.3E-15*
28	*< 4.3E-14*	*< 6.4E-16*	*< 4.2E-14*	*< 7.3E-16*	*< 4.1E-14*	*< 1.4E-16*	*< 4.5E-14*	*< 5.5E-16*	*< 4.3E-14*	*< 5.4E-16*	*< 4.1E-14*	*< 6.5E-16*
42	*< 7.3E-14*	*< 1.1E-15*	*< 7.1E-14*	*< 1.2E-15*	*< 6.9E-14*	*< 2.4E-16*	*< 7.6E-14*	*< 9.2E-16*	*< 7.2E-14*	*< 9.1E-16*	*< 7.0E-14*	*< 1.1E-15*
49	*< 3.8E-13*	*< 5.6E-15*	*< 3.7E-13*	*< 6.5E-15*	*< 3.6E-13*	*< 1.2E-15*	*< 4.0E-13*	*< 4.9E-15*	*< 3.8E-13*	*< 4.8E-15*	*< 3.7E-13*	*< 5.8E-15*
63	*< 1.2E-13*	*< 1.7E-15*	*< 1.1E-13*	*< 2.0E-15*	*< 1.1E-13*	*< 3.8E-16*	*< 1.3E-13*	*< 1.5E-15*	*< 1.2E-13*	*< 1.5E-15*	*< 1.1E-13*	*< 1.8E-15*

3.3 EPA Method 1313

EPA Method 1313 tests were performed on the six Cast Stone monolith mixes with a focus on measuring Tc, Cr and I in the leachates. The results of the pre-titration pH sweep on the Cast Stone (using T1) are shown in Figure 3-8. Due to the high alkaline nature of the Cast Stone from previous data, only acid additions were performed in the pre-titration (Pierce et al. 2010b). The pre-titration was performed to determine the approximate number of acid equivalents required to achieve a desired pH after the crushed Cast Stone samples equilibrated with DIW for 24 hr. Based on the pre-titration data and moisture content of the Cast Stone, 25.97 g of Cast Stone, < 300 µm particle size, was added to 200 mL of solution (DDI and varying amounts of 2 N HNO_3) to give a solution-to- dry solid ratio of 10 mL/g. The samples reacted for ~24 h before they were sampled for ICP-MS (Tc and I) and ICP-OES (Cr), pH, EC and E_h. With the 24 h contact time it is possible that the samples have not yet reached equilibrium, however the final leachates give a strong comparison of pH dependent release of constituents. The pH, EC and E_h measurements are shown in Table 3-2.

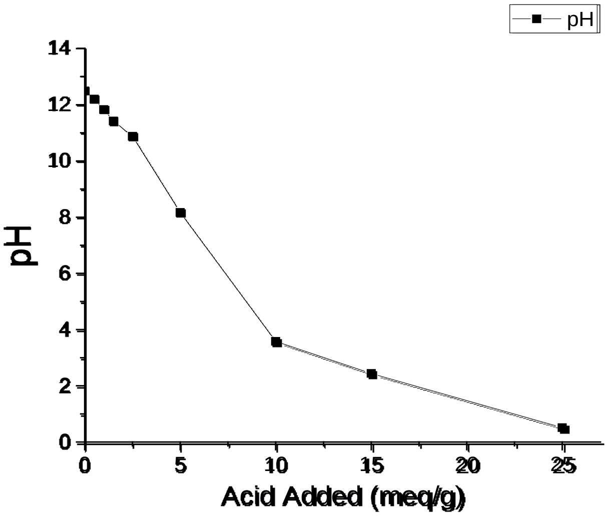

Figure 3-8 – Pre-titration curve for EPA 1313 testing using the T1 monolith and various acid additions using 2N HNO_3

Table 3-2 – Equilibrium pH, EC and E_h measurements for each EPA Method 1313 sample. The E_h measurements for T1 are not presented due to a probe error, and all E_h measurements are corrected for the standard hydrogen electrode and are FOR INFORMATION ONLY. The '-'indicates that the measurement was not taken.

pH	EC (mS/cm)	Eh (mV)	pH	EC (mS/cm)	Eh (mV)	pH	EC (mS/cm)	Eh (mV)
	T1			T2			T3	
12.77	33.1	-	12.77	32.6	-27.3	12.67	32.7	10.3
12.33	28.4	-	12.35	27.7	45.3	12.16	28	58.2
10.89	37	-	10.88	36.4	111.8	10.83	36.8	48
9.78	46	-	9.7	45.3	156.7	9.92	45.8	126.1
9.07	51.3	-	9.13	50.8	158.1	9.17	51	142.3
8.13	57.4	-	8.08	57	209	7.86	58.1	217.7
6.54	65.7	-	6.46	64.7	280	6.05	66.6	284.9
5.57	73.1	-	5.55	71	317.3	5.57	70.7	327.5
2.52	91.9	-	2.46	83.2	561.5	2.47	91.1	553.2
	T4			T5			T6	
12.56	32.7	-43.1	12.64	33.1	-45.3	12.52	30.4	-57.2
12.15	28.2	-28.1	12.21	28.7	-21.5	11.93	27	-26
10.82	36.6	24	10.92	37.1	26.6	10.05	37.5	55.3
9.68	45.9	103.5	9.88	46.3	71.8	8.83	46.8	102
8.94	51.1	113.7	9.25	51.4	107	7.82	52	144.6
8.03	57.1	146.3	8.29	56.8	137.5	6.65	56.8	181.6
6.56	65.8	214	6.69	64.2	220.1	5.95	65.5	226.1
5.58	72.2	292.2	5.6	71.8	326.8	5.47	72	254.4
2.72	88	553	2.71	92	541	2.86	95.2	525.2

With decreasing pH, the EC values increased due to the increased dissolved salt levels of the solutions as the acid dissolved more of the Cast Stone matrix as the higher amount of acid was added and the E_h values moved in the anodic direction (i.e. increased in value). The E_h values were made in the open atmosphere and, with the influx of atmospheric oxygen, stabilized readings are difficult to attain. The E_h measurements were taken as the first stable value after 10 s of entry of the E_h probe into solution.

Plots of the measured release of Tc, Cr and I at the corresponding pH's are shown in Figure 3-9. In the Tc measurements there was a slight increase in Tc release with increasing pH above pH 6 in the T3 and T4 tests, while all other Cast Stone composition leachates are relatively stable, Figure 3-9a). Above pH 3, T1 without getters added released the highest amount of Tc, while T3 and T4 had the lowest releases, likely due to the formation of Tc_2S_7-like insoluble species that increased the Tc solids' stability. For Cr, Figure 3-9b), a pH dependence was observed as Cr release was measurable below pH4 and above pH 8. All Cast Stone mix leachates had similar Cr releases. For iodide, Figure 3-9c), the impact of getter addition can be observed in the region <pH 9. T1 showed consistent iodide release from pH 5 and above. The I getter containing samples (T2-T6) did not have measurable I release between pH 5-6. Immediately above pH 6, the T4, T5 and T6 monoliths had measurable iodide releases. The T3 monolith, where some I

was sequestered prior to the fabrication of the Cast Stone (23%), release of I was not observed until > pH 7. T2, where >98% of the I was sequestered before fabrication of the Cast Stone, only a small amount of I was released at < pH 9. Above pH 9, similar I releases were measured for the tests, with T2 having the lowest iodide release, especially compared with T1. Due to the crushing of the monoliths prior to performing the EPA Method 1313 testing, the physical properties that lead to higher releases in the T2 monolith system were not observed in the EPA Method 1313 tests. This result suggests that there is a pH dependence on I release from the Ag containing getters. This is important in a disposal scenario as the Hanford sediment background pH is ~ 7.7 and differences at this pH still exist between the I getter containing Cast Stone mixes and the control mix (with no getters). This finding supports the results seen in the EPA Method 1315 testing, where little difference in I D_{obs} was observed between the GCCS mixes. The alkaline nature of the Cast Stone grouts may be deleterious to I loaded Ag-containing getters.

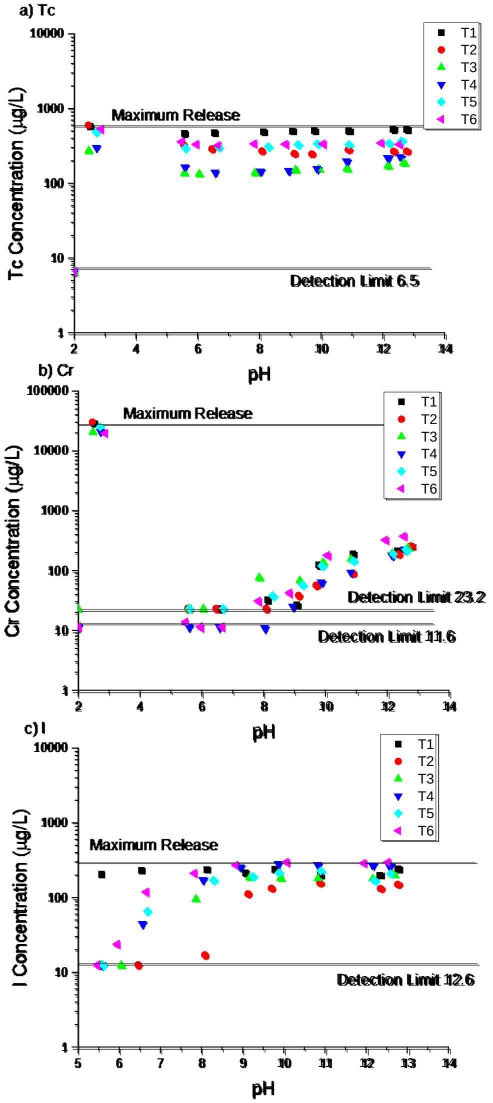

Figure 3-9 – Release plots for a) Tc, b) Cr and c) I as a function of pH in EPA Method 1313 testing. The detection limit and maximum theoretical release bases on complete release of the species are given by the horizontal lines.

3.4 Solid Phase Characterization

3.4.1 Monolith Opening Pictures

Following the 28-d curing, the four monoliths with the fewest defects were selected for EPA Method 1315 testing. One of remaining monoliths from each mix was selected to be crushed for EPA Method 1313 testing. The remaining three monoliths were archived for pre-leaching solid state characterizations. An photograph of each mix’s cured monoliths can be seen in Figure 3-10. A monolith for each mix that was destined for solid phase characterization was either manually cracked open using a hydraulic press, or sectioned into “pucks” using a circular saw with a diamond blade. Upon manually cracking the monoliths, their general interior characteristics can be seen in Figure 3-11.

All the monoliths show an outer grey exterior, and a dark green interior portion. This color difference is a result of differing Cr oxidation states in these locations, as discussed in section 3.4.6 in Figure 3-34. The T1 monolith, Figure 3-11a), showed some small blotches in the interior of the monolith, which may be a result of Cr re-oxidation from entrapped air at these locations. The origin of the blotches was not a focus of this work and not investigated further. The T2 monolith, Figure 3-11b), had the most diverse morphology. Large white clumps can be seen scattered throughout the interior of the monolith surrounded by grey regions. The identity of these white clumps will be discussed in sections 3.4.3 and 3.4.6. The KMS-2-SS containing monoliths in the T3-T6 mixes had similar interiors to the T1, as can be seen in the photograph of T4 in Figure 3-11c) and T5 in Figure 3-11d). T3 and T6 had identical interiors to T4 and T5 respectively.

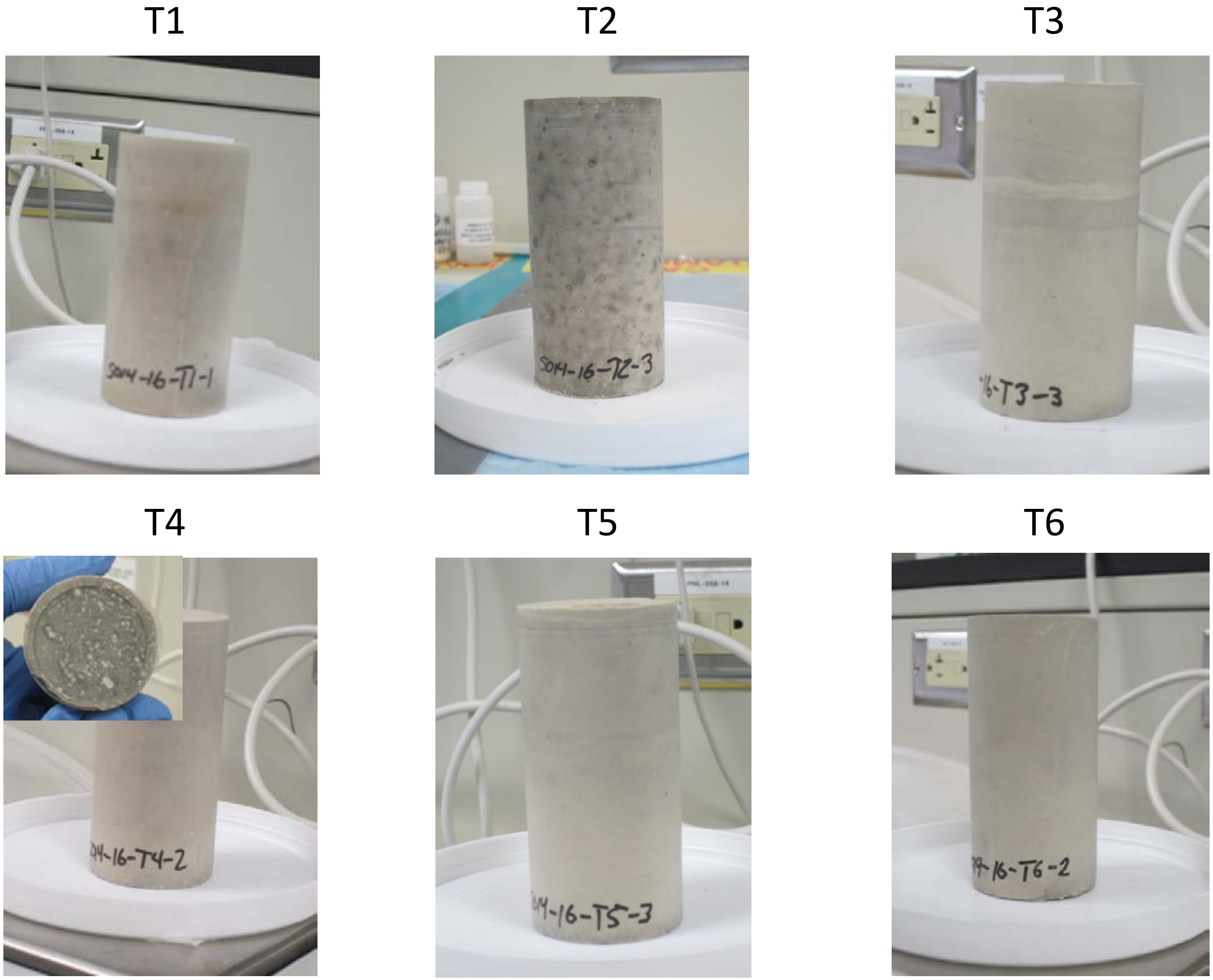

Figure 3-10 – Cast Stone monoliths fabricated in this study after 28-d curing. The insert of the T4 image shows the bottom face of the monolith.

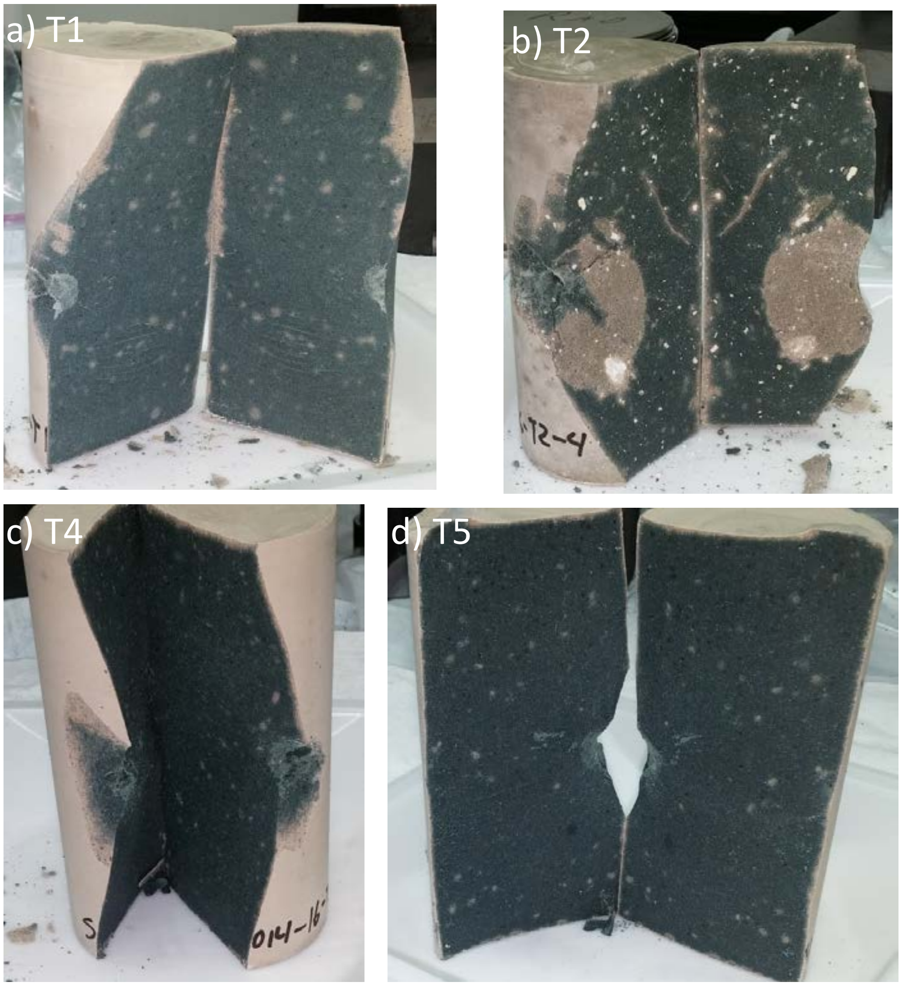

Figure 3-11 – Example unleached monoliths prior to preparation for solid state characterizations after initial manual cracking a) T1, b) T2, c) T4 and d) T5.

3.4.2 Leaching Progression

During each interval sampling of the EPA Method 1315 leachates, photos of the monoliths were taken in order to track the development of the physical features on the outer wall. Figure 3-12a) shows the progression of the T1-1 monolith leached in DIW. The surface remains clear of any outer deposits over the 63-d test. At 42 d, some micro-cracks begin to appear on the surface of the monolith that increase in size by 63 d. For the T1-4 monolith leached in VZPW, Figure 3-12b), the main characteristic is the growth of an outer white film which begins after the first interval. At 63 d, a dark line appeared on the monolith marked with a red arrow on the T1-7 monolith shown in the image. This dark line is similar to the other dark features on the monoliths leached in VZPW seen in the subsequent figures. A discussion of these features accompanies Figure 3-24.

a)

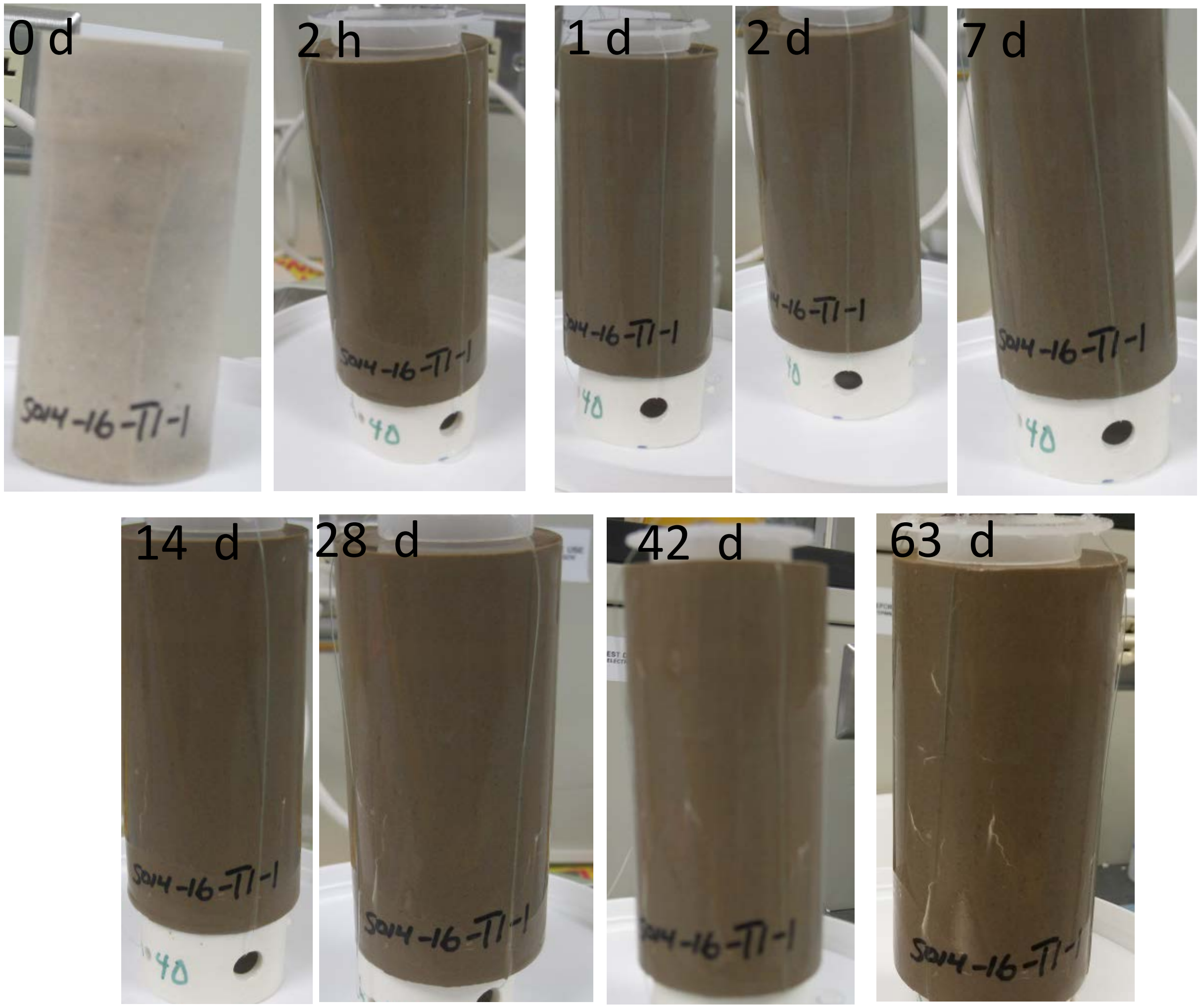

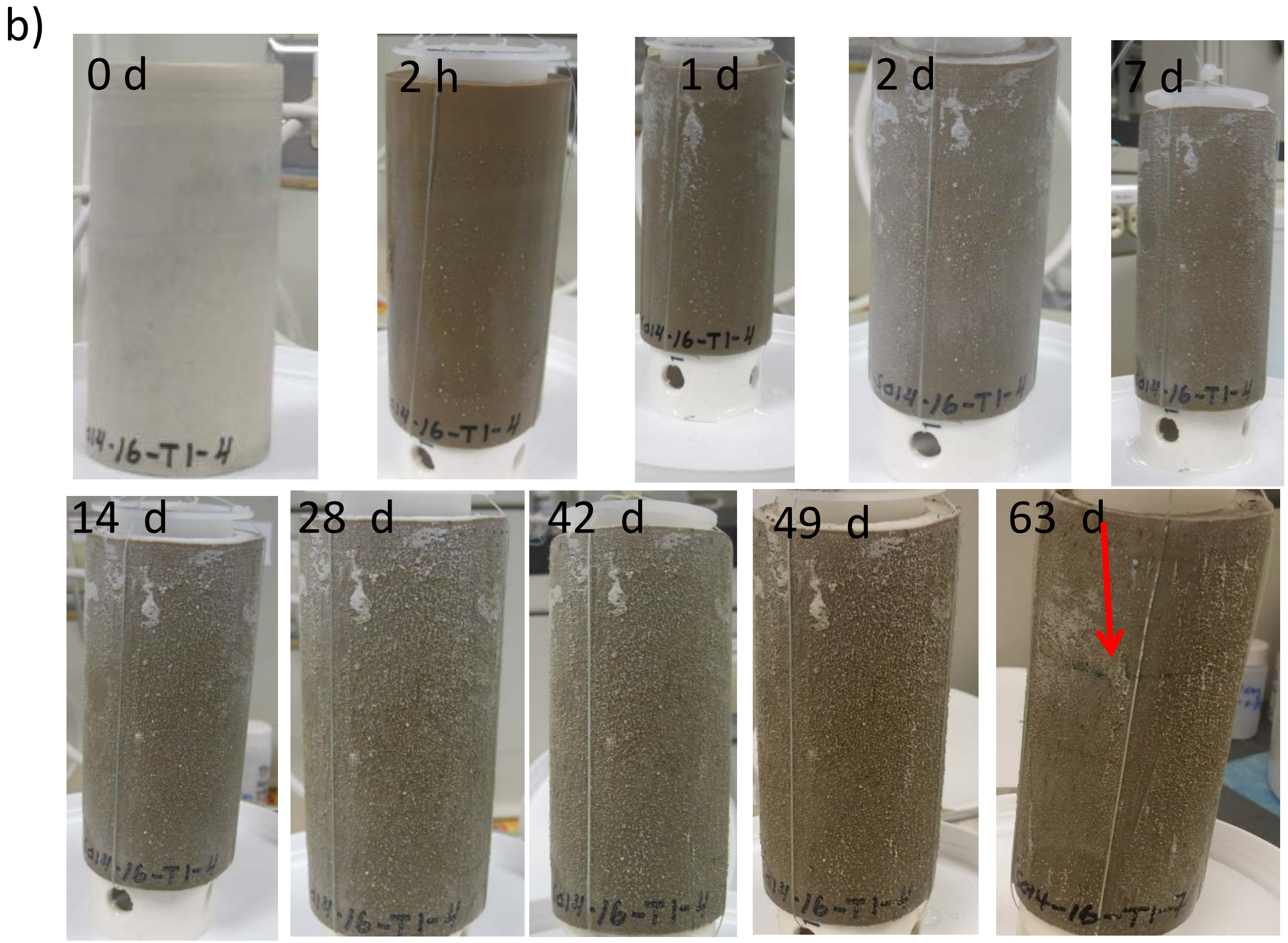

Figure 3-12 - The progression of the T1 monoliths leached in a) DIW and b) VZPW for the 63 d leaching period of EPA Method 1315.

The T2 monoliths, containing Sn-A and Ag-Z, show differing characteristics than the T1 control monolith. In DIW, Figure 3-13a), the T2-3 monolith displays “black dots” on the outer surface after 1 d of leaching and these black dots appear to “bleed” down the outer wall beginning at the 2d interval. The identity of these dots is discussed further in section 3.4.4. Additionally a white deposit appears to be exiting from the monolith interior after 1-d leaching. One of these white spots is highlighted with a red arrow at 63 d. There is no cracking observed in the T2 monoliths leached in DIW as is observed in all other monolith sets. The reason for this discrepancy is unknown. In the VZPW, Figure 3-13b), the T2-7 monolith displayed an outer deposit that was darker in color than the surface deposits formed on T1. The leachate from the T2 monoliths in DIW was also found to turn a brown color in all sampling intervals. Precipitate in the T2 bucket after the 28-d sampling interval was analyzed by XRD and found to be mainly brucite ($Mg(OH)_2$) with small amounts of calcite, hemicarbonate and hydrocalumite. The “bleeding dots” were not observed on the surface of the VZPW leached T2 monoliths.

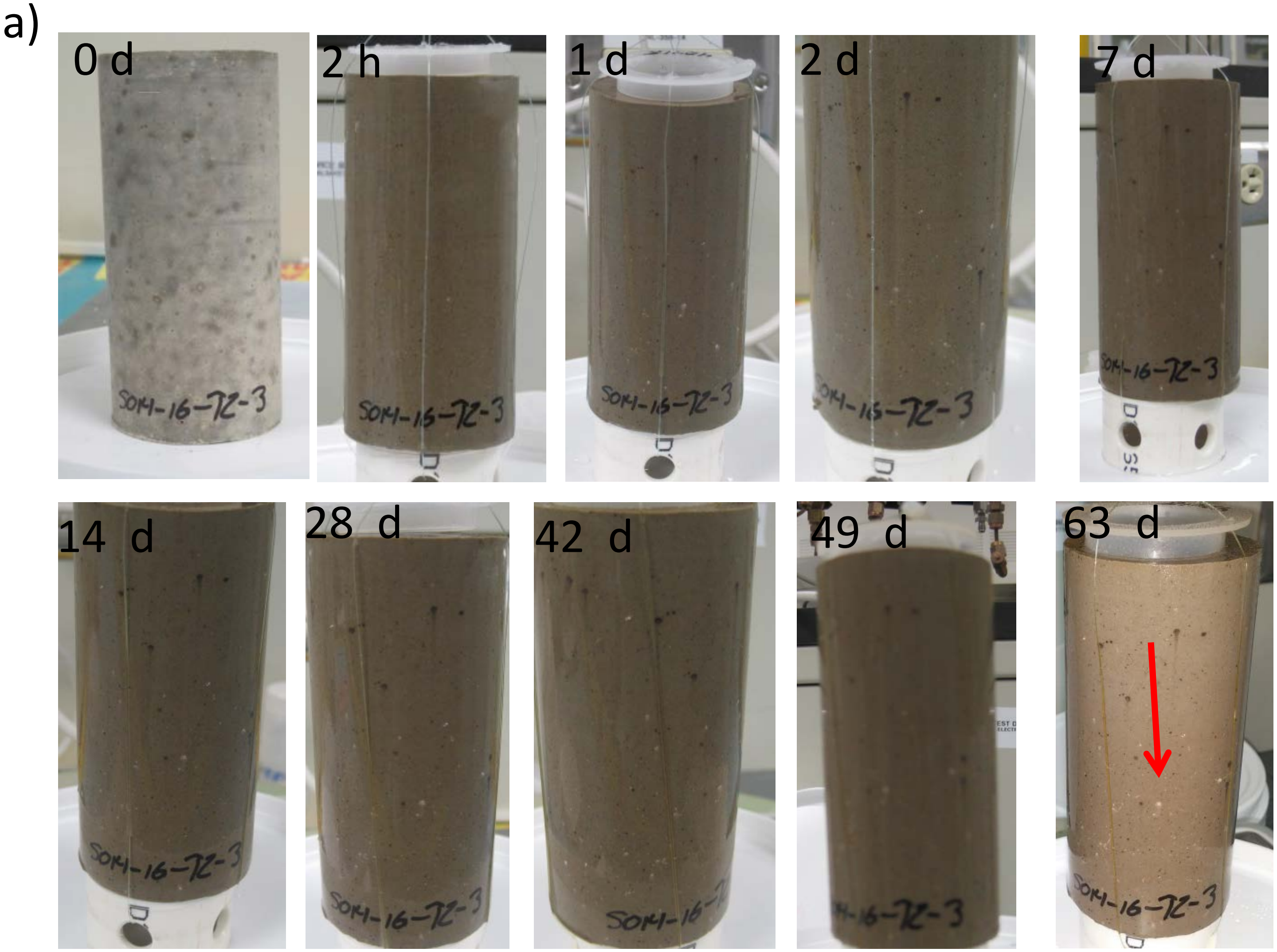
a)
0 d
2 h
1 d
2 d
7 d
14 d
28 d
42 d
49 d
63 d
SOM-16-TZ-3

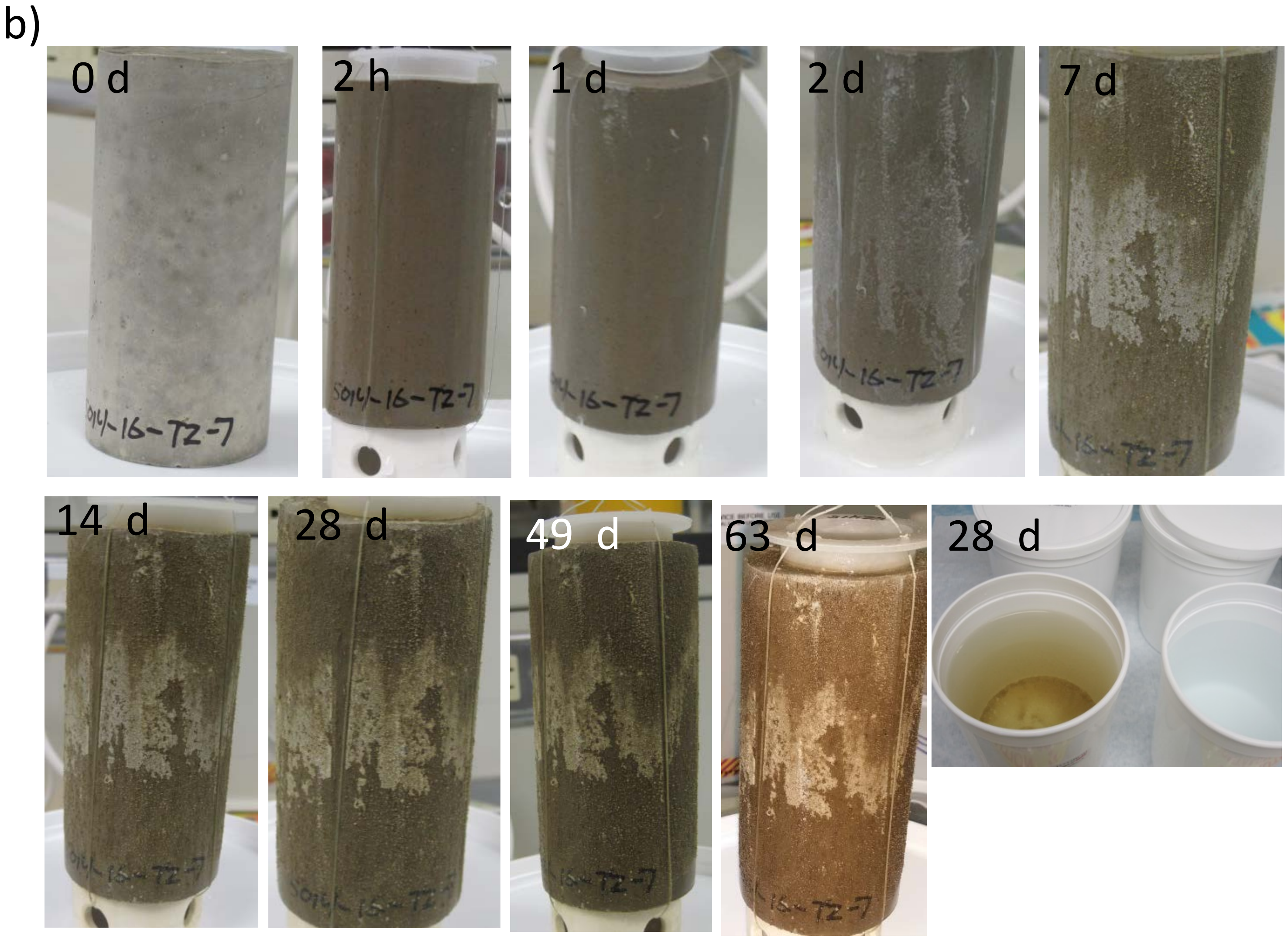

Figure 3-13- The progression of the T2 monoliths leached in a) DIW and b) VZPW for the 63 d leaching period of EPA Method 1315. No photo was available for the 42-d interval.

The KMS-2-SS and Ag-Z containing monoliths from the T3 mix had a similar morphological progression to the T1 set in DIW, Figure 3-14a). The T3 monoliths' surface remained bare, and at 14 d micro-cracks initiated on the outer surface and continuously propagated until the 63-d interval. In the VZPW, Figure 3-14b), the white outer film formed on the outer wall of the T3-4 monolith. At 42 d (the image shown is for the T3-8 monolith), a large black spot appeared and is highlighted in a red circle. This feature was similar in color to the line that appeared on the T1 monolith leached in VZPW. The characteristics of this spot will be discussed further in section 3.4.4. In the upper portion of the T3 monoliths leached in VZPW some dark particles were observed to be growing outward from each T3 monolith. These outcrops are biological growths.

Changing the I getter from argentite to Ag-Z did little to alter the morphology of the T4 monoliths compared with T3 monoliths. In DIW, Figure 3-15a), the T4-1 monolith first displayed micro-cracks at 28 d and they grew continuously to 63 d. Figure 3-15b) shows a T4-5 monolith that was leached in VZPW. As was the case with the T1 and T3 monoliths that were leached in VZPW, a black spot appeared at 28 d, and several others appeared by 63 d on T4 monoliths leached in VZPW.

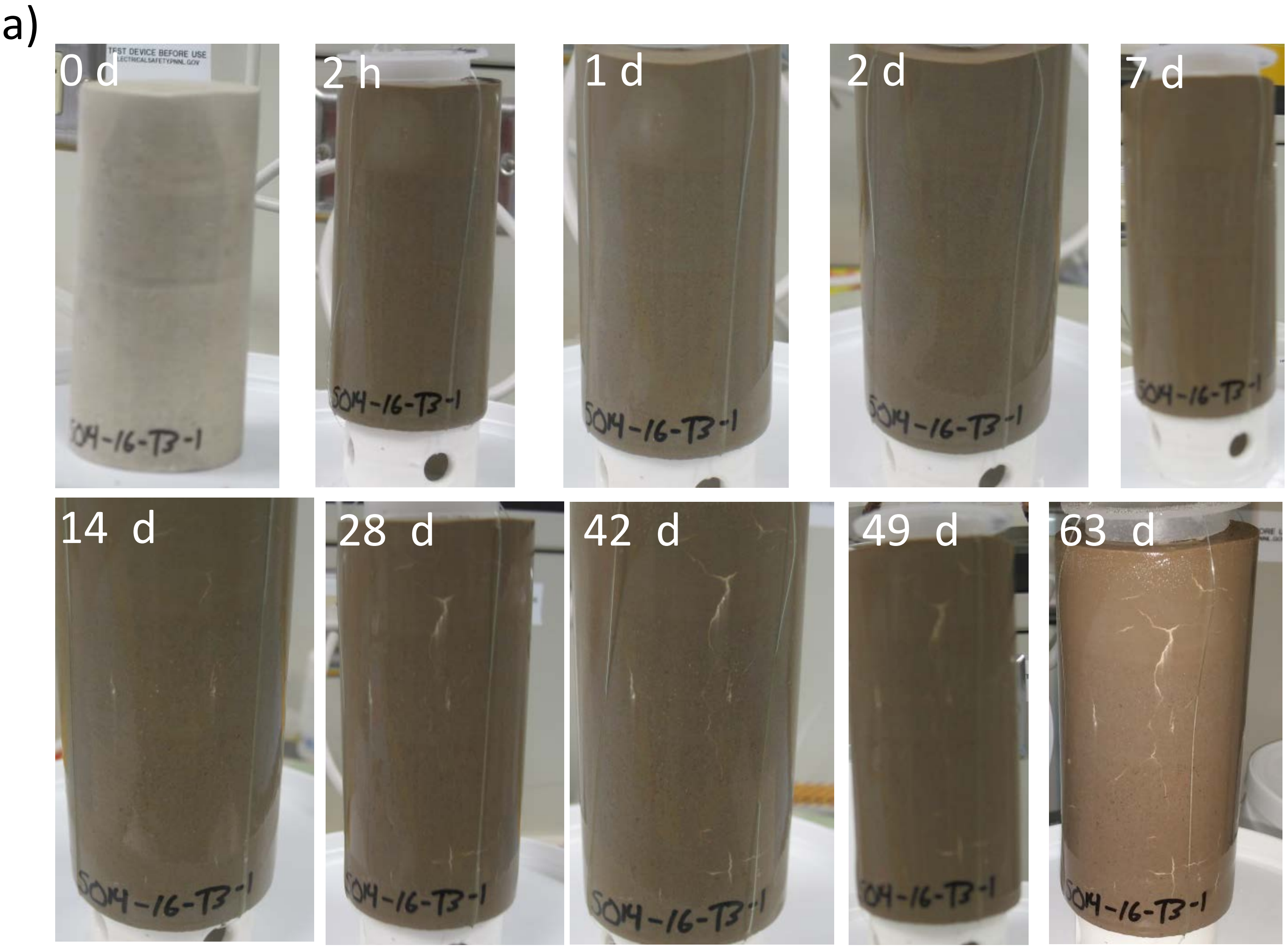
a)
0 d
2 h
1 d
2 d
7 d
14 d
28 d
42 d
49 d
63 d
SO14-16-T3-1
TEST DEVICE BEFORE USE

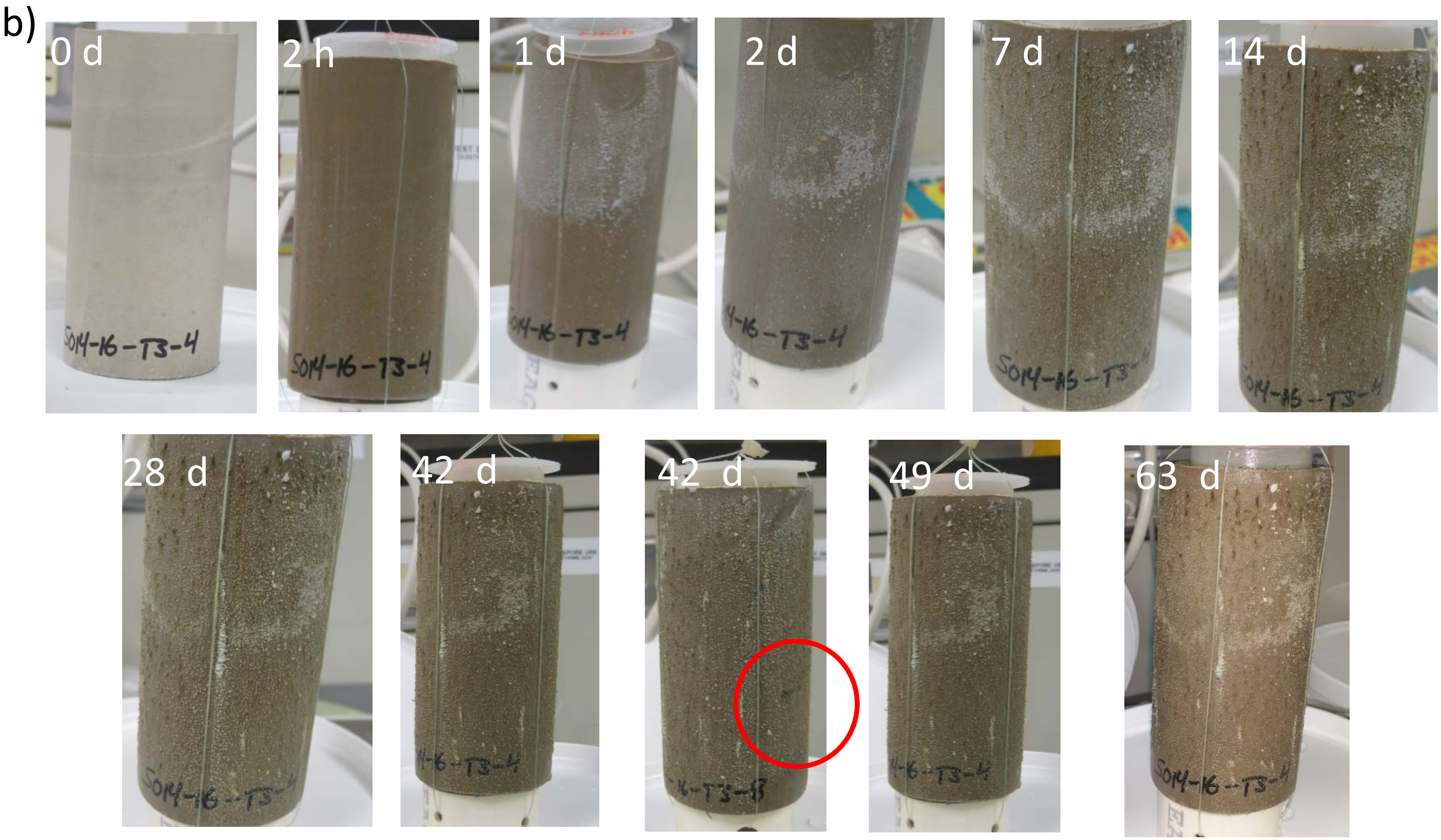

Figure 3-14 - The progression of the T3 monoliths leached in a) DIW and b) VZPW for the 63-d leaching period of EPA Method 1315. The red circle in b) highlights the appearance of a black spot on the T3-8 sample a)

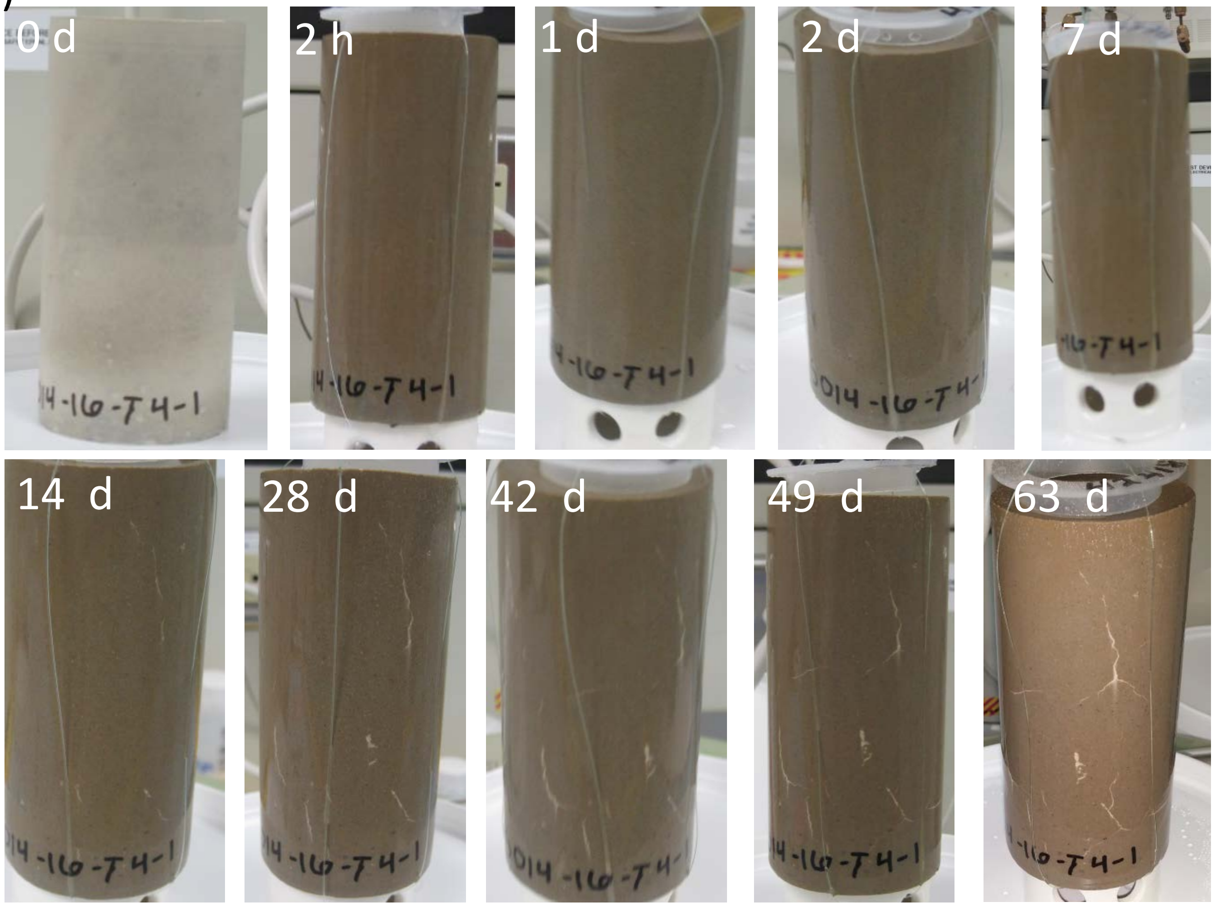

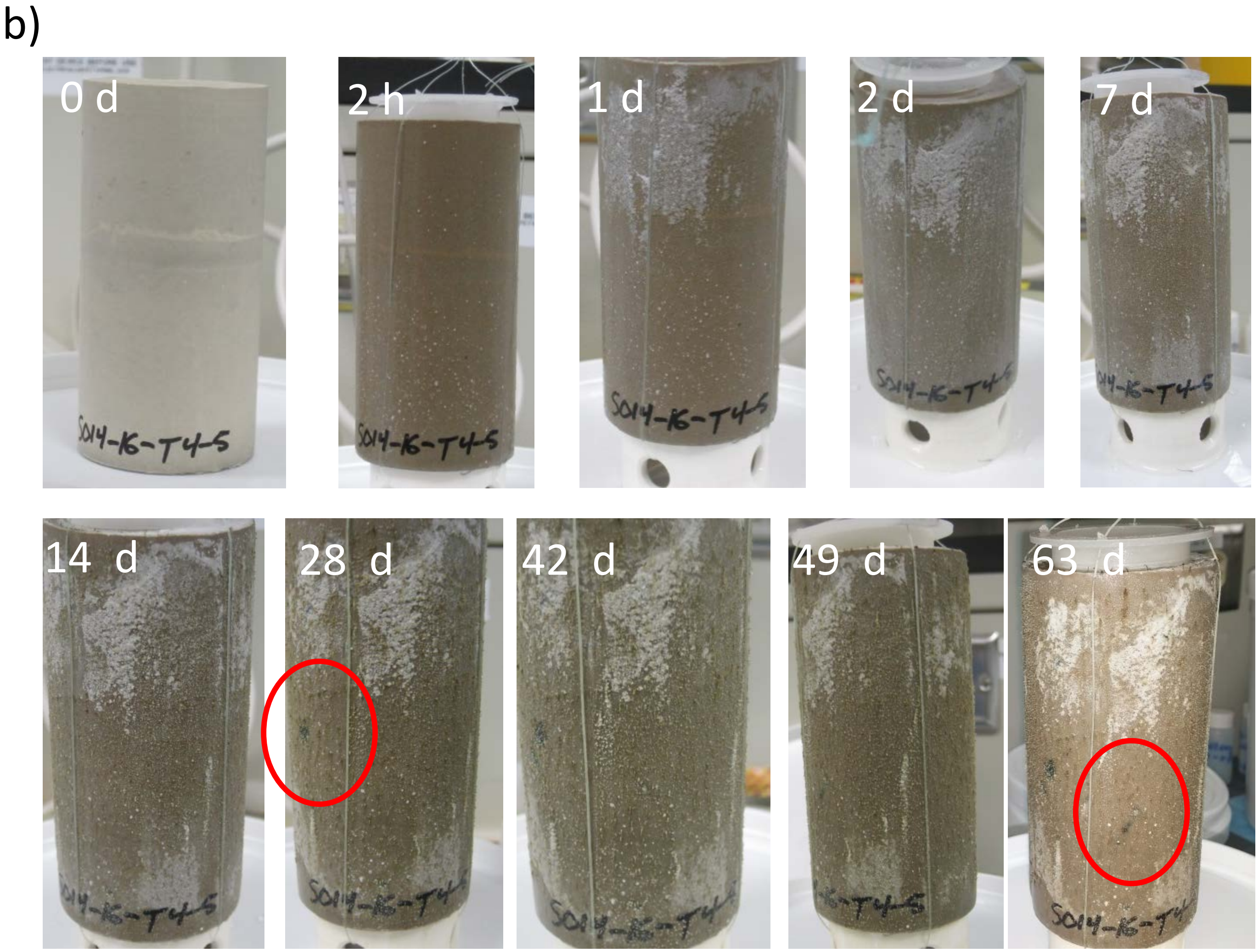

Figure 3-15 - The progression of the T4 monoliths leached in a) DIW and b) VZPW for the 63 d leaching period of EPA Method 1315.

T5 and T6 were also observed to have similar surface features to the T3 and T4 monoliths throughout their leaching in DIW and VZPW. Figure 3-16 shows the T5 and T6 monoliths at 63 d leaching. In DIW, micro-cracks can be seen on both the T5, Figure 3-16a), and the T6, Figure 3-16b), monoliths. The black dots also appeared on both the T5 and T6 monoliths leached in VZPW, in Figure 3-16b) and d) respectively

Figure 3-16 - Images of the T5 monoliths leached in a) DIW and b) VZPW and the T6 monolith leached in c) DIW and d) VZPW after 63 d

3.4.3 Digital Autoradiography and X-ray micro-fluorescence (µXRF)

To understand the mechanisms of contaminant retention and release in the GCCS monoliths, it is necessary to determine how the getters distribute within the monolith as it cures (hardens/set) and also how the getters bind the contaminants. However, the addition of relatively small amounts of the getters, relative to the dry blend mix, presents a challenge in identifying their locations in the cured monoliths. Radionuclide and contaminant detection in the Cast Stone is also challenging due to their low concentrations. Digital autoradiography was carried out on sectioned “pucks” from the Cast Stone samples to image β decay from radioactive ^{99}Tc, allowing identification of the distribution of Tc within the monolith samples. The “pucks” were cut from the central portion of the monolith. The scale in the autoradiograph images represents the relative number of β-decays at the corresponding pixel. This technique is not fully quantitative, although efforts have been initiated to develop quantitative Tc measurements in grouts. A higher intensity in the following images correlates to a higher number of measured β-decays at that pixel, and in turn a higher amount of Tc.

The monolith sections from T1 can be seen in Figure 3-17a), T1-7 which was leached in VZPW and T1-3 as an unleached control. The resulting radiographs of the two monoliths can be seen in Figure 3-17b). The scale bar on the image represents the relative numbers of β decays detected at that pixel (~ 50 µm × 50 µm). Tc appears to be evenly distributed through the T1-3 unleached monolith (right), however the Tc signal is amplified in the leached T1-7 monolith, with some congregation of Tc at the bottom outer edge of the monolith (left).

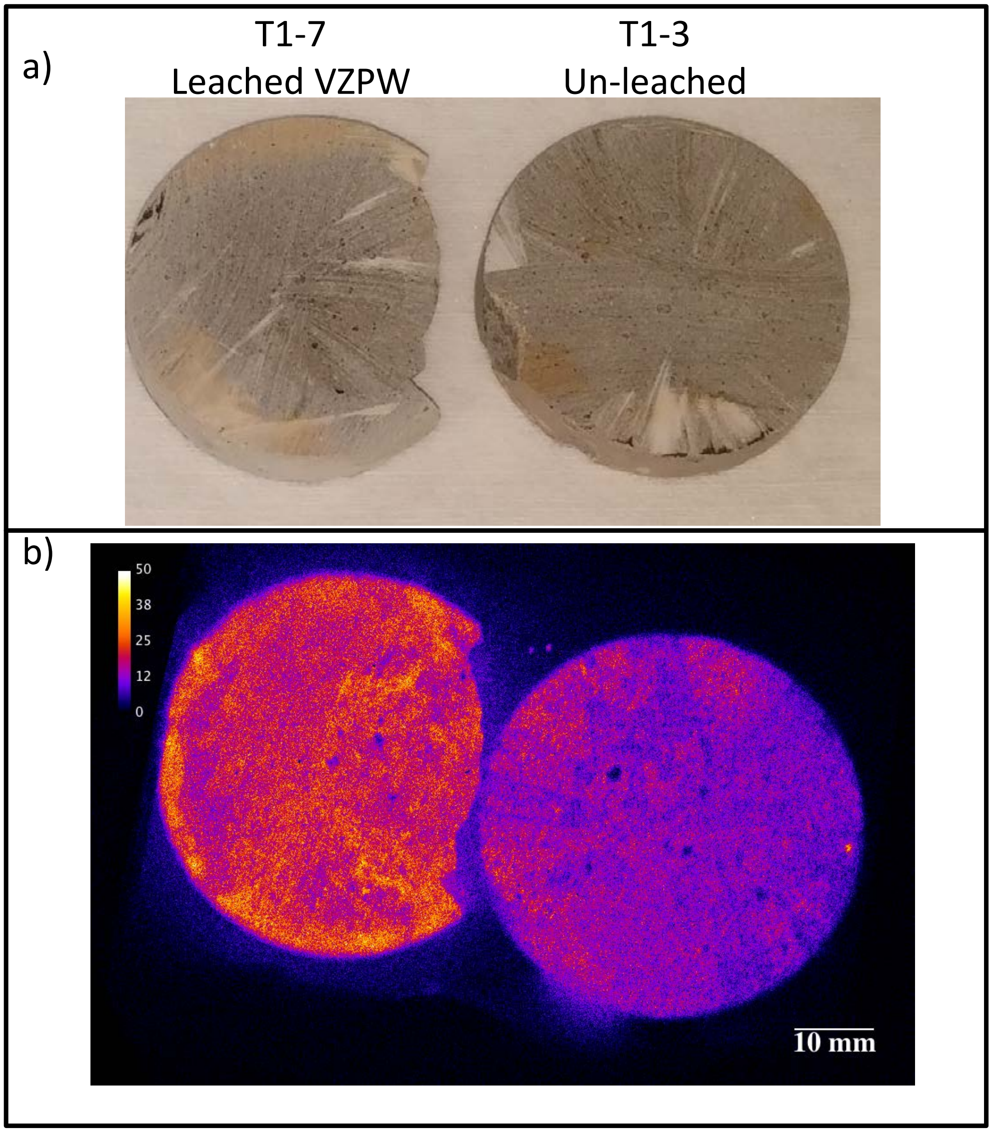

Figure 3-17 – a) photograph of the T1-7 (left, leached in VZPW) and T1-3 (right, unleached) monolith "pucks" analyzed with the iQid system, b) the resulting radiography maps produced after 45 h of β decays collection. The scale bar represents the relative number of β-decays detected at that specific pixel.

T-2 monoliths containing Sn-A as a Tc getter and Ag-Z as an I getter were sectioned and β decays measured. Unleached (T2-5) and T2-8 that had been leached in VZPW are shown in Figure 3-18; Figure 3-18a is the photograph of the pucks. In both monoliths, white isolations can be seen, just as was observed in the bulk T2 monolith Figure 3-11b). In the T2-5 radiograph before leaching (Figure 3-18 b) distinct isolations of Tc were observed. Upon leaching in VZPW, the Tc signal again increased throughout the monolith, and isolated regions of Tc were observed (Figure 3-18b). The presence of Tc "hot spots" suggests that it is associated with a particular mineral phase within the Cast Stone monolith, in this case, it is likely to be the Sn-A Tc getter and this possibility was further investigated using micro-XRF.

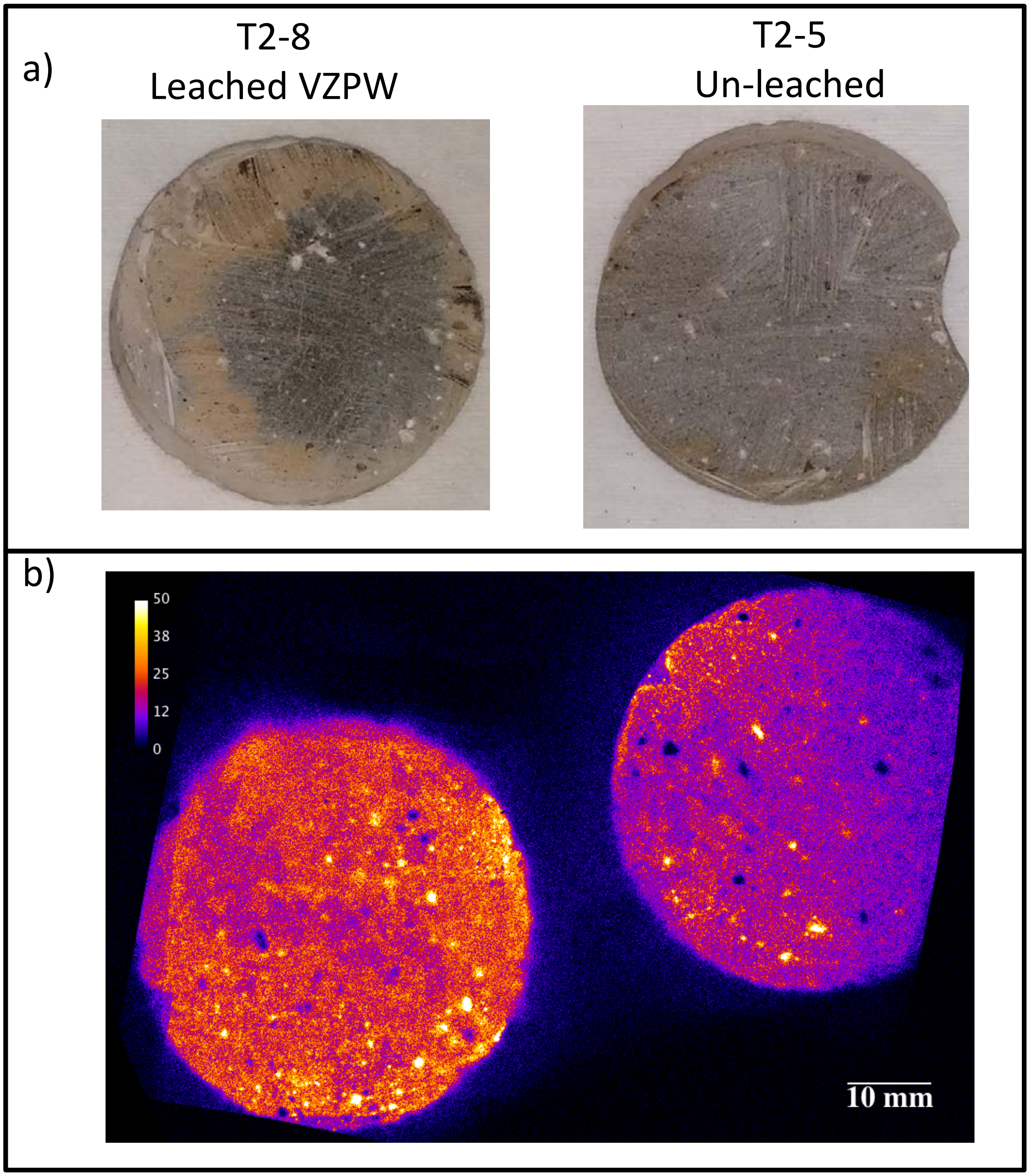

Figure 3-18– a) photograph of the T2-8 (left, leached in VZPW) and T2-5 (right, unleached) monolith "pucks" analyzed with the iQid system, b) the resulting radiography maps produced after 45 h of β decays collection. The scale bar represents the relative number of β-decays detected at that specific pixel.

A small sample of an unleached T2 monolith was extracted, mounted in epoxy, sectioned and polished to < 100 μm thickness. This T2 piece was imaged with the iQid system and the image can be seen in Figure 3-19a). Several Tc isolations are observed in the radiograph. The sample was next analyzed with μXRF (30 μm resolution) for its chemical composition. The resulting μXRF maps provide insight into the chemical composition at the Tc "hot spots". The bright regions in the μXRF image correspond to higher concentrations of that particular element. The Cr μXRF map (Figure 3-19b) also shows higher concentrations of Cr in the same isolated regions as the Tc. The phosphorous μXRF map (Figure 3-19c), and the Sn μXRF map (Figure 3-19d) also show higher concentrations in these specific locations. The white arrows in Figure 3-19a) – d) highlight one such region of high Tc, Cr, P and Sn concentrations. This would suggest that the isolated regions are comprised of Sn and P, the main chemical constituents of the Sn-A getter, thus Tc and Cr are likely reduced by the Sn-A and remain associated with it within the Cast Stone matrix. The large Sn and P signal in the top of the image is the large white “clump” visible in Figure 3-19f), and while this does not correspond to high concentrations of Tc or Cr, there is a higher concentration of Tc and Cr immediately adjacent to this location. This suggests that Tc and Cr are present on the outer surface of the Sn-A getter particles within the monolith. This result is of significance as it highlights the role that particle size will play in getter performance, i.e., getters with a smaller particle size and thus larger surface area likely will be more efficient Tc getters and will require a lower solid: solution ratio to achieve the same level of performance. Ag, present in the T2 monoliths as a result of the addition of the Ag-Z I getter, also appears as isolated areas in the sample (Figure 3-19e) and one of these spots has elevated I, Figure 3-19f). The I is also present near the Sn-P clump at the top of the image as it is likely sitting in the pore created around the clump. The full radiograph of the slice along with a photograph of the slice mounted in epoxy can be seen in Figure 3-19g).

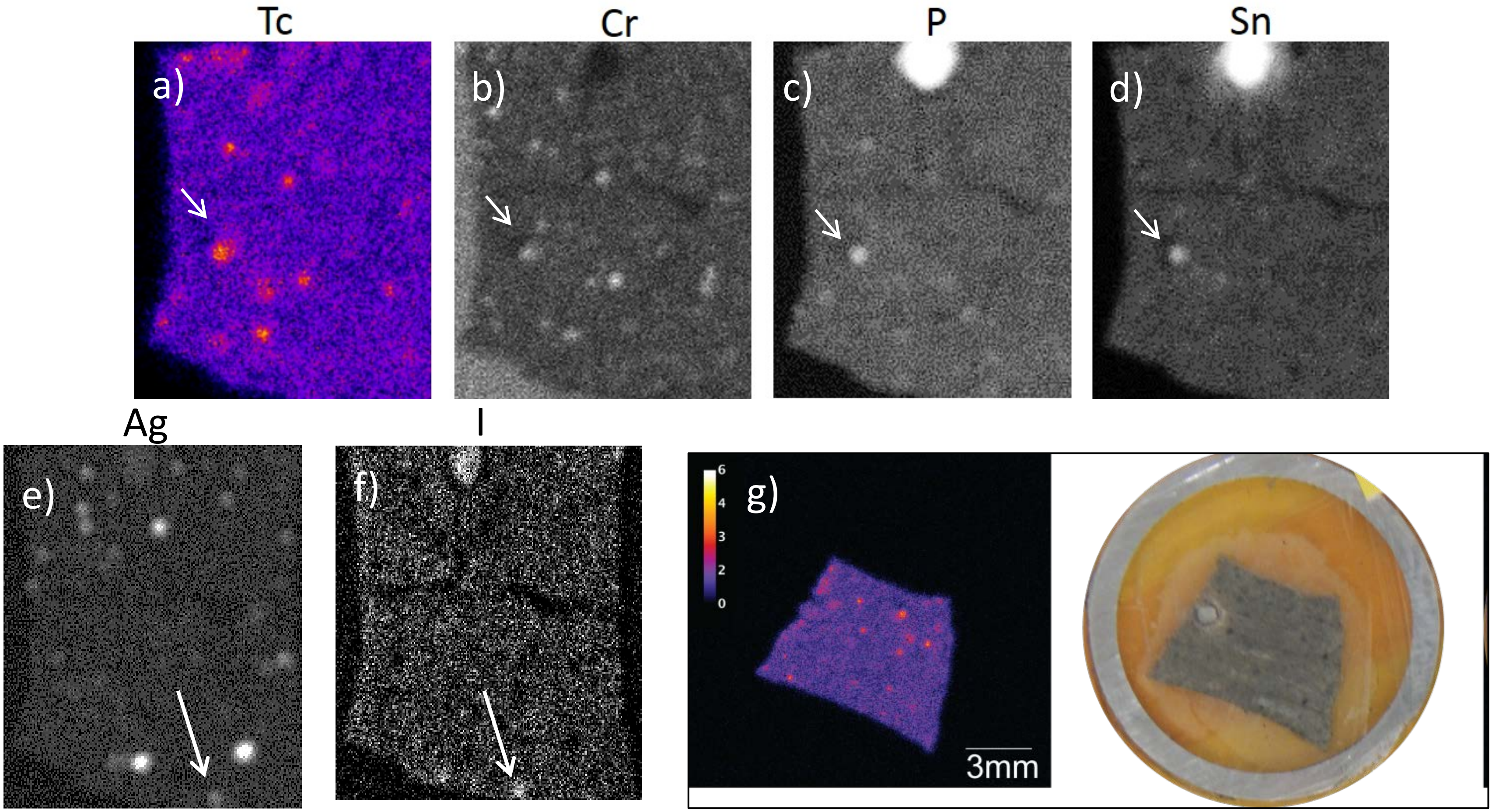

Figure 3-19 - a) digital radiograph of the T2 monolith slice showing Tc "hot spots", and the resulting µXRF elemental maps from the slice of b) Cr, c) P, d) Sn, e) Ag and f) I. g) shows the full radiograph of the T2 slice and a photograph of the slice mounted in epoxy. The increased brightness in the µXRF maps corresponds to highest concentration of that element at the location in the image.

KMS-2-SS containing monoliths (T5) were also imaged with the iQid system. Figure 3-20a) shows photographs of an unleached (T5-5) monolith and an DIW leached (T5-3) monolith. The resulting radiographs can be seen in Figure 3-20b). For the unleached T5-5 monolith, distinct Tc “hot spots” are observed in the puck, although smaller in size to those observed in the T2 monolith. Upon leaching, the Tc signal is again increased, and isolations of Tc were observed. These images suggest that the KMS-2-SS Tc getter also sequesters Tc into discrete locations within the monoliths.

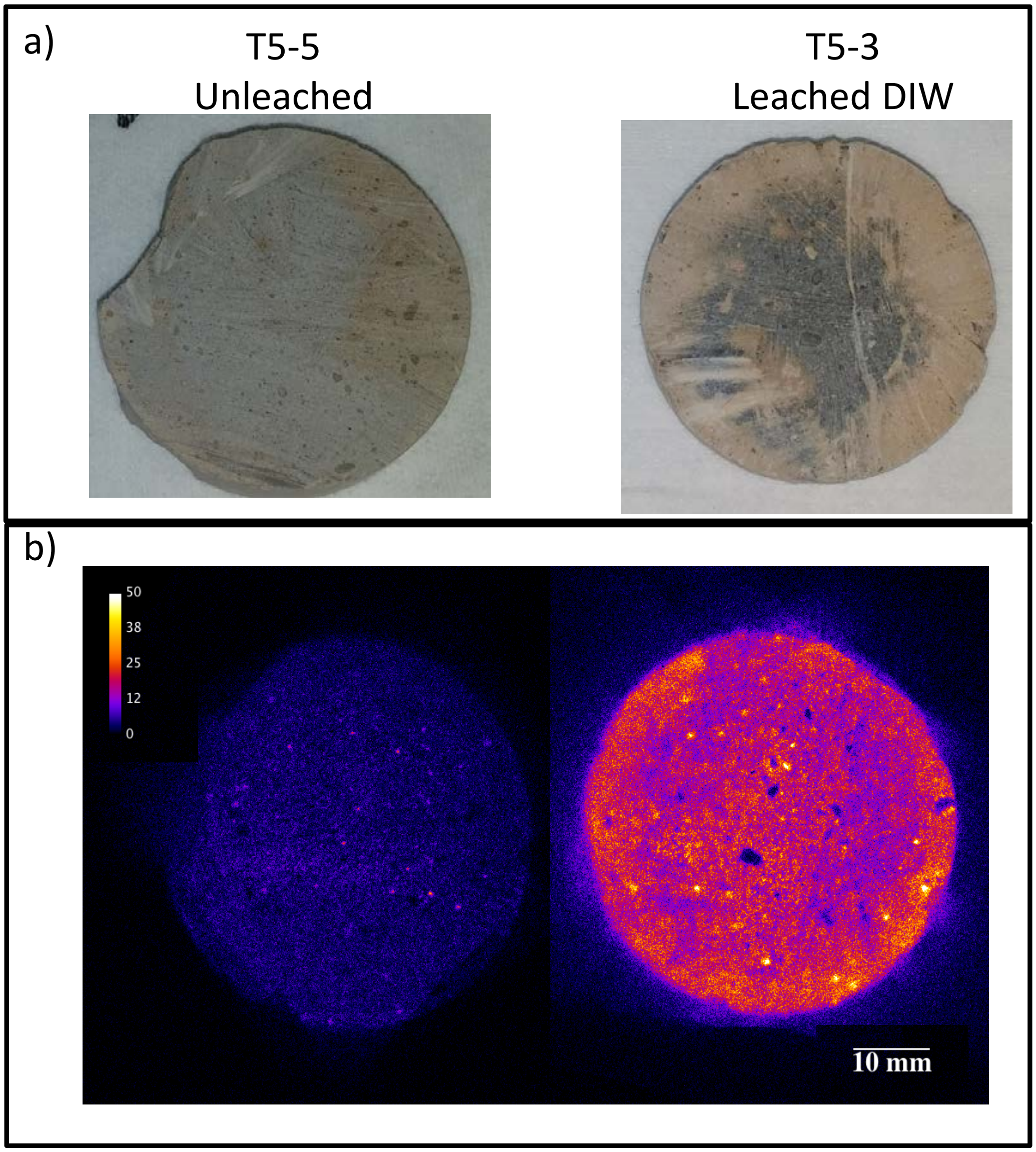

Figure 3-20– a) photograph of the T5-5 (left, unleached) and T5-3 (right, leached in DIW) monolith “pucks” analyzed with the iQid system, b) the resulting radiography maps produced after 45 h of β decays collection. The scale bar represents the relative number of β-decays detected at that specific pixel.

The T6-8 monolith leached in VZPW was analyzed for comparison with the T5-3 sample leached in DIW. The photographs of T6-6 and the T6-8 unleached and leached monoliths respectively are shown in Figure 3-21a). From the radiographs in Figure 3-21b) it can be seen that the isolated Tc “hot spots” are again present in both the unleached and leached monoliths. The sharp edge in the right image in Figure 3-

21 b) is due to the edge of the sample holder masking the surface. And after leaching, the Tc spread is minimal compared with the observations for T1, T2 and T5. As indicated by the calculated D_{obs} values, the release of Tc from the VZPW monoliths was far less than in DIW, and the β-digital radiographs suggest a similar trend, with fewer changes in the location of Tc in VZPW-leached monoliths compared with the DIW-leached monoliths for T5 and T6.

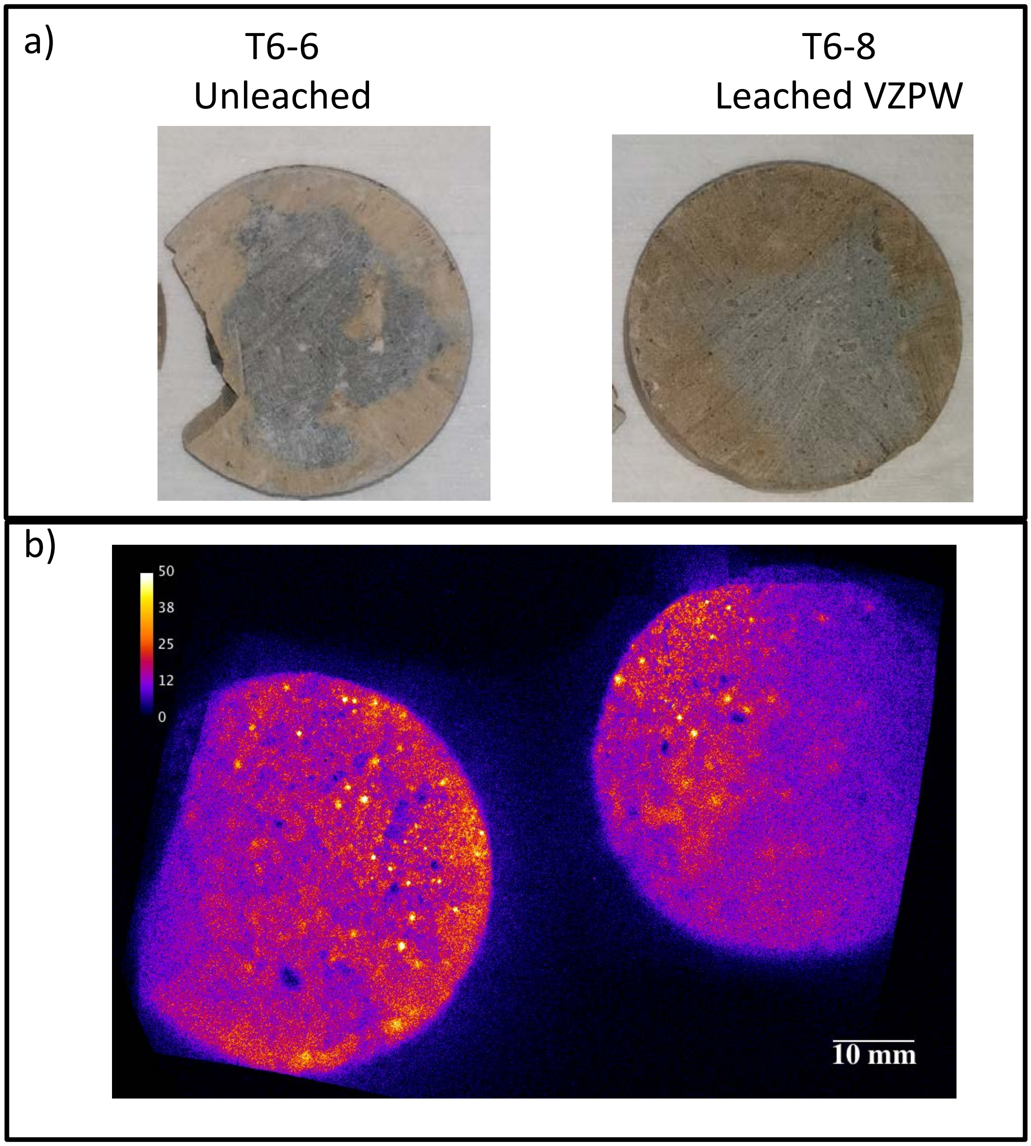

Figure 3-21– a) photograph of the T6-6 (left, unleached) and T6-8 (right, leached in VZPW) monolith "pucks" analyzed with the iQid system, b) the resulting radiography maps produced after 45 h of β decays collection. The scale bar represents the relative number of β-decays detected at that specific pixel.

A general feature of the autoradiographs produced by the iQid system is that, after leaching, the Tc signal increases in intensity. This could be the result of a combination of factors including the effect of water penetration into the monolith and the impact this has on both the porosity of the Cast Stone matrix and the Tc distribution. An increase in porosity will allow more β decay events to reach the detector, thus the signal will appear stronger, even if the Tc concentration is similar, as a result of the increase in effective sampling depth of the iQid detector. Further work involving the use of tomography to determine the relative porosity before and after leaching, in combination with Stopping and Range of Ions in Matter (SRIM) calculations to determine the true sampling depth is required, along with Tc standards (known Tc concentrations in known porosity geometries) measurements to quantify the radiography results in terms of absolute Tc concentration.

The results from the autoradiography analysis confirm that the addition of Tc getters leads to discrete isolations of Tc (and likely Cr) contaminants within the Cast Stone and that getter particle size will have an effect on the performance of the getters with respect to contaminant sequestration. The KMS-2-SS was relatively evenly distributed during the Cast Stone mixing, while the Sn-A formed small clumps in the wet slurry. The Tc “hot spots” observed in the KMS-2-SS containing cured monoliths were smaller in size compared with the Tc “hot spots” in cured Sn-A-containing monoliths and the KMS-2-SS monoliths exhibited the best performance in terms of D_{obs} values. Thus, KMS-2-SS distribution and performance may be further improved by reducing the initial particle size of the getter. Figure 3-22 shows SEM micrographs of the KMS-2-SS synthesized via the same method but with different heating and cooling regimes, resulting in differing particles sizes. The effect of particle size should be considered in future KMS-2 GCCS work.

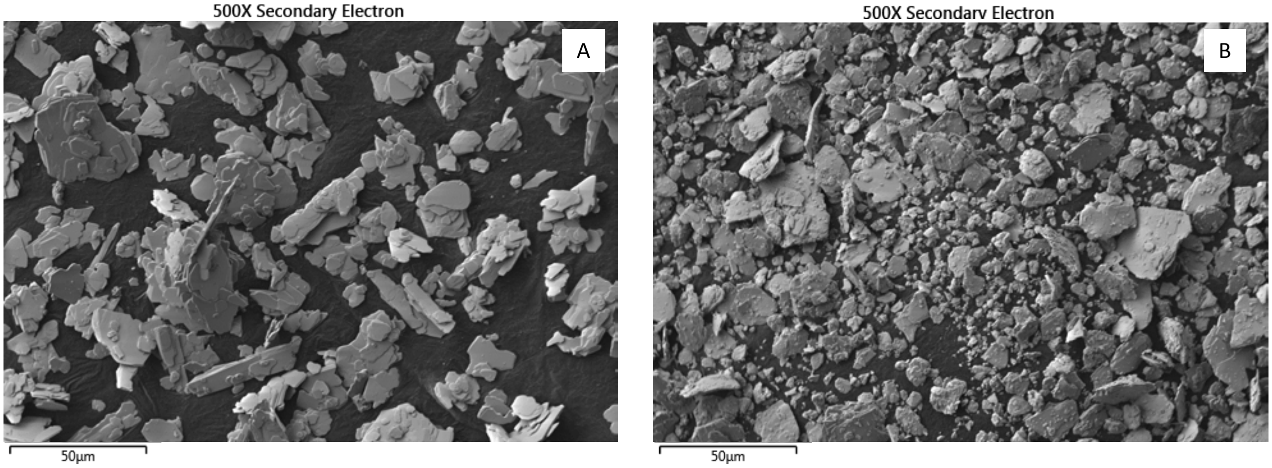

Figure 3-22 - SEM micrographs of KMS-2-SS particles from two different batches (A and B) showing a difference in particle size resulting from the synthesis temperature and cooling rate.

3.4.4 Scanning Electron Microscopy and X-ray Energy Dispersive Spectroscopy (SEM/EDS) Imaging

Several prominent features observed in the monoliths post-leaching were characterized by SEM/EDS. During leaching of the T2 monolith in DIW, black dots visible on the outer wall were observed to “bleed” down the side of the monolith (Figure 3-23a). This observation was also made during the leaching of Ag-Z containing monoliths studied in FY15(Asmussen et al. 2015). These FY15 monoliths were similar to T2, although Sn-A and Ag-Z were added simultaneously to the LAW simulant at 0.5 wt% of the total dry blend mass. A black dot was extracted from a FY15 monolith that had been leached in DIW and analyzed by SEM (the red box in the SEM micrograph in Figure 3-23b). A micrograph of the black dot, taken at higher magnification and in backscatter secondary electron mode, is shown in Figure 3-23c). EDS spot analyses were collected from both inside and outside the black dot (the pink boxes in Figure 3-23c). The

EDS spectrum from inside the black dot (Figure 3-23d), showed many elements, including Ag. The EDS spectrum from outside the black dot (Figure 3-23e) has many similar features, except that Ag is no longer present. The black dots are therefore Ag containing regions, possibly associated with I, which was not detectable under these conditions.

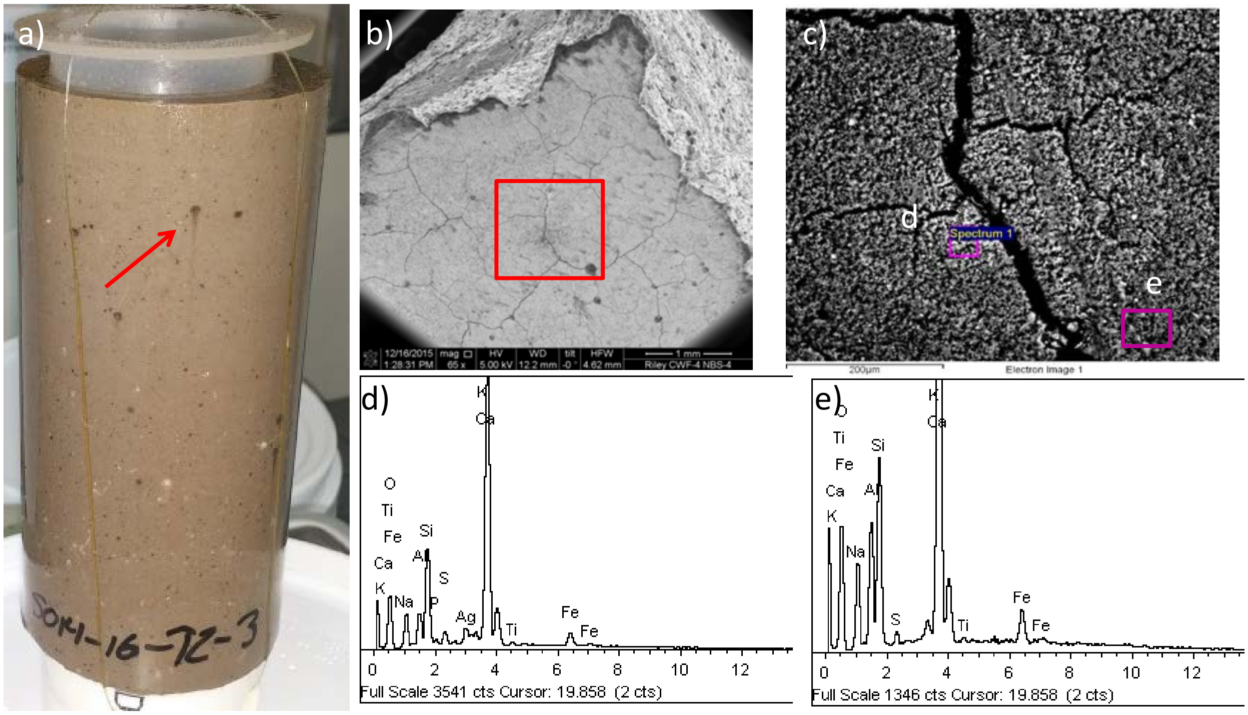

Figure 3-23 – a) image of the T2-3 monolith showing a bleeding dot at 63 d leaching, b) SEM micrograph of an extracted dot from the FY15 GCCS monoliths, c) magnified SEM micrograph of the bleeding dot with EDS analyses of the two spots in d) and e).

Black spots were also observed in the KMS-2-SS containing monoliths (mixes T3, T4, T5, and T6) leached in VZPW. One such spot is shown on the 63-d leached T3-8 monolith in Figure 3-24a). This spot was excised from the monolith and is shown in Figure 3-24b). The black region is the thin part of the slice, marked d), with the thicker part representative of the area outside the black spot, marked c). The SEM micrograph from the thick end is shown in Figure 3-24c). Five areas were analyzed with EDS and the corresponding elemental analyses are shown in the list below the image. Regions of high Ca (B/D), high Mg(C), Ca/Si (A) and Mg/Ca/Al/Si (E) were observed. Moving into the black spot region, Figure 3-24d), similar measurements with EDS were made for comparison. Unlike the area outside the black spot, Region E measured 2.7 wt% Tc, along with higher than normal levels of Mg (71.1 wt%), Sn (4.9%) and Cr (2.1%). Mg and Sn are components of the KMS-2-SS suggesting that the black spot is an isolated region of KMS-2-SS sequestering both Cr and Tc. This possibly represents a near-surface site from which Tc can be leached from the monolith. Tc was also detected at sites B and H (along with Mg), and C and F (with high levels of Ca). Detection of Tc by this technique is a significant result, as many techniques are unable to detect Tc in the concentrations present in the bulk Cast Stone.

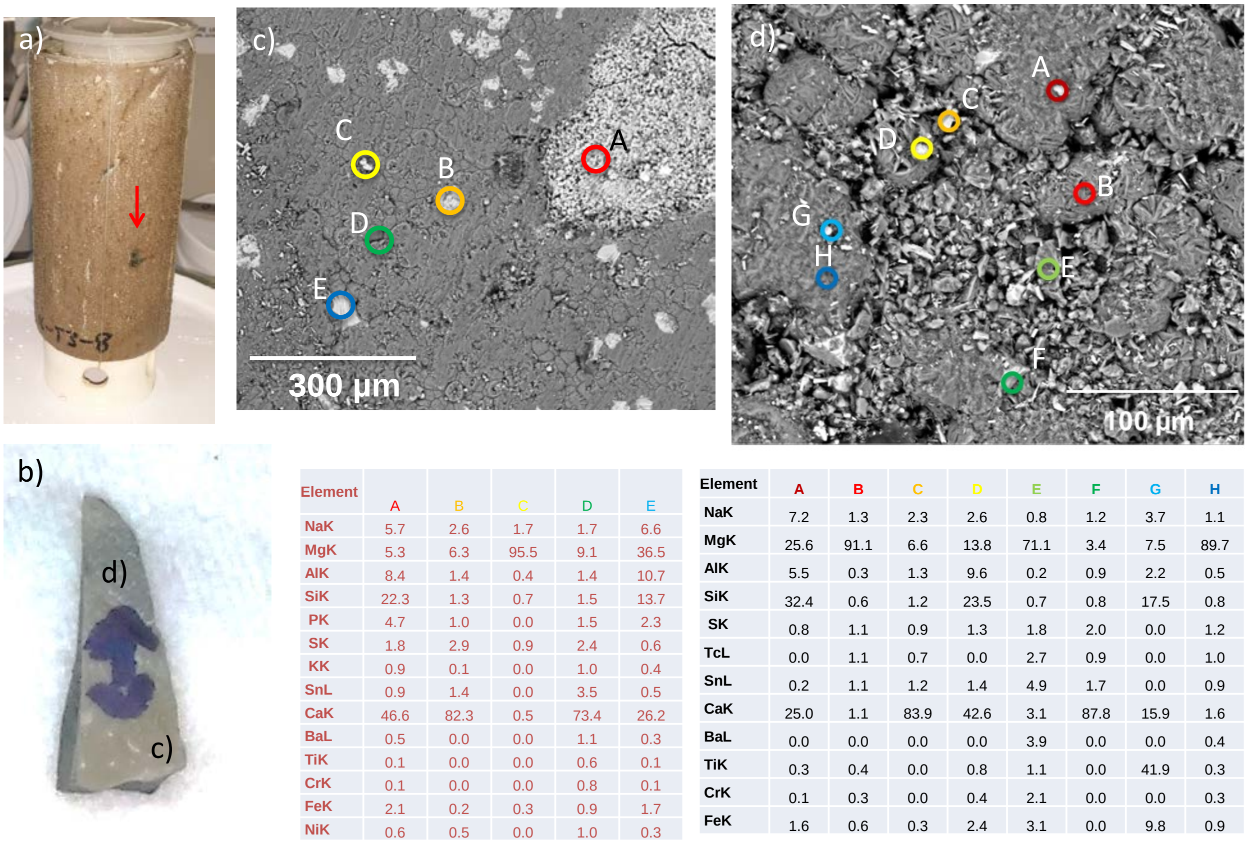

Element	A	B	C	D	E
NaK	5.7	2.6	1.7	1.7	6.6
MgK	5.3	6.3	95.5	9.1	36.5
AlK	8.4	1.4	0.4	1.4	10.7
SiK	22.3	1.3	0.7	1.5	13.7
PK	4.7	1.0	0.0	1.5	2.3
SK	1.8	2.9	0.9	2.4	0.6
KK	0.9	0.1	0.0	1.0	0.4
SnL	0.9	1.4	0.0	3.5	0.5
CaK	46.6	82.3	0.5	73.4	26.2
BaL	0.5	0.0	0.0	1.1	0.3
TiK	0.1	0.0	0.0	0.6	0.1
CrK	0.1	0.0	0.0	0.8	0.1
FeK	2.1	0.2	0.3	0.9	1.7
NiK	0.6	0.5	0.0	1.0	0.3

Element	A	B	C	D	E	F	G	H
NaK	7.2	1.3	2.3	2.6	0.8	1.2	3.7	1.1
MgK	25.6	91.1	6.6	13.8	71.1	3.4	7.5	89.7
AlK	5.5	0.3	1.3	9.6	0.2	0.9	2.2	0.5
SiK	32.4	0.6	1.2	23.5	0.7	0.8	17.5	0.8
SK	0.8	1.1	0.9	1.3	1.8	2.0	0.0	1.2
TcL	0.0	1.1	0.7	0.0	2.7	0.9	0.0	1.0
SnL	0.2	1.1	1.2	1.4	4.9	1.7	0.0	0.9
CaK	25.0	1.1	83.9	42.6	3.1	87.8	15.9	1.6
BaL	0.0	0.0	0.0	0.0	3.9	0.0	0.0	0.4
TiK	0.3	0.4	0.0	0.8	1.1	0.0	41.9	0.3
CrK	0.1	0.3	0.0	0.4	2.1	0.0	0.0	0.3
FeK	1.6	0.6	0.3	2.4	3.1	0.0	9.8	0.9

Figure 3-24 – a) image of the T3-8 monolith with a near-surface black spot that was extracted, b) the extracted black spot, from the region marked "d)", c) SEM micrograph of the T3 surface away from the black dot with the EDS elemental measurements in the table underneath, d) SEM micrograph of the region within the black dot and the EDS elemental measurements in the table below the image.

In the argentite-containing Cast Stone monoliths (T4 and T6), the bottom face of the cross-section (Figure 3-25a) has a different appearance compared with the other monoliths, for example T7 in Figure 3-25b). EDS maps were collected on a representative area of the argentite-containing samples to determine elemental composition. The resulting EDS maps are shown in Figure 3-25c). No "hotspots' of Ag or S were detected, suggesting that the darker color is due to a homogenous distribution of Ag and S throughout the monolith at concentrations too low to be detected by EDS. The overall darker color makes the lighter areas that are also present in Figure 3-25c) stand out. Veins of P and Ca are observed running through the surface and isolations of Si, Fe, Mg and Ti from components in the Cast Stone matrix were also observed.

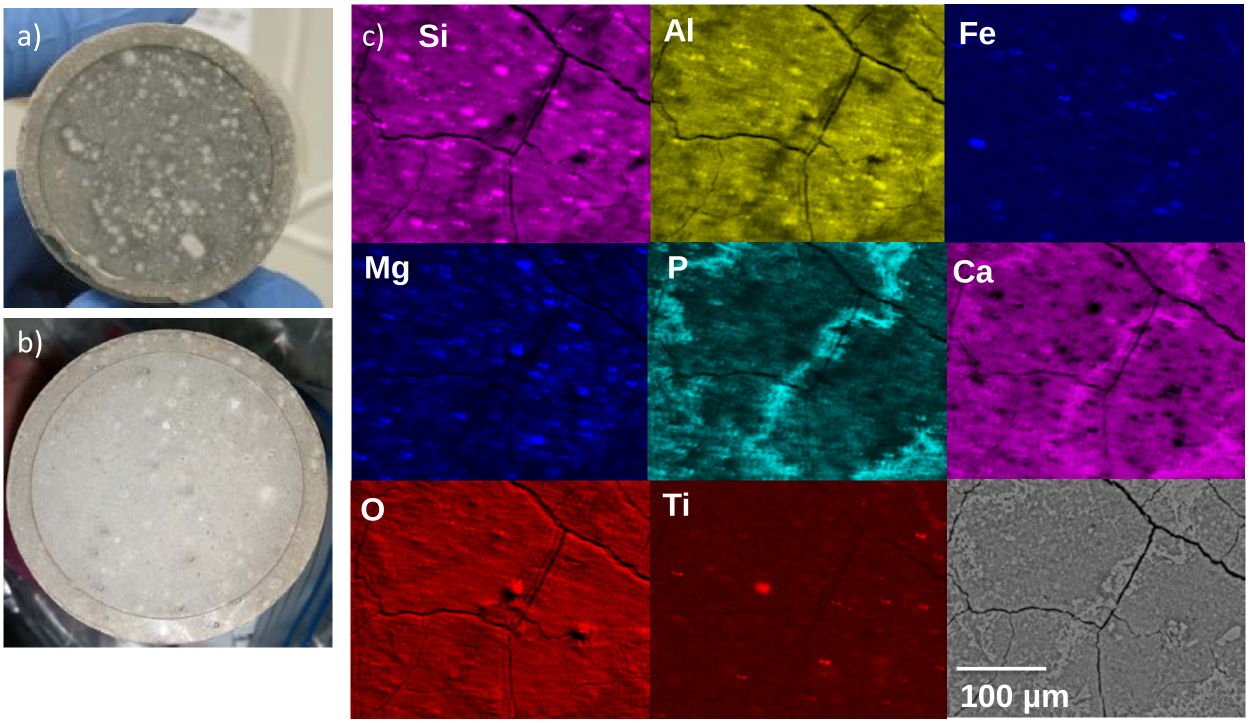

Figure 3-25 – a) image of the T4-1 monolith representative of the appearance of the T4 and T6 sets compared with the non-argentite containing monolith bottoms in b). c) EDS elemental maps of the T4-1 bottom face, taken from the surface shown in a).

3.4.5 X-ray Diffraction (XRD)

XRD patterns as a function of 2θ based on $Cu_{K\alpha}$ radiation (λ=1.5406 Å) were measured for samples from the interior and exterior of the monoliths to identify the mineral phases present and to quantify the amorphous component as a function of distance from the monolith's outer surface. The calculated and observed background-subtracted XRD pattern for the sample from the outside of the control monolith (T1) before leaching is shown in Figure 3-26, along with the fits from Rietveld refinement for the respective mineral phases present, including the rutile standard. Although TiO_2 is present in the BFS, it constitutes <0.6 wt.% (Westsik et al. 2013) and there is no evidence of rutile in the XRD patterns for samples measured without a standard, therefore addition of the rutile standard will allow semi- quantitative XRD results to be estimated. The crystalline solid phases identified by XRD as being present in the monoliths, including relative amounts, are summarized in Table 3-3. The errors associated with semi-quantitative XRD measurement of these challenging, predominantly amorphous samples, are ± 3 % (absolute) for the amorphous fraction (which includes unidentified phases) and an estimated uncertainty of ± 10% (relative) for the crystalline phases, however, trends in the data obtained by analyzing multiple samples in the same way provide useful semi-quantitative information.

All monoliths are dominated by amorphous phases (83-90% of the sample) with no evidence of variation as a function of distance from the monoliths' outer surface. In terms of crystalline phases, all monolith samples contain tobermorite $Ca_5Si_6O_{16}(OH)_2{\cdot}4H_2O$ (2.8-5.8%), quartz SiO_2 (1.3-4.6%), calcite $CaCO_3$ (0.7-3.5%) and larnite Ca_2SiO_4 (1.0-3.1%). A small peak present in all samples at low angle could be fit with varying amounts of the related hexagonal phases such as hydrocalumite $Ca_2Al(OH)_{6.5}Cl_{0.5}{\cdot}3H_2O$, hemicarbonate $(Ca_2Al(OH)_6)_2{\cdot}\ \tfrac{1}{2}CO_3{\cdot}OH{\cdot}nH_2O$ and hydrotalcite

$Mg_6Al_2(CO_3)(OH)_{16}•4(H_2O)$ (3.5-6.7%) with the peak angle increasing depending on the phase (hemicarbonate < hydrocalumite < hydrotalcite). Most of the mineral phases are evenly distributed throughout the monolith with the exception of the hydrous Ca and Al containing mineral hydrocalumite, which is present in higher quantities at the surface as compared to the interior of the monolith for all samples. XRD analysis of comparable monoliths after leaching, described in a concurrent report (Asmussen et al. 2016c) has shown that the monoliths transform over time resulting in an increase in the crystalline component and the transformation of mineral phases, particularly those that are less thermodynamically stable, such as hemicarbonate and larnite, into more thermodynamically stable phases such as sodalite ($Na_8(Al_6Si_6O_{24})Cl_2$).

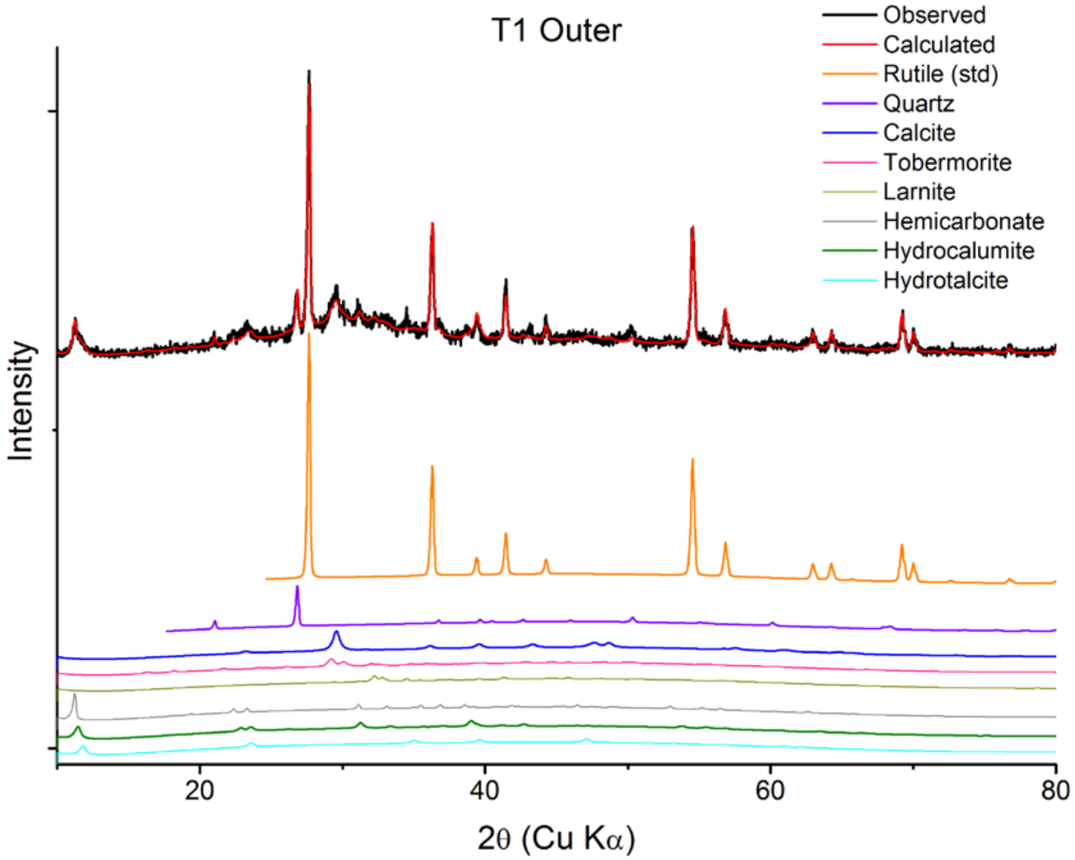

Figure 3-26 – Example of quantitative XRD fitting of the spectrum from the T1 Outer (near-surface) sample.

Table 3-3- Quantitative XRD measurements from the unleached Cast Stone samples

Sample	Hydrocalumite	Hemicarbonate	Hydrotalcite	Calcite	Larnite	Tobermorite	Burtite	Quartz	Amorphous
Inner T1	2.2%	1.4%	2.2%	1.2%	3.0%	5.6%		1.4%	83%
Outer T1	2.6%	1.8%	2.3%	3.2%	1.5%	3.1%		1.8%	84%
Inner T2	1.8%	2.6%	2.7%	2.0%	2.2%	3.2%	0.6%	2.0%	83%
Outer T2	2.7%	1.1%	1.5%	0.7%	1.4%	3.4%	0.5%	1.5%	87%
Inner T3	1.3%	0.8%	1.4%	1.1%	1.0%	2.7%		1.4%	90%
Outer T3	2.2%	1.0%	2.1%	0.9%	1.0%	5.1%		2.8%	85%
Inner T4	1.4%	1.4%	2.6%	2.4%	1.2%	5.3%		1.8%	84%
Outer T4	1.9%	1.0%	2.3%	1.0%	1.5%	3.8%		3.7%	85%
Top T4	1.5%	1.2%	2.2%	1.1%	1.1%	5.2%		2.1%	86%
Bottom T4	1.3%	1.1%	2.3%	1.1%	1.3%	3.7%		1.3%	88%
Inner T5	1.6%	1.0%	2.0%	1.3%	1.1%	5.1%		1.9%	86%
Outer T5	1.9%	1.4%	2.8%	0.8%	2.9%	4.8%		4.6%	81%

Although Sn-A was added to T2, there was no evidence that this phase was present in a crystalline form in the aliquots of T2 monoliths that were analyzed by XRD. This is in agreement with results from Duncan et al. (Duncan et al. 2012) who found that their manufactured Sn-A was a poorly crystallized hydroxyapatite. However, the Sn-containing phase burtite $Ca(Sn(OH)_6)$ was identified both in the interior and on the surface of our T2 monoliths, demonstrating that the reaction with the Tc- and Cr-containing LAW simulant and grout mixture had altered the Sn-A. The white clumps observed in the T2 monolith prior to the leach test (Figure 3-11b), were also identified as burtite, along with an additional Sn-containing phase, cassiterite (SnO_2).

Hexagonal KMS-2-SS, added to T3-T6 monoliths, exhibits a characteristic XRD pattern with intense basal reflections (002 and 004) corresponding to an interlayer spacing of 8.42Å (Fig. 3.27). However, there is no evidence for the presence of this crystalline phase in the cured monoliths. This is because exposure of the KMS-2-SS to the LAW simulant results in a major structural change as shown by the broader, low intensity peaks in the XRD pattern for KMS-2-SS after LAW exposure in Figure 3-27. These peaks were too weak to be observed in the XRD patterns for the unleached monolith.

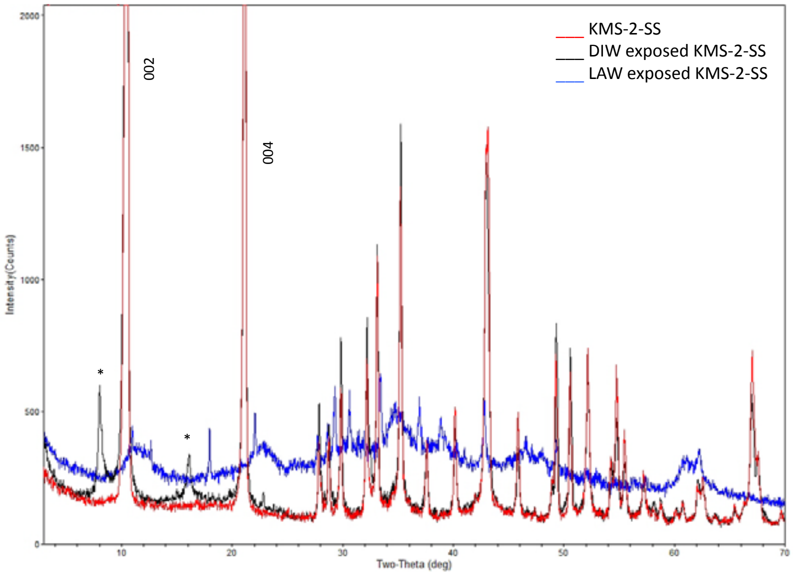

Figure 3-27- Comparison between the XRD patterns of KMS-2-SS unreacted, after exposure to DIW and after exposure to LAW.

3.4.6 X-ray photoelectron spectroscopy (XPS) and X-ray adsorption spectroscopy (XAS)

Powder samples of the GCCS monoliths containing Cr (806 ppm), Tc (56 ppm) and I (6 ppm) with 0.5 wt% Sn-A and Ag-Z getters, fabricated in FY15 (Asmussen et al. 2015) were analyzed using XPS to determine oxidation state by fitting the Tc 3d and the Cr 2p binding energies. These FY15 samples are denoted TT1. These FY15 samples can be used for comparison to the GCCS fabricated in this report as there was low getter addition amounts, similar LAW simulant used for fabrication, identical water: dry mix ratio and identical fabrication procedure. A survey XPS scan revealed that samples contained Na, Ca, O, C, and Si, but there was no observable signal for Cr or Tc (Figure 3-28). Regional scans for Cr 2p (80 sweeps), Tc 3d (200 sweeps), Ca 2p (5 sweeps), O 1s (5 sweeps), C 1s (5 sweeps) and Na 1s (5 sweeps) were collected (Figure 3-29). Both Tc 3d and Cr 2p concentrations were below the detection limit within the 5 nm probing depth for XPS, even with many (80 to 200) scans.

Given the low concentrations of Tc and Cr associated with the monolith solid phase both before and after leaching, synchrotron-based techniques were subsequently employed to determine Tc oxidation state and local bonding environment

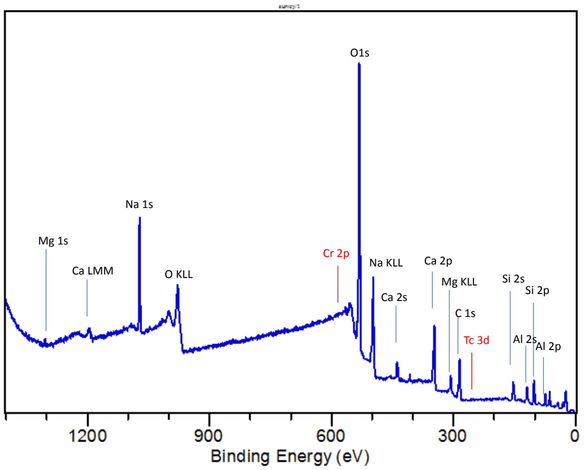

Figure 3-28 – XPS survey spectrum of the FY15 GCCS (TT1) powder. The position of Cr and Tc signals are identified in red.

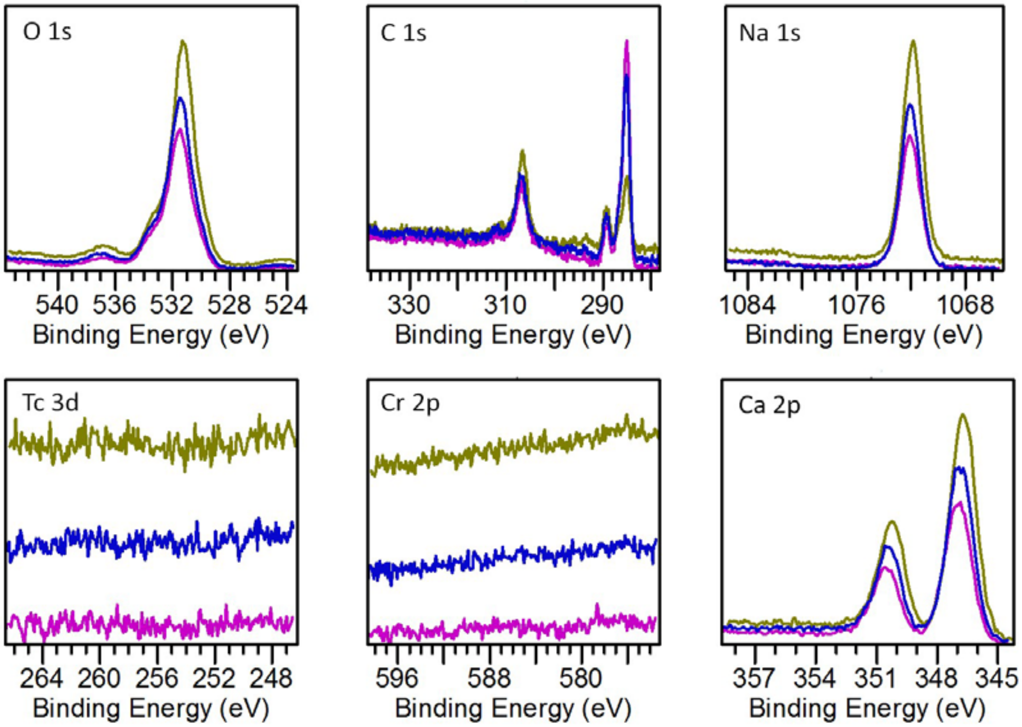

Figure 3-29 – Regional XPS scans for O, C, Na, Tc, Cr and Ca showing the absence of Tc and Cr in the FY15 GCCS (TT1) monolith measurement. Each line in the spectra is a separate scan of the sample.

Tc K-edge XANES spectra were collected to determine: (i) the Tc oxidation state after removal by Sn-A from DIW spiked with Tc(VII); (ii) the competitive effect of Cr on Tc removal from LAW simulant by Sn-A; (iii) the mechanism of Tc removal by KMS-2-SS from DI water and from LAW simulant; (iv) the effect of exposing KMS-2-SS to fresh DI water after Tc removal; and (v) the effect of monolith leaching on Tc present in Cast Stone prepared with LAW simulant (TT1), which contained KMS-2-SS.

Six standard spectra were used in the initial fitting of the Tc K-edge XANES spectra: TcO_4^-, $Tc(IV)_2S_7$, Tc(V)=O polyoxometallate, Tc(IV) gluconate, $TcO_2{\bullet}2H_2O$ and Tc(IV) EDTA complex. The latter three standards represent Tc(IV) with varying degrees of disorder in the first shell of 6 oxygen atoms. In Tc(IV) gluconate, the first shell consist of 6 oxygen atoms 2.0 Å from the Tc center in an octahedral geometry. In $TcO_2{\bullet}2H_2O$, there are 4 oxygen atoms 2.0 Å from the Tc center and two oxygen atoms at a longer distance (~2.4 Å). In Tc(IV) EDTA, the first shell is quite distorted with two oxygen atoms at 2 Å, two oxygen atoms at a longer distance, and two nitrogen atoms still farther away. These changes in the local environment of Tc produce changes in the structure of the Tc K-edge XANES spectrum as illustrated in Figure 3-30. Initially, all six Tc standard spectra were used to fit each Tc-XANES spectrum for the getter and Cast Stone specimens. Any non-pertechnetate standard spectrum for which the contribution was less than two standard deviations was removed from the fitting procedure, and the fitting process was repeated until TcO_4^-, $Tc(IV)_2S_7$, and a single Tc(IV) standard remained. The purpose of removing the Tc(IV) spectra that are not significant is to determine accurate standard deviations for the amount of Tc(IV) in the sample. If more than one Tc(IV) standard is used, the standard deviation of each becomes very large since their contributions are strongly correlated. The final fitting results are given in Table 3-4. The Tc(IV) standard that best fits the data is $TcO_2{\bullet}2H_2O$ and the KMS-2-SS samples contained a significant amount of Tc_2S_7.

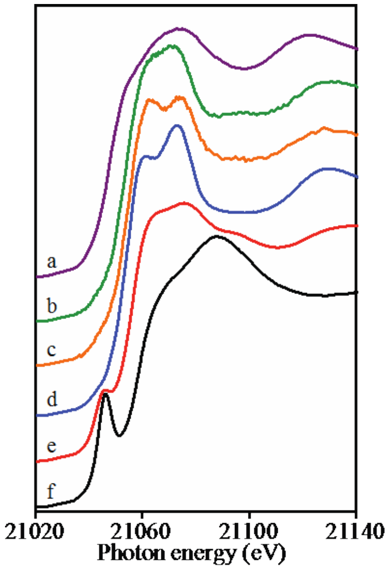

Figure 3-30 – The standard Tc K-edge XANES spectra for known standards used for fitting of the spectra collected in this work. From top to bottom, these are the Tc K-edge spectra of a) Tc_2S_7, b) Tc(IV) EDTA complex, c) $TcO_2{\bullet}2H_2O$, d) Tc(IV) gluconate, e)Tc(V)=O polyoxometallate, f) TcO_4^-.

As shown in Table 3-4 and Figure 3-31A, removal of Tc from DI water by Sn-A occurred via the reduction of the soluble $Tc(VII)O_4^-$ to form Tc(IV), presumably coordinated by oxygen atoms, with some Tc remaining in solution (see Figure 3-2, T2 for % Tc removal). In Table 3-4, the numbers in parentheses represent the standard deviations of the contribution of that component for the ending digit, p is the probability that improvement of the fit, when this standard is included, is due to random error. Only Tc(IV) contributes significantly to the spectrum but the local environment of Tc does not closely resemble that in $TcO_2{\bullet}xH_2O$ and the feature at the edge is considerably narrower, possibly because the Tc(IV) is adsorbed to apatite although this cannot be inferred from the XANES data alone. The Tc(IV) formed by removal of $Tc(VII)O_4^-$ from DIW by Sn-A showed high stability upon exposure to air. Figure 3-31B displays the XANES spectrum and resulting fits from Sn-A which was transferred to an oxic environment. Tc(IV) remained the dominant form, with only a small presence of $Tc(VII)O_4^-$ that was within error of having no Tc(VII)O_4^- being present. In LAW simulant, the TcO_4^- removal ability of the Sn-A was decreased due to the high alkalinity (see Figure 3-2, T2 for % Tc removal). Figure 3-31 C&D show the XANES spectra from the LAW simulant experiments (with Tc(VII) and without Cr(VI) added, c) and with an equimolar amount of Cr(VI) and Tc(VII) added d) performed in an anoxic chamber. The samples were prepared in the anoxic chamber for XAS and shipped at the same time, thus any oxygen exposure would be equal. These samples showed that a large percentage (45±2 % to 60±1 %) of the Tc associated with the solid phase is in the oxidized TcO_4^- form, with the rest present as Tc(IV), presumably coordinated by oxygen atoms. It should be noted that Sn-A did not exhibit a difference in final Tc product in the presence of Cr(VI) as a similar amount of Tc(VII)O_4^- was associated with the solid phase after removal from LAW simulant both with and without Cr(VI).

Table 3-4- Tc K-edge fitting results for the getter and Cast Stone samples analyzed. The numbers in parentheses represent the standard deviations of the contribution of that component for the ending digit, p is the probability that improvement of the fit, when this standard is included, is due to random error.

Sample	TcO_4^-	p	Tc_2S_7	p	Tc(IV)	p
KMS-2-SS DIW	0.00(1)	1	1.00(3)	<0.001	0.00(2)	1
KMS2-SS DIW Water Exposed	0.07(3)	0.066	0.55(7)	<0.001	0.38(5)	<0.001
KMS2-SS LAW	0.32(1)	<0.001	0.47(3)	<0.001	0.21(2)	<0.001
SnA DIW	0.00(7)	1.000	0.07(13)	0.784	0.93(9)	<0.001
SnA DIW Air Exposed	0.02(4)	0.391	0.00(7)	1	0.98(4)	<0.001
SnA LAW Exposed (no Cr)	0.60(1)	<0.001	0.00(1)	1	0.40(1)	<0.001
SnA LAW Exposed (Tc+Cr)	0.45(2)	<0.001	0.00(2)	1	0.55(2)	<0.001
Cast Stone TT1 4A	0.59(1)	<0.001	0.13(2)	<0.001	0.28(2)	<0.001
Cast Stone TT1 6 mo leach	0.76(1)	<0.001	0.11(2)	<0.001	0.13(2)	<0.001

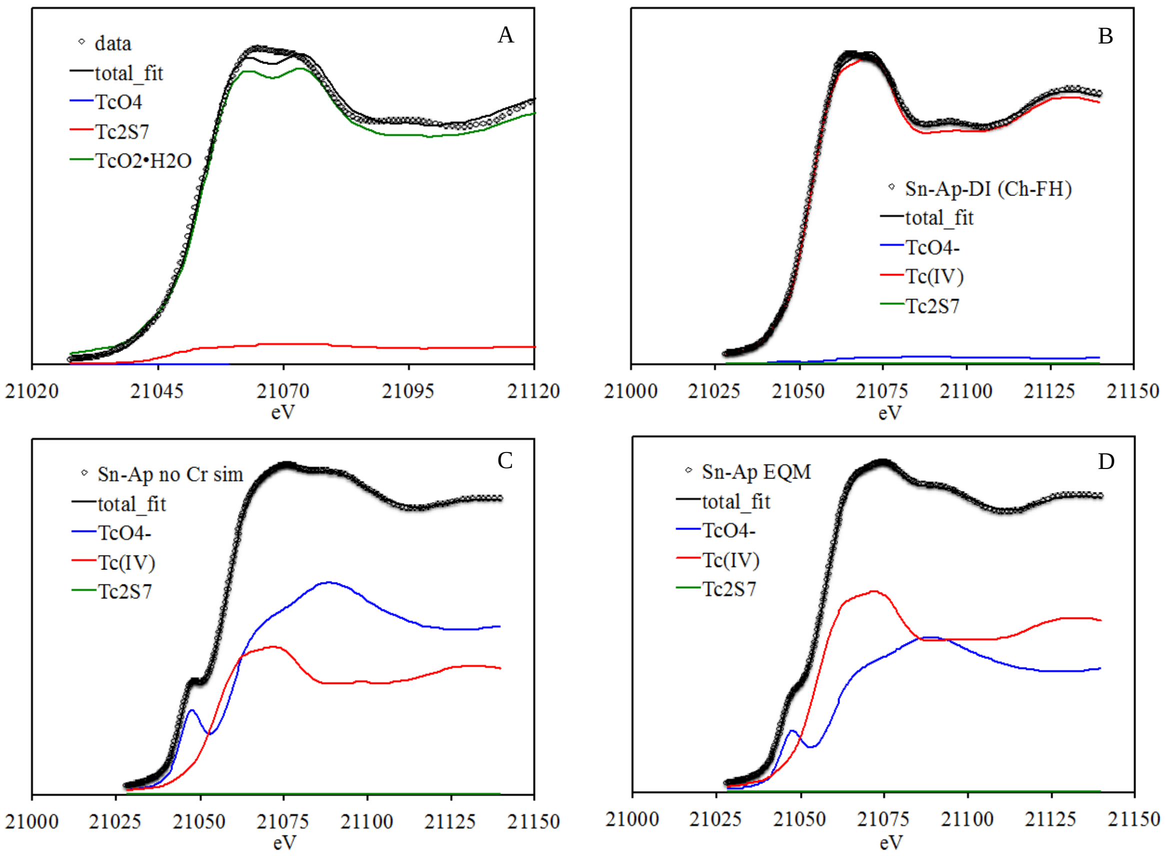

Figure 3-31 – Tc K-edge XANES spectrum and fit for sample Sn-A exposed to water A) before and B) after exposure to oxygen and exposed to LAW simulant without C) Cr and D) with Cr.

Removal of Tc from DI water by KMS-2-SS occurred via the complete reduction of the soluble Tc(VII)O_4^- to form a single insoluble Tc(IV)$_2S_7$ phase (Table 3-4 and Figure 3-32A). The Tc_2S_7 is a commonly reported Tc-S structure with Tc(IV) coordinated by disulfide ligands. The Tc_2S_7 formed by the removal of Tc(VII)O_4^- from DIW by KMS-2-SS showed high stability upon exposure to air (Neeway et al. 2016). However, exposure of the KMS-2-SS-associated Tc(IV)$_2S_7$ to fresh oxic DI water resulted in partial re-oxidation to form a mixture of Tc(IV)$_2S_7$ (55±7 %) and Tc(IV)O_2•2H_2O (38±5 %) (Table 3-4, Figure 3-32B). Including the presence of Tc(VII)O_4^- did not significantly improve the XANES fit indicating that the Tc associated with the solid KMS-2-SS phase remained as reduced Tc(IV), despite subsequent exposure to oxidizing conditions. The mismatch between the data and fit at ~21085 eV is most likely due to the presence of a Tc oxysulfide species. Almost complete removal of Tc by KMS-2-SS from LAW simulant was observed (see Figure 3-2, T3-T6 for % Tc removal)) but resulted in a mixture of Tc species (Table 3-4, Figure 3-32C). Including TcO_4^- significantly improved the fit suggesting two mechanisms of Tc removal from LAW simulant by KMS-2-SS: (i) sorption of 32 % Tc(VII)O_4^- onto the solid phase; and (ii) reduction of soluble Tc(VII)O_4^- to form a mixture of Tc(IV)$_2S_7$ (47±3 %) and Tc(IV)O_2•2H_2O (21±2 %). The different mechanisms for Tc(VII)O_4^- removal by KMS-2-SS in DI water versus LAW simulant could be explained by the difference in the KMS-2-SS structure. As shown by the XRD patterns in Figure 3-27, the KMS-2-SS exposed to DI water is isostructural with pristine KMS-2-SS except for a shift of the (002) and (004) basal Bragg peaks to lower 2θ (higher *d* spacing) due to hydration of the structure. These peaks are labeled with * in Figure 3-27. Under these conditions, the hydrated

KMS-2-SS efficiently removes Tc(VII)O_4^- from solution and produces a sulfide-coordinated Tc(IV). However, the KMS-2-SS sample after exposure to LAW simulant has undergone a major structural change with only small, broad peaks associated with a more random (less ordered) structure and/or small crystallite sizes. The increase in surface area associated with this less ordered material could result in efficient sorption of Tc(VII)O_4^- from solution, and a fraction of the starting Tc(VII)O_4^- is also reduced to Tc(IV)O_2•2H_2O, but the lack of structural order means that there is insufficient sulfide in the vicinity of the TcO_4^- to supplant the O and produce Tc(IV)$_2S_7$. It should also be noted that the LAW simulant contains 806 ppm Cr(VI) which will compete with Tc(VII)O_4^- for available reducing equivalents and could inhibit the reduction of Tc(VII)O_4^- to Tc(IV)O_2•2H_2O and then further to Tc(IV)$_2S_7$ by the KMS-2-SS, resulting in the observed, mixed phased product.

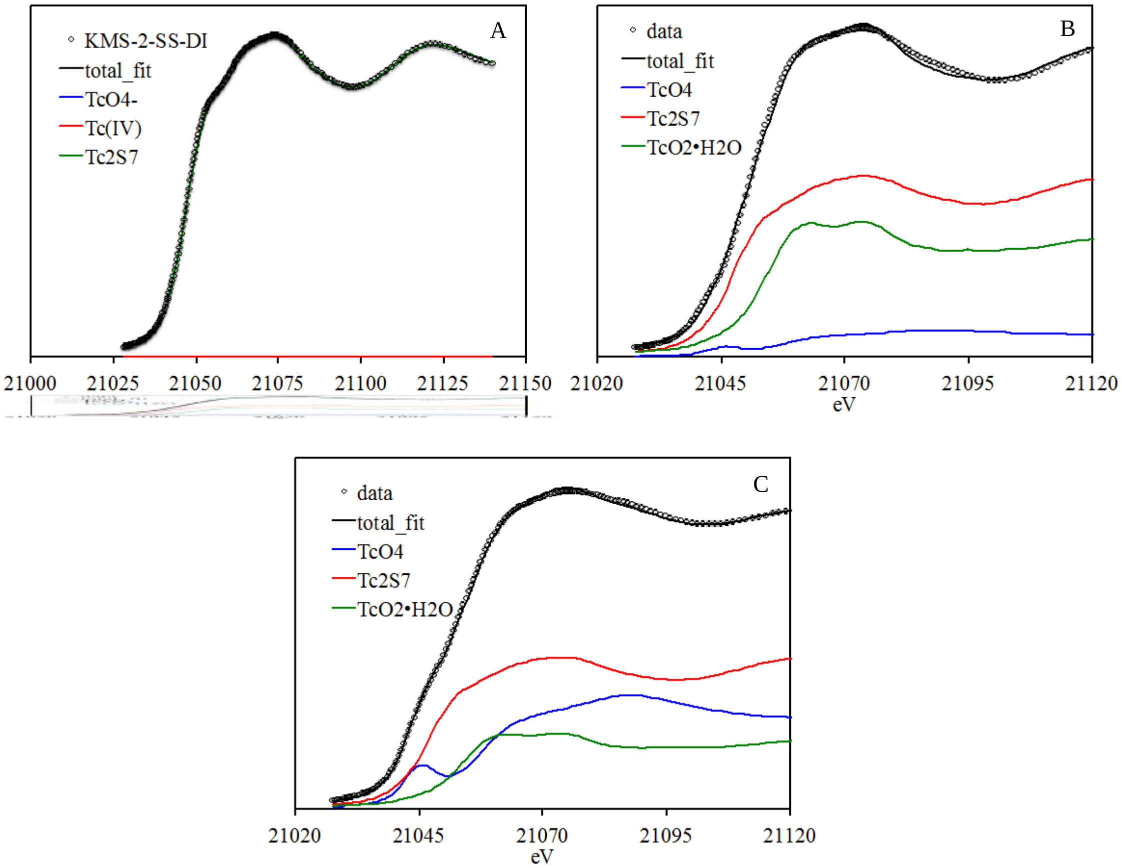

Figure 3-32 Tc K-edge XANES spectrum and fit for KMS-2 exposed to A) DDI, B) extracted from DDI and exposed to fresh DDI and C) exposed to LAW simulant

Figure 3-33 shows the Tc K-edge XANES spectra for Cast Stone TT1 sample from FY15 (Asmussen et al. 2015) made with LAW simulant before (A and after (B leaching in DIW. These spectra provide insight into the mechanism of release of Tc from the Cast Stone monoliths during the leaching process. Before leaching in DIW, the Cast Stone contains 13±2 % Tc(IV)$_2S_7$, 28±2 % Tc(IV)O_2•2H_2O and 59±1 % Tc(VII)O_4^-. After 6 months of leaching in DIW, the amount of Tc(IV)$_2S_7$ in the Cast Stone monolith remains the same within error (11±2 %) but the amount of Tc(IV)O_2•2H_2O has decreased to 13±2 %, with a corresponding increase in the amount of Tc(VII)O_4^- (76±1 %) (see Table 3-4). This suggests that Tc(IV)$_2S_7$ is stable under leaching conditions and the mechanism of Tc release from the monolith is via oxidation of the Tc(IV)O_2•2H_2O to form soluble Tc(VII)O_4^- that dissolves into the pore water and diffuses out of the monolith. Further work is required to optimize the performance of the KMS-2-SS containing Cast Stone by increasing the proportion of Tc(IV)$_2S_7$ present, thus lowering the Tc observed diffusivity. As the KMS-2-SS was observed to form Tc_2S_7, the Tc will exist within this Tc getter-laden Cast Stone in this form, and this may be the cause of the lower D_{obs} Tc values observed for T3-T6 in comparison to mix T2 and the control (no Tc getters) T1.

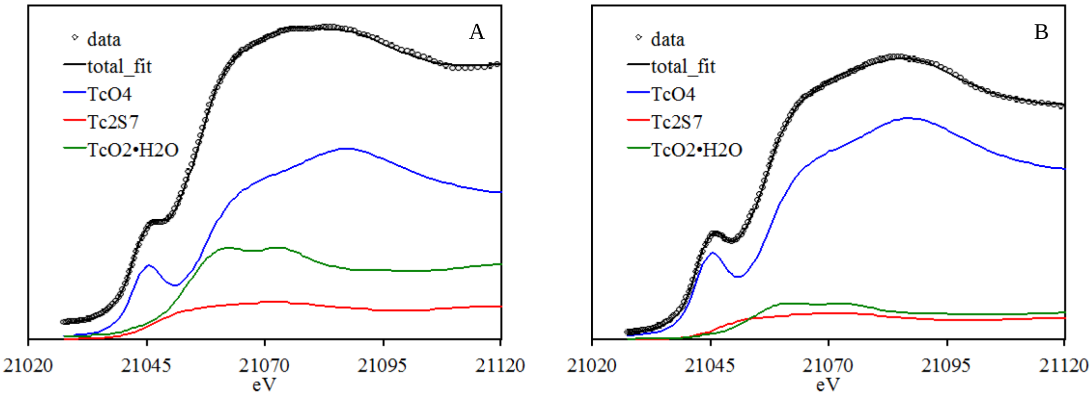

Figure 3-33 Tc K-edge XANES spectrum and fit for the FY15 TT1 GCCS A) prior to leaching and B) after 6 month leaching in VZPW.

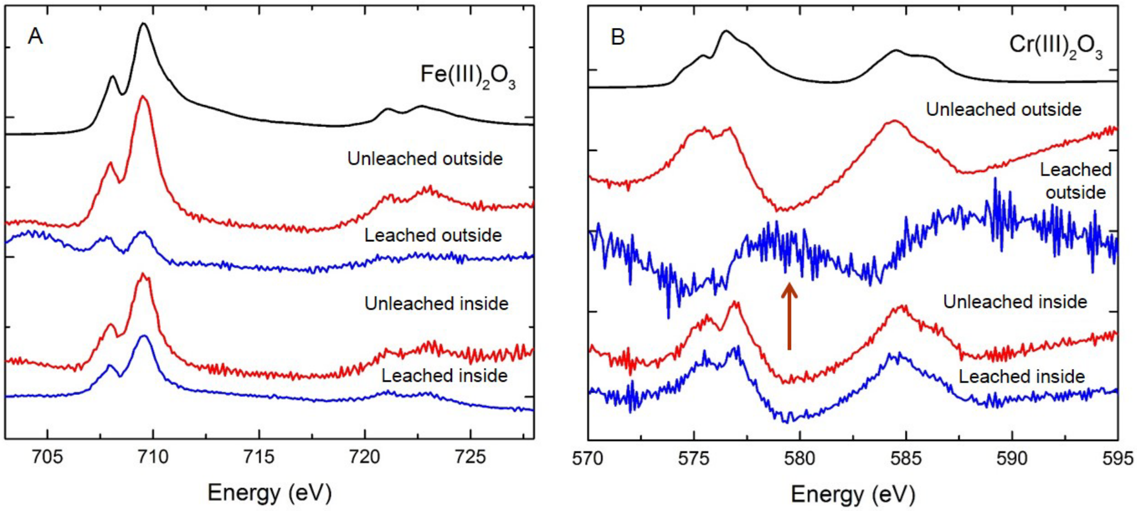

Figure 3-34- A) Fe L-edge and B) Cr L-edge XAS spectrum for T7 monolith prior to leaching and after 63-d leaching in VZPW. The “outside” samples were scraped from the outer wall of the monolith and the “inside” samples were taken from a minimum 20 mm from the outer wall.

Fe and Cr L-edge XAS spectra were collected to determine the extent of oxidation within the monolith as a function of distance from the surface. Figure 3-34A shows the Fe L-edge XAS spectra of samples taken from the outside and from the inside of the T7 monolith. Comparing the data to the hematite Fe(III) standard, it can be seen that the Fe is present as Fe(III) both inside and on the outer surface of the monolith, before and after leaching. Therefore, Fe oxidation state within the monolith is not influenced by a change in redox conditions promoted by the presence of KMS-2-SS in the mix and after the leaching process, which was performed in the presence of air. Leaching results in the removal of Fe from the monolith surface as can be seen by the decrease in intensity of the Fe XAS spectrum for the sample taken from the outside of the monolith after leaching.

Figure 3-34B shows the Cr L-edge XAS spectra of samples taken from the outside and from the inside of the T7 monolith. Comparing the data to the eskolaite $Cr(III)_2O_3$ standard, it can be seen that the Cr is present as Cr(III) both inside and on the surface of the monolith, before leaching. After leaching in VZPW, the Cr XAS spectrum for the sample taken from the monolith interior shows that the Cr remains reduced as Cr(III) but the Cr XAS Spectrum for the sample taken from the outer surface of the monolith after leaching is much less intense and shows a distinct shift to higher energy (brown arrow in Figure 3-34B), resembling the crocoite $PbCr(VI)O_4$ standard shown previous work (Telling 2010). Thus, the leaching process results in oxidation of Cr at the monolith surface and subsequent release of Cr(VI) into solution, although at a very low rate.

3.4.7 Nuclear Magnetic Resonance Spectroscopy (NMR)

Three Cast Stone samples were analyzed via ^{27}Al direct polarization (DP) nuclear magnetic resonance to characterize any local bonding changes relative to position within the monolith. The samples were collected from a region located ~ 5 mm from the monolith wall (OUT samples) and from ~ 25 mm depth in the monolith center (IN samples). The samples were crushed to < 300 µm particle size and mixed with StyCast resin to form a pellet to keep the specimen non-dispersible. The samples analyzed were:

- T1-3 which was fabricated as part of this report and was unleached.
- T1-7 which was fabricated in this report and leached for 63 d in VZPW
- TT2-5 which was fabricated as part of the FY15 effort (Asmussen et al. 2015) and leached for ~1 year in VZPW.

The TT2-5 sample was fabricated using the same recipe as this year's Cast Stone with the exception that ~ 8 M Na average LAW simulant was used and the monolith contained 0.5 wt% of Sn-A and Ag-Z (Asmussen et al. 2015).

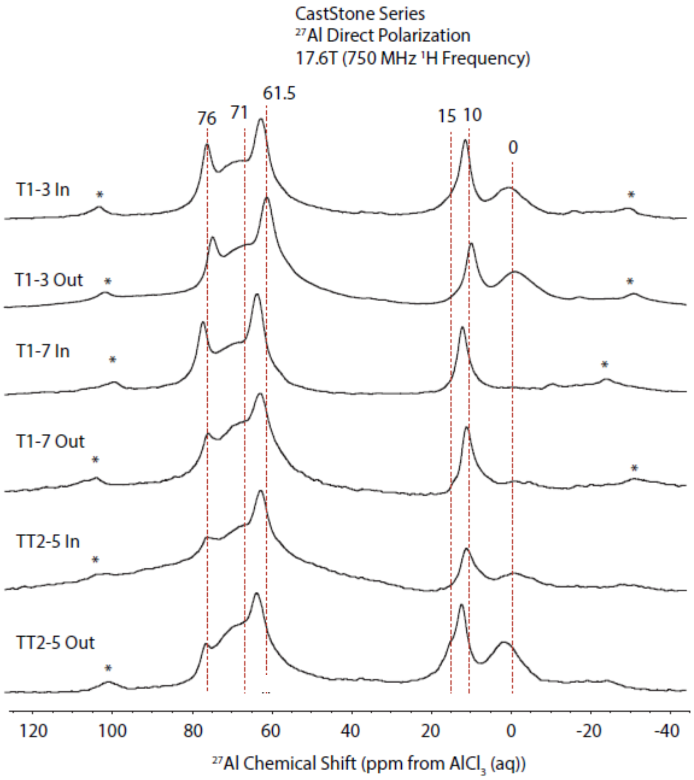

Figure 3-35 – ^{27}Al DP NMR spectra of the inner and outer samples taken from the T1-3 (unleached), T1-7 (63 d leached in VZPW) and TT2-5 (~1 year leached in VZPW) monoliths. * denotes a spinning sideband.

The ^{27}Al NMR spectra from these specimens are shown in Figure 3-35. The spectra displayed some similar features. In the tetrahedral region, two distinct ^{27}Al resonances were observed in the 61-63 ppm and 76 ppm regions. In the octahedral coordination region all spectra show a distinct resonance in the10-12 ppm region, with the unleached monoliths (T1-3) and TT2-5 samples exhibiting a resonance near 0 ppm. This resonance is greatly diminished in the 63 d leached T1-7 spectra, yet appears in the TT2-5 IN sample and strongly appears in the TT2-5 OUT sample. The evolution of this resonance may suggest an evolving octahedral species on the outer wall of the monoliths over long leaching time. The Cast Stone samples do show some heterogeneity from sample to sample, however not to the extent observed in long term leached monoliths, > 3 years (Asmussen et al, 2016c). It should be noted that due to the complexity of each monolith's structure, exact determinations of chemical environments are not attainable with NMR alone.

3.4.8 Biological Characterization

DNA sequencing was performed on a sample of the biological growths present on the T6-5 monolith leached in VZPW. The growths on the surface of the monolith can be seen in Figure 3-36 a). Following removal of low quality sequences, approximately 84,000 sequences were analyzed for the sample. Phylogenic analysis of the sample showed very low diversity with fewer than four phyla being represented in the samples (Figure 3-36b). *Proteobacteria* were the most dominant phylotype observed.

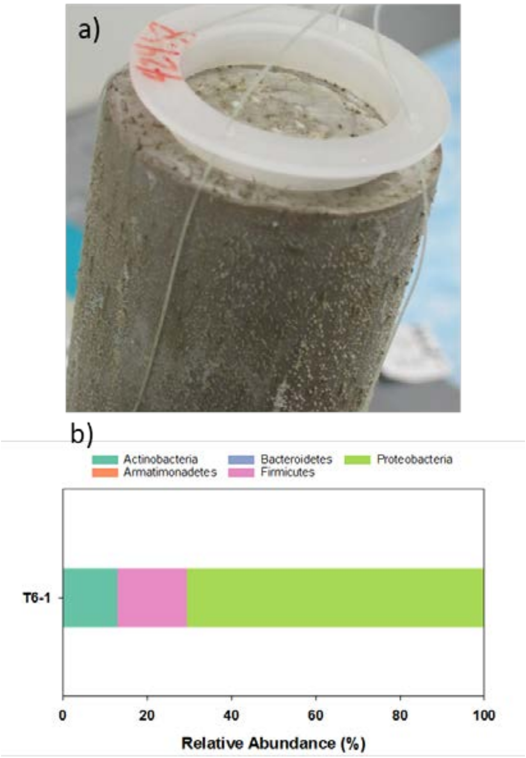

Figure 3-36 – a) image showing the biological growths on the surface of the T6-5 monolith leached in VZPW and b) relative abundance of bacterial phyla present in precipitates from the T6-5 sample

Genus level identification within these phyla indicates a mixture of species are present. Bacterial genera representing greater than 10% of the community are described in the Table 3-5. Bacteria related to those found on the Cast Stone surfaces have shown the ability to grow oxidatively on a range of carbon sources, and may be able to metabolize the acetate present in Cast Stone from the LAW simulant. Likewise, a number of the bacteria found, are halotolerant and some combine this phenotype with tolerance to alkaline conditions. Both of these characteristics would allow the bacteria to grow in the high salt, alkaline environment on the surface of the Cast Stone. Finally, resistance to metals, and the ability to use inorganic constituents in the waste including nitrate and radionuclides, in addition to oxygen would allow these microbes to grow~~n~~ on the surface of the Cast Stone.

Table 3-5- Bacterial genera found in Cast Stone precipitates and description of phenotypic characteristics.

Genus	Abundance (%)	Description
Solirubrobacter	12.6	*Actinobacteria*. Aerobic, chemoheterotroph isolated from soils and sediments. Dessication and possible radioresistance
***Bacillales* (Order)**	2.4	
Bacillus	6.0	
Geobacillus	1.4	
Salinococcus	6.5	
Brevundimonas	16.2	*Proteobacteria*. Facultative anaerobe, chemoheterotrophic (oligotrophic), halotolerant, alkaliphilic. Isolated from diverse environments. Some species have shown resistance to ionizing radiation.
Cupriavidus	30.7	*Proteobacteria*. Facultative anaerobe, chemoheterotroph/chemolithotrophic. Commonly found in soils. Known for resistance to metals, some strains have demonstrated the ability to chemically reduce metals.
Ralstonia	23.5	*Proteobacteria*. Facultative anaerobe, chemoheterotrophic. Isolated from numerous environments including soil and water. Resistant to metals, able to chemically reduce a variety of metals and metalloids.

4.0 Summary and Conclusions

This report includes the culmination of a multi-year effort into investigations on Tc and I getters performance on removing Tc and I from LAW simulants and after incorporation into Cast Stone. This effort was initiated in FY14 following the initial Cast Stone screening work in FY13 (Westsik et al. 2013). The addition of getters to Cast Stone can potentially lower release of radionuclides and COC's from the waste form through incorporation of these species into more stable forms controlled by the getters. Getter performance for selective sequestration of Tc (Sn-A and KMS-2) and I (Ag-Z and argentite) from LAW has been established in previous efforts (Qafoku et al. 2014). Deleterious interactions between the Tc and I getters when present together in solution have also been identified. Sequential addition of the getters to LAW liquid wastes with removal of the first getter by filtration and subsequent re-introduction to the final Cast Stone wet slurry can partially overcome these deleterious interactions (Asmussen et al. 2015). A sequential getter introduction process was utilized to develop a testing matrix designed to investigate the incorporation of Tc and I getters into Cast Stone, and the subsequent impact on Tc and I observed diffusivities during leach tests.

Seven sets of monoliths (T1 through T7) were fabricated with LAW simulant using different combinations and mixing orders of Tc and I getters, including two control sets of monoliths (either no getters added (T1) or AgI added as the I "waste" source (T7)). All the Cast Stone monoliths were cured for 28 days then they underwent performance testing using EPA Methods 1315 and 1313 followed by pre- and post-leach testing solid state characterization. EPA Method 1315 testing is representative of a fully saturated water exposure of the waste form. However, in a disposal scenario relevant to the IDF partially saturated water conditions are expected and the waste form might experience wet/dry cycles due to episodic recharge water wetting fronts. The authors are aware of limited work performed in these relevant disposal conditions. Work at Brookhaven National Laboratory investigated cement-based materials spiked with Cs and Sr surrounded by a porous medium which was exposed to wet/dry cycling. The authors reported that the grout was never truly "dry" as the water inside the grout from the "wet" cycle was retained and diffusion still occurred in this "dry" period (Dayal et al. 1983). Similar work has yet to be performed on grouts containing reductants, such as the BFS in Cast Stone, or those containing Tc and I in relevant IDF disposal conditions.

A control monolith, T1, was fabricated with LAW spiked with Tc and I but with no getters. As minor variations in the Cast Stone mix can lead to differences in D_{obs} values (Westsik et al., 2013), the T1 set represents a control system as it was fabricated using identical dry blend mix, LAW simulant, Tc and I spike levels, curing times, mix ratio and fabrication steps as the getter containing Cast Stone monoliths. After curing, iQid autoradiography imaging of the control monolith showed the Tc to be rather evenly distributed throughout the circular cross section cut from the middle of a T1 control monolith. Upon leaching an intact control monolith in VZPW, the Tc D_{obs} values for the control monolith continually increased until a maximum of 1.2×10^{-11} cm^2/s was reached at 49 d leaching. During leaching an intact control monolith in DIW, the Tc D_{obs} values increased from 3.7×10^{-13} cm^2/s at 2 h to 3.9×10^{-11} cm^2/s at 63 d. In initial screening tests of LAW Cast Stone (Westsik et al. 2013) an average Tc D_{obs} of 5.3×10^{-11} was reported (Cantrell et al. 2016). Leaching the control T1 monolith in VZPW gave an I D_{obs} of 3.5×10^{-8} cm^2/s at 1 d, followed by a continual decreasing to 6.6×10^{-9} cm^2/s at 63 d. During leaching of the control monolith in DIW for 63 d, the I D_{obs} steadily decreased to 8.3×10^{-9} cm^2/s after 63 d. In the initial screening tests of LAW Cast Stone (Westsik et al. 2013) an average I D_{obs} of 5.7×10^{-9} was reported (Cantrell et al. 2016). Following leaching of these T1 control monoliths, autoradiography imaging of cross-sections taken from the center of these leached monoliths showed that, although Tc was still present throughout the cross-section, the distribution had changed with a buildup in Tc concentration occurring closer to the outer wall of the control monoliths.

In T2 monoliths Sn-A was used as the Tc getter, in the highest quantity (2.85 wt% of the dry mix), in order to account for its lower reduction capacity and reduced performance in alkaline environments. The Sn-A was first added to the LAW simulant and this led to the removal of 65% of the Tc and 99.6% of the Cr. Sequestration of Tc by Sn-A occurred via the reduction of soluble $Tc(VII)O_4^-$ in the LAW simulant to form Tc(IV), presumably coordinated by oxygen atoms, as shown by Tc K-edge XANES analysis of the final cured Cast Stone. Ag-Z (0.5 wt% of the total dry blend mass) was added to the LAW simulant 24 h after the Sn-A had been added and the Ag-Z removed > 98% of the I. This confirms the ability of Ag-Z to sequester I^- from highly caustic-saline solutions such as LAW. After curing, the T2 monoliths were observed to contain white "clumps", identified by XRD as burtite ($CaSn(OH)_6$), which result from the reaction of Sn-A with the LAW simulant. The area around the burtite clumps was brown in color, in contrast to the dark green color of the rest of the Cast Stone T2 monoliths. From XRD, the brown colored areas contained the expected Cast Stone composition but with burtite present, showing limited incorporation of the altered Sn-A into the entire grout matrix. iQid autoradiography measurements of a horizontal circular cross section from the center of a T2 monolith showed distinct Tc "hot spots" spread through the cross section. A T2 thin section, analyzed by both autoradiography and µ-XRF, showed smaller isolations of Tc associated with Cr and in the same location as Sn and P. A larger white clump present in the thin section, similar in appearance to those identified as burtite by XRD, contained both Sn and P confirming that burtite is an altered form of original Sn-A. In contrast to the smaller Sn- and P-containing areas, no Tc was detected inside one of the larger burtite clumps, but Tc was present in the immediate area surrounding the clump. This suggests that the reduction of Tc and Cr by the Sn-A is a surface mediated process. Thus the reduction of Tc and Cr will be influenced by the available surface area of the Sn-A getter particles, and that these two redox-sensitive species remain closely associated (i.e., bound to the surfaces of the Sn-A getter within the Cast Stone bulk matrix.

Appendix D summarizes recent Savannah River National Laboratory (SRNL) studies on simulants of WTP off-gas (secondary wastes) liquid condensates and flush waters that were spiked with $^{99}Tc(VII)O_4^-$ and then treated with $SnCl_2$ or $SnCl_2$ and hydroxyapatite. These SRNL studies show similar removal of Tc from the secondary waste simulants as found in our studies of LAW simulants treated with Sn-A as long as the secondary waste streams were kept near neutral pH. When the secondary waste simulants were made caustic, the Sn(II) treatment was less effective at precipitating Tc as low solubility Tc(IV)-oxides, see Taylor-Pashow et al. (2014 and 2015) for more details.

Upon leaching, the T2 monolith had the highest Tc D_{obs} values in VZPW for the initial 14 d of leaching for all the getter containing Cast Stone mixes studied. This high Tc release may represent the fraction of Tc within the LAW simulant that was not sequestered by Sn-A; recall that 35% of the Tc remained in solution after adding Sn-A. This Tc after mixing in the dry blend and forming Cast Stone might have remained readily available to leach, however no proof of this hypothesis was provided in this work. Regardless, at 63 d leaching in VZPW the T2 monolith Tc D_{obs} (1.1×10^{-12} cm^2/s) had decreased to well below the getter-free T1 control's Tc D_{obs} value of 3.9×10^{-11}. Sn-A was previously studied as a getter for Tc from a neutral brine solution and incorporation into a fly ash free grout (65 wt % OPC, 35 wt % BFS and 3 wt % Sn-A) with a Tc loading of 0.7 ppm (Duncan et al. 2009). In 24-h leaching of their monoliths in DIW, an improvement in Tc release was observed. Our report shows that Sn-A can also be effective in lowering Tc release from grout waste forms fabricated with aggressive LAW simulant, over longer leaching periods in VZPW, which represents the conditions most relevant to the actual IDF disposal environment.

When leached in DIW, the Tc D_{obs} values for T2 monoliths were within the same range as the Tc D_{obs} values Tc D_{obs} as those for T1, T3 and T4 monoliths throughout the 63 d leaching, and higher than Tc D_{obs} values for monoliths leached in VZPW. This suggests that Tc release from getter containing Cast Stone is likely pH controlled as the pH of the leachate in DIW is higher (pH ~ 12) than in VZPW which buffers the leachate pH to 10.8. The significantly more alkaline pH in DIW leachates may increase the solubility of the reduced Tc(IV) phases and may also lead to increased dissolution of the bulk Cast Stone monolith, as evidenced by the measurable Al and Si releases in DIW leachates in comparison to non-detectable releases of Al and Si in VZPW leachates (see leachate data in Appendix B). As well, the calcium carbonate-based layer that forms on the outer monolith surfaces in the VZPW leached monoliths likely assists in lowering Tc release.

The I D_{obs} values for all the Cast Stone mixes that contained I getters in both DIW and VZPW were similar to each other and to the T1 control that did not contain an I getter. The I D_{obs} values decreased over time to 6.6×10^{-9} cm^2/s at 63 d in VZPW and to 4.4×10^{-9} cm^2/s in DIW. Despite the Ag-Z sequestering all the detectable I inventory as AgI in the LAW simulant prior to Cast Stone fabrication, little to no improvement in I release was attained when the cured Cast Stone monoliths, which contained between 0.083 to 0.5 wt % Ag-Z in the dry blend ingredients, were leached. This fact clearly indicates that other processes (e.g., AgI solubility in Cast Stone) were likely controlling the I release from the Cast Stone monoliths into the leachate. Following leaching in DIW, black dots were observed on the surface of the T2 monoliths that were confirmed by SEM/EDS to contain Ag. Evidence from µXRF also shows that I is associated with the Ag within the monolith. Therefore these surface black dots may represent sites of congregation of Ag (as black silver-oxide(Varkey et al. 1993)) and possibly I.

Autoradiography iQid imaging of the T2 monolith cross section after leaching showed Tc was distributed throughout the cross section but with Tc hot spots still present. The results from solid phase characterization of T2 samples suggest that the sequential addition of Sn-A and Ag-Z can effectively remove Cr and Tc and I, respectively, from LAW simulant. Tc retention in the Sn-A bearing Cast Stone during leaching is improved relative to the control without Tc getter. Further improvements in Tc sequestration and retention may be achieved through: (i) a reduction in Tc getter particle size, along with increased mixing time of the Cast Stone wet slurry, to homogenize Sn-A distribution and reduce Sn-A "clump" size; (ii) addition of higher concentrations of Sn-A getter; and (iii) using multiple sequential Sn-A treatments to the LAW liquid waste prior to adding an iodide getter.

In monoliths T3 and T4, KMS-2-SS was added to LAW simulant as the Tc getter at 0.14 wt % of the total dry blend. The KMS-2-SS was then removed from the LAW simulant by filtration and an I getter (Ag-Z for T3 and Arg for T4) was subsequently added to the LAW simulant. In the T3 and T4 compositions, KMS-2-SS removed 97% of the Tc inventory from LAW solution. Analysis showed that a majority of Cr (> 89%) remained in solution but a color change in the LAW simulant upon addition of KMS-2-SS suggested reduction of the yellow Cr(VI) to a green soluble Cr(III) species. Then the subsequent I getter addition to the LAW simulant was far less effective at removing iodide than the LAW simulant first treated with Sn-A (the T2 LAW testing). The T3 LAW test after removal of the KMS-2-SS showed that addition of Ag-Z removed 24 % of the I, a drastic drop compared with the iodide removal from LAW by the T2 mix. The Ag-Z I getter in T3 was added at a stoichiometric determined ratio (0.08 wt % of the total dry blend) to remove all of the I present in the LAW simulant. At this ratio Ag-Z was previously shown to be effective in removing all the I spiked into the LAW simulant. It is likely that either residual dissolved sulfide from the KMS-2-SS was present in the filtered LAW that reacted with the Ag-Z or small KMS-2-SS particles passed through the filter, limiting the Ag-Z's ability to remove I from the LAW simulant. The interfering mechanism is likely residual sulfide forming a more insoluble Ag compound, Ag_2S that releases iodide from AgI precipitates that are the product formed when Ag-Z is added to the LAW simulant.

The argentite used in T4 tests, added at 0.28 wt% of the dry blend, removed no measurable amount of I from the LAW simulant that was first contacted with KMS-2SS. Following the addition of the dry blend and curing, the T3 and T4 Cast Stone monoliths were visually similar to the T1 control Cast Stone monoliths, and had a similar mineralogical composition, as expected due to the low concentrations of getters added.

The EPA 1315 leach testing of T3 and T4 cured Cast Stone monoliths showed excellent results for Tc; that is low Tc D_{obs} values were measured. Tc K-edge XANES measurements on T3 and T4 monoliths showed that the addition of KMS-2-SS to the LAW simulant sequestered Tc(VII) as a $Tc(IV)_2S_7$ species within the cured Cast Stone. The use of KMS-2-SS led to the lowest measured Tc D_{obs} values for Cast Stone leached in VZPW, 5.4×10^{-13} cm^2/s and 6.1×10^{-13} cm^2/s at 63 d for T3 and T4 respectively, a near order of magnitude improvement over the getter-free T1 control in VZPW. This improved Tc retention is likely due to the stability of the reduced Tc-S solid phases in the Cast Stone. Tc K-edge XANES analyses of Cast Stone monoliths fabricated in FY15, with KMS-2-SS and a higher initial Tc loading of 46 ppm, showed that, after >6-month leaching, the proportion of the Tc inventory present as Tc(VII) in the leached monolith was higher compared with the proportion present as Tc(VII) in an unleached KMS-2-SS-containing monolith that had been exposed to air. The amount of $Tc(IV)O_2$ present in the leached monolith decreased proportionally to the increase in Tc(VII), while the amount of Tc_2S_7 in the leached monolith remained the same. This suggests that Tc(IV) oxides within the Cast Stone are preferentially re-oxidized to Tc(VII) during leaching and that Tc(IV) sulfides exhibit much greater long-term stability. It is therefore likely that through treatment with sufficient amounts of the KMS-2-SS, nearly all Tc will be present in the monolith as a Tc(IV) sulfide, which can resist re-oxidation and lead to lower D_{obs} in the VZPW over long leaching times.

In leach testing conducted with DIW, the T3 and T4 cured Cast Stone monoliths , the measured Tc D_{obs} values were similar to the Tc D_{obs} values for the T1 and T2 mixes leached in DIW and higher than the Tc D_{obs} values in VZPW, possibly due to the influence of pH as described for T1. The I D_{obs} values for T3 and T4 in both VZPW and DIW were similar to the I D_{obs} values for the T1 control as little of the I was sequestered by either I getter prior to their incorporation into the Cast Stone.

During the leaching of T3 and T4 Cast Stone monoliths, irregularly shaped black spots developed on the monolith surfaces in VZPW at >14 d leaching. An example black spot was excised from the T3-8 monolith and imaged with SEM/EDS. Tc was found in these EDS spot measurements, along with Mg and Sn, within the black spot, but not in the adjacent region near the black spots in the rest of the monolith's surface. The Mg and Sn are also components of the KMS-2-SS, and this may be evidence of Tc being released at these surface black spots from the KMS-2-SS structure, demonstrating that Tc is retained by the KMS-2-SS getter after leaching and that Tc release from the monoliths may occur at discrete locations instead of homogeneously from all surface pores.

In T5 and T6, KMS-2-SS (0.14 wt%) was again used as the Tc getter and added to the LAW simulant but it was not filtered out before adding the I getters, Ag-Z in T5 (0.08 wt%) and argentite in T6 (0.28 wt%). These iodide getters were combined with the dry blend instead of being as added directly to the LAW simulant. The KMS-2-SS removed 97 % of the Tc in T5's LAW simulant and 99.9 % from the LAW simulant in T6. Following the curing, the T5 and T6 Cast Stone monoliths were visually similar to the T1 control, and had a similar mineralogical composition (from XRD). iQid radiography imaging of cured T5 and T6 monolith cross-sections revealed distinct Tc "hot spots", showing that Tc was sequestered by KMS-2-SS in discrete areas within the cross section through the middle of the monolith.

After EPA 1315 leach testing of the T5 and T6 monoliths in VZPW for 63 d, a Tc D_{obs} of 8.0×10^{-13} cm^2/s and 6.9×10^{-13} cm^2/s were calculated, respectively. These Tc D_{obs} values are very similar to those for the leached T3 and T4 mixes wherein the KMS-2-SS had first been filtered out of the LAW simulant before adding the iodide getters and then both getters and the Law simulant were mixed with the dry blend, suggesting that removal of the Tc getter through filtration does not have a major impact on Tc retention In the final cured Cast Stone. iQid autoradiography of a T6 monolith cross-section after leaching in VZPW showed minimal change in Tc distribution between the leached and unleached monoliths, with Tc hot spots still present.

After leaching in DIW, the T5 and T6 monoliths exhibited slightly higher Tc D_{obs} values at 63 d, than the other Tc D_{obs} values for T2, T3, and T4 monoliths leached in DIW. iQid imaging of a T5 monolith following DIW leaching showed Tc hot spots, with an apparent increase in Tc concentrations around the outer ring of the monolith's cross . The Tc "hot spots" in the KMS-2-SS monoliths are smaller than those observed in T2 (containing Sn-A), and this is likely a result of the difference in particle size for the two Tc getters. It is possible that getter particle size has an impact on Tc retention as the monoliths with the smaller Tc hot spots gave lower Tc D_{obs} in VZPW, but this requires further investigation.

Adding the I getters to the dry blend before fabricating the Cast Stone did not have a measurable effect on I D_{obs} values compared to first adding the I getters to the LAW simulant and allowing the I getters to interact with the LAW solution for 24 hr before fabricating the Cast Stone. The I D_{obs} values for all of the GCCS monoliths were very similar to that for the T1 control. The I D_{obs} values at 63 d in both DIW and VZPW (~ $4 – 8 \times 10^{-9}$ cm^2/s) are similar to the I D_{obs} values for other mobile constituents at 63 d; values for Na, NO_3^- and NO_2^- ranged from ($3\text{-}6 \times 10^{-9}$ cm^2/s). The similar D_{obs} values for iodide and the other mobile constituents suggest that I does not form a strong chemical bond with iodide getters or components in the Cast Stone matrix. Thus iodide in cured Cast Stone, regardless of the presence of Ag-Z orArg, is free to diffuse out of the monolith at the same rate as the mobile constituents, at least when the iodide getters are present in the cured Cast Stone at low loadings (0.08 to 0.50 and 0.28 wt % of the dry blend) for Ag-Z and Arg, respectively.

The I getters selected for this study function through precipitation of AgI. The T7 monolith mix was fabricated using solid AgI as the source of I, equivalent to putting 20 ppm iodide in the LAW simulant. The T7 monoliths contained no other getters and were thus similar to the T1 control monoliths excepting the source of added iodide. If the Ag-containing getters are to be effective, then the AgI must be stable in the grout. However, the measured I D_{obs} in VZPW for T7 at 63 d is very similar to that for all the GCCS monoliths. Thus, it is likely that the rate of I release is controlled by the solubility of AgI within all the Cast Stone mixes studied, regardless as to whether silver-based iodide getters are present or not at the low loadings used. We speculate that if adequate sulfide ions (from BFS and/or KMS-2-SS) are present they could compete with iodide to sequester the getter's Ag as the more insoluble Ag_2S compound thus also releasing the iodide back into the Cast Stone's pore water. A similar finding was suggested from previous work in fabrication of OPC and BFS containing grout (Atkins et al. 1990).

Previous work by Lockrem (2005) showed an improvement in I retention in Cast Stone monoliths that contained Ag-Z. However, Lockrem's liquid waste that was solidified was a caustic but more dilute Na (0.8 M Na vs our 6.5 M Na) simulant. The simulant to dry blend mix ratio between Lockrem (2005) and our Cast Stone monoliths were similar. Lockrem spiked aliquots of his simulant with three iodide concentrations that ranged from 4.25 to 17 mg/L vs our use of ~6 mg/L. Lockrem's 28-d cured monoliths were very small (1.5 cm diameter by 1.5 cm tall; volume = 2.65 cm^3 and surface area = 10.6 cm^2) compared to our monoliths with volume ~206 cm^3 and surface area ~203 cm^2. Both sets of monoliths were leached in the appropriate volume of leachant for their geometric surface areas but the Lockrem (2005) monoliths were leached only for 19 d and many of the leachates had no detectable iodide present that makes accurate calculations of I D_{obs} values difficult. In Lockrem (2005) the Ag-Z was added at loadings of 1 wt%, 2.5 wt% and 5 wt % ; however, the highest Ag-Z loading used in our study was 0.5 wt% in T2 and 0.08 wt% for T3 and T5, which is much smaller than the amount used in the study by Lockrem. The higher I getter loadings may be responsible for the improvement (a factor of at least 10 drop in calculated I D_{obs} values observed at 19 d leaching). However, Lockrem (2005) reported an uptick in I D_{obs} values as the initial iodide loading in the simulant increased from 4.25 ppm to 17 ppm. (Lockrem

2005) also noted that addition of more than 5 wt% Ag-Z to the Cast Stone dry blend generated monoliths that would not set (harden) within 72 hrs.

We hypothesize that higher Ag-based iodide getter loadings can give lower initial I D_{obs} values, however this will eventually be overcome by the dissolution of AgI as leaching periods are extended. pH may also influence AgI solubility, as a notable release in I was observed with increasing pH in the EPA Method 1313 tests, compared with the getter free control monolith. A test of higher Ag-containing getter loading in Cast Stone is warranted to confirm this hypothesis. In addition, alternate methods of I sequestration will be required in future getter development. Examples of other iodide getters include layered double hydroxides, incorporation of iodide into organic structures and chemical transformations of iodide (e.g. moving to a more positive oxidation state or being part of a chemical bond).

The results of this study show that Cast Stone monoliths containing either of two Tc getters when leached under full saturation with VZPW, can be very effective in lowering significantly Tc diffusivities. Sulfide containing Tc getters, such as KMS-2-SS, show the greatest promise as a method of sequestering Tc from LAW and other harsh liquid waste streams that are solidified as final cementitious waste forms. Ag-containing I getters, while highly successful in sequestering I from LAW, are likely flawed as iodide getters after their incorporation into Cast Stone at the low Ag loadings used to date. There also appears to be a finite limit of around 5 wt% Ag-Z loading into the dry blend before Cast Stone set problems occur based on Lockrem (2005) results.

Additional studies should address the following issues:

1) Develop getter materials which can sequester both Tc and I from different waste streams.
2) Determine the re-oxidation rate of Tc-S formed within cementitious waste forms containing KMS-2-SS getters.
3) Identify chemical composition and mineral identity of Tc “hot spots” observed in the Cast Stone samples with Tc getters. Single particle digital autoradiography imaging can be used to find Tc hot spots, which can then be effectively interrogated with microscopic and spectroscopic techniques.
4) Perform leaching studies on cementitious waste forms containing reductants in partially saturated conditions, and with wet/dry cycling, in relevant conditions to the IDF.
5) Perform tests with higher Tc getter loading within Cast Stone to determine optimal compositions that may lead to even lower Tc release.
6) Determine the evolution of these Tc “hot spots” during leaching by imaging the unleached monolith surface with iQid, followed by time-dependent leaching to observe if preferential dissolution of Tc occurs from specific locations/Tc bonding environments. This would allow for further waste form tailoring and accurate long-term prediction of Tc release from the waste form.
7) Perform tests with higher I getter loading in Cast Stone, to confirm the hypothesis that I release is controlled by AgI solubility and previous Ag-based getter Cast Stone poor testing results can be improved by using higher I getter loading amounts.
8) Develop non-Ag based I getters to overcome the I release caused by competition for the available Ag by other reactants/soluble species (such as sulfide).
9) Develop a quantitative standard to apply for single particle digital autoradiography imaging to correlate Tc locations with absolute Tc concentrations and follow concentration changes as a function of leaching time.
10) Determine the influence of biological growths on cementitious waste forms on Tc and I releases.

11) Study sulfide-based materials as Tc getters in cementitious waste forms fabricated with other liquid waste streams (e.g., ETF).
12) Measure the influence of pH on reduced Tc(IV) species solubility to determine if this is the factor controlling the higher Tc D_{obs} values measured in DIW compared with VZPW.

5.0 References

Asmussen, RM, JJ Neeway, AR Lawter, TG Levitskaia, WW Lukens and N Qafoku. 2016a. "The Function of Sn(II)-Apatite as a Tc Immobilzing Agent." *Journal Of Nuclear Materials* 480: 393-402.

Asmussen, RM, JJ Neeway, AR Lawter, A Wilson and N Qafoku. 2016b. "Silver Based Getters for 129-I Removal from Low Activity Waste." *Radiochimica Acta* Accepted: DOI:http://dx.doi.org/10.1515/ract-2016-2598.

Asmussen, RM, CI Pearce, KE Parker, BW Miller, BD Lee, EC Buck, N Washton, ME Bowden, AR Lawter, E Cordova and J Serne. 2016c. "Solid State Characterizations of Long Term Leached Cast Stone Monoliths." *PNNL-25578* Pacific Northwest National Laboratory(Richland, WA, USA).

Asmussen, RM, N Qafoku, AR Lawter and JJ Neeway. 2015. "Interim Report: Getters and Cast Stone with Getters: Tc and I Sorption and Release Rates." *PNNL-24700* Pacific Northwest National Laboratory, Richland, Washington(Rev. 0).

ASTM. 2005. "Standard Test Method for Laboratory Determination of Water (Moisture) Content of Soil and Rock by Mass." *ASTM D2216-98* ASTM Standards, USA.

Atkins, M, A Kindness, FP Glasser and I Gibson. 1990. "The use of silver as a selective precipitant for 129I in radioactive waste management." *Waste Management* 10(4): 303-308.

Bannochie, C, T Fellinger and J Pareizs. 2005. "Tank 40 Final SB4 Chemical Characterization Results." *US Department of Energy Report SRNL-STI-2010* 441.

Brown, CF, RJ Serne, BN Bjornstad, DG Horton, DC Lanigan, RE Clayton, MM Valenta, TS Vickerman, IV Kutnyakov and KN Geiszler. 2006. "Characterization of Vadose Zone Sediments Below the C Tank Farm: Borehole C4297 and RCRA Borehole 299-E27-22." *PNNL-15503, Rev. 1* Pacific Northwest National Laboratory (PNNL), Richland, WA (US).

Cantrell, KJ and BD Williams. 2013. "Solubility control of technetium release from Saltstone by TcO 2· xH 2 O." *Journal of Nuclear Materials* 437(1): 424-431.

Caporaso, JG, J Kuczynski, J Stombaugh, K Bittinger, FD Bushman, EK Costello, N Fierer, AG Pena, JK Goodrich and JI Gordon. 2010. "QIIME allows analysis of high-throughput community sequencing data." *Nature Methods* 7(5): 335-336.

Certa, PJ and PA Empey. 2011. "River Protection Project System Plan." *ORP-11242* Revision 6, Washington River Protection Solutions, LLC, Richland, Washington.

Dayal, R, RE Davis and DG Schweitzer. 1983. "Wet and dry cycle leaching: Aspects of releases in the unsaturated zone." *BNL-NUREG-33580* Brookhaven National Laboratory, Upton, NY(Rev. 0).

DOE, USDoE. 2012. "Final Tank Closure and Waste Management Environmental Impact Statement for the Hanford Site, Richland, Washington." *DOE/EIS-0391* Office of River Protection, U.S. Department of Energy, Richland, WA.

Duncan, JB, GA Cooke and LL Lockrem. 2009. "Assessment of Technetium Leachability in Cement Stabilized Basin 43 Groundwater Brine." *RPP-RPT-29195* Washington River Protection Solutions, Richland, WA, USA.

Duncan, JB, K Hagerty, WP Moore, RN Rhodes, JM Johnson and RC Moore. 2012. "Laboratory Report on the Reduction and Stabilization (Immobilization) of Pertechnetate to Technetium Dioxide using Tin(II)apatite." *LAB-RPT-12-00001* Washington River Protection Solutions(Rev.0).

EPA. 2012. "Liquid-solid partitioning as a function of extract pH using a parallel batch extraction procedure." *Method 1313* USA Environmental Protection Agencu, Washington, DC(Rev.0).

EPA. 2013. "Mass transfer rates of constituents in monolithic or compacted granulated materials using a semi-dynamic tank leaching procedure." *Method 1315* US Environmental Protection Agency, Washington, DC(Rev.0).

Eriksen, TE, P Ndalamba, J Bruno and M Caceci. 1992. "The solubility of TcO2· nH2O in neutral to alkaline solutions under constant pCO2." *Radiochimica Acta* 58(1): 67-70.

Hassanzadeh Fard, Z, CD Malliakas, JL Mertz and MG Kanatzidis. 2015. "Direct Extraction of Ag+ and Hg2+ from Cyanide Complexes and Mode of Binding by the Layered K2MgSn2S6 (KMS-2)." *Chemistry of Materials* 27(6): 1925-1928.

Kaplan, DI, SV Mattigod, KE Parker and G Iversen. 2000. "Experimental Work in Support of the ^{129}I Disposal Special Analysis." *WSRC-TR-2000-00283* Westinghouse Savannah River Company, Aiken, South Carolina.

Kuczynski, J, J Stombaugh, WA Walters, A González, JG Caporaso and R Knight. 2012. "Using QIIME to analyze 16S rRNA gene sequences from microbial communities." *Current Protocols in Microbiology*: 1E. 5.1-1E. 5.20.

Lockrem, LL. 2005. "Cast Stone Technology for Treatment and Disposal of Iodine-rich Caustic Waste Demonstration - Final Report." *RPP-RPT-26725* U.S. Department of Energy Office of River Protection(Richland, WA, USA).

Mattigod, SV, RJ Serne and GE Fryxell. 2003. "Selection and Testing of "Getters" for Adsorption of Iodine-129 and Technetium-99: A Review." *PNNL-14208* Pacific Northwest National Laboratory, Richland, Washington.

Mattigod, SV, JH Westsik Jr., CW Chung, MJ Lindberg and KE Parker. 2011. "Waste Acceptance Testing of Secondary Waste Forms: Cast Stone, Ceramicrete and DuraLith." *PNNL-20632* Pacific Northwest National Laboratory(Richland, WA).

McCabe, DJ, WR Wilmarth and CA Nash. 2013. *Waste Treatment Technology Process Development Plan for Hanford Waste Treatment Plant Low Activity Waste Recycle*, SRNL-STI-2013-00351, July.

Miller, BW, SH Frost, SL Frayo, AL Kenoyer, E Santos, JC Jones, DJ Green, DK Hamlin, DS Wilbur and DR Fisher. 2015. "Quantitative single-particle digital autoradiography with α-particle emitters for targeted radionuclide therapy using the iQID camera." *Medical physics* 42(7): 4094-4105.

Neeway, JJ, RM Asmussen, AR Lawter, ME Bowden, WW Lukens, D Sarma, BJ Riley, MG Kanatzidis and NP Qafoku. 2016. "Removal of TcO4-from Representative Nuclear Waste Streams with Layered Potassium Metal Sulfide Materials." *Chemistry of Materials* 28(11): 3976-3983.

Neeway, JJ, N Qafoku, RJ Serne, AJ Lawter, JR Stephenson, WW Lukens and JH Westsik Jr. 2015. "Evaluation of Technetium Getters to Improve the Performance of Cast Stone." *PNNL-23667* Pacific Northwest National Laboratory, Richland, Washington(Rev. 1).

Pierce, EM, SV Mattigod, RJ Serne, JP Icenhower, RD Scheele, W Um, N Qafoku and JH Westsik. 2010a. "Review of Potential Candiate Stabilization Technologies for Liquid and Solid Secondary Waste Streams." *PNNL-19122* Pacific Northwest National Laboratory, Richland, Washington.

Pierce, EM, W Um, K Cantrell, M Valenta, J Westsik Jr, R Serne and K Parker. 2010b. "Secondary Waste Form Screening Test Results–Cast Stone and Alkali Alumino-Silicate Geopolymer." *PNNL-19505* Pacific Northwest National Laboratory, Richland, WA, USA.

Qafoku, N, JJ Neeway, AR Lawter, TG Levitskaia, RJ Serne, J Westsik, J.H. and MM Valenta Snyder. 2014. "Technetium and Iodine Getters to Improve Cast Stone Performance." *PNNL-23282* Pacific Northwest National Laboratory(Rev. 1).

Ravel, B and M Newville. 2005. "ATHENA and ARTEMIS: interactive graphical data analysis using IFEFFIT." *Physica Scripta* 2005(T115): 1007.

Russel, RL, J Westsik Jr, DJ Swanberg, RE Eibling, AD Cozzi, MJ Lindberg, GB Josephson and DE Rinehart. 2013. "Letter Report: LAW Simulant Development for Cast Stone Screening Tests." *PNNL-22352* Rev.0, Pacific Northwest National Laboratory, Richland, WA.

Serne, J, DC Lanigan, J Westsik Jr, BD Williams, HB Jung and G Wang. 2016. "Extended leach testing of simulated LAW cast stone monoliths." *PNNL-24297, RPT-SLAW-001* Pacific Northwest National Laboratory, Richland, WA, USA(Rev.1).

Taylor-Pashow, K and D McCabe. 2015. "Laboratory Optimization Tests of Technetium Decontamination of Hanford Waste Treatment Plant Low Activity Waste Melter Off-Gas Condensate Simulant." *SRNL-STI-2015-00645, Rev.0* Savannah River National Laboratory, Aiken SC.

Taylor-Pashow, K, C Nash, C Crawford, D McCabe and W Wilmarth. 2014. "Laboratory Scoping Tests of Decontamination of Hanford Waste Treatment Plant Low Activity Waste Off-Gas Condensate Simulant." *SRNL-STI-2013-00719, Rev. 0* Savannah River National Laboratory, Aiken , SC.

Telling, N. 2010. "Remediation of Cr (VI) by biogenic magnetic nanoparticles: an X-ray magnetic circular dichroism study." *LBNL-2702E* Lawrence Berkeley National Laboratory, Berkeley, CA.

Um, W, BD Williams, MM Valenta Snyder and G Wang. 2016. "Liquid Secondary Waste Grout Formulation and Waste Form Qualification." *PNNL-25129* Pacific Norhtwest National Laboratory, Richland, WA(Rev.0).

Varkey, AJ and AF Fort. 1993. "Some optical properties of silver peroxide (AgO) and silver oxide (Ag2O) films produced by chemical-bath deposition." *Solar Energy Materials and Solar Cells* 29(3): 253-259.

Warwick, P, S Aldridge, N Evans and S Vines. 2007. "The solubility of technetium (IV) at high pH." *Radiochimica Acta* 95(12): 709-716.

Webb, SM. 2005. "SIXpack: a graphical user interface for XAS analysis using IFEFFIT." *Physica Scripta* 2005(T115): 1011.

Westsik, JH, GF Piepel, MJ Lindberg, PG Heasler, TM Mercier, RL Russel, AD Cozzi, WE Daniel, RE Eibling, EK Hansen, MR Reigal and DJ Swanberg. 2013. "Supplemental Immobilization of Hanford Low-Activity Waste: Cast Stone Screening Tests." *PNNL-22747, SRNL-STI-2013-00465* Rev. 0, Pacific Northwest National Laboratory, Richland, Washington and Savannah River National Laboratory, Aiken, South Carolina.

Xu, K, P Hrma, JA Rice, MJ Schweiger, BJ Riley, NR Overman and AA Kruger. 2016. "Conversion of Nuclear Waste to Molten Glass: Cold-Cap Reactions in Crucible Tests." *Journal of the American Ceramic Society* 99(9): 2964-2970.

Appendix A

Simulant Fabrication Pictures

Initial Water Addition

Soluble Salts

NaOH + $Al(NO_3)_3$

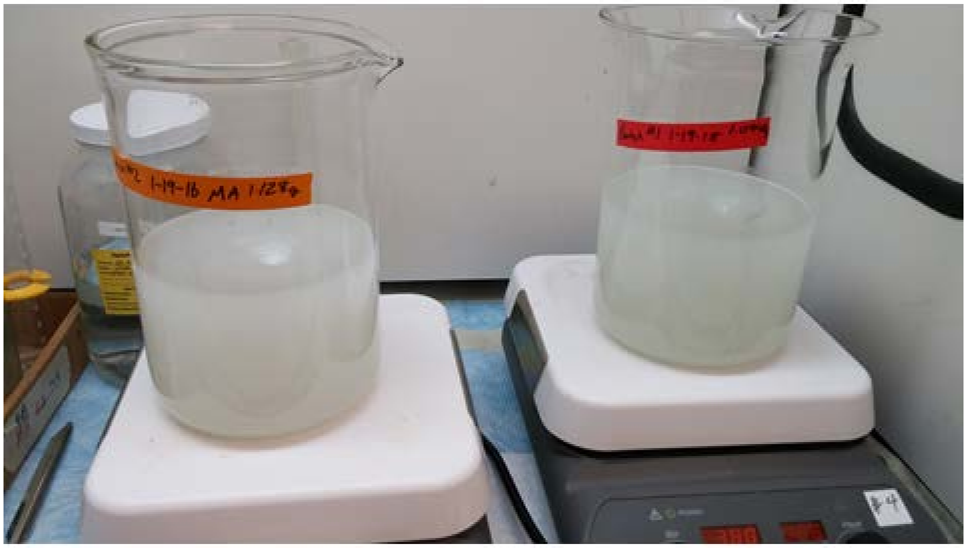

Phosphate

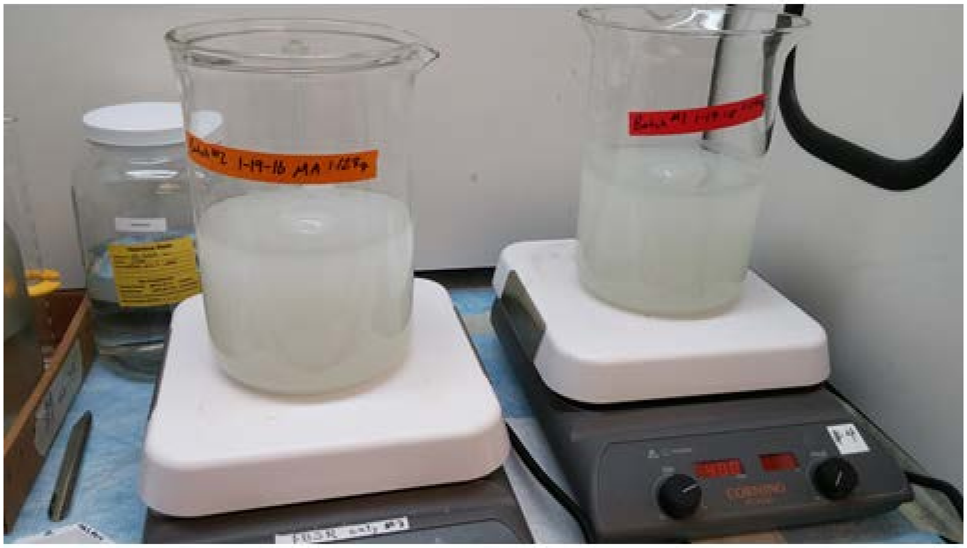

Acetate and Carbonate

Chromate

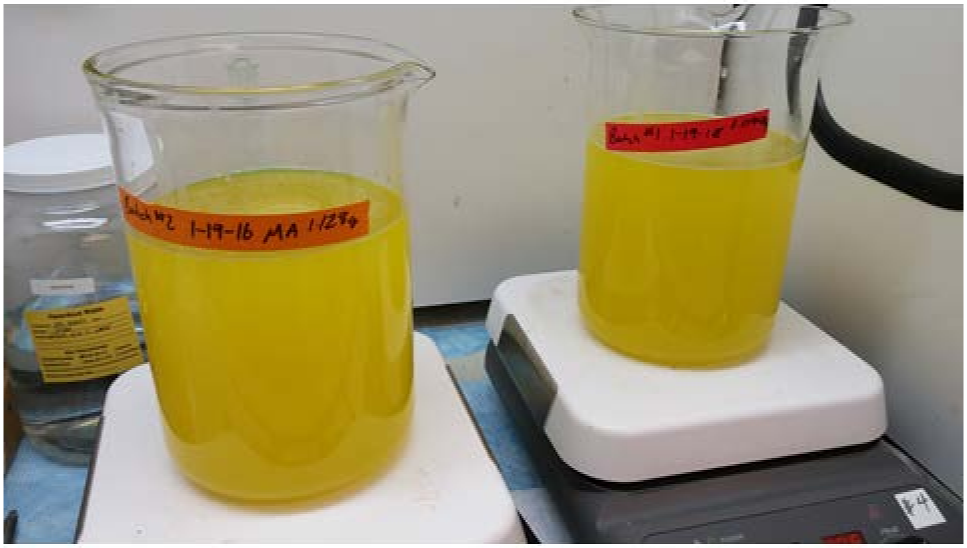

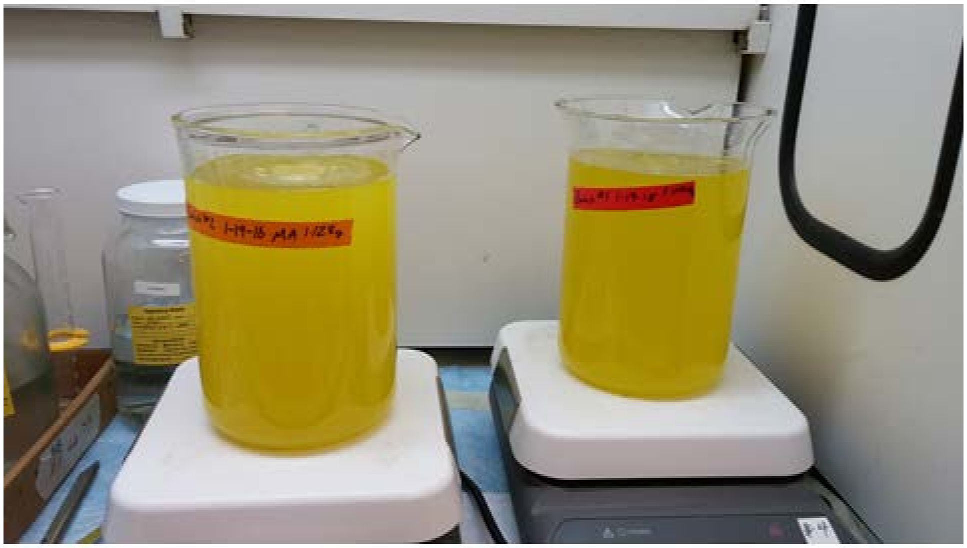

Before Transferring to Volumetric Flask

Figure A-1– Appendix A – Sequence of images showing 6.5 M LAW Simulant Prep.

Appendix B

EPA 1315 pH, EC and Al/Si Releases

Getter monolith pH graphs

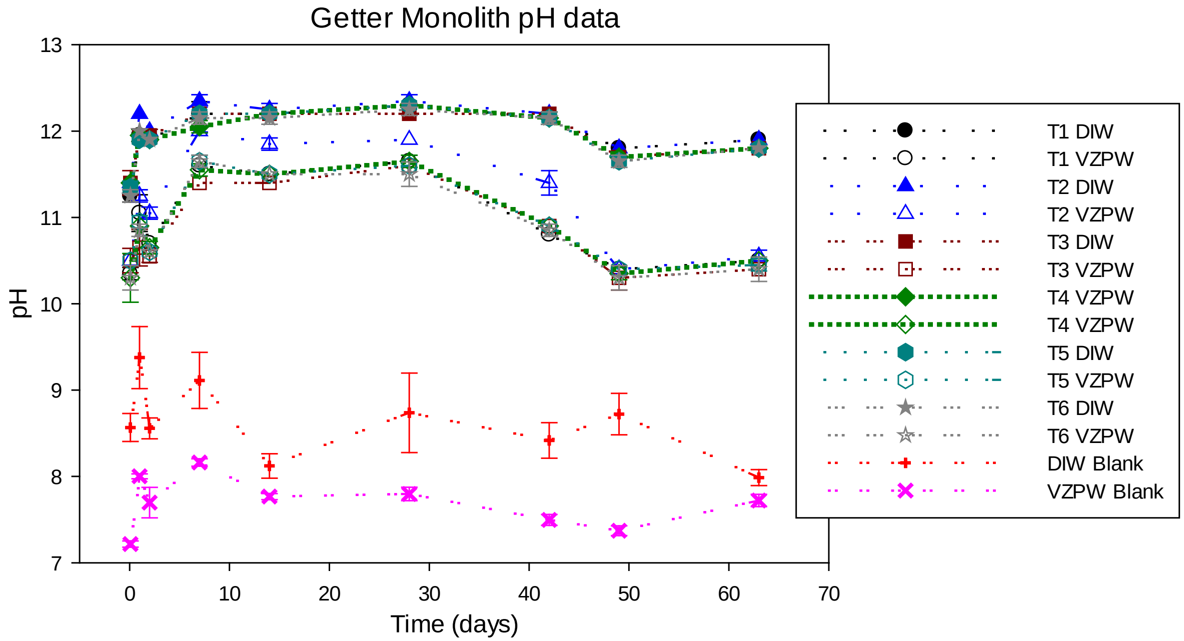

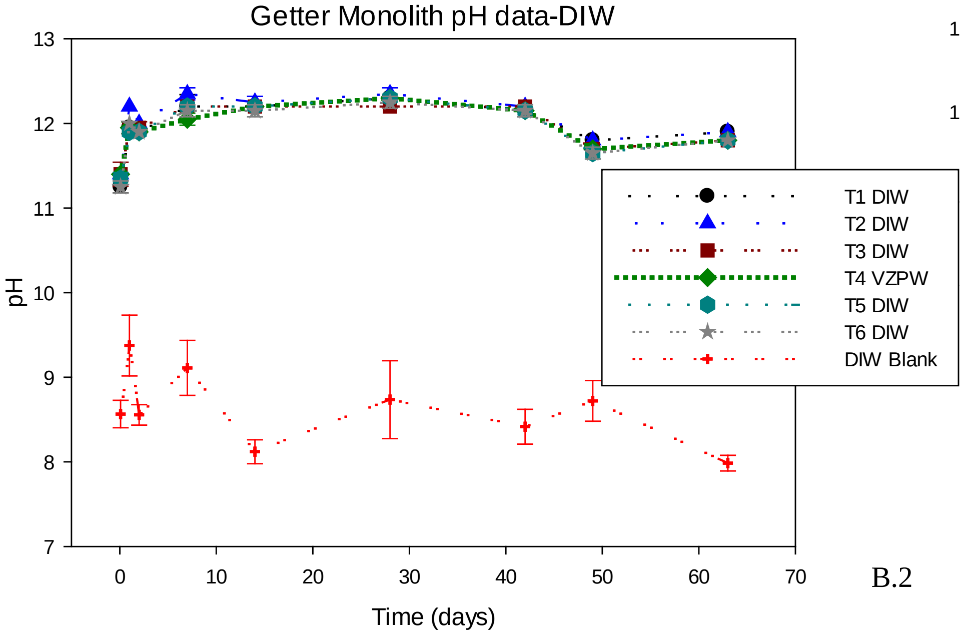

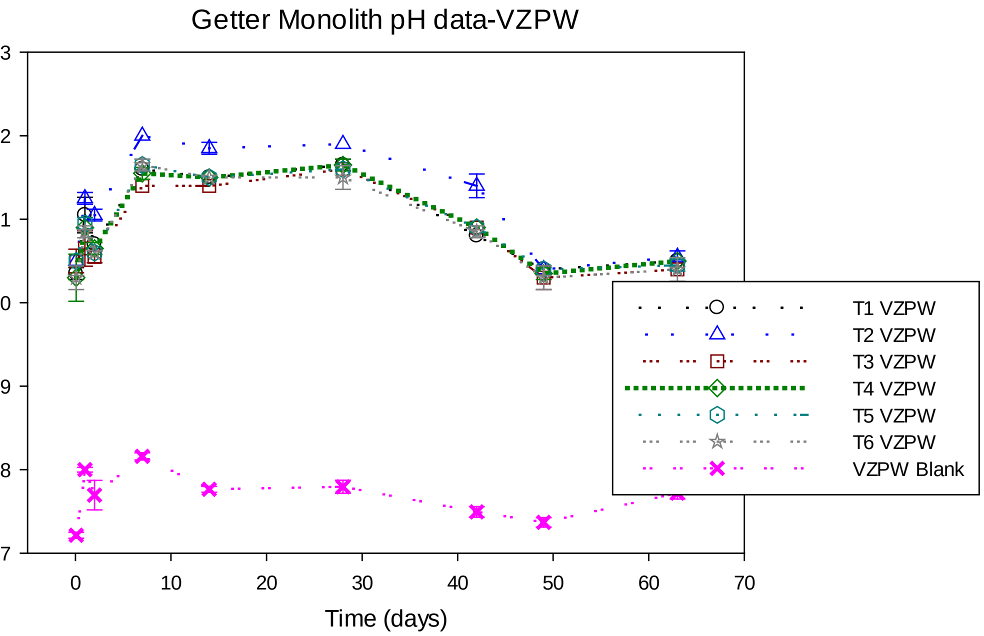

Getter monolith EC graphs

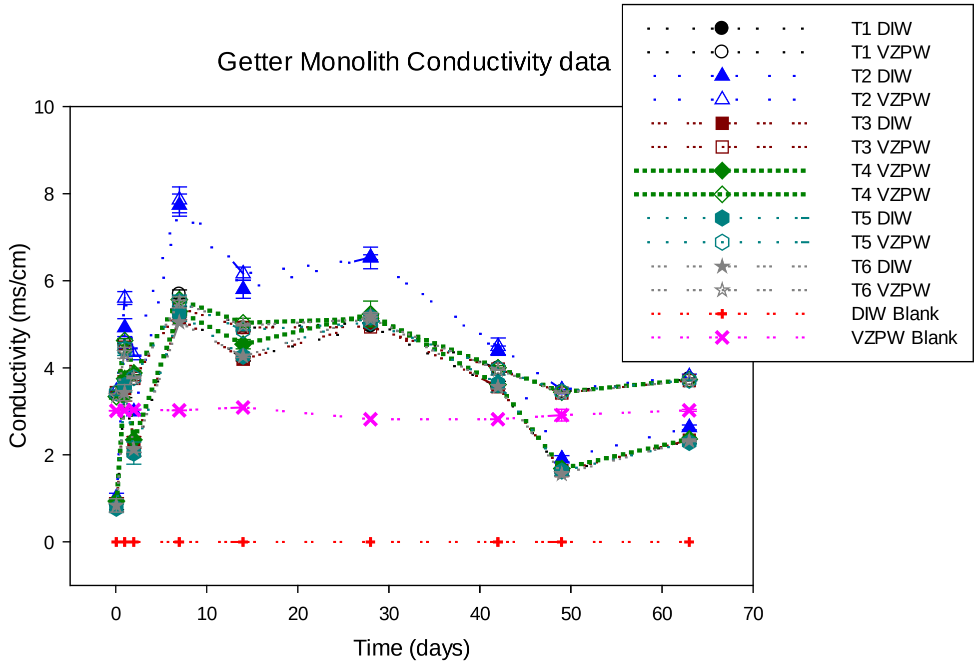

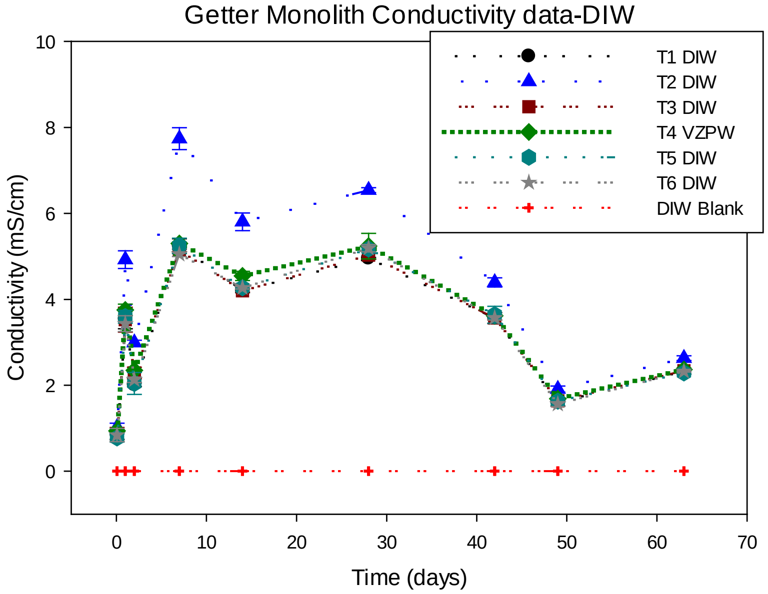

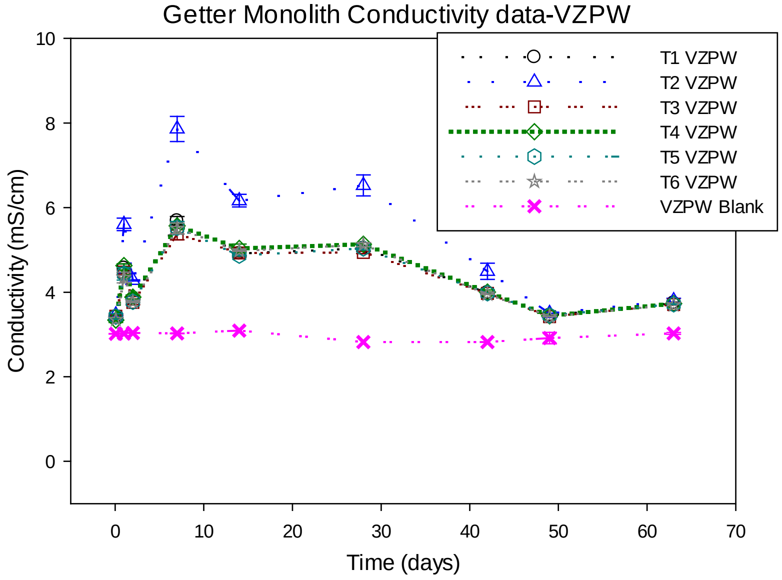

Getter monolith Al Graphs

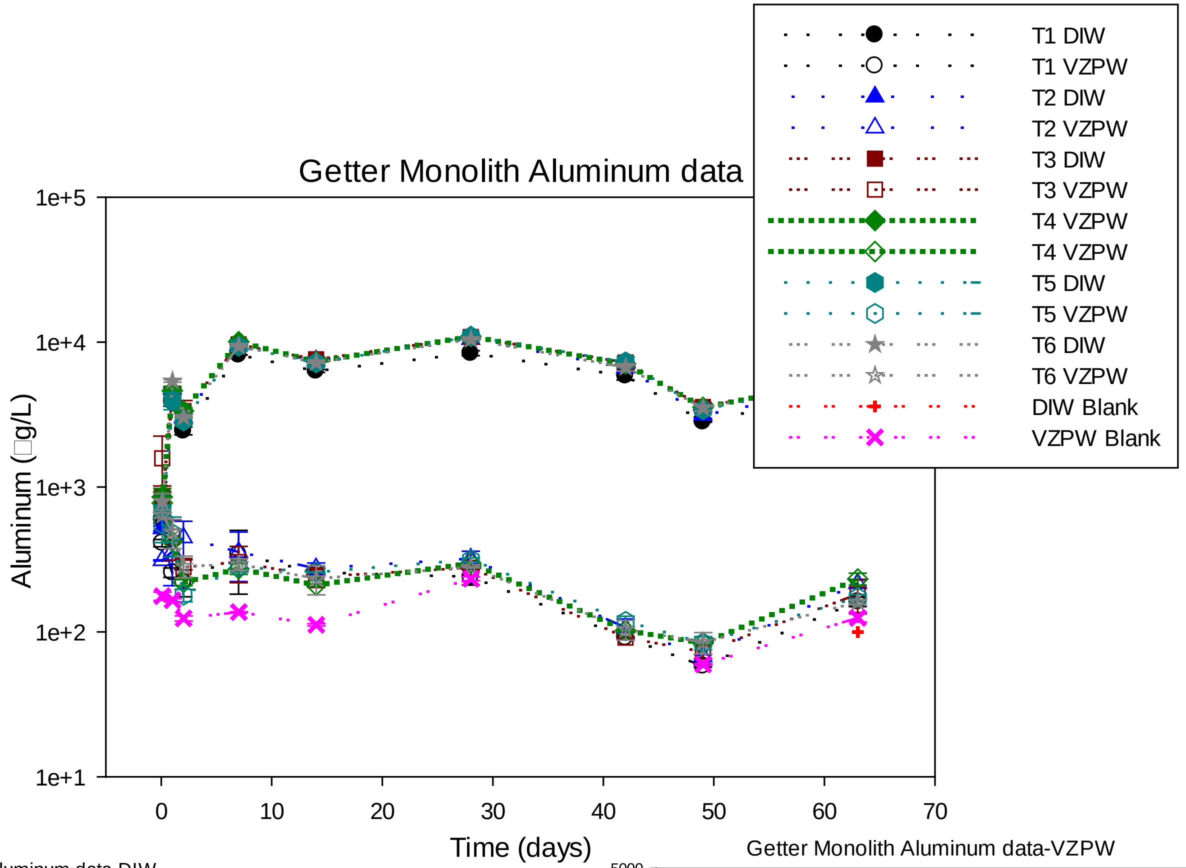

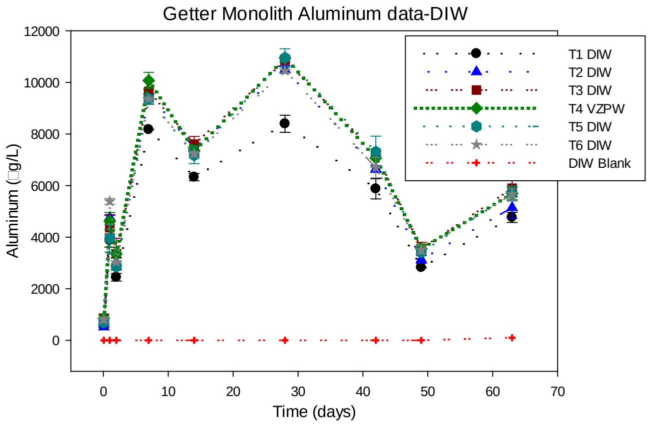

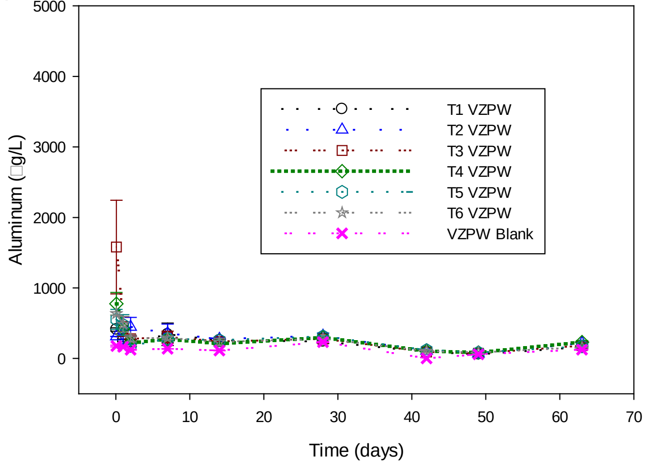

Getter monolith Si graphs

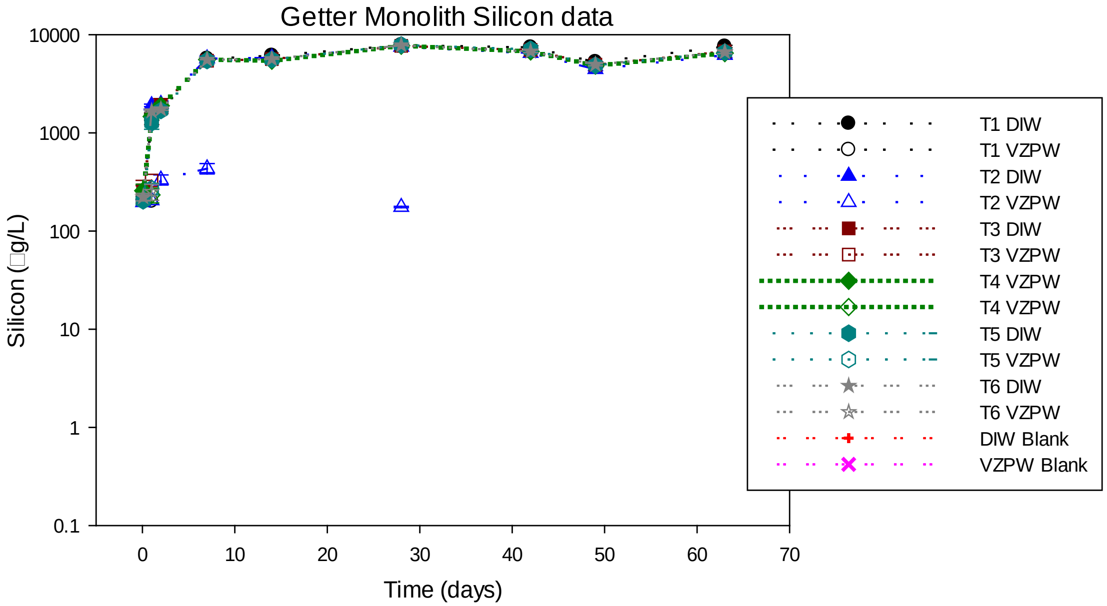

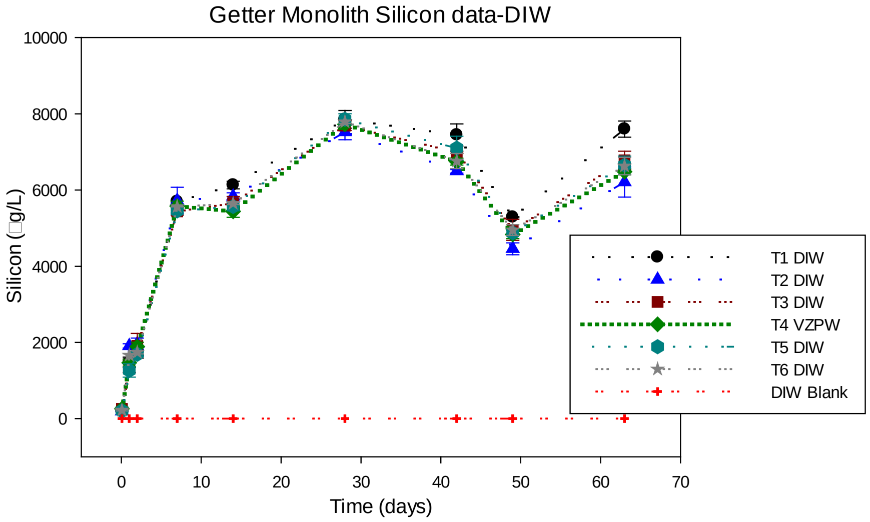

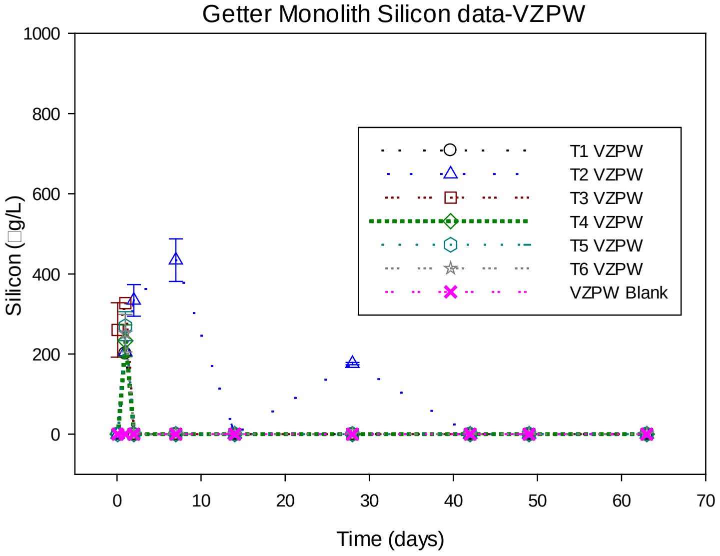

Appendix C- EPA 1315 Data

Monolith Measurements and Data

The “Permissible Leachate Volume (mL)” listed is the volume of solution used in the EPA Method 1315 leach testing and in calculations of D_{obs} for the individual monoliths. Monoliths used in the EPA Method 1315 testing are highlighted in green.

CALC-SLAW-014, Rev. 0

Batch ID	Mass (g)	Diameter 1 (mm)	Diameter 2 (mm)	Diameter 3 (mm)	Average Diameter (mm)	Average Diameter (cm)	Length 1 (mm)	Length 2 (mm)	Length 3 (mm)	Average Length (mm)	Average Length (cm)	Surface Area (cm^2)	Permissible Leachant Volume (mL)	Maximum Permissible Volume (mL)	Minimum Permissible Volume (mL)
S014-16-T1-															
T1-1	359.63	48.85	48.90	48.75	48.83	4.883	101.86	100.67	100.72	101.08	10.108	192.53	1732.8	1925.35	1540.28
T1-2	365.20	49.93	49.54	49.26	49.58	4.958	103.52	103.04	102.73	103.10	10.310	199.18	1792.6	1991.80	1593.44
T1-3	360.76	49.47	49.40	49.31	49.39	4.939	101.05	100.93	101.08	101.02	10.102	195.08	1755.7	1950.79	1560.63
T1-4	360.86	49.83	49.40	49.31	49.51	4.951	101.24	101.13	101.04	101.14	10.114	195.83	1762.5	1958.28	1566.62
T1-5	362.63	49.15	49.17	48.96	49.09	4.909	101.59	101.87	102.60	102.02	10.202	195.21	1756.8	1952.05	1561.64
T1-6	360.90	49.58	49.29	49.20	49.36	4.936	101.43	101.45	101.23	101.37	10.137	195.45	1759.0	1954.49	1563.59
T1-7	361.60	49.05	49.20	49.33	49.19	4.919	101.13	101.04	101.31	101.16	10.116	194.35	1749.2	1943.51	1554.81
T1-8	359.71	49.15	49.23	49.14	49.17	4.917	100.82	100.64	100.78	100.75	10.075	193.62	1742.6	1936.18	1548.94
S014-16-T2-															
T2-1	363.63	49.57	49.27	48.83	49.22	4.922	102.64	101.98	101.46	102.03	10.203	195.83	1762.5	1958.33	1566.66
T2-2	362.16	49.04	49.12	48.86	49.01	4.901	101.78	101.76	101.92	101.82	10.182	194.49	1750.4	1944.86	1555.89
T2-3	364.71	48.90	48.75	48.81	48.82	4.882	102.34	102.43	102.28	102.35	10.235	194.41	1749.7	1944.15	1555.32
T2-4	366.51	48.85	49.19	49.66	49.23	4.923	102.81	102.91	103.04	102.92	10.292	197.26	1775.4	1972.62	1578.10
T2-5	367.59	49.40	49.21	49.21	49.27	4.927	103.02	103.29	103.39	103.23	10.323	197.94	1781.4	1979.38	1583.51
T2-6	367.70	49.44	49.27	49.10	49.27	4.927	103.06	103.11	103.36	103.18	10.318	197.83	1780.5	1978.35	1582.68
T2-7	366.00	49.10	49.28	49.54	49.31	4.931	102.44	102.46	102.22	102.37	10.237	196.77	1770.9	1967.66	1574.13
T2-8	363.14	49.29	49.76	49.58	49.54	4.954	102.36	102.31	102.46	102.38	10.238	197.90	1781.1	1979.00	1583.20
S014-16-T3-															
T3-1	366.62	49.10	49.03	48.83	48.99	4.899	102.85	102.87	102.63	102.78	10.278	195.87	1762.9	1958.74	1566.99
T3-2	368.67	49.11	49.08	49.18	49.12	4.912	103.79	102.79	103.48	103.35	10.335	197.41	1776.6	1974.05	1579.24
T3-3	364.46	49.14	49.45	49.29	49.29	4.929	101.67	101.62	101.55	101.61	10.161	195.53	1759.7	1955.26	1564.20
T3-4	362.76	49.05	49.21	49.40	49.22	4.922	101.37	100.70	101.47	101.18	10.118	194.51	1750.6	1945.08	1556.06
T3-5	364.88	49.95	49.87	49.64	49.82	4.982	102.65	101.95	101.46	102.02	10.202	198.66	1788.0	1986.63	1589.31
T3-6	363.01	50.34	49.91	49.88	50.04	5.004	101.12	100.97	101.66	101.25	10.125	198.52	1786.7	1985.19	1588.15
T3-7	362.43	49.45	49.31	49.28	49.35	4.935	101.60	100.92	101.40	101.31	10.131	195.30	1757.7	1953.03	1562.42
T3-8	360.88	49.49	49.21	49.08	49.26	4.926	101.64	100.73	100.14	100.84	10.084	194.17	1747.5	1941.66	1553.32
S014-16-T4-															
T4-1	364.02	49.48	49.42	49.30	49.40	4.940	101.18	101.47	101.52	101.39	10.139	195.68	1761.2	1956.85	1565.48
T4-2	369.27	49.77	49.51	49.35	49.54	4.954	103.09	103.30	103.28	103.22	10.322	199.22	1793.0	1992.18	1593.74
T4-3	369.43	49.34	49.48	49.48	49.43	4.943	103.29	103.17	103.28	103.25	10.325	198.73	1788.5	1987.26	1589.81
T4-4	366.79	49.68	49.15	49.00	49.28	4.928	101.91	102.18	101.95	102.01	10.201	196.07	1764.6	1960.66	1568.53
T4-5	365.37	49.24	49.43	49.24	49.30	4.930	101.91	101.91	101.70	101.84	10.184	195.92	1763.3	1959.24	1567.39
T4-6	366.01	50.09	49.90	49.39	49.79	4.979	103.04	102.38	102.31	102.58	10.258	199.41	1794.7	1994.07	1595.25
T4-7	363.93	49.80	49.44	49.62	49.62	4.962	101.30	101.14	101.50	101.31	10.131	196.61	1769.5	1966.08	1572.87
T4-8	368.74	49.51	49.37	49.29	49.39	4.939	102.64	102.50	102.74	102.63	10.263	197.56	1778.0	1975.56	1580.45
S014-16-T5-															
T5-1	365.95	49.65	49.55	49.53	49.58	4.958	102.23	102.83	103.18	102.75	10.275	198.64	1787.7	1986.35	1589.08
T5-2	365.93	49.37	49.39	49.45	49.40	4.940	102.15	102.73	103.46	102.78	10.278	197.86	1780.7	1978.58	1582.86
T5-3	364.75	48.84	48.89	48.82	48.85	4.885	102.88	102.27	102.82	102.66	10.266	195.03	1755.3	1950.28	1560.22
T5-4	366.62	49.17	49.20	48.86	49.08	4.908	103.51	102.84	102.94	103.10	10.310	196.79	1771.1	1967.86	1574.29
T5-5	367.50	49.70	49.57	49.49	49.59	4.959	104.00	102.75	103.35	103.37	10.337	199.65	1796.8	1996.49	1597.19
T5-6	365.56	49.53	49.23	49.03	49.26	4.926	102.09	103.02	103.00	102.70	10.270	197.07	1773.6	1970.70	1576.56
T5-7	365.76	49.46	49.40	49.21	49.36	4.936	102.82	102.40	103.75	102.99	10.299	197.96	1781.6	1979.60	1583.68
T5-8	362.23	49.11	49.00	48.82	48.98	4.898	101.71	101.97	102.10	101.93	10.193	194.51	1750.6	1945.08	1556.06
S014-16-T6-															
T6-1	365.08	48.98	49.19	49.58	49.25	4.925	102.51	102.66	102.17	102.45	10.245	196.61	1769.5	1966.09	1572.88
T6-2	363.78	49.51	49.34	49.17	49.34	4.934	102.56	101.81	102.31	102.23	10.223	196.70	1770.3	1966.98	1573.58
T6-3	364.78	49.44	49.45	49.27	49.39	4.939	102.71	102.38	102.30	102.46	10.246	197.29	1775.6	1972.87	1578.30
T6-4	364.73	49.48	49.29	48.95	49.24	4.924	102.34	102.51	103.29	102.71	10.271	196.97	1772.8	1969.74	1575.79
T6-5	362.95	49.32	49.26	49.24	49.27	4.927	101.76	102.63	102.31	102.23	10.223	196.39	1767.5	1963.90	1571.12
T6-6	360.98	48.67	49.02	49.02	48.90	4.890	101.12	101.46	102.24	101.61	10.161	193.67	1743.0	1936.69	1549.35
T6-7	363.47	49.09	49.53	49.58	49.40	4.940	101.89	101.84	102.47	102.07	10.207	196.73	1770.6	1967.35	1573.88
T6-8	364.61	49.14	49.38	49.43	49.32	4.932	102.57	102.77	103.01	102.78	10.278	197.45	1777.0	1974.49	1579.59

* Leachant volumes can be found on pg C.2 for each monolith.*

EPA Method 1315 Sampling Times

Interval Time	Start Time	End Time
2 h	3/1/16 8:30	3/1/16 10:30
1 d	3/1/16 10:30	3/2/16 8:30
2 d	3/2/16 8:30	3/3/16 8:40
7 d	3/3/16 8:40	3/8/16 8:40
14 d	3/8/16/ 8:40	3/15/16 8:50
28 d	3/15/16 8:50	3/29/16 8:00
42 d	3/29/16 8:00	4/12/16 8:30
49 d	4/12/16 8:30	4/19/16 8:40
63 d	4/19/16 8:40	5/3/16 9:00

Tc 2 h Sampling

		Experiment Start	3/1/16 8:30:00												

T1

Name	Tc (µg/L)	Interval Begin	Sampling Date	Monlith mass (g)	Monlith Dry Mass (g)	Surface Area (cm^2)	Solution Volume (mL)	Monolith Volume (m^3)	M_{ti} (mg/m^2)	ρ (kg/m^3)	Co (mg$_{Tc}$/kg$_{mono}$)	D_e (m^2/s)	D_e (cm^2/s)	Average D_e (cm^2/s)	Standard Deviation of Average De
S014-16-T1-1	0.0828	3/1/2016 8:30:	3/1/2016 10:30:0	359.63	277.23	192.53	1732.8	1.89E-04	7.45E-03	1.46E+03	8.37	4.0E-17	4.0E-13	3.7E-13	3.3E-14
S014-16-T1-2	0.0731	3/1/2016 8:30:	3/1/2016 10:30:0	365.20	281.52	199.18	1792.6	1.99E-04	6.58E-03	1.41E+03	8.37	3.4E-17	3.4E-13		
S014-16-T1-4	0.0426	3/1/2016 8:30:	3/1/2016 10:30:0	360.86	278.18	195.83	1762.5	1.95E-04	3.83E-03	1.43E+03	8.37	1.1E-17	1.1E-13	1.5E-13	3.3E-14
S014-16-T1-7	0.0544	3/1/2016 8:30:	3/1/2016 10:30:0	361.60	278.75	194.35	1749.2	1.92E-04	4.90E-03	1.45E+03	8.37	1.8E-17	1.8E-13		

T2

Name	Tc (µg/L)	Interval Begin	Sampling Date	Monlith mass (g)	Monlith Dry Mass (g)	Surface Area (cm^2)	Solution Volume (mL)	Monolith Volume (m^3)	M_{ti} (mg/m^2)	ρ (kg/m^3)	Co (mg$_{Tc}$/kg$_{mono}$)	D_e (m^2/s)	D_e (cm^2/s)	Average D_e (cm^2/s)	Standard Deviation of Average De
S014-16-T2-3	0.197	3/1/2016 8:30:	3/1/2016 10:30:0	364.71	283.41	195.83	1749.7	1.92E-04	1.76E-02	1.48E+03	8.23	2.3E-16	2.3E-12	2.3E-12	1.2E-14
S014-16-T2-6	0.191	3/1/2016 8:30:	3/1/2016 10:30:0	367.70	285.74	197.83	1780.5	1.97E-04	1.72E-02	1.45E+03	8.23	2.3E-16	2.3E-12		
S014-16-T2-7	0.155	3/1/2016 8:30:	3/1/2016 10:30:0	366.00	284.41	196.77	1770.9	1.95E-04	1.40E-02	1.46E+03	8.23	1.5E-16	1.5E-12	1.3E-12	1.7E-13
S014-16-T2-8	0.134	3/1/2016 8:30:	3/1/2016 10:30:0	363.14	282.19	197.90	1781.1	1.97E-04	1.21E-02	1.43E+03	8.23	1.1E-16	1.1E-12		

T3

Name	Tc (µg/L)	Interval Begin	Sampling Date	Monlith mass (g)	Monlith Dry Mass (g)	Surface Area (cm^2)	Solution Volume (mL)	Monolith Volume (m^3)	M_{ti} (mg/m^2)	ρ (kg/m^3)	Co (mg$_{Tc}$/kg$_{mono}$)	D_e (m^2/s)	D_e (cm^2/s)	Average D_e (cm^2/s)	Standard Deviation of Average De
S014-16-T3-1	0.117	3/1/2016 8:30:	3/1/2016 10:30:0	366.62	285.46	195.87	1762.9	1.94E-04	1.05E-02	1.47E+03	7.45	1.0E-16	1.0E-12	1.2E-12	2.2E-13
S014-16-T3-3	0.139	3/1/2016 8:30:	3/1/2016 10:30:0	364.46	283.78	195.53	1759.7	1.94E-04	1.25E-02	1.46E+03	7.45	1.4E-16	1.4E-12		
S014-16-T3-4	0.219	3/1/2016 8:30:	3/1/2016 10:30:0	362.76	282.46	194.51	1750.6	1.93E-04	1.97E-02	1.47E+03	7.45	3.6E-16	3.6E-12	3.2E-12	3.4E-13
S014-16-T3-8	0.196	3/1/2016 8:30:	3/1/2016 10:30:0	360.88	280.99	194.17	1747.5	1.92E-04	1.76E-02	1.46E+03	7.45	2.9E-16	2.9E-12		

T4

Name	Tc (µg/L)	Interval Begin	Sampling Date	Monlith mass (g)	Monlith Dry Mass (g)	Surface Area (cm^2)	Solution Volume (mL)	Monolith Volume (m^3)	M_{ti} (mg/m^2)	ρ (kg/m^3)	Co (mg$_{Tc}$/kg$_{mono}$)	D_e (m^2/s)	D_e (cm^2/s)	Average D_e (cm^2/s)	Standard Deviation of Average De
S014-16-T4-1	0.201	3/1/2016 8:30:	3/1/2016 10:30:0	364.02	284.12	195.68	1761.2	1.94E-04	1.81E-02	1.46E+03	8.79	2.2E-16	2.2E-12	1.9E-12	2.9E-13
S014-16-T4-2	0.17	3/1/2016 8:30:	3/1/2016 10:30:0	369.27	288.22	199.22	1793.0	1.99E-04	1.53E-02	1.45E+03	8.79	1.6E-16	1.6E-12		
S014-16-T4-5	0.174	3/1/2016 8:30:	3/1/2016 10:30:0	365.37	285.18	195.92	1763.3	1.94E-04	1.57E-02	1.47E+03	8.79	1.6E-16	1.6E-12	2.7E-12	1.0E-12
S014-16-T4-7	0.261	3/1/2016 8:30:	3/1/2016 10:30:0	363.93	284.05	196.69	1770.2	1.96E-04	2.35E-02	1.45E+03	8.79	3.7E-16	3.7E-12		

T5

Name	Tc (µg/L)	Interval Begin	Sampling Date	Monlith mass (g)	Monlith Dry Mass (g)	Surface Area (cm^2)	Solution Volume (mL)	Monolith Volume (m^3)	M_{ti} (mg/m^2)	ρ (kg/m^3)	Co (mg$_{Tc}$/kg$_{mono}$)	D_e (m^2/s)	D_e (cm^2/s)	Average D_e (cm^2/s)	Standard Deviation of Average De
S014-16-T5-2	0.126	3/1/2016 8:30:	3/1/2016 10:30:0	365.93	283.58	197.86	1780.7	1.97E-04	1.13E-02	1.44E+03	7.67	1.2E-16	1.2E-12	1.1E-12	1.4E-14
S014-16-T5-3	0.127	3/1/2016 8:30:	3/1/2016 10:30:0	364.75	282.66	195.03	1755.3	1.92E-04	1.14E-02	1.47E+03	7.67	1.1E-16	1.1E-12		
S014-16-T5-4	0.192	3/1/2016 8:30:	3/1/2016 10:30:0	366.62	284.11	196.79	1771.1	1.95E-04	1.73E-02	1.46E+03	7.67	2.6E-16	2.6E-12	2.3E-12	2.8E-13
S014-16-T5-7	0.168	3/1/2016 8:30:	3/1/2016 10:30:0	365.76	283.44	197.96	1781.6	1.97E-04	1.51E-02	1.44E+03	7.67	2.0E-16	2.0E-12		

T6

Name	Tc (µg/L)	Interval Begin	Sampling Date	Monlith mass (g)	Monlith Dry Mass (g)	Surface Area (cm^2)	Solution Volume (mL)	Monolith Volume (m^3)	M_{ti} (mg/m^2)	ρ (kg/m^3)	Co (mg$_{Tc}$/kg$_{mono}$)	D_e (m^2/s)	D_e (cm^2/s)	Average D_e (cm^2/s)	Standard Deviation of Average De
S014-16-T6-2	0.13	3/1/2016 8:30:	3/1/2016 10:30:0	363.78	284.09	196.70	1770.3	1.95E-04	1.17E-02	1.45E+03	7.95	1.1E-16	1.1E-12	1.4E-12	2.6E-13
S014-16-T6-3	0.157	3/1/2016 8:30:	3/1/2016 10:30:0	364.78	284.87	197.29	1775.6	1.96E-04	1.41E-02	1.45E+03	7.95	1.6E-16	1.6E-12		
S014-16-T6-5	0.124	3/1/2016 8:30:	3/1/2016 10:30:0	362.95	283.44	196.39	1767.5	1.95E-04	1.12E-02	1.45E+03	7.95	1.0E-16	1.0E-12	8.0E-13	2.1E-13
S014-16-T6-6	0.0962	3/1/2016 8:30:	3/1/2016 10:30:0	360.98	281.90	193.67	1743.0	1.91E-04	8.66E-03	1.48E+03	7.95	5.9E-17	5.9E-13		

Tc 1 d Sampling Data

Experiment Start 3/1/16 8:30:00

T1

Name	Tc (μg/L)	Interval Begin	Sampling Date	Monlith mass (g)	Monlith Dry Mass (g)	Surface Area (cm^2)	Solution Volume (mL)	Monolith Volume (m^3)	M_{ti} (mg/m^2)	ρ (kg/m^3)	Co (mg$_{Tc}$/kg$_{mono}$)	D_e (m^2/s)	D_e (cm^2/s)	Average D_e (cm^2/s)	Standard Deviation of Average De
S014-16-T1-1	0.602	3/1/2016 10:30:00	3/2/2016 8:30:00	359.63	277.23	192.53	1732.8	1.89E-04	5.42E-02	1.46E+03	8.37	3.5E-16	3.5E-12	3.0E-12	5.2E-13
S014-16-T1-2	0.488	3/1/2016 10:30:00	3/2/2016 8:30:00	365.20	281.52	199.18	1792.6	1.99E-04	4.39E-02	1.41E+03	8.37	2.5E-16	2.5E-12		
S014-16-T1-4	0.155	3/1/2016 10:30:00	3/2/2016 8:30:00	360.86	278.18	195.83	1762.5	1.95E-04	1.40E-02	1.43E+03	8.37	2.4E-17	2.4E-13	5.3E-13	2.9E-13
S014-16-T1-7	0.288	3/1/2016 10:30:00	3/2/2016 8:30:00	361.60	278.75	194.35	1749.2	1.92E-04	2.59E-02	1.45E+03	8.37	8.2E-17	8.2E-13		

T2

Name	Tc (μg/L)	Interval Begin	Sampling Date	Monlith mass (g)	Monlith Dry Mass (g)	Surface Area (cm^2)	Solution Volume (mL)	Monolith Volume (m^3)	M_{ti} (mg/m^2)	ρ (kg/m^3)	Co (mg$_{Tc}$/kg$_{mono}$)	D_e (m^2/s)	D_e (cm^2/s)	Average D_e (cm^2/s)	Standard Deviation of Average De
S014-16-T2-3	1.3	3/1/2016 10:30:00	3/2/2016 8:30:00	364.71	283.41	195.83	1749.7	1.92E-04	1.16E-01	1.48E+03	8.23	1.6E-15	1.6E-11	2.0E-11	3.3E-12
S014-16-T2-6	1.5	3/1/2016 10:30:00	3/2/2016 8:30:00	367.70	285.74	197.83	1780.5	1.97E-04	1.35E-01	1.45E+03	8.23	2.3E-15	2.3E-11		
S014-16-T2-7	0.559	3/1/2016 10:30:00	3/2/2016 8:30:00	366.00	284.41	196.77	1770.9	1.95E-04	5.03E-02	1.46E+03	8.23	3.2E-16	3.2E-12	3.2E-12	6.2E-14
S014-16-T2-8	0.56	3/1/2016 10:30:00	3/2/2016 8:30:00	363.14	282.19	197.90	1781.1	1.97E-04	5.04E-02	1.43E+03	8.23	3.3E-16	3.3E-12		

T3

Name	Tc (μg/L)	Interval Begin	Sampling Date	Monlith mass (g)	Monlith Dry Mass (g)	Surface Area (cm^2)	Solution Volume (mL)	Monolith Volume (m^3)	M_{ti} (mg/m^2)	ρ (kg/m^3)	Co (mg$_{Tc}$/kg$_{mono}$)	D_e (m^2/s)	D_e (cm^2/s)	Average D_e (cm^2/s)	Standard Deviation of Average De
S014-16-T3-1	0.63	3/1/2016 10:30:00	3/2/2016 8:30:00	366.62	285.46	195.87	1762.9	1.94E-04	5.67E-02	1.47E+03	7.45	4.8E-16	4.8E-12	4.8E-12	4.3E-14
S014-16-T3-3	0.62	3/1/2016 10:30:00	3/2/2016 8:30:00	364.46	283.78	195.53	1759.7	1.94E-04	5.58E-02	1.46E+03	7.45	4.7E-16	4.7E-12		
S014-16-T3-4	0.27	3/1/2016 10:30:00	3/2/2016 8:30:00	362.76	282.46	194.51	1750.6	1.93E-04	2.43E-02	1.47E+03	7.45	8.9E-17	8.9E-13	1.6E-12	7.3E-13
S014-16-T3-8	0.437	3/1/2016 10:30:00	3/2/2016 8:30:00	360.88	280.99	194.17	1747.5	1.92E-04	3.93E-02	1.46E+03	7.45	2.3E-16	2.3E-12		

T4

Name	Tc (μg/L)	Interval Begin	Sampling Date	Monlith mass (g)	Monlith Dry Mass (g)	Surface Area (cm^2)	Solution Volume (mL)	Monolith Volume (m^3)	M_{ti} (mg/m^2)	ρ (kg/m^3)	Co (mg$_{Tc}$/kg$_{mono}$)	D_e (m^2/s)	D_e (cm^2/s)	Average D_e (cm^2/s)	Standard Deviation of Average De
S014-16-T4-1	0.926	3/1/2016 10:30:00	3/2/2016 8:30:00	364.02	284.12	195.68	1761.2	1.94E-04	8.33E-02	1.46E+03	8.79	7.6E-16	7.6E-12	8.0E-12	4.4E-13
S014-16-T4-2	0.969	3/1/2016 10:30:00	3/2/2016 8:30:00	369.27	288.22	199.22	1793.0	1.99E-04	8.72E-02	1.45E+03	8.79	8.4E-16	8.4E-12		
S014-16-T4-5	0.571	3/1/2016 10:30:00	3/2/2016 8:30:00	365.37	285.18	195.92	1763.3	1.94E-04	5.14E-02	1.47E+03	8.79	2.9E-16	2.9E-12	2.6E-12	2.1E-13
S014-16-T4-7	0.521	3/1/2016 10:30:00	3/2/2016 8:30:00	363.93	284.05	196.69	1770.2	1.96E-04	4.69E-02	1.45E+03	8.79	2.4E-16	2.4E-12		

T5

Name	Tc (μg/L)	Interval Begin	Sampling Date	Monlith mass (g)	Monlith Dry Mass (g)	Surface Area (cm^2)	Solution Volume (mL)	Monolith Volume (m^3)	M_{ti} (mg/m^2)	ρ (kg/m^3)	Co (mg$_{Tc}$/kg$_{mono}$)	D_e (m^2/s)	D_e (cm^2/s)	Average D_e (cm^2/s)	Standard Deviation of Average De
S014-16-T5-2	0.885	3/1/2016 10:30:00	3/2/2016 8:30:00	365.93	283.58	197.86	1780.7	1.97E-04	7.97E-02	1.44E+03	7.67	9.4E-16	9.4E-12	1.1E-11	2.0E-12
S014-16-T5-3	1.08	3/1/2016 10:30:00	3/2/2016 8:30:00	364.75	282.66	195.03	1755.3	1.92E-04	9.72E-02	1.47E+03	7.67	1.3E-15	1.3E-11		
S014-16-T5-4	0.818	3/1/2016 10:30:00	3/2/2016 8:30:00	366.62	284.11	196.79	1771.1	1.95E-04	7.36E-02	1.46E+03	7.67	7.8E-16	7.8E-12	6.9E-12	8.7E-13
S014-16-T5-7	0.712	3/1/2016 10:30:00	3/2/2016 8:30:00	365.76	283.44	197.96	1781.6	1.97E-04	6.41E-02	1.44E+03	7.67	6.1E-16	6.1E-12		

T6

Name	Tc (μg/L)	Interval Begin	Sampling Date	Monlith mass (g)	Monlith Dry Mass (g)	Surface Area (cm^2)	Solution Volume (mL)	Monolith Volume (m^3)	M_{ti} (mg/m^2)	ρ (kg/m^3)	Co (mg$_{Tc}$/kg$_{mono}$)	D_e (m^2/s)	D_e (cm^2/s)	Average D_e (cm^2/s)	Standard Deviation of Average De
S014-16-T6-2	1.7	3/1/2016 10:30:00	3/2/2016 8:30:00	363.78	284.09	196.70	1770.3	1.95E-04	1.53E-01	1.45E+03	7.95	3.1E-15	3.1E-11	2.8E-11	3.6E-12
S014-16-T6-3	1.49	3/1/2016 10:30:00	3/2/2016 8:30:00	364.78	284.87	197.29	1775.6	1.96E-04	1.34E-01	1.45E+03	7.95	2.4E-15	2.4E-11		
S014-16-T6-5	0.716	3/1/2016 10:30:00	3/2/2016 8:30:00	362.95	283.44	196.39	1767.5	1.95E-04	6.44E-02	1.45E+03	7.95	5.6E-16	5.6E-12	5.0E-12	6.3E-13
S014-16-T6-6	0.64	3/1/2016 10:30:00	3/2/2016 8:30:00	360.98	281.90	193.67	1743.0	1.91E-04	5.76E-02	1.48E+03	7.95	4.3E-16	4.3E-12		

Tc 2 d Sampling

Experiment Start 3/1/16 8:30:00

T1

Name	Tc (µg/L)	Interval Begin	Sampling Date	Monlith mass (g)	Monlith Dry Mass (g)	Surface Area (cm^2)	Solution Volume (mL)	Monolith Volume (m^3)	M_{ti} (mg/m^2)	ρ (kg/m^3)	Co (mg$_{Tc}$/kg$_{mono}$)	D_e (m^2/s)	D_e (cm^2/s)	Average D_e (cm^2/s)	Standard Deviation of Average De
S014-16-T1-1	0.387	3/2/2016 8:30:0	3/3/2016 8:40:00	359.63	277.23	192.53	1732.8	1.89E-04	3.48E-02	1.46E+03	8.37	4.2E-16	4.2E-12	4.3E-12	3.6E-14
S014-16-T1-2	0.377	3/2/2016 8:30:0	3/3/2016 8:40:00	365.20	281.52	199.18	1792.6	1.99E-04	3.39E-02	1.41E+03	8.37	4.3E-16	4.3E-12		
S014-16-T1-4	0.101	3/2/2016 8:30:0	3/3/2016 8:40:00	360.86	278.18	195.83	1762.5	1.95E-04	9.09E-03	1.43E+03	8.37	3.0E-17	3.0E-13	3.2E-13	2.0E-14
S014-16-T1-7	0.109	3/2/2016 8:30:0	3/3/2016 8:40:00	361.60	278.75	194.35	1749.2	1.92E-04	9.81E-03	1.45E+03	8.37	3.4E-17	3.4E-13		

T2

Name	Tc (µg/L)	Interval Begin	Sampling Date	Monlith mass (g)	Monlith Dry Mass (g)	Surface Area (cm^2)	Solution Volume (mL)	Monolith Volume (m^3)	M_{ti} (mg/m^2)	ρ (kg/m^3)	Co (mg$_{Tc}$/kg$_{mono}$)	D_e (m^2/s)	D_e (cm^2/s)	Average D_e (cm^2/s)	Standard Deviation of Average De
S014-16-T2-3	0.531	3/2/2016 8:30:0	3/3/2016 8:40:00	364.71	283.41	195.83	1749.7	1.92E-04	4.74E-02	1.48E+03	8.23	8.0E-16	8.0E-12	1.0E-11	2.0E-12
S014-16-T2-6	0.635	3/2/2016 8:30:0	3/3/2016 8:40:00	367.70	285.74	197.83	1780.5	1.97E-04	5.72E-02	1.45E+03	8.23	1.2E-15	1.2E-11		
S014-16-T2-7	0.359	3/2/2016 8:30:0	3/3/2016 8:40:00	366.00	284.41	196.77	1770.9	1.95E-04	3.23E-02	1.46E+03	8.23	3.8E-16	3.8E-12	3.7E-12	1.4E-13
S014-16-T2-8	0.34	3/2/2016 8:30:0	3/3/2016 8:40:00	363.14	282.19	197.90	1781.1	1.97E-04	3.06E-02	1.43E+03	8.23	3.5E-16	3.5E-12		

T3

Name	Tc (µg/L)	Interval Begin	Sampling Date	Monlith mass (g)	Monlith Dry Mass (g)	Surface Area (cm^2)	Solution Volume (mL)	Monolith Volume (m^3)	M_{ti} (mg/m^2)	ρ (kg/m^3)	Co (mg$_{Tc}$/kg$_{mono}$)	D_e (m^2/s)	D_e (cm^2/s)	Average D_e (cm^2/s)	Standard Deviation of Average De
S014-16-T3-1	0.392	3/2/2016 8:30:0	3/3/2016 8:40:00	366.62	285.46	195.87	1762.9	1.94E-04	3.53E-02	1.47E+03	7.45	5.4E-16	5.4E-12	6.8E-12	1.4E-12
S014-16-T3-3	0.48	3/2/2016 8:30:0	3/3/2016 8:40:00	364.46	283.78	195.53	1759.7	1.94E-04	4.32E-02	1.46E+03	7.45	8.2E-16	8.2E-12		
S014-16-T3-4	0.167	3/2/2016 8:30:0	3/3/2016 8:40:00	362.76	282.46	194.51	1750.6	1.93E-04	1.50E-02	1.47E+03	7.45	9.9E-17	9.9E-13	9.2E-13	7.1E-14
S014-16-T3-8	0.154	3/2/2016 8:30:0	3/3/2016 8:40:00	360.88	280.99	194.17	1747.5	1.92E-04	1.39E-02	1.46E+03	7.45	8.5E-17	8.5E-13		

T4

Name	Tc (µg/L)	Interval Begin	Sampling Date	Monlith mass (g)	Monlith Dry Mass (g)	Surface Area (cm^2)	Solution Volume (mL)	Monolith Volume (m^3)	M_{ti} (mg/m^2)	ρ (kg/m^3)	Co (mg$_{Tc}$/kg$_{mono}$)	D_e (m^2/s)	D_e (cm^2/s)	Average D_e (cm^2/s)	Standard Deviation of Average De
S014-16-T4-1	0.665	3/2/2016 8:30:0	3/3/2016 8:40:00	364.02	284.12	195.68	1761.2	1.94E-04	5.99E-02	1.46E+03	8.79	1.1E-15	1.1E-11	1.0E-11	9.8E-13
S014-16-T4-2	0.599	3/2/2016 8:30:0	3/3/2016 8:40:00	369.27	288.22	199.22	1793.0	1.99E-04	5.39E-02	1.45E+03	8.79	9.4E-16	9.4E-12		
S014-16-T4-5	0.243	3/2/2016 8:30:0	3/3/2016 8:40:00	365.37	285.18	195.92	1763.3	1.94E-04	2.19E-02	1.47E+03	8.79	1.5E-16	1.5E-12	1.2E-12	2.9E-13
S014-16-T4-7	0.189	3/2/2016 8:30:0	3/3/2016 8:40:00	363.93	284.05	196.69	1770.2	1.96E-04	1.70E-02	1.45E+03	8.79	9.3E-17	9.3E-13		

T5

Name	Tc (µg/L)	Interval Begin	Sampling Date	Monlith mass (g)	Monlith Dry Mass (g)	Surface Area (cm^2)	Solution Volume (mL)	Monolith Volume (m^3)	M_{ti} (mg/m^2)	ρ (kg/m^3)	Co (mg$_{Tc}$/kg$_{mono}$)	D_e (m^2/s)	D_e (cm^2/s)	Average D_e (cm^2/s)	Standard Deviation of Average De
S014-16-T5-2	0.759	3/2/2016 8:30:0	3/3/2016 8:40:00	365.93	283.58	197.86	1780.7	1.97E-04	6.83E-02	1.44E+03	7.67	2.0E-15	2.0E-11	2.3E-11	3.4E-12
S014-16-T5-3	0.898	3/2/2016 8:30:0	3/3/2016 8:40:00	364.75	282.66	195.03	1755.3	1.92E-04	8.08E-02	1.47E+03	7.67	2.7E-15	2.7E-11		
S014-16-T5-4	0.264	3/2/2016 8:30:0	3/3/2016 8:40:00	366.62	284.11	196.79	1771.1	1.95E-04	2.38E-02	1.46E+03	7.67	2.4E-16	2.4E-12	2.5E-12	9.6E-14
S014-16-T5-7	0.271	3/2/2016 8:30:0	3/3/2016 8:40:00	365.76	283.44	197.96	1781.6	1.97E-04	2.44E-02	1.44E+03	7.67	2.6E-16	2.6E-12		

T6

Name	Tc (µg/L)	Interval Begin	Sampling Date	Monlith mass (g)	Monlith Dry Mass (g)	Surface Area (cm^2)	Solution Volume (mL)	Monolith Volume (m^3)	M_{ti} (mg/m^2)	ρ (kg/m^3)	Co (mg$_{Tc}$/kg$_{mono}$)	D_e (m^2/s)	D_e (cm^2/s)	Average D_e (cm^2/s)	Standard Deviation of Average De
S014-16-T6-2	0.975	3/2/2016 8:30:0	3/3/2016 8:40:00	363.78	284.09	196.70	1770.3	1.95E-04	8.78E-02	1.45E+03	7.95	3.0E-15	3.0E-11	2.7E-11	2.9E-12
S014-16-T6-3	0.874	3/2/2016 8:30:0	3/3/2016 8:40:00	364.78	284.87	197.29	1775.6	1.96E-04	7.87E-02	1.45E+03	7.95	2.4E-15	2.4E-11		
S014-16-T6-5	0.267	3/2/2016 8:30:0	3/3/2016 8:40:00	362.95	283.44	196.39	1767.5	1.95E-04	2.40E-02	1.45E+03	7.95	2.3E-16	2.3E-12	2.1E-12	2.1E-13
S014-16-T6-6	0.245	3/2/2016 8:30:0	3/3/2016 8:40:00	360.98	281.90	193.67	1743.0	1.91E-04	2.21E-02	1.48E+03	7.95	1.8E-16	1.8E-12		

Tc 7 d Sampling

Experiment Start 3/1/16 8:30:00

T1

Name	Tc (µg/L)	Interval Begin	Sampling Date	Monlith mass (g)	Monlith Dry Mass (g)	Surface Area (cm^2)	Solution Volume (mL)	Monolith Volume (m^3)	M_{ti} (mg/m^2)	ρ (kg/m^3)	Co (mg$_{Tc}$/kg$_{mono}$)	D_e (m^2/s)	D_e (cm^2/s)	Average D_e (cm^2/s)	Standard Deviation of Average De
S014-16-T1-1	1.48	3/3/2016 8:40:	3/8/2016 8:40:00	359.63	277.23	192.53	1732.8	1.89E-04	1.33E-01	1.46E+03	8.37	7.1E-16	7.1E-12	7.8E-12	6.8E-13
S014-16-T1-2	1.56	3/3/2016 8:40:	3/8/2016 8:40:00	365.20	281.52	199.18	1792.6	1.99E-04	1.40E-01	1.41E+03	8.37	8.5E-16	8.45E-12		
S014-16-T1-4	0.384	3/3/2016 8:40:	3/8/2016 8:40:00	360.86	278.18	195.83	1762.5	1.95E-04	3.46E-02	1.43E+03	8.37	5.0E-17	5.02E-13	9.3E-13	4.2E-13
S014-16-T1-7	0.639	3/3/2016 8:40:	3/8/2016 8:40:00	361.60	278.75	194.35	1749.2	1.92E-04	5.75E-02	1.45E+03	8.37	1.4E-16	1.35E-12		

T2

Name	Tc (µg/L)	Interval Begin	Sampling Date	Monlith mass (g)	Monlith Dry Mass (g)	Surface Area (cm^2)	Solution Volume (mL)	Monolith Volume (m^3)	M_{ti} (mg/m^2)	ρ (kg/m^3)	Co (mg$_{Tc}$/kg$_{mono}$)	D_e (m^2/s)	D_e (cm^2/s)	Average D_e (cm^2/s)	Standard Deviation of Average De
S014-16-T2-3	1.82	3/3/2016 8:40:	3/8/2016 8:40:00	364.71	283.41	195.83	1749.7	1.92E-04	1.63E-01	1.48E+03	8.23	1.1E-15	1.07E-11	1.1E-11	4.0E-13
S014-16-T2-6	1.84	3/3/2016 8:40:	3/8/2016 8:40:00	367.70	285.74	197.83	1780.5	1.97E-04	1.66E-01	1.45E+03	8.23	1.2E-15	1.15E-11		
S014-16-T2-7	0.964	3/3/2016 8:40:	3/8/2016 8:40:00	366.00	284.41	196.77	1770.9	1.95E-04	8.68E-02	1.46E+03	8.23	3.2E-16	3.15E-12	3.6E-12	4.7E-13
S014-16-T2-8	1.08	3/3/2016 8:40:	3/8/2016 8:40:00	363.14	282.19	197.90	1781.1	1.97E-04	9.72E-02	1.43E+03	8.23	4.1E-16	4.1E-12		

T3

Name	Tc (µg/L)	Interval Begin	Sampling Date	Monlith mass (g)	Monlith Dry Mass (g)	Surface Area (cm^2)	Solution Volume (mL)	Monolith Volume (m^3)	M_{ti} (mg/m^2)	ρ (kg/m^3)	Co (mg$_{Tc}$/kg$_{mono}$)	D_e (m^2/s)	D_e (cm^2/s)	Average D_e (cm^2/s)	Standard Deviation of Average De
S014-16-T3-1	1.62	3/3/2016 8:40:	3/8/2016 8:40:00	366.62	285.46	195.87	1762.9	1.94E-04	1.46E-01	1.47E+03	7.45	1.1E-15	1.06E-11	1.1E-11	8.0E-15
S014-16-T3-3	1.61	3/3/2016 8:40:	3/8/2016 8:40:00	364.46	283.78	195.53	1759.7	1.94E-04	1.45E-01	1.46E+03	7.45	1.1E-15	1.06E-11		
S014-16-T3-4	0.396	3/3/2016 8:40:	3/8/2016 8:40:00	362.76	282.46	194.51	1750.6	1.93E-04	3.56E-02	1.47E+03	7.45	6.4E-17	6.39E-13	7.6E-13	1.2E-13
S014-16-T3-8	0.464	3/3/2016 8:40:	3/8/2016 8:40:00	360.88	280.99	194.17	1747.5	1.92E-04	4.18E-02	1.46E+03	7.45	8.8E-17	8.84E-13		

T4

Name	Tc (µg/L)	Interval Begin	Sampling Date	Monlith mass (g)	Monlith Dry Mass (g)	Surface Area (cm^2)	Solution Volume (mL)	Monolith Volume (m^3)	M_{ti} (mg/m^2)	ρ (kg/m^3)	Co (mg$_{Tc}$/kg$_{mono}$)	D_e (m^2/s)	D_e (cm^2/s)	Average D_e (cm^2/s)	Standard Deviation of Average De
S014-16-T4-1	2.32	3/3/2016 8:40:	3/8/2016 8:40:00	364.02	284.12	195.68	1761.2	1.94E-04	2.09E-01	1.46E+03	8.79	1.6E-15	1.58E-11	1.5E-11	9.3E-13
S014-16-T4-2	2.16	3/3/2016 8:40:	3/8/2016 8:40:00	369.27	288.22	199.22	1793.0	1.99E-04	1.94E-01	1.45E+03	8.79	1.4E-15	1.4E-11		
S014-16-T4-5	0.522	3/3/2016 8:40:	3/8/2016 8:40:00	365.37	285.18	195.92	1763.3	1.94E-04	4.70E-02	1.47E+03	8.79	8.0E-17	7.97E-13	8.2E-13	2.2E-14
S014-16-T4-7	0.53	3/3/2016 8:40:	3/8/2016 8:40:00	363.93	284.05	196.69	1770.2	1.96E-04	4.77E-02	1.45E+03	8.79	8.4E-17	8.41E-13		

T5

Name	Tc (µg/L)	Interval Begin	Sampling Date	Monlith mass (g)	Monlith Dry Mass (g)	Surface Area (cm^2)	Solution Volume (mL)	Monolith Volume (m^3)	M_{ti} (mg/m^2)	ρ (kg/m^3)	Co (mg$_{Tc}$/kg$_{mono}$)	D_e (m^2/s)	D_e (cm^2/s)	Average D_e (cm^2/s)	Standard Deviation of Average De
S014-16-T5-2	3.07	3/3/2016 8:40:	3/8/2016 8:40:00	365.93	283.58	197.86	1780.7	1.97E-04	2.76E-01	1.44E+03	7.67	3.8E-15	3.76E-11	4.0E-11	2.6E-12
S014-16-T5-3	3.34	3/3/2016 8:40:	3/8/2016 8:40:00	364.75	282.66	195.03	1755.3	1.92E-04	3.01E-01	1.47E+03	7.67	4.3E-15	4.27E-11		
S014-16-T5-4	0.636	3/3/2016 8:40:	3/8/2016 8:40:00	366.62	284.11	196.79	1771.1	1.95E-04	5.72E-02	1.46E+03	7.67	1.6E-16	1.58E-12	1.9E-12	2.8E-13
S014-16-T5-7	0.731	3/3/2016 8:40:	3/8/2016 8:40:00	365.76	283.44	197.96	1781.6	1.97E-04	6.58E-02	1.44E+03	7.67	2.1E-16	2.14E-12		

T6

Name	Tc (µg/L)	Interval Begin	Sampling Date	Monlith mass (g)	Monlith Dry Mass (g)	Surface Area (cm^2)	Solution Volume (mL)	Monolith Volume (m^3)	M_{ti} (mg/m^2)	ρ (kg/m^3)	Co (mg$_{Tc}$/kg$_{mono}$)	D_e (m^2/s)	D_e (cm^2/s)	Average D_e (cm^2/s)	Standard Deviation of Average De
S014-16-T6-2	3.11	3/3/2016 8:40:	3/8/2016 8:40:00	363.78	284.09	196.70	1770.3	1.95E-04	2.80E-01	1.45E+03	7.95	3.5E-15	3.52E-11	3.6E-11	3.9E-13
S014-16-T6-3	3.14	3/3/2016 8:40:	3/8/2016 8:40:00	364.78	284.87	197.29	1775.6	1.96E-04	2.83E-01	1.45E+03	7.95	3.6E-15	3.6E-11		
S014-16-T6-5	0.567	3/3/2016 8:40:	3/8/2016 8:40:00	362.95	283.44	196.39	1767.5	1.95E-04	5.10E-02	1.45E+03	7.95	1.2E-16	1.17E-12	1.4E-12	2.2E-13
S014-16-T6-6	0.674	3/3/2016 8:40:	3/8/2016 8:40:00	360.98	281.90	193.67	1743.0	1.91E-04	6.07E-02	1.48E+03	7.95	1.6E-16	1.6E-12		

Tc 14 d Sampling

Experiment Start	3/1/16 8:30:00

T1

Name	Tc (µg/L)	Interval Begin	Sampling Date	Monlith mass (g)	Monlith Dry Mass (g)	Surface Area (cm^2)	Solution Volume (mL)	Monolith Volume (m^3)	M_{ti} (mg/m^2)	ρ (kg/m^3)	Co (mg$_{Tc}$/kg$_{mono}$)	D_e (m^2/s)	D_e (cm^2/s)	Average D_e (cm^2/s)	Standard Deviation of Average De
S014-16-T1-1	1.47	3/8/2016 8:40:0	3/15/2016 8:50:0	359.63	277.23	192.53	1732.8	1.89E-04	1.32E-01	1.46E+03	8.37	8.8E-16	8.8E-12	9.6E-12	7.8E-13
S014-16-T1-2	1.54	3/8/2016 8:40:0	3/15/2016 8:50:0	365.20	281.52	199.18	1792.6	1.99E-04	1.39E-01	1.41E+03	8.37	1.0E-15	1.0E-11		
S014-16-T1-4	0.644	3/8/2016 8:40:0	3/15/2016 8:50:0	360.86	278.18	195.83	1762.5	1.95E-04	5.80E-02	1.43E+03	8.37	1.8E-16	1.8E-12	2.1E-12	2.8E-13
S014-16-T1-7	0.749	3/8/2016 8:40:0	3/15/2016 8:50:0	361.60	278.75	194.35	1749.2	1.92E-04	6.74E-02	1.45E+03	8.37	2.3E-16	2.3E-12		

T2

Name	Tc (µg/L)	Interval Begin	Sampling Date	Monlith mass (g)	Monlith Dry Mass (g)	Surface Area (cm^2)	Solution Volume (mL)	Monolith Volume (m^3)	M_{ti} (mg/m^2)	ρ (kg/m^3)	Co (mg$_{Tc}$/kg$_{mono}$)	D_e (m^2/s)	D_e (cm^2/s)	Average D_e (cm^2/s)	Standard Deviation of Average De
S014-16-T2-3	1.75	3/8/2016 8:40:0	3/15/2016 8:50:0	364.71	283.41	195.83	1749.7	1.92E-04	1.56E-01	1.48E+03	8.23	1.2E-15	1.2E-11	1.4E-11	1.2E-12
S014-16-T2-6	1.86	3/8/2016 8:40:0	3/15/2016 8:50:0	367.70	285.74	197.83	1780.5	1.97E-04	1.67E-01	1.45E+03	8.23	1.5E-15	1.5E-11		
S014-16-T2-7	1.06	3/8/2016 8:40:0	3/15/2016 8:50:0	366.00	284.41	196.77	1770.9	1.95E-04	9.54E-02	1.46E+03	8.23	4.8E-16	4.8E-12	3.7E-12	1.1E-12
S014-16-T2-8	0.758	3/8/2016 8:40:0	3/15/2016 8:50:0	363.14	282.19	197.90	1781.1	1.97E-04	6.82E-02	1.43E+03	8.23	2.5E-16	2.5E-12		

T3

Name	Tc (µg/L)	Interval Begin	Sampling Date	Monlith mass (g)	Monlith Dry Mass (g)	Surface Area (cm^2)	Solution Volume (mL)	Monolith Volume (m^3)	M_{ti} (mg/m^2)	ρ (kg/m^3)	Co (mg$_{Tc}$/kg$_{mono}$)	D_e (m^2/s)	D_e (cm^2/s)	Average D_e (cm^2/s)	Standard Deviation of Average De
S014-16-T3-1	1.69	3/8/2016 8:40:0	3/15/2016 8:50:0	366.62	285.46	195.87	1762.9	1.94E-04	1.52E-01	1.47E+03	7.45	1.5E-15	1.5E-11	1.5E-11	9.1E-13
S014-16-T3-3	1.78	3/8/2016 8:40:0	3/15/2016 8:50:0	364.46	283.78	195.53	1759.7	1.94E-04	1.60E-01	1.46E+03	7.45	1.6E-15	1.6E-11		
S014-16-T3-4	0.282	3/8/2016 8:40:0	3/15/2016 8:50:0	362.76	282.46	194.51	1750.6	1.93E-04	2.54E-02	1.47E+03	7.45	4.1E-17	4.1E-13	5.0E-13	8.8E-14
S014-16-T3-8	0.336	3/8/2016 8:40:0	3/15/2016 8:50:0	360.88	280.99	194.17	1747.5	1.92E-04	3.02E-02	1.46E+03	7.45	5.8E-17	5.8E-13		

T4

Name	Tc (µg/L)	Interval Begin	Sampling Date	Monlith mass (g)	Monlith Dry Mass (g)	Surface Area (cm^2)	Solution Volume (mL)	Monolith Volume (m^3)	M_{ti} (mg/m^2)	ρ (kg/m^3)	Co (mg$_{Tc}$/kg$_{mono}$)	D_e (m^2/s)	D_e (cm^2/s)	Average D_e (cm^2/s)	Standard Deviation of Average De
S014-16-T4-1	2.06	3/8/2016 8:40:0	3/15/2016 8:50:0	364.02	284.12	195.68	1761.2	1.94E-04	1.85E-01	1.46E+03	8.79	1.6E-15	1.6E-11	1.7E-11	1.7E-12
S014-16-T4-2	2.25	3/8/2016 8:40:0	3/15/2016 8:50:0	369.27	288.22	199.22	1793.0	1.99E-04	2.03E-01	1.45E+03	8.79	1.9E-15	1.9E-11		
S014-16-T4-5	0.406	3/8/2016 8:40:0	3/15/2016 8:50:0	365.37	285.18	195.92	1763.3	1.94E-04	3.65E-02	1.47E+03	8.79	6.1E-17	6.1E-13	5.8E-13	2.9E-14
S014-16-T4-7	0.382	3/8/2016 8:40:0	3/15/2016 8:50:0	363.93	284.05	196.69	1770.2	1.96E-04	3.44E-02	1.45E+03	8.79	5.5E-17	5.5E-13		

T5

Name	Tc (µg/L)	Interval Begin	Sampling Date	Monlith mass (g)	Monlith Dry Mass (g)	Surface Area (cm^2)	Solution Volume (mL)	Monolith Volume (m^3)	M_{ti} (mg/m^2)	ρ (kg/m^3)	Co (mg$_{Tc}$/kg$_{mono}$)	D_e (m^2/s)	D_e (cm^2/s)	Average D_e (cm^2/s)	Standard Deviation of Average De
S014-16-T5-2	2.92	3/8/2016 8:40:0	3/15/2016 8:50:0	365.93	283.58	197.86	1780.7	1.97E-04	2.63E-01	1.44E+03	7.67	4.3E-15	4.3E-11	4.6E-11	3.0E-12
S014-16-T5-3	3.18	3/8/2016 8:40:0	3/15/2016 8:50:0	364.75	282.66	195.03	1755.3	1.92E-04	2.86E-01	1.47E+03	7.67	4.9E-15	4.9E-11		
S014-16-T5-4	0.588	3/8/2016 8:40:0	3/15/2016 8:50:0	366.62	284.11	196.79	1771.1	1.95E-04	5.29E-02	1.46E+03	7.67	1.7E-16	1.7E-12	1.5E-12	1.5E-13
S014-16-T5-7	0.527	3/8/2016 8:40:0	3/15/2016 8:50:0	365.76	283.44	197.96	1781.6	1.97E-04	4.74E-02	1.44E+03	7.67	1.4E-16	1.4E-12		

T6

Name	Tc (µg/L)	Interval Begin	Sampling Date	Monlith mass (g)	Monlith Dry Mass (g)	Surface Area (cm^2)	Solution Volume (mL)	Monolith Volume (m^3)	M_{ti} (mg/m^2)	ρ (kg/m^3)	Co (mg$_{Tc}$/kg$_{mono}$)	D_e (m^2/s)	D_e (cm^2/s)	Average D_e (cm^2/s)	Standard Deviation of Average De
S014-16-T6-2	2.94	3/8/2016 8:40:0	3/15/2016 8:50:0	363.78	284.09	196.70	1770.3	1.95E-04	2.65E-01	1.45E+03	7.95	4.0E-15	4.0E-11	4.0E-11	3.3E-13
S014-16-T6-3	2.96	3/8/2016 8:40:0	3/15/2016 8:50:0	364.78	284.87	197.29	1775.6	1.96E-04	2.66E-01	1.45E+03	7.95	4.0E-15	4.0E-11		
S014-16-T6-5	0.473	3/8/2016 8:40:0	3/15/2016 8:50:0	362.95	283.44	196.39	1767.5	1.95E-04	4.26E-02	1.45E+03	7.95	1.0E-16	1.0E-12	1.1E-12	5.6E-14
S014-16-T6-6	0.506	3/8/2016 8:40:0	3/15/2016 8:50:0	360.98	281.90	193.67	1743.0	1.91E-04	4.55E-02	1.48E+03	7.95	1.1E-16	1.1E-12		

Tc Sampling 28 d

Experiment Start 3/1/16 8:30:00

T1

Name	Tc (µg/L)	Interval Begin	Sampling Date	Monlith mass (g)	Monlith Dry Mass (g)	Surface Area (cm^2)	Solution Volume (mL)	Monolith Volume (m^3)	M_{ti} (mg/m^2)	ρ (kg/m^3)	Co (mg$_{Tc}$/kg$_{mono}$)	D_e (m^2/s)	D_e (cm^2/s)	Average D_e (cm^2/s)	Standard Deviation of Average De
S014-16-T1-1	2.84	03/15/2016 08:50:00	03/29/2016 08:00:0	359.63	277.23	192.53	1732.8	1.89E-04	2.56E-01	1.46E+03	8.37	1.7E-15	1.7E-11	1.7E-11	2.1E-14
S014-16-T1-2	2.74	03/15/2016 08:50:00	03/29/2016 08:00:0	365.20	281.52	199.18	1792.6	1.99E-04	2.47E-01	1.41E+03	8.37	1.7E-15	1.7E-11		
S014-16-T1-4	1.34	03/15/2016 08:50:00	03/29/2016 08:00:0	360.86	278.18	195.83	1762.5	1.95E-04	1.21E-01	1.43E+03	8.37	3.9E-16	3.9E-12	3.7E-12	1.7E-13
S014-16-T1-7	1.3	03/15/2016 08:50:00	03/29/2016 08:00:0	361.60	278.75	194.35	1749.2	1.92E-04	1.17E-01	1.45E+03	8.37	3.5E-16	3.5E-12		

T2

Name	Tc (µg/L)	Interval Begin	Sampling Date	Monlith mass (g)	Monlith Dry Mass (g)	Surface Area (cm^2)	Solution Volume (mL)	Monolith Volume (m^3)	M_{ti} (mg/m^2)	ρ (kg/m^3)	Co (mg$_{Tc}$/kg$_{mono}$)	D_e (m^2/s)	D_e (cm^2/s)	Average D_e (cm^2/s)	Standard Deviation of Average De
S014-16-T2-3	2.95	03/15/2016 08:50:00	03/29/2016 08:00:0	364.71	283.41	195.83	1749.7	1.92E-04	2.64E-01	1.48E+03	8.23	1.8E-15	1.8E-11	1.9E-11	1.2E-12
S014-16-T2-6	3.07	03/15/2016 08:50:00	03/29/2016 08:00:0	367.70	285.74	197.83	1780.5	1.97E-04	2.76E-01	1.45E+03	8.23	2.0E-15	2.0E-11		
S014-16-T2-7	1.23	03/15/2016 08:50:00	03/29/2016 08:00:0	366.00	284.41	196.77	1770.9	1.95E-04	1.11E-01	1.46E+03	8.23	3.2E-16	3.2E-12	3.2E-12	2.3E-14
S014-16-T2-8	1.2	03/15/2016 08:50:00	03/29/2016 08:00:0	363.14	282.19	197.90	1781.1	1.97E-04	1.08E-01	1.43E+03	8.23	3.2E-16	3.2E-12		

T3

Name	Tc (µg/L)	Interval Begin	Sampling Date	Monlith mass (g)	Monlith Dry Mass (g)	Surface Area (cm^2)	Solution Volume (mL)	Monolith Volume (m^3)	M_{ti} (mg/m^2)	ρ (kg/m^3)	Co (mg$_{Tc}$/kg$_{mono}$)	D_e (m^2/s)	D_e (cm^2/s)	Average D_e (cm^2/s)	Standard Deviation of Average De
S014-16-T3-1	2.71	03/15/2016 08:50:00	03/29/2016 08:00:0	366.62	285.46	195.87	1762.9	1.94E-04	2.44E-01	1.47E+03	7.45	1.9E-15	1.9E-11	2.0E-11	7.7E-13
S014-16-T3-3	2.8	03/15/2016 08:50:00	03/29/2016 08:00:0	364.46	283.78	195.53	1759.7	1.94E-04	2.52E-01	1.46E+03	7.45	2.0E-15	2.0E-11		
S014-16-T3-4	0.416	03/15/2016 08:50:00	03/29/2016 08:00:0	362.76	282.46	194.51	1750.6	1.93E-04	3.74E-02	1.47E+03	7.45	4.5E-17	4.5E-13	5.3E-13	8.5E-14
S014-16-T3-8	0.487	03/15/2016 08:50:00	03/29/2016 08:00:0	360.88	280.99	194.17	1747.5	1.92E-04	4.38E-02	1.46E+03	7.45	6.2E-17	6.2E-13		

T4

Name	Tc (µg/L)	Interval Begin	Sampling Date	Monlith mass (g)	Monlith Dry Mass (g)	Surface Area (cm^2)	Solution Volume (mL)	Monolith Volume (m^3)	M_{ti} (mg/m^2)	ρ (kg/m^3)	Co (mg$_{Tc}$/kg$_{mono}$)	D_e (m^2/s)	D_e (cm^2/s)	Average D_e (cm^2/s)	Standard Deviation of Average De
S014-16-T4-1	3.43	03/15/2016 08:50:00	03/29/2016 08:00:0	364.02	284.12	195.68	1761.2	1.94E-04	3.09E-01	1.46E+03	8.79	2.2E-15	2.2E-11	2.2E-11	1.4E-13
S014-16-T4-2	3.42	03/15/2016 08:50:00	03/29/2016 08:00:0	369.27	288.22	199.22	1793.0	1.99E-04	3.08E-01	1.45E+03	8.79	2.2E-15	2.2E-11		
S014-16-T4-5	0.545	03/15/2016 08:50:00	03/29/2016 08:00:0	365.37	285.18	195.92	1763.3	1.94E-04	4.91E-02	1.47E+03	8.79	5.5E-17	5.5E-13	6.9E-13	1.4E-13
S014-16-T4-7	0.659	03/15/2016 08:50:00	03/29/2016 08:00:0	363.93	284.05	196.69	1770.2	1.96E-04	5.93E-02	1.45E+03	8.79	8.2E-17	8.2E-13		

T5

Name	Tc (µg/L)	Interval Begin	Sampling Date	Monlith mass (g)	Monlith Dry Mass (g)	Surface Area (cm^2)	Solution Volume (mL)	Monolith Volume (m^3)	M_{ti} (mg/m^2)	ρ (kg/m^3)	Co (mg$_{Tc}$/kg$_{mono}$)	D_e (m^2/s)	D_e (cm^2/s)	Average D_e (cm^2/s)	Standard Deviation of Average De
S014-16-T5-2	4.63	03/15/2016 08:50:00	03/29/2016 08:00:0	365.93	283.58	197.86	1780.7	1.97E-04	4.17E-01	1.44E+03	7.67	5.4E-15	5.4E-11	5.1E-11	3.5E-12
S014-16-T5-3	4.41	03/15/2016 08:50:00	03/29/2016 08:00:0	364.75	282.66	195.03	1755.3	1.92E-04	3.97E-01	1.47E+03	7.67	4.7E-15	4.7E-11		
S014-16-T5-4	0.662	03/15/2016 08:50:00	03/29/2016 08:00:0	366.62	284.11	196.79	1771.1	1.95E-04	5.96E-02	1.46E+03	7.67	1.1E-16	1.1E-12	1.2E-12	9.2E-14
S014-16-T5-7	0.707	03/15/2016 08:50:00	03/29/2016 08:00:0	365.76	283.44	197.96	1781.6	1.97E-04	6.36E-02	1.44E+03	7.67	1.3E-16	1.3E-12		

T6

Name	Tc (µg/L)	Interval Begin	Sampling Date	Monlith mass (g)	Monlith Dry Mass (g)	Surface Area (cm^2)	Solution Volume (mL)	Monolith Volume (m^3)	M_{ti} (mg/m^2)	ρ (kg/m^3)	Co (mg$_{Tc}$/kg$_{mono}$)	D_e (m^2/s)	D_e (cm^2/s)	Average D_e (cm^2/s)	Standard Deviation of Average De
S014-16-T6-2	4.03	03/15/2016 08:50:00	03/29/2016 08:00:0	363.78	284.09	196.70	1770.3	1.95E-04	3.63E-01	1.45E+03	7.95	3.7E-15	3.7E-11	4.0E-11	2.4E-12
S014-16-T6-3	4.27	03/15/2016 08:50:00	03/29/2016 08:00:0	364.78	284.87	197.29	1775.6	1.96E-04	3.84E-01	1.45E+03	7.95	4.2E-15	4.2E-11		
S014-16-T6-5	0.659	03/15/2016 08:50:00	03/29/2016 08:00:0	362.95	283.44	196.39	1767.5	1.95E-04	5.93E-02	1.45E+03	7.95	1.0E-16	1.0E-12	1.0E-12	4.8E-14
S014-16-T6-6	0.701	03/15/2016 08:50:00	03/29/2016 08:00:0	360.98	281.90	193.67	1743.0	1.91E-04	6.31E-02	1.48E+03	7.95	1.1E-16	1.1E-12		

Tc 42 d Sampling

Experiment Start 3/1/16 8:30:00

T1

Name	Tc (µg/L)	Interval Begin	Sampling Date	Monlith mass (g)	Monlith Dry Mass (g)	Surface Area (cm^2)	Solution Volume (mL)	Monolith Volume (m^3)	M_{ti} (mg/m^2)	ρ (kg/m^3)	Co (mg$_{Tc}$/kg$_{mono}$)	D_e (m^2/s)	D_e (cm^2/s)	Average D_e (cm^2/s)	Standard Deviation of Average De
S014-16-T1-1	2.69	03/29/2016 08:00:0	04/12/2016 08:30:0	359.63	277.23	192.53	1732.8	1.89E-04	2.42E-01	1.46E+03	8.37	2.5E-15	2.5E-11	2.4E-11	1.4E-12
S014-16-T1-2	2.45	03/29/2016 08:00:0	04/12/2016 08:30:0	365.20	281.52	199.18	1792.6	1.99E-04	2.21E-01	1.41E+03	8.37	2.2E-15	2.2E-11		
S014-16-T1-4	1.22	03/29/2016 08:00:0	04/12/2016 08:30:0	360.86	278.18	195.83	1762.5	1.95E-04	1.10E-01	1.43E+03	8.37	5.4E-16	5.4E-12	5.6E-12	1.9E-13
S014-16-T1-7	1.28	03/29/2016 08:00:0	04/12/2016 08:30:0	361.60	278.75	194.35	1749.2	1.92E-04	1.15E-01	1.45E+03	8.37	5.8E-16	5.8E-12		

T2

Name	Tc (µg/L)	Interval Begin	Sampling Date	Monlith mass (g)	Monlith Dry Mass (g)	Surface Area (cm^2)	Solution Volume (mL)	Monolith Volume (m^3)	M_{ti} (mg/m^2)	ρ (kg/m^3)	Co (mg$_{Tc}$/kg$_{mono}$)	D_e (m^2/s)	D_e (cm^2/s)	Average D_e (cm^2/s)	Standard Deviation of Average De
S014-16-T2-3	2.42	03/29/2016 08:00:0	04/12/2016 08:30:0	364.71	283.41	195.83	1749.7	1.92E-04	2.16E-01	1.48E+03	8.23	2.0E-15	2.0E-11	2.1E-11	4.4E-13
S014-16-T2-6	2.41	03/29/2016 08:00:0	04/12/2016 08:30:0	367.70	285.74	197.83	1780.5	1.97E-04	2.17E-01	1.45E+03	8.23	2.1E-15	2.1E-11		
S014-16-T2-7	0.565	03/29/2016 08:00:0	04/12/2016 08:30:0	366.00	284.41	196.77	1770.9	1.95E-04	5.09E-02	1.46E+03	8.23	1.2E-16	1.2E-12	1.0E-12	1.1E-13
S014-16-T2-8	0.5	03/29/2016 08:00:0	04/12/2016 08:30:0	363.14	282.19	197.90	1781.1	1.97E-04	4.50E-02	1.43E+03	8.23	9.4E-17	9.4E-13		

T3

Name	Tc (µg/L)	Interval Begin	Sampling Date	Monlith mass (g)	Monlith Dry Mass (g)	Surface Area (cm^2)	Solution Volume (mL)	Monolith Volume (m^3)	M_{ti} (mg/m^2)	ρ (kg/m^3)	Co (mg$_{Tc}$/kg$_{mono}$)	D_e (m^2/s)	D_e (cm^2/s)	Average D_e (cm^2/s)	Standard Deviation of Average De
S014-16-T3-1	2.21	03/29/2016 08:00:0	04/12/2016 08:30:0	366.62	285.46	195.87	1762.9	1.94E-04	1.99E-01	1.47E+03	7.45	2.1E-15	2.1E-11	2.1E-11	4.2E-13
S014-16-T3-3	2.15	03/29/2016 08:00:0	04/12/2016 08:30:0	364.46	283.78	195.53	1759.7	1.94E-04	1.94E-01	1.46E+03	7.45	2.0E-15	2.0E-11		
S014-16-T3-4	0.361	03/29/2016 08:00:0	04/12/2016 08:30:0	362.76	282.46	194.51	1750.6	1.93E-04	3.25E-02	1.47E+03	7.45	5.7E-17	5.7E-13	5.7E-13	3.5E-15
S014-16-T3-8	0.362	03/29/2016 08:00:0	04/12/2016 08:30:0	360.88	280.99	194.17	1747.5	1.92E-04	3.26E-02	1.46E+03	7.45	5.7E-17	5.7E-13		

T4

Name	Tc (µg/L)	Interval Begin	Sampling Date	Monlith mass (g)	Monlith Dry Mass (g)	Surface Area (cm^2)	Solution Volume (mL)	Monolith Volume (m^3)	M_{ti} (mg/m^2)	ρ (kg/m^3)	Co (mg$_{Tc}$/kg$_{mono}$)	D_e (m^2/s)	D_e (cm^2/s)	Average D_e (cm^2/s)	Standard Deviation of Average De
S014-16-T4-1	2.69	03/29/2016 08:00:0	04/12/2016 08:30:0	364.02	284.12	195.68	1761.2	1.94E-04	2.42E-01	1.46E+03	8.79	2.3E-15	2.3E-11	2.3E-11	3.9E-13
S014-16-T4-2	2.71	03/29/2016 08:00:0	04/12/2016 08:30:0	369.27	288.22	199.22	1793.0	1.99E-04	2.44E-01	1.45E+03	8.79	2.4E-15	2.4E-11		
S014-16-T4-5	0.472	03/29/2016 08:00:0	04/12/2016 08:30:0	365.37	285.18	195.92	1763.3	1.94E-04	4.25E-02	1.47E+03	8.79	7.0E-17	7.0E-13	7.0E-13	2.1E-15
S014-16-T4-7	0.468	03/29/2016 08:00:0	04/12/2016 08:30:0	363.93	284.05	196.69	1770.2	1.96E-04	4.21E-02	1.45E+03	8.79	7.0E-17	7.0E-13		

T5

Name	Tc (µg/L)	Interval Begin	Sampling Date	Monlith mass (g)	Monlith Dry Mass (g)	Surface Area (cm^2)	Solution Volume (mL)	Monolith Volume (m^3)	M_{ti} (mg/m^2)	ρ (kg/m^3)	Co (mg$_{Tc}$/kg$_{mono}$)	D_e (m^2/s)	D_e (cm^2/s)	Average D_e (cm^2/s)	Standard Deviation of Average De
S014-16-T5-2	3.43	03/29/2016 08:00:0	04/12/2016 08:30:0	365.93	283.58	197.86	1780.7	1.97E-04	3.09E-01	1.44E+03	7.67	5.0E-15	5.0E-11	5.4E-11	4.0E-12
S014-16-T5-3	3.77	03/29/2016 08:00:0	04/12/2016 08:30:0	364.75	282.66	195.03	1755.3	1.92E-04	3.39E-01	1.47E+03	7.67	5.8E-15	5.8E-11		
S014-16-T5-4	0.472	03/29/2016 08:00:0	04/12/2016 08:30:0	366.62	284.11	196.79	1771.1	1.95E-04	4.25E-02	1.46E+03	7.67	9.3E-17	9.3E-13	1.1E-12	2.2E-13
S014-16-T5-7	0.565	03/29/2016 08:00:0	04/12/2016 08:30:0	365.76	283.44	197.96	1781.6	1.97E-04	5.09E-02	1.44E+03	7.67	1.4E-16	1.4E-12		

T6

Name	Tc (µg/L)	Interval Begin	Sampling Date	Monlith mass (g)	Monlith Dry Mass (g)	Surface Area (cm^2)	Solution Volume (mL)	Monolith Volume (m^3)	M_{ti} (mg/m^2)	ρ (kg/m^3)	Co (mg$_{Tc}$/kg$_{mono}$)	D_e (m^2/s)	D_e (cm^2/s)	Average D_e (cm^2/s)	Standard Deviation of Average De
S014-16-T6-2	3.26	03/29/2016 08:00:0	04/12/2016 08:30:0	363.78	284.09	196.70	1770.3	1.95E-04	2.93E-01	1.45E+03	7.95	4.1E-15	4.1E-11	3.7E-11	4.5E-12
S014-16-T6-3	2.88	03/29/2016 08:00:0	04/12/2016 08:30:0	364.78	284.87	197.29	1775.6	1.96E-04	2.59E-01	1.45E+03	7.95	3.2E-15	3.2E-11		
S014-16-T6-5	0.467	03/29/2016 08:00:0	04/12/2016 08:30:0	362.95	283.44	196.39	1767.5	1.95E-04	4.20E-02	1.45E+03	7.95	8.5E-17	8.5E-13	9.0E-13	5.3E-14
S014-16-T6-6	0.503	03/29/2016 08:00:0	04/12/2016 08:30:0	360.98	281.90	193.67	1743.0	1.91E-04	4.53E-02	1.48E+03	7.95	9.5E-17	9.5E-13		

Tc 49 d Sampling

Experiment Start 3/1/16 8:30:00

T1

Name	Tc (µg/L)	Interval Begin	Sampling Date	Monlith mass (g)	Monlith Dry Mass (g)	Surface Area (cm^2)	Solution Volume (mL)	Monolith Volume (m^3)	M$_{ti}$ (mg/m^2)	ρ (kg/m^3)	Co (mg$_{Tc}$/kg$_{mono}$)	D$_e$ (m^2/s)	D$_e$ (cm^2/s)	Average D$_e$ (cm^2/s)	Standard Deviation of Average De
S014-16-T1-1	1.22	04/12/2016 08:30:0	04/19/2016 08:40:0	359.63	277.23	192.53	1732.8	1.89E-04	1.10E-01	1.46E+03	8.37	2.7E-15	2.7E-11	2.7E-11	3.3E-14
S014-16-T1-2	1.18	04/12/2016 08:30:0	04/19/2016 08:40:0	365.20	281.52	199.18	1792.6	1.99E-04	1.06E-01	1.41E+03	8.37	2.7E-15	2.7E-11		
S014-16-T1-4	0.863	04/12/2016 08:30:0	04/19/2016 08:40:0	360.86	278.18	195.83	1762.5	1.95E-04	7.77E-02	1.43E+03	8.37	1.4E-15	1.4E-11	1.3E-11	1.5E-12
S014-16-T1-7	0.776	04/12/2016 08:30:0	04/19/2016 08:40:0	361.60	278.75	194.35	1749.2	1.92E-04	6.98E-02	1.45E+03	8.37	1.1E-15	1.1E-11		

T2

Name	Tc (µg/L)	Interval Begin	Sampling Date	Monlith mass (g)	Monlith Dry Mass (g)	Surface Area (cm^2)	Solution Volume (mL)	Monolith Volume (m^3)	M$_{ti}$ (mg/m^2)	ρ (kg/m^3)	Co (mg$_{Tc}$/kg$_{mono}$)	D$_e$ (m^2/s)	D$_e$ (cm^2/s)	Average D$_e$ (cm^2/s)	Standard Deviation of Average De
S014-16-T2-3	1.13	04/12/2016 08:30:0	04/19/2016 08:40:0	364.71	283.41	195.83	1749.7	1.92E-04	1.01E-01	1.48E+03	8.23	2.3E-15	2.3E-11	2.2E-11	8.6E-13
S014-16-T2-6	1.06	04/12/2016 08:30:0	04/19/2016 08:40:0	367.70	285.74	197.83	1780.5	1.97E-04	9.54E-02	1.45E+03	8.23	2.1E-15	2.1E-11		
S014-16-T2-7	0.329	04/12/2016 08:30:0	04/19/2016 08:40:0	366.00	284.41	196.77	1770.9	1.95E-04	2.96E-02	1.46E+03	8.23	2.1E-16	2.1E-12	2.4E-12	3.8E-13
S014-16-T2-8	0.379	04/12/2016 08:30:0	04/19/2016 08:40:0	363.14	282.19	197.90	1781.1	1.97E-04	3.41E-02	1.43E+03	8.23	2.8E-16	2.8E-12		

T3

Name	Tc (µg/L)	Interval Begin	Sampling Date	Monlith mass (g)	Monlith Dry Mass (g)	Surface Area (cm^2)	Solution Volume (mL)	Monolith Volume (m^3)	M$_{ti}$ (mg/m^2)	ρ (kg/m^3)	Co (mg$_{Tc}$/kg$_{mono}$)	D$_e$ (m^2/s)	D$_e$ (cm^2/s)	Average D$_e$ (cm^2/s)	Standard Deviation of Average De
S014-16-T3-1	1.06	04/12/2016 08:30:0	04/19/2016 08:40:0	366.62	285.46	195.87	1762.9	1.94E-04	9.54E-02	1.47E+03	7.45	2.5E-15	2.5E-11	2.3E-11	2.5E-12
S014-16-T3-3	0.943	04/12/2016 08:30:0	04/19/2016 08:40:0	364.46	283.78	195.53	1759.7	1.94E-04	8.49E-02	1.46E+03	7.45	2.0E-15	2.0E-11		
S014-16-T3-4	0.229	04/12/2016 08:30:0	04/19/2016 08:40:0	362.76	282.46	194.51	1750.6	1.93E-04	2.06E-02	1.47E+03	7.45	1.2E-16	1.2E-12	1.3E-12	8.0E-14
S014-16-T3-8	0.243	04/12/2016 08:30:0	04/19/2016 08:40:0	360.88	280.99	194.17	1747.5	1.92E-04	2.19E-02	1.46E+03	7.45	1.4E-16	1.4E-12		

T4

Name	Tc (µg/L)	Interval Begin	Sampling Date	Monlith mass (g)	Monlith Dry Mass (g)	Surface Area (cm^2)	Solution Volume (mL)	Monolith Volume (m^3)	M$_{ti}$ (mg/m^2)	ρ (kg/m^3)	Co (mg$_{Tc}$/kg$_{mono}$)	D$_e$ (m^2/s)	D$_e$ (cm^2/s)	Average D$_e$ (cm^2/s)	Standard Deviation of Average De
S014-16-T4-1	1.27	04/12/2016 08:30:0	04/19/2016 08:40:0	364.02	284.12	195.68	1761.2	1.94E-04	1.14E-01	1.46E+03	8.79	2.7E-15	2.7E-11	2.5E-11	1.4E-12
S014-16-T4-2	1.19	04/12/2016 08:30:0	04/19/2016 08:40:0	369.27	288.22	199.22	1793.0	1.99E-04	1.07E-01	1.45E+03	8.79	2.4E-15	2.4E-11		
S014-16-T4-5	0.233	04/12/2016 08:30:0	04/19/2016 08:40:0	365.37	285.18	195.92	1763.3	1.94E-04	2.10E-02	1.47E+03	8.79	8.9E-17	8.9E-13	1.2E-12	3.1E-13
S014-16-T4-7	0.3	04/12/2016 08:30:0	04/19/2016 08:40:0	363.93	284.05	196.69	1770.2	1.96E-04	2.70E-02	1.45E+03	8.79	1.5E-16	1.5E-12		

T5

Name	Tc (µg/L)	Interval Begin	Sampling Date	Monlith mass (g)	Monlith Dry Mass (g)	Surface Area (cm^2)	Solution Volume (mL)	Monolith Volume (m^3)	M$_{ti}$ (mg/m^2)	ρ (kg/m^3)	Co (mg$_{Tc}$/kg$_{mono}$)	D$_e$ (m^2/s)	D$_e$ (cm^2/s)	Average D$_e$ (cm^2/s)	Standard Deviation of Average De
S014-16-T5-2	1.51	04/12/2016 08:30:0	04/19/2016 08:40:0	365.93	283.58	197.86	1780.7	1.97E-04	1.36E-01	1.44E+03	7.67	5.1E-15	5.1E-11	5.5E-11	4.1E-12
S014-16-T5-3	1.66	04/12/2016 08:30:0	04/19/2016 08:40:0	364.75	282.66	195.03	1755.3	1.92E-04	1.49E-01	1.47E+03	7.67	5.9E-15	5.9E-11		
S014-16-T5-4	0.293	04/12/2016 08:30:0	04/19/2016 08:40:0	366.62	284.11	196.79	1771.1	1.95E-04	2.64E-02	1.46E+03	7.67	1.9E-16	1.9E-12	2.1E-12	2.2E-13
S014-16-T5-7	0.322	04/12/2016 08:30:0	04/19/2016 08:40:0	365.76	283.44	197.96	1781.6	1.97E-04	2.90E-02	1.44E+03	7.67	2.3E-16	2.3E-12		

T6

Name	Tc (µg/L)	Interval Begin	Sampling Date	Monlith mass (g)	Monlith Dry Mass (g)	Surface Area (cm^2)	Solution Volume (mL)	Monolith Volume (m^3)	M$_{ti}$ (mg/m^2)	ρ (kg/m^3)	Co (mg$_{Tc}$/kg$_{mono}$)	D$_e$ (m^2/s)	D$_e$ (cm^2/s)	Average D$_e$ (cm^2/s)	Standard Deviation of Average De
S014-16-T6-2	1.5	04/12/2016 08:30:0	04/19/2016 08:40:0	363.78	284.09	196.70	1770.3	1.95E-04	1.35E-01	1.45E+03	7.95	4.6E-15	4.6E-11	4.2E-11	4.3E-12
S014-16-T6-3	1.35	04/12/2016 08:30:0	04/19/2016 08:40:0	364.78	284.87	197.29	1775.6	1.96E-04	1.22E-01	1.45E+03	7.95	3.7E-15	3.7E-11		
S014-16-T6-5	0.256	04/12/2016 08:30:0	04/19/2016 08:40:0	362.95	283.44	196.39	1767.5	1.95E-04	2.30E-02	1.45E+03	7.95	1.3E-16	1.3E-12	1.4E-12	6.3E-14
S014-16-T6-6	0.272	04/12/2016 08:30:0	04/19/2016 08:40:0	360.98	281.90	193.67	1743.0	1.91E-04	2.45E-02	1.48E+03	7.95	1.5E-16	1.5E-12		

Tc 63 d Sampling

Experiment Start 3/1/16 8:30:00

T1

Name	Tc (µg/L)	Interval Begin	Sampling Date	Monlith mass (g)	Monlith Dry Mass (g)	Surface Area (cm^2)	Solution Volume (mL)	Monolith Volume (m^3)	M_{ti} (mg/m^2)	ρ (kg/m^3)	Co (mg$_{Tc}$/kg$_{mono}$)	D_e (m^2/s)	D_e (cm^2/s)	Average D_e (cm^2/s)	Standard Deviation of Average De
S014-16-T1-1	2.69	04/19/2016 08:40:0	05/3/2016 09:00:00	359.63	277.23	192.53	1732.8	1.89E-04	2.42E-01	1.46E+03	8.37	4.0E-15	4.0E-11	3.9E-11	1.1E-12
S014-16-T1-2	2.53	04/19/2016 08:40:0	05/3/2016 09:00:00	365.20	281.52	199.18	1792.6	1.99E-04	2.28E-01	1.41E+03	8.37	3.8E-15	3.8E-11		
S014-16-T1-4	0.904	04/19/2016 08:40:0	05/3/2016 09:00:00	360.86	278.18	195.83	1762.5	1.95E-04	8.14E-02	1.43E+03	8.37	4.8E-16	4.8E-12	4.6E-12	2.2E-13
S014-16-T1-7	0.875	04/19/2016 08:40:0	05/3/2016 09:00:00	361.60	278.75	194.35	1749.2	1.92E-04	7.88E-02	1.45E+03	8.37	4.4E-16	4.4E-12		

T2

Name	Tc (µg/L)	Interval Begin	Sampling Date	Monlith mass (g)	Monlith Dry Mass (g)	Surface Area (cm^2)	Solution Volume (mL)	Monolith Volume (m^3)	M_{ti} (mg/m^2)	ρ (kg/m^3)	Co (mg$_{Tc}$/kg$_{mono}$)	D_e (m^2/s)	D_e (cm^2/s)	Average D_e (cm^2/s)	Standard Deviation of Average De
S014-16-T2-3	2.18	04/12/2016 08:30:0	05/3/2016 09:00:00	364.71	283.41	195.83	1749.7	1.92E-04	1.95E-01	1.48E+03	8.23	1.1E-15	1.1E-11	1.0E-11	5.8E-13
S014-16-T2-6	2.01	04/12/2016 08:30:0	05/3/2016 09:00:00	367.70	285.74	197.83	1780.5	1.97E-04	1.81E-01	1.45E+03	8.23	9.8E-16	9.8E-12		
S014-16-T2-7	0.437	04/12/2016 08:30:0	05/3/2016 09:00:00	366.00	284.41	196.77	1770.9	1.95E-04	3.93E-02	1.46E+03	8.23	4.6E-17	4.6E-13	4.6E-13	2.6E-15
S014-16-T2-8	0.427	04/12/2016 08:30:0	05/3/2016 09:00:00	363.14	282.19	197.90	1781.1	1.97E-04	3.84E-02	1.43E+03	8.23	4.6E-17	4.6E-13		

T3

Name	Tc (µg/L)	Interval Begin	Sampling Date	Monlith mass (g)	Monlith Dry Mass (g)	Surface Area (cm^2)	Solution Volume (mL)	Monolith Volume (m^3)	M_{ti} (mg/m^2)	ρ (kg/m^3)	Co (mg$_{Tc}$/kg$_{mono}$)	D_e (m^2/s)	D_e (cm^2/s)	Average D_e (cm^2/s)	Standard Deviation of Average De
S014-16-T3-1	2.09	04/12/2016 08:30:0	05/3/2016 09:00:00	366.62	285.46	195.87	1762.9	1.94E-04	1.88E-01	1.47E+03	7.45	1.3E-15	1.3E-11	1.2E-11	9.1E-13
S014-16-T3-3	1.92	04/12/2016 08:30:0	05/3/2016 09:00:00	364.46	283.78	195.53	1759.7	1.94E-04	1.73E-01	1.46E+03	7.45	1.1E-15	1.1E-11		
S014-16-T3-4	0.289	04/12/2016 08:30:0	05/3/2016 09:00:00	362.76	282.46	194.51	1750.6	1.93E-04	2.60E-02	1.47E+03	7.45	2.4E-17	2.4E-13	2.2E-13	1.8E-14
S014-16-T3-8	0.266	04/12/2016 08:30:0	05/3/2016 09:00:00	360.88	280.99	194.17	1747.5	1.92E-04	2.39E-02	1.46E+03	7.45	2.1E-17	2.1E-13		

T4

Name	Tc (µg/L)	Interval Begin	Sampling Date	Monlith mass (g)	Monlith Dry Mass (g)	Surface Area (cm^2)	Solution Volume (mL)	Monolith Volume (m^3)	M_{ti} (mg/m^2)	ρ (kg/m^3)	Co (mg$_{Tc}$/kg$_{mono}$)	D_e (m^2/s)	D_e (cm^2/s)	Average D_e (cm^2/s)	Standard Deviation of Average De
S014-16-T4-1	2.55	04/12/2016 08:30:0	05/3/2016 09:00:00	364.02	284.12	195.68	1761.2	1.94E-04	2.30E-01	1.46E+03	8.79	1.4E-15	1.4E-11	1.3E-11	5.6E-13
S014-16-T4-2	2.42	04/12/2016 08:30:0	05/3/2016 09:00:00	369.27	288.22	199.22	1793.0	1.99E-04	2.18E-01	1.45E+03	8.79	1.3E-15	1.3E-11		
S014-16-T4-5	0.377	04/12/2016 08:30:0	05/3/2016 09:00:00	365.37	285.18	195.92	1763.3	1.94E-04	3.39E-02	1.47E+03	8.79	3.0E-17	3.0E-13	2.5E-13	4.4E-14
S014-16-T4-7	0.313	04/12/2016 08:30:0	05/3/2016 09:00:00	363.93	284.05	196.69	1770.2	1.96E-04	2.82E-02	1.45E+03	8.79	2.1E-17	2.1E-13		

T5

Name	Tc (µg/L)	Interval Begin	Sampling Date	Monlith mass (g)	Monlith Dry Mass (g)	Surface Area (cm^2)	Solution Volume (mL)	Monolith Volume (m^3)	M_{ti} (mg/m^2)	ρ (kg/m^3)	Co (mg$_{Tc}$/kg$_{mono}$)	D_e (m^2/s)	D_e (cm^2/s)	Average D_e (cm^2/s)	Standard Deviation of Average De
S014-16-T5-2	3.21	04/12/2016 08:30:0	05/3/2016 09:00:00	365.93	283.58	197.86	1780.7	1.97E-04	2.89E-01	1.44E+03	7.67	2.9E-15	2.9E-11	2.7E-11	2.2E-12
S014-16-T5-3	3.02	04/12/2016 08:30:0	05/3/2016 09:00:00	364.75	282.66	195.03	1755.3	1.92E-04	2.72E-01	1.47E+03	7.67	2.5E-15	2.5E-11		
S014-16-T5-4	0.324	04/12/2016 08:30:0	05/3/2016 09:00:00	366.62	284.11	196.79	1771.1	1.95E-04	2.92E-02	1.46E+03	7.67	2.9E-17	2.9E-13	3.3E-13	4.3E-14
S014-16-T5-7	0.364	04/12/2016 08:30:0	05/3/2016 09:00:00	365.76	283.44	197.96	1781.6	1.97E-04	3.28E-02	1.44E+03	7.67	3.8E-17	3.8E-13		

T6

Name	Tc (µg/L)	Interval Begin	Sampling Date	Monlith mass (g)	Monlith Dry Mass (g)	Surface Area (cm^2)	Solution Volume (mL)	Monolith Volume (m^3)	M_{ti} (mg/m^2)	ρ (kg/m^3)	Co (mg$_{Tc}$/kg$_{mono}$)	D_e (m^2/s)	D_e (cm^2/s)	Average D_e (cm^2/s)	Standard Deviation of Average De
S014-16-T6-2	3.02	04/12/2016 08:30:0	05/3/2016 09:00:00	363.78	284.09	196.70	1770.3	1.95E-04	2.72E-01	1.45E+03	7.95	2.4E-15	2.4E-11	2.2E-11	1.8E-12
S014-16-T6-3	2.77	04/12/2016 08:30:0	05/3/2016 09:00:00	364.78	284.87	197.29	1775.6	1.96E-04	2.49E-01	1.45E+03	7.95	2.0E-15	2.0E-11		
S014-16-T6-5	0.315	04/12/2016 08:30:0	05/3/2016 09:00:00	362.95	283.44	196.39	1767.5	1.95E-04	2.84E-02	1.45E+03	7.95	2.6E-17	2.6E-13	2.9E-13	3.0E-14
S014-16-T6-6	0.355	04/12/2016 08:30:0	05/3/2016 09:00:00	360.98	281.90	193.67	1743.0	1.91E-04	3.20E-02	1.48E+03	7.95	3.2E-17	3.2E-13		

Moisture and Solids Content Calculation

Test	Monolith ID	Mass of tin	Mass of tin+ sample (g)	Final Dry Mass of sample + tin(g)	Mass of sample- M_{test} (g)	Dry mass of sample - M_{dry} (g)	Solids Content	Moisture Content	Average Solids Content	Average Moisture Content
T1 #1	S014-16-T1-9	33.2525	35.6244	35.0789	2.37	1.83	0.77	0.23	0.77	0.23
T1 #2	S014-16-T1-9	33.4181	35.1077	34.7220	1.69	1.30	0.77	0.23		
T2 #1	S014-16-T2-9	33.3539	35.3388	34.8938	1.98	1.54	0.78	0.22	0.78	0.22
T2 #2	S014-16-T2-9	33.3010	35.8891	35.3155	2.59	2.01	0.78	0.22		
T3 #1	S014-16-T3-9	33.3404	35.0038	34.6367	1.66	1.30	0.78	0.22	0.78	0.22
T3 #2	S014-16-T3-9	33.3936	35.6278	35.1317	2.23	1.74	0.78	0.22		
T4 #1	S014-16-T4-9	33.2818	35.0115	34.6307	1.73	1.35	0.78	0.22	0.78	0.22
T4 #2	S014-16-T4-9	33.2891	35.5722	35.0726	2.28	1.78	0.78	0.22		
T5 #1	S014-16-T5-9	33.4410	34.6813	34.4047	1.24	0.96	0.78	0.22	0.77	0.23
T5 #2	S014-16-T5-9	33.4081	34.4244	34.1936	1.02	0.79	0.77	0.23		
T6 #1	S014-16-T6-9	33.2984	34.5803	34.2994	1.28	1.00	0.78	0.22	0.78	0.22
T6#2	S014-16-T6-9	33.2771	34.4953	34.2285	1.22	0.95	0.78	0.22		

Tc Co Calculation

Tc Co Calculation

LIMS Data

LIMS data on Tc concentration measurement from the spiked 6.5 M Na simulants

These values show the initial Tc content of the simulant prior to any getter addition

Test	LabNumber	SampleName	Result	Units	EQL
T1	1601042-01	T1 Initial	17800	ug/L	16.5
T2	1601042-03	T2 Initial	17700	ug/L	16.5
T3	1601042-05	T3 Initial	16000	ug/L	16.5
T4	1601042-08	T4 Initial	18900	ug/L	16.5
T5	1601042-11	T5 Initial	16400	ug/L	16.5
T6	1601042-13	T6 Initial	17100	ug/L	16.5
			3		

Simulant Volume

Density of the 6.5 M Na Average simulant [g/mL] 1.31

Test	Simulant Bottle Tare (g)	Bottle + Simulant (g)	Simulant Mass	Simulant Volume-(mL)	Simulant Volume after sampling (mL)	Dry Blend (g)	Total Weight of Slurry [g]
T1	100.1	1407.8	1307.7	998.244275	994.2443	1750.0	2744.24427
T2	100.3	1408.1	1307.8	998.320611	994.3206	1757.3	2751.57061
T3	100.1	1407.9	1307.8	998.320611	994.3206	1750.0	2744.32061
T4	100	1408	1308	998.473282	994.4733	1745.0	2739.42328
T5	99.8	1408	1308.2	998.625954	994.626	1750.0	2744.62595
T6	99.9	1410.2	1310.3	1000.22901	996.229	1747.6	2743.77901

Co

Calculation on Tc C_0 in dry Cast Stone (mg/kg) monolith

	T1	T2	T3	T4	T5	T6
Dry solid fraction in Cast Stone Monolith	0.771	0.78	0.78	0.78	0.77	0.78

Test	Tc (ug/g wet Cast Stone)-analytical	C_0 (mg/kg) in dry Cast Stone - analytical
T1	6.449	**8.366**
T2	6.396	**8.231**
T3	5.797	**7.445**
T4	6.861	**8.791**
T5	5.943	**7.669**
T6	6.209	**7.950**

I Sampling 2h

Experiment Start 3/1/16 8:30:00

T1

Name	I (µg/L)	Interval Begin	Sampling Date	Monlith mass (g)	Monlith Dry Mass (g)	Surface Area (cm^2)	Solution Volume (mL)	Monolith Volume (m^3)	M_{ti} (mg/m^2)	ρ (kg/m^3)	Co (mg$_{Tc}$/kg$_{mono}$)	D_e (m^2/s)	D_e (cm^2/s)	Average D_e (cm^2/s)	Standard Deviation of Average De
S014-16-T1-1	2.46	3/1/2016 8:30:	3/1/2016 10:30:0	359.63	277.23	192.53	1732.8	1.89E-04	2.21E-01	1.46E+03	2.21	5.1E-13	5.1E-09	5.0E-09	7.7E-11
S014-16-T1-2	2.34	3/1/2016 8:30:	3/1/2016 10:30:0	365.20	281.52	199.18	1792.6	1.99E-04	2.11E-01	1.41E+03	2.21	4.9E-13	4.9E-09		
S014-16-T1-4	3.56	3/1/2016 8:30:	3/1/2016 10:30:0	360.86	278.18	195.83	1762.5	1.95E-04	3.20E-01	1.43E+03	2.21	1.1E-12	1.1E-08	1.1E-08	2.2E-10
S014-16-T1-7	3.54	3/1/2016 8:30:	3/1/2016 10:30:0	361.60	278.75	194.35	1749.2	1.92E-04	3.19E-01	1.45E+03	2.21	1.1E-12	1.1E-08		

T2

Name	I (µg/L)	Interval Begin	Sampling Date	Monlith mass (g)	Monlith Dry Mass (g)	Surface Area (cm^2)	Solution Volume (mL)	Monolith Volume (m^3)	M_{ti} (mg/m^2)	ρ (kg/m^3)	Co (mg$_{Tc}$/kg$_{mono}$)	D_e (m^2/s)	D_e (cm^2/s)	Average D_e (cm^2/s)	Standard Deviation of Average De
S014-16-T2-3	1.94	3/1/2016 8:30:	3/1/2016 10:30:0	364.71	283.41	195.83	1749.7	1.92E-04	1.73E-01	1.48E+03	2.24	3.0E-13	3.0E-09	3.4E-09	4.0E-10
S014-16-T2-6	2.13	3/1/2016 8:30:	3/1/2016 10:30:0	367.70	285.74	197.83	1780.5	1.97E-04	1.92E-01	1.45E+03	2.24	3.8E-13	3.8E-09		
S014-16-T2-7	3.39	3/1/2016 8:30:	3/1/2016 10:30:0	366.00	284.41	196.77	1770.9	1.95E-04	3.05E-01	1.46E+03	2.24	9.6E-13	9.6E-09	8.5E-09	1.1E-09
S014-16-T2-8	2.91	3/1/2016 8:30:	3/1/2016 10:30:0	363.14	282.19	197.90	1781.1	1.97E-04	2.62E-01	1.43E+03	2.24	7.3E-13	7.3E-09		

T3

Name	I (µg/L)	Interval Begin	Sampling Date	Monlith mass (g)	Monlith Dry Mass (g)	Surface Area (cm^2)	Solution Volume (mL)	Monolith Volume (m^3)	M_{ti} (mg/m^2)	ρ (kg/m^3)	Co (mg$_{Tc}$/kg$_{mono}$)	D_e (m^2/s)	D_e (cm^2/s)	Average D_e (cm^2/s)	Standard Deviation of Average De
S014-16-T3-1	2.55	3/1/2016 8:30:	3/1/2016 10:30:0	366.62	285.46	195.87	1762.9	1.94E-04	2.30E-01	1.47E+03	2.45	4.4E-13	4.4E-09	6.4E-09	2.0E-09
S014-16-T3-3	3.48	3/1/2016 8:30:	3/1/2016 10:30:0	364.46	283.78	195.53	1759.7	1.94E-04	3.13E-01	1.46E+03	2.45	8.3E-13	8.3E-09		
S014-16-T3-4	3.92	3/1/2016 8:30:	3/1/2016 10:30:0	362.76	282.46	194.51	1750.6	1.93E-04	3.53E-01	1.47E+03	2.45	1.1E-12	1.1E-08	1.3E-08	2.6E-09
S014-16-T3-8	4.77	3/1/2016 8:30:	3/1/2016 10:30:0	360.88	280.99	194.17	1747.5	1.92E-04	4.29E-01	1.46E+03	2.45	1.6E-12	1.6E-08		

T4

Name	I (µg/L)	Interval Begin	Sampling Date	Monlith mass (g)	Monlith Dry Mass (g)	Surface Area (cm^2)	Solution Volume (mL)	Monolith Volume (m^3)	M_{ti} (mg/m^2)	ρ (kg/m^3)	Co (mg$_{Tc}$/kg$_{mono}$)	D_e (m^2/s)	D_e (cm^2/s)	Average D_e (cm^2/s)	Standard Deviation of Average De
S014-16-T4-1	3.74	3/1/2016 8:30:	3/1/2016 10:30:0	364.02	284.12	195.68	1761.2	1.94E-04	3.37E-01	1.46E+03	2.14	1.3E-12	1.3E-08	1.0E-08	2.3E-09
S014-16-T4-2	2.96	3/1/2016 8:30:	3/1/2016 10:30:0	369.27	288.22	199.22	1793.0	1.99E-04	2.66E-01	1.45E+03	2.14	8.1E-13	8.1E-09		
S014-16-T4-5	2.65	3/1/2016 8:30:	3/1/2016 10:30:0	365.37	285.18	195.92	1763.3	1.94E-04	2.39E-01	1.47E+03	2.14	6.3E-13	6.3E-09	1.1E-08	4.6E-09
S014-16-T4-7	4.1	3/1/2016 8:30:	3/1/2016 10:30:0	363.93	284.05	196.69	1770.2	1.96E-04	3.69E-01	1.45E+03	2.14	1.5E-12	1.5E-08		

T5

Name	I (µg/L)	Interval Begin	Sampling Date	Monlith mass (g)	Monlith Dry Mass (g)	Surface Area (cm^2)	Solution Volume (mL)	Monolith Volume (m^3)	M_{ti} (mg/m^2)	ρ (kg/m^3)	Co (mg$_{Tc}$/kg$_{mono}$)	D_e (m^2/s)	D_e (cm^2/s)	Average D_e (cm^2/s)	Standard Deviation of Average De
S014-16-T5-2	2.51	3/1/2016 8:30:	3/1/2016 10:30:0	365.93	283.58	197.86	1780.7	1.97E-04	2.26E-01	1.44E+03	2.15	5.8E-13	5.8E-09	5.3E-09	5.2E-10
S014-16-T5-3	2.32	3/1/2016 8:30:	3/1/2016 10:30:0	364.75	282.66	195.03	1755.3	1.92E-04	2.09E-01	1.47E+03	2.15	4.8E-13	4.8E-09		
S014-16-T5-4	4.17	3/1/2016 8:30:	3/1/2016 10:30:0	366.62	284.11	196.79	1771.1	1.95E-04	3.75E-01	1.46E+03	2.15	1.6E-12	1.6E-08	1.6E-08	2.8E-11
S014-16-T5-7	4.11	3/1/2016 8:30:	3/1/2016 10:30:0	365.76	283.44	197.96	1781.6	1.97E-04	3.70E-01	1.44E+03	2.15	1.6E-12	1.6E-08		

T6

Name	I (µg/L)	Interval Begin	Sampling Date	Monlith mass (g)	Monlith Dry Mass (g)	Surface Area (cm^2)	Solution Volume (mL)	Monolith Volume (m^3)	M_{ti} (mg/m^2)	ρ (kg/m^3)	Co (mg$_{Tc}$/kg$_{mono}$)	D_e (m^2/s)	D_e (cm^2/s)	Average D_e (cm^2/s)	Standard Deviation of Average De
S014-16-T6-2	2.86	3/1/2016 8:30:	3/1/2016 10:30:0	363.78	284.09	196.70	1770.3	1.95E-04	2.57E-01	1.45E+03	2.15	7.4E-13	7.4E-09	8.0E-09	6.6E-10
S014-16-T6-3	3.1	3/1/2016 8:30:	3/1/2016 10:30:0	364.78	284.87	197.29	1775.6	1.96E-04	2.79E-01	1.45E+03	2.15	8.7E-13	8.7E-09		
S014-16-T6-5	4.02	3/1/2016 8:30:	3/1/2016 10:30:0	362.95	283.44	196.39	1767.5	1.95E-04	3.62E-01	1.45E+03	2.15	1.5E-12	1.5E-08	1.1E-08	3.6E-09
S014-16-T6-6	2.91	3/1/2016 8:30:	3/1/2016 10:30:0	360.98	281.90	193.67	1743.0	1.91E-04	2.62E-01	1.48E+03	2.15	7.4E-13	7.4E-09		

I Sampling 1 d

Experiment Start 3/1/16 8:30:00

T1

Name	I (µg/L)	Interval Begin	Sampling Date	Monlith mass (g)	Monlith Dry Mass (g)	Surface Area (cm^2)	Solution Volume (mL)	Monolith Volume (m^3)	M_{ti} (mg/m^2)	ρ (kg/m^3)	Co (mg$_{Tc}$/kg$_{mono}$)	D_e (m^2/s)	D_e (cm^2/s)	Average D_e (cm^2/s)	Standard Deviation of Average De
S014-16-T1-1	12.1	3/1/2016 10:30:00	3/2/2016 8:30:00	359.63	277.23	192.53	1732.8	1.89E-04	1.09E+00	1.46E+03	2.21	2.0E-12	2.0E-08	2.0E-08	6.6E-10
S014-16-T1-2	11.3	3/1/2016 10:30:00	3/2/2016 8:30:00	365.20	281.52	199.18	1792.6	1.99E-04	1.02E+00	1.41E+03	2.21	1.9E-12	1.9E-08		
S014-16-T1-4	12.1	3/1/2016 10:30:00	3/2/2016 8:30:00	360.86	278.18	195.83	1762.5	1.95E-04	1.09E+00	1.43E+03	2.21	2.1E-12	2.1E-08	3.5E-08	1.4E-08
S014-16-T1-7	18.5	3/1/2016 10:30:00	3/2/2016 8:30:00	361.60	278.75	194.35	1749.2	1.92E-04	1.67E+00	1.45E+03	2.21	4.8E-12	4.8E-08		

T2

Name	I (µg/L)	Interval Begin	Sampling Date	Monlith mass (g)	Monlith Dry Mass (g)	Surface Area (cm^2)	Solution Volume (mL)	Monolith Volume (m^3)	M_{ti} (mg/m^2)	ρ (kg/m^3)	Co (mg$_{Tc}$/kg$_{mono}$)	D_e (m^2/s)	D_e (cm^2/s)	Average D_e (cm^2/s)	Standard Deviation of Average De
S014-16-T2-3	16.1	3/1/2016 10:30:00	3/2/2016 8:30:00	364.71	283.41	195.83	1749.7	1.92E-04	1.44E+00	1.48E+03	2.24	3.4E-12	3.4E-08	3.6E-08	2.0E-09
S014-16-T2-6	16.6	3/1/2016 10:30:00	3/2/2016 8:30:00	367.70	285.74	197.83	1780.5	1.97E-04	1.49E+00	1.45E+03	2.24	3.8E-12	3.8E-08		
S014-16-T2-7	13.2	3/1/2016 10:30:00	3/2/2016 8:30:00	366.00	284.41	196.77	1770.9	1.95E-04	1.19E+00	1.46E+03	2.24	2.4E-12	2.4E-08	2.8E-08	3.8E-09
S014-16-T2-8	14.9	3/1/2016 10:30:00	3/2/2016 8:30:00	363.14	282.19	197.90	1781.1	1.97E-04	1.34E+00	1.43E+03	2.24	3.2E-12	3.2E-08		

T3

Name	I (µg/L)	Interval Begin	Sampling Date	Monlith mass (g)	Monlith Dry Mass (g)	Surface Area (cm^2)	Solution Volume (mL)	Monolith Volume (m^3)	M_{ti} (mg/m^2)	ρ (kg/m^3)	Co (mg$_{Tc}$/kg$_{mono}$)	D_e (m^2/s)	D_e (cm^2/s)	Average D_e (cm^2/s)	Standard Deviation of Average De
S014-16-T3-1	9.42	3/1/2016 10:30:00	3/2/2016 8:30:00	366.62	285.46	195.87	1762.9	1.94E-04	8.48E-01	1.47E+03	2.45	9.9E-13	9.9E-09	1.1E-08	1.4E-09
S014-16-T3-3	10.6	3/1/2016 10:30:00	3/2/2016 8:30:00	364.46	283.78	195.53	1759.7	1.94E-04	9.54E-01	1.46E+03	2.45	1.3E-12	1.3E-08		
S014-16-T3-4	7.1	3/1/2016 10:30:00	3/2/2016 8:30:00	362.76	282.46	194.51	1750.6	1.93E-04	6.39E-01	1.47E+03	2.45	5.7E-13	5.7E-09	1.3E-08	7.7E-09
S014-16-T3-8	13.6	3/1/2016 10:30:00	3/2/2016 8:30:00	360.88	280.99	194.17	1747.5	1.92E-04	1.22E+00	1.46E+03	2.45	2.1E-12	2.1E-08		

T4

Name	I (µg/L)	Interval Begin	Sampling Date	Monlith mass (g)	Monlith Dry Mass (g)	Surface Area (cm^2)	Solution Volume (mL)	Monolith Volume (m^3)	M_{ti} (mg/m^2)	ρ (kg/m^3)	Co (mg$_{Tc}$/kg$_{mono}$)	D_e (m^2/s)	D_e (cm^2/s)	Average D_e (cm^2/s)	Standard Deviation of Average De
S014-16-T4-1	11.9	3/1/2016 10:30:00	3/2/2016 8:30:00	364.02	284.12	195.68	1761.2	1.94E-04	1.07E+00	1.46E+03	2.14	2.1E-12	2.1E-08	2.4E-08	2.5E-09
S014-16-T4-2	13.1	3/1/2016 10:30:00	3/2/2016 8:30:00	369.27	288.22	199.22	1793.0	1.99E-04	1.18E+00	1.45E+03	2.14	2.6E-12	2.6E-08		
S014-16-T4-5	11.9	3/1/2016 10:30:00	3/2/2016 8:30:00	365.37	285.18	195.92	1763.3	1.94E-04	1.07E+00	1.47E+03	2.14	2.1E-12	2.1E-08	2.1E-08	2.9E-10
S014-16-T4-7	11.6	3/1/2016 10:30:00	3/2/2016 8:30:00	363.93	284.05	196.69	1770.2	1.96E-04	1.04E+00	1.45E+03	2.14	2.0E-12	2.0E-08		

T5

Name	I (µg/L)	Interval Begin	Sampling Date	Monlith mass (g)	Monlith Dry Mass (g)	Surface Area (cm^2)	Solution Volume (mL)	Monolith Volume (m^3)	M_{ti} (mg/m^2)	ρ (kg/m^3)	Co (mg$_{Tc}$/kg$_{mono}$)	D_e (m^2/s)	D_e (cm^2/s)	Average D_e (cm^2/s)	Standard Deviation of Average De
S014-16-T5-2	8.95	3/1/2016 10:30:00	3/2/2016 8:30:00	365.93	283.58	197.86	1780.7	1.97E-04	8.06E-01	1.44E+03	2.15	1.2E-12	1.2E-08	1.5E-08	2.7E-09
S014-16-T5-3	11	3/1/2016 10:30:00	3/2/2016 8:30:00	364.75	282.66	195.03	1755.3	1.92E-04	9.90E-01	1.47E+03	2.15	1.8E-12	1.8E-08		
S014-16-T5-4	13.9	3/1/2016 10:30:00	3/2/2016 8:30:00	366.62	284.11	196.79	1771.1	1.95E-04	1.25E+00	1.46E+03	2.15	2.9E-12	2.9E-08	2.8E-08	1.1E-09
S014-16-T5-7	13.2	3/1/2016 10:30:00	3/2/2016 8:30:00	365.76	283.44	197.96	1781.6	1.97E-04	1.19E+00	1.44E+03	2.15	2.7E-12	2.7E-08		

T6

Name	I (µg/L)	Interval Begin	Sampling Date	Monlith mass (g)	Monlith Dry Mass (g)	Surface Area (cm^2)	Solution Volume (mL)	Monolith Volume (m^3)	M_{ti} (mg/m^2)	ρ (kg/m^3)	Co (mg$_{Tc}$/kg$_{mono}$)	D_e (m^2/s)	D_e (cm^2/s)	Average D_e (cm^2/s)	Standard Deviation of Average De
S014-16-T6-2	13.9	3/1/2016 10:30:00	3/2/2016 8:30:00	363.78	284.09	196.70	1770.3	1.95E-04	1.25E+00	1.45E+03	2.15	2.9E-12	2.9E-08	2.7E-08	1.4E-09
S014-16-T6-3	13.2	3/1/2016 10:30:00	3/2/2016 8:30:00	364.78	284.87	197.29	1775.6	1.96E-04	1.19E+00	1.45E+03	2.15	2.6E-12	2.6E-08		
S014-16-T6-5	13.7	3/1/2016 10:30:00	3/2/2016 8:30:00	362.95	283.44	196.39	1767.5	1.95E-04	1.23E+00	1.45E+03	2.15	2.8E-12	2.8E-08	2.5E-08	3.1E-09
S014-16-T6-6	12.3	3/1/2016 10:30:00	3/2/2016 8:30:00	360.98	281.90	193.67	1743.0	1.91E-04	1.11E+00	1.48E+03	2.15	2.2E-12	2.2E-08		

I Sampling 2 d

		Experiment Start	3/1/16 8:30:00												

T1

Name	I (μg/L)	Interval Begin	Sampling Date	Monlith mass (g)	Monlith Dry Mass (g)	Surface Area (cm^2)	Solution Volume (mL)	Monolith Volume (m^3)	M_{ti} (mg/m^2)	ρ (kg/m^3)	Co (mg$_{Tc}$/kg$_{mono}$)	D_e (m^2/s)	D_e (cm^2/s)	Average D_e (cm^2/s)	Standard Deviation of Average De
S014-16-T1-1	6.74	3/2/2016 8:30:(	3/3/2016 8:30:00	359.63	277.23	192.53	1732.8	1.89E-04	6.07E-01	1.46E+03	2.21	1.9E-12	1.9E-08	1.9E-08	3.1E-11
S014-16-T1-2	6.5	3/2/2016 8:30:(	3/3/2016 8:30:00	365.20	281.52	199.18	1792.6	1.99E-04	5.85E-01	1.41E+03	2.21	1.8E-12	1.8E-08		
S014-16-T1-4	8.32	3/2/2016 8:30:(	3/3/2016 8:30:00	360.86	278.18	195.83	1762.5	1.95E-04	7.49E-01	1.43E+03	2.21	3.0E-12	3.0E-08	2.9E-08	9.1E-10
S014-16-T1-7	8.18	3/2/2016 8:30:(	3/3/2016 8:30:00	361.60	278.75	194.35	1749.2	1.92E-04	7.36E-01	1.45E+03	2.21	2.8E-12	2.8E-08		

T2

Name	I (μg/L)	Interval Begin	Sampling Date	Monlith mass (g)	Monlith Dry Mass (g)	Surface Area (cm^2)	Solution Volume (mL)	Monolith Volume (m^3)	M_{ti} (mg/m^2)	ρ (kg/m^3)	Co (mg$_{Tc}$/kg$_{mono}$)	D_e (m^2/s)	D_e (cm^2/s)	Average D_e (cm^2/s)	Standard Deviation of Average De
S014-16-T2-3	12.1	3/2/2016 8:30:(	3/3/2016 8:30:00	364.71	283.41	195.83	1749.7	1.92E-04	1.08E+00	1.48E+03	2.24	5.7E-12	5.7E-08	6.3E-08	6.6E-09
S014-16-T2-6	13.1	3/2/2016 8:30:(	3/3/2016 8:30:00	367.70	285.74	197.83	1780.5	1.97E-04	1.18E+00	1.45E+03	2.24	7.0E-12	7.0E-08		
S014-16-T2-7	12.5	3/2/2016 8:30:(	3/3/2016 8:30:00	366.00	284.41	196.77	1770.9	1.95E-04	1.13E+00	1.46E+03	2.24	6.3E-12	6.3E-08	6.1E-08	1.9E-09
S014-16-T2-8	11.9	3/2/2016 8:30:(	3/3/2016 8:30:00	363.14	282.19	197.90	1781.1	1.97E-04	1.07E+00	1.43E+03	2.24	5.9E-12	5.9E-08		

T3

Name	I (μg/L)	Interval Begin	Sampling Date	Monlith mass (g)	Monlith Dry Mass (g)	Surface Area (cm^2)	Solution Volume (mL)	Monolith Volume (m^3)	M_{ti} (mg/m^2)	ρ (kg/m^3)	Co (mg$_{Tc}$/kg$_{mono}$)	D_e (m^2/s)	D_e (cm^2/s)	Average D_e (cm^2/s)	Standard Deviation of Average De
S014-16-T3-1	5.74	3/2/2016 8:30:(	3/3/2016 8:40:00	366.62	285.46	195.87	1762.9	1.94E-04	5.17E-01	1.47E+03	2.45	1.1E-12	1.1E-08	1.4E-08	3.3E-09
S014-16-T3-3	7.25	3/2/2016 8:30:(	3/3/2016 8:40:01	364.46	283.78	195.53	1759.7	1.94E-04	6.53E-01	1.46E+03	2.45	1.7E-12	1.7E-08		
S014-16-T3-4	7.28	3/2/2016 8:30:(	3/3/2016 8:40:02	362.76	282.46	194.51	1750.6	1.93E-04	6.55E-01	1.47E+03	2.45	1.7E-12	1.7E-08	1.7E-08	3.5E-10
S014-16-T3-8	7.11	3/2/2016 8:30:(	3/3/2016 8:40:03	360.88	280.99	194.17	1747.5	1.92E-04	6.40E-01	1.46E+03	2.45	1.7E-12	1.7E-08		

T4

Name	I (μg/L)	Interval Begin	Sampling Date	Monlith mass (g)	Monlith Dry Mass (g)	Surface Area (cm^2)	Solution Volume (mL)	Monolith Volume (m^3)	M_{ti} (mg/m^2)	ρ (kg/m^3)	Co (mg$_{Tc}$/kg$_{mono}$)	D_e (m^2/s)	D_e (cm^2/s)	Average D_e (cm^2/s)	Standard Deviation of Average De
S014-16-T4-1	8.32	3/2/2016 8:30:(	3/3/2016 8:40:00	364.02	284.12	195.68	1761.2	1.94E-04	7.49E-01	1.46E+03	2.14	3.0E-12	3.0E-08	2.8E-08	1.9E-09
S014-16-T4-2	7.7	3/2/2016 8:30:(	3/3/2016 8:40:01	369.27	288.22	199.22	1793.0	1.99E-04	6.93E-01	1.45E+03	2.14	2.6E-12	2.6E-08		
S014-16-T4-5	9.3	3/2/2016 8:30:(	3/3/2016 8:40:02	365.37	285.18	195.92	1763.3	1.94E-04	8.37E-01	1.47E+03	2.14	3.7E-12	3.7E-08	3.3E-08	4.4E-09
S014-16-T4-7	8.04	3/2/2016 8:30:(	3/3/2016 8:40:03	363.93	284.05	196.69	1770.2	1.96E-04	7.24E-01	1.45E+03	2.14	2.8E-12	2.8E-08		

T5

Name	I (μg/L)	Interval Begin	Sampling Date	Monlith mass (g)	Monlith Dry Mass (g)	Surface Area (cm^2)	Solution Volume (mL)	Monolith Volume (m^3)	M_{ti} (mg/m^2)	ρ (kg/m^3)	Co (mg$_{Tc}$/kg$_{mono}$)	D_e (m^2/s)	D_e (cm^2/s)	Average D_e (cm^2/s)	Standard Deviation of Average De
S014-16-T5-2	6.03	3/2/2016 8:30:(	3/3/2016 8:40:00	365.93	283.58	197.86	1780.7	1.97E-04	5.43E-01	1.44E+03	2.15	1.6E-12	1.6E-08	1.7E-08	1.2E-09
S014-16-T5-3	6.58	3/2/2016 8:30:(	3/3/2016 8:40:01	364.75	282.66	195.03	1755.3	1.92E-04	5.92E-01	1.47E+03	2.15	1.8E-12	1.8E-08		
S014-16-T5-4	7.83	3/2/2016 8:30:(	3/3/2016 8:40:02	366.62	284.11	196.79	1771.1	1.95E-04	7.05E-01	1.46E+03	2.15	2.7E-12	2.7E-08	2.8E-08	1.8E-09
S014-16-T5-7	8.24	3/2/2016 8:30:(	3/3/2016 8:40:03	365.76	283.44	197.96	1781.6	1.97E-04	7.42E-01	1.44E+03	2.15	3.0E-12	3.0E-08		

T6

Name	I (μg/L)	Interval Begin	Sampling Date	Monlith mass (g)	Monlith Dry Mass (g)	Surface Area (cm^2)	Solution Volume (mL)	Monolith Volume (m^3)	M_{ti} (mg/m^2)	ρ (kg/m^3)	Co (mg$_{Tc}$/kg$_{mono}$)	D_e (m^2/s)	D_e (cm^2/s)	Average D_e (cm^2/s)	Standard Deviation of Average De
S014-16-T6-2	7.15	3/2/2016 8:30:(	3/3/2016 8:40:00	363.78	284.09	196.70	1770.3	1.95E-04	6.44E-01	1.45E+03	2.15	2.2E-12	2.2E-08	2.1E-08	8.8E-10
S014-16-T6-3	6.85	3/2/2016 8:30:(	3/3/2016 8:40:01	364.78	284.87	197.29	1775.6	1.96E-04	6.17E-01	1.45E+03	2.15	2.0E-12	2.0E-08		
S014-16-T6-5	8.55	3/2/2016 8:30:(	3/3/2016 8:40:02	362.95	283.44	196.39	1767.5	1.95E-04	7.70E-01	1.45E+03	2.15	3.2E-12	3.2E-08	3.0E-08	2.0E-09
S014-16-T6-6	8.11	3/2/2016 8:30:(	3/3/2016 8:40:03	360.98	281.90	193.67	1743.0	1.91E-04	7.30E-01	1.48E+03	2.15	2.8E-12	2.8E-08		

I Sampling 7 d

		Experiment Start	3/1/16 8:30:00

T1

Name	I (µg/L)	Interval Begin	Sampling Date	Monlith mass (g)	Monlith Dry Mass (g)	Surface Area (cm^2)	Solution Volume (mL)	Monolith Volume (m^3)	M_{ti} (mg/m^2)	ρ (kg/m^3)	Co (mg$_{Tc}$/kg$_{mono}$)	D_e (m^2/s)	D_e (cm^2/s)	Average D_e (cm^2/s)	Standard Deviation of Average De
S014-16-T1-1	24.5	3/3/2016 8:40:0	3/8/2016 8:40:00	359.63	277.23	192.53	1732.8	1.89E-04	2.21E+00	1.46E+03	2.21	2.8E-12	2.8E-08	2.9E-08	8.7E-10
S014-16-T1-2	24.4	3/3/2016 8:40:0	3/8/2016 8:40:00	365.20	281.52	199.18	1792.6	1.99E-04	2.20E+00	1.41E+03	2.21	3.0E-12	3.0E-08		
S014-16-T1-4	22.9	3/3/2016 8:40:0	3/8/2016 8:40:00	360.86	278.18	195.83	1762.5	1.95E-04	2.06E+00	1.43E+03	2.21	2.6E-12	2.6E-08	2.6E-08	8.5E-10
S014-16-T1-7	24	3/3/2016 8:40:0	3/8/2016 8:40:00	361.60	278.75	194.35	1749.2	1.92E-04	2.16E+00	1.45E+03	2.21	2.7E-12	2.7E-08		

T2

Name	I (µg/L)	Interval Begin	Sampling Date	Monlith mass (g)	Monlith Dry Mass (g)	Surface Area (cm^2)	Solution Volume (mL)	Monolith Volume (m^3)	M_{ti} (mg/m^2)	ρ (kg/m^3)	Co (mg$_{Tc}$/kg$_{mono}$)	D_e (m^2/s)	D_e (cm^2/s)	Average D_e (cm^2/s)	Standard Deviation of Average De
S014-16-T2-3	32.3	3/3/2016 8:40:0	3/8/2016 8:40:00	364.71	283.41	195.83	1749.7	1.92E-04	2.89E+00	1.48E+03	2.24	4.6E-12	4.6E-08	4.9E-08	3.5E-09
S014-16-T2-6	33.8	3/3/2016 8:40:0	3/8/2016 8:40:00	367.70	285.74	197.83	1780.5	1.97E-04	3.04E+00	1.45E+03	2.24	5.3E-12	5.3E-08		
S014-16-T2-7	29.3	3/3/2016 8:40:0	3/8/2016 8:40:00	366.00	284.41	196.77	1770.9	1.95E-04	2.64E+00	1.46E+03	2.24	3.9E-12	3.9E-08	4.3E-08	3.3E-09
S014-16-T2-8	31.1	3/3/2016 8:40:0	3/8/2016 8:40:00	363.14	282.19	197.90	1781.1	1.97E-04	2.80E+00	1.43E+03	2.24	4.6E-12	4.6E-08		

T3

Name	I (µg/L)	Interval Begin	Sampling Date	Monlith mass (g)	Monlith Dry Mass (g)	Surface Area (cm^2)	Solution Volume (mL)	Monolith Volume (m^3)	M_{ti} (mg/m^2)	ρ (kg/m^3)	Co (mg$_{Tc}$/kg$_{mono}$)	D_e (m^2/s)	D_e (cm^2/s)	Average D_e (cm^2/s)	Standard Deviation of Average De
S014-16-T3-1	20.1	3/3/2016 8:40:0	3/8/2016 8:40:00	366.62	285.46	195.87	1762.9	1.94E-04	1.81E+00	1.47E+03	2.45	1.5E-12	1.5E-08	1.5E-08	2.0E-10
S014-16-T3-3	19.7	3/3/2016 8:40:0	3/8/2016 8:40:00	364.46	283.78	195.53	1759.7	1.94E-04	1.77E+00	1.46E+03	2.45	1.5E-12	1.5E-08		
S014-16-T3-4	19.5	3/3/2016 8:40:0	3/8/2016 8:40:00	362.76	282.46	194.51	1750.6	1.93E-04	1.76E+00	1.47E+03	2.45	1.4E-12	1.4E-08	1.5E-08	9.7E-10
S014-16-T3-8	20.7	3/3/2016 8:40:0	3/8/2016 8:40:00	360.88	280.99	194.17	1747.5	1.92E-04	1.86E+00	1.46E+03	2.45	1.6E-12	1.6E-08		

T4

Name	I (µg/L)	Interval Begin	Sampling Date	Monlith mass (g)	Monlith Dry Mass (g)	Surface Area (cm^2)	Solution Volume (mL)	Monolith Volume (m^3)	M_{ti} (mg/m^2)	ρ (kg/m^3)	Co (mg$_{Tc}$/kg$_{mono}$)	D_e (m^2/s)	D_e (cm^2/s)	Average D_e (cm^2/s)	Standard Deviation of Average De
S014-16-T4-1	25.7	3/3/2016 8:40:0	3/8/2016 8:40:00	364.02	284.12	195.68	1761.2	1.94E-04	2.31E+00	1.46E+03	2.14	3.3E-12	3.3E-08	3.1E-08	1.3E-09
S014-16-T4-2	24.4	3/3/2016 8:40:0	3/8/2016 8:40:00	369.27	288.22	199.22	1793.0	1.99E-04	2.20E+00	1.45E+03	2.14	3.0E-12	3.0E-08		
S014-16-T4-5	23.9	3/3/2016 8:40:0	3/8/2016 8:40:00	365.37	285.18	195.92	1763.3	1.94E-04	2.15E+00	1.47E+03	2.14	2.8E-12	2.8E-08	3.0E-08	1.4E-09
S014-16-T4-7	24.8	3/3/2016 8:40:0	3/8/2016 8:40:00	363.93	284.05	196.69	1770.2	1.96E-04	2.23E+00	1.45E+03	2.14	3.1E-12	3.1E-08		

T5

Name	I (µg/L)	Interval Begin	Sampling Date	Monlith mass (g)	Monlith Dry Mass (g)	Surface Area (cm^2)	Solution Volume (mL)	Monolith Volume (m^3)	M_{ti} (mg/m^2)	ρ (kg/m^3)	Co (mg$_{Tc}$/kg$_{mono}$)	D_e (m^2/s)	D_e (cm^2/s)	Average D_e (cm^2/s)	Standard Deviation of Average De
S014-16-T5-2	20.9	3/3/2016 8:40:0	3/8/2016 8:40:00	365.93	283.58	197.86	1780.7	1.97E-04	1.88E+00	1.44E+03	2.15	2.2E-12	2.2E-08	2.3E-08	4.9E-10
S014-16-T5-3	21.8	3/3/2016 8:40:0	3/8/2016 8:40:00	364.75	282.66	195.03	1755.3	1.92E-04	1.96E+00	1.47E+03	2.15	2.3E-12	2.3E-08		
S014-16-T5-4	21.9	3/3/2016 8:40:0	3/8/2016 8:40:00	366.62	284.11	196.79	1771.1	1.95E-04	1.97E+00	1.46E+03	2.15	2.4E-12	2.4E-08	2.7E-08	3.3E-09
S014-16-T5-7	24.4	3/3/2016 8:40:0	3/8/2016 8:40:00	365.76	283.44	197.96	1781.6	1.97E-04	2.20E+00	1.44E+03	2.15	3.0E-12	3.0E-08		

T6

Name	I (µg/L)	Interval Begin	Sampling Date	Monlith mass (g)	Monlith Dry Mass (g)	Surface Area (cm^2)	Solution Volume (mL)	Monolith Volume (m^3)	M_{ti} (mg/m^2)	ρ (kg/m^3)	Co (mg$_{Tc}$/kg$_{mono}$)	D_e (m^2/s)	D_e (cm^2/s)	Average D_e (cm^2/s)	Standard Deviation of Average De
S014-16-T6-2	22.2	3/3/2016 8:40:0	3/8/2016 8:40:00	363.78	284.09	196.70	1770.3	1.95E-04	2.00E+00	1.45E+03	2.15	2.4E-12	2.4E-08	2.5E-08	1.5E-10
S014-16-T6-3	22.3	3/3/2016 8:40:0	3/8/2016 8:40:00	364.78	284.87	197.29	1775.6	1.96E-04	2.01E+00	1.45E+03	2.15	2.5E-12	2.5E-08		
S014-16-T6-5	23.5	3/3/2016 8:40:0	3/8/2016 8:40:00	362.95	283.44	196.39	1767.5	1.95E-04	2.12E+00	1.45E+03	2.15	2.7E-12	2.7E-08	2.8E-08	7.3E-10
S014-16-T6-6	24.5	3/3/2016 8:40:0	3/8/2016 8:40:00	360.98	281.90	193.67	1743.0	1.91E-04	2.21E+00	1.48E+03	2.15	2.9E-12	2.9E-08		

I Sampling 14 d

Experiment Start 3/1/16 8:30:00

T1

Name	I (µg/L)	Interval Begin	Sampling Date	Monlith mass (g)	Monlith Dry Mass (g)	Surface Area (cm^2)	Solution Volume (mL)	Monolith Volume (m^3)	M_{ti} (mg/m^2)	ρ (kg/m^3)	Co (mg$_{Tc}$/kg$_{mono}$)	D_e (m^2/s)	D_e (cm^2/s)	Average D_e (cm^2/s)	Standard Deviation of Average De
S014-16-T1-1	17.7	3/8/2016 8:40:0	3/15/2016 8:50:0	359.63	277.23	192.53	1732.8	1.89E-04	1.59E+00	1.46E+03	2.21	1.8E-12	1.8E-08	1.9E-08	5.4E-10
S014-16-T1-2	17.6	3/8/2016 8:40:0	3/15/2016 8:50:0	365.20	281.52	199.18	1792.6	1.99E-04	1.58E+00	1.41E+03	2.21	1.9E-12	1.9E-08		
S014-16-T1-4	17.7	3/8/2016 8:40:0	3/15/2016 8:50:0	360.86	278.18	195.83	1762.5	1.95E-04	1.59E+00	1.43E+03	2.21	1.9E-12	1.9E-08	2.0E-08	9.1E-10
S014-16-T1-7	18.8	3/8/2016 8:40:0	3/15/2016 8:50:0	361.60	278.75	194.35	1749.2	1.92E-04	1.69E+00	1.45E+03	2.21	2.1E-12	2.1E-08		

T2

Name	I (µg/L)	Interval Begin	Sampling Date	Monlith mass (g)	Monlith Dry Mass (g)	Surface Area (cm^2)	Solution Volume (mL)	Monolith Volume (m^3)	M_{ti} (mg/m^2)	ρ (kg/m^3)	Co (mg$_{Tc}$/kg$_{mono}$)	D_e (m^2/s)	D_e (cm^2/s)	Average D_e (cm^2/s)	Standard Deviation of Average De
S014-16-T2-3	19	3/8/2016 8:40:0	3/15/2016 8:50:0	364.71	283.41	195.83	1749.7	1.92E-04	1.70E+00	1.48E+03	2.24	2.0E-12	2.0E-08	2.2E-08	2.5E-09
S014-16-T2-6	20.7	3/8/2016 8:40:0	3/15/2016 8:50:0	367.70	285.74	197.83	1780.5	1.97E-04	1.86E+00	1.45E+03	2.24	2.5E-12	2.5E-08		
S014-16-T2-7	21.4	3/8/2016 8:40:0	3/15/2016 8:50:0	366.00	284.41	196.77	1770.9	1.95E-04	1.93E+00	1.46E+03	2.24	2.6E-12	2.6E-08	2.5E-08	1.6E-09
S014-16-T2-8	19.7	3/8/2016 8:40:0	3/15/2016 8:50:0	363.14	282.19	197.90	1781.1	1.97E-04	1.77E+00	1.43E+03	2.24	2.3E-12	2.3E-08		

T3

Name	I (µg/L)	Interval Begin	Sampling Date	Monlith mass (g)	Monlith Dry Mass (g)	Surface Area (cm^2)	Solution Volume (mL)	Monolith Volume (m^3)	M_{ti} (mg/m^2)	ρ (kg/m^3)	Co (mg$_{Tc}$/kg$_{mono}$)	D_e (m^2/s)	D_e (cm^2/s)	Average D_e (cm^2/s)	Standard Deviation of Average De
S014-16-T3-1	15.3	3/8/2016 8:40:0	3/15/2016 8:50:0	366.62	285.46	195.87	1762.9	1.94E-04	1.38E+00	1.47E+03	2.45	1.1E-12	1.1E-08	1.1E-08	2.8E-10
S014-16-T3-3	14.8	3/8/2016 8:40:0	3/15/2016 8:50:0	364.46	283.78	195.53	1759.7	1.94E-04	1.33E+00	1.46E+03	2.45	1.0E-12	1.0E-08		
S014-16-T3-4	13.5	3/8/2016 8:40:0	3/15/2016 8:50:0	362.76	282.46	194.51	1750.6	1.93E-04	1.22E+00	1.47E+03	2.45	8.7E-13	8.7E-09	9.9E-09	1.2E-09
S014-16-T3-8	15.2	3/8/2016 8:40:0	3/15/2016 8:50:0	360.88	280.99	194.17	1747.5	1.92E-04	1.37E+00	1.46E+03	2.45	1.1E-12	1.1E-08		

T4

Name	I (µg/L)	Interval Begin	Sampling Date	Monlith mass (g)	Monlith Dry Mass (g)	Surface Area (cm^2)	Solution Volume (mL)	Monolith Volume (m^3)	M_{ti} (mg/m^2)	ρ (kg/m^3)	Co (mg$_{Tc}$/kg$_{mono}$)	D_e (m^2/s)	D_e (cm^2/s)	Average D_e (cm^2/s)	Standard Deviation of Average De
S014-16-T4-1	16.8	3/8/2016 8:40:0	3/15/2016 8:50:0	364.02	284.12	195.68	1761.2	1.94E-04	1.51E+00	1.46E+03	2.14	1.8E-12	1.8E-08	1.9E-08	1.2E-09
S014-16-T4-2	17.7	3/8/2016 8:40:0	3/15/2016 8:50:0	369.27	288.22	199.22	1793.0	1.99E-04	1.59E+00	1.45E+03	2.14	2.0E-12	2.0E-08		
S014-16-T4-5	18.3	3/8/2016 8:40:0	3/15/2016 8:50:0	365.37	285.18	195.92	1763.3	1.94E-04	1.65E+00	1.47E+03	2.14	2.1E-12	2.1E-08	2.1E-08	3.6E-10
S014-16-T4-7	18.4	3/8/2016 8:40:0	3/15/2016 8:50:0	363.93	284.05	196.69	1770.2	1.96E-04	1.66E+00	1.45E+03	2.14	2.2E-12	2.2E-08		

T5

Name	I (µg/L)	Interval Begin	Sampling Date	Monlith mass (g)	Monlith Dry Mass (g)	Surface Area (cm^2)	Solution Volume (mL)	Monolith Volume (m^3)	M_{ti} (mg/m^2)	ρ (kg/m^3)	Co (mg$_{Tc}$/kg$_{mono}$)	D_e (m^2/s)	D_e (cm^2/s)	Average D_e (cm^2/s)	Standard Deviation of Average De
S014-16-T5-2	15.7	3/8/2016 8:40:0	3/15/2016 8:50:0	365.93	283.58	197.86	1780.7	1.97E-04	1.41E+00	1.44E+03	2.15	1.6E-12	1.6E-08	1.6E-08	3.7E-10
S014-16-T5-3	16.4	3/8/2016 8:40:0	3/15/2016 8:50:0	364.75	282.66	195.03	1755.3	1.92E-04	1.48E+00	1.47E+03	2.15	1.7E-12	1.7E-08		
S014-16-T5-4	16.6	3/8/2016 8:40:0	3/15/2016 8:50:0	366.62	284.11	196.79	1771.1	1.95E-04	1.49E+00	1.46E+03	2.15	1.7E-12	1.7E-08	1.9E-08	1.9E-09
S014-16-T5-7	18.1	3/8/2016 8:40:0	3/15/2016 8:50:0	365.76	283.44	197.96	1781.6	1.97E-04	1.63E+00	1.44E+03	2.15	2.1E-12	2.1E-08		

T6

Name	I (µg/L)	Interval Begin	Sampling Date	Monlith mass (g)	Monlith Dry Mass (g)	Surface Area (cm^2)	Solution Volume (mL)	Monolith Volume (m^3)	M_{ti} (mg/m^2)	ρ (kg/m^3)	Co (mg$_{Tc}$/kg$_{mono}$)	D_e (m^2/s)	D_e (cm^2/s)	Average D_e (cm^2/s)	Standard Deviation of Average De
S014-16-T6-2	17.2	3/8/2016 8:40:0	3/15/2016 8:50:0	363.78	284.09	196.70	1770.3	1.95E-04	1.55E+00	1.45E+03	2.15	1.9E-12	1.9E-08	1.9E-08	6.9E-10
S014-16-T6-3	17.8	3/8/2016 8:40:0	3/15/2016 8:50:0	364.78	284.87	197.29	1775.6	1.96E-04	1.60E+00	1.45E+03	2.15	2.0E-12	2.0E-08		
S014-16-T6-5	17.8	3/8/2016 8:40:0	3/15/2016 8:50:0	362.95	283.44	196.39	1767.5	1.95E-04	1.60E+00	1.45E+03	2.15	2.0E-12	2.0E-08	2.0E-08	4.6E-10
S014-16-T6-6	18.5	3/8/2016 8:40:0	3/15/2016 8:50:0	360.98	281.90	193.67	1743.0	1.91E-04	1.67E+00	1.48E+03	2.15	2.1E-12	2.1E-08		

I Sampling 28 d

Experiment Start 3/1/16 8:30:00

T1

Name	I (µg/L)	Interval Begin	Sampling Date	Monlith mass (g)	Monlith Dry Mass (g)	Surface Area (cm^2)	Solution Volume (mL)	Monolith Volume (m^3)	M$_{ti}$ (mg/m^2)	ρ (kg/m^3)	Co (mg$_{Tc}$/kg$_{mono}$)	D$_e$ (m^2/s)	D$_e$ (cm^2/s)	Average D$_e$ (cm^2/s)	Standard Deviation of Average De
S014-16-T1-1	23	03/15/2016 08:50:00	03/29/2016 08:00:0	359.63	277.23	192.53	1732.8	1.89E-04	2.07E+00	1.46E+03	2.21	1.6E-12	1.6E-08	1.5E-08	2.2E-10
S014-16-T1-2	21.9	03/15/2016 08:50:00	03/29/2016 08:00:0	365.20	281.52	199.18	1792.6	1.99E-04	1.97E+00	1.41E+03	2.21	1.5E-12	1.5E-08		
S014-16-T1-4	21.9	03/15/2016 08:50:00	03/29/2016 08:00:0	360.86	278.18	195.83	1762.5	1.95E-04	1.97E+00	1.43E+03	2.21	1.5E-12	1.5E-08	1.4E-08	4.1E-10
S014-16-T1-7	21.6	03/15/2016 08:50:00	03/29/2016 08:00:0	361.60	278.75	194.35	1749.2	1.92E-04	1.94E+00	1.45E+03	2.21	1.4E-12	1.4E-08		

T2

Name	I (µg/L)	Interval Begin	Sampling Date	Monlith mass (g)	Monlith Dry Mass (g)	Surface Area (cm^2)	Solution Volume (mL)	Monolith Volume (m^3)	M$_{ti}$ (mg/m^2)	ρ (kg/m^3)	Co (mg$_{Tc}$/kg$_{mono}$)	D$_e$ (m^2/s)	D$_e$ (cm^2/s)	Average D$_e$ (cm^2/s)	Standard Deviation of Average De
S014-16-T2-3	23.3	03/15/2016 08:50:00	03/29/2016 08:00:0	364.71	283.41	195.83	1749.7	1.92E-04	2.08E+00	1.48E+03	2.24	1.5E-12	1.5E-08	1.7E-08	1.4E-09
S014-16-T2-6	24.8	03/15/2016 08:50:00	03/29/2016 08:00:0	367.70	285.74	197.83	1780.5	1.97E-04	2.23E+00	1.45E+03	2.24	1.8E-12	1.8E-08		
S014-16-T2-7	24.3	03/15/2016 08:50:00	03/29/2016 08:00:0	366.00	284.41	196.77	1770.9	1.95E-04	2.19E+00	1.46E+03	2.24	1.7E-12	1.7E-08	1.8E-08	5.3E-10
S014-16-T2-8	24.6	03/15/2016 08:50:00	03/29/2016 08:00:0	363.14	282.19	197.90	1781.1	1.97E-04	2.21E+00	1.43E+03	2.24	1.8E-12	1.8E-08		

T3

Name	I (µg/L)	Interval Begin	Sampling Date	Monlith mass (g)	Monlith Dry Mass (g)	Surface Area (cm^2)	Solution Volume (mL)	Monolith Volume (m^3)	M$_{ti}$ (mg/m^2)	ρ (kg/m^3)	Co (mg$_{Tc}$/kg$_{mono}$)	D$_e$ (m^2/s)	D$_e$ (cm^2/s)	Average D$_e$ (cm^2/s)	Standard Deviation of Average De
S014-16-T3-1	19.9	03/15/2016 08:50:00	03/29/2016 08:00:0	366.62	285.46	195.87	1762.9	1.94E-04	1.79E+00	1.47E+03	2.45	9.4E-13	9.4E-09	9.4E-09	1.8E-11
S014-16-T3-3	19.8	03/15/2016 08:50:00	03/29/2016 08:00:0	364.46	283.78	195.53	1759.7	1.94E-04	1.78E+00	1.46E+03	2.45	9.4E-13	9.4E-09		
S014-16-T3-4	16.8	03/15/2016 08:50:00	03/29/2016 08:00:0	362.76	282.46	194.51	1750.6	1.93E-04	1.51E+00	1.47E+03	2.45	6.7E-13	6.7E-09	7.2E-09	4.8E-10
S014-16-T3-8	17.9	03/15/2016 08:50:00	03/29/2016 08:00:0	360.88	280.99	194.17	1747.5	1.92E-04	1.61E+00	1.46E+03	2.45	7.7E-13	7.7E-09		

T4

Name	I (µg/L)	Interval Begin	Sampling Date	Monlith mass (g)	Monlith Dry Mass (g)	Surface Area (cm^2)	Solution Volume (mL)	Monolith Volume (m^3)	M$_{ti}$ (mg/m^2)	ρ (kg/m^3)	Co (mg$_{Tc}$/kg$_{mono}$)	D$_e$ (m^2/s)	D$_e$ (cm^2/s)	Average D$_e$ (cm^2/s)	Standard Deviation of Average De
S014-16-T4-1	22.9	03/15/2016 08:50:00	03/29/2016 08:00:0	364.02	284.12	195.68	1761.2	1.94E-04	2.06E+00	1.46E+03	2.14	1.7E-12	1.7E-08	1.6E-08	6.2E-11
S014-16-T4-2	22.6	03/15/2016 08:50:00	03/29/2016 08:00:0	369.27	288.22	199.22	1793.0	1.99E-04	2.03E+00	1.45E+03	2.14	1.6E-12	1.6E-08		
S014-16-T4-5	21.2	03/15/2016 08:50:00	03/29/2016 08:00:0	365.37	285.18	195.92	1763.3	1.94E-04	1.91E+00	1.47E+03	2.14	1.4E-12	1.4E-08	1.5E-08	1.1E-09
S014-16-T4-7	22.6	03/15/2016 08:50:00	03/29/2016 08:00:0	363.93	284.05	196.69	1770.2	1.96E-04	2.03E+00	1.45E+03	2.14	1.6E-12	1.6E-08		

T5

Name	I (µg/L)	Interval Begin	Sampling Date	Monlith mass (g)	Monlith Dry Mass (g)	Surface Area (cm^2)	Solution Volume (mL)	Monolith Volume (m^3)	M$_{ti}$ (mg/m^2)	ρ (kg/m^3)	Co (mg$_{Tc}$/kg$_{mono}$)	D$_e$ (m^2/s)	D$_e$ (cm^2/s)	Average D$_e$ (cm^2/s)	Standard Deviation of Average De
S014-16-T5-2	22.8	03/15/2016 08:50:00	03/29/2016 08:00:0	365.93	283.58	197.86	1780.7	1.97E-04	2.05E+00	1.44E+03	2.15	1.7E-12	1.7E-08	1.5E-08	1.4E-09
S014-16-T5-3	21.2	03/15/2016 08:50:00	03/29/2016 08:00:0	364.75	282.66	195.03	1755.3	1.92E-04	1.91E+00	1.47E+03	2.15	1.4E-12	1.4E-08		
S014-16-T5-4	20.5	03/15/2016 08:50:00	03/29/2016 08:00:0	366.62	284.11	196.79	1771.1	1.95E-04	1.85E+00	1.46E+03	2.15	1.3E-12	1.3E-08	1.3E-08	2.4E-10
S014-16-T5-7	20.6	03/15/2016 08:50:00	03/29/2016 08:00:0	365.76	283.44	197.96	1781.6	1.97E-04	1.85E+00	1.44E+03	2.15	1.4E-12	1.4E-08		

T6

Name	I (µg/L)	Interval Begin	Sampling Date	Monlith mass (g)	Monlith Dry Mass (g)	Surface Area (cm^2)	Solution Volume (mL)	Monolith Volume (m^3)	M$_{ti}$ (mg/m^2)	ρ (kg/m^3)	Co (mg$_{Tc}$/kg$_{mono}$)	D$_e$ (m^2/s)	D$_e$ (cm^2/s)	Average D$_e$ (cm^2/s)	Standard Deviation of Average De
S014-16-T6-2	22.4	03/15/2016 08:50:00	03/29/2016 08:00:0	363.78	284.09	196.70	1770.3	1.95E-04	2.02E+00	1.45E+03	2.15	1.6E-12	1.6E-08	1.5E-08	4.6E-10
S014-16-T6-3	21.7	03/15/2016 08:50:00	03/29/2016 08:00:0	364.78	284.87	197.29	1775.6	1.96E-04	1.95E+00	1.45E+03	2.15	1.5E-12	1.5E-08		
S014-16-T6-5	21.6	03/15/2016 08:50:00	03/29/2016 08:00:0	362.95	283.44	196.39	1767.5	1.95E-04	1.94E+00	1.45E+03	2.15	1.5E-12	1.5E-08	1.5E-08	2.4E-10
S014-16-T6-6	22.3	03/15/2016 08:50:00	03/29/2016 08:00:0	360.98	281.90	193.67	1743.0	1.91E-04	2.01E+00	1.48E+03	2.15	1.5E-12	1.5E-08		

I Sampling 42 d

Experiment Start 3/1/16 8:30:00

T1

Name	I (µg/L)	Interval Begin	Sampling Date	Monlith mass (g)	Monlith Dry Mass (g)	Surface Area (cm^2)	Solution Volume (mL)	Monolith Volume (m^3)	M_{ti} (mg/m^2)	ρ (kg/m^3)	Co (mg$_{Tc}$/kg$_{mono}$)	D_e (m^2/s)	D_e (cm^2/s)	Average D_e (cm^2/s)	Standard Deviation of Average De
S014-16-T1-1	15.6	03/29/2016 08:00:0	04/12/2016 08:30:00	359.63	277.23	192.53	1732.8	1.89E-04	1.40E+00	1.46E+03	2.21	1.2E-12	1.2E-08	1.1E-08	7.5E-10
S014-16-T1-2	14.1	03/29/2016 08:00:0	04/12/2016 08:30:00	365.20	281.52	199.18	1792.6	1.99E-04	1.27E+00	1.41E+03	2.21	1.1E-12	1.1E-08		
S014-16-T1-4	15.1	03/29/2016 08:00:0	04/12/2016 08:30:00	360.86	278.18	195.83	1762.5	1.95E-04	1.36E+00	1.43E+03	2.21	1.2E-12	1.2E-08	1.1E-08	4.7E-10
S014-16-T1-7	14.7	03/29/2016 08:00:0	04/12/2016 08:30:00	361.60	278.75	194.35	1749.2	1.92E-04	1.32E+00	1.45E+03	2.21	1.1E-12	1.1E-08		

T2

Name	I (µg/L)	Interval Begin	Sampling Date	Monlith mass (g)	Monlith Dry Mass (g)	Surface Area (cm^2)	Solution Volume (mL)	Monolith Volume (m^3)	M_{ti} (mg/m^2)	ρ (kg/m^3)	Co (mg$_{Tc}$/kg$_{mono}$)	D_e (m^2/s)	D_e (cm^2/s)	Average D_e (cm^2/s)	Standard Deviation of Average De
S014-16-T2-3	13.5	03/29/2016 08:00:0	04/12/2016 08:30:00	364.71	283.41	195.83	1749.7	1.92E-04	1.21E+00	1.48E+03	2.24	8.5E-13	8.5E-09	9.2E-09	7.0E-10
S014-16-T2-6	14.2	03/29/2016 08:00:0	04/12/2016 08:30:00	367.70	285.74	197.83	1780.5	1.97E-04	1.28E+00	1.45E+03	2.24	9.9E-13	9.9E-09		
S014-16-T2-7	13.5	03/29/2016 08:00:0	04/12/2016 08:30:00	366.00	284.41	196.77	1770.9	1.95E-04	1.22E+00	1.46E+03	2.24	8.9E-13	8.9E-09	9.4E-09	5.1E-10
S014-16-T2-8	14	03/29/2016 08:00:0	04/12/2016 08:30:00	363.14	282.19	197.90	1781.1	1.97E-04	1.26E+00	1.43E+03	2.24	9.9E-13	9.9E-09		

T3

Name	I (µg/L)	Interval Begin	Sampling Date	Monlith mass (g)	Monlith Dry Mass (g)	Surface Area (cm^2)	Solution Volume (mL)	Monolith Volume (m^3)	M_{ti} (mg/m^2)	ρ (kg/m^3)	Co (mg$_{Tc}$/kg$_{mono}$)	D_e (m^2/s)	D_e (cm^2/s)	Average D_e (cm^2/s)	Standard Deviation of Average De
S014-16-T3-1	13	03/29/2016 08:00:0	04/12/2016 08:30:00	366.62	285.46	195.87	1762.9	1.94E-04	1.17E+00	1.47E+03	2.45	6.7E-13	6.7E-09	6.5E-09	2.1E-10
S014-16-T3-3	12.5	03/29/2016 08:00:0	04/12/2016 08:30:00	364.46	283.78	195.53	1759.7	1.94E-04	1.13E+00	1.46E+03	2.45	6.3E-13	6.3E-09		
S014-16-T3-4	12.4	03/29/2016 08:00:0	04/12/2016 08:30:00	362.76	282.46	194.51	1750.6	1.93E-04	1.12E+00	1.47E+03	2.45	6.2E-13	6.2E-09	6.1E-09	1.3E-10
S014-16-T3-8	12.1	03/29/2016 08:00:0	04/12/2016 08:30:00	360.88	280.99	194.17	1747.5	1.92E-04	1.09E+00	1.46E+03	2.45	5.9E-13	5.9E-09		

T4

Name	I (µg/L)	Interval Begin	Sampling Date	Monlith mass (g)	Monlith Dry Mass (g)	Surface Area (cm^2)	Solution Volume (mL)	Monolith Volume (m^3)	M_{ti} (mg/m^2)	ρ (kg/m^3)	Co (mg$_{Tc}$/kg$_{mono}$)	D_e (m^2/s)	D_e (cm^2/s)	Average D_e (cm^2/s)	Standard Deviation of Average De
S014-16-T4-1	15	03/29/2016 08:00:0	04/12/2016 08:30:00	364.02	284.12	195.68	1761.2	1.94E-04	1.35E+00	1.46E+03	2.14	1.2E-12	1.2E-08	1.2E-08	2.1E-10
S014-16-T4-2	14.6	03/29/2016 08:00:0	04/12/2016 08:30:00	369.27	288.22	199.22	1793.0	1.99E-04	1.31E+00	1.45E+03	2.14	1.2E-12	1.2E-08		
S014-16-T4-5	14.7	03/29/2016 08:00:0	04/12/2016 08:30:00	365.37	285.18	195.92	1763.3	1.94E-04	1.32E+00	1.47E+03	2.14	1.1E-12	1.1E-08	1.2E-08	3.7E-10
S014-16-T4-7	15	03/29/2016 08:00:0	04/12/2016 08:30:00	363.93	284.05	196.69	1770.2	1.96E-04	1.35E+00	1.45E+03	2.14	1.2E-12	1.2E-08		

T5

Name	I (µg/L)	Interval Begin	Sampling Date	Monlith mass (g)	Monlith Dry Mass (g)	Surface Area (cm^2)	Solution Volume (mL)	Monolith Volume (m^3)	M_{ti} (mg/m^2)	ρ (kg/m^3)	Co (mg$_{Tc}$/kg$_{mono}$)	D_e (m^2/s)	D_e (cm^2/s)	Average D_e (cm^2/s)	Standard Deviation of Average De
S014-16-T5-2	14.3	03/29/2016 08:00:0	04/12/2016 08:30:00	365.93	283.58	197.86	1780.7	1.97E-04	1.29E+00	1.44E+03	2.15	1.1E-12	1.1E-08	1.2E-08	1.0E-09
S014-16-T5-3	15.9	03/29/2016 08:00:0	04/12/2016 08:30:00	364.75	282.66	195.03	1755.3	1.92E-04	1.43E+00	1.47E+03	2.15	1.3E-12	1.3E-08		
S014-16-T5-4	13.8	03/29/2016 08:00:0	04/12/2016 08:30:00	366.62	284.11	196.79	1771.1	1.95E-04	1.24E+00	1.46E+03	2.15	1.0E-12	1.0E-08	1.0E-08	2.8E-10
S014-16-T5-7	14	03/29/2016 08:00:0	04/12/2016 08:30:00	365.76	283.44	197.96	1781.6	1.97E-04	1.26E+00	1.44E+03	2.15	1.1E-12	1.1E-08		

T6

Name	I (µg/L)	Interval Begin	Sampling Date	Monlith mass (g)	Monlith Dry Mass (g)	Surface Area (cm^2)	Solution Volume (mL)	Monolith Volume (m^3)	M_{ti} (mg/m^2)	ρ (kg/m^3)	Co (mg$_{Tc}$/kg$_{mono}$)	D_e (m^2/s)	D_e (cm^2/s)	Average D_e (cm^2/s)	Standard Deviation of Average De
S014-16-T6-2	14.9	03/29/2016 08:00:0	04/12/2016 08:30:00	363.78	284.09	196.70	1770.3	1.95E-04	1.34E+00	1.45E+03	2.15	1.2E-12	1.2E-08	1.1E-08	1.0E-09
S014-16-T6-3	13.5	03/29/2016 08:00:0	04/12/2016 08:30:00	364.78	284.87	197.29	1775.6	1.96E-04	1.22E+00	1.45E+03	2.15	9.7E-13	9.7E-09		
S014-16-T6-5	14.4	03/29/2016 08:00:0	04/12/2016 08:30:00	362.95	283.44	196.39	1767.5	1.95E-04	1.30E+00	1.45E+03	2.15	1.1E-12	1.1E-08	1.1E-08	2.4E-10
S014-16-T6-6	14.3	03/29/2016 08:00:0	04/12/2016 08:30:00	360.98	281.90	193.67	1743.0	1.91E-04	1.29E+00	1.48E+03	2.15	1.0E-12	1.0E-08		

I Sampling 49 d

Experiment Start 3/1/16 8:30:00

T1

Name	I (µg/L)	Interval Begin	Sampling Date	Monlith mass (g)	Monlith Dry Mass (g)	Surface Area (cm^2)	Solution Volume (mL)	Monolith Volume (m^3)	M_{ti} (mg/m^2)	ρ (kg/m^3)	Co (mg$_{Tc}$/kg$_{mono}$)	D_e (m^2/s)	D_e (cm^2/s)	Average D_e (cm^2/s)	Standard Deviation of Average De
S014-16-T1-1	5.48	04/12/2016 08:30:0	04/19/2016 08:40:00	359.63	277.23	192.53	1732.8	1.89E-04	4.93E-01	1.46E+03	2.21	7.8E-13	7.8E-09	7.5E-09	2.7E-10
S014-16-T1-2	5.11	04/12/2016 08:30:0	04/19/2016 08:40:00	365.20	281.52	199.18	1792.6	1.99E-04	4.60E-01	1.41E+03	2.21	7.3E-13	7.3E-09		
S014-16-T1-4	5.78	04/12/2016 08:30:0	04/19/2016 08:40:00	360.86	278.18	195.83	1762.5	1.95E-04	5.20E-01	1.43E+03	2.21	9.1E-13	9.1E-09	8.8E-09	3.3E-10
S014-16-T1-7	5.65	04/12/2016 08:30:0	04/19/2016 08:40:00	361.60	278.75	194.35	1749.2	1.92E-04	5.09E-01	1.45E+03	2.21	8.4E-13	8.4E-09		

T2

Name	I (µg/L)	Interval Begin	Sampling Date	Monlith mass (g)	Monlith Dry Mass (g)	Surface Area (cm^2)	Solution Volume (mL)	Monolith Volume (m^3)	M_{ti} (mg/m^2)	ρ (kg/m^3)	Co (mg$_{Tc}$/kg$_{mono}$)	D_e (m^2/s)	D_e (cm^2/s)	Average D_e (cm^2/s)	Standard Deviation of Average De
S014-16-T2-3	4.63	04/12/2016 08:30:0	04/19/2016 08:40:00	364.71	283.41	195.83	1749.7	1.92E-04	4.14E-01	1.48E+03	2.24	5.3E-13	5.3E-09	5.5E-09	2.1E-10
S014-16-T2-6	4.69	04/12/2016 08:30:0	04/19/2016 08:40:00	367.70	285.74	197.83	1780.5	1.97E-04	4.22E-01	1.45E+03	2.24	5.7E-13	5.7E-09		
S014-16-T2-7	5.35	04/12/2016 08:30:0	04/19/2016 08:40:00	366.00	284.41	196.77	1770.9	1.95E-04	4.82E-01	1.46E+03	2.24	7.4E-13	7.4E-09	7.1E-09	2.3E-10
S014-16-T2-8	5.09	04/12/2016 08:30:0	04/19/2016 08:40:00	363.14	282.19	197.90	1781.1	1.97E-04	4.58E-01	1.43E+03	2.24	6.9E-13	6.9E-09		

T3

Name	I (µg/L)	Interval Begin	Sampling Date	Monlith mass (g)	Monlith Dry Mass (g)	Surface Area (cm^2)	Solution Volume (mL)	Monolith Volume (m^3)	M_{ti} (mg/m^2)	ρ (kg/m^3)	Co (mg$_{Tc}$/kg$_{mono}$)	D_e (m^2/s)	D_e (cm^2/s)	Average D_e (cm^2/s)	Standard Deviation of Average De
S014-16-T3-1	4.97	04/12/2016 08:30:0	04/19/2016 08:40:00	366.62	285.46	195.87	1762.9	1.94E-04	4.47E-01	1.47E+03	2.45	5.2E-13	5.2E-09	4.7E-09	5.2E-10
S014-16-T3-3	4.41	04/12/2016 08:30:0	04/19/2016 08:40:00	364.46	283.78	195.53	1759.7	1.94E-04	3.97E-01	1.46E+03	2.45	4.1E-13	4.1E-09		
S014-16-T3-4	5.07	04/12/2016 08:30:0	04/19/2016 08:40:00	362.76	282.46	194.51	1750.6	1.93E-04	4.56E-01	1.47E+03	2.45	5.4E-13	5.4E-09	5.2E-09	2.0E-10
S014-16-T3-8	4.86	04/12/2016 08:30:0	04/19/2016 08:40:00	360.88	280.99	194.17	1747.5	1.92E-04	4.37E-01	1.46E+03	2.45	5.0E-13	5.0E-09		

T4

Name	I (µg/L)	Interval Begin	Sampling Date	Monlith mass (g)	Monlith Dry Mass (g)	Surface Area (cm^2)	Solution Volume (mL)	Monolith Volume (m^3)	M_{ti} (mg/m^2)	ρ (kg/m^3)	Co (mg$_{Tc}$/kg$_{mono}$)	D_e (m^2/s)	D_e (cm^2/s)	Average D_e (cm^2/s)	Standard Deviation of Average De
S014-16-T4-1	5.41	04/12/2016 08:30:0	04/19/2016 08:40:00	364.02	284.12	195.68	1761.2	1.94E-04	4.87E-01	1.46E+03	2.14	8.2E-13	8.2E-09	7.9E-09	2.1E-10
S014-16-T4-2	5.22	04/12/2016 08:30:0	04/19/2016 08:40:00	369.27	288.22	199.22	1793.0	1.99E-04	4.70E-01	1.45E+03	2.14	7.7E-13	7.7E-09		
S014-16-T4-5	5.44	04/12/2016 08:30:0	04/19/2016 08:40:00	365.37	285.18	195.92	1763.3	1.94E-04	4.90E-01	1.47E+03	2.14	8.2E-13	8.2E-09	8.5E-09	3.3E-10
S014-16-T4-7	5.59	04/12/2016 08:30:0	04/19/2016 08:40:00	363.93	284.05	196.69	1770.2	1.96E-04	5.03E-01	1.45E+03	2.14	8.9E-13	8.9E-09		

T5

Name	I (µg/L)	Interval Begin	Sampling Date	Monlith mass (g)	Monlith Dry Mass (g)	Surface Area (cm^2)	Solution Volume (mL)	Monolith Volume (m^3)	M_{ti} (mg/m^2)	ρ (kg/m^3)	Co (mg$_{Tc}$/kg$_{mono}$)	D_e (m^2/s)	D_e (cm^2/s)	Average D_e (cm^2/s)	Standard Deviation of Average De
S014-16-T5-2	4.93	04/12/2016 08:30:0	04/19/2016 08:40:00	365.93	283.58	197.86	1780.7	1.97E-04	4.44E-01	1.44E+03	2.15	6.9E-13	6.9E-09	7.5E-09	6.0E-10
S014-16-T5-3	5.45	04/12/2016 08:30:0	04/19/2016 08:40:00	364.75	282.66	195.03	1755.3	1.92E-04	4.91E-01	1.47E+03	2.15	8.1E-13	8.1E-09		
S014-16-T5-4	5.32	04/12/2016 08:30:0	04/19/2016 08:40:00	366.62	284.11	196.79	1771.1	1.95E-04	4.79E-01	1.46E+03	2.15	7.9E-13	7.9E-09	8.1E-09	1.9E-10
S014-16-T5-7	5.38	04/12/2016 08:30:0	04/19/2016 08:40:00	365.76	283.44	197.96	1781.6	1.97E-04	4.84E-01	1.44E+03	2.15	8.3E-13	8.3E-09		

T6

Name	I (µg/L)	Interval Begin	Sampling Date	Monlith mass (g)	Monlith Dry Mass (g)	Surface Area (cm^2)	Solution Volume (mL)	Monolith Volume (m^3)	M_{ti} (mg/m^2)	ρ (kg/m^3)	Co (mg$_{Tc}$/kg$_{mono}$)	D_e (m^2/s)	D_e (cm^2/s)	Average D_e (cm^2/s)	Standard Deviation of Average De
S014-16-T6-2	5.36	04/12/2016 08:30:0	04/19/2016 08:40:00	363.78	284.09	196.70	1770.3	1.95E-04	4.82E-01	1.45E+03	2.15	8.0E-13	8.0E-09	7.6E-09	4.0E-10
S014-16-T6-3	5.08	04/12/2016 08:30:0	04/19/2016 08:40:00	364.78	284.87	197.29	1775.6	1.96E-04	4.57E-01	1.45E+03	2.15	7.2E-13	7.2E-09		
S014-16-T6-5	5.3	04/12/2016 08:30:0	04/19/2016 08:40:00	362.95	283.44	196.39	1767.5	1.95E-04	4.77E-01	1.45E+03	2.15	7.8E-13	7.8E-09	7.9E-09	3.7E-11
S014-16-T6-6	5.41	04/12/2016 08:30:0	04/19/2016 08:40:00	360.98	281.90	193.67	1743.0	1.91E-04	4.87E-01	1.48E+03	2.15	7.9E-13	7.9E-09		

I Sampling 63 d

Experiment Start 3/1/16 8:30:00

T1

Name	I (µg/L)	Interval Begin	Sampling Date	Monlith mass (g)	Monlith Dry Mass (g)	Surface Area (cm^2)	Solution Volume (mL)	Monolith Volume (m^3)	M_{ti} (mg/m^2)	ρ (kg/m^3)	Co (mg$_{Tc}$/kg$_{mono}$)	D_e (m^2/s)	D_e (cm^2/s)	Average D_e (cm^2/s)	Standard Deviation of Average De
S014-16-T1-1	10.5	04/19/2016 08:40:0	05/03/2016 09:00:0	359.63	277.23	192.53	1732.8	1.89E-04	9.45E-01	1.46E+03	2.21	8.8E-13	8.8E-09	8.4E-09	3.5E-10
S014-16-T1-2	9.73	04/19/2016 08:40:0	05/03/2016 09:00:0	365.20	281.52	199.18	1792.6	1.99E-04	8.76E-01	1.41E+03	2.21	8.1E-13	8.1E-09		
S014-16-T1-4	9.25	04/19/2016 08:40:0	05/03/2016 09:00:0	360.86	278.18	195.83	1762.5	1.95E-04	8.33E-01	1.43E+03	2.21	7.2E-13	7.2E-09	6.7E-09	4.6E-10
S014-16-T1-7	8.76	04/19/2016 08:40:0	05/03/2016 09:00:0	361.60	278.75	194.35	1749.2	1.92E-04	7.88E-01	1.45E+03	2.21	6.2E-13	6.2E-09		

T2

Name	I (µg/L)	Interval Begin	Sampling Date	Monlith mass (g)	Monlith Dry Mass (g)	Surface Area (cm^2)	Solution Volume (mL)	Monolith Volume (m^3)	M_{ti} (mg/m^2)	ρ (kg/m^3)	Co (mg$_{Tc}$/kg$_{mono}$)	D_e (m^2/s)	D_e (cm^2/s)	Average D_e (cm^2/s)	Standard Deviation of Average De
S014-16-T2-3	7.72	04/19/2016 08:40:0	05/03/2016 09:00:0	364.71	283.41	195.83	1749.7	1.92E-04	6.90E-01	1.48E+03	2.24	4.5E-13	4.5E-09	4.5E-09	3.3E-11
S014-16-T2-6	7.47	04/19/2016 08:40:0	05/03/2016 09:00:0	367.70	285.74	197.83	1780.5	1.97E-04	6.72E-01	1.45E+03	2.24	4.4E-13	4.4E-09		
S014-16-T2-7	8.32	04/19/2016 08:40:0	05/03/2016 09:00:0	366.00	284.41	196.77	1770.9	1.95E-04	7.49E-01	1.46E+03	2.24	5.5E-13	5.5E-09	5.1E-09	4.0E-10
S014-16-T2-8	7.56	04/19/2016 08:40:0	05/03/2016 09:00:0	363.14	282.19	197.90	1781.1	1.97E-04	6.80E-01	1.43E+03	2.24	4.7E-13	4.7E-09		

T3

Name	I (µg/L)	Interval Begin	Sampling Date	Monlith mass (g)	Monlith Dry Mass (g)	Surface Area (cm^2)	Solution Volume (mL)	Monolith Volume (m^3)	M_{ti} (mg/m^2)	ρ (kg/m^3)	Co (mg$_{Tc}$/kg$_{mono}$)	D_e (m^2/s)	D_e (cm^2/s)	Average D_e (cm^2/s)	Standard Deviation of Average De
S014-16-T3-1	9	04/19/2016 08:40:0	05/03/2016 09:00:0	366.62	285.46	195.87	1762.9	1.94E-04	8.10E-01	1.47E+03	2.45	5.2E-13	5.2E-09	4.9E-09	3.3E-10
S014-16-T3-3	8.35	04/19/2016 08:40:0	05/03/2016 09:00:0	364.46	283.78	195.53	1759.7	1.94E-04	7.52E-01	1.46E+03	2.45	4.5E-13	4.5E-09		
S014-16-T3-4	7.69	04/19/2016 08:40:0	05/03/2016 09:00:0	362.76	282.46	194.51	1750.6	1.93E-04	6.92E-01	1.47E+03	2.45	3.8E-13	3.8E-09	3.7E-09	1.3E-10
S014-16-T3-8	7.4	04/19/2016 08:40:0	05/03/2016 09:00:0	360.88	280.99	194.17	1747.5	1.92E-04	6.66E-01	1.46E+03	2.45	3.6E-13	3.6E-09		

T4

Name	I (µg/L)	Interval Begin	Sampling Date	Monlith mass (g)	Monlith Dry Mass (g)	Surface Area (cm^2)	Solution Volume (mL)	Monolith Volume (m^3)	M_{ti} (mg/m^2)	ρ (kg/m^3)	Co (mg$_{Tc}$/kg$_{mono}$)	D_e (m^2/s)	D_e (cm^2/s)	Average D_e (cm^2/s)	Standard Deviation of Average De
S014-16-T4-1	10.2	04/19/2016 08:40:0	05/03/2016 09:00:0	364.02	284.12	195.68	1761.2	1.94E-04	9.18E-01	1.46E+03	2.14	8.9E-13	8.9E-09	8.0E-09	8.5E-10
S014-16-T4-2	9.09	04/19/2016 08:40:0	05/03/2016 09:00:0	369.27	288.22	199.22	1793.0	1.99E-04	8.18E-01	1.45E+03	2.14	7.2E-13	7.2E-09		
S014-16-T4-5	8.58	04/19/2016 08:40:0	05/03/2016 09:00:0	365.37	285.18	195.92	1763.3	1.94E-04	7.72E-01	1.47E+03	2.14	6.3E-13	6.3E-09	6.3E-09	5.1E-11
S014-16-T4-7	8.55	04/19/2016 08:40:0	05/03/2016 09:00:0	363.93	284.05	196.69	1770.2	1.96E-04	7.70E-01	1.45E+03	2.14	6.4E-13	6.4E-09		

T5

Name	I (µg/L)	Interval Begin	Sampling Date	Monlith mass (g)	Monlith Dry Mass (g)	Surface Area (cm^2)	Solution Volume (mL)	Monolith Volume (m^3)	M_{ti} (mg/m^2)	ρ (kg/m^3)	Co (mg$_{Tc}$/kg$_{mono}$)	D_e (m^2/s)	D_e (cm^2/s)	Average D_e (cm^2/s)	Standard Deviation of Average De
S014-16-T5-2	9.49	04/19/2016 08:40:0	05/03/2016 09:00:0	365.93	283.58	197.86	1780.7	1.97E-04	8.54E-01	1.44E+03	2.15	7.9E-13	7.9E-09	7.3E-09	5.9E-10
S014-16-T5-3	8.94	04/19/2016 08:40:0	05/03/2016 09:00:0	364.75	282.66	195.03	1755.3	1.92E-04	8.05E-01	1.47E+03	2.15	6.7E-13	6.7E-09		
S014-16-T5-4	8.66	04/19/2016 08:40:0	05/03/2016 09:00:0	366.62	284.11	196.79	1771.1	1.95E-04	7.79E-01	1.46E+03	2.15	6.4E-13	6.4E-09	6.5E-09	3.7E-11
S014-16-T5-7	8.6	04/19/2016 08:40:0	05/03/2016 09:00:0	365.76	283.44	197.96	1781.6	1.97E-04	7.74E-01	1.44E+03	2.15	6.5E-13	6.5E-09		

T6

Name	I (µg/L)	Interval Begin	Sampling Date	Monlith mass (g)	Monlith Dry Mass (g)	Surface Area (cm^2)	Solution Volume (mL)	Monolith Volume (m^3)	M_{ti} (mg/m^2)	ρ (kg/m^3)	Co (mg$_{Tc}$/kg$_{mono}$)	D_e (m^2/s)	D_e (cm^2/s)	Average D_e (cm^2/s)	Standard Deviation of Average De
S014-16-T6-2	10.2	04/19/2016 08:40:0	05/03/2016 09:00:0	363.78	284.09	196.70	1770.3	1.95E-04	9.18E-01	1.45E+03	2.15	8.9E-13	8.9E-09	8.0E-09	8.7E-10
S014-16-T6-3	9.14	04/19/2016 08:40:0	05/03/2016 09:00:0	364.78	284.87	197.29	1775.6	1.96E-04	8.23E-01	1.45E+03	2.15	7.2E-13	7.2E-09		
S014-16-T6-5	8.55	04/19/2016 08:40:0	05/03/2016 09:00:0	362.95	283.44	196.39	1767.5	1.95E-04	7.70E-01	1.45E+03	2.15	6.2E-13	6.2E-09	6.0E-09	2.5E-10
S014-16-T6-6	8.33	04/19/2016 08:40:0	05/03/2016 09:00:0	360.98	281.90	193.67	1743.0	1.91E-04	7.50E-01	1.48E+03	2.15	5.7E-13	5.7E-09		

I Sampling Co calculations

I Co Calculation

LIMS Data

LIMS data on I concentration measurement from the spiked 6.5 M Na simulants

These values show the initial I content of the simulant prior to any getter addition

Test	LabNumber	SampleName	Result	Units	EQL
T1	1601042-01	T1 Initial	4710	ug/L	250
T2	1601042-03	T2 Initial	4810	ug/L	250
T3	1601042-05	T3 Initial	5260	ug/L	250
T4	1601042-10	T4 Final	4600	ug/L	250
T5	1601042-11	T5 Initial	4590	ug/L	250
T6	1601042-13	T6 Initial	4630	ug/L	250

Simulant Volume

Density of the 6.5 M Na Average simulant [g 1.31

Test	Simulant Bottle Tare (g)	Bottle + Simulant (g)	Simulant Mass	Simulant Volume-(mL)	Simulant Volume after sampling (mL)	Dry Blend (g)	Total Weight of Slurry [g]
T1	100.1	1407.8	1307.7	998.2	994.2	1750.0	2744.2
T2	100.3	1408.1	1307.8	998.3	994.3	1757.3	2751.6
T3	100.1	1407.9	1307.8	998.3	994.3	1750.0	2744.3
T4	100	1408	1308	998.5	994.5	1745.0	2739.4
T5	99.8	1408	1308.2	998.6	994.6	1750.0	2744.6
T6	99.9	1410.2	1310.3	1000.2	996.2	1747.6	2743.8

Co

Calculation on I C_0 in dry Cast Stone (mg/kg) monolith

	T1	T2	T3	T4	T5	T6
Dry solid fraction in Cast Stone Monolith	0.771	0.78	0.78	0.78	0.77	0.78

Test	I (ug/g wet Cast Stone)-analytical	C_0 (mg/kg) in dry Cast Stone -analytical
T1	1.706	**2.214**
T2	1.738	**2.237**
T3	1.906	**2.448**
T4	1.670	**2.140**
T5	1.663	**2.146**
T6	1.681	**2.153**

I Sampling T7

		Experiment Start	3/23/16 11:00:00												
2h															
Name	I (µg/L)	Interval Begin	Sampling Date	Monlith mass (g)	Monlith Dry Mass (g)	Surface Area (cm^2)	Solution Volume (mL)	Monolith Volume (m^3)	M_{ti} (mg/m^2)	ρ (kg/m^3)	Co (mg_{Tc}/kg_{mono})	D_e (m^2/s)	D_e (cm^2/s)	Average D_e (cm^2/s)	Standard Deviation of Average De
T7-1	15.7	3/23/16 11:00:00	3/23/2016 13:00:0	366.49	282.52	200.19	1801.7	2.01E-04	1.41E+00	1.41E+03	9.08	1.3E-12	1.3E-08	1.3E-08	6.8E-10
T7-2	15	3/23/16 11:00:00	3/23/2016 13:00:0	363.36	280.10	198.06	1782.5	1.97E-04	1.35E+00	1.42E+03	9.08	1.2E-12	1.2E-08		
1d															
T7-1	47.3	3/23/2016 13:00:	3/24/2016 11:00:0	366.49	282.52	200.19	1801.7	2.01E-04	4.26E+00	1.41E+03	9.08	2.0E-12	2.0E-08	1.8E-08	2.3E-09
T7-2	41.7	3/23/2016 13:00:	3/24/2016 11:00:0	363.36	280.10	198.06	1782.5	1.97E-04	3.75E+00	1.42E+03	9.08	1.5E-12	1.5E-08		
2d															
T7-1	24.9	3/24/2016 11:00:	3/25/2016 11:00:0	366.49	282.52	200.19	1801.7	2.01E-04	2.24E+00	1.41E+03	9.08	1.6E-12	1.6E-08	1.7E-08	1.1E-09
T7-2	26.7	3/24/2016 11:00:	3/25/2016 11:00:0	363.36	280.10	198.06	1782.5	1.97E-04	2.40E+00	1.42E+03	9.08	1.8E-12	1.8E-08		
7d															
T7-1	53.8	3/25/2016 11:00:	3/30/2016 11:00:0	366.49	282.52	200.19	1801.7	2.01E-04	4.84E+00	1.41E+03	9.08	8.6E-13	8.6E-09	9.1E-09	5.0E-10
T7-2	57.3	3/25/2016 11:00:	3/30/2016 11:00:0	363.36	280.10	198.06	1782.5	1.97E-04	5.16E+00	1.42E+03	9.08	9.6E-13	9.6E-09		
14d															
T7-1	46.7	3/30/2016 11:00:	4/6/2016 11:00:00	366.49	282.52	200.19	1801.7	2.01E-04	4.20E+00	1.41E+03	9.08	8.2E-13	8.2E-09	8.5E-09	3.2E-10
T7-2	48.9	3/30/2016 11:00:	4/6/2016 11:00:00	363.36	280.10	198.06	1782.5	1.97E-04	4.40E+00	1.42E+03	9.08	8.8E-13	8.8E-09		
28d															
T7-1	56.9	4/6/2016 11:00:0	4/20/2016 11:00:0	366.49	282.52	200.19	1801.7	2.01E-04	5.12E+00	1.41E+03	9.08	6.1E-13	6.1E-09	4.9E-09	1.2E-09
T7-2	45	4/6/2016 11:00:0	4/20/2016 11:00:0	363.36	280.10	198.06	1782.5	1.97E-04	4.05E+00	1.42E+03	9.08	3.7E-13	3.7E-09		
42d															
T7-1	37	4/20/2016 11:00:	5/4/2016 12:30:00	366.49	282.52	200.19	1801.7	2.01E-04	3.33E+00	1.41E+03	9.08	4.3E-13	4.3E-09	4.0E-09	3.7E-10
T7-2	34	4/20/2016 11:00:	5/4/2016 12:30:00	363.36	280.10	198.06	1782.5	1.97E-04	3.06E+00	1.42E+03	9.08	3.6E-13	3.6E-09		
51d															
T7-1	19	5/4/2016 12:30:0	5/13/2016 14:00:0	366.49	282.52	200.19	1801.7	2.01E-04	1.71E+00	1.41E+03	9.08	3.7E-13	3.7E-09	3.5E-09	2.1E-10
T7-2	18	5/4/2016 12:30:0	5/13/2016 14:00:0	363.36	280.10	198.06	1782.5	1.97E-04	1.62E+00	1.42E+03	9.08	3.2E-13	3.2E-09		
63d															
T7-1	18	5/13/2016 14:00:	5/24/2016 13:00:0	366.49	282.52	200.19	1801.7	2.01E-04	1.62E+00	1.41E+03	9.08	2.7E-13	2.7E-09	2.5E-09	2.3E-10
T7-2	18	5/13/2016 14:00:	5/25/2016 13:00:0	363.36	280.10	198.06	1782.5	1.97E-04	1.62E+00	1.42E+03	9.08	2.3E-13	2.3E-09		

Cr Sampling 2h

Experiment Start 3/1/16 8:30:00

T1

Name	Cr (µg/L)	Interval Begin	Sampling Date	Monlith mass (g)	Monlith Dry Mass (g)	Surface Area (cm^2)	Solution Volume (mL)	Monolith Volume (m^3)	M_{ti} (mg/m^2)	ρ (kg/m^3)	Co (mg_{Cr} /kg_{mono})	D_e (m^2/s)	D_e (cm^2/s)	Average D_e (cm^2/s)	Standard Deviation of Average De
S014-16-T1-1	6.95	3/1/2016 8:30:	3/1/2016 10:30:0	359.63	277.23	192.53	1732.8	1.89E-04	6.26E-01	1.46E+03	407.95	1.2E-16	1.2E-12	1.2E-12	4.3E-14
S014-16-T1-2	6.95	3/1/2016 8:30:	3/1/2016 10:30:0	365.20	281.52	199.18	1792.6	1.99E-04	6.26E-01	1.41E+03	407.95	1.3E-16	1.3E-12		
S014-16-T1-4	6.95	3/1/2016 8:30:	3/1/2016 10:30:0	360.86	278.18	195.83	1762.5	1.95E-04	6.26E-01	1.43E+03	407.95	1.3E-16	1.3E-12	1.2E-12	1.8E-14
S014-16-T1-7	6.95	3/1/2016 8:30:	3/1/2016 10:30:0	361.60	278.75	194.35	1749.2	1.92E-04	6.26E-01	1.45E+03	407.95	1.2E-16	1.2E-12		

T2

Name	Cr (µg/L)	Interval Begin	Sampling Date	Monlith mass (g)	Monlith Dry Mass (g)	Surface Area (cm^2)	Solution Volume (mL)	Monolith Volume (m^3)	M_{ti} (mg/m^2)	ρ (kg/m^3)	Co (mg_{Cr} /kg_{mono})	D_e (m^2/s)	D_e (cm^2/s)	Average D_e (cm^2/s)	Standard Deviation of Average De
S014-16-T2-3	6.95	3/1/2016 8:30:	3/1/2016 10:30:0	364.71	283.41	195.83	1749.7	1.92E-04	6.21E-01	1.48E+03	412.01	1.1E-16	1.1E-12	1.2E-12	3.0E-14
S014-16-T2-6	6.95	3/1/2016 8:30:	3/1/2016 10:30:0	367.70	285.74	197.83	1780.5	1.97E-04	6.26E-01	1.45E+03	412.01	1.2E-16	1.2E-12		
S014-16-T2-7	6.95	3/1/2016 8:30:	3/1/2016 10:30:0	366.00	284.41	196.77	1770.9	1.95E-04	6.26E-01	1.46E+03	412.01	1.2E-16	1.2E-12	1.2E-12	2.1E-14
S014-16-T2-8	6.95	3/1/2016 8:30:	3/1/2016 10:30:0	363.14	282.19	197.90	1781.1	1.97E-04	6.26E-01	1.43E+03	412.01	1.2E-16	1.2E-12		

T3

Name	Cr (µg/L)	Interval Begin	Sampling Date	Monlith mass (g)	Monlith Dry Mass (g)	Surface Area (cm^2)	Solution Volume (mL)	Monolith Volume (m^3)	M_{ti} (mg/m^2)	ρ (kg/m^3)	Co (mg_{Cr} /kg_{mono})	D_e (m^2/s)	D_e (cm^2/s)	Average D_e (cm^2/s)	Standard Deviation of Average De
S014-16-T3-1	6.95	3/1/2016 8:30:	3/1/2016 10:30:0	366.62	285.46	195.87	1762.9	1.94E-04	6.26E-01	1.47E+03	411.82	1.2E-16	1.2E-12	1.2E-12	8.1E-15
S014-16-T3-3	6.95	3/1/2016 8:30:	3/1/2016 10:30:0	364.46	283.78	195.53	1759.7	1.94E-04	6.26E-01	1.46E+03	411.82	1.2E-16	1.2E-12		
S014-16-T3-4	6.95	3/1/2016 8:30:	3/1/2016 10:30:0	362.76	282.46	194.51	1750.6	1.93E-04	6.26E-01	1.47E+03	411.82	1.2E-16	1.2E-12	1.2E-12	4.0E-15
S014-16-T3-8	6.95	3/1/2016 8:30:	3/1/2016 10:30:0	360.88	280.99	194.17	1747.5	1.92E-04	6.26E-01	1.46E+03	411.82	1.2E-16	1.2E-12		

T4

Name	Cr (µg/L)	Interval Begin	Sampling Date	Monlith mass (g)	Monlith Dry Mass (g)	Surface Area (cm^2)	Solution Volume (mL)	Monolith Volume (m^3)	M_{ti} (mg/m^2)	ρ (kg/m^3)	Co (mg_{Cr} /kg_{mono})	D_e (m^2/s)	D_e (cm^2/s)	Average D_e (cm^2/s)	Standard Deviation of Average De
S014-16-T4-1	6.95	3/1/2016 8:30:	3/1/2016 10:30:0	364.02	284.12	195.68	1761.2	1.94E-04	6.26E-01	1.46E+03	393.48	1.3E-16	1.3E-12	1.3E-12	1.2E-14
S014-16-T4-2	6.95	3/1/2016 8:30:	3/1/2016 10:30:0	369.27	288.22	199.22	1793.0	1.99E-04	6.26E-01	1.45E+03	393.48	1.3E-16	1.3E-12		
S014-16-T4-5	6.95	3/1/2016 8:30:	3/1/2016 10:30:0	365.37	285.18	195.92	1763.3	1.94E-04	6.26E-01	1.47E+03	393.48	1.3E-16	1.3E-12	1.3E-12	1.6E-14
S014-16-T4-7	6.95	3/1/2016 8:30:	3/1/2016 10:30:0	363.93	284.05	196.69	1770.2	1.96E-04	6.26E-01	1.45E+03	393.48	1.3E-16	1.3E-12		

T5

Name	Cr (µg/L)	Interval Begin	Sampling Date	Monlith mass (g)	Monlith Dry Mass (g)	Surface Area (cm^2)	Solution Volume (mL)	Monolith Volume (m^3)	M_{ti} (mg/m^2)	ρ (kg/m^3)	Co (mg_{Cr} /kg_{mono})	D_e (m^2/s)	D_e (cm^2/s)	Average D_e (cm^2/s)	Standard Deviation of Average De
S014-16-T5-2	6.95	3/1/2016 8:30:	3/1/2016 10:30:0	365.93	283.58	197.86	1780.7	1.97E-04	6.26E-01	1.44E+03	408.71	1.2E-16	1.2E-12	1.2E-12	2.5E-14
S014-16-T5-3	6.95	3/1/2016 8:30:	3/1/2016 10:30:0	364.75	282.66	195.03	1755.3	1.92E-04	6.26E-01	1.47E+03	408.71	1.2E-16	1.2E-12		
S014-16-T5-4	6.95	3/1/2016 8:30:	3/1/2016 10:30:0	366.62	284.11	196.79	1771.1	1.95E-04	6.26E-01	1.46E+03	408.71	1.2E-16	1.2E-12	1.2E-12	1.5E-14
S014-16-T5-7	6.95	3/1/2016 8:30:	3/1/2016 10:30:0	365.76	283.44	197.96	1781.6	1.97E-04	6.26E-01	1.44E+03	408.71	1.2E-16	1.2E-12		

T6

Name	Cr (µg/L)	Interval Begin	Sampling Date	Monlith mass (g)	Monlith Dry Mass (g)	Surface Area (cm^2)	Solution Volume (mL)	Monolith Volume (m^3)	M_{ti} (mg/m^2)	ρ (kg/m^3)	Co (mg_{Cr} /kg_{mono})	D_e (m^2/s)	D_e (cm^2/s)	Average D_e (cm^2/s)	Standard Deviation of Average De
S014-16-T6-2	6.95	3/1/2016 8:30:	3/1/2016 10:30:0	363.78	284.0868039	196.70	1770.3	1.95E-04	6.26E-01	1.45E+03	410.08	1.2E-16	1.2E-12	1.2E-12	1.8E-15
S014-16-T6-3	6.95	3/1/2016 8:30:	3/1/2016 10:30:0	364.78	284.8677341	197.29	1775.6	1.96E-04	6.26E-01	1.45E+03	410.08	1.2E-16	1.2E-12		
S014-16-T6-5	6.95	3/1/2016 8:30:	3/1/2016 10:30:0	362.95	283.4386318	196.39	1767.5	1.95E-04	6.26E-01	1.45E+03	410.08	1.2E-16	1.2E-12	1.2E-12	1.9E-14
S014-16-T6-6	6.95	3/1/2016 8:30:	3/1/2016 10:30:0	360.98	281.9001992	193.67	1743.0	1.91E-04	6.26E-01	1.48E+03	410.08	1.2E-16	1.2E-12		

Cr Sampling 1 d

		Experiment Start	3/1/16 8:30:00												

T1

Name	Cr (μg/L)	Interval Begin	Sampling Date	Monlith mass (g)	Monlith Dry Mass (g)	Surface Area (cm^2)	Solution Volume (mL)	Monolith Volume (m^3)	M_{ti} (mg/m^2)	ρ (kg/m^3)	Co (mg$_{Cr}$ /kg$_{mono}$)	D_e (m^2/s)	D_e (cm^2/s)	Average D_e (cm^2/s)	Standard Deviation of Average De
S014-16-T1-1	6.95	3/1/2016 10:30:0	3/2/2016 8:30:00	359.63	277.23	192.53	1732.8	1.89E-04	6.26E-01	1.46E+03	407.95	2.0E-17	2.0E-13	2.0E-13	7.0E-15
S014-16-T1-2	6.95	3/1/2016 10:30:0	3/2/2016 8:30:00	365.20	281.52	199.18	1792.6	1.99E-04	6.26E-01	1.41E+03	407.95	2.1E-17	2.1E-13		
S014-16-T1-4	6.95	3/1/2016 10:30:0	3/2/2016 8:30:00	360.86	278.18	195.83	1762.5	1.95E-04	6.26E-01	1.43E+03	407.95	2.1E-17	2.1E-13	2.0E-13	3.0E-15
S014-16-T1-7	6.95	3/1/2016 10:30:0	3/2/2016 8:30:00	361.60	278.75	194.35	1749.2	1.92E-04	6.26E-01	1.45E+03	407.95	2.0E-17	2.0E-13		

T2

Name	Cr (μg/L)	Interval Begin	Sampling Date	Monlith mass (g)	Monlith Dry Mass (g)	Surface Area (cm^2)	Solution Volume (mL)	Monolith Volume (m^3)	M_{ti} (mg/m^2)	ρ (kg/m^3)	Co (mg$_{Cr}$ /kg$_{mono}$)	D_e (m^2/s)	D_e (cm^2/s)	Average D_e (cm^2/s)	Standard Deviation of Average De
S014-16-T2-3	6.95	3/1/2016 10:30:0	3/2/2016 8:30:00	364.71	283.41	195.83	1749.7	1.92E-04	6.21E-01	1.48E+03	412.01	1.9E-17	1.9E-13	1.9E-13	4.9E-15
S014-16-T2-6	6.95	3/1/2016 10:30:0	3/2/2016 8:30:00	367.70	285.74	197.83	1780.5	1.97E-04	6.26E-01	1.45E+03	412.01	2.0E-17	2.0E-13		
S014-16-T2-7	6.95	3/1/2016 10:30:0	3/2/2016 8:30:00	366.00	284.41	196.77	1770.9	1.95E-04	6.26E-01	1.46E+03	412.01	2.0E-17	2.0E-13	2.0E-13	3.5E-15
S014-16-T2-8	6.95	3/1/2016 10:30:0	3/2/2016 8:30:00	363.14	282.19	197.90	1781.1	1.97E-04	6.26E-01	1.43E+03	412.01	2.0E-17	2.0E-13		

T3

Name	Cr (μg/L)	Interval Begin	Sampling Date	Monlith mass (g)	Monlith Dry Mass (g)	Surface Area (cm^2)	Solution Volume (mL)	Monolith Volume (m^3)	M_{ti} (mg/m^2)	ρ (kg/m^3)	Co (mg$_{Cr}$ /kg$_{mono}$)	D_e (m^2/s)	D_e (cm^2/s)	Average D_e (cm^2/s)	Standard Deviation of Average De
S014-16-T3-1	6.95	3/1/2016 10:30:0	3/2/2016 8:30:00	366.62	285.46	195.87	1762.9	1.94E-04	6.26E-01	1.47E+03	411.82	1.9E-17	1.9E-13	1.9E-13	1.3E-15
S014-16-T3-3	6.95	3/1/2016 10:30:0	3/2/2016 8:30:00	364.46	283.78	195.53	1759.7	1.94E-04	6.26E-01	1.46E+03	411.82	1.9E-17	1.9E-13		
S014-16-T3-4	6.95	3/1/2016 10:30:0	3/2/2016 8:30:00	362.76	282.46	194.51	1750.6	1.93E-04	6.26E-01	1.47E+03	411.82	1.9E-17	1.9E-13	1.9E-13	6.6E-16
S014-16-T3-8	6.95	3/1/2016 10:30:0	3/2/2016 8:30:00	360.88	280.99	194.17	1747.5	1.92E-04	6.26E-01	1.46E+03	411.82	1.9E-17	1.9E-13		

T4

Name	Cr (μg/L)	Interval Begin	Sampling Date	Monlith mass (g)	Monlith Dry Mass (g)	Surface Area (cm^2)	Solution Volume (mL)	Monolith Volume (m^3)	M_{ti} (mg/m^2)	ρ (kg/m^3)	Co (mg$_{Cr}$ /kg$_{mono}$)	D_e (m^2/s)	D_e (cm^2/s)	Average D_e (cm^2/s)	Standard Deviation of Average De
S014-16-T4-1	6.95	3/1/2016 10:30:0	3/2/2016 8:30:00	364.02	284.12	195.68	1761.2	1.94E-04	6.26E-01	1.46E+03	393.48	2.1E-17	2.1E-13	2.1E-13	2.0E-15
S014-16-T4-2	6.95	3/1/2016 10:30:0	3/2/2016 8:30:00	369.27	288.22	199.22	1793.0	1.99E-04	6.26E-01	1.45E+03	393.48	2.2E-17	2.2E-13		
S014-16-T4-5	6.95	3/1/2016 10:30:0	3/2/2016 8:30:00	365.37	285.18	195.92	1763.3	1.94E-04	6.26E-01	1.47E+03	393.48	2.1E-17	2.1E-13	2.1E-13	2.6E-15
S014-16-T4-7	6.95	3/1/2016 10:30:0	3/2/2016 8:30:00	363.93	284.05	196.69	1770.2	1.96E-04	6.26E-01	1.45E+03	393.48	2.2E-17	2.2E-13		

T5

Name	Cr (μg/L)	Interval Begin	Sampling Date	Monlith mass (g)	Monlith Dry Mass (g)	Surface Area (cm^2)	Solution Volume (mL)	Monolith Volume (m^3)	M_{ti} (mg/m^2)	ρ (kg/m^3)	Co (mg$_{Cr}$ /kg$_{mono}$)	D_e (m^2/s)	D_e (cm^2/s)	Average D_e (cm^2/s)	Standard Deviation of Average De
S014-16-T5-2	6.95	3/1/2016 10:30:0	3/2/2016 8:30:00	365.93	283.58	197.86	1780.7	1.97E-04	6.26E-01	1.44E+03	408.71	2.0E-17	2.0E-13	2.0E-13	4.1E-15
S014-16-T5-3	6.95	3/1/2016 10:30:0	3/2/2016 8:30:00	364.75	282.66	195.03	1755.3	1.92E-04	6.26E-01	1.47E+03	408.71	1.9E-17	1.9E-13		
S014-16-T5-4	6.95	3/1/2016 10:30:0	3/2/2016 8:30:00	366.62	284.11	196.79	1771.1	1.95E-04	6.26E-01	1.46E+03	408.71	2.0E-17	2.0E-13	2.0E-13	2.5E-15
S014-16-T5-7	6.95	3/1/2016 10:30:0	3/2/2016 8:30:00	365.76	283.44	197.96	1781.6	1.97E-04	6.26E-01	1.44E+03	408.71	2.0E-17	2.0E-13		

T6

Name	Cr (μg/L)	Interval Begin	Sampling Date	Monlith mass (g)	Monlith Dry Mass (g)	Surface Area (cm^2)	Solution Volume (mL)	Monolith Volume (m^3)	M_{ti} (mg/m^2)	ρ (kg/m^3)	Co (mg$_{Cr}$ /kg$_{mono}$)	D_e (m^2/s)	D_e (cm^2/s)	Average D_e (cm^2/s)	Standard Deviation of Average De
S014-16-T6-2	6.95	3/1/2016 10:30:0	3/2/2016 8:30:00	363.78	284.0868039	196.70	1770.3	1.95E-04	6.26E-01	1.45E+03	410.08	2.0E-17	2.0E-13	2.0E-13	2.9E-16
S014-16-T6-3	6.95	3/1/2016 10:30:0	3/2/2016 8:30:00	364.78	284.8677341	197.29	1775.6	1.96E-04	6.26E-01	1.45E+03	410.08	2.0E-17	2.0E-13		
S014-16-T6-5	6.95	3/1/2016 10:30:0	3/2/2016 8:30:00	362.95	283.4386318	196.39	1767.5	1.95E-04	6.26E-01	1.45E+03	410.08	2.0E-17	2.0E-13	1.9E-13	3.1E-15
S014-16-T6-6	6.95	3/1/2016 10:30:0	3/2/2016 8:30:00	360.98	281.9001992	193.67	1743.0	1.91E-04	6.26E-01	1.48E+03	410.08	1.9E-17	1.9E-13		

Cr Sampling 2 d

Experiment Start 3/1/16 8:30:00

T1

Name	Cr (µg/L)	Interval Begin	Sampling Date	Monlith mass (g)	Monlith Dry Mass (g)	Surface Area (cm^2)	Solution Volume (mL)	Monolith Volume (m^3)	M_{ti} (mg/m^2)	ρ (kg/m^3)	Co (mg$_{Cr}$ /kg$_{mono}$)	D_e (m^2/s)	D_e (cm^2/s)	Average D_e (cm^2/s)	Standard Deviation of Average De
S014-16-T1-1	6.95	3/2/2016 8:30:0	3/3/2016 8:40:00	359.63	277.23	192.53	1732.8	1.89E-04	6.26E-01	1.46E+03	407.95	5.7E-17	5.7E-13	5.9E-13	2.1E-14
S014-16-T1-2	6.95	3/2/2016 8:30:0	3/3/2016 8:40:00	365.20	281.52	199.18	1792.6	1.99E-04	6.26E-01	1.41E+03	407.95	6.2E-17	6.2E-13		
S014-16-T1-4	6.95	3/2/2016 8:30:0	3/3/2016 8:40:00	360.86	278.18	195.83	1762.5	1.95E-04	6.26E-01	1.43E+03	407.95	6.0E-17	6.0E-13	5.9E-13	8.8E-15
S014-16-T1-7	6.95	3/2/2016 8:30:0	3/3/2016 8:40:00	361.60	278.75	194.35	1749.2	1.92E-04	6.26E-01	1.45E+03	407.95	5.9E-17	5.9E-13		

T2

Name	Cr (µg/L)	Interval Begin	Sampling Date	Monlith mass (g)	Monlith Dry Mass (g)	Surface Area (cm^2)	Solution Volume (mL)	Monolith Volume (m^3)	M_{ti} (mg/m^2)	ρ (kg/m^3)	Co (mg$_{Cr}$ /kg$_{mono}$)	D_e (m^2/s)	D_e (cm^2/s)	Average D_e (cm^2/s)	Standard Deviation of Average De
S014-16-T2-3	6.95	3/2/2016 8:30:0	3/3/2016 8:40:00	364.71	283.41	195.83	1749.7	1.92E-04	6.21E-01	1.48E+03	412.01	5.4E-17	5.4E-13	5.6E-13	1.4E-14
S014-16-T2-6	6.95	3/2/2016 8:30:0	3/3/2016 8:40:00	367.70	285.74	197.83	1780.5	1.97E-04	6.26E-01	1.45E+03	412.01	5.7E-17	5.7E-13		
S014-16-T2-7	6.95	3/2/2016 8:30:0	3/3/2016 8:40:00	366.00	284.41	196.77	1770.9	1.95E-04	6.26E-01	1.46E+03	412.01	5.7E-17	5.7E-13	5.8E-13	1.0E-14
S014-16-T2-8	6.95	3/2/2016 8:30:0	3/3/2016 8:40:00	363.14	282.19	197.90	1781.1	1.97E-04	6.26E-01	1.43E+03	412.01	5.9E-17	5.9E-13		

T3

Name	Cr (µg/L)	Interval Begin	Sampling Date	Monlith mass (g)	Monlith Dry Mass (g)	Surface Area (cm^2)	Solution Volume (mL)	Monolith Volume (m^3)	M_{ti} (mg/m^2)	ρ (kg/m^3)	Co (mg$_{Cr}$ /kg$_{mono}$)	D_e (m^2/s)	D_e (cm^2/s)	Average D_e (cm^2/s)	Standard Deviation of Average De
S014-16-T3-1	6.95	3/2/2016 8:30:0	3/3/2016 8:40:00	366.62	285.46	195.87	1762.9	1.94E-04	6.26E-01	1.47E+03	411.82	5.6E-17	5.6E-13	5.6E-13	3.9E-15
S014-16-T3-3	6.95	3/2/2016 8:30:0	3/3/2016 8:40:00	364.46	283.78	195.53	1759.7	1.94E-04	6.26E-01	1.46E+03	411.82	5.6E-17	5.6E-13		
S014-16-T3-4	6.95	3/2/2016 8:30:0	3/3/2016 8:40:00	362.76	282.46	194.51	1750.6	1.93E-04	6.26E-01	1.47E+03	411.82	5.6E-17	5.6E-13	5.6E-13	1.9E-15
S014-16-T3-8	6.95	3/2/2016 8:30:0	3/3/2016 8:40:00	360.88	280.99	194.17	1747.5	1.92E-04	6.26E-01	1.46E+03	411.82	5.7E-17	5.7E-13		

T4

Name	Cr (µg/L)	Interval Begin	Sampling Date	Monlith mass (g)	Monlith Dry Mass (g)	Surface Area (cm^2)	Solution Volume (mL)	Monolith Volume (m^3)	M_{ti} (mg/m^2)	ρ (kg/m^3)	Co (mg$_{Cr}$ /kg$_{mono}$)	D_e (m^2/s)	D_e (cm^2/s)	Average D_e (cm^2/s)	Standard Deviation of Average De
S014-16-T4-1	6.95	3/2/2016 8:30:0	3/3/2016 8:40:00	364.02	284.12	195.68	1761.2	1.94E-04	6.26E-01	1.46E+03	393.48	6.2E-17	6.2E-13	6.2E-13	5.9E-15
S014-16-T4-2	6.95	3/2/2016 8:30:0	3/3/2016 8:40:00	369.27	288.22	199.22	1793.0	1.99E-04	6.26E-01	1.45E+03	393.48	6.3E-17	6.3E-13		
S014-16-T4-5	6.95	3/2/2016 8:30:0	3/3/2016 8:40:00	365.37	285.18	195.92	1763.3	1.94E-04	6.26E-01	1.47E+03	393.48	6.2E-17	6.2E-13	6.2E-13	7.5E-15
S014-16-T4-7	6.95	3/2/2016 8:30:0	3/3/2016 8:40:00	363.93	284.05	196.69	1770.2	1.96E-04	6.26E-01	1.45E+03	393.48	6.3E-17	6.3E-13		

T5

Name	Cr (µg/L)	Interval Begin	Sampling Date	Monlith mass (g)	Monlith Dry Mass (g)	Surface Area (cm^2)	Solution Volume (mL)	Monolith Volume (m^3)	M_{ti} (mg/m^2)	ρ (kg/m^3)	Co (mg$_{Cr}$ /kg$_{mono}$)	D_e (m^2/s)	D_e (cm^2/s)	Average D_e (cm^2/s)	Standard Deviation of Average De
S014-16-T5-2	6.95	3/2/2016 8:30:0	3/3/2016 8:40:00	365.93	283.58	197.86	1780.7	1.97E-04	6.26E-01	1.44E+03	408.71	5.9E-17	5.9E-13	5.8E-13	1.2E-14
S014-16-T5-3	6.95	3/2/2016 8:30:0	3/3/2016 8:40:00	364.75	282.66	195.03	1755.3	1.92E-04	6.26E-01	1.47E+03	408.71	5.7E-17	5.7E-13		
S014-16-T5-4	6.95	3/2/2016 8:30:0	3/3/2016 8:40:00	366.62	284.11	196.79	1771.1	1.95E-04	6.26E-01	1.46E+03	408.71	5.8E-17	5.8E-13	5.9E-13	7.4E-15
S014-16-T5-7	6.95	3/2/2016 8:30:0	3/3/2016 8:40:00	365.76	283.44	197.96	1781.6	1.97E-04	6.26E-01	1.44E+03	408.71	5.9E-17	5.9E-13		

T6

Name	Cr (µg/L)	Interval Begin	Sampling Date	Monlith mass (g)	Monlith Dry Mass (g)	Surface Area (cm^2)	Solution Volume (mL)	Monolith Volume (m^3)	M_{ti} (mg/m^2)	ρ (kg/m^3)	Co (mg$_{Cr}$ /kg$_{mono}$)	D_e (m^2/s)	D_e (cm^2/s)	Average D_e (cm^2/s)	Standard Deviation of Average De
S014-16-T6-2	6.95	3/2/2016 8:30:0	3/3/2016 8:40:00	363.78	284.0868039	196.70	1770.3	1.95E-04	6.26E-01	1.45E+03	410.08	5.8E-17	5.8E-13	5.8E-13	8.4E-16
S014-16-T6-3	6.95	3/2/2016 8:30:0	3/3/2016 8:40:00	364.78	284.8677341	197.29	1775.6	1.96E-04	6.26E-01	1.45E+03	410.08	5.8E-17	5.8E-13		
S014-16-T6-5	6.95	3/2/2016 8:30:0	3/3/2016 8:40:00	362.95	283.4386318	196.39	1767.5	1.95E-04	6.26E-01	1.45E+03	410.08	5.8E-17	5.8E-13	5.7E-13	9.0E-15
S014-16-T6-6	6.95	3/2/2016 8:30:0	3/3/2016 8:40:00	360.98	281.9001992	193.67	1743.0	1.91E-04	6.26E-01	1.48E+03	410.08	5.6E-17	5.6E-13		

Cr Sampling 7d

Experiment Start	3/1/16 8:30:00

T1

Name	Cr (µg/L)	Interval Begin	Sampling Date	Monlith mass (g)	Monlith Dry Mass (g)	Surface Area (cm^2)	Solution Volume (mL)	Monolith Volume (m^3)	M_{ti} (mg/m^2)	ρ (kg/m^3)	Co (mg$_{Cr}$ /kg$_{mono}$)	D_e (m^2/s)	D_e (cm^2/s)	Average D_e (cm^2/s)	Standard Deviation of Average De
S014-16-T1-1	7.86	3/3/2016 8:40:0	3/8/2016 8:40:00	359.63	277.23	192.53	1732.8	1.89E-04	7.07E-01	1.46E+03	407.95	8.4E-18	8.4E-14	9.2E-14	7.7E-15
S014-16-T1-2	8.26	3/3/2016 8:40:0	3/8/2016 8:40:00	365.20	281.52	199.18	1792.6	1.99E-04	7.43E-01	1.41E+03	407.95	1.0E-17	1.0E-13		
S014-16-T1-4	6.95	3/3/2016 8:40:0	3/8/2016 8:40:00	360.86	278.18	195.83	1762.5	1.95E-04	6.26E-01	1.43E+03	407.95	6.9E-18	6.9E-14	6.8E-14	1.0E-15
S014-16-T1-7	6.95	3/3/2016 8:40:0	3/8/2016 8:40:00	361.60	278.75	194.35	1749.2	1.92E-04	6.26E-01	1.45E+03	407.95	6.7E-18	6.7E-14		

T2

Name	Cr (µg/L)	Interval Begin	Sampling Date	Monlith mass (g)	Monlith Dry Mass (g)	Surface Area (cm^2)	Solution Volume (mL)	Monolith Volume (m^3)	M_{ti} (mg/m^2)	ρ (kg/m^3)	Co (mg$_{Cr}$ /kg$_{mono}$)	D_e (m^2/s)	D_e (cm^2/s)	Average D_e (cm^2/s)	Standard Deviation of Average De
S014-16-T2-3	8.29	3/3/2016 8:40:0	3/8/2016 8:40:00	364.71	283.41	195.83	1749.7	1.92E-04	7.41E-01	1.48E+03	412.01	8.9E-18	8.9E-14	9.4E-14	5.8E-15
S014-16-T2-6	8.59	3/3/2016 8:40:0	3/8/2016 8:40:00	367.70	285.74	197.83	1780.5	1.97E-04	7.73E-01	1.45E+03	412.01	1.0E-17	1.0E-13		
S014-16-T2-7	6.95	3/3/2016 8:40:0	3/8/2016 8:40:00	366.00	284.41	196.77	1770.9	1.95E-04	6.26E-01	1.46E+03	412.01	6.5E-18	6.5E-14	6.7E-14	1.2E-15
S014-16-T2-8	6.95	3/3/2016 8:40:0	3/8/2016 8:40:00	363.14	282.19	197.90	1781.1	1.97E-04	6.26E-01	1.43E+03	412.01	6.8E-18	6.8E-14		

T3

Name	Cr (µg/L)	Interval Begin	Sampling Date	Monlith mass (g)	Monlith Dry Mass (g)	Surface Area (cm^2)	Solution Volume (mL)	Monolith Volume (m^3)	M_{ti} (mg/m^2)	ρ (kg/m^3)	Co (mg$_{Cr}$ /kg$_{mono}$)	D_e (m^2/s)	D_e (cm^2/s)	Average D_e (cm^2/s)	Standard Deviation of Average De
S014-16-T3-1	9	3/3/2016 8:40:0	3/8/2016 8:40:00	366.62	285.46	195.87	1762.9	1.94E-04	8.10E-01	1.47E+03	411.82	1.1E-17	1.1E-13	1.0E-13	2.2E-15
S014-16-T3-3	8.75	3/3/2016 8:40:0	3/8/2016 8:40:00	364.46	283.78	195.53	1759.7	1.94E-04	7.88E-01	1.46E+03	411.82	1.0E-17	1.0E-13		
S014-16-T3-4	6.95	3/3/2016 8:40:0	3/8/2016 8:40:00	362.76	282.46	194.51	1750.6	1.93E-04	6.26E-01	1.47E+03	411.82	6.4E-18	6.4E-14	6.5E-14	2.2E-16
S014-16-T3-8	6.95	3/3/2016 8:40:0	3/8/2016 8:40:00	360.88	280.99	194.17	1747.5	1.92E-04	6.26E-01	1.46E+03	411.82	6.5E-18	6.5E-14		

T4

Name	Cr (µg/L)	Interval Begin	Sampling Date	Monlith mass (g)	Monlith Dry Mass (g)	Surface Area (cm^2)	Solution Volume (mL)	Monolith Volume (m^3)	M_{ti} (mg/m^2)	ρ (kg/m^3)	Co (mg$_{Cr}$ /kg$_{mono}$)	D_e (m^2/s)	D_e (cm^2/s)	Average D_e (cm^2/s)	Standard Deviation of Average De
S014-16-T4-1	8.52	3/3/2016 8:40:0	3/8/2016 8:40:00	364.02	284.12	195.68	1761.2	1.94E-04	7.67E-01	1.46E+03	393.48	1.1E-17	1.1E-13	1.0E-13	4.2E-15
S014-16-T4-2	8.1	3/3/2016 8:40:0	3/8/2016 8:40:00	369.27	288.22	199.22	1793.0	1.99E-04	7.29E-01	1.45E+03	393.48	9.8E-18	9.8E-14		
S014-16-T4-5	6.95	3/3/2016 8:40:0	3/8/2016 8:40:00	365.37	285.18	195.92	1763.3	1.94E-04	6.26E-01	1.47E+03	393.48	7.1E-18	7.1E-14	7.1E-14	8.6E-16
S014-16-T4-7	6.95	3/3/2016 8:40:0	3/8/2016 8:40:00	363.93	284.05	196.69	1770.2	1.96E-04	6.26E-01	1.45E+03	393.48	7.2E-18	7.2E-14		

T5

Name	Cr (µg/L)	Interval Begin	Sampling Date	Monlith mass (g)	Monlith Dry Mass (g)	Surface Area (cm^2)	Solution Volume (mL)	Monolith Volume (m^3)	M_{ti} (mg/m^2)	ρ (kg/m^3)	Co (mg$_{Cr}$ /kg$_{mono}$)	D_e (m^2/s)	D_e (cm^2/s)	Average D_e (cm^2/s)	Standard Deviation of Average De
S014-16-T5-2	7.85	3/3/2016 8:40:0	3/8/2016 8:40:00	365.93	283.58	197.86	1780.7	1.97E-04	7.07E-01	1.44E+03	408.71	8.7E-18	8.7E-14	8.0E-14	6.7E-15
S014-16-T5-3	7.37	3/3/2016 8:40:0	3/8/2016 8:40:00	364.75	282.66	195.03	1755.3	1.92E-04	6.63E-01	1.47E+03	408.71	7.3E-18	7.3E-14		
S014-16-T5-4	6.95	3/3/2016 8:40:0	3/8/2016 8:40:00	366.62	284.11	196.79	1771.1	1.95E-04	6.26E-01	1.46E+03	408.71	6.6E-18	6.6E-14	6.7E-14	8.5E-16
S014-16-T5-7	6.95	3/3/2016 8:40:0	3/8/2016 8:40:00	365.76	283.44	197.96	1781.6	1.97E-04	6.26E-01	1.44E+03	408.71	6.8E-18	6.8E-14		

T6

Name	Cr (µg/L)	Interval Begin	Sampling Date	Monlith mass (g)	Monlith Dry Mass (g)	Surface Area (cm^2)	Solution Volume (mL)	Monolith Volume (m^3)	M_{ti} (mg/m^2)	ρ (kg/m^3)	Co (mg$_{Cr}$ /kg$_{mono}$)	D_e (m^2/s)	D_e (cm^2/s)	Average D_e (cm^2/s)	Standard Deviation of Average De
S014-16-T6-2	7.75	3/3/2016 8:40:0	3/8/2016 8:40:00	363.78	284.0868039	196.70	1770.3	1.95E-04	6.98E-01	1.45E+03	410.08	8.2E-18	8.2E-14	8.6E-14	4.3E-15
S014-16-T6-3	8.13	3/3/2016 8:40:0	3/8/2016 8:40:00	364.78	284.8677341	197.29	1775.6	1.96E-04	7.32E-01	1.45E+03	410.08	9.1E-18	9.1E-14		
S014-16-T6-5	6.95	3/3/2016 8:40:0	3/8/2016 8:40:00	362.95	283.4386318	196.39	1767.5	1.95E-04	6.26E-01	1.45E+03	410.08	6.6E-18	6.6E-14	6.5E-14	1.0E-15
S014-16-T6-6	6.95	3/3/2016 8:40:0	3/8/2016 8:40:00	360.98	281.9001992	193.67	1743.0	1.91E-04	6.26E-01	1.48E+03	410.08	6.4E-18	6.4E-14		

Cr Sampling 14 d

Experiment Start	3/1/16 8:30:00

T1

Name	Cr (µg/L)	Interval Begin	Sampling Date	Monlith mass (g)	Monlith Dry Mass (g)	Surface Area (cm^2)	Solution Volume (mL)	Monolith Volume (m^3)	M_{ti} (mg/m^2)	ρ (kg/m^3)	Co (mg$_{Cr}$ /kg$_{mono}$)	D_e (m^2/s)	D_e (cm^2/s)	Average D_e (cm^2/s)	Standard Deviation of Average De
S014-16-T1-1	6.95	3/8/2016 8:40:0	3/15/2016 8:50:0	359.63	277.23	192.53	1732.8	1.89E-04	6.26E-01	1.46E+03	407.95	8.3E-18	8.3E-14	8.6E-14	3.0E-15
S014-16-T1-2	6.95	3/8/2016 8:40:0	3/15/2016 8:50:0	365.20	281.52	199.18	1792.6	1.99E-04	6.26E-01	1.41E+03	407.95	8.9E-18	8.9E-14		
S014-16-T1-4	6.95	3/8/2016 8:40:0	3/15/2016 8:50:0	360.86	278.18	195.83	1762.5	1.95E-04	6.26E-01	1.43E+03	407.95	8.7E-18	8.7E-14	8.6E-14	1.3E-15
S014-16-T1-7	6.95	3/8/2016 8:40:0	3/15/2016 8:50:0	361.60	278.75	194.35	1749.2	1.92E-04	6.26E-01	1.45E+03	407.95	8.5E-18	8.5E-14		

T2

Name	Cr (µg/L)	Interval Begin	Sampling Date	Monlith mass (g)	Monlith Dry Mass (g)	Surface Area (cm^2)	Solution Volume (mL)	Monolith Volume (m^3)	M_{ti} (mg/m^2)	ρ (kg/m^3)	Co (mg$_{Cr}$ /kg$_{mono}$)	D_e (m^2/s)	D_e (cm^2/s)	Average D_e (cm^2/s)	Standard Deviation of Average De
S014-16-T2-3	6.95	3/8/2016 8:40:0	3/15/2016 8:50:0	364.71	283.41	195.83	1749.7	1.92E-04	6.21E-01	1.48E+03	412.01	7.8E-18	7.8E-14	8.1E-14	2.1E-15
S014-16-T2-6	6.95	3/8/2016 8:40:0	3/15/2016 8:50:0	367.70	285.74	197.83	1780.5	1.97E-04	6.26E-01	1.45E+03	412.01	8.3E-18	8.3E-14		
S014-16-T2-7	6.95	3/8/2016 8:40:0	3/15/2016 8:50:0	366.00	284.41	196.77	1770.9	1.95E-04	6.26E-01	1.46E+03	412.01	8.2E-18	8.2E-14	8.4E-14	1.5E-15
S014-16-T2-8	6.95	3/8/2016 8:40:0	3/15/2016 8:50:0	363.14	282.19	197.90	1781.1	1.97E-04	6.26E-01	1.43E+03	412.01	8.5E-18	8.5E-14		

T3

Name	Cr (µg/L)	Interval Begin	Sampling Date	Monlith mass (g)	Monlith Dry Mass (g)	Surface Area (cm^2)	Solution Volume (mL)	Monolith Volume (m^3)	M_{ti} (mg/m^2)	ρ (kg/m^3)	Co (mg$_{Cr}$ /kg$_{mono}$)	D_e (m^2/s)	D_e (cm^2/s)	Average D_e (cm^2/s)	Standard Deviation of Average De
S014-16-T3-1	6.95	3/8/2016 8:40:0	3/15/2016 8:50:0	366.62	285.46	195.87	1762.9	1.94E-04	6.26E-01	1.47E+03	411.82	8.0E-18	8.0E-14	8.1E-14	5.6E-16
S014-16-T3-3	6.95	3/8/2016 8:40:0	3/15/2016 8:50:0	364.46	283.78	195.53	1759.7	1.94E-04	6.26E-01	1.46E+03	411.82	8.1E-18	8.1E-14		
S014-16-T3-4	6.95	3/8/2016 8:40:0	3/15/2016 8:50:0	362.76	282.46	194.51	1750.6	1.93E-04	6.26E-01	1.47E+03	411.82	8.1E-18	8.1E-14	8.1E-14	2.8E-16
S014-16-T3-8	6.95	3/8/2016 8:40:0	3/15/2016 8:50:0	360.88	280.99	194.17	1747.5	1.92E-04	6.26E-01	1.46E+03	411.82	8.2E-18	8.2E-14		

T4

Name	Cr (µg/L)	Interval Begin	Sampling Date	Monlith mass (g)	Monlith Dry Mass (g)	Surface Area (cm^2)	Solution Volume (mL)	Monolith Volume (m^3)	M_{ti} (mg/m^2)	ρ (kg/m^3)	Co (mg$_{Cr}$ /kg$_{mono}$)	D_e (m^2/s)	D_e (cm^2/s)	Average D_e (cm^2/s)	Standard Deviation of Average De
S014-16-T4-1	6.95	3/8/2016 8:40:0	3/15/2016 8:50:0	364.02	284.12	195.68	1761.2	1.94E-04	6.26E-01	1.46E+03	393.48	8.9E-18	8.9E-14	9.0E-14	8.5E-16
S014-16-T4-2	6.95	3/8/2016 8:40:0	3/15/2016 8:50:0	369.27	288.22	199.22	1793.0	1.99E-04	6.26E-01	1.45E+03	393.48	9.1E-18	9.1E-14		
S014-16-T4-5	6.95	3/8/2016 8:40:0	3/15/2016 8:50:0	365.37	285.18	195.92	1763.3	1.94E-04	6.26E-01	1.47E+03	393.48	8.9E-18	8.9E-14	9.0E-14	1.1E-15
S014-16-T4-7	6.95	3/8/2016 8:40:0	3/15/2016 8:50:0	363.93	284.05	196.69	1770.2	1.96E-04	6.26E-01	1.45E+03	393.48	9.1E-18	9.1E-14		

T5

Name	Cr (µg/L)	Interval Begin	Sampling Date	Monlith mass (g)	Monlith Dry Mass (g)	Surface Area (cm^2)	Solution Volume (mL)	Monolith Volume (m^3)	M_{ti} (mg/m^2)	ρ (kg/m^3)	Co (mg$_{Cr}$ /kg$_{mono}$)	D_e (m^2/s)	D_e (cm^2/s)	Average D_e (cm^2/s)	Standard Deviation of Average De
S014-16-T5-2	6.95	3/8/2016 8:40:0	3/15/2016 8:50:0	365.93	283.58	197.86	1780.7	1.97E-04	6.26E-01	1.44E+03	408.71	8.5E-18	8.5E-14	8.4E-14	1.7E-15
S014-16-T5-3	6.95	3/8/2016 8:40:0	3/15/2016 8:50:0	364.75	282.66	195.03	1755.3	1.92E-04	6.26E-01	1.47E+03	408.71	8.2E-18	8.2E-14		
S014-16-T5-4	6.95	3/8/2016 8:40:0	3/15/2016 8:50:0	366.62	284.11	196.79	1771.1	1.95E-04	6.26E-01	1.46E+03	408.71	8.3E-18	8.3E-14	8.5E-14	1.1E-15
S014-16-T5-7	6.95	3/8/2016 8:40:0	3/15/2016 8:50:0	365.76	283.44	197.96	1781.6	1.97E-04	6.26E-01	1.44E+03	408.71	8.6E-18	8.6E-14		

T6

Name	Cr (µg/L)	Interval Begin	Sampling Date	Monlith mass (g)	Monlith Dry Mass (g)	Surface Area (cm^2)	Solution Volume (mL)	Monolith Volume (m^3)	M_{ti} (mg/m^2)	ρ (kg/m^3)	Co (mg$_{Cr}$ /kg$_{mono}$)	D_e (m^2/s)	D_e (cm^2/s)	Average D_e (cm^2/s)	Standard Deviation of Average De
S014-16-T6-2	6.95	3/8/2016 8:40:0	3/15/2016 8:50:0	363.78	284.0868039	196.70	1770.3	1.95E-04	6.26E-01	1.45E+03	410.08	8.3E-18	8.3E-14	8.3E-14	1.2E-16
S014-16-T6-3	6.95	3/8/2016 8:40:0	3/15/2016 8:50:0	364.78	284.8677341	197.29	1775.6	1.96E-04	6.26E-01	1.45E+03	410.08	8.4E-18	8.4E-14		
S014-16-T6-5	6.95	3/8/2016 8:40:0	3/15/2016 8:50:0	362.95	283.4386318	196.39	1767.5	1.95E-04	6.26E-01	1.45E+03	410.08	8.3E-18	8.3E-14	8.2E-14	1.3E-15
S014-16-T6-6	6.95	3/8/2016 8:40:0	3/15/2016 8:50:0	360.98	281.9001992	193.67	1743.0	1.91E-04	6.26E-01	1.48E+03	410.08	8.1E-18	8.1E-14		

Cr Sampling 28 d

Experiment Start 3/1/16 8:30:00

T1

Name	Cr (µg/L)	Interval Begin	Sampling Date	Monlith mass (g)	Monlith Dry Mass (g)	Surface Area (cm^2)	Solution Volume (mL)	Monolith Volume (m^3)	M_{ti} (mg/m^2)	ρ (kg/m^3)	Co (mg$_{Cr}$ /kg$_{mono}$)	D_e (m^2/s)	D_e (cm^2/s)	Average D_e (cm^2/s)	Standard Deviation of Average De
S014-16-T1-1	6.95	03/15/2016 08:50:0	03/29/2016 08:00:0	359.63	277.23	192.53	1732.8	1.89E-04	6.26E-01	1.46E+03	407.95	4.2E-18	4.2E-14	4.3E-14	1.5E-15
S014-16-T1-2	6.95	03/15/2016 08:50:0	03/29/2016 08:00:0	365.20	281.52	199.18	1792.6	1.99E-04	6.26E-01	1.41E+03	407.95	4.5E-18	4.5E-14		
S014-16-T1-4	6.95	03/15/2016 08:50:0	03/29/2016 08:00:0	360.86	278.18	195.83	1762.5	1.95E-04	6.26E-01	1.43E+03	407.95	4.4E-18	4.4E-14	4.3E-14	6.4E-16
S014-16-T1-7	6.95	03/15/2016 08:50:0	03/29/2016 08:00:0	361.60	278.75	194.35	1749.2	1.92E-04	6.26E-01	1.45E+03	407.95	4.3E-18	4.3E-14		

T2

Name	Cr (µg/L)	Interval Begin	Sampling Date	Monlith mass (g)	Monlith Dry Mass (g)	Surface Area (cm^2)	Solution Volume (mL)	Monolith Volume (m^3)	M_{ti} (mg/m^2)	ρ (kg/m^3)	Co (mg$_{Cr}$ /kg$_{mono}$)	D_e (m^2/s)	D_e (cm^2/s)	Average D_e (cm^2/s)	Standard Deviation of Average De
S014-16-T2-3	6.95	03/15/2016 08:50:0	03/29/2016 08:00:0	364.71	283.41	195.83	1749.7	1.92E-04	6.21E-01	1.48E+03	412.01	3.9E-18	3.9E-14	4.1E-14	1.0E-15
S014-16-T2-6	6.95	03/15/2016 08:50:0	03/29/2016 08:00:0	367.70	285.74	197.83	1780.5	1.97E-04	6.26E-01	1.45E+03	412.01	4.2E-18	4.2E-14		
S014-16-T2-7	6.95	03/15/2016 08:50:0	03/29/2016 08:00:0	366.00	284.41	196.77	1770.9	1.95E-04	6.26E-01	1.46E+03	412.01	4.1E-18	4.1E-14	4.2E-14	7.4E-16
S014-16-T2-8	6.95	03/15/2016 08:50:0	03/29/2016 08:00:0	363.14	282.19	197.90	1781.1	1.97E-04	6.26E-01	1.43E+03	412.01	4.3E-18	4.3E-14		

T3

Name	Cr (µg/L)	Interval Begin	Sampling Date	Monlith mass (g)	Monlith Dry Mass (g)	Surface Area (cm^2)	Solution Volume (mL)	Monolith Volume (m^3)	M_{ti} (mg/m^2)	ρ (kg/m^3)	Co (mg$_{Cr}$ /kg$_{mono}$)	D_e (m^2/s)	D_e (cm^2/s)	Average D_e (cm^2/s)	Standard Deviation of Average De
S014-16-T3-1	8.36	03/15/2016 08:50:0	03/29/2016 08:00:0	366.62	285.46	195.87	1762.9	1.94E-04	7.52E-01	1.47E+03	411.82	5.8E-18	5.8E-14	6.1E-14	2.4E-15
S014-16-T3-3	8.64	03/15/2016 08:50:0	03/29/2016 08:00:0	364.46	283.78	195.53	1759.7	1.94E-04	7.78E-01	1.46E+03	411.82	6.3E-18	6.3E-14		
S014-16-T3-4	6.95	03/15/2016 08:50:0	03/29/2016 08:00:0	362.76	282.46	194.51	1750.6	1.93E-04	6.26E-01	1.47E+03	411.82	4.1E-18	4.1E-14	4.1E-14	1.4E-16
S014-16-T3-8	6.95	03/15/2016 08:50:0	03/29/2016 08:00:0	360.88	280.99	194.17	1747.5	1.92E-04	6.26E-01	1.46E+03	411.82	4.1E-18	4.1E-14		

T4

Name	Cr (µg/L)	Interval Begin	Sampling Date	Monlith mass (g)	Monlith Dry Mass (g)	Surface Area (cm^2)	Solution Volume (mL)	Monolith Volume (m^3)	M_{ti} (mg/m^2)	ρ (kg/m^3)	Co (mg$_{Cr}$ /kg$_{mono}$)	D_e (m^2/s)	D_e (cm^2/s)	Average D_e (cm^2/s)	Standard Deviation of Average De
S014-16-T4-1	6.95	03/15/2016 08:50:0	03/29/2016 08:00:0	364.02	284.12	195.68	1761.2	1.94E-04	6.26E-01	1.46E+03	393.48	4.5E-18	4.5E-14	4.9E-14	3.8E-15
S014-16-T4-2	7.45	03/15/2016 08:50:0	03/29/2016 08:00:0	369.27	288.22	199.22	1793.0	1.99E-04	6.71E-01	1.45E+03	393.48	5.3E-18	5.3E-14		
S014-16-T4-5	6.95	03/15/2016 08:50:0	03/29/2016 08:00:0	365.37	285.18	195.92	1763.3	1.94E-04	6.26E-01	1.47E+03	393.48	4.5E-18	4.5E-14	4.5E-14	5.5E-16
S014-16-T4-7	6.95	03/15/2016 08:50:0	03/29/2016 08:00:0	363.93	284.05	196.69	1770.2	1.96E-04	6.26E-01	1.45E+03	393.48	4.6E-18	4.6E-14		

T5

Name	Cr (µg/L)	Interval Begin	Sampling Date	Monlith mass (g)	Monlith Dry Mass (g)	Surface Area (cm^2)	Solution Volume (mL)	Monolith Volume (m^3)	M_{ti} (mg/m^2)	ρ (kg/m^3)	Co (mg$_{Cr}$ /kg$_{mono}$)	D_e (m^2/s)	D_e (cm^2/s)	Average D_e (cm^2/s)	Standard Deviation of Average De
S014-16-T5-2	9.02	03/15/2016 08:50:0	03/29/2016 08:00:0	365.93	283.58	197.86	1780.7	1.97E-04	8.12E-01	1.44E+03	408.71	7.2E-18	7.2E-14	6.5E-14	7.3E-15
S014-16-T5-3	8.22	03/15/2016 08:50:0	03/29/2016 08:00:0	364.75	282.66	195.03	1755.3	1.92E-04	7.40E-01	1.47E+03	408.71	5.8E-18	5.8E-14		
S014-16-T5-4	6.95	03/15/2016 08:50:0	03/29/2016 08:00:0	366.62	284.11	196.79	1771.1	1.95E-04	6.26E-01	1.46E+03	408.71	4.2E-18	4.2E-14	4.3E-14	5.4E-16
S014-16-T5-7	6.95	03/15/2016 08:50:0	03/29/2016 08:00:0	365.76	283.44	197.96	1781.6	1.97E-04	6.26E-01	1.44E+03	408.71	4.3E-18	4.3E-14		

T6

Name	Cr (µg/L)	Interval Begin	Sampling Date	Monlith mass (g)	Monlith Dry Mass (g)	Surface Area (cm^2)	Solution Volume (mL)	Monolith Volume (m^3)	M_{ti} (mg/m^2)	ρ (kg/m^3)	Co (mg$_{Cr}$ /kg$_{mono}$)	D_e (m^2/s)	D_e (cm^2/s)	Average D_e (cm^2/s)	Standard Deviation of Average De
S014-16-T6-2	6.95	03/15/2016 08:50:0	03/29/2016 08:00:0	363.78	284.0868039	196.70	1770.3	1.95E-04	6.26E-01	1.45E+03	410.08	4.2E-18	4.2E-14	5.1E-14	8.9E-15
S014-16-T6-3	8.28	03/15/2016 08:50:0	03/29/2016 08:00:0	364.78	284.8677341	197.29	1775.6	1.96E-04	7.45E-01	1.45E+03	410.08	6.0E-18	6.0E-14		
S014-16-T6-5	6.95	03/15/2016 08:50:0	03/29/2016 08:00:0	362.95	283.4386318	196.39	1767.5	1.95E-04	6.26E-01	1.45E+03	410.08	4.2E-18	4.2E-14	4.1E-14	6.5E-16
S014-16-T6-6	6.95	03/15/2016 08:50:0	03/29/2016 08:00:0	360.98	281.9001992	193.67	1743.0	1.91E-04	6.26E-01	1.48E+03	410.08	4.1E-18	4.1E-14		

Cr Sampling 42 d

Experiment Start 3/1/16 8:30:00

T1

Name	I (µg/L)	Interval Begin	Sampling Date	Monlith mass (g)	Monlith Dry Mass (g)	Surface Area (cm^2)	Solution Volume (mL)	Monolith Volume (m^3)	M_{ti} (mg/m^2)	ρ (kg/m^3)	Co (mg$_{Cr}$ /kg$_{mono}$)	D_e (m^2/s)	D_e (cm^2/s)	Average D_e (cm^2/s)	Standard Deviation of Average De
S014-16-T1-1	6.95	03/29/2016 08:00:0	4/12/16 8:30:00	359.63	277.23	192.53	1732.8	1.89E-04	6.26E-01	1.46E+03	407.95	7.0E-18	7.0E-14	7.3E-14	2.5E-15
S014-16-T1-2	6.95	03/29/2016 08:00:0	4/12/16 8:30:00	365.20	281.52	199.18	1792.6	1.99E-04	6.26E-01	1.41E+03	407.95	7.5E-18	7.5E-14		
S014-16-T1-4	6.95	03/29/2016 08:00:0	4/12/16 8:30:00	360.86	278.18	195.83	1762.5	1.95E-04	6.26E-01	1.43E+03	407.95	7.4E-18	7.4E-14	7.3E-14	1.1E-15
S014-16-T1-7	6.95	03/29/2016 08:00:0	4/12/16 8:30:00	361.60	278.75	194.35	1749.2	1.92E-04	6.26E-01	1.45E+03	407.95	7.2E-18	7.2E-14		

T2

Name	Cr (µg/L)	Interval Begin	Sampling Date	Monlith mass (g)	Monlith Dry Mass (g)	Surface Area (cm^2)	Solution Volume (mL)	Monolith Volume (m^3)	M_{ti} (mg/m^2)	ρ (kg/m^3)	Co (mg$_{Cr}$ /kg$_{mono}$)	D_e (m^2/s)	D_e (cm^2/s)	Average D_e (cm^2/s)	Standard Deviation of Average De
S014-16-T2-3	6.95	03/29/2016 08:00:0	4/12/16 8:30:00	364.71	283.41	195.83	1749.7	1.92E-04	6.21E-01	1.48E+03	412.01	6.7E-18	6.7E-14	6.8E-14	1.7E-15
S014-16-T2-6	6.95	03/29/2016 08:00:0	4/12/16 8:30:00	367.70	285.74	197.83	1780.5	1.97E-04	6.26E-01	1.45E+03	412.01	7.0E-18	7.0E-14		
S014-16-T2-7	6.95	03/29/2016 08:00:0	4/12/16 8:30:00	366.00	284.41	196.77	1770.9	1.95E-04	6.26E-01	1.46E+03	412.01	7.0E-18	7.0E-14	7.1E-14	1.2E-15
S014-16-T2-8	6.95	03/29/2016 08:00:0	4/12/16 8:30:00	363.14	282.19	197.90	1781.1	1.97E-04	6.26E-01	1.43E+03	412.01	7.2E-18	7.2E-14		

T3

Name	Cr (µg/L)	Interval Begin	Sampling Date	Monlith mass (g)	Monlith Dry Mass (g)	Surface Area (cm^2)	Solution Volume (mL)	Monolith Volume (m^3)	M_{ti} (mg/m^2)	ρ (kg/m^3)	Co (mg$_{Cr}$ /kg$_{mono}$)	D_e (m^2/s)	D_e (cm^2/s)	Average D_e (cm^2/s)	Standard Deviation of Average De
S014-16-T3-1	6.95	03/29/2016 08:00:0	4/12/16 8:30:00	366.62	285.46	195.87	1762.9	1.94E-04	6.26E-01	1.47E+03	411.82	6.8E-18	6.8E-14	6.9E-14	4.8E-16
S014-16-T3-3	6.95	03/29/2016 08:00:0	4/12/16 8:30:00	364.46	283.78	195.53	1759.7	1.94E-04	6.26E-01	1.46E+03	411.82	6.9E-18	6.9E-14		
S014-16-T3-4	6.95	03/29/2016 08:00:0	4/12/16 8:30:00	362.76	282.46	194.51	1750.6	1.93E-04	6.26E-01	1.47E+03	411.82	6.9E-18	6.9E-14	6.9E-14	2.4E-16
S014-16-T3-8	6.95	03/29/2016 08:00:0	4/12/16 8:30:00	360.88	280.99	194.17	1747.5	1.92E-04	6.26E-01	1.46E+03	411.82	6.9E-18	6.9E-14		

T4

Name	Cr (µg/L)	Interval Begin	Sampling Date	Monlith mass (g)	Monlith Dry Mass (g)	Surface Area (cm^2)	Solution Volume (mL)	Monolith Volume (m^3)	M_{ti} (mg/m^2)	ρ (kg/m^3)	Co (mg$_{Cr}$ /kg$_{mono}$)	D_e (m^2/s)	D_e (cm^2/s)	Average D_e (cm^2/s)	Standard Deviation of Average De
S014-16-T4-1	6.95	03/29/2016 08:00:0	4/12/16 8:30:00	364.02	284.12	195.68	1761.2	1.94E-04	6.26E-01	1.46E+03	393.48	7.6E-18	7.6E-14	7.6E-14	7.2E-16
S014-16-T4-2	6.95	03/29/2016 08:00:0	4/12/16 8:30:00	369.27	288.22	199.22	1793.0	1.99E-04	6.26E-01	1.45E+03	393.48	7.7E-18	7.7E-14		
S014-16-T4-5	6.95	03/29/2016 08:00:0	4/12/16 8:30:00	365.37	285.18	195.92	1763.3	1.94E-04	6.26E-01	1.47E+03	393.48	7.5E-18	7.5E-14	7.6E-14	9.2E-16
S014-16-T4-7	6.95	03/29/2016 08:00:0	4/12/16 8:30:00	363.93	284.05	196.69	1770.2	1.96E-04	6.26E-01	1.45E+03	393.48	7.7E-18	7.7E-14		

T5

Name	Cr (µg/L)	Interval Begin	Sampling Date	Monlith mass (g)	Monlith Dry Mass (g)	Surface Area (cm^2)	Solution Volume (mL)	Monolith Volume (m^3)	M_{ti} (mg/m^2)	ρ (kg/m^3)	Co (mg$_{Cr}$ /kg$_{mono}$)	D_e (m^2/s)	D_e (cm^2/s)	Average D_e (cm^2/s)	Standard Deviation of Average De
S014-16-T5-2	6.95	03/29/2016 08:00:0	4/12/16 8:30:00	365.93	283.58	197.86	1780.7	1.97E-04	6.26E-01	1.44E+03	408.71	7.2E-18	7.2E-14	7.1E-14	1.5E-15
S014-16-T5-3	6.95	03/29/2016 08:00:0	4/12/16 8:30:00	364.75	282.66	195.03	1755.3	1.92E-04	6.26E-01	1.47E+03	408.71	7.0E-18	7.0E-14		
S014-16-T5-4	6.95	03/29/2016 08:00:0	4/12/16 8:30:00	366.62	284.11	196.79	1771.1	1.95E-04	6.26E-01	1.46E+03	408.71	7.1E-18	7.1E-14	7.2E-14	9.1E-16
S014-16-T5-7	6.95	03/29/2016 08:00:0	4/12/16 8:30:00	365.76	283.44	197.96	1781.6	1.97E-04	6.26E-01	1.44E+03	408.71	7.3E-18	7.3E-14		

T6

Name	Cr (µg/L)	Interval Begin	Sampling Date	Monlith mass (g)	Monlith Dry Mass (g)	Surface Area (cm^2)	Solution Volume (mL)	Monolith Volume (m^3)	M_{ti} (mg/m^2)	ρ (kg/m^3)	Co (mg$_{Cr}$ /kg$_{mono}$)	D_e (m^2/s)	D_e (cm^2/s)	Average D_e (cm^2/s)	Standard Deviation of Average De
S014-16-T6-2	6.95	03/29/2016 08:00:0	4/12/16 8:30:00	363.78	284.0868039	196.70	1770.3	1.95E-04	6.26E-01	1.45E+03	410.08	7.1E-18	7.1E-14	7.1E-14	1.0E-16
S014-16-T6-3	6.95	03/29/2016 08:00:0	4/12/16 8:30:00	364.78	284.8677341	197.29	1775.6	1.96E-04	6.26E-01	1.45E+03	410.08	7.1E-18	7.1E-14		
S014-16-T6-5	6.95	03/29/2016 08:00:0	4/12/16 8:30:00	362.95	283.4386318	196.39	1767.5	1.95E-04	6.26E-01	1.45E+03	410.08	7.1E-18	7.1E-14	6.9E-14	1.1E-15
S014-16-T6-6	6.95	03/29/2016 08:00:0	4/12/16 8:30:00	360.98	281.9001992	193.67	1743.0	1.91E-04	6.26E-01	1.48E+03	410.08	6.8E-18	6.8E-14		

Cr Sampling 49 d

Experiment Start 3/1/16 8:30:00

T1

Name	Cr (µg/L)	Interval Begin	Sampling Date	Monlith mass (g)	Monlith Dry Mass (g)	Surface Area (cm^2)	Solution Volume (mL)	Monolith Volume (m^3)	M_{ti} (mg/m^2)	ρ (kg/m^3)	Co (mg$_{Cr}$ /kg$_{mono}$)	D_e (m^2/s)	D_e (cm^2/s)	Average D_e (cm^2/s)	Standard Deviation of Average De
S014-16-T1-1	6.95	4/12/16 8:30:0	4/19/16 8:40:00	359.63	277.23	192.53	1732.8	1.89E-04	6.26E-01	1.46E+03	407.95	3.7E-17	3.7E-13	3.8E-13	1.3E-14
S014-16-T1-2	6.95	4/12/16 8:30:0	4/19/16 8:40:00	365.20	281.52	199.18	1792.6	1.99E-04	6.26E-01	1.41E+03	407.95	4.0E-17	4.0E-13		
S014-16-T1-4	6.95	4/12/16 8:30:0	4/19/16 8:40:00	360.86	278.18	195.83	1762.5	1.95E-04	6.26E-01	1.43E+03	407.95	3.9E-17	3.9E-13	3.8E-13	5.6E-15
S014-16-T1-7	6.95	4/12/16 8:30:0	4/19/16 8:40:00	361.60	278.75	194.35	1749.2	1.92E-04	6.26E-01	1.45E+03	407.95	3.8E-17	3.8E-13		

T2

Name	Cr (µg/L)	Interval Begin	Sampling Date	Monlith mass (g)	Monlith Dry Mass (g)	Surface Area (cm^2)	Solution Volume (mL)	Monolith Volume (m^3)	M_{ti} (mg/m^2)	ρ (kg/m^3)	Co (mg$_{Cr}$ /kg$_{mono}$)	D_e (m^2/s)	D_e (cm^2/s)	Average D_e (cm^2/s)	Standard Deviation of Average De
S014-16-T2-3	6.95	4/12/16 8:30:0	4/19/16 8:40:00	364.71	283.41	195.83	1749.7	1.92E-04	6.21E-01	1.48E+03	412.01	3.5E-17	3.5E-13	3.6E-13	9.1E-15
S014-16-T2-6	6.95	4/12/16 8:30:0	4/19/16 8:40:00	367.70	285.74	197.83	1780.5	1.97E-04	6.26E-01	1.45E+03	412.01	3.7E-17	3.7E-13		
S014-16-T2-7	6.95	4/12/16 8:30:0	4/19/16 8:40:00	366.00	284.41	196.77	1770.9	1.95E-04	6.26E-01	1.46E+03	412.01	3.7E-17	3.7E-13	3.7E-13	6.5E-15
S014-16-T2-8	6.95	4/12/16 8:30:0	4/19/16 8:40:00	363.14	282.19	197.90	1781.1	1.97E-04	6.26E-01	1.43E+03	412.01	3.8E-17	3.8E-13		

T3

Name	Cr (µg/L)	Interval Begin	Sampling Date	Monlith mass (g)	Monlith Dry Mass (g)	Surface Area (cm^2)	Solution Volume (mL)	Monolith Volume (m^3)	M_{ti} (mg/m^2)	ρ (kg/m^3)	Co (mg$_{Cr}$ /kg$_{mono}$)	D_e (m^2/s)	D_e (cm^2/s)	Average D_e (cm^2/s)	Standard Deviation of Average De
S014-16-T3-1	6.95	4/12/16 8:30:0	4/19/16 8:40:00	366.62	285.46	195.87	1762.9	1.94E-04	6.26E-01	1.47E+03	411.82	3.6E-17	3.6E-13	3.6E-13	2.5E-15
S014-16-T3-3	6.95	4/12/16 8:30:0	4/19/16 8:40:00	364.46	283.78	195.53	1759.7	1.94E-04	6.26E-01	1.46E+03	411.82	3.6E-17	3.6E-13		
S014-16-T3-4	6.95	4/12/16 8:30:0	4/19/16 8:40:00	362.76	282.46	194.51	1750.6	1.93E-04	6.26E-01	1.47E+03	411.82	3.6E-17	3.6E-13	3.6E-13	1.2E-15
S014-16-T3-8	6.95	4/12/16 8:30:0	4/19/16 8:40:00	360.88	280.99	194.17	1747.5	1.92E-04	6.26E-01	1.46E+03	411.82	3.6E-17	3.6E-13		

T4

Name	Cr (µg/L)	Interval Begin	Sampling Date	Monlith mass (g)	Monlith Dry Mass (g)	Surface Area (cm^2)	Solution Volume (mL)	Monolith Volume (m^3)	M_{ti} (mg/m^2)	ρ (kg/m^3)	Co (mg$_{Cr}$ /kg$_{mono}$)	D_e (m^2/s)	D_e (cm^2/s)	Average D_e (cm^2/s)	Standard Deviation of Average De
S014-16-T4-1	6.95	4/12/16 8:30:0	4/19/16 8:40:00	364.02	284.12	195.68	1761.2	1.94E-04	6.26E-01	1.46E+03	393.48	4.0E-17	4.0E-13	4.0E-13	3.8E-15
S014-16-T4-2	6.95	4/12/16 8:30:0	4/19/16 8:40:00	369.27	288.22	199.22	1793.0	1.99E-04	6.26E-01	1.45E+03	393.48	4.1E-17	4.1E-13		
S014-16-T4-5	6.95	4/12/16 8:30:0	4/19/16 8:40:00	365.37	285.18	195.92	1763.3	1.94E-04	6.26E-01	1.47E+03	393.48	4.0E-17	4.0E-13	4.0E-13	4.8E-15
S014-16-T4-7	6.95	4/12/16 8:30:0	4/19/16 8:40:00	363.93	284.05	196.69	1770.2	1.96E-04	6.26E-01	1.45E+03	393.48	4.0E-17	4.0E-13		

T5

Name	Cr (µg/L)	Interval Begin	Sampling Date	Monlith mass (g)	Monlith Dry Mass (g)	Surface Area (cm^2)	Solution Volume (mL)	Monolith Volume (m^3)	M_{ti} (mg/m^2)	ρ (kg/m^3)	Co (mg$_{Cr}$ /kg$_{mono}$)	D_e (m^2/s)	D_e (cm^2/s)	Average D_e (cm^2/s)	Standard Deviation of Average De
S014-16-T5-2	6.95	4/12/16 8:30:0	4/19/16 8:40:00	365.93	283.58	197.86	1780.7	1.97E-04	6.26E-01	1.44E+03	408.71	3.8E-17	3.8E-13	3.7E-13	7.6E-15
S014-16-T5-3	6.95	4/12/16 8:30:0	4/19/16 8:40:00	364.75	282.66	195.03	1755.3	1.92E-04	6.26E-01	1.47E+03	408.71	3.7E-17	3.7E-13		
S014-16-T5-4	6.95	4/12/16 8:30:0	4/19/16 8:40:00	366.62	284.11	196.79	1771.1	1.95E-04	6.26E-01	1.46E+03	408.71	3.7E-17	3.7E-13	3.8E-13	4.8E-15
S014-16-T5-7	6.95	4/12/16 8:30:0	4/19/16 8:40:00	365.76	283.44	197.96	1781.6	1.97E-04	6.26E-01	1.44E+03	408.71	3.8E-17	3.8E-13		

T6

Name	Cr (µg/L)	Interval Begin	Sampling Date	Monlith mass (g)	Monlith Dry Mass (g)	Surface Area (cm^2)	Solution Volume (mL)	Monolith Volume (m^3)	M_{ti} (mg/m^2)	ρ (kg/m^3)	Co (mg$_{Cr}$ /kg$_{mono}$)	D_e (m^2/s)	D_e (cm^2/s)	Average D_e (cm^2/s)	Standard Deviation of Average De
S014-16-T6-2	6.95	4/12/16 8:30:0	4/19/16 8:40:00	363.78	284.0868039	196.70	1770.3	1.95E-04	6.26E-01	1.45E+03	410.08	3.7E-17	3.7E-13	3.7E-13	5.4E-16
S014-16-T6-3	6.95	4/12/16 8:30:0	4/19/16 8:40:00	364.78	284.8677341	197.29	1775.6	1.96E-04	6.26E-01	1.45E+03	410.08	3.7E-17	3.7E-13		
S014-16-T6-5	6.95	4/12/16 8:30:0	4/19/16 8:40:00	362.95	283.4386318	196.39	1767.5	1.95E-04	6.26E-01	1.45E+03	410.08	3.7E-17	3.7E-13	3.6E-13	5.8E-15
S014-16-T6-6	6.95	4/12/16 8:30:0	4/19/16 8:40:00	360.98	281.9001992	193.67	1743.0	1.91E-04	6.26E-01	1.48E+03	410.08	3.6E-17	3.6E-13		

Cr Sampling 63 d

Experiment Start 3/1/16 8:30:00

T1

Name	Cr (μg/L)	Interval Begin	Sampling Date	Monlith mass (g)	Monlith Dry Mass (g)	Surface Area (cm^2)	Solution Volume (mL)	Monolith Volume (m^3)	M_{ti} (mg/m^2)	ρ (kg/m^3)	Co (mg$_{Cr}$ /kg$_{mono}$)	D_e (m^2/s)	D_e (cm^2/s)	Average D_e (cm^2/s)	Standard Deviation of Average De
S014-16-T1-1	11.6	4/19/16 8:40:0	05/3/2016 09:00:0	359.63	279.46	192.53	1732.8	1.89E-04	1.04E+00	1.48E+03	407.95	3.1E-17	3.1E-13	3.2E-13	1.1E-14
S014-16-T1-2	11.6	4/19/16 8:40:0	05/3/2016 09:00:0	365.20	283.79	199.18	1792.6	1.99E-04	1.04E+00	1.43E+03	407.95	3.3E-17	3.3E-13		
S014-16-T1-4	11.6	4/19/16 8:40:0	05/3/2016 09:00:0	360.86	280.42	195.83	1762.5	1.95E-04	1.04E+00	1.44E+03	407.95	3.3E-17	3.3E-13	3.2E-13	4.8E-15
S014-16-T1-7	11.6	4/19/16 8:40:0	05/3/2016 09:00:0	361.60	281.00	194.35	1749.2	1.92E-04	1.04E+00	1.46E+03	407.95	3.2E-17	3.2E-13		

T2

Name	Cr (μg/L)	Interval Begin	Sampling Date	Monlith mass (g)	Monlith Dry Mass (g)	Surface Area (cm^2)	Solution Volume (mL)	Monolith Volume (m^3)	M_{ti} (mg/m^2)	ρ (kg/m^3)	Co (mg$_{Cr}$ /kg$_{mono}$)	D_e (m^2/s)	D_e (cm^2/s)	Average D_e (cm^2/s)	Standard Deviation of Average De
S014-16-T2-3	11.6	4/19/16 8:40:0	05/3/2016 09:00:0	364.71	283.97	195.83	1749.7	1.92E-04	1.04E+00	1.48E+03	412.01	3.0E-17	3.0E-13	3.1E-13	7.8E-15
S014-16-T2-6	11.6	4/19/16 8:40:0	05/3/2016 09:00:0	367.70	286.30	197.83	1780.5	1.97E-04	1.04E+00	1.46E+03	412.01	3.1E-17	3.1E-13		
S014-16-T2-7	11.6	4/19/16 8:40:0	05/3/2016 09:00:0	366.00	284.98	196.77	1770.9	1.95E-04	1.04E+00	1.46E+03	412.01	3.1E-17	3.1E-13	3.2E-13	5.5E-15
S014-16-T2-8	11.6	4/19/16 8:40:0	05/3/2016 09:00:0	363.14	282.75	197.90	1781.1	1.97E-04	1.04E+00	1.43E+03	412.01	3.2E-17	3.2E-13		

T3

Name	Cr (μg/L)	Interval Begin	Sampling Date	Monlith mass (g)	Monlith Dry Mass (g)	Surface Area (cm^2)	Solution Volume (mL)	Monolith Volume (m^3)	M_{ti} (mg/m^2)	ρ (kg/m^3)	Co (mg$_{Cr}$ /kg$_{mono}$)	D_e (m^2/s)	D_e (cm^2/s)	Average D_e (cm^2/s)	Standard Deviation of Average De
S014-16-T3-1	11.6	4/19/16 8:40:0	05/3/2016 09:00:0	366.62	286.15	195.87	1762.9	1.94E-04	1.04E+00	1.48E+03	411.82	3.0E-17	3.0E-13	3.1E-13	2.1E-15
S014-16-T3-3	11.6	4/19/16 8:40:0	05/3/2016 09:00:0	364.46	284.46	195.53	1759.7	1.94E-04	1.04E+00	1.47E+03	411.82	3.1E-17	3.1E-13		
S014-16-T3-4	11.6	4/19/16 8:40:0	05/3/2016 09:00:0	362.76	283.14	194.51	1750.6	1.93E-04	1.04E+00	1.47E+03	411.82	3.1E-17	3.1E-13	3.1E-13	1.1E-15
S014-16-T3-8	11.6	4/19/16 8:40:0	05/3/2016 09:00:0	360.88	281.67	194.17	1747.5	1.92E-04	1.04E+00	1.47E+03	411.82	3.1E-17	3.1E-13		

T4

Name	Cr (μg/L)	Interval Begin	Sampling Date	Monlith mass (g)	Monlith Dry Mass (g)	Surface Area (cm^2)	Solution Volume (mL)	Monolith Volume (m^3)	M_{ti} (mg/m^2)	ρ (kg/m^3)	Co (mg$_{Cr}$ /kg$_{mono}$)	D_e (m^2/s)	D_e (cm^2/s)	Average D_e (cm^2/s)	Standard Deviation of Average De
S014-16-T4-1	11.6	4/19/16 8:40:0	05/3/2016 09:00:0	364.02	282.10	195.68	1761.2	1.94E-04	1.04E+00	1.45E+03	393.48	3.5E-17	3.5E-13	3.5E-13	3.3E-15
S014-16-T4-2	11.6	4/19/16 8:40:0	05/3/2016 09:00:0	369.27	286.16	199.22	1793.0	1.99E-04	1.04E+00	1.44E+03	393.48	3.5E-17	3.5E-13		
S014-16-T4-5	11.6	4/19/16 8:40:0	05/3/2016 09:00:0	365.37	283.14	195.92	1763.3	1.94E-04	1.04E+00	1.46E+03	393.48	3.4E-17	3.4E-13	3.5E-13	4.2E-15
S014-16-T4-7	11.6	4/19/16 8:40:0	05/3/2016 09:00:0	363.93	282.03	196.69	1770.2	1.96E-04	1.04E+00	1.44E+03	393.48	3.5E-17	3.5E-13		

T5

Name	Cr (μg/L)	Interval Begin	Sampling Date	Monlith mass (g)	Monlith Dry Mass (g)	Surface Area (cm^2)	Solution Volume (mL)	Monolith Volume (m^3)	M_{ti} (mg/m^2)	ρ (kg/m^3)	Co (mg$_{Cr}$ /kg$_{mono}$)	D_e (m^2/s)	D_e (cm^2/s)	Average D_e (cm^2/s)	Standard Deviation of Average De
S014-16-T5-2	11.6	4/19/16 8:40:0	05/3/2016 09:00:0	365.93	283.58	197.86	1780.7	1.97E-04	1.04E+00	1.44E+03	408.71	3.3E-17	3.3E-13	3.2E-13	6.5E-15
S014-16-T5-3	11.6	4/19/16 8:40:0	05/3/2016 09:00:0	364.75	282.66	195.03	1755.3	1.92E-04	1.04E+00	1.47E+03	408.71	3.1E-17	3.1E-13		
S014-16-T5-4	11.6	4/19/16 8:40:0	05/3/2016 09:00:0	366.62	284.11	196.79	1771.1	1.95E-04	1.04E+00	1.46E+03	408.71	3.2E-17	3.2E-13	3.2E-13	4.1E-15
S014-16-T5-7	11.6	4/19/16 8:40:0	05/3/2016 09:00:0	365.76	283.44	197.96	1781.6	1.97E-04	1.04E+00	1.44E+03	408.71	3.3E-17	3.3E-13		

T6

Name	Cr (μg/L)	Interval Begin	Sampling Date	Monlith mass (g)	Monlith Dry Mass (g)	Surface Area (cm^2)	Solution Volume (mL)	Monolith Volume (m^3)	M_{ti} (mg/m^2)	ρ (kg/m^3)	Co (mg$_{Cr}$ /kg$_{mono}$)	D_e (m^2/s)	D_e (cm^2/s)	Average D_e (cm^2/s)	Standard Deviation of Average De
S014-16-T6-2	11.6	4/19/16 8:40:0	05/3/2016 09:00:0	363.78	284.0868039	196.70	1770.3	1.95E-04	1.04E+00	1.45E+03	410.08	3.2E-17	3.2E-13	3.2E-13	4.6E-16
S014-16-T6-3	11.6	4/19/16 8:40:0	05/3/2016 09:00:0	364.78	284.8677341	197.29	1775.6	1.96E-04	1.04E+00	1.45E+03	410.08	3.2E-17	3.2E-13		
S014-16-T6-5	11.6	4/19/16 8:40:0	05/3/2016 09:00:0	362.95	283.4386318	196.39	1767.5	1.95E-04	1.04E+00	1.45E+03	410.08	3.2E-17	3.2E-13	3.1E-13	4.9E-15
S014-16-T6-6	11.6	4/19/16 8:40:0	05/3/2016 09:00:0	360.98	281.9001992	193.67	1743.0	1.91E-04	1.04E+00	1.48E+03	410.08	3.1E-17	3.1E-13		

Cr Co Calculation

LIMS Data

LIMS data on Cr concentration measurement from the spiked 6.5 M Na simulants

These values show the initial Cr content of the simulant prior to any getter addition

Test	LabNumber	SampleName	Result	Units	EQL
T1	1601042-01	T1 Initial	868000	ug/L	2320
T2	1601042-03	T2 Initial	886000	ug/L	2320
T3	1601042-05	T3 Initial	885000	ug/L	2320
T4	1601042-10	T4 Final	846000	ug/L	2320
T5	1601042-11	T5 Initial	874000	ug/L	2320
T6	1601042-13	T6 Initial	882000	ug/L	2320

Simulant Volume

Density of the 6.5 M Na Average simulant [g 1.31

Test	Simulant Bottle Tare (g)	Bottle + Simulant (g)	Simulant Mass	Simulant Volume- (mL)	Simulant Volume after sampling (mL)	Dry Blend (g)	Total Weight of Slurry [g]
T1	100.1	1407.8	1307.7	998.2	994.2	1750.0	2744.2
T2	100.3	1408.1	1307.8	998.3	994.3	1757.3	2751.6
T3	100.1	1407.9	1307.8	998.3	994.3	1750.0	2744.3
T4	100	1408	1308	998.5	994.5	1745.0	2739.4
T5	99.8	1408	1308.2	998.6	994.6	1750.0	2744.6
T6	99.9	1410.2	1310.3	1000.2	996.2	1747.6	2743.8

Co

Calculation on Cr C_0 in dry Cast Stone (mg/kg) monolith

	T1	T2	T3	T4	T5	T6
Dry solid fraction in Cast Stone Monolith	0.771	0.78	0.78	0.78	0.77	0.78

Test	Cr (ug/g wet Cast Stone)-analytical	C_0 (mg/kg) in dry Cast Stone -analytical
T1	314.478	**407.953**
T2	320.169	**412.011**
T3	320.653	**411.817**
T4	307.117	**393.483**
T5	316.729	**408.711**
T6	320.242	**410.078**

Na Sampling 2 h

Experiment Start 3/1/16 8:30:00

T1

Name	Na (µg/L)	Interval Begin	Sampling Date	Monlith mass (g)	Monlith Dry Mass (g)	Surface Area (cm^2)	Solution Volume (mL)	Monolith Volume (m^3)	M_{ti} (mg/m^2)	ρ (kg/m^3)	Co (mgNa/kgmono)	D_e (m^2/s)	D_e (cm^2/s)	Average D_e (cm^2/s)	Standard Deviation of Average De
S014-16-T1-1	62300	3/1/2016 8:30:	3/1/2016 10:30:0	359.63	277.23	192.53	1732.8	1.89E-04	5.61E+03	1.46E+03	7.61E+04	2.8E-13	2.8E-09	2.8E-09	1.9E-11
S014-16-T1-2	60600	3/1/2016 8:30:	3/1/2016 10:30:0	365.20	281.52	199.18	1792.6	1.99E-04	5.45E+03	1.41E+03	7.61E+04	2.8E-13	2.8E-09		
S014-16-T1-4	79500	3/1/2016 8:30:	3/1/2016 10:30:0	360.86	278.18	195.83	1762.5	1.95E-04	7.16E+03	1.43E+03	7.61E+04	4.7E-13	4.7E-09	4.4E-09	3.5E-10
S014-16-T1-7	74500	3/1/2016 8:30:	3/1/2016 10:30:0	361.60	278.75	194.35	1749.2	1.92E-04	6.71E+03	1.45E+03	7.61E+04	4.0E-13	4.0E-09		

T2

Name	Na (µg/L)	Interval Begin	Sampling Date	Monlith mass (g)	Monlith Dry Mass (g)	Surface Area (cm^2)	Solution Volume (mL)	Monolith Volume (m^3)	M_{ti} (mg/m^2)	ρ (kg/m^3)	Co (mgNa/kgmono)	D_e (m^2/s)	D_e (cm^2/s)	Average D_e (cm^2/s)	Standard Deviation of Average De
S014-16-T2-3	72300	3/1/2016 8:30:	3/1/2016 10:30:0	364.71	283.41	195.83	1749.7	1.92E-04	6.46E+03	1.48E+03	7.44E+04	3.8E-13	3.8E-09	4.1E-09	3.6E-10
S014-16-T2-6	77000	3/1/2016 8:30:	3/1/2016 10:30:0	367.70	285.74	197.83	1780.5	1.97E-04	6.93E+03	1.45E+03	7.44E+04	4.5E-13	4.5E-09		
S014-16-T2-7	95500	3/1/2016 8:30:	3/1/2016 10:30:0	366.00	284.41	196.77	1770.9	1.95E-04	8.60E+03	1.46E+03	7.44E+04	6.9E-13	6.9E-09	5.8E-09	1.0E-09
S014-16-T2-8	78500	3/1/2016 8:30:	3/1/2016 10:30:0	363.14	282.19	197.90	1781.1	1.97E-04	7.07E+03	1.43E+03	7.44E+04	4.8E-13	4.8E-09		

T3

Name	Na (µg/L)	Interval Begin	Sampling Date	Monlith mass (g)	Monlith Dry Mass (g)	Surface Area (cm^2)	Solution Volume (mL)	Monolith Volume (m^3)	M_{ti} (mg/m^2)	ρ (kg/m^3)	Co (mgNa/kgmono)	D_e (m^2/s)	D_e (cm^2/s)	Average D_e (cm^2/s)	Standard Deviation of Average De
S014-16-T3-1	76600	3/1/2016 8:30:	3/1/2016 10:30:0	366.62	285.46	195.87	1762.9	1.94E-04	6.89E+03	1.47E+03	7.82E+04	3.9E-13	3.9E-09	5.2E-09	1.3E-09
S014-16-T3-3	98800	3/1/2016 8:30:	3/1/2016 10:30:0	364.46	283.78	195.53	1759.7	1.94E-04	8.89E+03	1.46E+03	7.82E+04	6.6E-13	6.6E-09		
S014-16-T3-4	99500	3/1/2016 8:30:	3/1/2016 10:30:0	362.76	282.46	194.51	1750.6	1.93E-04	8.96E+03	1.47E+03	7.82E+04	6.6E-13	6.6E-09	8.4E-09	1.7E-09
S014-16-T3-8	122500	3/1/2016 8:30:	3/1/2016 10:30:0	360.88	280.99	194.17	1747.5	1.92E-04	1.10E+04	1.46E+03	7.82E+04	1.0E-12	1.0E-08		

T4

Name	Na (µg/L)	Interval Begin	Sampling Date	Monlith mass (g)	Monlith Dry Mass (g)	Surface Area (cm^2)	Solution Volume (mL)	Monolith Volume (m^3)	M_{ti} (mg/m^2)	ρ (kg/m^3)	Co (mgNa/kgmono)	D_e (m^2/s)	D_e (cm^2/s)	Average D_e (cm^2/s)	Standard Deviation of Average De
S014-16-T4-1	97700	3/1/2016 8:30:	3/1/2016 10:30:0	364.02	284.12	195.68	1761.2	1.94E-04	8.79E+03	1.46E+03	7.44E+04	7.1E-13	7.1E-09	5.8E-09	1.3E-09
S014-16-T4-2	77200	3/1/2016 8:30:	3/1/2016 10:30:0	369.27	288.22	199.22	1793.0	1.99E-04	6.95E+03	1.45E+03	7.44E+04	4.5E-13	4.5E-09		
S014-16-T4-5	59500	3/1/2016 8:30:	3/1/2016 10:30:0	365.37	285.18	195.92	1763.3	1.94E-04	5.36E+03	1.47E+03	7.44E+04	2.6E-13	2.6E-09	4.2E-09	1.6E-09
S014-16-T4-7	87500	3/1/2016 8:30:	3/1/2016 10:30:0	363.93	284.05	196.69	1770.2	1.96E-04	7.88E+03	1.45E+03	7.44E+04	5.8E-13	5.8E-09		

T5

Name	Na (µg/L)	Interval Begin	Sampling Date	Monlith mass (g)	Monlith Dry Mass (g)	Surface Area (cm^2)	Solution Volume (mL)	Monolith Volume (m^3)	M_{ti} (mg/m^2)	ρ (kg/m^3)	Co (mgNa/kgmono)	D_e (m^2/s)	D_e (cm^2/s)	Average D_e (cm^2/s)	Standard Deviation of Average De
S014-16-T5-2	69300	3/1/2016 8:30:	3/1/2016 10:30:0	365.93	283.58	197.86	1780.7	1.97E-04	6.24E+03	1.44E+03	7.72E+04	3.4E-13	3.4E-09	3.1E-09	3.0E-10
S014-16-T5-3	64300	3/1/2016 8:30:	3/1/2016 10:30:0	364.75	282.66	195.03	1755.3	1.92E-04	5.79E+03	1.47E+03	7.72E+04	2.8E-13	2.8E-09		
S014-16-T5-4	95500	3/1/2016 8:30:	3/1/2016 10:30:0	366.62	284.11	196.79	1771.1	1.95E-04	8.60E+03	1.46E+03	7.72E+04	6.4E-13	6.4E-09	6.3E-09	5.4E-11
S014-16-T5-7	93500	3/1/2016 8:30:	3/1/2016 10:30:0	365.76	283.44	197.96	1781.6	1.97E-04	8.42E+03	1.44E+03	7.72E+04	6.3E-13	6.3E-09		

T6

Name	Na (µg/L)	Interval Begin	Sampling Date	Monlith mass (g)	Monlith Dry Mass (g)	Surface Area (cm^2)	Solution Volume (mL)	Monolith Volume (m^3)	M_{ti} (mg/m^2)	ρ (kg/m^3)	Co (mgNa/kgmono)	D_e (m^2/s)	D_e (cm^2/s)	Average D_e (cm^2/s)	Standard Deviation of Average De
S014-16-T6-2	75200	3/1/2016 8:30:	3/1/2016 10:30:0	363.78	284.09	196.70	1770.3	1.95E-04	6.77E+03	1.45E+03	7.86E+04	3.8E-13	3.8E-09	4.2E-09	3.8E-10
S014-16-T6-3	82200	3/1/2016 8:30:	3/1/2016 10:30:0	364.78	284.87	197.29	1775.6	1.96E-04	7.40E+03	1.45E+03	7.86E+04	4.6E-13	4.6E-09		
S014-16-T6-5	89500	3/1/2016 8:30:	3/1/2016 10:30:0	362.95	283.44	196.39	1767.5	1.95E-04	8.06E+03	1.45E+03	7.86E+04	5.4E-13	5.4E-09	4.0E-09	1.4E-09
S014-16-T6-6	62500	3/1/2016 8:30:	3/1/2016 10:30:0	360.98	281.90	193.67	1743.0	1.91E-04	5.63E+03	1.48E+03	7.86E+04	2.6E-13	2.6E-09		

Na Sampling 1 d

		Experiment Start	3/1/16 8:30:00

T1

Name	Na (μg/L)	Interval Begin	Sampling Date	Monlith mass (g)	Monlith Dry Mass (g)	Surface Area (cm^2)	Solution Volume (mL)	Monolith Volume (m^3)	M_{ti} (mg/m^2)	ρ (kg/m^3)	Co (mgNa/kgmono)	D_e (m^2/s)	D_e (cm^2/s)	Average D_e (cm^2/s)	Standard Deviation of Average De
S014-16-T1-1	290000	3/1/2016 10:30:	3/2/2016 8:30:00	359.63	277.23	192.53	1732.8	1.89E-04	2.61E+04	1.46E+03	7.61E+04	9.8E-13	9.8E-09	9.4E-09	4.2E-10
S014-16-T1-2	268000	3/1/2016 10:30:	3/2/2016 8:30:00	365.20	281.52	199.18	1792.6	1.99E-04	2.41E+04	1.41E+03	7.61E+04	9.0E-13	9.0E-09		
S014-16-T1-4	292500	3/1/2016 10:30:	3/2/2016 8:30:00	360.86	278.18	195.83	1762.5	1.95E-04	2.63E+04	1.43E+03	7.61E+04	1.1E-12	1.1E-08	1.7E-08	6.6E-09
S014-16-T1-7	446500	3/1/2016 10:30:	3/2/2016 8:30:00	361.60	278.75	194.35	1749.2	1.92E-04	4.02E+04	1.45E+03	7.61E+04	2.4E-12	2.4E-08		

T2

Name	Na (μg/L)	Interval Begin	Sampling Date	Monlith mass (g)	Monlith Dry Mass (g)	Surface Area (cm^2)	Solution Volume (mL)	Monolith Volume (m^3)	M_{ti} (mg/m^2)	ρ (kg/m^3)	Co (mgNa/kgmono)	D_e (m^2/s)	D_e (cm^2/s)	Average D_e (cm^2/s)	Standard Deviation of Average De
S014-16-T2-3	424000	3/1/2016 10:30:	3/2/2016 8:30:00	364.71	283.41	195.83	1749.7	1.92E-04	3.79E+04	1.48E+03	7.44E+04	2.1E-12	2.1E-08	2.2E-08	1.1E-09
S014-16-T2-6	435000	3/1/2016 10:30:	3/2/2016 8:30:00	367.70	285.74	197.83	1780.5	1.97E-04	3.92E+04	1.45E+03	7.44E+04	2.4E-12	2.4E-08		
S014-16-T2-7	344500	3/1/2016 10:30:	3/2/2016 8:30:00	366.00	284.41	196.77	1770.9	1.95E-04	3.10E+04	1.46E+03	7.44E+04	1.5E-12	1.5E-08	1.6E-08	9.9E-10
S014-16-T2-8	360500	3/1/2016 10:30:	3/2/2016 8:30:00	363.14	282.19	197.90	1781.1	1.97E-04	3.24E+04	1.43E+03	7.44E+04	1.7E-12	1.7E-08		

T3

Name	Na (μg/L)	Interval Begin	Sampling Date	Monlith mass (g)	Monlith Dry Mass (g)	Surface Area (cm^2)	Solution Volume (mL)	Monolith Volume (m^3)	M_{ti} (mg/m^2)	ρ (kg/m^3)	Co (mgNa/kgmono)	D_e (m^2/s)	D_e (cm^2/s)	Average D_e (cm^2/s)	Standard Deviation of Average De
S014-16-T3-1	254000	3/1/2016 10:30:	3/2/2016 8:30:00	366.62	285.46	195.87	1762.9	1.94E-04	2.29E+04	1.47E+03	7.82E+04	7.1E-13	7.1E-09	8.1E-09	1.1E-09
S014-16-T3-3	288000	3/1/2016 10:30:	3/2/2016 8:30:00	364.46	283.78	195.53	1759.7	1.94E-04	2.59E+04	1.46E+03	7.82E+04	9.2E-13	9.2E-09		
S014-16-T3-4	195500	3/1/2016 10:30:	3/2/2016 8:30:00	362.76	282.46	194.51	1750.6	1.93E-04	1.76E+04	1.47E+03	7.82E+04	4.2E-13	4.2E-09	9.6E-09	5.4E-09
S014-16-T3-8	367500	3/1/2016 10:30:	3/2/2016 8:30:00	360.88	280.99	194.17	1747.5	1.92E-04	3.31E+04	1.46E+03	7.82E+04	1.5E-12	1.5E-08		

T4

Name	Na (μg/L)	Interval Begin	Sampling Date	Monlith mass (g)	Monlith Dry Mass (g)	Surface Area (cm^2)	Solution Volume (mL)	Monolith Volume (m^3)	M_{ti} (mg/m^2)	ρ (kg/m^3)	Co (mgNa/kgmono)	D_e (m^2/s)	D_e (cm^2/s)	Average D_e (cm^2/s)	Standard Deviation of Average De
S014-16-T4-1	291000	3/1/2016 10:30:	3/2/2016 8:30:00	364.02	284.12	195.68	1761.2	1.94E-04	2.62E+04	1.46E+03	7.44E+04	1.0E-12	1.0E-08	1.1E-08	9.7E-10
S014-16-T4-2	314000	3/1/2016 10:30:	3/2/2016 8:30:00	369.27	288.22	199.22	1793.0	1.99E-04	2.83E+04	1.45E+03	7.44E+04	1.2E-12	1.2E-08		
S014-16-T4-5	277500	3/1/2016 10:30:	3/2/2016 8:30:00	365.37	285.18	195.92	1763.3	1.94E-04	2.50E+04	1.47E+03	7.44E+04	9.4E-13	9.4E-09	9.5E-09	1.2E-10
S014-16-T4-7	277500	3/1/2016 10:30:	3/2/2016 8:30:00	363.93	284.05	196.69	1770.2	1.96E-04	2.50E+04	1.45E+03	7.44E+04	9.6E-13	9.6E-09		

T5

Name	Na (μg/L)	Interval Begin	Sampling Date	Monlith mass (g)	Monlith Dry Mass (g)	Surface Area (cm^2)	Solution Volume (mL)	Monolith Volume (m^3)	M_{ti} (mg/m^2)	ρ (kg/m^3)	Co (mgNa/kgmono)	D_e (m^2/s)	D_e (cm^2/s)	Average D_e (cm^2/s)	Standard Deviation of Average De
S014-16-T5-2	234000	3/1/2016 10:30:	3/2/2016 8:30:00	365.93	283.58	197.86	1780.7	1.97E-04	2.11E+04	1.44E+03	7.72E+04	6.5E-13	6.5E-09	7.7E-09	1.2E-09
S014-16-T5-3	280000	3/1/2016 10:30:	3/2/2016 8:30:00	364.75	282.66	195.03	1755.3	1.92E-04	2.52E+04	1.47E+03	7.72E+04	8.9E-13	8.9E-09		
S014-16-T5-4	352500	3/1/2016 10:30:	3/2/2016 8:30:00	366.62	284.11	196.79	1771.1	1.95E-04	3.17E+04	1.46E+03	7.72E+04	1.4E-12	1.4E-08	1.4E-08	6.0E-11
S014-16-T5-7	349500	3/1/2016 10:30:	3/2/2016 8:30:00	365.76	283.44	197.96	1781.6	1.97E-04	3.15E+04	1.44E+03	7.72E+04	1.4E-12	1.4E-08		

T6

Name	Na (μg/L)	Interval Begin	Sampling Date	Monlith mass (g)	Monlith Dry Mass (g)	Surface Area (cm^2)	Solution Volume (mL)	Monolith Volume (m^3)	M_{ti} (mg/m^2)	ρ (kg/m^3)	Co (mgNa/kgmono)	D_e (m^2/s)	D_e (cm^2/s)	Average D_e (cm^2/s)	Standard Deviation of Average De
S014-16-T6-2	331000	3/1/2016 10:30:	3/2/2016 8:30:00	363.78	284.09	196.70	1770.3	1.95E-04	2.98E+04	1.45E+03	7.86E+04	1.2E-12	1.2E-08	1.2E-08	1.7E-10
S014-16-T6-3	326000	3/1/2016 10:30:	3/2/2016 8:30:00	364.78	284.87	197.29	1775.6	1.96E-04	2.93E+04	1.45E+03	7.86E+04	1.2E-12	1.2E-08		
S014-16-T6-5	353500	3/1/2016 10:30:	3/2/2016 8:30:00	362.95	283.44	196.39	1767.5	1.95E-04	3.18E+04	1.45E+03	7.86E+04	1.4E-12	1.4E-08	1.2E-08	2.4E-09
S014-16-T6-6	291500	3/1/2016 10:30:	3/2/2016 8:30:00	360.98	281.90	193.67	1743.0	1.91E-04	2.62E+04	1.48E+03	7.86E+04	9.2E-13	9.2E-09		

Na Sampling 2 d

Experiment Start 3/1/16 8:30:00

T1

Name	Na (µg/L)	Interval Begin	Sampling Date	Monlith mass (g)	Monlith Dry Mass (g)	Surface Area (cm^2)	Solution Volume (mL)	Monolith Volume (m^3)	M_{ti} (mg/m^2)	ρ (kg/m^3)	Co (mgNa/kgmono)	D_e (m^2/s)	D_e (cm^2/s)	Average D_e (cm^2/s)	Standard Deviation of Average De
S014-16-T1-1	168000	3/2/2016 8:30:0	3/3/2016 8:40:00	359.63	277.23	192.53	1732.8	1.89E-04	1.51E+04	1.46E+03	7.61E+04	9.6E-13	9.6E-09	9.3E-09	3.1E-10
S014-16-T1-2	157000	3/2/2016 8:30:0	3/3/2016 8:40:00	365.20	281.52	199.18	1792.6	1.99E-04	1.41E+04	1.41E+03	7.61E+04	9.0E-13	9.0E-09		
S014-16-T1-4	186500	3/2/2016 8:30:0	3/3/2016 8:40:00	360.86	278.18	195.83	1762.5	1.95E-04	1.68E+04	1.43E+03	7.61E+04	1.2E-12	1.2E-08	1.3E-08	7.6E-10
S014-16-T1-7	200500	3/2/2016 8:30:0	3/3/2016 8:40:00	361.60	278.75	194.35	1749.2	1.92E-04	1.80E+04	1.45E+03	7.61E+04	1.4E-12	1.4E-08		

T2

Name	Na (µg/L)	Interval Begin	Sampling Date	Monlith mass (g)	Monlith Dry Mass (g)	Surface Area (cm^2)	Solution Volume (mL)	Monolith Volume (m^3)	M_{ti} (mg/m^2)	ρ (kg/m^3)	Co (mgNa/kgmono)	D_e (m^2/s)	D_e (cm^2/s)	Average D_e (cm^2/s)	Standard Deviation of Average De
S014-16-T2-3	240000	3/2/2016 8:30:0	3/3/2016 8:40:00	364.71	283.41	195.83	1749.7	1.92E-04	2.14E+04	1.48E+03	7.44E+04	2.0E-12	2.0E-08	2.2E-08	1.7E-09
S014-16-T2-6	253000	3/2/2016 8:30:0	3/3/2016 8:40:00	367.70	285.74	197.83	1780.5	1.97E-04	2.28E+04	1.45E+03	7.44E+04	2.3E-12	2.3E-08		
S014-16-T2-7	273500	3/2/2016 8:30:0	3/3/2016 8:40:00	366.00	284.41	196.77	1770.9	1.95E-04	2.46E+04	1.46E+03	7.44E+04	2.7E-12	2.7E-08	2.7E-08	2.7E-11
S014-16-T2-8	268500	3/2/2016 8:30:0	3/3/2016 8:40:00	363.14	282.19	197.90	1781.1	1.97E-04	2.42E+04	1.43E+03	7.44E+04	2.7E-12	2.7E-08		

T3

Name	Na (µg/L)	Interval Begin	Sampling Date	Monlith mass (g)	Monlith Dry Mass (g)	Surface Area (cm^2)	Solution Volume (mL)	Monolith Volume (m^3)	M_{ti} (mg/m^2)	ρ (kg/m^3)	Co (mgNa/kgmono)	D_e (m^2/s)	D_e (cm^2/s)	Average D_e (cm^2/s)	Standard Deviation of Average De
S014-16-T3-1	160000	3/2/2016 8:30:0	3/3/2016 8:40:00	366.62	285.46	195.87	1762.9	1.94E-04	1.44E+04	1.47E+03	7.82E+04	8.2E-13	8.2E-09	1.1E-08	2.5E-09
S014-16-T3-3	201000	3/2/2016 8:30:0	3/3/2016 8:40:00	364.46	283.78	195.53	1759.7	1.94E-04	1.81E+04	1.46E+03	7.82E+04	1.3E-12	1.3E-08		
S014-16-T3-4	190500	3/2/2016 8:30:0	3/3/2016 8:40:00	362.76	282.46	194.51	1750.6	1.93E-04	1.71E+04	1.47E+03	7.82E+04	1.2E-12	1.2E-08	1.1E-08	4.4E-10
S014-16-T3-8	182500	3/2/2016 8:30:0	3/3/2016 8:40:00	360.88	280.99	194.17	1747.5	1.92E-04	1.64E+04	1.46E+03	7.82E+04	1.1E-12	1.1E-08		

T4

Name	Na (µg/L)	Interval Begin	Sampling Date	Monlith mass (g)	Monlith Dry Mass (g)	Surface Area (cm^2)	Solution Volume (mL)	Monolith Volume (m^3)	M_{ti} (mg/m^2)	ρ (kg/m^3)	Co (mgNa/kgmono)	D_e (m^2/s)	D_e (cm^2/s)	Average D_e (cm^2/s)	Standard Deviation of Average De
S014-16-T4-1	197000	3/2/2016 8:30:0	3/3/2016 8:40:00	364.02	284.12	195.68	1761.2	1.94E-04	1.77E+04	1.46E+03	7.44E+04	1.4E-12	1.4E-08	1.3E-08	7.0E-10
S014-16-T4-2	185000	3/2/2016 8:30:0	3/3/2016 8:40:00	369.27	288.22	199.22	1793.0	1.99E-04	1.67E+04	1.45E+03	7.44E+04	1.2E-12	1.2E-08		
S014-16-T4-5	210500	3/2/2016 8:30:0	3/3/2016 8:40:00	365.37	285.18	195.92	1763.3	1.94E-04	1.89E+04	1.47E+03	7.44E+04	1.6E-12	1.6E-08	1.4E-08	1.5E-09
S014-16-T4-7	187500	3/2/2016 8:30:0	3/3/2016 8:40:00	363.93	284.05	196.69	1770.2	1.96E-04	1.69E+04	1.45E+03	7.44E+04	1.3E-12	1.3E-08		

T5

Name	Na (µg/L)	Interval Begin	Sampling Date	Monlith mass (g)	Monlith Dry Mass (g)	Surface Area (cm^2)	Solution Volume (mL)	Monolith Volume (m^3)	M_{ti} (mg/m^2)	ρ (kg/m^3)	Co (mgNa/kgmono)	D_e (m^2/s)	D_e (cm^2/s)	Average D_e (cm^2/s)	Standard Deviation of Average De
S014-16-T5-2	154000	3/2/2016 8:30:0	3/3/2016 8:40:00	365.93	283.58	197.86	1780.7	1.97E-04	1.39E+04	1.44E+03	7.72E+04	8.2E-13	8.2E-09	8.7E-09	5.2E-10
S014-16-T5-3	167000	3/2/2016 8:30:0	3/3/2016 8:40:00	364.75	282.66	195.03	1755.3	1.92E-04	1.50E+04	1.47E+03	7.72E+04	9.2E-13	9.2E-09		
S014-16-T5-4	196500	3/2/2016 8:30:0	3/3/2016 8:40:00	366.62	284.11	196.79	1771.1	1.95E-04	1.77E+04	1.46E+03	7.72E+04	1.3E-12	1.3E-08	1.4E-08	6.5E-10
S014-16-T5-7	203500	3/2/2016 8:30:0	3/3/2016 8:40:00	365.76	283.44	197.96	1781.6	1.97E-04	1.83E+04	1.44E+03	7.72E+04	1.4E-12	1.4E-08		

T6

Name	Na (µg/L)	Interval Begin	Sampling Date	Monlith mass (g)	Monlith Dry Mass (g)	Surface Area (cm^2)	Solution Volume (mL)	Monolith Volume (m^3)	M_{ti} (mg/m^2)	ρ (kg/m^3)	Co (mgNa/kgmono)	D_e (m^2/s)	D_e (cm^2/s)	Average D_e (cm^2/s)	Standard Deviation of Average De
S014-16-T6-2	173000	3/2/2016 8:30:0	3/3/2016 8:40:00	363.78	284.09	196.70	1770.3	1.95E-04	1.56E+04	1.45E+03	7.86E+04	9.7E-13	9.7E-09	9.5E-09	2.6E-10
S014-16-T6-3	168000	3/2/2016 8:30:0	3/3/2016 8:40:00	364.78	284.87	197.29	1775.6	1.96E-04	1.51E+04	1.45E+03	7.86E+04	9.2E-13	9.2E-09		
S014-16-T6-5	200500	3/2/2016 8:30:0	3/3/2016 8:40:00	362.95	283.44	196.39	1767.5	1.95E-04	1.80E+04	1.45E+03	7.86E+04	1.3E-12	1.3E-08	1.3E-08	3.9E-10
S014-16-T6-6	197500	3/2/2016 8:30:0	3/3/2016 8:40:00	360.98	281.90	193.67	1743.0	1.91E-04	1.78E+04	1.48E+03	7.86E+04	1.2E-12	1.2E-08		

Na Sampling 7d

Experiment Start 3/1/16 8:30:00

T1

Name	Na (µg/L)	Interval Begin	Sampling Date	Monlith mass (g)	Monlith Dry Mass (g)	Surface Area (cm^2)	Solution Volume (mL)	Monolith Volume (m^3)	M_{ti} (mg/m^2)	ρ (kg/m^3)	Co (mgNa/kgmono)	D_e (m^2/s)	D_e (cm^2/s)	Average D_e (cm^2/s)	Standard Deviation of Average De
S014-16-T1-1	575000	3/3/2016 8:40:0	3/8/2016 8:40:00	359.63	277.23	192.53	1732.8	1.89E-04	5.18E+04	1.46E+03	7.61E+04	1.3E-12	1.3E-08	1.4E-08	8.0E-10
S014-16-T1-2	589000	3/3/2016 8:40:0	3/8/2016 8:40:00	365.20	281.52	199.18	1792.6	1.99E-04	5.30E+04	1.41E+03	7.61E+04	1.5E-12	1.5E-08		
S014-16-T1-4	534000	3/3/2016 8:40:0	3/8/2016 8:40:00	360.86	278.18	195.83	1762.5	1.95E-04	4.81E+04	1.43E+03	7.61E+04	1.2E-12	1.2E-08	1.2E-08	6.6E-11
S014-16-T1-7	545000	3/3/2016 8:40:0	3/8/2016 8:40:00	361.60	278.75	194.35	1749.2	1.92E-04	4.91E+04	1.45E+03	7.61E+04	1.2E-12	1.2E-08		

T2

Name	Na (µg/L)	Interval Begin	Sampling Date	Monlith mass (g)	Monlith Dry Mass (g)	Surface Area (cm^2)	Solution Volume (mL)	Monolith Volume (m^3)	M_{ti} (mg/m^2)	ρ (kg/m^3)	Co (mgNa/kgmono)	D_e (m^2/s)	D_e (cm^2/s)	Average D_e (cm^2/s)	Standard Deviation of Average De
S014-16-T2-3	795000	3/3/2016 8:40:0	3/8/2016 8:40:00	364.71	283.41	195.83	1749.7	1.92E-04	7.10E+04	1.48E+03	7.44E+04	2.5E-12	2.5E-08	2.7E-08	1.7E-09
S014-16-T2-6	827000	3/3/2016 8:40:0	3/8/2016 8:40:00	367.70	285.74	197.83	1780.5	1.97E-04	7.44E+04	1.45E+03	7.44E+04	2.8E-12	2.8E-08		
S014-16-T2-7	737000	3/3/2016 8:40:0	3/8/2016 8:40:00	366.00	284.41	196.77	1770.9	1.95E-04	6.63E+04	1.46E+03	7.44E+04	2.3E-12	2.3E-08	2.4E-08	1.1E-09
S014-16-T2-8	759000	3/3/2016 8:40:0	3/8/2016 8:40:00	363.14	282.19	197.90	1781.1	1.97E-04	6.83E+04	1.43E+03	7.44E+04	2.5E-12	2.5E-08		

T3

Name	Na (µg/L)	Interval Begin	Sampling Date	Monlith mass (g)	Monlith Dry Mass (g)	Surface Area (cm^2)	Solution Volume (mL)	Monolith Volume (m^3)	M_{ti} (mg/m^2)	ρ (kg/m^3)	Co (mgNa/kgmono)	D_e (m^2/s)	D_e (cm^2/s)	Average D_e (cm^2/s)	Standard Deviation of Average De
S014-16-T3-1	555000	3/3/2016 8:40:0	3/8/2016 8:40:00	366.62	285.46	195.87	1762.9	1.94E-04	5.00E+04	1.47E+03	7.82E+04	1.1E-12	1.1E-08	1.2E-08	3.9E-10
S014-16-T3-3	570000	3/3/2016 8:40:0	3/8/2016 8:40:00	364.46	283.78	195.53	1759.7	1.94E-04	5.13E+04	1.46E+03	7.82E+04	1.2E-12	1.2E-08		
S014-16-T3-4	521000	3/3/2016 8:40:0	3/8/2016 8:40:00	362.76	282.46	194.51	1750.6	1.93E-04	4.69E+04	1.47E+03	7.82E+04	1.0E-12	1.0E-08	1.1E-08	8.2E-10
S014-16-T3-8	560000	3/3/2016 8:40:0	3/8/2016 8:40:00	360.88	280.99	194.17	1747.5	1.92E-04	5.04E+04	1.46E+03	7.82E+04	1.2E-12	1.2E-08		

T4

Name	Na (µg/L)	Interval Begin	Sampling Date	Monlith mass (g)	Monlith Dry Mass (g)	Surface Area (cm^2)	Solution Volume (mL)	Monolith Volume (m^3)	M_{ti} (mg/m^2)	ρ (kg/m^3)	Co (mgNa/kgmono)	D_e (m^2/s)	D_e (cm^2/s)	Average D_e (cm^2/s)	Standard Deviation of Average De
S014-16-T4-1	603000	3/3/2016 8:40:0	3/8/2016 8:40:00	364.02	284.12	195.68	1761.2	1.94E-04	5.43E+04	1.46E+03	7.44E+04	1.5E-12	1.5E-08	1.4E-08	4.8E-10
S014-16-T4-2	578000	3/3/2016 8:40:0	3/8/2016 8:40:00	369.27	288.22	199.22	1793.0	1.99E-04	5.20E+04	1.45E+03	7.44E+04	1.4E-12	1.4E-08		
S014-16-T4-5	565000	3/3/2016 8:40:0	3/8/2016 8:40:00	365.37	285.18	195.92	1763.3	1.94E-04	5.09E+04	1.47E+03	7.44E+04	1.3E-12	1.3E-08	1.4E-08	4.7E-10
S014-16-T4-7	578000	3/3/2016 8:40:0	3/8/2016 8:40:00	363.93	284.05	196.69	1770.2	1.96E-04	5.20E+04	1.45E+03	7.44E+04	1.4E-12	1.4E-08		

T5

Name	Na (µg/L)	Interval Begin	Sampling Date	Monlith mass (g)	Monlith Dry Mass (g)	Surface Area (cm^2)	Solution Volume (mL)	Monolith Volume (m^3)	M_{ti} (mg/m^2)	ρ (kg/m^3)	Co (mgNa/kgmono)	D_e (m^2/s)	D_e (cm^2/s)	Average D_e (cm^2/s)	Standard Deviation of Average De
S014-16-T5-2	546000	3/3/2016 8:40:0	3/8/2016 8:40:00	365.93	283.58	197.86	1780.7	1.97E-04	4.91E+04	1.44E+03	7.72E+04	1.2E-12	1.2E-08	1.2E-08	7.8E-11
S014-16-T5-3	561000	3/3/2016 8:40:0	3/8/2016 8:40:00	364.75	282.66	195.03	1755.3	1.92E-04	5.05E+04	1.47E+03	7.72E+04	1.2E-12	1.2E-08		
S014-16-T5-4	540000	3/3/2016 8:40:0	3/8/2016 8:40:00	366.62	284.11	196.79	1771.1	1.95E-04	4.86E+04	1.46E+03	7.72E+04	1.1E-12	1.1E-08	1.3E-08	1.4E-09
S014-16-T5-7	598000	3/3/2016 8:40:0	3/8/2016 8:40:00	365.76	283.44	197.96	1781.6	1.97E-04	5.38E+04	1.44E+03	7.72E+04	1.4E-12	1.4E-08		

T6

Name	Na (µg/L)	Interval Begin	Sampling Date	Monlith mass (g)	Monlith Dry Mass (g)	Surface Area (cm^2)	Solution Volume (mL)	Monolith Volume (m^3)	M_{ti} (mg/m^2)	ρ (kg/m^3)	Co (mgNa/kgmono)	D_e (m^2/s)	D_e (cm^2/s)	Average D_e (cm^2/s)	Standard Deviation of Average De
S014-16-T6-2	555000	3/3/2016 8:40:0	3/8/2016 8:40:00	363.78	284.09	196.70	1770.3	1.95E-04	5.00E+04	1.45E+03	7.86E+04	1.1E-12	1.1E-08	1.1E-08	6.6E-11
S014-16-T6-3	551000	3/3/2016 8:40:0	3/8/2016 8:40:00	364.78	284.87	197.29	1775.6	1.96E-04	4.96E+04	1.45E+03	7.86E+04	1.1E-12	1.1E-08		
S014-16-T6-5	569000	3/3/2016 8:40:0	3/8/2016 8:40:00	362.95	283.44	196.39	1767.5	1.95E-04	5.12E+04	1.45E+03	7.86E+04	1.2E-12	1.2E-08	1.2E-08	1.1E-12
S014-16-T6-6	578000	3/3/2016 8:40:0	3/8/2016 8:40:00	360.98	281.90	193.67	1743.0	1.91E-04	5.20E+04	1.48E+03	7.86E+04	1.2E-12	1.2E-08		

Na Sampling 14 d

		Experiment Start	3/1/16 8:30:00

T1

Name	Na (µg/L)	Interval Begin	Sampling Date	Monlith mass (g)	Monlith Dry Mass (g)	Surface Area (cm^2)	Solution Volume (mL)	Monolith Volume (m^3)	M_{ti} (mg/m^2)	ρ (kg/m^3)	Co (mgNa/kgmono)	D_e (m^2/s)	D_e (cm^2/s)	Average D_e (cm^2/s)	Standard Deviation of Average De
S014-16-T1-1	456000	3/8/2016 8:40:0	3/15/2016 8:50:0	359.63	277.23	192.53	1732.8	1.89E-04	4.10E+04	1.46E+03	7.61E+04	1.0E-12	1.0E-08	1.0E-08	1.0E-10
S014-16-T1-2	436000	3/8/2016 8:40:0	3/15/2016 8:50:0	365.20	281.52	199.18	1792.6	1.99E-04	3.92E+04	1.41E+03	7.61E+04	1.0E-12	1.0E-08		
S014-16-T1-4	439000	3/8/2016 8:40:0	3/15/2016 8:50:0	360.86	278.18	195.83	1762.5	1.95E-04	3.95E+04	1.43E+03	7.61E+04	1.0E-12	1.0E-08	1.1E-08	6.1E-10
S014-16-T1-7	472000	3/8/2016 8:40:0	3/15/2016 8:50:0	361.60	278.75	194.35	1749.2	1.92E-04	4.25E+04	1.45E+03	7.61E+04	1.1E-12	1.1E-08		

T2

Name	Na (µg/L)	Interval Begin	Sampling Date	Monlith mass (g)	Monlith Dry Mass (g)	Surface Area (cm^2)	Solution Volume (mL)	Monolith Volume (m^3)	M_{ti} (mg/m^2)	ρ (kg/m^3)	Co (mgNa/kgmono)	D_e (m^2/s)	D_e (cm^2/s)	Average D_e (cm^2/s)	Standard Deviation of Average De
S014-16-T2-3	610000	3/8/2016 8:40:0	3/15/2016 8:50:0	364.71	283.41	195.83	1749.7	1.92E-04	5.45E+04	1.48E+03	7.44E+04	1.9E-12	1.9E-08	2.0E-08	1.6E-09
S014-16-T2-6	644000	3/8/2016 8:40:0	3/15/2016 8:50:0	367.70	285.74	197.83	1780.5	1.97E-04	5.80E+04	1.45E+03	7.44E+04	2.2E-12	2.2E-08		
S014-16-T2-7	615000	3/8/2016 8:40:0	3/15/2016 8:50:0	366.00	284.41	196.77	1770.9	1.95E-04	5.54E+04	1.46E+03	7.44E+04	2.0E-12	2.0E-08	1.8E-08	1.6E-09
S014-16-T2-8	552000	3/8/2016 8:40:0	3/15/2016 8:50:0	363.14	282.19	197.90	1781.1	1.97E-04	4.97E+04	1.43E+03	7.44E+04	1.6E-12	1.6E-08		

T3

Name	Na (µg/L)	Interval Begin	Sampling Date	Monlith mass (g)	Monlith Dry Mass (g)	Surface Area (cm^2)	Solution Volume (mL)	Monolith Volume (m^3)	M_{ti} (mg/m^2)	ρ (kg/m^3)	Co (mgNa/kgmono)	D_e (m^2/s)	D_e (cm^2/s)	Average D_e (cm^2/s)	Standard Deviation of Average De
S014-16-T3-1	466000	3/8/2016 8:40:0	3/15/2016 8:50:0	366.62	285.46	195.87	1762.9	1.94E-04	4.19E+04	1.47E+03	7.82E+04	1.0E-12	1.0E-08	9.7E-09	2.9E-10
S014-16-T3-3	449000	3/8/2016 8:40:0	3/15/2016 8:50:0	364.46	283.78	195.53	1759.7	1.94E-04	4.04E+04	1.46E+03	7.82E+04	9.4E-13	9.4E-09		
S014-16-T3-4	392000	3/8/2016 8:40:0	3/15/2016 8:50:0	362.76	282.46	194.51	1750.6	1.93E-04	3.53E+04	1.47E+03	7.82E+04	7.2E-13	7.2E-09	8.2E-09	1.0E-09
S014-16-T3-8	443000	3/8/2016 8:40:0	3/15/2016 8:50:0	360.88	280.99	194.17	1747.5	1.92E-04	3.99E+04	1.46E+03	7.82E+04	9.2E-13	9.2E-09		

T4

Name	Na (µg/L)	Interval Begin	Sampling Date	Monlith mass (g)	Monlith Dry Mass (g)	Surface Area (cm^2)	Solution Volume (mL)	Monolith Volume (m^3)	M_{ti} (mg/m^2)	ρ (kg/m^3)	Co (mgNa/kgmono)	D_e (m^2/s)	D_e (cm^2/s)	Average D_e (cm^2/s)	Standard Deviation of Average De
S014-16-T4-1	444000	3/8/2016 8:40:0	3/15/2016 8:50:0	364.02	284.12	195.68	1761.2	1.94E-04	4.00E+04	1.46E+03	7.44E+04	1.0E-12	1.0E-08	1.1E-08	6.5E-10
S014-16-T4-2	467000	3/8/2016 8:40:0	3/15/2016 8:50:0	369.27	288.22	199.22	1793.0	1.99E-04	4.20E+04	1.45E+03	7.44E+04	1.1E-12	1.1E-08		
S014-16-T4-5	479000	3/8/2016 8:40:0	3/15/2016 8:50:0	365.37	285.18	195.92	1763.3	1.94E-04	4.31E+04	1.47E+03	7.44E+04	1.2E-12	1.2E-08	1.2E-08	1.8E-10
S014-16-T4-7	466000	3/8/2016 8:40:0	3/15/2016 8:50:0	363.93	284.05	196.69	1770.2	1.96E-04	4.19E+04	1.45E+03	7.44E+04	1.1E-12	1.1E-08		

T5

Name	Na (µg/L)	Interval Begin	Sampling Date	Monlith mass (g)	Monlith Dry Mass (g)	Surface Area (cm^2)	Solution Volume (mL)	Monolith Volume (m^3)	M_{ti} (mg/m^2)	ρ (kg/m^3)	Co (mgNa/kgmono)	D_e (m^2/s)	D_e (cm^2/s)	Average D_e (cm^2/s)	Standard Deviation of Average De
S014-16-T5-2	420000	3/8/2016 8:40:0	3/15/2016 8:50:0	365.93	283.58	197.86	1780.7	1.97E-04	3.78E+04	1.44E+03	7.72E+04	8.8E-13	8.8E-09	9.3E-09	5.5E-10
S014-16-T5-3	455000	3/8/2016 8:40:0	3/15/2016 8:50:0	364.75	282.66	195.03	1755.3	1.92E-04	4.10E+04	1.47E+03	7.72E+04	9.9E-13	9.9E-09		
S014-16-T5-4	451000	3/8/2016 8:40:0	3/15/2016 8:50:0	366.62	284.11	196.79	1771.1	1.95E-04	4.06E+04	1.46E+03	7.72E+04	9.9E-13	9.9E-09	1.1E-08	1.0E-09
S014-16-T5-7	489000	3/8/2016 8:40:0	3/15/2016 8:50:0	365.76	283.44	197.96	1781.6	1.97E-04	4.40E+04	1.44E+03	7.72E+04	1.2E-12	1.2E-08		

T6

Name	Na (µg/L)	Interval Begin	Sampling Date	Monlith mass (g)	Monlith Dry Mass (g)	Surface Area (cm^2)	Solution Volume (mL)	Monolith Volume (m^3)	M_{ti} (mg/m^2)	ρ (kg/m^3)	Co (mgNa/kgmono)	D_e (m^2/s)	D_e (cm^2/s)	Average D_e (cm^2/s)	Standard Deviation of Average De
S014-16-T6-2	430000	3/8/2016 8:40:0	3/15/2016 8:50:0	363.78	284.09	196.70	1770.3	1.95E-04	3.87E+04	1.45E+03	7.86E+04	8.7E-13	8.7E-09	9.2E-09	4.9E-10
S014-16-T6-3	453000	3/8/2016 8:40:0	3/15/2016 8:50:0	364.78	284.87	197.29	1775.6	1.96E-04	4.08E+04	1.45E+03	7.86E+04	9.7E-13	9.7E-09		
S014-16-T6-5	457000	3/8/2016 8:40:0	3/15/2016 8:50:0	362.95	283.44	196.39	1767.5	1.95E-04	4.11E+04	1.45E+03	7.86E+04	9.8E-13	9.8E-09	1.0E-08	5.1E-10
S014-16-T6-6	488000	3/8/2016 8:40:0	3/15/2016 8:50:0	360.98	281.90	193.67	1743.0	1.91E-04	4.39E+04	1.48E+03	7.86E+04	1.1E-12	1.1E-08		

Na Sampling 28 d

Experiment Start 3/1/16 8:30:00

T1

Name	Na (μg/L)	Interval Begin	Sampling Date	Monlith mass (g)	Monlith Dry Mass (g)	Surface Area (cm^2)	Solution Volume (mL)	Monolith Volume (m^3)	M_{ti} (mg/m^2)	ρ (kg/m^3)	Co (mgNa/kgmono)	D_e (m^2/s)	D_e (cm^2/s)	Average D_e (cm^2/s)	Standard Deviation of Average De
S014-16-T1-1	557000	03/15/2016 08:50:0	03/29/2016 08:00:00	359.63	277.23	192.53	1732.8	1.89E-04	5.01E+04	1.46E+03	7.61E+04	7.7E-13	7.7E-09	7.6E-09	1.0E-10
S014-16-T1-2	531000	03/15/2016 08:50:0	03/29/2016 08:00:00	365.20	281.52	199.18	1792.6	1.99E-04	4.78E+04	1.41E+03	7.61E+04	7.5E-13	7.5E-09		
S014-16-T1-4	529500	03/15/2016 08:50:0	03/29/2016 08:00:00	360.86	278.18	195.83	1762.5	1.95E-04	4.77E+04	1.43E+03	7.61E+04	7.3E-13	7.3E-09	7.3E-09	1.5E-12
S014-16-T1-7	537500	03/15/2016 08:50:0	03/29/2016 08:00:00	361.60	278.75	194.35	1749.2	1.92E-04	4.84E+04	1.45E+03	7.61E+04	7.3E-13	7.3E-09		

T2

Name	Na (μg/L)	Interval Begin	Sampling Date	Monlith mass (g)	Monlith Dry Mass (g)	Surface Area (cm^2)	Solution Volume (mL)	Monolith Volume (m^3)	M_{ti} (mg/m^2)	ρ (kg/m^3)	Co (mgNa/kgmono)	D_e (m^2/s)	D_e (cm^2/s)	Average D_e (cm^2/s)	Standard Deviation of Average De
S014-16-T2-3	761000	03/15/2016 08:50:0	03/29/2016 08:00:00	364.71	283.41	195.83	1749.7	1.92E-04	6.80E+04	1.48E+03	7.44E+04	1.5E-12	1.5E-08	1.6E-08	1.6E-09
S014-16-T2-6	819000	03/15/2016 08:50:0	03/29/2016 08:00:00	367.70	285.74	197.83	1780.5	1.97E-04	7.37E+04	1.45E+03	7.44E+04	1.8E-12	1.8E-08		
S014-16-T2-7	742500	03/15/2016 08:50:0	03/29/2016 08:00:00	366.00	284.41	196.77	1770.9	1.95E-04	6.68E+04	1.46E+03	7.44E+04	1.4E-12	1.4E-08	1.4E-08	5.1E-10
S014-16-T2-8	703500	03/15/2016 08:50:0	03/29/2016 08:00:00	363.14	282.19	197.90	1781.1	1.97E-04	6.33E+04	1.43E+03	7.44E+04	1.3E-12	1.3E-08		

T3

Name	Na (μg/L)	Interval Begin	Sampling Date	Monlith mass (g)	Monlith Dry Mass (g)	Surface Area (cm^2)	Solution Volume (mL)	Monolith Volume (m^3)	M_{ti} (mg/m^2)	ρ (kg/m^3)	Co (mgNa/kgmono)	D_e (m^2/s)	D_e (cm^2/s)	Average D_e (cm^2/s)	Standard Deviation of Average De
S014-16-T3-1	603000	03/15/2016 08:50:0	03/29/2016 08:00:00	366.62	285.46	195.87	1762.9	1.94E-04	5.43E+04	1.47E+03	7.82E+04	8.4E-13	8.4E-09	8.5E-09	7.3E-11
S014-16-T3-3	604000	03/15/2016 08:50:0	03/29/2016 08:00:00	364.46	283.78	195.53	1759.7	1.94E-04	5.44E+04	1.46E+03	7.82E+04	8.6E-13	8.6E-09		
S014-16-T3-4	503500	03/15/2016 08:50:0	03/29/2016 08:00:00	362.76	282.46	194.51	1750.6	1.93E-04	4.53E+04	1.47E+03	7.82E+04	5.9E-13	5.9E-09	6.2E-09	3.0E-10
S014-16-T3-8	526500	03/15/2016 08:50:0	03/29/2016 08:00:00	360.88	280.99	194.17	1747.5	1.92E-04	4.74E+04	1.46E+03	7.82E+04	6.5E-13	6.5E-09		

T4

Name	Na (μg/L)	Interval Begin	Sampling Date	Monlith mass (g)	Monlith Dry Mass (g)	Surface Area (cm^2)	Solution Volume (mL)	Monolith Volume (m^3)	M_{ti} (mg/m^2)	ρ (kg/m^3)	Co (mgNa/kgmono)	D_e (m^2/s)	D_e (cm^2/s)	Average D_e (cm^2/s)	Standard Deviation of Average De
S014-16-T4-1	625000	03/15/2016 08:50:0	03/29/2016 08:00:00	364.02	284.12	195.68	1761.2	1.94E-04	5.63E+04	1.46E+03	7.44E+04	1.0E-12	1.0E-08	1.0E-08	1.7E-10
S014-16-T4-2	609000	03/15/2016 08:50:0	03/29/2016 08:00:00	369.27	288.22	199.22	1793.0	1.99E-04	5.48E+04	1.45E+03	7.44E+04	9.8E-13	9.8E-09		
S014-16-T4-5	574500	03/15/2016 08:50:0	03/29/2016 08:00:00	365.37	285.18	195.92	1763.3	1.94E-04	5.17E+04	1.47E+03	7.44E+04	8.5E-13	8.5E-09	8.8E-09	2.7E-10
S014-16-T4-7	585500	03/15/2016 08:50:0	03/29/2016 08:00:00	363.93	284.05	196.69	1770.2	1.96E-04	5.27E+04	1.45E+03	7.44E+04	9.1E-13	9.1E-09		

T5

Name	Na (μg/L)	Interval Begin	Sampling Date	Monlith mass (g)	Monlith Dry Mass (g)	Surface Area (cm^2)	Solution Volume (mL)	Monolith Volume (m^3)	M_{ti} (mg/m^2)	ρ (kg/m^3)	Co (mgNa/kgmono)	D_e (m^2/s)	D_e (cm^2/s)	Average D_e (cm^2/s)	Standard Deviation of Average De
S014-16-T5-2	650000	03/15/2016 08:50:0	03/29/2016 08:00:00	365.93	283.58	197.86	1780.7	1.97E-04	5.85E+04	1.44E+03	7.72E+04	1.1E-12	1.1E-08	9.8E-09	8.0E-10
S014-16-T5-3	611000	03/15/2016 08:50:0	03/29/2016 08:00:00	364.75	282.66	195.03	1755.3	1.92E-04	5.50E+04	1.47E+03	7.72E+04	8.9E-13	8.9E-09		
S014-16-T5-4	583500	03/15/2016 08:50:0	03/29/2016 08:00:00	366.62	284.11	196.79	1771.1	1.95E-04	5.25E+04	1.46E+03	7.72E+04	8.3E-13	8.3E-09	8.4E-09	1.4E-10
S014-16-T5-7	585500	03/15/2016 08:50:0	03/29/2016 08:00:00	365.76	283.44	197.96	1781.6	1.97E-04	5.27E+04	1.44E+03	7.72E+04	8.6E-13	8.6E-09		

T6

Name	Na (μg/L)	Interval Begin	Sampling Date	Monlith mass (g)	Monlith Dry Mass (g)	Surface Area (cm^2)	Solution Volume (mL)	Monolith Volume (m^3)	M_{ti} (mg/m^2)	ρ (kg/m^3)	Co (mgNa/kgmono)	D_e (m^2/s)	D_e (cm^2/s)	Average D_e (cm^2/s)	Standard Deviation of Average De
S014-16-T6-2	612000	03/15/2016 08:50:0	03/29/2016 08:00:00	363.78	284.09	196.70	1770.3	1.95E-04	5.51E+04	1.45E+03	7.86E+04	8.8E-13	8.8E-09	8.7E-09	1.9E-10
S014-16-T6-3	598000	03/15/2016 08:50:0	03/29/2016 08:00:00	364.78	284.87	197.29	1775.6	1.96E-04	5.38E+04	1.45E+03	7.86E+04	8.5E-13	8.5E-09		
S014-16-T6-5	571500	03/15/2016 08:50:0	03/29/2016 08:00:00	362.95	283.44	196.39	1767.5	1.95E-04	5.14E+04	1.45E+03	7.86E+04	7.7E-13	7.7E-09	8.0E-09	3.4E-10
S014-16-T6-6	605500	03/15/2016 08:50:0	03/29/2016 08:00:00	360.98	281.90	193.67	1743.0	1.91E-04	5.45E+04	1.48E+03	7.86E+04	8.4E-13	8.4E-09		

Na 42 d Sampling

Experiment Start 3/1/16 8:30:00

T1

Name	Na (µg/L)	Interval Begin	Sampling Date	Monlith mass (g)	Monlith Dry Mass (g)	Surface Area (cm^2)	Solution Volume (mL)	Monolith Volume (m^3)	M_{ti} (mg/m^2)	ρ (kg/m^3)	Co (mgNa/kgmono)	D_e (m^2/s)	D_e (cm^2/s)	Average D_e (cm^2/s)	Standard Deviation of Average De
S014-16-T1-1	454000	03/29/2016 08:00:	04/12/2016 08:30:0	359.63	277.23	192.53	1732.8	1.89E-04	4.09E+04	1.46E+03	7.61E+04	8.6E-13	8.6E-09	7.9E-09	7.2E-10
S014-16-T1-2	400000	03/29/2016 08:00:	04/12/2016 08:30:0	365.20	281.52	199.18	1792.6	1.99E-04	3.60E+04	1.41E+03	7.61E+04	7.2E-13	7.2E-09		
S014-16-T1-4	438000	03/29/2016 08:00:	04/12/2016 08:30:0	360.86	278.18	195.83	1762.5	1.95E-04	3.94E+04	1.43E+03	7.61E+04	8.4E-13	8.4E-09	8.1E-09	3.1E-10
S014-16-T1-7	428000	03/29/2016 08:00:	04/12/2016 08:30:0	361.60	278.75	194.35	1749.2	1.92E-04	3.85E+04	1.45E+03	7.61E+04	7.8E-13	7.8E-09		

T2

Name	Na (µg/L)	Interval Begin	Sampling Date	Monlith mass (g)	Monlith Dry Mass (g)	Surface Area (cm^2)	Solution Volume (mL)	Monolith Volume (m^3)	M_{ti} (mg/m^2)	ρ (kg/m^3)	Co (mgNa/kgmono)	D_e (m^2/s)	D_e (cm^2/s)	Average D_e (cm^2/s)	Standard Deviation of Average De
S014-16-T2-3	521000	03/29/2016 08:00:	04/12/2016 08:30:0	364.71	283.41	195.83	1749.7	1.92E-04	4.66E+04	1.48E+03	7.44E+04	1.1E-12	1.1E-08	1.2E-08	6.8E-10
S014-16-T2-6	537000	03/29/2016 08:00:	04/12/2016 08:30:0	367.70	285.74	197.83	1780.5	1.97E-04	4.83E+04	1.45E+03	7.44E+04	1.3E-12	1.3E-08		
S014-16-T2-7	480000	03/29/2016 08:00:	04/12/2016 08:30:0	366.00	284.41	196.77	1770.9	1.95E-04	4.32E+04	1.46E+03	7.44E+04	1.0E-12	1.0E-08	1.1E-08	3.4E-10
S014-16-T2-8	487000	03/29/2016 08:00:	04/12/2016 08:30:0	363.14	282.19	197.90	1781.1	1.97E-04	4.38E+04	1.43E+03	7.44E+04	1.1E-12	1.1E-08		

T3

Name	Na (µg/L)	Interval Begin	Sampling Date	Monlith mass (g)	Monlith Dry Mass (g)	Surface Area (cm^2)	Solution Volume (mL)	Monolith Volume (m^3)	M_{ti} (mg/m^2)	ρ (kg/m^3)	Co (mgNa/kgmono)	D_e (m^2/s)	D_e (cm^2/s)	Average D_e (cm^2/s)	Standard Deviation of Average De
S014-16-T3-1	433000	03/29/2016 08:00:	04/12/2016 08:30:0	366.62	285.46	195.87	1762.9	1.94E-04	3.90E+04	1.47E+03	7.82E+04	7.3E-13	7.3E-09	7.2E-09	1.4E-10
S014-16-T3-3	422000	03/29/2016 08:00:	04/12/2016 08:30:0	364.46	283.78	195.53	1759.7	1.94E-04	3.80E+04	1.46E+03	7.82E+04	7.1E-13	7.1E-09		
S014-16-T3-4	420000	03/29/2016 08:00:	04/12/2016 08:30:0	362.76	282.46	194.51	1750.6	1.93E-04	3.78E+04	1.47E+03	7.82E+04	7.0E-13	7.0E-09	6.6E-09	3.3E-10
S014-16-T3-8	398000	03/29/2016 08:00:	04/12/2016 08:30:0	360.88	280.99	194.17	1747.5	1.92E-04	3.58E+04	1.46E+03	7.82E+04	6.3E-13	6.3E-09		

T4

Name	Na (µg/L)	Interval Begin	Sampling Date	Monlith mass (g)	Monlith Dry Mass (g)	Surface Area (cm^2)	Solution Volume (mL)	Monolith Volume (m^3)	M_{ti} (mg/m^2)	ρ (kg/m^3)	Co (mgNa/kgmono)	D_e (m^2/s)	D_e (cm^2/s)	Average D_e (cm^2/s)	Standard Deviation of Average De
S014-16-T4-1	426000	03/29/2016 08:00:	04/12/2016 08:30:0	364.02	284.12	195.68	1761.2	1.94E-04	3.83E+04	1.46E+03	7.44E+04	8.0E-13	8.0E-09	8.0E-09	1.9E-11
S014-16-T4-2	423000	03/29/2016 08:00:	04/12/2016 08:30:0	369.27	288.22	199.22	1793.0	1.99E-04	3.81E+04	1.45E+03	7.44E+04	8.0E-13	8.0E-09		
S014-16-T4-5	424000	03/29/2016 08:00:	04/12/2016 08:30:0	365.37	285.18	195.92	1763.3	1.94E-04	3.82E+04	1.47E+03	7.44E+04	7.8E-13	7.8E-09	8.0E-09	1.7E-10
S014-16-T4-7	428000	03/29/2016 08:00:	04/12/2016 08:30:0	363.93	284.05	196.69	1770.2	1.96E-04	3.85E+04	1.45E+03	7.44E+04	8.2E-13	8.2E-09		

T5

Name	Na (µg/L)	Interval Begin	Sampling Date	Monlith mass (g)	Monlith Dry Mass (g)	Surface Area (cm^2)	Solution Volume (mL)	Monolith Volume (m^3)	M_{ti} (mg/m^2)	ρ (kg/m^3)	Co (mgNa/kgmono)	D_e (m^2/s)	D_e (cm^2/s)	Average D_e (cm^2/s)	Standard Deviation of Average De
S014-16-T5-2	419000	03/29/2016 08:00:	04/12/2016 08:30:0	365.93	283.58	197.86	1780.7	1.97E-04	3.77E+04	1.44E+03	7.72E+04	7.4E-13	7.4E-09	8.3E-09	8.8E-10
S014-16-T5-3	476000	03/29/2016 08:00:	04/12/2016 08:30:0	364.75	282.66	195.03	1755.3	1.92E-04	4.28E+04	1.47E+03	7.72E+04	9.1E-13	9.1E-09		
S014-16-T5-4	404000	03/29/2016 08:00:	04/12/2016 08:30:0	366.62	284.11	196.79	1771.1	1.95E-04	3.64E+04	1.46E+03	7.72E+04	6.7E-13	6.7E-09	7.2E-09	5.1E-10
S014-16-T5-7	428000	03/29/2016 08:00:	04/12/2016 08:30:0	365.76	283.44	197.96	1781.6	1.97E-04	3.85E+04	1.44E+03	7.72E+04	7.7E-13	7.7E-09		

T6

Name	Na (µg/L)	Interval Begin	Sampling Date	Monlith mass (g)	Monlith Dry Mass (g)	Surface Area (cm^2)	Solution Volume (mL)	Monolith Volume (m^3)	M_{ti} (mg/m^2)	ρ (kg/m^3)	Co (mgNa/kgmono)	D_e (m^2/s)	D_e (cm^2/s)	Average D_e (cm^2/s)	Standard Deviation of Average De
S014-16-T6-2	434000	03/29/2016 08:00:	04/12/2016 08:30:0	363.78	284.09	196.70	1770.3	1.95E-04	3.91E+04	1.45E+03	7.86E+04	7.5E-13	7.5E-09	6.8E-09	6.7E-10
S014-16-T6-3	393000	03/29/2016 08:00:	04/12/2016 08:30:0	364.78	284.87	197.29	1775.6	1.96E-04	3.54E+04	1.45E+03	7.86E+04	6.2E-13	6.2E-09		
S014-16-T6-5	407000	03/29/2016 08:00:	04/12/2016 08:30:0	362.95	283.44	196.39	1767.5	1.95E-04	3.66E+04	1.45E+03	7.86E+04	6.6E-13	6.6E-09	6.5E-09	3.9E-11
S014-16-T6-6	411000	03/29/2016 08:00:	04/12/2016 08:30:0	360.98	281.90	193.67	1743.0	1.91E-04	3.70E+04	1.48E+03	7.86E+04	6.5E-13	6.5E-09		

Na Sampling 49 d

Experiment Start 3/1/16 8:30:00

T1

Name	Na (µg/L)	Interval Begin	Sampling Date	Monlith mass (g)	Monlith Dry Mass (g)	Surface Area (cm^2)	Solution Volume (mL)	Monolith Volume (m^3)	M_{ti} (mg/m^2)	ρ (kg/m^3)	Co (mgNa/kgmono)	D_e (m^2/s)	D_e (cm^2/s)	Average D_e (cm^2/s)	Standard Deviation of Average De
S014-16-T1-1	167000	04/12/2016 08:30:00	04/19/2016 08:40:00	359.63	277.23	192.53	1732.8	1.89E-04	1.50E+04	1.46E+03	7.61E+04	6.1E-13	6.1E-09	5.8E-09	2.7E-10
S014-16-T1-2	154000	04/12/2016 08:30:00	04/19/2016 08:40:01	365.20	281.52	199.18	1792.6	1.99E-04	1.39E+04	1.41E+03	7.61E+04	5.6E-13	5.6E-09		
S014-16-T1-4	157500	04/12/2016 08:30:00	04/19/2016 08:40:02	360.86	278.18	195.83	1762.5	1.95E-04	1.42E+04	1.43E+03	7.61E+04	5.7E-13	5.7E-09	5.6E-09	1.2E-10
S014-16-T1-7	156500	04/12/2016 08:30:00	04/19/2016 08:40:03	361.60	278.75	194.35	1749.2	1.92E-04	1.41E+04	1.45E+03	7.61E+04	5.5E-13	5.5E-09		

T2

Name	Na (µg/L)	Interval Begin	Sampling Date	Monlith mass (g)	Monlith Dry Mass (g)	Surface Area (cm^2)	Solution Volume (mL)	Monolith Volume (m^3)	M_{ti} (mg/m^2)	ρ (kg/m^3)	Co (mgNa/kgmono)	D_e (m^2/s)	D_e (cm^2/s)	Average D_e (cm^2/s)	Standard Deviation of Average De
S014-16-T2-3	185000	04/12/2016 08:30:00	04/19/2016 08:40:00	364.71	283.41	195.83	1749.7	1.92E-04	1.65E+04	1.48E+03	7.44E+04	7.6E-13	7.6E-09	7.8E-09	2.4E-10
S014-16-T2-6	186000	04/12/2016 08:30:00	04/19/2016 08:40:01	367.70	285.74	197.83	1780.5	1.97E-04	1.67E+04	1.45E+03	7.44E+04	8.1E-13	8.1E-09		
S014-16-T2-7	193500	04/12/2016 08:30:00	04/19/2016 08:40:02	366.00	284.41	196.77	1770.9	1.95E-04	1.74E+04	1.46E+03	7.44E+04	8.7E-13	8.7E-09	8.5E-09	2.5E-10
S014-16-T2-8	184500	04/12/2016 08:30:00	04/19/2016 08:40:03	363.14	282.19	197.90	1781.1	1.97E-04	1.66E+04	1.43E+03	7.44E+04	8.2E-13	8.2E-09		

T3

Name	Na (µg/L)	Interval Begin	Sampling Date	Monlith mass (g)	Monlith Dry Mass (g)	Surface Area (cm^2)	Solution Volume (mL)	Monolith Volume (m^3)	M_{ti} (mg/m^2)	ρ (kg/m^3)	Co (mgNa/kgmono)	D_e (m^2/s)	D_e (cm^2/s)	Average D_e (cm^2/s)	Standard Deviation of Average De
S014-16-T3-1	170000	04/12/2016 08:30:00	04/19/2016 08:40:00	366.62	285.46	195.87	1762.9	1.94E-04	1.53E+04	1.47E+03	7.82E+04	5.9E-13	5.9E-09	5.4E-09	5.3E-10
S014-16-T3-3	153000	04/12/2016 08:30:00	04/19/2016 08:40:01	364.46	283.78	195.53	1759.7	1.94E-04	1.38E+04	1.46E+03	7.82E+04	4.9E-13	4.9E-09		
S014-16-T3-4	149500	04/12/2016 08:30:00	04/19/2016 08:40:02	362.76	282.46	194.51	1750.6	1.93E-04	1.35E+04	1.47E+03	7.82E+04	4.6E-13	4.6E-09	4.6E-09	1.5E-11
S014-16-T3-8	148500	04/12/2016 08:30:00	04/19/2016 08:40:03	360.88	280.99	194.17	1747.5	1.92E-04	1.34E+04	1.46E+03	7.82E+04	4.6E-13	4.6E-09		

T4

Name	Na (µg/L)	Interval Begin	Sampling Date	Monlith mass (g)	Monlith Dry Mass (g)	Surface Area (cm^2)	Solution Volume (mL)	Monolith Volume (m^3)	M_{ti} (mg/m^2)	ρ (kg/m^3)	Co (mgNa/kgmono)	D_e (m^2/s)	D_e (cm^2/s)	Average D_e (cm^2/s)	Standard Deviation of Average De
S014-16-T4-1	164000	04/12/2016 08:30:00	04/19/2016 08:40:00	364.02	284.12	195.68	1761.2	1.94E-04	1.48E+04	1.46E+03	7.44E+04	6.2E-13	6.2E-09	6.1E-09	1.3E-10
S014-16-T4-2	159000	04/12/2016 08:30:00	04/19/2016 08:40:01	369.27	288.22	199.22	1793.0	1.99E-04	1.43E+04	1.45E+03	7.44E+04	5.9E-13	5.9E-09		
S014-16-T4-5	151500	04/12/2016 08:30:00	04/19/2016 08:40:02	365.37	285.18	195.92	1763.3	1.94E-04	1.36E+04	1.47E+03	7.44E+04	5.3E-13	5.3E-09	5.5E-09	2.1E-10
S014-16-T4-7	155500	04/12/2016 08:30:00	04/19/2016 08:40:03	363.93	284.05	196.69	1770.2	1.96E-04	1.40E+04	1.45E+03	7.44E+04	5.7E-13	5.7E-09		

T5

Name	Na (µg/L)	Interval Begin	Sampling Date	Monlith mass (g)	Monlith Dry Mass (g)	Surface Area (cm^2)	Solution Volume (mL)	Monolith Volume (m^3)	M_{ti} (mg/m^2)	ρ (kg/m^3)	Co (mgNa/kgmono)	D_e (m^2/s)	D_e (cm^2/s)	Average D_e (cm^2/s)	Standard Deviation of Average De
S014-16-T5-2	156000	04/12/2016 08:30:00	04/19/2016 08:40:00	365.93	283.58	197.86	1780.7	1.97E-04	1.40E+04	1.44E+03	7.72E+04	5.4E-13	5.4E-09	2.7E-09	2.7E-09
S014-16-T5-3		04/12/2016 08:30:00	04/19/2016 08:40:01	364.75	282.66	195.03	1755.3	1.92E-04	0.00E+00	1.47E+03	7.72E+04	0.0E+00	0.0E+00		
S014-16-T5-4	155500	04/12/2016 08:30:00	04/19/2016 08:40:02	366.62	284.11	196.79	1771.1	1.95E-04	1.40E+04	1.46E+03	7.72E+04	5.2E-13	5.2E-09	5.2E-09	1.3E-12
S014-16-T5-7	153500	04/12/2016 08:30:00	04/19/2016 08:40:03	365.76	283.44	197.96	1781.6	1.97E-04	1.38E+04	1.44E+03	7.72E+04	5.2E-13	5.2E-09		

T6

Name	Na (µg/L)	Interval Begin	Sampling Date	Monlith mass (g)	Monlith Dry Mass (g)	Surface Area (cm^2)	Solution Volume (mL)	Monolith Volume (m^3)	M_{ti} (mg/m^2)	ρ (kg/m^3)	Co (mgNa/kgmono)	D_e (m^2/s)	D_e (cm^2/s)	Average D_e (cm^2/s)	Standard Deviation of Average De
S014-16-T6-2	165000	04/12/2016 08:30:00	04/19/2016 08:40:00	363.78	284.09	196.70	1770.3	1.95E-04	1.49E+04	1.45E+03	7.86E+04	5.7E-13	5.7E-09	5.4E-09	2.6E-10
S014-16-T6-3	157000	04/12/2016 08:30:00	04/19/2016 08:40:01	364.78	284.87	197.29	1775.6	1.96E-04	1.41E+04	1.45E+03	7.86E+04	5.2E-13	5.2E-09		
S014-16-T6-5	150500	04/12/2016 08:30:00	04/19/2016 08:40:02	362.95	283.44	196.39	1767.5	1.95E-04	1.35E+04	1.45E+03	7.86E+04	4.7E-13	4.7E-09	4.6E-09	1.6E-10
S014-16-T6-6	147500	04/12/2016 08:30:00	04/19/2016 08:40:03	360.98	281.90	193.67	1743.0	1.91E-04	1.33E+04	1.48E+03	7.86E+04	4.4E-13	4.4E-09		

Na Sampling 63 d

Experiment Start 3/1/16 8:30:00

T1

Name	Na (µg/L)	Interval Begin	Sampling Date	Monlith mass (g)	Monlith Dry Mass (g)	Surface Area (cm^2)	Solution Volume (mL)	Monolith Volume (m^3)	M_{ti} (mg/m^2)	ρ (kg/m^3)	Co (mgNa/kgmono)	D_e (m^2/s)	D_e (cm^2/s)	Average D_e (cm^2/s)	Standard Deviation of Average De
S014-16-T1-1	271000	04/19/2016 08:40:00	05/3/2016 09:00:	359.63	277.23	192.53	1732.8	1.89E-04	2.44E+04	1.46E+03	7.61E+04	4.9E-13	4.9E-09	4.8E-09	1.1E-10
S014-16-T1-2	256000	04/19/2016 08:40:00	05/3/2016 09:00:	365.20	281.52	199.18	1792.6	1.99E-04	2.30E+04	1.41E+03	7.61E+04	4.7E-13	4.7E-09		
S014-16-T1-4	239000	04/19/2016 08:40:00	05/3/2016 09:00:	360.86	278.18	195.83	1762.5	1.95E-04	2.15E+04	1.43E+03	7.61E+04	4.0E-13	4.0E-09	3.9E-09	1.2E-10
S014-16-T1-7	235000	04/19/2016 08:40:00	05/3/2016 09:00:	361.60	278.75	194.35	1749.2	1.92E-04	2.12E+04	1.45E+03	7.61E+04	3.8E-13	3.8E-09		

T2

Name	Na (µg/L)	Interval Begin	Sampling Date	Monlith mass (g)	Monlith Dry Mass (g)	Surface Area (cm^2)	Solution Volume (mL)	Monolith Volume (m^3)	M_{ti} (mg/m^2)	ρ (kg/m^3)	Co (mgNa/kgmono)	D_e (m^2/s)	D_e (cm^2/s)	Average D_e (cm^2/s)	Standard Deviation of Average De
S014-16-T2-3	282000	04/19/2016 08:40:00	05/3/2016 09:00:	364.71	283.41	195.83	1749.7	1.92E-04	2.52E+04	1.48E+03	7.44E+04	5.4E-13	5.4E-09	5.3E-09	1.3E-10
S014-16-T2-6	268000	04/19/2016 08:40:00	05/3/2016 09:00:	367.70	285.74	197.83	1780.5	1.97E-04	2.41E+04	1.45E+03	7.44E+04	5.1E-13	5.1E-09		
S014-16-T2-7	270000	04/19/2016 08:40:00	05/3/2016 09:00:	366.00	284.41	196.77	1770.9	1.95E-04	2.43E+04	1.46E+03	7.44E+04	5.2E-13	5.2E-09	5.0E-09	2.0E-10
S014-16-T2-8	255000	04/19/2016 08:40:00	05/3/2016 09:00:	363.14	282.19	197.90	1781.1	1.97E-04	2.30E+04	1.43E+03	7.44E+04	4.8E-13	4.8E-09		

T3

Name	Na (µg/L)	Interval Begin	Sampling Date	Monlith mass (g)	Monlith Dry Mass (g)	Surface Area (cm^2)	Solution Volume (mL)	Monolith Volume (m^3)	M_{ti} (mg/m^2)	ρ (kg/m^3)	Co (mgNa/kgmono)	D_e (m^2/s)	D_e (cm^2/s)	Average D_e (cm^2/s)	Standard Deviation of Average De
S014-16-T3-1	275000	04/19/2016 08:40:00	05/3/2016 09:00:	366.62	285.46	195.87	1762.9	1.94E-04	2.48E+04	1.47E+03	7.82E+04	4.8E-13	4.8E-09	4.4E-09	3.9E-10
S014-16-T3-3	250000	04/19/2016 08:40:00	05/3/2016 09:00:	364.46	283.78	195.53	1759.7	1.94E-04	2.25E+04	1.46E+03	7.82E+04	4.0E-13	4.0E-09		
S014-16-T3-4	234000	04/19/2016 08:40:00	05/3/2016 09:00:	362.76	282.46	194.51	1750.6	1.93E-04	2.11E+04	1.47E+03	7.82E+04	3.5E-13	3.5E-09	3.6E-09	7.2E-11
S014-16-T3-8	238000	04/19/2016 08:40:00	05/3/2016 09:00:	360.88	280.99	194.17	1747.5	1.92E-04	2.14E+04	1.46E+03	7.82E+04	3.6E-13	3.6E-09		

T4

Name	Na (µg/L)	Interval Begin	Sampling Date	Monlith mass (g)	Monlith Dry Mass (g)	Surface Area (cm^2)	Solution Volume (mL)	Monolith Volume (m^3)	M_{ti} (mg/m^2)	ρ (kg/m^3)	Co (mgNa/kgmono)	D_e (m^2/s)	D_e (cm^2/s)	Average D_e (cm^2/s)	Standard Deviation of Average De
S014-16-T4-1	260000	04/19/2016 08:40:00	05/3/2016 09:00:	364.02	284.12	195.68	1761.2	1.94E-04	2.34E+04	1.46E+03	7.44E+04	4.8E-13	4.8E-09	4.4E-09	3.3E-10
S014-16-T4-2	239000	04/19/2016 08:40:00	05/3/2016 09:00:	369.27	288.22	199.22	1793.0	1.99E-04	2.15E+04	1.45E+03	7.44E+04	4.1E-13	4.1E-09		
S014-16-T4-5	249000	04/19/2016 08:40:00	05/3/2016 09:00:	365.37	285.18	195.92	1763.3	1.94E-04	2.24E+04	1.47E+03	7.44E+04	4.4E-13	4.4E-09	4.2E-09	1.9E-10
S014-16-T4-7	235000	04/19/2016 08:40:00	05/3/2016 09:00:	363.93	284.05	196.69	1770.2	1.96E-04	2.12E+04	1.45E+03	7.44E+04	4.0E-13	4.0E-09		

T5

Name	Na (µg/L)	Interval Begin	Sampling Date	Monlith mass (g)	Monlith Dry Mass (g)	Surface Area (cm^2)	Solution Volume (mL)	Monolith Volume (m^3)	M_{ti} (mg/m^2)	ρ (kg/m^3)	Co (mgNa/kgmono)	D_e (m^2/s)	D_e (cm^2/s)	Average D_e (cm^2/s)	Standard Deviation of Average De
S014-16-T5-2	258000	04/19/2016 08:40:00	05/3/2016 09:00:	365.93	283.58	197.86	1780.7	1.97E-04	2.32E+04	1.44E+03	7.72E+04	4.5E-13	4.5E-09	4.2E-09	3.4E-10
S014-16-T5-3	243000	04/19/2016 08:40:00	05/3/2016 09:00:	364.75	282.66	195.03	1755.3	1.92E-04	2.19E+04	1.47E+03	7.72E+04	3.8E-13	3.8E-09		
S014-16-T5-4	249000	04/19/2016 08:40:00	05/3/2016 09:00:	366.62	284.11	196.79	1771.1	1.95E-04	2.24E+04	1.46E+03	7.72E+04	4.1E-13	4.1E-09	3.8E-09	2.6E-10
S014-16-T5-7	230000	04/19/2016 08:40:00	05/3/2016 09:00:	365.76	283.44	197.96	1781.6	1.97E-04	2.07E+04	1.44E+03	7.72E+04	3.6E-13	3.6E-09		

T6

Name	Na (µg/L)	Interval Begin	Sampling Date	Monlith mass (g)	Monlith Dry Mass (g)	Surface Area (cm^2)	Solution Volume (mL)	Monolith Volume (m^3)	M_{ti} (mg/m^2)	ρ (kg/m^3)	Co (mgNa/kgmono)	D_e (m^2/s)	D_e (cm^2/s)	Average D_e (cm^2/s)	Standard Deviation of Average De
S014-16-T6-2	257000	04/19/2016 08:40:00	05/3/2016 09:00:	363.78	284.09	196.70	1770.3	1.95E-04	2.31E+04	1.45E+03	7.86E+04	4.2E-13	4.2E-09	4.0E-09	2.2E-10
S014-16-T6-3	243000	04/19/2016 08:40:00	05/3/2016 09:00:	364.78	284.87	197.29	1775.6	1.96E-04	2.19E+04	1.45E+03	7.86E+04	3.8E-13	3.8E-09		
S014-16-T6-5	229000	04/19/2016 08:40:00	05/3/2016 09:00:	362.95	283.44	196.39	1767.5	1.95E-04	2.06E+04	1.45E+03	7.86E+04	3.4E-13	3.4E-09	3.5E-09	1.4E-10
S014-16-T6-6	242000	04/19/2016 08:40:00	05/3/2016 09:00:	360.98	281.90	193.67	1743.0	1.91E-04	2.18E+04	1.48E+03	7.86E+04	3.6E-13	3.6E-09		

Na Co Calculation

LIMS Data

LIMS data on Na concentration measurement from the spiked 6.5 M Na simulants

These values show the initial Na content of the simulant prior to any getter addition

Test	LabNumber	SampleName	Result	Units	EQL
T1	1601042-01	T1 Initial	162000000	ug/L	44700
T2	1601042-03	T2 Initial	160000000	ug/L	44700
T3	1601042-05	T3 Initial	168000000	ug/L	44700
T4	1601042-08	T4 Initial	160000000	ug/L	44700
T5	1601042-11	T5 Initial	165000000	ug/L	44700
T6	1601042-13	T6 Initial	169000000	ug/L	44700
			3		

Simulant Volume

Density of the 6.5 M Na Average simulant [g/mL] 1.31

Test	Simulant Bottle Tare (g)	Bottle + Simulant (g)	Simulant Mass	Simulant Volume-(mL)	Simulant Volume after sampling (mL)	Dry Blend (g)	Total Weight of Slurry [g]
T1	100.1	1407.8	1307.7	998.2	994.2	1750.0	2744.2
T2	100.3	1408.1	1307.8	998.3	994.3	1757.3	2751.6
T3	100.1	1407.9	1307.8	998.3	994.3	1750.0	2744.3
T4	100	1408	1308	998.5	994.5	1745.0	2739.4
T5	99.8	1408	1308.2	998.6	994.6	1750.0	2744.6
T6	99.9	1410.2	1310.3	1000.2	996.2	1747.6	2743.8

Co

Calculation on Na C_0 in dry Cast Stone (mg/kg) monolith

	T1	T2	T3	T4	T5	T6
Dry solid fraction in Cast Stone Monolith	0.771	0.78	0.78	0.78	0.77	0.78

Test	Na (ug/g wet Cast Stone)-analytical	C_0 (mg/kg) in dry Cast Stone - analytical
T1	58692.87	**76138.64**
T2	57818.36	**74403.80**
T3	60869.66	**78175.37**
T4	58083.66	**74417.53**
T5	59794.41	**77159.49**
T6	61361.61	**78575.02**

NO3 Sampling 2h

Experiment Start	3/1/16 8:30:00

T1

Name	NO3 (µg/L	Interval Begin	Sampling Date	Monlith mass (g)	Monlith Dry Mass (g)	Surface Area (cm^2)	Solution Volume (mL)	Monolith Volume (m^3)	M$_{ti}$ (mg/m^2)	ρ (kg/m^3)	Co (mgNO3/kg mono)	D$_e$ (m^2/s)	D$_e$ (cm^2/s)	Average D$_e$ (cm^2/s)	Standard Deviation of Average De
S014-16-T1-1	55100	3/1/2016 8:30:	3/1/2016 10:30:0	359.63	277.23	192.53	1732.8	1.89E-04	4.96E+03	1.46E+03	6.81E+04	2.7E-13	2.7E-09	2.6E-09	7.1E-11
S014-16-T1-2	51800	3/1/2016 8:30:	3/1/2016 10:30:0	365.20	281.52	199.18	1792.6	1.99E-04	4.66E+03	1.41E+03	6.81E+04	2.6E-13	2.6E-09		
S014-16-T1-4	73500	3/1/2016 8:30:	3/1/2016 10:30:0	360.86	278.18	195.83	1762.5	1.95E-04	6.62E+03	1.43E+03	6.81E+04	5.0E-13	5.0E-09	4.8E-09	2.7E-10
S014-16-T1-7	70500	3/1/2016 8:30:	3/1/2016 10:30:0	361.60	278.75	194.35	1749.2	1.92E-04	6.35E+03	1.45E+03	6.81E+04	4.5E-13	4.5E-09		

T2

Name	NO3 (µg/L	Interval Begin	Sampling Date	Monlith mass (g)	Monlith Dry Mass (g)	Surface Area (cm^2)	Solution Volume (mL)	Monolith Volume (m^3)	M$_{ti}$ (mg/m^2)	ρ (kg/m^3)	Co (mgNO3/kg mono)	D$_e$ (m^2/s)	D$_e$ (cm^2/s)	Average D$_e$ (cm^2/s)	Standard Deviation of Average De
S014-16-T2-3	62300	3/1/2016 8:30:	3/1/2016 10:30:0	364.71	283.41	195.83	1749.7	1.92E-04	5.57E+03	1.48E+03	6.74E+04	3.4E-13	3.4E-09	3.6E-09	2.2E-10
S014-16-T2-6	64600	3/1/2016 8:30:	3/1/2016 10:30:0	367.70	285.74	197.83	1780.5	1.97E-04	5.81E+03	1.45E+03	6.74E+04	3.8E-13	3.8E-09		
S014-16-T2-7	90500	3/1/2016 8:30:	3/1/2016 10:30:0	366.00	284.41	196.77	1770.9	1.95E-04	8.15E+03	1.46E+03	6.74E+04	7.5E-13	7.5E-09	6.5E-09	9.8E-10
S014-16-T2-8	76500	3/1/2016 8:30:	3/1/2016 10:30:0	363.14	282.19	197.90	1781.1	1.97E-04	6.89E+03	1.43E+03	6.74E+04	5.6E-13	5.6E-09		

T3

Name	NO3 (µg/L	Interval Begin	Sampling Date	Monlith mass (g)	Monlith Dry Mass (g)	Surface Area (cm^2)	Solution Volume (mL)	Monolith Volume (m^3)	M$_{ti}$ (mg/m^2)	ρ (kg/m^3)	Co (mgNO3/kg mono)	D$_e$ (m^2/s)	D$_e$ (cm^2/s)	Average D$_e$ (cm^2/s)	Standard Deviation of Average De
S014-16-T3-1	64800	3/1/2016 8:30:	3/1/2016 10:30:0	366.62	285.46	195.87	1762.9	1.94E-04	5.83E+03	1.47E+03	6.75E+04	3.8E-13	3.8E-09	1.9E-09	1.8E-09
S014-16-T3-3	8780	3/1/2016 8:30:	3/1/2016 10:30:0	364.46	283.78	195.53	1759.7	1.94E-04	7.90E+02	1.46E+03	6.75E+04	7.0E-15	7.0E-11		
S014-16-T3-4	94500	3/1/2016 8:30:	3/1/2016 10:30:0	362.76	282.46	194.51	1750.6	1.93E-04	8.51E+03	1.47E+03	6.75E+04	8.1E-13	8.1E-09	1.0E-08	2.1E-09
S014-16-T3-8	116500	3/1/2016 8:30:	3/1/2016 10:30:0	360.88	280.99	194.17	1747.5	1.92E-04	1.05E+04	1.46E+03	6.75E+04	1.2E-12	1.2E-08		

T4

Name	NO3 (µg/L	Interval Begin	Sampling Date	Monlith mass (g)	Monlith Dry Mass (g)	Surface Area (cm^2)	Solution Volume (mL)	Monolith Volume (m^3)	M$_{ti}$ (mg/m^2)	ρ (kg/m^3)	Co (mgNO3/kg mono)	D$_e$ (m^2/s)	D$_e$ (cm^2/s)	Average D$_e$ (cm^2/s)	Standard Deviation of Average De
S014-16-T4-1	84400	3/1/2016 8:30:	3/1/2016 10:30:0	364.02	284.12	195.68	1761.2	1.94E-04	7.60E+03	1.46E+03	6.88E+04	6.2E-13	6.2E-09	5.1E-09	1.1E-09
S014-16-T4-2	66400	3/1/2016 8:30:	3/1/2016 10:30:0	369.27	288.22	199.22	1793.0	1.99E-04	5.98E+03	1.45E+03	6.88E+04	3.9E-13	3.9E-09		
S014-16-T4-5	56500	3/1/2016 8:30:	3/1/2016 10:30:0	365.37	285.18	195.92	1763.3	1.94E-04	5.09E+03	1.47E+03	6.88E+04	2.8E-13	2.8E-09	4.9E-09	2.2E-09
S014-16-T4-7	89500	3/1/2016 8:30:	3/1/2016 10:30:0	363.93	284.05	196.69	1770.2	1.96E-04	8.06E+03	1.45E+03	6.88E+04	7.1E-13	7.1E-09		

T5

Name	NO3 (µg/L	Interval Begin	Sampling Date	Monlith mass (g)	Monlith Dry Mass (g)	Surface Area (cm^2)	Solution Volume (mL)	Monolith Volume (m^3)	M$_{ti}$ (mg/m^2)	ρ (kg/m^3)	Co (mgNO3/kg mono)	D$_e$ (m^2/s)	D$_e$ (cm^2/s)	Average D$_e$ (cm^2/s)	Standard Deviation of Average De
S014-16-T5-2	58200	3/1/2016 8:30:	3/1/2016 10:30:0	365.93	283.58	197.86	1780.7	1.97E-04	5.24E+03	1.44E+03	6.78E+04	3.1E-13	3.1E-09	2.9E-09	2.8E-10
S014-16-T5-3	53900	3/1/2016 8:30:	3/1/2016 10:30:0	364.75	282.66	195.03	1755.3	1.92E-04	4.85E+03	1.47E+03	6.78E+04	2.6E-13	2.6E-09		
S014-16-T5-4	95500	3/1/2016 8:30:	3/1/2016 10:30:0	366.62	284.11	196.79	1771.1	1.95E-04	8.60E+03	1.46E+03	6.78E+04	8.3E-13	8.3E-09	7.8E-09	4.9E-10
S014-16-T5-7	88500	3/1/2016 8:30:	3/1/2016 10:30:0	365.76	283.44	197.96	1781.6	1.97E-04	7.97E+03	1.44E+03	6.78E+04	7.3E-13	7.3E-09		

T6

Name	NO3 (µg/L	Interval Begin	Sampling Date	Monlith mass (g)	Monlith Dry Mass (g)	Surface Area (cm^2)	Solution Volume (mL)	Monolith Volume (m^3)	M$_{ti}$ (mg/m^2)	ρ (kg/m^3)	Co (mgNO3/kg mono)	D$_e$ (m^2/s)	D$_e$ (cm^2/s)	Average D$_e$ (cm^2/s)	Standard Deviation of Average De
S014-16-T6-2	63100	3/1/2016 8:30:	3/1/2016 10:30:0	363.78	284.09	196.70	1770.3	1.95E-04	5.68E+03	1.45E+03	6.74E+04	3.7E-13	3.7E-09	4.1E-09	4.3E-10
S014-16-T6-3	70000	3/1/2016 8:30:	3/1/2016 10:30:0	364.78	284.87	197.29	1775.6	1.96E-04	6.30E+03	1.45E+03	6.74E+04	4.5E-13	4.5E-09		
S014-16-T6-5	85500	3/1/2016 8:30:	3/1/2016 10:30:0	362.95	283.44	196.39	1767.5	1.95E-04	7.70E+03	1.45E+03	6.74E+04	6.7E-13	6.7E-09	5.0E-09	1.7E-09
S014-16-T6-6	61500	3/1/2016 8:30:	3/1/2016 10:30:0	360.98	281.90	193.67	1743.0	1.91E-04	5.54E+03	1.48E+03	6.74E+04	3.4E-13	3.4E-09		

NO3 Sampling 1 d

Experiment Start 3/1/16 8:30:00

T1

Name	NO3 (µg/L	Interval Begin	Sampling Date	Monlith mass (g)	Monlith Dry Mass (g)	Surface Area (cm^2)	Solution Volume (mL)	Monolith Volume (m^3)	M_{ti} (mg/m^2)	ρ (kg/m^3)	Co (mgNO3/kg mono)	D_e (m^2/s)	D_e (cm^2/s)	Average D_e (cm^2/s)	Standard Deviation of Average De
S014-16-T1-1	262000	3/1/2016 10:30:00	3/2/2016 8:30:00	359.63	277.23	192.53	1732.8	1.89E-04	2.36E+04	1.46E+03	6.81E+04	1.0E-12	1.0E-08	9.6E-09	3.9E-10
S014-16-T1-2	243000	3/1/2016 10:30:00	3/2/2016 8:30:00	365.20	281.52	199.18	1792.6	1.99E-04	2.19E+04	1.41E+03	6.81E+04	9.2E-13	9.2E-09		
S014-16-T1-4	260500	3/1/2016 10:30:00	3/2/2016 8:30:00	360.86	278.18	195.83	1762.5	1.95E-04	2.34E+04	1.43E+03	6.81E+04	1.0E-12	1.0E-08	1.6E-08	5.9E-09
S014-16-T1-7	385500	3/1/2016 10:30:00	3/2/2016 8:30:00	361.60	278.75	194.35	1749.2	1.92E-04	3.47E+04	1.45E+03	6.81E+04	2.2E-12	2.2E-08		

T2

Name	NO3 (µg/L	Interval Begin	Sampling Date	Monlith mass (g)	Monlith Dry Mass (g)	Surface Area (cm^2)	Solution Volume (mL)	Monolith Volume (m^3)	M_{ti} (mg/m^2)	ρ (kg/m^3)	Co (mgNO3/kg mono)	D_e (m^2/s)	D_e (cm^2/s)	Average D_e (cm^2/s)	Standard Deviation of Average De
S014-16-T2-3	377000	3/1/2016 10:30:00	3/2/2016 8:30:00	364.71	283.41	195.83	1749.7	1.92E-04	3.37E+04	1.48E+03	6.74E+04	2.0E-12	2.0E-08	2.3E-08	2.1E-09
S014-16-T2-6	404000	3/1/2016 10:30:00	3/2/2016 8:30:00	367.70	285.74	197.83	1780.5	1.97E-04	3.64E+04	1.45E+03	6.74E+04	2.5E-12	2.5E-08		
S014-16-T2-7	306500	3/1/2016 10:30:00	3/2/2016 8:30:00	366.00	284.41	196.77	1770.9	1.95E-04	2.76E+04	1.46E+03	6.74E+04	1.4E-12	1.4E-08	1.6E-08	1.4E-09
S014-16-T2-8	329500	3/1/2016 10:30:00	3/2/2016 8:30:00	363.14	282.19	197.90	1781.1	1.97E-04	2.97E+04	1.43E+03	6.74E+04	1.7E-12	1.7E-08		

T3

Name	NO3 (µg/L	Interval Begin	Sampling Date	Monlith mass (g)	Monlith Dry Mass (g)	Surface Area (cm^2)	Solution Volume (mL)	Monolith Volume (m^3)	M_{ti} (mg/m^2)	ρ (kg/m^3)	Co (mgNO3/kg mono)	D_e (m^2/s)	D_e (cm^2/s)	Average D_e (cm^2/s)	Standard Deviation of Average De
S014-16-T3-1	235000	3/1/2016 10:30:00	3/2/2016 8:30:00	366.62	285.46	195.87	1762.9	1.94E-04	2.12E+04	1.47E+03	6.75E+04	8.1E-13	8.1E-09	9.3E-09	1.2E-09
S014-16-T3-3	266000	3/1/2016 10:30:00	3/2/2016 8:30:00	364.46	283.78	195.53	1759.7	1.94E-04	2.39E+04	1.46E+03	6.75E+04	1.1E-12	1.1E-08		
S014-16-T3-4	177500	3/1/2016 10:30:00	3/2/2016 8:30:00	362.76	282.46	194.51	1750.6	1.93E-04	1.60E+04	1.47E+03	6.75E+04	4.7E-13	4.7E-09	9.7E-09	5.0E-09
S014-16-T3-8	313500	3/1/2016 10:30:00	3/2/2016 8:30:00	360.88	280.99	194.17	1747.5	1.92E-04	2.82E+04	1.46E+03	6.75E+04	1.5E-12	1.5E-08		

T4

Name	NO3 (µg/L	Interval Begin	Sampling Date	Monlith mass (g)	Monlith Dry Mass (g)	Surface Area (cm^2)	Solution Volume (mL)	Monolith Volume (m^3)	M_{ti} (mg/m^2)	ρ (kg/m^3)	Co (mgNO3/kg mono)	D_e (m^2/s)	D_e (cm^2/s)	Average D_e (cm^2/s)	Standard Deviation of Average De
S014-16-T4-1	257000	3/1/2016 10:30:00	3/2/2016 8:30:00	364.02	284.12	195.68	1761.2	1.94E-04	2.31E+04	1.46E+03	6.88E+04	9.5E-13	9.5E-09	1.1E-08	1.1E-09
S014-16-T4-2	283000	3/1/2016 10:30:00	3/2/2016 8:30:00	369.27	288.22	199.22	1793.0	1.99E-04	2.55E+04	1.45E+03	6.88E+04	1.2E-12	1.2E-08		
S014-16-T4-5	255500	3/1/2016 10:30:00	3/2/2016 8:30:00	365.37	285.18	195.92	1763.3	1.94E-04	2.30E+04	1.47E+03	6.88E+04	9.3E-13	9.3E-09	8.7E-09	5.7E-10
S014-16-T4-7	236500	3/1/2016 10:30:00	3/2/2016 8:30:00	363.93	284.05	196.69	1770.2	1.96E-04	2.13E+04	1.45E+03	6.88E+04	8.2E-13	8.2E-09		

T5

Name	NO3 (µg/L	Interval Begin	Sampling Date	Monlith mass (g)	Monlith Dry Mass (g)	Surface Area (cm^2)	Solution Volume (mL)	Monolith Volume (m^3)	M_{ti} (mg/m^2)	ρ (kg/m^3)	Co (mgNO3/kg mono)	D_e (m^2/s)	D_e (cm^2/s)	Average D_e (cm^2/s)	Standard Deviation of Average De
S014-16-T5-2	204000	3/1/2016 10:30:00	3/2/2016 8:30:00	365.93	283.58	197.86	1780.7	1.97E-04	1.84E+04	1.44E+03	6.78E+04	6.4E-13	6.4E-09	7.8E-09	1.4E-09
S014-16-T5-3	251000	3/1/2016 10:30:00	3/2/2016 8:30:00	364.75	282.66	195.03	1755.3	1.92E-04	2.26E+04	1.47E+03	6.78E+04	9.2E-13	9.2E-09		
S014-16-T5-4	312500	3/1/2016 10:30:00	3/2/2016 8:30:00	366.62	284.11	196.79	1771.1	1.95E-04	2.81E+04	1.46E+03	6.78E+04	1.5E-12	1.5E-08	1.4E-08	4.7E-10
S014-16-T5-7	298500	3/1/2016 10:30:00	3/2/2016 8:30:00	365.76	283.44	197.96	1781.6	1.97E-04	2.69E+04	1.44E+03	6.78E+04	1.4E-12	1.4E-08		

T6

Name	NO3 (µg/L	Interval Begin	Sampling Date	Monlith mass (g)	Monlith Dry Mass (g)	Surface Area (cm^2)	Solution Volume (mL)	Monolith Volume (m^3)	M_{ti} (mg/m^2)	ρ (kg/m^3)	Co (mgNO3/kg mono)	D_e (m^2/s)	D_e (cm^2/s)	Average D_e (cm^2/s)	Standard Deviation of Average De
S014-16-T6-2	298000	3/1/2016 10:30:00	3/2/2016 8:30:00	363.78	284.09	196.70	1770.3	1.95E-04	2.68E+04	1.45E+03	6.74E+04	1.3E-12	1.3E-08	1.3E-08	4.7E-10
S014-16-T6-3	287000	3/1/2016 10:30:00	3/2/2016 8:30:00	364.78	284.87	197.29	1775.6	1.96E-04	2.58E+04	1.45E+03	6.74E+04	1.3E-12	1.3E-08		
S014-16-T6-5	292500	3/1/2016 10:30:00	3/2/2016 8:30:00	362.95	283.44	196.39	1767.5	1.95E-04	2.63E+04	1.45E+03	6.74E+04	1.3E-12	1.3E-08	1.1E-08	1.5E-09
S014-16-T6-6	259500	3/1/2016 10:30:00	3/2/2016 8:30:00	360.98	281.90	193.67	1743.0	1.91E-04	2.34E+04	1.48E+03	6.74E+04	9.9E-13	9.9E-09		

NO3 Sampling 2 d

Experiment Start 3/1/16 8:30:00

T1

Name	NO3 (µg/L	Interval Begin	Sampling Date	Monlith mass (g)	Monlith Dry Mass (g)	Surface Area (cm^2)	Solution Volume (mL)	Monolith Volume (m^3)	M_{ti} (mg/m^2)	ρ (kg/m^3)	Co (mgNO3/kg mono)	D_e (m^2/s)	D_e (cm^2/s)	Average D_e (cm^2/s)	Standard Deviation of Average De
S014-16-T1-1	142000	3/2/2016 8:30:0	3/3/2016 8:40:00	359.63	277.23	192.53	1732.8	1.89E-04	1.28E+04	1.46E+03	6.81E+04	8.6E-13	8.6E-09	8.8E-09	1.8E-10
S014-16-T1-2	140000	3/2/2016 8:30:0	3/3/2016 8:40:00	365.20	281.52	199.18	1792.6	1.99E-04	1.26E+04	1.41E+03	6.81E+04	8.9E-13	8.9E-09		
S014-16-T1-4	173500	3/2/2016 8:30:0	3/3/2016 8:40:00	360.86	278.18	195.83	1762.5	1.95E-04	1.56E+04	1.43E+03	6.81E+04	1.3E-12	1.3E-08	1.3E-08	2.7E-10
S014-16-T1-7	172500	3/2/2016 8:30:0	3/3/2016 8:40:00	361.60	278.75	194.35	1749.2	1.92E-04	1.55E+04	1.45E+03	6.81E+04	1.3E-12	1.3E-08		

T2

Name	NO3 (µg/L	Interval Begin	Sampling Date	Monlith mass (g)	Monlith Dry Mass (g)	Surface Area (cm^2)	Solution Volume (mL)	Monolith Volume (m^3)	M_{ti} (mg/m^2)	ρ (kg/m^3)	Co (mgNO3/kg mono)	D_e (m^2/s)	D_e (cm^2/s)	Average D_e (cm^2/s)	Standard Deviation of Average De
S014-16-T2-3	213000	3/2/2016 8:30:0	3/3/2016 8:40:00	364.71	283.41	195.83	1749.7	1.92E-04	1.90E+04	1.48E+03	6.74E+04	1.9E-12	1.9E-08	2.2E-08	2.9E-09
S014-16-T2-6	237000	3/2/2016 8:30:0	3/3/2016 8:40:00	367.70	285.74	197.83	1780.5	1.97E-04	2.13E+04	1.45E+03	6.74E+04	2.5E-12	2.5E-08		
S014-16-T2-7	251500	3/2/2016 8:30:0	3/3/2016 8:40:00	366.00	284.41	196.77	1770.9	1.95E-04	2.26E+04	1.46E+03	6.74E+04	2.8E-12	2.8E-08	2.7E-08	8.5E-10
S014-16-T2-8	239500	3/2/2016 8:30:0	3/3/2016 8:40:00	363.14	282.19	197.90	1781.1	1.97E-04	2.16E+04	1.43E+03	6.74E+04	2.6E-12	2.6E-08		

T3

Name	NO3 (µg/L	Interval Begin	Sampling Date	Monlith mass (g)	Monlith Dry Mass (g)	Surface Area (cm^2)	Solution Volume (mL)	Monolith Volume (m^3)	M_{ti} (mg/m^2)	ρ (kg/m^3)	Co (mgNO3/kg mono)	D_e (m^2/s)	D_e (cm^2/s)	Average D_e (cm^2/s)	Standard Deviation of Average De
S014-16-T3-1	140000	3/2/2016 8:30:0	3/3/2016 8:40:00	366.62	285.46	195.87	1762.9	1.94E-04	1.26E+04	1.47E+03	6.75E+04	8.4E-13	8.4E-09	1.1E-08	3.0E-09
S014-16-T3-3	182000	3/2/2016 8:30:0	3/3/2016 8:40:00	364.46	283.78	195.53	1759.7	1.94E-04	1.64E+04	1.46E+03	6.75E+04	1.4E-12	1.4E-08		
S014-16-T3-4	177500	3/2/2016 8:30:0	3/3/2016 8:40:00	362.76	282.46	194.51	1750.6	1.93E-04	1.60E+04	1.47E+03	6.75E+04	1.4E-12	1.4E-08	1.3E-08	4.8E-10
S014-16-T3-8	170500	3/2/2016 8:30:0	3/3/2016 8:40:00	360.88	280.99	194.17	1747.5	1.92E-04	1.53E+04	1.46E+03	6.75E+04	1.3E-12	1.3E-08		

T4

Name	NO3 (µg/L	Interval Begin	Sampling Date	Monlith mass (g)	Monlith Dry Mass (g)	Surface Area (cm^2)	Solution Volume (mL)	Monolith Volume (m^3)	M_{ti} (mg/m^2)	ρ (kg/m^3)	Co (mgNO3/kg mono)	D_e (m^2/s)	D_e (cm^2/s)	Average D_e (cm^2/s)	Standard Deviation of Average De
S014-16-T4-1	174000	3/2/2016 8:30:0	3/3/2016 8:40:00	364.02	284.12	195.68	1761.2	1.94E-04	1.57E+04	1.46E+03	6.88E+04	1.3E-12	1.3E-08	1.2E-08	8.1E-10
S014-16-T4-2	161000	3/2/2016 8:30:0	3/3/2016 8:40:00	369.27	288.22	199.22	1793.0	1.99E-04	1.45E+04	1.45E+03	6.88E+04	1.1E-12	1.1E-08		
S014-16-T4-5	189500	3/2/2016 8:30:0	3/3/2016 8:40:00	365.37	285.18	195.92	1763.3	1.94E-04	1.71E+04	1.47E+03	6.88E+04	1.5E-12	1.5E-08	1.3E-08	1.8E-09
S014-16-T4-7	163500	3/2/2016 8:30:0	3/3/2016 8:40:00	363.93	284.05	196.69	1770.2	1.96E-04	1.47E+04	1.45E+03	6.88E+04	1.1E-12	1.1E-08		

T5

Name	NO3 (µg/L	Interval Begin	Sampling Date	Monlith mass (g)	Monlith Dry Mass (g)	Surface Area (cm^2)	Solution Volume (mL)	Monolith Volume (m^3)	M_{ti} (mg/m^2)	ρ (kg/m^3)	Co (mgNO3/kg mono)	D_e (m^2/s)	D_e (cm^2/s)	Average D_e (cm^2/s)	Standard Deviation of Average De
S014-16-T5-2	133000	3/2/2016 8:30:0	3/3/2016 8:40:00	365.93	283.58	197.86	1780.7	1.97E-04	1.20E+04	1.44E+03	6.78E+04	7.9E-13	7.9E-09	8.5E-09	6.2E-10
S014-16-T5-3	146000	3/2/2016 8:30:0	3/3/2016 8:40:00	364.75	282.66	195.03	1755.3	1.92E-04	1.31E+04	1.47E+03	6.78E+04	9.1E-13	9.1E-09		
S014-16-T5-4	171500	3/2/2016 8:30:0	3/3/2016 8:40:00	366.62	284.11	196.79	1771.1	1.95E-04	1.54E+04	1.46E+03	6.78E+04	1.3E-12	1.3E-08	1.3E-08	4.7E-10
S014-16-T5-7	175500	3/2/2016 8:30:0	3/3/2016 8:40:00	365.76	283.44	197.96	1781.6	1.97E-04	1.58E+04	1.44E+03	6.78E+04	1.4E-12	1.4E-08		

T6

Name	NO3 (µg/L	Interval Begin	Sampling Date	Monlith mass (g)	Monlith Dry Mass (g)	Surface Area (cm^2)	Solution Volume (mL)	Monolith Volume (m^3)	M_{ti} (mg/m^2)	ρ (kg/m^3)	Co (mgNO3/kg mono)	D_e (m^2/s)	D_e (cm^2/s)	Average D_e (cm^2/s)	Standard Deviation of Average De
S014-16-T6-2	150000	3/2/2016 8:30:0	3/3/2016 8:40:00	363.78	284.09	196.70	1770.3	1.95E-04	1.35E+04	1.45E+03	6.74E+04	9.9E-13	9.9E-09	9.5E-09	4.4E-10
S014-16-T6-3	143000	3/2/2016 8:30:0	3/3/2016 8:40:00	364.78	284.87	197.29	1775.6	1.96E-04	1.29E+04	1.45E+03	6.74E+04	9.1E-13	9.1E-09		
S014-16-T6-5	176500	3/2/2016 8:30:0	3/3/2016 8:40:00	362.95	283.44	196.39	1767.5	1.95E-04	1.59E+04	1.45E+03	6.74E+04	1.4E-12	1.4E-08	1.3E-08	9.5E-10
S014-16-T6-6	166500	3/2/2016 8:30:0	3/3/2016 8:40:00	360.98	281.90	193.67	1743.0	1.91E-04	1.50E+04	1.48E+03	6.74E+04	1.2E-12	1.2E-08		

NO3 Sampling 7 d

Experiment Start 3/1/16 8:30:00

T1

Name	NO3 (µg/L	Interval Begin	Sampling Date	Monlith mass (g)	Monlith Dry Mass (g)	Surface Area (cm^2)	Solution Volume (mL)	Monolith Volume (m^3)	M_{ti} (mg/m^2)	ρ (kg/m^3)	Co (mgNO3/kg mono)	D_e (m^2/s)	D_e (cm^2/s)	Average D_e (cm^2/s)	Standard Deviation of Average De
S014-16-T1-1	522000	3/3/2016 8:40:0	3/8/2016 8:40:00	359.63	277.23	192.53	1732.8	1.89E-04	4.70E+04	1.46E+03	6.81E+04	1.3E-12	1.3E-08	1.4E-08	5.0E-10
S014-16-T1-2	523000	3/3/2016 8:40:0	3/8/2016 8:40:00	365.20	281.52	199.18	1792.6	1.99E-04	4.71E+04	1.41E+03	6.81E+04	1.4E-12	1.4E-08		
S014-16-T1-4	477000	3/3/2016 8:40:0	3/8/2016 8:40:00	360.86	278.18	195.83	1762.5	1.95E-04	4.29E+04	1.43E+03	6.81E+04	1.2E-12	1.2E-08	1.2E-08	5.1E-10
S014-16-T1-7	505000	3/3/2016 8:40:0	3/8/2016 8:40:00	361.60	278.75	194.35	1749.2	1.92E-04	4.55E+04	1.45E+03	6.81E+04	1.3E-12	1.3E-08		

T2

Name	NO3 (µg/L	Interval Begin	Sampling Date	Monlith mass (g)	Monlith Dry Mass (g)	Surface Area (cm^2)	Solution Volume (mL)	Monolith Volume (m^3)	M_{ti} (mg/m^2)	ρ (kg/m^3)	Co (mgNO3/kg mono)	D_e (m^2/s)	D_e (cm^2/s)	Average D_e (cm^2/s)	Standard Deviation of Average De
S014-16-T2-3	724000	3/3/2016 8:40:0	3/8/2016 8:40:00	364.71	283.41	195.83	1749.7	1.92E-04	6.47E+04	1.48E+03	6.74E+04	2.5E-12	2.5E-08	2.7E-08	1.9E-09
S014-16-T2-6	757000	3/3/2016 8:40:0	3/8/2016 8:40:00	367.70	285.74	197.83	1780.5	1.97E-04	6.81E+04	1.45E+03	6.74E+04	2.9E-12	2.9E-08		
S014-16-T2-7	659000	3/3/2016 8:40:0	3/8/2016 8:40:00	366.00	284.41	196.77	1770.9	1.95E-04	5.93E+04	1.46E+03	6.74E+04	2.2E-12	2.2E-08	2.4E-08	1.6E-09
S014-16-T2-8	692000	3/3/2016 8:40:0	3/8/2016 8:40:00	363.14	282.19	197.90	1781.1	1.97E-04	6.23E+04	1.43E+03	6.74E+04	2.5E-12	2.5E-08		

T3

Name	NO3 (µg/L	Interval Begin	Sampling Date	Monlith mass (g)	Monlith Dry Mass (g)	Surface Area (cm^2)	Solution Volume (mL)	Monolith Volume (m^3)	M_{ti} (mg/m^2)	ρ (kg/m^3)	Co (mgNO3/kg mono)	D_e (m^2/s)	D_e (cm^2/s)	Average D_e (cm^2/s)	Standard Deviation of Average De
S014-16-T3-1	507000	3/3/2016 8:40:0	3/8/2016 8:40:00	366.62	285.46	195.87	1762.9	1.94E-04	4.56E+04	1.47E+03	6.75E+04	1.3E-12	1.3E-08	1.3E-08	3.8E-11
S014-16-T3-3	505000	3/3/2016 8:40:0	3/8/2016 8:40:00	364.46	283.78	195.53	1759.7	1.94E-04	4.55E+04	1.46E+03	6.75E+04	1.3E-12	1.3E-08		
S014-16-T3-4	480000	3/3/2016 8:40:0	3/8/2016 8:40:00	362.76	282.46	194.51	1750.6	1.93E-04	4.32E+04	1.47E+03	6.75E+04	1.1E-12	1.1E-08	1.2E-08	7.8E-10
S014-16-T3-8	510000	3/3/2016 8:40:0	3/8/2016 8:40:00	360.88	280.99	194.17	1747.5	1.92E-04	4.59E+04	1.46E+03	6.75E+04	1.3E-12	1.3E-08		

T4

Name	NO3 (µg/L	Interval Begin	Sampling Date	Monlith mass (g)	Monlith Dry Mass (g)	Surface Area (cm^2)	Solution Volume (mL)	Monolith Volume (m^3)	M_{ti} (mg/m^2)	ρ (kg/m^3)	Co (mgNO3/kg mono)	D_e (m^2/s)	D_e (cm^2/s)	Average D_e (cm^2/s)	Standard Deviation of Average De
S014-16-T4-1	547000	3/3/2016 8:40:0	3/8/2016 8:40:00	364.02	284.12	195.68	1761.2	1.94E-04	4.92E+04	1.46E+03	6.88E+04	1.4E-12	1.4E-08	1.4E-08	3.9E-10
S014-16-T4-2	527000	3/3/2016 8:40:0	3/8/2016 8:40:00	369.27	288.22	199.22	1793.0	1.99E-04	4.74E+04	1.45E+03	6.88E+04	1.4E-12	1.4E-08		
S014-16-T4-5	510000	3/3/2016 8:40:0	3/8/2016 8:40:00	365.37	285.18	195.92	1763.3	1.94E-04	4.59E+04	1.47E+03	6.88E+04	1.2E-12	1.2E-08	1.3E-08	4.8E-10
S014-16-T4-7	523000	3/3/2016 8:40:0	3/8/2016 8:40:00	363.93	284.05	196.69	1770.2	1.96E-04	4.71E+04	1.45E+03	6.88E+04	1.3E-12	1.3E-08		

T5

Name	NO3 (µg/L	Interval Begin	Sampling Date	Monlith mass (g)	Monlith Dry Mass (g)	Surface Area (cm^2)	Solution Volume (mL)	Monolith Volume (m^3)	M_{ti} (mg/m^2)	ρ (kg/m^3)	Co (mgNO3/kg mono)	D_e (m^2/s)	D_e (cm^2/s)	Average D_e (cm^2/s)	Standard Deviation of Average De
S014-16-T5-2	475000	3/3/2016 8:40:0	3/8/2016 8:40:00	365.93	283.58	197.86	1780.7	1.97E-04	4.28E+04	1.44E+03	6.78E+04	1.2E-12	1.2E-08	1.2E-08	3.7E-10
S014-16-T5-3	500000	3/3/2016 8:40:0	3/8/2016 8:40:00	364.75	282.66	195.03	1755.3	1.92E-04	4.50E+04	1.47E+03	6.78E+04	1.2E-12	1.2E-08		
S014-16-T5-4	489000	3/3/2016 8:40:0	3/8/2016 8:40:00	366.62	284.11	196.79	1771.1	1.95E-04	4.40E+04	1.46E+03	6.78E+04	1.2E-12	1.2E-08	1.4E-08	1.7E-09
S014-16-T5-7	548000	3/3/2016 8:40:0	3/8/2016 8:40:00	365.76	283.44	197.96	1781.6	1.97E-04	4.93E+04	1.44E+03	6.78E+04	1.5E-12	1.5E-08		

T6

Name	NO3 (µg/L	Interval Begin	Sampling Date	Monlith mass (g)	Monlith Dry Mass (g)	Surface Area (cm^2)	Solution Volume (mL)	Monolith Volume (m^3)	M_{ti} (mg/m^2)	ρ (kg/m^3)	Co (mgNO3/kg mono)	D_e (m^2/s)	D_e (cm^2/s)	Average D_e (cm^2/s)	Standard Deviation of Average De
S014-16-T6-2	484000	3/3/2016 8:40:0	3/8/2016 8:40:00	363.78	284.09	196.70	1770.3	1.95E-04	4.36E+04	1.45E+03	6.74E+04	1.2E-12	1.2E-08	1.2E-08	1.7E-10
S014-16-T6-3	490000	3/3/2016 8:40:0	3/8/2016 8:40:00	364.78	284.87	197.29	1775.6	1.96E-04	4.41E+04	1.45E+03	6.74E+04	1.2E-12	1.2E-08		
S014-16-T6-5	501000	3/3/2016 8:40:0	3/8/2016 8:40:00	362.95	283.44	196.39	1767.5	1.95E-04	4.51E+04	1.45E+03	6.74E+04	1.3E-12	1.3E-08	1.3E-08	2.5E-10
S014-16-T6-6	519000	3/3/2016 8:40:0	3/8/2016 8:40:00	360.98	281.90	193.67	1743.0	1.91E-04	4.67E+04	1.48E+03	6.74E+04	1.3E-12	1.3E-08		

NO3 Sampling 14 d

Experiment Start 3/1/16 8:30:00

T1

Name	NO3 (µg/L	Interval Begin	Sampling Date	Monlith mass (g)	Monlith Dry Mass (g)	Surface Area (cm^2)	Solution Volume (mL)	Monolith Volume (m^3)	M_{ti} (mg/m^2)	ρ (kg/m^3)	Co (mgNO3/kg mono)	D_e (m^2/s)	D_e (cm^2/s)	Average D_e (cm^2/s)	Standard Deviation of Average De
S014-16-T1-1	395000	3/8/2016 8:40:0	3/15/2016 8:50:0	359.63	277.23	192.53	1732.8	1.89E-04	3.56E+04	1.46E+03	6.81E+04	9.6E-13	9.6E-09	9.8E-09	1.9E-10
S014-16-T1-2	389000	3/8/2016 8:40:0	3/15/2016 8:50:0	365.20	281.52	199.18	1792.6	1.99E-04	3.50E+04	1.41E+03	6.81E+04	1.0E-12	1.0E-08		
S014-16-T1-4	379000	3/8/2016 8:40:0	3/15/2016 8:50:0	360.86	278.18	195.83	1762.5	1.95E-04	3.41E+04	1.43E+03	6.81E+04	9.3E-13	9.3E-09	1.0E-08	6.8E-10
S014-16-T1-7	412000	3/8/2016 8:40:0	3/15/2016 8:50:0	361.60	278.75	194.35	1749.2	1.92E-04	3.71E+04	1.45E+03	6.81E+04	1.1E-12	1.1E-08		

T2

Name	NO3 (µg/L	Interval Begin	Sampling Date	Monlith mass (g)	Monlith Dry Mass (g)	Surface Area (cm^2)	Solution Volume (mL)	Monolith Volume (m^3)	M_{ti} (mg/m^2)	ρ (kg/m^3)	Co (mgNO3/kg mono)	D_e (m^2/s)	D_e (cm^2/s)	Average D_e (cm^2/s)	Standard Deviation of Average De
S014-16-T2-3	543000	3/8/2016 8:40:0	3/15/2016 8:50:0	364.71	283.41	195.83	1749.7	1.92E-04	4.85E+04	1.48E+03	6.74E+04	1.8E-12	1.8E-08	2.0E-08	2.0E-09
S014-16-T2-6	586000	3/8/2016 8:40:0	3/15/2016 8:50:0	367.70	285.74	197.83	1780.5	1.97E-04	5.27E+04	1.45E+03	6.74E+04	2.2E-12	2.2E-08		
S014-16-T2-7	562000	3/8/2016 8:40:0	3/15/2016 8:50:0	366.00	284.41	196.77	1770.9	1.95E-04	5.06E+04	1.46E+03	6.74E+04	2.0E-12	2.0E-08	1.9E-08	1.1E-09
S014-16-T2-8	522000	3/8/2016 8:40:0	3/15/2016 8:50:0	363.14	282.19	197.90	1781.1	1.97E-04	4.70E+04	1.43E+03	6.74E+04	1.8E-12	1.8E-08		

T3

Name	NO3 (µg/L	Interval Begin	Sampling Date	Monlith mass (g)	Monlith Dry Mass (g)	Surface Area (cm^2)	Solution Volume (mL)	Monolith Volume (m^3)	M_{ti} (mg/m^2)	ρ (kg/m^3)	Co (mgNO3/kg mono)	D_e (m^2/s)	D_e (cm^2/s)	Average D_e (cm^2/s)	Standard Deviation of Average De
S014-16-T3-1	401000	3/8/2016 8:40:0	3/15/2016 8:50:0	366.62	285.46	195.87	1762.9	1.94E-04	3.61E+04	1.47E+03	6.75E+04	1.0E-12	1.0E-08	9.8E-09	1.3E-10
S014-16-T3-3	393000	3/8/2016 8:40:0	3/15/2016 8:50:0	364.46	283.78	195.53	1759.7	1.94E-04	3.54E+04	1.46E+03	6.75E+04	9.7E-13	9.7E-09		
S014-16-T3-4	348000	3/8/2016 8:40:0	3/15/2016 8:50:0	362.76	282.46	194.51	1750.6	1.93E-04	3.13E+04	1.47E+03	6.75E+04	7.6E-13	7.6E-09	8.6E-09	1.0E-09
S014-16-T3-8	391000	3/8/2016 8:40:0	3/15/2016 8:50:0	360.88	280.99	194.17	1747.5	1.92E-04	3.52E+04	1.46E+03	6.75E+04	9.6E-13	9.6E-09		

T4

Name	NO3 (µg/L	Interval Begin	Sampling Date	Monlith mass (g)	Monlith Dry Mass (g)	Surface Area (cm^2)	Solution Volume (mL)	Monolith Volume (m^3)	M_{ti} (mg/m^2)	ρ (kg/m^3)	Co (mgNO3/kg mono)	D_e (m^2/s)	D_e (cm^2/s)	Average D_e (cm^2/s)	Standard Deviation of Average De
S014-16-T4-1	384000	3/8/2016 8:40:0	3/15/2016 8:50:0	364.02	284.12	195.68	1761.2	1.94E-04	3.46E+04	1.46E+03	6.88E+04	8.9E-13	8.9E-09	9.6E-09	7.0E-10
S014-16-T4-2	409000	3/8/2016 8:40:0	3/15/2016 8:50:0	369.27	288.22	199.22	1793.0	1.99E-04	3.68E+04	1.45E+03	6.88E+04	1.0E-12	1.0E-08		
S014-16-T4-5	412000	3/8/2016 8:40:0	3/15/2016 8:50:0	365.37	285.18	195.92	1763.3	1.94E-04	3.71E+04	1.47E+03	6.88E+04	1.0E-12	1.0E-08	1.0E-08	2.0E-10
S014-16-T4-7	415000	3/8/2016 8:40:0	3/15/2016 8:50:0	363.93	284.05	196.69	1770.2	1.96E-04	3.74E+04	1.45E+03	6.88E+04	1.1E-12	1.1E-08		

T5

Name	NO3 (µg/L	Interval Begin	Sampling Date	Monlith mass (g)	Monlith Dry Mass (g)	Surface Area (cm^2)	Solution Volume (mL)	Monolith Volume (m^3)	M_{ti} (mg/m^2)	ρ (kg/m^3)	Co (mgNO3/kg mono)	D_e (m^2/s)	D_e (cm^2/s)	Average D_e (cm^2/s)	Standard Deviation of Average De
S014-16-T5-2	373000	3/8/2016 8:40:0	3/15/2016 8:50:0	365.93	283.58	197.86	1780.7	1.97E-04	3.36E+04	1.44E+03	6.78E+04	8.9E-13	8.9E-09	9.2E-09	2.2E-10
S014-16-T5-3	390000	3/8/2016 8:40:0	3/15/2016 8:50:0	364.75	282.66	195.03	1755.3	1.92E-04	3.51E+04	1.47E+03	6.78E+04	9.4E-13	9.4E-09		
S014-16-T5-4	391000	3/8/2016 8:40:0	3/15/2016 8:50:0	366.62	284.11	196.79	1771.1	1.95E-04	3.52E+04	1.46E+03	6.78E+04	9.6E-13	9.6E-09	1.0E-08	8.3E-10
S014-16-T5-7	418000	3/8/2016 8:40:0	3/15/2016 8:50:0	365.76	283.44	197.96	1781.6	1.97E-04	3.76E+04	1.44E+03	6.78E+04	1.1E-12	1.1E-08		

T6

Name	NO3 (µg/L	Interval Begin	Sampling Date	Monlith mass (g)	Monlith Dry Mass (g)	Surface Area (cm^2)	Solution Volume (mL)	Monolith Volume (m^3)	M_{ti} (mg/m^2)	ρ (kg/m^3)	Co (mgNO3/kg mono)	D_e (m^2/s)	D_e (cm^2/s)	Average D_e (cm^2/s)	Standard Deviation of Average De
S014-16-T6-2	382000	3/8/2016 8:40:0	3/15/2016 8:50:0	363.78	284.09	196.70	1770.3	1.95E-04	3.44E+04	1.45E+03	6.74E+04	9.3E-13	9.3E-09	1.0E-08	7.5E-10
S014-16-T6-3	411000	3/8/2016 8:40:0	3/15/2016 8:50:0	364.78	284.87	197.29	1775.6	1.96E-04	3.70E+04	1.45E+03	6.74E+04	1.1E-12	1.1E-08		
S014-16-T6-5	402000	3/8/2016 8:40:0	3/15/2016 8:50:0	362.95	283.44	196.39	1767.5	1.95E-04	3.62E+04	1.45E+03	6.74E+04	1.0E-12	1.0E-08	1.0E-08	1.4E-10
S014-16-T6-6	414000	3/8/2016 8:40:0	3/15/2016 8:50:0	360.98	281.90	193.67	1743.0	1.91E-04	3.73E+04	1.48E+03	6.74E+04	1.1E-12	1.1E-08		

NO3 Sampling 28 d

Experiment Start 3/1/16 8:30:00

T1

Name	NO3 (µg/L	Interval Begin	Sampling Date	Monlith mass (g)	Monlith Dry Mass (g)	Surface Area (cm^2)	Solution Volume (mL)	Monolith Volume (m^3)	M_{ti} (mg/m^2)	ρ (kg/m^3)	Co (mgNO3/kg mono)	D_e (m^2/s)	D_e (cm^2/s)	Average D_e (cm^2/s)	Standard Deviation of Average De
S014-16-T1-1	534000	03/15/2016 08:50:0	03/29/2016 08:00:	359.63	277.23	192.53	1732.8	1.89E-04	4.81E+04	1.46E+03	6.81E+04	8.8E-13	8.8E-09	8.6E-09	1.8E-10
S014-16-T1-2	505000	03/15/2016 08:50:0	03/29/2016 08:00:	365.20	281.52	199.18	1792.6	1.99E-04	4.55E+04	1.41E+03	6.81E+04	8.5E-13	8.5E-09		
S014-16-T1-4	499500	03/15/2016 08:50:0	03/29/2016 08:00:	360.86	278.18	195.83	1762.5	1.95E-04	4.50E+04	1.43E+03	6.81E+04	8.1E-13	8.1E-09	7.8E-09	3.1E-10
S014-16-T1-7	487500	03/15/2016 08:50:0	03/29/2016 08:00:	361.60	278.75	194.35	1749.2	1.92E-04	4.39E+04	1.45E+03	6.81E+04	7.5E-13	7.5E-09		

T2

Name	NO3 (µg/L	Interval Begin	Sampling Date	Monlith mass (g)	Monlith Dry Mass (g)	Surface Area (cm^2)	Solution Volume (mL)	Monolith Volume (m^3)	M_{ti} (mg/m^2)	ρ (kg/m^3)	Co (mgNO3/kg mono)	D_e (m^2/s)	D_e (cm^2/s)	Average D_e (cm^2/s)	Standard Deviation of Average De
S014-16-T2-3	739000	03/15/2016 08:50:0	03/29/2016 08:00:	364.71	283.41	195.83	1749.7	1.92E-04	6.60E+04	1.48E+03	6.74E+04	1.7E-12	1.7E-08	1.8E-08	1.5E-09
S014-16-T2-6	782000	03/15/2016 08:50:0	03/29/2016 08:00:	367.70	285.74	197.83	1780.5	1.97E-04	7.04E+04	1.45E+03	6.74E+04	2.0E-12	2.0E-08		
S014-16-T2-7	692500	03/15/2016 08:50:0	03/29/2016 08:00:	366.00	284.41	196.77	1770.9	1.95E-04	6.23E+04	1.46E+03	6.74E+04	1.5E-12	1.5E-08	1.5E-08	4.5E-11
S014-16-T2-8	682500	03/15/2016 08:50:0	03/29/2016 08:00:	363.14	282.19	197.90	1781.1	1.97E-04	6.14E+04	1.43E+03	6.74E+04	1.5E-12	1.5E-08		

T3

Name	NO3 (µg/L	Interval Begin	Sampling Date	Monlith mass (g)	Monlith Dry Mass (g)	Surface Area (cm^2)	Solution Volume (mL)	Monolith Volume (m^3)	M_{ti} (mg/m^2)	ρ (kg/m^3)	Co (mgNO3/kg mono)	D_e (m^2/s)	D_e (cm^2/s)	Average D_e (cm^2/s)	Standard Deviation of Average De
S014-16-T3-1	540000	03/15/2016 08:50:0	03/29/2016 08:00:	366.62	285.46	195.87	1762.9	1.94E-04	4.86E+04	1.47E+03	6.75E+04	9.1E-13	9.1E-09	9.2E-09	6.4E-11
S014-16-T3-3	540000	03/15/2016 08:50:0	03/29/2016 08:00:	364.46	283.78	195.53	1759.7	1.94E-04	4.86E+04	1.46E+03	6.75E+04	9.2E-13	9.2E-09		
S014-16-T3-4	444500	03/15/2016 08:50:0	03/29/2016 08:00:	362.76	282.46	194.51	1750.6	1.93E-04	4.00E+04	1.47E+03	6.75E+04	6.2E-13	6.2E-09	6.6E-09	3.8E-10
S014-16-T3-8	469500	03/15/2016 08:50:0	03/29/2016 08:00:	360.88	280.99	194.17	1747.5	1.92E-04	4.23E+04	1.46E+03	6.75E+04	7.0E-13	7.0E-09		

T4

Name	NO3 (µg/L	Interval Begin	Sampling Date	Monlith mass (g)	Monlith Dry Mass (g)	Surface Area (cm^2)	Solution Volume (mL)	Monolith Volume (m^3)	M_{ti} (mg/m^2)	ρ (kg/m^3)	Co (mgNO3/kg mono)	D_e (m^2/s)	D_e (cm^2/s)	Average D_e (cm^2/s)	Standard Deviation of Average De
S014-16-T4-1	549000	03/15/2016 08:50:0	03/29/2016 08:00:	364.02	284.12	195.68	1761.2	1.94E-04	4.94E+04	1.46E+03	6.88E+04	9.2E-13	9.2E-09	9.1E-09	6.5E-11
S014-16-T4-2	540000	03/15/2016 08:50:0	03/29/2016 08:00:	369.27	288.22	199.22	1793.0	1.99E-04	4.86E+04	1.45E+03	6.88E+04	9.0E-13	9.0E-09		
S014-16-T4-5	498500	03/15/2016 08:50:0	03/29/2016 08:00:	365.37	285.18	195.92	1763.3	1.94E-04	4.49E+04	1.47E+03	6.88E+04	7.5E-13	7.5E-09	7.9E-09	4.4E-10
S014-16-T4-7	520500	03/15/2016 08:50:0	03/29/2016 08:00:	363.93	284.05	196.69	1770.2	1.96E-04	4.68E+04	1.45E+03	6.88E+04	8.4E-13	8.4E-09		

T5

Name	NO3 (µg/L	Interval Begin	Sampling Date	Monlith mass (g)	Monlith Dry Mass (g)	Surface Area (cm^2)	Solution Volume (mL)	Monolith Volume (m^3)	M_{ti} (mg/m^2)	ρ (kg/m^3)	Co (mgNO3/kg mono)	D_e (m^2/s)	D_e (cm^2/s)	Average D_e (cm^2/s)	Standard Deviation of Average De
S014-16-T5-2	570000	03/15/2016 08:50:0	03/29/2016 08:00:	365.93	283.58	197.86	1780.7	1.97E-04	5.13E+04	1.44E+03	6.78E+04	1.1E-12	1.1E-08	9.6E-09	9.3E-10
S014-16-T5-3	528000	03/15/2016 08:50:0	03/29/2016 08:00:	364.75	282.66	195.03	1755.3	1.92E-04	4.75E+04	1.47E+03	6.78E+04	8.7E-13	8.7E-09		
S014-16-T5-4	495500	03/15/2016 08:50:0	03/29/2016 08:00:	366.62	284.11	196.79	1771.1	1.95E-04	4.46E+04	1.46E+03	6.78E+04	7.8E-13	7.8E-09	7.9E-09	1.3E-10
S014-16-T5-7	497500	03/15/2016 08:50:0	03/29/2016 08:00:	365.76	283.44	197.96	1781.6	1.97E-04	4.48E+04	1.44E+03	6.78E+04	8.0E-13	8.0E-09		

T6

Name	NO3 (µg/L	Interval Begin	Sampling Date	Monlith mass (g)	Monlith Dry Mass (g)	Surface Area (cm^2)	Solution Volume (mL)	Monolith Volume (m^3)	M_{ti} (mg/m^2)	ρ (kg/m^3)	Co (mgNO3/kg mono)	D_e (m^2/s)	D_e (cm^2/s)	Average D_e (cm^2/s)	Standard Deviation of Average De
S014-16-T6-2	529000	03/15/2016 08:50:0	03/29/2016 08:00:	363.78	284.09	196.70	1770.3	1.95E-04	4.76E+04	1.45E+03	6.74E+04	9.0E-13	9.0E-09	8.8E-09	1.9E-10
S014-16-T6-3	517000	03/15/2016 08:50:0	03/29/2016 08:00:	364.78	284.87	197.29	1775.6	1.96E-04	4.65E+04	1.45E+03	6.74E+04	8.6E-13	8.6E-09		
S014-16-T6-5	500500	03/15/2016 08:50:0	03/29/2016 08:00:	362.95	283.44	196.39	1767.5	1.95E-04	4.50E+04	1.45E+03	6.74E+04	8.0E-13	8.0E-09	8.1E-09	6.4E-11
S014-16-T6-6	512500	03/15/2016 08:50:0	03/29/2016 08:00:	360.98	281.90	193.67	1743.0	1.91E-04	4.61E+04	1.48E+03	6.74E+04	8.2E-13	8.2E-09		

NO3 Sampling 42 d

Experiment Start 3/1/16 8:30:00

T1

Name	NO3 (µg/L	Interval Begin	Sampling Date	Monlith mass (g)	Monlith Dry Mass (g)	Surface Area (cm^2)	Solution Volume (mL)	Monolith Volume (m^3)	M_{ti} (mg/m^2)	ρ (kg/m^3)	Co (mgNO3/kg mono)	D_e (m^2/s)	D_e (cm^2/s)	Average D_e (cm^2/s)	Standard Deviation of Average De
S014-16-T1-1	361000	03/29/2016 08:00:(	04/12/2016 08:30:0(	359.63	277.23	192.53	1732.8	1.89E-04	3.25E+04	1.46E+03	6.81E+04	6.8E-13	6.8E-09	6.2E-09	6.3E-10
S014-16-T1-2	315000	03/29/2016 08:00:(	04/12/2016 08:30:0(	365.20	281.52	199.18	1792.6	1.99E-04	2.84E+04	1.41E+03	6.81E+04	5.5E-13	5.5E-09		
S014-16-T1-4	338500	03/29/2016 08:00:(	04/12/2016 08:30:0(	360.86	278.18	195.83	1762.5	1.95E-04	3.05E+04	1.43E+03	6.81E+04	6.3E-13	6.3E-09	5.9E-09	3.4E-10
S014-16-T1-7	324500	03/29/2016 08:00:(	04/12/2016 08:30:0(	361.60	278.75	194.35	1749.2	1.92E-04	2.92E+04	1.45E+03	6.81E+04	5.6E-13	5.6E-09		

T2

Name	NO3 (µg/L	Interval Begin	Sampling Date	Monlith mass (g)	Monlith Dry Mass (g)	Surface Area (cm^2)	Solution Volume (mL)	Monolith Volume (m^3)	M_{ti} (mg/m^2)	ρ (kg/m^3)	Co (mgNO3/kg mono)	D_e (m^2/s)	D_e (cm^2/s)	Average D_e (cm^2/s)	Standard Deviation of Average De
S014-16-T2-3	423000	03/29/2016 08:00:(	04/12/2016 08:30:0(	364.71	283.41	195.83	1749.7	1.92E-04	3.78E+04	1.48E+03	6.74E+04	9.2E-13	9.2E-09	9.9E-09	6.9E-10
S014-16-T2-6	442000	03/29/2016 08:00:(	04/12/2016 08:30:0(	367.70	285.74	197.83	1780.5	1.97E-04	3.98E+04	1.45E+03	6.74E+04	1.1E-12	1.1E-08		
S014-16-T2-7	396500	03/29/2016 08:00:(	04/12/2016 08:30:0(	366.00	284.41	196.77	1770.9	1.95E-04	3.57E+04	1.46E+03	6.74E+04	8.5E-13	8.5E-09	8.6E-09	1.3E-10
S014-16-T2-8	395500	03/29/2016 08:00:(	04/12/2016 08:30:0(	363.14	282.19	197.90	1781.1	1.97E-04	3.56E+04	1.43E+03	6.74E+04	8.7E-13	8.7E-09		

T3

Name	NO3 (µg/L	Interval Begin	Sampling Date	Monlith mass (g)	Monlith Dry Mass (g)	Surface Area (cm^2)	Solution Volume (mL)	Monolith Volume (m^3)	M_{ti} (mg/m^2)	ρ (kg/m^3)	Co (mgNO3/kg mono)	D_e (m^2/s)	D_e (cm^2/s)	Average D_e (cm^2/s)	Standard Deviation of Average De
S014-16-T3-1	344000	03/29/2016 08:00:(	04/12/2016 08:30:0(	366.62	285.46	195.87	1762.9	1.94E-04	3.10E+04	1.47E+03	6.75E+04	6.2E-13	6.2E-09	6.0E-09	2.4E-10
S014-16-T3-3	328000	03/29/2016 08:00:(	04/12/2016 08:30:0(	364.46	283.78	195.53	1759.7	1.94E-04	2.95E+04	1.46E+03	6.75E+04	5.7E-13	5.7E-09		
S014-16-T3-4	320500	03/29/2016 08:00:(	04/12/2016 08:30:0(	362.76	282.46	194.51	1750.6	1.93E-04	2.88E+04	1.47E+03	6.75E+04	5.4E-13	5.4E-09	5.3E-09	1.5E-10
S014-16-T3-8	310500	03/29/2016 08:00:(	04/12/2016 08:30:0(	360.88	280.99	194.17	1747.5	1.92E-04	2.79E+04	1.46E+03	6.75E+04	5.1E-13	5.1E-09		

T4

Name	NO3 (µg/L	Interval Begin	Sampling Date	Monlith mass (g)	Monlith Dry Mass (g)	Surface Area (cm^2)	Solution Volume (mL)	Monolith Volume (m^3)	M_{ti} (mg/m^2)	ρ (kg/m^3)	Co (mgNO3/kg mono)	D_e (m^2/s)	D_e (cm^2/s)	Average D_e (cm^2/s)	Standard Deviation of Average De
S014-16-T4-1	344000	03/29/2016 08:00:(	04/12/2016 08:30:0(	364.02	284.12	195.68	1761.2	1.94E-04	3.10E+04	1.46E+03	6.88E+04	6.1E-13	6.1E-09	5.9E-09	1.4E-10
S014-16-T4-2	333000	03/29/2016 08:00:(	04/12/2016 08:30:0(	369.27	288.22	199.22	1793.0	1.99E-04	3.00E+04	1.45E+03	6.88E+04	5.8E-13	5.8E-09		
S014-16-T4-5	323500	03/29/2016 08:00:(	04/12/2016 08:30:0(	365.37	285.18	195.92	1763.3	1.94E-04	2.91E+04	1.47E+03	6.88E+04	5.3E-13	5.3E-09	5.5E-09	1.7E-10
S014-16-T4-7	329500	03/29/2016 08:00:(	04/12/2016 08:30:0(	363.93	284.05	196.69	1770.2	1.96E-04	2.97E+04	1.45E+03	6.88E+04	5.7E-13	5.7E-09		

T5

Name	NO3 (µg/L	Interval Begin	Sampling Date	Monlith mass (g)	Monlith Dry Mass (g)	Surface Area (cm^2)	Solution Volume (mL)	Monolith Volume (m^3)	M_{ti} (mg/m^2)	ρ (kg/m^3)	Co (mgNO3/kg mono)	D_e (m^2/s)	D_e (cm^2/s)	Average D_e (cm^2/s)	Standard Deviation of Average De
S014-16-T5-2	340000	03/29/2016 08:00:(	04/12/2016 08:30:0(	365.93	283.58	197.86	1780.7	1.97E-04	3.06E+04	1.44E+03	6.78E+04	6.3E-13	6.3E-09	6.9E-09	6.3E-10
S014-16-T5-3	380000	03/29/2016 08:00:(	04/12/2016 08:30:0(	364.75	282.66	195.03	1755.3	1.92E-04	3.42E+04	1.47E+03	6.78E+04	7.6E-13	7.6E-09		
S014-16-T5-4	319500	03/29/2016 08:00:(	04/12/2016 08:30:0(	366.62	284.11	196.79	1771.1	1.95E-04	2.88E+04	1.46E+03	6.78E+04	5.4E-13	5.4E-09	5.7E-09	3.0E-10
S014-16-T5-7	332500	03/29/2016 08:00:(	04/12/2016 08:30:0(	365.76	283.44	197.96	1781.6	1.97E-04	2.99E+04	1.44E+03	6.78E+04	6.0E-13	6.0E-09		

T6

Name	NO3 (µg/L	Interval Begin	Sampling Date	Monlith mass (g)	Monlith Dry Mass (g)	Surface Area (cm^2)	Solution Volume (mL)	Monolith Volume (m^3)	M_{ti} (mg/m^2)	ρ (kg/m^3)	Co (mgNO3/kg mono)	D_e (m^2/s)	D_e (cm^2/s)	Average D_e (cm^2/s)	Standard Deviation of Average De
S014-16-T6-2	342000	03/29/2016 08:00:(	04/12/2016 08:30:0(	363.78	284.09	196.70	1770.3	1.95E-04	3.08E+04	1.45E+03	6.74E+04	6.3E-13	6.3E-09	5.8E-09	5.6E-10
S014-16-T6-3	310000	03/29/2016 08:00:(	04/12/2016 08:30:0(	364.78	284.87	197.29	1775.6	1.96E-04	2.79E+04	1.45E+03	6.74E+04	5.2E-13	5.2E-09		
S014-16-T6-5	319500	03/29/2016 08:00:(	04/12/2016 08:30:0(	362.95	283.44	196.39	1767.5	1.95E-04	2.88E+04	1.45E+03	6.74E+04	5.5E-13	5.5E-09	5.4E-09	1.4E-10
S014-16-T6-6	316500	03/29/2016 08:00:(	04/12/2016 08:30:0(	360.98	281.90	193.67	1743.0	1.91E-04	2.85E+04	1.48E+03	6.74E+04	5.2E-13	5.2E-09		

NO3 Sampling 49 d

Experiment Start 3/1/16 8:30:00

T1

Name	NO3 (µg/L	Interval Begin	Sampling Date	Monlith mass (g)	Monlith Dry Mass (g)	Surface Area (cm^2)	Solution Volume (mL)	Monolith Volume (m^3)	M_{ti} (mg/m^2)	ρ (kg/m^3)	Co (mgNO3/kg mono)	D_e (m^2/s)	D_e (cm^2/s)	Average D_e (cm^2/s)	Standard Deviation of Average De
S014-16-T1-1	124000	04/12/2016 08:30:	04/19/2016 08:40:0	359.63	277.23	192.53	1732.8	1.89E-04	1.12E+04	1.46E+03	6.81E+04	4.2E-13	4.2E-09	4.1E-09	9.7E-11
S014-16-T1-2	117000	04/12/2016 08:30:	04/19/2016 08:40:0	365.20	281.52	199.18	1792.6	1.99E-04	1.05E+04	1.41E+03	6.81E+04	4.0E-13	4.0E-09		
S014-16-T1-4	132500	04/12/2016 08:30:	04/19/2016 08:40:0	360.86	278.18	195.83	1762.5	1.95E-04	1.19E+04	1.43E+03	6.81E+04	5.0E-13	5.0E-09	4.8E-09	2.9E-10
S014-16-T1-7	126500	04/12/2016 08:30:	04/19/2016 08:40:0	361.60	278.75	194.35	1749.2	1.92E-04	1.14E+04	1.45E+03	6.81E+04	4.5E-13	4.5E-09		

T2

Name	NO3 (µg/L	Interval Begin	Sampling Date	Monlith mass (g)	Monlith Dry Mass (g)	Surface Area (cm^2)	Solution Volume (mL)	Monolith Volume (m^3)	M_{ti} (mg/m^2)	ρ (kg/m^3)	Co (mgNO3/kg mono)	D_e (m^2/s)	D_e (cm^2/s)	Average D_e (cm^2/s)	Standard Deviation of Average De
S014-16-T2-3	144000	04/12/2016 08:30:	04/19/2016 08:40:0	364.71	283.41	195.83	1749.7	1.92E-04	1.29E+04	1.48E+03	6.74E+04	5.6E-13	5.6E-09	5.8E-09	2.3E-10
S014-16-T2-6	146000	04/12/2016 08:30:	04/19/2016 08:40:0	367.70	285.74	197.83	1780.5	1.97E-04	1.31E+04	1.45E+03	6.74E+04	6.1E-13	6.1E-09		
S014-16-T2-7	155500	04/12/2016 08:30:	04/19/2016 08:40:0	366.00	284.41	196.77	1770.9	1.95E-04	1.40E+04	1.46E+03	6.74E+04	6.8E-13	6.8E-09	6.9E-09	3.1E-11
S014-16-T2-8	153500	04/12/2016 08:30:	04/19/2016 08:40:0	363.14	282.19	197.90	1781.1	1.97E-04	1.38E+04	1.43E+03	6.74E+04	6.9E-13	6.9E-09		

T3

Name	NO3 (µg/L	Interval Begin	Sampling Date	Monlith mass (g)	Monlith Dry Mass (g)	Surface Area (cm^2)	Solution Volume (mL)	Monolith Volume (m^3)	M_{ti} (mg/m^2)	ρ (kg/m^3)	Co (mgNO3/kg mono)	D_e (m^2/s)	D_e (cm^2/s)	Average D_e (cm^2/s)	Standard Deviation of Average De
S014-16-T3-1	131000	04/12/2016 08:30:	04/19/2016 08:40:0	366.62	285.46	195.87	1762.9	1.94E-04	1.18E+04	1.47E+03	6.75E+04	4.7E-13	4.7E-09	4.2E-09	5.2E-10
S014-16-T3-3	115000	04/12/2016 08:30:	04/19/2016 08:40:0	364.46	283.78	195.53	1759.7	1.94E-04	1.04E+04	1.46E+03	6.75E+04	3.7E-13	3.7E-09		
S014-16-T3-4	120500	04/12/2016 08:30:	04/19/2016 08:40:0	362.76	282.46	194.51	1750.6	1.93E-04	1.08E+04	1.47E+03	6.75E+04	4.0E-13	4.0E-09	4.1E-09	8.2E-11
S014-16-T3-8	122500	04/12/2016 08:30:	04/19/2016 08:40:0	360.88	280.99	194.17	1747.5	1.92E-04	1.10E+04	1.46E+03	6.75E+04	4.2E-13	4.2E-09		

T4

Name	NO3 (µg/L	Interval Begin	Sampling Date	Monlith mass (g)	Monlith Dry Mass (g)	Surface Area (cm^2)	Solution Volume (mL)	Monolith Volume (m^3)	M_{ti} (mg/m^2)	ρ (kg/m^3)	Co (mgNO3/kg mono)	D_e (m^2/s)	D_e (cm^2/s)	Average D_e (cm^2/s)	Standard Deviation of Average De
S014-16-T4-1	122000	04/12/2016 08:30:	04/19/2016 08:40:0	364.02	284.12	195.68	1761.2	1.94E-04	1.10E+04	1.46E+03	6.88E+04	4.0E-13	4.0E-09	3.9E-09	6.1E-11
S014-16-T4-2	119000	04/12/2016 08:30:	04/19/2016 08:40:0	369.27	288.22	199.22	1793.0	1.99E-04	1.07E+04	1.45E+03	6.88E+04	3.9E-13	3.9E-09		
S014-16-T4-5	123500	04/12/2016 08:30:	04/19/2016 08:40:0	365.37	285.18	195.92	1763.3	1.94E-04	1.11E+04	1.47E+03	6.88E+04	4.1E-13	4.1E-09	4.3E-09	1.9E-10
S014-16-T4-7	127500	04/12/2016 08:30:	04/19/2016 08:40:0	363.93	284.05	196.69	1770.2	1.96E-04	1.15E+04	1.45E+03	6.88E+04	4.5E-13	4.5E-09		

T5

Name	NO3 (µg/L	Interval Begin	Sampling Date	Monlith mass (g)	Monlith Dry Mass (g)	Surface Area (cm^2)	Solution Volume (mL)	Monolith Volume (m^3)	M_{ti} (mg/m^2)	ρ (kg/m^3)	Co (mgNO3/kg mono)	D_e (m^2/s)	D_e (cm^2/s)	Average D_e (cm^2/s)	Standard Deviation of Average De
S014-16-T5-2	117000	04/12/2016 08:30:	04/19/2016 08:40:0	365.93	283.58	197.86	1780.7	1.97E-04	1.05E+04	1.44E+03	6.78E+04	3.9E-13	3.9E-09	4.2E-09	3.3E-10
S014-16-T5-3	129000	04/12/2016 08:30:	04/19/2016 08:40:0	364.75	282.66	195.03	1755.3	1.92E-04	1.16E+04	1.47E+03	6.78E+04	4.6E-13	4.6E-09		
S014-16-T5-4	126500	04/12/2016 08:30:	04/19/2016 08:40:0	366.62	284.11	196.79	1771.1	1.95E-04	1.14E+04	1.46E+03	6.78E+04	4.5E-13	4.5E-09	4.5E-09	5.7E-11
S014-16-T5-7	126500	04/12/2016 08:30:	04/19/2016 08:40:0	365.76	283.44	197.96	1781.6	1.97E-04	1.14E+04	1.44E+03	6.78E+04	4.6E-13	4.6E-09		

T6

Name	NO3 (µg/L	Interval Begin	Sampling Date	Monlith mass (g)	Monlith Dry Mass (g)	Surface Area (cm^2)	Solution Volume (mL)	Monolith Volume (m^3)	M_{ti} (mg/m^2)	ρ (kg/m^3)	Co (mgNO3/kg mono)	D_e (m^2/s)	D_e (cm^2/s)	Average D_e (cm^2/s)	Standard Deviation of Average De
S014-16-T6-2	124000	04/12/2016 08:30:	04/19/2016 08:40:0	363.78	284.09	196.70	1770.3	1.95E-04	1.12E+04	1.45E+03	6.74E+04	4.4E-13	4.4E-09	4.1E-09	2.7E-10
S014-16-T6-3	116000	04/12/2016 08:30:	04/19/2016 08:40:0	364.78	284.87	197.29	1775.6	1.96E-04	1.04E+04	1.45E+03	6.74E+04	3.8E-13	3.8E-09		
S014-16-T6-5	122500	04/12/2016 08:30:	04/19/2016 08:40:0	362.95	283.44	196.39	1767.5	1.95E-04	1.10E+04	1.45E+03	6.74E+04	4.3E-13	4.3E-09	4.2E-09	6.6E-11
S014-16-T6-6	122500	04/12/2016 08:30:	04/19/2016 08:40:0	360.98	281.90	193.67	1743.0	1.91E-04	1.10E+04	1.48E+03	6.74E+04	4.1E-13	4.1E-09		

NO3 Sampling 63 d

Experiment Start 3/1/16 8:30:00

T1

Name	NO3 (µg/L	Interval Begin	Sampling Date	Monlith mass (g)	Monlith Dry Mass (g)	Surface Area (cm^2)	Solution Volume (mL)	Monolith Volume (m^3)	M_{ti} (mg/m^2)	ρ (kg/m^3)	Co (mgNO3/kg mono)	D_e (m^2/s)	D_e (cm^2/s)	Average D_e (cm^2/s)	Standard Deviation of Average De
S014-16-T1-1	249000	04/19/2016 08:40:0	05/3/2016 09:00:	359.63	277.23	192.53	1732.8	1.89E-04	2.24E+04	1.46E+03	6.81E+04	5.2E-13	5.2E-09	4.9E-09	2.8E-10
S014-16-T1-2	227000	04/19/2016 08:40:0	05/3/2016 09:00:	365.20	281.52	199.18	1792.6	1.99E-04	2.04E+04	1.41E+03	6.81E+04	4.6E-13	4.6E-09		
S014-16-T1-4	210500	04/19/2016 08:40:0	05/3/2016 09:00:	360.86	278.18	195.83	1762.5	1.95E-04	1.89E+04	1.43E+03	6.81E+04	3.9E-13	3.9E-09	3.7E-09	2.0E-10
S014-16-T1-7	202500	04/19/2016 08:40:0	05/3/2016 09:00:	361.60	278.75	194.35	1749.2	1.92E-04	1.82E+04	1.45E+03	6.81E+04	3.5E-13	3.5E-09		

T2

Name	NO3 (µg/L	Interval Begin	Sampling Date	Monlith mass (g)	Monlith Dry Mass (g)	Surface Area (cm^2)	Solution Volume (mL)	Monolith Volume (m^3)	M_{ti} (mg/m^2)	ρ (kg/m^3)	Co (mgNO3/kg mono)	D_e (m^2/s)	D_e (cm^2/s)	Average D_e (cm^2/s)	Standard Deviation of Average De
S014-16-T2-3	259000	04/19/2016 08:40:0	05/3/2016 09:00:	364.71	283.41	195.83	1749.7	1.92E-04	2.31E+04	1.48E+03	6.74E+04	5.6E-13	5.6E-09	5.4E-09	1.8E-10
S014-16-T2-6	244000	04/19/2016 08:40:0	05/3/2016 09:00:	367.70	285.74	197.83	1780.5	1.97E-04	2.20E+04	1.45E+03	6.74E+04	5.2E-13	5.2E-09		
S014-16-T2-7	247500	04/19/2016 08:40:0	05/3/2016 09:00:	366.00	284.41	196.77	1770.9	1.95E-04	2.23E+04	1.46E+03	6.74E+04	5.3E-13	5.3E-09	5.0E-09	3.5E-10
S014-16-T2-8	226500	04/19/2016 08:40:0	05/3/2016 09:00:	363.14	282.19	197.90	1781.1	1.97E-04	2.04E+04	1.43E+03	6.74E+04	4.6E-13	4.6E-09		

T3

Name	NO3 (µg/L	Interval Begin	Sampling Date	Monlith mass (g)	Monlith Dry Mass (g)	Surface Area (cm^2)	Solution Volume (mL)	Monolith Volume (m^3)	M_{ti} (mg/m^2)	ρ (kg/m^3)	Co (mgNO3/kg mono)	D_e (m^2/s)	D_e (cm^2/s)	Average D_e (cm^2/s)	Standard Deviation of Average De
S014-16-T3-1	243000	04/19/2016 08:40:0	05/3/2016 09:00:	366.62	285.46	195.87	1762.9	1.94E-04	2.19E+04	1.47E+03	6.75E+04	5.0E-13	5.0E-09	4.7E-09	2.9E-10
S014-16-T3-3	227000	04/19/2016 08:40:0	05/3/2016 09:00:	364.46	283.78	195.53	1759.7	1.94E-04	2.04E+04	1.46E+03	6.75E+04	4.4E-13	4.4E-09		
S014-16-T3-4	202500	04/19/2016 08:40:0	05/3/2016 09:00:	362.76	282.46	194.51	1750.6	1.93E-04	1.82E+04	1.47E+03	6.75E+04	3.5E-13	3.5E-09	3.4E-09	7.4E-11
S014-16-T3-8	197500	04/19/2016 08:40:0	05/3/2016 09:00:	360.88	280.99	194.17	1747.5	1.92E-04	1.78E+04	1.46E+03	6.75E+04	3.4E-13	3.4E-09		

T4

Name	NO3 (µg/L	Interval Begin	Sampling Date	Monlith mass (g)	Monlith Dry Mass (g)	Surface Area (cm^2)	Solution Volume (mL)	Monolith Volume (m^3)	M_{ti} (mg/m^2)	ρ (kg/m^3)	Co (mgNO3/kg mono)	D_e (m^2/s)	D_e (cm^2/s)	Average D_e (cm^2/s)	Standard Deviation of Average De
S014-16-T4-1	239000	04/19/2016 08:40:0	05/3/2016 09:00:	364.02	284.12	195.68	1761.2	1.94E-04	2.15E+04	1.46E+03	6.88E+04	4.7E-13	4.7E-09	4.3E-09	4.3E-10
S014-16-T4-2	214000	04/19/2016 08:40:0	05/3/2016 09:00:	369.27	288.22	199.22	1793.0	1.99E-04	1.93E+04	1.45E+03	6.88E+04	3.9E-13	3.9E-09		
S014-16-T4-5	204500	04/19/2016 08:40:0	05/3/2016 09:00:	365.37	285.18	195.92	1763.3	1.94E-04	1.84E+04	1.47E+03	6.88E+04	3.4E-13	3.4E-09	3.4E-09	7.6E-11
S014-16-T4-7	197500	04/19/2016 08:40:0	05/3/2016 09:00:	363.93	284.05	196.69	1770.2	1.96E-04	1.78E+04	1.45E+03	6.88E+04	3.3E-13	3.3E-09		

T5

Name	NO3 (µg/L	Interval Begin	Sampling Date	Monlith mass (g)	Monlith Dry Mass (g)	Surface Area (cm^2)	Solution Volume (mL)	Monolith Volume (m^3)	M_{ti} (mg/m^2)	ρ (kg/m^3)	Co (mgNO3/kg mono)	D_e (m^2/s)	D_e (cm^2/s)	Average D_e (cm^2/s)	Standard Deviation of Average De
S014-16-T5-2	234000	04/19/2016 08:40:0	05/3/2016 09:00:	365.93	283.58	197.86	1780.7	1.97E-04	2.11E+04	1.44E+03	6.78E+04	4.8E-13	4.8E-09	4.4E-09	3.6E-10
S014-16-T5-3	220000	04/19/2016 08:40:0	05/3/2016 09:00:	364.75	282.66	195.03	1755.3	1.92E-04	1.98E+04	1.47E+03	6.78E+04	4.1E-13	4.1E-09		
S014-16-T5-4	203500	04/19/2016 08:40:0	05/3/2016 09:00:	366.62	284.11	196.79	1771.1	1.95E-04	1.83E+04	1.46E+03	6.78E+04	3.6E-13	3.6E-09	3.4E-09	1.3E-10
S014-16-T5-7	193500	04/19/2016 08:40:0	05/3/2016 09:00:	365.76	283.44	197.96	1781.6	1.97E-04	1.74E+04	1.44E+03	6.78E+04	3.3E-13	3.3E-09		

T6

Name	NO3 (µg/L	Interval Begin	Sampling Date	Monlith mass (g)	Monlith Dry Mass (g)	Surface Area (cm^2)	Solution Volume (mL)	Monolith Volume (m^3)	M_{ti} (mg/m^2)	ρ (kg/m^3)	Co (mgNO3/kg mono)	D_e (m^2/s)	D_e (cm^2/s)	Average D_e (cm^2/s)	Standard Deviation of Average De
S014-16-T6-2	235000	04/19/2016 08:40:0	05/3/2016 09:00:	363.78	284.09	196.70	1770.3	1.95E-04	2.12E+04	1.45E+03	6.74E+04	4.8E-13	4.8E-09	4.4E-09	4.4E-10
S014-16-T6-3	212000	04/19/2016 08:40:0	05/3/2016 09:00:	364.78	284.87	197.29	1775.6	1.96E-04	1.91E+04	1.45E+03	6.74E+04	3.9E-13	3.9E-09		
S014-16-T6-5	206500	04/19/2016 08:40:0	05/3/2016 09:00:	362.95	283.44	196.39	1767.5	1.95E-04	1.86E+04	1.45E+03	6.74E+04	3.7E-13	3.7E-09	3.4E-09	2.9E-10
S014-16-T6-6	192500	04/19/2016 08:40:0	05/3/2016 09:00:	360.98	281.90	193.67	1743.0	1.91E-04	1.73E+04	1.48E+03	6.74E+04	3.1E-13	3.1E-09		

NO3 Co Calculation

LIMS Data

LIMS data on NO3 concentration measurement from the spiked 6.5 M Na simulants

These values show the initial NO3 content of the simulant prior to any getter addition

Test	LabNumber	SampleName	Result	Units	EQL
T1	1601042-01	T1 Initial	145000000	ug/L	5000
T2	1601042-03	T2 Initial	145000000	ug/L	5000
T3	1601042-05	T3 Initial	145000000	ug/L	5000
T4	1601042-08	T4 Initial	148000000	ug/L	5000
T5	1601042-11	T5 Initial	145000000	ug/L	5000
T6	1601042-13	T6 Initial	145000000	ug/L	5000

3

Simulant Volume

Density of the 6.5 M Na Average simulant [g/mL] 1.31

Test	Simulant Bottle Tare (g)	Bottle + Simulant (g)	Simulant Mass	Simulant Volume- (mL)	Simulant Volume after sampling (mL)	Dry Blend (g)	Total Weight of Slurry [g]
T1	100.1	1407.8	1307.7	998.244275	994.2443	1750.0	2744.24427
T2	100.3	1408.1	1307.8	998.320611	994.3206	1757.3	2751.57061
T3	100.1	1407.9	1307.8	998.320611	994.3206	1750.0	2744.32061
T4	100	1408	1308	998.473282	994.4733	1745.0	2739.42328
T5	99.8	1408	1308.2	998.625954	994.626	1750.0	2744.62595
T6	99.9	1410.2	1310.3	1000.22901	996.229	1747.6	2743.77901

Co

Calculation on NO3 C_0 in dry Cast Stone (mg/kg) monolith

	T1	T2	T3	T4	T5	T6
Dry solid fraction in Cast Stone Monolith	0.771	0.78	0.78	0.78	0.77	0.78

Test	NO3 (ug/g wet Cast Stone)-analytical	C_0 (mg/kg) in dry Cast Stone - analytical
T1	52533.742	**68148.785**
T2	52397.888	**67428.444**
T3	52536.314	**67472.789**
T4	53727.384	**68836.212**
T5	52546.600	**67806.827**
T6	52647.537	**67416.440**

NO2 Sampling 2h

Experiment Start 3/1/16 8:30:00

T1

Name	NO2 (μg/L	Interval Begin	Sampling Date	Monlith mass (g)	Monlith Dry Mass (g)	Surface Area (cm^2)	Solution Volume (mL)	Monolith Volume (m^3)	M_{ti} (mg/m^2)	ρ (kg/m^3)	Co (mgNO2/kg mono)	D_e (m^2/s)	D_e (cm^2/s)	Average D_e (cm^2/s)	Standard Deviation of Average De
S014-16-T1-1	15800	3/1/2016 8:30:	3/1/2016 10:30:0	359.63	277.23	192.53	1732.8	1.89E-04	1.42E+03	1.46E+03	1.80E+04	3.2E-13	3.2E-09	3.1E-09	7.5E-11
S014-16-T1-2	14900	3/1/2016 8:30:	3/1/2016 10:30:0	365.20	281.52	199.18	1792.6	1.99E-04	1.34E+03	1.41E+03	1.80E+04	3.0E-13	3.0E-09		
S014-16-T1-4	22100	3/1/2016 8:30:	3/1/2016 10:30:0	360.86	278.18	195.83	1762.5	1.95E-04	1.99E+03	1.43E+03	1.80E+04	6.6E-13	6.6E-09	6.0E-09	5.7E-10
S014-16-T1-7	20400	3/1/2016 8:30:	3/1/2016 10:30:0	361.60	278.75	194.35	1749.2	1.92E-04	1.84E+03	1.45E+03	1.80E+04	5.4E-13	5.4E-09		

T2

Name	NO2 (μg/L	Interval Begin	Sampling Date	Monlith mass (g)	Monlith Dry Mass (g)	Surface Area (cm^2)	Solution Volume (mL)	Monolith Volume (m^3)	M_{ti} (mg/m^2)	ρ (kg/m^3)	Co (mgNO2/kg mono)	D_e (m^2/s)	D_e (cm^2/s)	Average D_e (cm^2/s)	Standard Deviation of Average De
S014-16-T2-3	18400	3/1/2016 8:30:	3/1/2016 10:30:0	364.71	283.41	195.83	1749.7	1.92E-04	1.64E+03	1.48E+03	1.78E+04	4.2E-13	4.2E-09	4.6E-09	3.1E-10
S014-16-T2-6	19200	3/1/2016 8:30:	3/1/2016 10:30:0	367.70	285.74	197.83	1780.5	1.97E-04	1.73E+03	1.45E+03	1.78E+04	4.9E-13	4.9E-09		
S014-16-T2-7	27200	3/1/2016 8:30:	3/1/2016 10:30:0	366.00	284.41	196.77	1770.9	1.95E-04	2.45E+03	1.46E+03	1.78E+04	9.7E-13	9.7E-09	8.6E-09	1.2E-09
S014-16-T2-8	23300	3/1/2016 8:30:	3/1/2016 10:30:0	363.14	282.19	197.90	1781.1	1.97E-04	2.10E+03	1.43E+03	1.78E+04	7.4E-13	7.4E-09		

T3

Name	NO2 (μg/L	Interval Begin	Sampling Date	Monlith mass (g)	Monlith Dry Mass (g)	Surface Area (cm^2)	Solution Volume (mL)	Monolith Volume (m^3)	M_{ti} (mg/m^2)	ρ (kg/m^3)	Co (mgNO2/kg mono)	D_e (m^2/s)	D_e (cm^2/s)	Average D_e (cm^2/s)	Standard Deviation of Average De
S014-16-T3-1	18400	3/1/2016 8:30:	3/1/2016 10:30:0	366.62	285.46	195.87	1762.9	1.94E-04	1.66E+03	1.47E+03	1.78E+04	4.4E-13	4.4E-09	2.2E-09	2.1E-09
S014-16-T3-3	2500	3/1/2016 8:30:	3/1/2016 10:30:0	364.46	283.78	195.53	1759.7	1.94E-04	2.25E+02	1.46E+03	1.78E+04	8.2E-15	8.2E-11		
S014-16-T3-4	26800	3/1/2016 8:30:	3/1/2016 10:30:0	362.76	282.46	194.51	1750.6	1.93E-04	2.41E+03	1.47E+03	1.78E+04	9.3E-13	9.3E-09	1.2E-08	2.5E-09
S014-16-T3-8	33000	3/1/2016 8:30:	3/1/2016 10:30:0	360.88	280.99	194.17	1747.5	1.92E-04	2.97E+03	1.46E+03	1.78E+04	1.4E-12	1.4E-08		

T4

Name	NO2 (μg/L	Interval Begin	Sampling Date	Monlith mass (g)	Monlith Dry Mass (g)	Surface Area (cm^2)	Solution Volume (mL)	Monolith Volume (m^3)	M_{ti} (mg/m^2)	ρ (kg/m^3)	Co (mgNO2/kg mono)	D_e (m^2/s)	D_e (cm^2/s)	Average D_e (cm^2/s)	Standard Deviation of Average De
S014-16-T4-1	24100	3/1/2016 8:30:	3/1/2016 10:30:0	364.02	284.12	195.68	1761.2	1.94E-04	2.17E+03	1.46E+03	1.83E+04	7.2E-13	7.2E-09	5.8E-09	1.3E-09
S014-16-T4-2	18900	3/1/2016 8:30:	3/1/2016 10:30:0	369.27	288.22	199.22	1793.0	1.99E-04	1.70E+03	1.45E+03	1.83E+04	4.5E-13	4.5E-09		
S014-16-T4-5	16600	3/1/2016 8:30:	3/1/2016 10:30:0	365.37	285.18	195.92	1763.3	1.94E-04	1.49E+03	1.47E+03	1.83E+04	3.4E-13	3.4E-09	5.8E-09	2.4E-09
S014-16-T4-7	25600	3/1/2016 8:30:	3/1/2016 10:30:0	363.93	284.05	196.69	1770.2	1.96E-04	2.30E+03	1.45E+03	1.83E+04	8.3E-13	8.3E-09		

T5

Name	NO2 (μg/L	Interval Begin	Sampling Date	Monlith mass (g)	Monlith Dry Mass (g)	Surface Area (cm^2)	Solution Volume (mL)	Monolith Volume (m^3)	M_{ti} (mg/m^2)	ρ (kg/m^3)	Co (mgNO2/kg mono)	D_e (m^2/s)	D_e (cm^2/s)	Average D_e (cm^2/s)	Standard Deviation of Average De
S014-16-T5-2	16600	3/1/2016 8:30:	3/1/2016 10:30:0	365.93	283.58	197.86	1780.7	1.97E-04	1.49E+03	1.44E+03	1.80E+04	3.6E-13	3.6E-09	3.3E-09	3.4E-10
S014-16-T5-3	15300	3/1/2016 8:30:	3/1/2016 10:30:0	364.75	282.66	195.03	1755.3	1.92E-04	1.38E+03	1.47E+03	1.80E+04	3.0E-13	3.0E-09		
S014-16-T5-4	27400	3/1/2016 8:30:	3/1/2016 10:30:0	366.62	284.11	196.79	1771.1	1.95E-04	2.47E+03	1.46E+03	1.80E+04	9.7E-13	9.7E-09	9.4E-09	3.4E-10
S014-16-T5-7	26100	3/1/2016 8:30:	3/1/2016 10:30:0	365.76	283.44	197.96	1781.6	1.97E-04	2.35E+03	1.44E+03	1.80E+04	9.0E-13	9.0E-09		

T6

Name	NO2 (μg/L	Interval Begin	Sampling Date	Monlith mass (g)	Monlith Dry Mass (g)	Surface Area (cm^2)	Solution Volume (mL)	Monolith Volume (m^3)	M_{ti} (mg/m^2)	ρ (kg/m^3)	Co (mgNO2/kg mono)	D_e (m^2/s)	D_e (cm^2/s)	Average D_e (cm^2/s)	Standard Deviation of Average De
S014-16-T6-2	18000	3/1/2016 8:30:	3/1/2016 10:30:0	363.78	284.09	196.70	1770.3	1.95E-04	1.62E+03	1.45E+03	1.78E+04	4.3E-13	4.3E-09	4.8E-09	5.1E-10
S014-16-T6-3	20000	3/1/2016 8:30:	3/1/2016 10:30:0	364.78	284.87	197.29	1775.6	1.96E-04	1.80E+03	1.45E+03	1.78E+04	5.3E-13	5.3E-09		
S014-16-T6-5	24800	3/1/2016 8:30:	3/1/2016 10:30:0	362.95	283.44	196.39	1767.5	1.95E-04	2.23E+03	1.45E+03	1.78E+04	8.1E-13	8.1E-09	6.1E-09	2.0E-09
S014-16-T6-6	17800	3/1/2016 8:30:	3/1/2016 10:30:0	360.98	281.90	193.67	1743.0	1.91E-04	1.60E+03	1.48E+03	1.78E+04	4.1E-13	4.1E-09		

NO2 Sampling 1d

		Experiment Start	3/1/16 8:30:00												

T1

Name	NO2 (µg/L	Interval Begin	Sampling Date	Monlith mass (g)	Monlith Dry Mass (g)	Surface Area (cm^2)	Solution Volume (mL)	Monolith Volume (m^3)	M$_{ti}$ (mg/m^2)	ρ (kg/m^3)	Co (mgNO2/kg mono)	D$_e$ (m^2/s)	D$_e$ (cm^2/s)	Average D$_e$ (cm^2/s)	Standard Deviation of Average De
S014-16-T1-1	73900	3/1/2016 10:30:0	3/2/2016 8:30:00	359.63	277.23	192.53	1732.8	1.89E-04	6.65E+03	1.46E+03	1.80E+04	1.1E-12	1.1E-08	1.1E-08	4.1E-10
S014-16-T1-2	68800	3/1/2016 10:30:0	3/2/2016 8:30:00	365.20	281.52	199.18	1792.6	1.99E-04	6.19E+03	1.41E+03	1.80E+04	1.1E-12	1.1E-08		
S014-16-T1-4	73500	3/1/2016 10:30:0	3/2/2016 8:30:00	360.86	278.18	195.83	1762.5	1.95E-04	6.62E+03	1.43E+03	1.80E+04	1.2E-12	1.2E-08	1.8E-08	6.3E-09
S014-16-T1-7	107000	3/1/2016 10:30:0	3/2/2016 8:30:00	361.60	278.75	194.35	1749.2	1.92E-04	9.63E+03	1.45E+03	1.80E+04	2.5E-12	2.5E-08		

T2

Name	NO2 (µg/L	Interval Begin	Sampling Date	Monlith mass (g)	Monlith Dry Mass (g)	Surface Area (cm^2)	Solution Volume (mL)	Monolith Volume (m^3)	M$_{ti}$ (mg/m^2)	ρ (kg/m^3)	Co (mgNO2/kg mono)	D$_e$ (m^2/s)	D$_e$ (cm^2/s)	Average D$_e$ (cm^2/s)	Standard Deviation of Average De
S014-16-T2-3	107000	3/1/2016 10:30:0	3/2/2016 8:30:00	364.71	283.41	195.83	1749.7	1.92E-04	9.56E+03	1.48E+03	1.78E+04	2.4E-12	2.4E-08	2.6E-08	2.3E-09
S014-16-T2-6	114000	3/1/2016 10:30:0	3/2/2016 8:30:00	367.70	285.74	197.83	1780.5	1.97E-04	1.03E+04	1.45E+03	1.78E+04	2.8E-12	2.8E-08		
S014-16-T2-7	88100	3/1/2016 10:30:0	3/2/2016 8:30:00	366.00	284.41	196.77	1770.9	1.95E-04	7.93E+03	1.46E+03	1.78E+04	1.7E-12	1.7E-08	1.9E-08	1.8E-09
S014-16-T2-8	95200	3/1/2016 10:30:0	3/2/2016 8:30:00	363.14	282.19	197.90	1781.1	1.97E-04	8.57E+03	1.43E+03	1.78E+04	2.0E-12	2.0E-08		

T3

Name	NO2 (µg/L	Interval Begin	Sampling Date	Monlith mass (g)	Monlith Dry Mass (g)	Surface Area (cm^2)	Solution Volume (mL)	Monolith Volume (m^3)	M$_{ti}$ (mg/m^2)	ρ (kg/m^3)	Co (mgNO2/kg mono)	D$_e$ (m^2/s)	D$_e$ (cm^2/s)	Average D$_e$ (cm^2/s)	Standard Deviation of Average De
S014-16-T3-1	65600	3/1/2016 10:30:0	3/2/2016 8:30:00	366.62	285.46	195.87	1762.9	1.94E-04	5.90E+03	1.47E+03	1.78E+04	9.1E-13	9.1E-09	1.0E-08	1.3E-09
S014-16-T3-3	74000	3/1/2016 10:30:0	3/2/2016 8:30:00	364.46	283.78	195.53	1759.7	1.94E-04	6.66E+03	1.46E+03	1.78E+04	1.2E-12	1.2E-08		
S014-16-T3-4	49700	3/1/2016 10:30:0	3/2/2016 8:30:00	362.76	282.46	194.51	1750.6	1.93E-04	4.47E+03	1.47E+03	1.78E+04	5.3E-13	5.3E-09	1.1E-08	5.3E-09
S014-16-T3-8	86000	3/1/2016 10:30:0	3/2/2016 8:30:00	360.88	280.99	194.17	1747.5	1.92E-04	7.74E+03	1.46E+03	1.78E+04	1.6E-12	1.6E-08		

T4

Name	NO2 (µg/L	Interval Begin	Sampling Date	Monlith mass (g)	Monlith Dry Mass (g)	Surface Area (cm^2)	Solution Volume (mL)	Monolith Volume (m^3)	M$_{ti}$ (mg/m^2)	ρ (kg/m^3)	Co (mgNO2/kg mono)	D$_e$ (m^2/s)	D$_e$ (cm^2/s)	Average D$_e$ (cm^2/s)	Standard Deviation of Average De
S014-16-T4-1	71600	3/1/2016 10:30:0	3/2/2016 8:30:00	364.02	284.12	195.68	1761.2	1.94E-04	6.44E+03	1.46E+03	1.83E+04	1.0E-12	1.0E-08	1.2E-08	1.2E-09
S014-16-T4-2	78600	3/1/2016 10:30:0	3/2/2016 8:30:00	369.27	288.22	199.22	1793.0	1.99E-04	7.07E+03	1.45E+03	1.83E+04	1.3E-12	1.3E-08		
S014-16-T4-5	71100	3/1/2016 10:30:0	3/2/2016 8:30:00	365.37	285.18	195.92	1763.3	1.94E-04	6.40E+03	1.47E+03	1.83E+04	1.0E-12	1.0E-08	9.8E-09	4.8E-10
S014-16-T4-7	66900	3/1/2016 10:30:0	3/2/2016 8:30:00	363.93	284.05	196.69	1770.2	1.96E-04	6.02E+03	1.45E+03	1.83E+04	9.3E-13	9.3E-09		

T5

Name	NO2 (µg/L	Interval Begin	Sampling Date	Monlith mass (g)	Monlith Dry Mass (g)	Surface Area (cm^2)	Solution Volume (mL)	Monolith Volume (m^3)	M$_{ti}$ (mg/m^2)	ρ (kg/m^3)	Co (mgNO2/kg mono)	D$_e$ (m^2/s)	D$_e$ (cm^2/s)	Average D$_e$ (cm^2/s)	Standard Deviation of Average De
S014-16-T5-2	58000	3/1/2016 10:30:0	3/2/2016 8:30:00	365.93	283.58	197.86	1780.7	1.97E-04	5.22E+03	1.44E+03	1.80E+04	7.3E-13	7.3E-09	8.9E-09	1.6E-09
S014-16-T5-3	70700	3/1/2016 10:30:0	3/2/2016 8:30:00	364.75	282.66	195.03	1755.3	1.92E-04	6.36E+03	1.47E+03	1.80E+04	1.0E-12	1.0E-08		
S014-16-T5-4	87200	3/1/2016 10:30:0	3/2/2016 8:30:00	366.62	284.11	196.79	1771.1	1.95E-04	7.85E+03	1.46E+03	1.80E+04	1.6E-12	1.6E-08	1.6E-08	5.0E-10
S014-16-T5-7	83400	3/1/2016 10:30:0	3/2/2016 8:30:00	365.76	283.44	197.96	1781.6	1.97E-04	7.51E+03	1.44E+03	1.80E+04	1.5E-12	1.5E-08		

T6

Name	NO2 (µg/L	Interval Begin	Sampling Date	Monlith mass (g)	Monlith Dry Mass (g)	Surface Area (cm^2)	Solution Volume (mL)	Monolith Volume (m^3)	M$_{ti}$ (mg/m^2)	ρ (kg/m^3)	Co (mgNO2/kg mono)	D$_e$ (m^2/s)	D$_e$ (cm^2/s)	Average D$_e$ (cm^2/s)	Standard Deviation of Average De
S014-16-T6-2	83000	3/1/2016 10:30:0	3/2/2016 8:30:00	363.78	284.09	196.70	1770.3	1.95E-04	7.47E+03	1.45E+03	1.78E+04	1.5E-12	1.5E-08	1.5E-08	4.8E-10
S014-16-T6-3	80200	3/1/2016 10:30:0	3/2/2016 8:30:00	364.78	284.87	197.29	1775.6	1.96E-04	7.22E+03	1.45E+03	1.78E+04	1.4E-12	1.4E-08		
S014-16-T6-5	81100	3/1/2016 10:30:0	3/2/2016 8:30:00	362.95	283.44	196.39	1767.5	1.95E-04	7.30E+03	1.45E+03	1.78E+04	1.4E-12	1.4E-08	1.3E-08	1.6E-09
S014-16-T6-6	72800	3/1/2016 10:30:0	3/2/2016 8:30:00	360.98	281.90	193.67	1743.0	1.91E-04	6.55E+03	1.48E+03	1.78E+04	1.1E-12	1.1E-08		

NO2 Sampling 2d

Experiment Start 3/1/16 8:30:00

T1

Name	NO2 (µg/L	Interval Begin	Sampling Date	Monlith mass (g)	Monlith Dry Mass (g)	Surface Area (cm^2)	Solution Volume (mL)	Monolith Volume (m^3)	M_{ti} (mg/m^2)	ρ (kg/m^3)	Co (mgNO2/kg mono)	D_e (m^2/s)	D_e (cm^2/s)	Average D_e (cm^2/s)	Standard Deviation of Average De
S014-16-T1-1	41100	3/2/2016 8:30:	3/3/2016 8:40:0	359.63	277.23	192.53	1732.8	1.89E-04	3.70E+03	1.46E+03	1.80E+04	1.0E-12	1.0E-08	1.1E-08	1.6E-10
S014-16-T1-2	40300	3/2/2016 8:30:	3/3/2016 8:40:0	365.20	281.52	199.18	1792.6	1.99E-04	3.63E+03	1.41E+03	1.80E+04	1.1E-12	1.1E-08		
S014-16-T1-4	49900	3/2/2016 8:30:	3/3/2016 8:40:0	360.86	278.18	195.83	1762.5	1.95E-04	4.49E+03	1.43E+03	1.80E+04	1.6E-12	1.6E-08	1.6E-08	4.2E-10
S014-16-T1-7	49300	3/2/2016 8:30:	3/3/2016 8:40:0	361.60	278.75	194.35	1749.2	1.92E-04	4.44E+03	1.45E+03	1.80E+04	1.5E-12	1.5E-08		

T2

Name	NO2 (µg/L	Interval Begin	Sampling Date	Monlith mass (g)	Monlith Dry Mass (g)	Surface Area (cm^2)	Solution Volume (mL)	Monolith Volume (m^3)	M_{ti} (mg/m^2)	ρ (kg/m^3)	Co (mgNO2/kg mono)	D_e (m^2/s)	D_e (cm^2/s)	Average D_e (cm^2/s)	Standard Deviation of Average De
S014-16-T2-3	62200	3/2/2016 8:30:	3/3/2016 8:40:0	364.71	283.41	195.83	1749.7	1.92E-04	5.56E+03	1.48E+03	1.78E+04	2.3E-12	2.3E-08	2.7E-08	3.4E-09
S014-16-T2-6	68900	3/2/2016 8:30:	3/3/2016 8:40:0	367.70	285.74	197.83	1780.5	1.97E-04	6.20E+03	1.45E+03	1.78E+04	3.0E-12	3.0E-08		
S014-16-T2-7	73700	3/2/2016 8:30:	3/3/2016 8:40:0	366.00	284.41	196.77	1770.9	1.95E-04	6.63E+03	1.46E+03	1.78E+04	3.4E-12	3.4E-08	3.3E-08	8.5E-10
S014-16-T2-8	70600	3/2/2016 8:30:	3/3/2016 8:40:0	363.14	282.19	197.90	1781.1	1.97E-04	6.35E+03	1.43E+03	1.78E+04	3.3E-12	3.3E-08		

T3

Name	NO2 (µg/L	Interval Begin	Sampling Date	Monlith mass (g)	Monlith Dry Mass (g)	Surface Area (cm^2)	Solution Volume (mL)	Monolith Volume (m^3)	M_{ti} (mg/m^2)	ρ (kg/m^3)	Co (mgNO2/kg mono)	D_e (m^2/s)	D_e (cm^2/s)	Average D_e (cm^2/s)	Standard Deviation of Average De
S014-16-T3-1	40200	3/2/2016 8:30:	3/3/2016 8:40:0	366.62	285.46	195.87	1762.9	1.94E-04	3.62E+03	1.47E+03	1.78E+04	1.0E-12	1.0E-08	1.3E-08	3.3E-09
S014-16-T3-3	51600	3/2/2016 8:30:	3/3/2016 8:40:0	364.46	283.78	195.53	1759.7	1.94E-04	4.64E+03	1.46E+03	1.78E+04	1.7E-12	1.7E-08		
S014-16-T3-4	49900	3/2/2016 8:30:	3/3/2016 8:40:0	362.76	282.46	194.51	1750.6	1.93E-04	4.49E+03	1.47E+03	1.78E+04	1.6E-12	1.6E-08	1.5E-08	4.4E-10
S014-16-T3-8	48300	3/2/2016 8:30:	3/3/2016 8:40:0	360.88	280.99	194.17	1747.5	1.92E-04	4.35E+03	1.46E+03	1.78E+04	1.5E-12	1.5E-08		

T4

Name	NO2 (µg/L	Interval Begin	Sampling Date	Monlith mass (g)	Monlith Dry Mass (g)	Surface Area (cm^2)	Solution Volume (mL)	Monolith Volume (m^3)	M_{ti} (mg/m^2)	ρ (kg/m^3)	Co (mgNO2/kg mono)	D_e (m^2/s)	D_e (cm^2/s)	Average D_e (cm^2/s)	Standard Deviation of Average De
S014-16-T4-1	49800	3/2/2016 8:30:	3/3/2016 8:40:0	364.02	284.12	195.68	1761.2	1.94E-04	4.48E+03	1.46E+03	1.83E+04	1.5E-12	1.5E-08	1.4E-08	1.0E-09
S014-16-T4-2	45700	3/2/2016 8:30:	3/3/2016 8:40:0	369.27	288.22	199.22	1793.0	1.99E-04	4.11E+03	1.45E+03	1.83E+04	1.3E-12	1.3E-08		
S014-16-T4-5	54000	3/2/2016 8:30:	3/3/2016 8:40:0	365.37	285.18	195.92	1763.3	1.94E-04	4.86E+03	1.47E+03	1.83E+04	1.7E-12	1.7E-08	1.5E-08	2.0E-09
S014-16-T4-7	46800	3/2/2016 8:30:	3/3/2016 8:40:0	363.93	284.05	196.69	1770.2	1.96E-04	4.21E+03	1.45E+03	1.83E+04	1.3E-12	1.3E-08		

T5

Name	NO2 (µg/L	Interval Begin	Sampling Date	Monlith mass (g)	Monlith Dry Mass (g)	Surface Area (cm^2)	Solution Volume (mL)	Monolith Volume (m^3)	M_{ti} (mg/m^2)	ρ (kg/m^3)	Co (mgNO2/kg mono)	D_e (m^2/s)	D_e (cm^2/s)	Average D_e (cm^2/s)	Standard Deviation of Average De
S014-16-T5-2	38500	3/2/2016 8:30:	3/3/2016 8:40:0	365.93	283.58	197.86	1780.7	1.97E-04	3.47E+03	1.44E+03	1.80E+04	9.4E-13	9.4E-09	1.0E-08	6.2E-10
S014-16-T5-3	41800	3/2/2016 8:30:	3/3/2016 8:40:0	364.75	282.66	195.03	1755.3	1.92E-04	3.76E+03	1.47E+03	1.80E+04	1.1E-12	1.1E-08		
S014-16-T5-4	49000	3/2/2016 8:30:	3/3/2016 8:40:0	366.62	284.11	196.79	1771.1	1.95E-04	4.41E+03	1.46E+03	1.80E+04	1.5E-12	1.5E-08	1.6E-08	6.3E-10
S014-16-T5-7	50400	3/2/2016 8:30:	3/3/2016 8:40:0	365.76	283.44	197.96	1781.6	1.97E-04	4.54E+03	1.44E+03	1.80E+04	1.6E-12	1.6E-08		

T6

Name	NO2 (µg/L	Interval Begin	Sampling Date	Monlith mass (g)	Monlith Dry Mass (g)	Surface Area (cm^2)	Solution Volume (mL)	Monolith Volume (m^3)	M_{ti} (mg/m^2)	ρ (kg/m^3)	Co (mgNO2/kg mono)	D_e (m^2/s)	D_e (cm^2/s)	Average D_e (cm^2/s)	Standard Deviation of Average De
S014-16-T6-2	43100	3/2/2016 8:30:	3/3/2016 8:40:0	363.78	284.09	196.70	1770.3	1.95E-04	3.88E+03	1.45E+03	1.78E+04	1.2E-12	1.2E-08	1.1E-08	4.7E-10
S014-16-T6-3	41300	3/2/2016 8:30:	3/3/2016 8:40:0	364.78	284.87	197.29	1775.6	1.96E-04	3.72E+03	1.45E+03	1.78E+04	1.1E-12	1.1E-08		
S014-16-T6-5	50600	3/2/2016 8:30:	3/3/2016 8:40:0	362.95	283.44	196.39	1767.5	1.95E-04	4.55E+03	1.45E+03	1.78E+04	1.6E-12	1.6E-08	1.5E-08	1.0E-09
S014-16-T6-6	48000	3/2/2016 8:30:	3/3/2016 8:40:0	360.98	281.90	193.67	1743.0	1.91E-04	4.32E+03	1.48E+03	1.78E+04	1.4E-12	1.4E-08		

NO2 Sampling 7d

		Experiment Start	3/1/16 8:30:00

T1

Name	NO2 (µg/L	Interval Begin	Sampling Date	Monlith mass (g)	Monlith Dry Mass (g)	Surface Area (cm^2)	Solution Volume (mL)	Monolith Volume (m^3)	M_{ti} (mg/m^2)	ρ (kg/m^3)	Co (mgNO2/kg mono)	D_e (m^2/s)	D_e (cm^2/s)	Average D_e (cm^2/s)	Standard Deviation of Average De
S014-16-T1-1	141000	3/3/2016 8:40:0	3/8/2016 8:40:00	359.63	277.23	192.53	1732.8	1.89E-04	1.27E+04	1.46E+03	1.80E+04	1.4E-12	1.4E-08	1.4E-08	5.0E-10
S014-16-T1-2	141000	3/3/2016 8:40:0	3/8/2016 8:40:00	365.20	281.52	199.18	1792.6	1.99E-04	1.27E+04	1.41E+03	1.80E+04	1.5E-12	1.5E-08		
S014-16-T1-4	131000	3/3/2016 8:40:0	3/8/2016 8:40:00	360.86	278.18	195.83	1762.5	1.95E-04	1.18E+04	1.43E+03	1.80E+04	1.3E-12	1.3E-08	1.3E-08	3.9E-10
S014-16-T1-7	137000	3/3/2016 8:40:0	3/8/2016 8:40:00	361.60	278.75	194.35	1749.2	1.92E-04	1.23E+04	1.45E+03	1.80E+04	1.3E-12	1.3E-08		

T2

Name	NO2 (µg/L	Interval Begin	Sampling Date	Monlith mass (g)	Monlith Dry Mass (g)	Surface Area (cm^2)	Solution Volume (mL)	Monolith Volume (m^3)	M_{ti} (mg/m^2)	ρ (kg/m^3)	Co (mgNO2/kg mono)	D_e (m^2/s)	D_e (cm^2/s)	Average D_e (cm^2/s)	Standard Deviation of Average De
S014-16-T2-3	196000	3/3/2016 8:40:0	3/8/2016 8:40:00	364.71	283.41	195.83	1749.7	1.92E-04	1.75E+04	1.48E+03	1.78E+04	2.7E-12	2.7E-08	2.9E-08	2.2E-09
S014-16-T2-6	206000	3/3/2016 8:40:0	3/8/2016 8:40:00	367.70	285.74	197.83	1780.5	1.97E-04	1.85E+04	1.45E+03	1.78E+04	3.1E-12	3.1E-08		
S014-16-T2-7	182000	3/3/2016 8:40:0	3/8/2016 8:40:00	366.00	284.41	196.77	1770.9	1.95E-04	1.64E+04	1.46E+03	1.78E+04	2.4E-12	2.4E-08	2.6E-08	1.8E-09
S014-16-T2-8	192000	3/3/2016 8:40:0	3/8/2016 8:40:00	363.14	282.19	197.90	1781.1	1.97E-04	1.73E+04	1.43E+03	1.78E+04	2.8E-12	2.8E-08		

T3

Name	NO2 (µg/L	Interval Begin	Sampling Date	Monlith mass (g)	Monlith Dry Mass (g)	Surface Area (cm^2)	Solution Volume (mL)	Monolith Volume (m^3)	M_{ti} (mg/m^2)	ρ (kg/m^3)	Co (mgNO2/kg mono)	D_e (m^2/s)	D_e (cm^2/s)	Average D_e (cm^2/s)	Standard Deviation of Average De
S014-16-T3-1	139000	3/3/2016 8:40:0	3/8/2016 8:40:00	366.62	285.46	195.87	1762.9	1.94E-04	1.25E+04	1.47E+03	1.78E+04	1.4E-12	1.4E-08	1.4E-08	3.8E-12
S014-16-T3-3	138000	3/3/2016 8:40:0	3/8/2016 8:40:00	364.46	283.78	195.53	1759.7	1.94E-04	1.24E+04	1.46E+03	1.78E+04	1.4E-12	1.4E-08		
S014-16-T3-4	132000	3/3/2016 8:40:0	3/8/2016 8:40:00	362.76	282.46	194.51	1750.6	1.93E-04	1.19E+04	1.47E+03	1.78E+04	1.2E-12	1.2E-08	1.3E-08	6.3E-10
S014-16-T3-8	138000	3/3/2016 8:40:0	3/8/2016 8:40:00	360.88	280.99	194.17	1747.5	1.92E-04	1.24E+04	1.46E+03	1.78E+04	1.4E-12	1.4E-08		

T4

Name	NO2 (µg/L	Interval Begin	Sampling Date	Monlith mass (g)	Monlith Dry Mass (g)	Surface Area (cm^2)	Solution Volume (mL)	Monolith Volume (m^3)	M_{ti} (mg/m^2)	ρ (kg/m^3)	Co (mgNO2/kg mono)	D_e (m^2/s)	D_e (cm^2/s)	Average D_e (cm^2/s)	Standard Deviation of Average De
S014-16-T4-1	149000	3/3/2016 8:40:0	3/8/2016 8:40:00	364.02	284.12	195.68	1761.2	1.94E-04	1.34E+04	1.46E+03	1.83E+04	1.5E-12	1.5E-08	1.5E-08	3.6E-10
S014-16-T4-2	144000	3/3/2016 8:40:0	3/8/2016 8:40:00	369.27	288.22	199.22	1793.0	1.99E-04	1.30E+04	1.45E+03	1.83E+04	1.4E-12	1.4E-08		
S014-16-T4-5	140000	3/3/2016 8:40:0	3/8/2016 8:40:00	365.37	285.18	195.92	1763.3	1.94E-04	1.26E+04	1.47E+03	1.83E+04	1.3E-12	1.3E-08	1.4E-08	5.6E-10
S014-16-T4-7	144000	3/3/2016 8:40:0	3/8/2016 8:40:00	363.93	284.05	196.69	1770.2	1.96E-04	1.30E+04	1.45E+03	1.83E+04	1.4E-12	1.4E-08		

T5

Name	NO2 (µg/L	Interval Begin	Sampling Date	Monlith mass (g)	Monlith Dry Mass (g)	Surface Area (cm^2)	Solution Volume (mL)	Monolith Volume (m^3)	M_{ti} (mg/m^2)	ρ (kg/m^3)	Co (mgNO2/kg mono)	D_e (m^2/s)	D_e (cm^2/s)	Average D_e (cm^2/s)	Standard Deviation of Average De
S014-16-T5-2	131000	3/3/2016 8:40:0	3/8/2016 8:40:00	365.93	283.58	197.86	1780.7	1.97E-04	1.18E+04	1.44E+03	1.80E+04	1.2E-12	1.2E-08	1.3E-08	4.1E-10
S014-16-T5-3	138000	3/3/2016 8:40:0	3/8/2016 8:40:00	364.75	282.66	195.03	1755.3	1.92E-04	1.24E+04	1.47E+03	1.80E+04	1.3E-12	1.3E-08		
S014-16-T5-4	134000	3/3/2016 8:40:0	3/8/2016 8:40:00	366.62	284.11	196.79	1771.1	1.95E-04	1.21E+04	1.46E+03	1.80E+04	1.3E-12	1.3E-08	1.5E-08	1.8E-09
S014-16-T5-7	150000	3/3/2016 8:40:0	3/8/2016 8:40:00	365.76	283.44	197.96	1781.6	1.97E-04	1.35E+04	1.44E+03	1.80E+04	1.6E-12	1.6E-08		

T6

Name	NO2 (µg/L	Interval Begin	Sampling Date	Monlith mass (g)	Monlith Dry Mass (g)	Surface Area (cm^2)	Solution Volume (mL)	Monolith Volume (m^3)	M_{ti} (mg/m^2)	ρ (kg/m^3)	Co (mgNO2/kg mono)	D_e (m^2/s)	D_e (cm^2/s)	Average D_e (cm^2/s)	Standard Deviation of Average De
S014-16-T6-2	134000	3/3/2016 8:40:0	3/8/2016 8:40:00	363.78	284.09	196.70	1770.3	1.95E-04	1.21E+04	1.45E+03	1.78E+04	1.3E-12	1.3E-08	1.3E-08	2.2E-10
S014-16-T6-3	136000	3/3/2016 8:40:0	3/8/2016 8:40:00	364.78	284.87	197.29	1775.6	1.96E-04	1.22E+04	1.45E+03	1.78E+04	1.4E-12	1.4E-08		
S014-16-T6-5	139000	3/3/2016 8:40:0	3/8/2016 8:40:00	362.95	283.44	196.39	1767.5	1.95E-04	1.25E+04	1.45E+03	1.78E+04	1.4E-12	1.4E-08	1.4E-08	1.8E-10
S014-16-T6-6	143000	3/3/2016 8:40:0	3/8/2016 8:40:00	360.98	281.90	193.67	1743.0	1.91E-04	1.29E+04	1.48E+03	1.78E+04	1.4E-12	1.4E-08		

NO2 Sampling 14 d

		Experiment Start	3/1/16 8:30:00

T1

Name	NO2 (µg/L	Interval Begin	Sampling Date	Monlith mass (g)	Monlith Dry Mass (g)	Surface Area (cm^2)	Solution Volume (mL)	Monolith Volume (m^3)	M_{ti} (mg/m^2)	ρ (kg/m^3)	Co (mgNO2/kg mono)	D_e (m^2/s)	D_e (cm^2/s)	Average D_e (cm^2/s)	Standard Deviation of Average De
S014-16-T1-1	108000	3/8/2016 8:40:0	3/15/2016 8:50:0	359.63	277.23	192.53	1732.8	1.89E-04	9.72E+03	1.46E+03	1.80E+04	1.0E-12	1.0E-08	1.1E-08	1.7E-10
S014-16-T1-2	106000	3/8/2016 8:40:0	3/15/2016 8:50:0	365.20	281.52	199.18	1792.6	1.99E-04	9.54E+03	1.41E+03	1.80E+04	1.1E-12	1.1E-08		
S014-16-T1-4	105000	3/8/2016 8:40:0	3/15/2016 8:50:0	360.86	278.18	195.83	1762.5	1.95E-04	9.45E+03	1.43E+03	1.80E+04	1.0E-12	1.0E-08	1.1E-08	5.4E-10
S014-16-T1-7	112000	3/8/2016 8:40:0	3/15/2016 8:50:0	361.60	278.75	194.35	1749.2	1.92E-04	1.01E+04	1.45E+03	1.80E+04	1.1E-12	1.1E-08		

T2

Name	NO2 (µg/L	Interval Begin	Sampling Date	Monlith mass (g)	Monlith Dry Mass (g)	Surface Area (cm^2)	Solution Volume (mL)	Monolith Volume (m^3)	M_{ti} (mg/m^2)	ρ (kg/m^3)	Co (mgNO2/kg mono)	D_e (m^2/s)	D_e (cm^2/s)	Average D_e (cm^2/s)	Standard Deviation of Average De
S014-16-T2-3	150000	3/8/2016 8:40:0	3/15/2016 8:50:0	364.71	283.41	195.83	1749.7	1.92E-04	1.34E+04	1.48E+03	1.78E+04	2.0E-12	2.0E-08	2.2E-08	2.1E-09
S014-16-T2-6	161000	3/8/2016 8:40:0	3/15/2016 8:50:0	367.70	285.74	197.83	1780.5	1.97E-04	1.45E+04	1.45E+03	1.78E+04	2.4E-12	2.4E-08		
S014-16-T2-7	155000	3/8/2016 8:40:0	3/15/2016 8:50:0	366.00	284.41	196.77	1770.9	1.95E-04	1.40E+04	1.46E+03	1.78E+04	2.2E-12	2.2E-08	2.1E-08	1.0E-09
S014-16-T2-8	145000	3/8/2016 8:40:0	3/15/2016 8:50:0	363.14	282.19	197.90	1781.1	1.97E-04	1.31E+04	1.43E+03	1.78E+04	2.0E-12	2.0E-08		

T3

Name	NO2 (µg/L	Interval Begin	Sampling Date	Monlith mass (g)	Monlith Dry Mass (g)	Surface Area (cm^2)	Solution Volume (mL)	Monolith Volume (m^3)	M_{ti} (mg/m^2)	ρ (kg/m^3)	Co (mgNO2/kg mono)	D_e (m^2/s)	D_e (cm^2/s)	Average D_e (cm^2/s)	Standard Deviation of Average De
S014-16-T3-1	110000	3/8/2016 8:40:0	3/15/2016 8:50:0	366.62	285.46	195.87	1762.9	1.94E-04	9.90E+03	1.47E+03	1.78E+04	1.1E-12	1.1E-08	1.1E-08	2.2E-10
S014-16-T3-3	107000	3/8/2016 8:40:0	3/15/2016 8:50:0	364.46	283.78	195.53	1759.7	1.94E-04	9.63E+03	1.46E+03	1.78E+04	1.0E-12	1.0E-08		
S014-16-T3-4	95600	3/8/2016 8:40:0	3/15/2016 8:50:0	362.76	282.46	194.51	1750.6	1.93E-04	8.60E+03	1.47E+03	1.78E+04	8.2E-13	8.2E-09	9.2E-09	9.8E-10
S014-16-T3-8	106000	3/8/2016 8:40:0	3/15/2016 8:50:0	360.88	280.99	194.17	1747.5	1.92E-04	9.54E+03	1.46E+03	1.78E+04	1.0E-12	1.0E-08		

T4

Name	NO2 (µg/L	Interval Begin	Sampling Date	Monlith mass (g)	Monlith Dry Mass (g)	Surface Area (cm^2)	Solution Volume (mL)	Monolith Volume (m^3)	M_{ti} (mg/m^2)	ρ (kg/m^3)	Co (mgNO2/kg mono)	D_e (m^2/s)	D_e (cm^2/s)	Average D_e (cm^2/s)	Standard Deviation of Average De
S014-16-T4-1	106000	3/8/2016 8:40:0	3/15/2016 8:50:0	364.02	284.12	195.68	1761.2	1.94E-04	9.54E+03	1.46E+03	1.83E+04	9.6E-13	9.6E-09	1.0E-08	5.7E-10
S014-16-T4-2	111000	3/8/2016 8:40:0	3/15/2016 8:50:0	369.27	288.22	199.22	1793.0	1.99E-04	9.99E+03	1.45E+03	1.83E+04	1.1E-12	1.1E-08		
S014-16-T4-5	113000	3/8/2016 8:40:0	3/15/2016 8:50:0	365.37	285.18	195.92	1763.3	1.94E-04	1.02E+04	1.47E+03	1.83E+04	1.1E-12	1.1E-08	1.1E-08	1.3E-10
S014-16-T4-7	113000	3/8/2016 8:40:0	3/15/2016 8:50:0	363.93	284.05	196.69	1770.2	1.96E-04	1.02E+04	1.45E+03	1.83E+04	1.1E-12	1.1E-08		

T5

Name	NO2 (µg/L	Interval Begin	Sampling Date	Monlith mass (g)	Monlith Dry Mass (g)	Surface Area (cm^2)	Solution Volume (mL)	Monolith Volume (m^3)	M_{ti} (mg/m^2)	ρ (kg/m^3)	Co (mgNO2/kg mono)	D_e (m^2/s)	D_e (cm^2/s)	Average D_e (cm^2/s)	Standard Deviation of Average De
S014-16-T5-2	103000	3/8/2016 8:40:0	3/15/2016 8:50:0	365.93	283.58	197.86	1780.7	1.97E-04	9.27E+03	1.44E+03	1.80E+04	9.7E-13	9.7E-09	9.9E-09	1.7E-10
S014-16-T5-3	107000	3/8/2016 8:40:0	3/15/2016 8:50:0	364.75	282.66	195.03	1755.3	1.92E-04	9.63E+03	1.47E+03	1.80E+04	1.0E-12	1.0E-08		
S014-16-T5-4	107000	3/8/2016 8:40:0	3/15/2016 8:50:0	366.62	284.11	196.79	1771.1	1.95E-04	9.63E+03	1.46E+03	1.80E+04	1.0E-12	1.0E-08	1.1E-08	9.5E-10
S014-16-T5-7	115000	3/8/2016 8:40:0	3/15/2016 8:50:0	365.76	283.44	197.96	1781.6	1.97E-04	1.04E+04	1.44E+03	1.80E+04	1.2E-12	1.2E-08		

T6

Name	NO2 (µg/L	Interval Begin	Sampling Date	Monlith mass (g)	Monlith Dry Mass (g)	Surface Area (cm^2)	Solution Volume (mL)	Monolith Volume (m^3)	M_{ti} (mg/m^2)	ρ (kg/m^3)	Co (mgNO2/kg mono)	D_e (m^2/s)	D_e (cm^2/s)	Average D_e (cm^2/s)	Standard Deviation of Average De
S014-16-T6-2	105000	3/8/2016 8:40:0	3/15/2016 8:50:0	363.78	284.09	196.70	1770.3	1.95E-04	9.45E+03	1.45E+03	1.78E+04	1.0E-12	1.0E-08	1.1E-08	7.1E-10
S014-16-T6-3	112000	3/8/2016 8:40:0	3/15/2016 8:50:0	364.78	284.87	197.29	1775.6	1.96E-04	1.01E+04	1.45E+03	1.78E+04	1.2E-12	1.2E-08		
S014-16-T6-5	110000	3/8/2016 8:40:0	3/15/2016 8:50:0	362.95	283.44	196.39	1767.5	1.95E-04	9.90E+03	1.45E+03	1.78E+04	1.1E-12	1.1E-08	1.1E-08	1.3E-10
S014-16-T6-6	113000	3/8/2016 8:40:0	3/15/2016 8:50:0	360.98	281.90	193.67	1743.0	1.91E-04	1.02E+04	1.48E+03	1.78E+04	1.1E-12	1.1E-08		

NO2 Sampling 28 d

Experiment Start 3/1/16 8:30:00

T1

Name	NO2 (μg/L	Interval Begin	Sampling Date	Monlith mass (g)	Monlith Dry Mass (g)	Surface Area (cm^2)	Solution Volume (mL)	Monolith Volume (m^3)	M_{ti} (mg/m^2)	ρ (kg/m^3)	Co (mgNO2/kg mono)	D_e (m^2/s)	D_e (cm^2/s)	Average D_e (cm^2/s)	Standard Deviation of Average De
S014-16-T1-1	135000	03/15/2016 08:50:00	03/29/2016 08:00	359.63	277.23	192.53	1732.8	1.89E-04	1.22E+04	1.46E+03	1.80E+04	8.1E-13	8.1E-09	8.0E-09	8.8E-11
S014-16-T1-2	129000	03/15/2016 08:50:00	03/29/2016 08:00	365.20	281.52	199.18	1792.6	1.99E-04	1.16E+04	1.41E+03	1.80E+04	7.9E-13	7.9E-09		
S014-16-T1-4	128000	03/15/2016 08:50:00	03/29/2016 08:00	360.86	278.18	195.83	1762.5	1.95E-04	1.15E+04	1.43E+03	1.80E+04	7.7E-13	7.7E-09	7.4E-09	2.3E-10
S014-16-T1-7	126000	03/15/2016 08:50:00	03/29/2016 08:00	361.60	278.75	194.35	1749.2	1.92E-04	1.13E+04	1.45E+03	1.80E+04	7.2E-13	7.2E-09		

T2

Name	NO2 (μg/L	Interval Begin	Sampling Date	Monlith mass (g)	Monlith Dry Mass (g)	Surface Area (cm^2)	Solution Volume (mL)	Monolith Volume (m^3)	M_{ti} (mg/m^2)	ρ (kg/m^3)	Co (mgNO2/kg mono)	D_e (m^2/s)	D_e (cm^2/s)	Average D_e (cm^2/s)	Standard Deviation of Average De
S014-16-T2-3	191000	03/15/2016 08:50:00	03/29/2016 08:00	364.71	283.41	195.83	1749.7	1.92E-04	1.71E+04	1.48E+03	1.78E+04	1.6E-12	1.6E-08	1.7E-08	1.5E-09
S014-16-T2-6	203000	03/15/2016 08:50:00	03/29/2016 08:00	367.70	285.74	197.83	1780.5	1.97E-04	1.83E+04	1.45E+03	1.78E+04	1.9E-12	1.9E-08		
S014-16-T2-7	181000	03/15/2016 08:50:00	03/29/2016 08:00	366.00	284.41	196.77	1770.9	1.95E-04	1.63E+04	1.46E+03	1.78E+04	1.5E-12	1.5E-08	1.5E-08	1.8E-10
S014-16-T2-8	180000	03/15/2016 08:50:00	03/29/2016 08:00	363.14	282.19	197.90	1781.1	1.97E-04	1.62E+04	1.43E+03	1.78E+04	1.5E-12	1.5E-08		

T3

Name	NO2 (μg/L	Interval Begin	Sampling Date	Monlith mass (g)	Monlith Dry Mass (g)	Surface Area (cm^2)	Solution Volume (mL)	Monolith Volume (m^3)	M_{ti} (mg/m^2)	ρ (kg/m^3)	Co (mgNO2/kg mono)	D_e (m^2/s)	D_e (cm^2/s)	Average D_e (cm^2/s)	Standard Deviation of Average De
S014-16-T3-1	141000	03/15/2016 08:50:00	03/29/2016 08:00	366.62	285.46	195.87	1762.9	1.94E-04	1.27E+04	1.47E+03	1.78E+04	8.9E-13	8.9E-09	9.0E-09	6.2E-11
S014-16-T3-3	141000	03/15/2016 08:50:00	03/29/2016 08:00	364.46	283.78	195.53	1759.7	1.94E-04	1.27E+04	1.46E+03	1.78E+04	9.1E-13	9.1E-09		
S014-16-T3-4	119000	03/15/2016 08:50:00	03/29/2016 08:00	362.76	282.46	194.51	1750.6	1.93E-04	1.07E+04	1.47E+03	1.78E+04	6.4E-13	6.4E-09	6.8E-09	3.6E-10
S014-16-T3-8	125000	03/15/2016 08:50:00	03/29/2016 08:00	360.88	280.99	194.17	1747.5	1.92E-04	1.13E+04	1.46E+03	1.78E+04	7.1E-13	7.1E-09		

T4

Name	NO2 (μg/L	Interval Begin	Sampling Date	Monlith mass (g)	Monlith Dry Mass (g)	Surface Area (cm^2)	Solution Volume (mL)	Monolith Volume (m^3)	M_{ti} (mg/m^2)	ρ (kg/m^3)	Co (mgNO2/kg mono)	D_e (m^2/s)	D_e (cm^2/s)	Average D_e (cm^2/s)	Standard Deviation of Average De
S014-16-T4-1	144000	03/15/2016 08:50:00	03/29/2016 08:00	364.02	284.12	195.68	1761.2	1.94E-04	1.30E+04	1.46E+03	1.83E+04	8.9E-13	8.9E-09	8.9E-09	4.1E-11
S014-16-T4-2	142000	03/15/2016 08:50:00	03/29/2016 08:00	369.27	288.22	199.22	1793.0	1.99E-04	1.28E+04	1.45E+03	1.83E+04	8.9E-13	8.9E-09		
S014-16-T4-5	132000	03/15/2016 08:50:00	03/29/2016 08:00	365.37	285.18	195.92	1763.3	1.94E-04	1.19E+04	1.47E+03	1.83E+04	7.5E-13	7.5E-09	7.9E-09	4.5E-10
S014-16-T4-7	138000	03/15/2016 08:50:00	03/29/2016 08:00	363.93	284.05	196.69	1770.2	1.96E-04	1.24E+04	1.45E+03	1.83E+04	8.4E-13	8.4E-09		

T5

Name	NO2 (μg/L	Interval Begin	Sampling Date	Monlith mass (g)	Monlith Dry Mass (g)	Surface Area (cm^2)	Solution Volume (mL)	Monolith Volume (m^3)	M_{ti} (mg/m^2)	ρ (kg/m^3)	Co (mgNO2/kg mono)	D_e (m^2/s)	D_e (cm^2/s)	Average D_e (cm^2/s)	Standard Deviation of Average De
S014-16-T5-2	152000	03/15/2016 08:50:00	03/29/2016 08:00	365.93	283.58	197.86	1780.7	1.97E-04	1.37E+04	1.44E+03	1.80E+04	1.1E-12	1.1E-08	9.7E-09	9.9E-10
S014-16-T5-3	140000	03/15/2016 08:50:00	03/29/2016 08:00	364.75	282.66	195.03	1755.3	1.92E-04	1.26E+04	1.47E+03	1.80E+04	8.7E-13	8.7E-09		
S014-16-T5-4	133000	03/15/2016 08:50:00	03/29/2016 08:00	366.62	284.11	196.79	1771.1	1.95E-04	1.20E+04	1.46E+03	1.80E+04	8.0E-13	8.0E-09	8.1E-09	1.0E-10
S014-16-T5-7	133000	03/15/2016 08:50:00	03/29/2016 08:00	365.76	283.44	197.96	1781.6	1.97E-04	1.20E+04	1.44E+03	1.80E+04	8.2E-13	8.2E-09		

T6

Name	NO2 (μg/L	Interval Begin	Sampling Date	Monlith mass (g)	Monlith Dry Mass (g)	Surface Area (cm^2)	Solution Volume (mL)	Monolith Volume (m^3)	M_{ti} (mg/m^2)	ρ (kg/m^3)	Co (mgNO2/kg mono)	D_e (m^2/s)	D_e (cm^2/s)	Average D_e (cm^2/s)	Standard Deviation of Average De
S014-16-T6-2	140000	03/15/2016 08:50:00	03/29/2016 08:00	363.78	284.09	196.70	1770.3	1.95E-04	1.26E+04	1.45E+03	1.78E+04	9.1E-13	9.1E-09	8.9E-09	1.2E-10
S014-16-T6-3	138000	03/15/2016 08:50:00	03/29/2016 08:00	364.78	284.87	197.29	1775.6	1.96E-04	1.24E+04	1.45E+03	1.78E+04	8.8E-13	8.8E-09		
S014-16-T6-5	133000	03/15/2016 08:50:00	03/29/2016 08:00	362.95	283.44	196.39	1767.5	1.95E-04	1.20E+04	1.45E+03	1.78E+04	8.2E-13	8.2E-09	8.3E-09	1.1E-10
S014-16-T6-6	137000	03/15/2016 08:50:00	03/29/2016 08:00	360.98	281.90	193.67	1743.0	1.91E-04	1.23E+04	1.48E+03	1.78E+04	8.4E-13	8.4E-09		

NO2 Sampling 42 d

Experiment Start 3/1/16 8:30:00

T1

Name	NO2 (µg/L	Interval Begin	Sampling Date	Monlith mass (g)	Monlith Dry Mass (g)	Surface Area (cm^2)	Solution Volume (mL)	Monolith Volume (m^3)	M_{ti} (mg/m^2)	ρ (kg/m^3)	Co (mgNO2/kg mono)	D_e (m^2/s)	D_e (cm^2/s)	Average D_e (cm^2/s)	Standard Deviation of Average De
S014-16-T1-1	94300	03/29/2016 08:00:0	04/12/2016 08:30:	359.63	277.23	192.53	1732.8	1.89E-04	8.49E+03	1.46E+03	1.80E+04	6.7E-13	6.7E-09	6.1E-09	5.3E-10
S014-16-T1-2	83500	03/29/2016 08:00:0	04/12/2016 08:30:	365.20	281.52	199.18	1792.6	1.99E-04	7.52E+03	1.41E+03	1.80E+04	5.6E-13	5.6E-09		
S014-16-T1-4	89600	03/29/2016 08:00:0	04/12/2016 08:30:	360.86	278.18	195.83	1762.5	1.95E-04	8.06E+03	1.43E+03	1.80E+04	6.3E-13	6.3E-09	6.0E-09	2.9E-10
S014-16-T1-7	86600	03/29/2016 08:00:0	04/12/2016 08:30:	361.60	278.75	194.35	1749.2	1.92E-04	7.79E+03	1.45E+03	1.80E+04	5.7E-13	5.7E-09		

T2

Name	NO2 (µg/L	Interval Begin	Sampling Date	Monlith mass (g)	Monlith Dry Mass (g)	Surface Area (cm^2)	Solution Volume (mL)	Monolith Volume (m^3)	M_{ti} (mg/m^2)	ρ (kg/m^3)	Co (mgNO2/kg mono)	D_e (m^2/s)	D_e (cm^2/s)	Average D_e (cm^2/s)	Standard Deviation of Average De
S014-16-T2-3	113000	03/29/2016 08:00:0	04/12/2016 08:30:	364.71	283.41	195.83	1749.7	1.92E-04	1.01E+04	1.48E+03	1.78E+04	9.4E-13	9.4E-09	1.0E-08	6.9E-10
S014-16-T2-6	118000	03/29/2016 08:00:0	04/12/2016 08:30:	367.70	285.74	197.83	1780.5	1.97E-04	1.06E+04	1.45E+03	1.78E+04	1.1E-12	1.1E-08		
S014-16-T2-7	106000	03/29/2016 08:00:0	04/12/2016 08:30:	366.00	284.41	196.77	1770.9	1.95E-04	9.54E+03	1.46E+03	1.78E+04	8.7E-13	8.7E-09	8.8E-09	1.5E-10
S014-16-T2-8	106000	03/29/2016 08:00:0	04/12/2016 08:30:	363.14	282.19	197.90	1781.1	1.97E-04	9.54E+03	1.43E+03	1.78E+04	9.0E-13	9.0E-09		

T3

Name	NO2 (µg/L	Interval Begin	Sampling Date	Monlith mass (g)	Monlith Dry Mass (g)	Surface Area (cm^2)	Solution Volume (mL)	Monolith Volume (m^3)	M_{ti} (mg/m^2)	ρ (kg/m^3)	Co (mgNO2/kg mono)	D_e (m^2/s)	D_e (cm^2/s)	Average D_e (cm^2/s)	Standard Deviation of Average De
S014-16-T3-1	91900	03/29/2016 08:00:0	04/12/2016 08:30:	366.62	285.46	195.87	1762.9	1.94E-04	8.27E+03	1.47E+03	1.78E+04	6.4E-13	6.4E-09	6.2E-09	2.3E-10
S014-16-T3-3	87900	03/29/2016 08:00:0	04/12/2016 08:30:	364.46	283.78	195.53	1759.7	1.94E-04	7.91E+03	1.46E+03	1.78E+04	5.9E-13	5.9E-09		
S014-16-T3-4	86500	03/29/2016 08:00:0	04/12/2016 08:30:	362.76	282.46	194.51	1750.6	1.93E-04	7.79E+03	1.47E+03	1.78E+04	5.7E-13	5.7E-09	5.6E-09	1.2E-10
S014-16-T3-8	84300	03/29/2016 08:00:0	04/12/2016 08:30:	360.88	280.99	194.17	1747.5	1.92E-04	7.59E+03	1.46E+03	1.78E+04	5.5E-13	5.5E-09		

T4

Name	NO2 (µg/L	Interval Begin	Sampling Date	Monlith mass (g)	Monlith Dry Mass (g)	Surface Area (cm^2)	Solution Volume (mL)	Monolith Volume (m^3)	M_{ti} (mg/m^2)	ρ (kg/m^3)	Co (mgNO2/kg mono)	D_e (m^2/s)	D_e (cm^2/s)	Average D_e (cm^2/s)	Standard Deviation of Average De
S014-16-T4-1	92800	03/29/2016 08:00:0	04/12/2016 08:30:	364.02	284.12	195.68	1761.2	1.94E-04	8.35E+03	1.46E+03	1.83E+04	6.3E-13	6.3E-09	6.1E-09	1.4E-10
S014-16-T4-2	89800	03/29/2016 08:00:0	04/12/2016 08:30:	369.27	288.22	199.22	1793.0	1.99E-04	8.08E+03	1.45E+03	1.83E+04	6.0E-13	6.0E-09		
S014-16-T4-5	88900	03/29/2016 08:00:0	04/12/2016 08:30:	365.37	285.18	195.92	1763.3	1.94E-04	8.00E+03	1.47E+03	1.83E+04	5.7E-13	5.7E-09	5.8E-09	8.3E-11
S014-16-T4-7	89100	03/29/2016 08:00:0	04/12/2016 08:30:	363.93	284.05	196.69	1770.2	1.96E-04	8.02E+03	1.45E+03	1.83E+04	5.9E-13	5.9E-09		

T5

Name	NO2 (µg/L	Interval Begin	Sampling Date	Monlith mass (g)	Monlith Dry Mass (g)	Surface Area (cm^2)	Solution Volume (mL)	Monolith Volume (m^3)	M_{ti} (mg/m^2)	ρ (kg/m^3)	Co (mgNO2/kg mono)	D_e (m^2/s)	D_e (cm^2/s)	Average D_e (cm^2/s)	Standard Deviation of Average De
S014-16-T5-2	92100	03/29/2016 08:00:0	04/12/2016 08:30:	365.93	283.58	197.86	1780.7	1.97E-04	8.29E+03	1.44E+03	1.80E+04	6.6E-13	6.6E-09	7.2E-09	6.6E-10
S014-16-T5-3	103000	03/29/2016 08:00:0	04/12/2016 08:30:	364.75	282.66	195.03	1755.3	1.92E-04	9.27E+03	1.47E+03	1.80E+04	7.9E-13	7.9E-09		
S014-16-T5-4	87900	03/29/2016 08:00:0	04/12/2016 08:30:	366.62	284.11	196.79	1771.1	1.95E-04	7.91E+03	1.46E+03	1.80E+04	5.9E-13	5.9E-09	6.1E-09	2.9E-10
S014-16-T5-7	91000	03/29/2016 08:00:0	04/12/2016 08:30:	365.76	283.44	197.96	1781.6	1.97E-04	8.19E+03	1.44E+03	1.80E+04	6.4E-13	6.4E-09		

T6

Name	NO2 (µg/L	Interval Begin	Sampling Date	Monlith mass (g)	Monlith Dry Mass (g)	Surface Area (cm^2)	Solution Volume (mL)	Monolith Volume (m^3)	M_{ti} (mg/m^2)	ρ (kg/m^3)	Co (mgNO2/kg mono)	D_e (m^2/s)	D_e (cm^2/s)	Average D_e (cm^2/s)	Standard Deviation of Average De
S014-16-T6-2	93600	03/29/2016 08:00:0	04/12/2016 08:30:	363.78	284.09	196.70	1770.3	1.95E-04	8.42E+03	1.45E+03	1.78E+04	6.8E-13	6.8E-09	6.2E-09	6.1E-10
S014-16-T6-3	84700	03/29/2016 08:00:0	04/12/2016 08:30:	364.78	284.87	197.29	1775.6	1.96E-04	7.62E+03	1.45E+03	1.78E+04	5.6E-13	5.6E-09		
S014-16-T6-5	88000	03/29/2016 08:00:0	04/12/2016 08:30:	362.95	283.44	196.39	1767.5	1.95E-04	7.92E+03	1.45E+03	1.78E+04	6.0E-13	6.0E-09	5.9E-09	1.5E-10
S014-16-T6-6	87100	03/29/2016 08:00:0	04/12/2016 08:30:	360.98	281.90	193.67	1743.0	1.91E-04	7.84E+03	1.48E+03	1.78E+04	5.7E-13	5.7E-09		

NO2 Sampling 49 d

Experiment Start 3/1/16 8:30:00

T1

Name	NO2 (µg/L	Interval Begin	Sampling Date	Monlith mass (g)	Monlith Dry Mass (g)	Surface Area (cm^2)	Solution Volume (mL)	Monolith Volume (m^3)	M_{ti} (mg/m^2)	ρ (kg/m^3)	Co (mgNO2/kg mono)	D_e (m^2/s)	D_e (cm^2/s)	Average D_e (cm^2/s)	Standard Deviation of Average De
S014-16-T1-1	34600	04/12/2016 08:30:(	04/19/2016 08:40:00	359.63	277.23	192.53	1732.8	1.89E-04	3.11E+03	1.46E+03	1.80E+04	4.7E-13	4.7E-09	4.6E-09	8.7E-11
S014-16-T1-2	32800	04/12/2016 08:30:(	04/19/2016 08:40:01	365.20	281.52	199.18	1792.6	1.99E-04	2.95E+03	1.41E+03	1.80E+04	4.5E-13	4.5E-09		
S014-16-T1-4	38600	04/12/2016 08:30:(	04/19/2016 08:40:02	360.86	278.18	195.83	1762.5	1.95E-04	3.47E+03	1.43E+03	1.80E+04	6.2E-13	6.2E-09	5.9E-09	2.9E-10
S014-16-T1-7	37300	04/12/2016 08:30:(	04/19/2016 08:40:03	361.60	278.75	194.35	1749.2	1.92E-04	3.36E+03	1.45E+03	1.80E+04	5.6E-13	5.6E-09		

T2

Name	NO2 (µg/L	Interval Begin	Sampling Date	Monlith mass (g)	Monlith Dry Mass (g)	Surface Area (cm^2)	Solution Volume (mL)	Monolith Volume (m^3)	M_{ti} (mg/m^2)	ρ (kg/m^3)	Co (mgNO2/kg mono)	D_e (m^2/s)	D_e (cm^2/s)	Average D_e (cm^2/s)	Standard Deviation of Average De
S014-16-T2-3	41200	04/12/2016 08:30:(	04/19/2016 08:40:00	364.71	283.41	195.83	1749.7	1.92E-04	3.68E+03	1.48E+03	1.78E+04	6.6E-13	6.6E-09	6.8E-09	2.6E-10
S014-16-T2-6	41700	04/12/2016 08:30:(	04/19/2016 08:40:01	367.70	285.74	197.83	1780.5	1.97E-04	3.75E+03	1.45E+03	1.78E+04	7.1E-13	7.1E-09		
S014-16-T2-7	45600	04/12/2016 08:30:(	04/19/2016 08:40:02	366.00	284.41	196.77	1770.9	1.95E-04	4.10E+03	1.46E+03	1.78E+04	8.4E-13	8.4E-09	8.6E-09	1.1E-10
S014-16-T2-8	45400	04/12/2016 08:30:(	04/19/2016 08:40:03	363.14	282.19	197.90	1781.1	1.97E-04	4.09E+03	1.43E+03	1.78E+04	8.7E-13	8.7E-09		

T3

Name	NO2 (µg/L	Interval Begin	Sampling Date	Monlith mass (g)	Monlith Dry Mass (g)	Surface Area (cm^2)	Solution Volume (mL)	Monolith Volume (m^3)	M_{ti} (mg/m^2)	ρ (kg/m^3)	Co (mgNO2/kg mono)	D_e (m^2/s)	D_e (cm^2/s)	Average D_e (cm^2/s)	Standard Deviation of Average De
S014-16-T3-1	36400	04/12/2016 08:30:(	04/19/2016 08:40:00	366.62	285.46	195.87	1762.9	1.94E-04	3.28E+03	1.47E+03	1.78E+04	5.3E-13	5.3E-09	4.7E-09	5.6E-10
S014-16-T3-3	32100	04/12/2016 08:30:(	04/19/2016 08:40:01	364.46	283.78	195.53	1759.7	1.94E-04	2.89E+03	1.46E+03	1.78E+04	4.2E-13	4.2E-09		
S014-16-T3-4	35600	04/12/2016 08:30:(	04/19/2016 08:40:02	362.76	282.46	194.51	1750.6	1.93E-04	3.20E+03	1.47E+03	1.78E+04	5.1E-13	5.1E-09	5.2E-09	9.0E-11
S014-16-T3-8	36100	04/12/2016 08:30:(	04/19/2016 08:40:03	360.88	280.99	194.17	1747.5	1.92E-04	3.25E+03	1.46E+03	1.78E+04	5.3E-13	5.3E-09		

T4

Name	NO2 (µg/L	Interval Begin	Sampling Date	Monlith mass (g)	Monlith Dry Mass (g)	Surface Area (cm^2)	Solution Volume (mL)	Monolith Volume (m^3)	M_{ti} (mg/m^2)	ρ (kg/m^3)	Co (mgNO2/kg mono)	D_e (m^2/s)	D_e (cm^2/s)	Average D_e (cm^2/s)	Standard Deviation of Average De
S014-16-T4-1	34100	04/12/2016 08:30:(	04/19/2016 08:40:00	364.02	284.12	195.68	1761.2	1.94E-04	3.07E+03	1.46E+03	1.83E+04	4.4E-13	4.4E-09	4.4E-09	6.3E-11
S014-16-T4-2	33300	04/12/2016 08:30:(	04/19/2016 08:40:01	369.27	288.22	199.22	1793.0	1.99E-04	3.00E+03	1.45E+03	1.83E+04	4.3E-13	4.3E-09		
S014-16-T4-5	36300	04/12/2016 08:30:(	04/19/2016 08:40:02	365.37	285.18	195.92	1763.3	1.94E-04	3.27E+03	1.47E+03	1.83E+04	5.0E-13	5.0E-09	5.1E-09	1.5E-10
S014-16-T4-7	36900	04/12/2016 08:30:(	04/19/2016 08:40:03	363.93	284.05	196.69	1770.2	1.96E-04	3.32E+03	1.45E+03	1.83E+04	5.3E-13	5.3E-09		

T5

Name	NO2 (µg/L	Interval Begin	Sampling Date	Monlith mass (g)	Monlith Dry Mass (g)	Surface Area (cm^2)	Solution Volume (mL)	Monolith Volume (m^3)	M_{ti} (mg/m^2)	ρ (kg/m^3)	Co (mgNO2/kg mono)	D_e (m^2/s)	D_e (cm^2/s)	Average D_e (cm^2/s)	Standard Deviation of Average De
S014-16-T5-2	32600	04/12/2016 08:30:(	04/19/2016 08:40:00	365.93	283.58	197.86	1780.7	1.97E-04	2.93E+03	1.44E+03	1.80E+04	4.3E-13	4.3E-09	4.7E-09	3.8E-10
S014-16-T5-3	36100	04/12/2016 08:30:(	04/19/2016 08:40:01	364.75	282.66	195.03	1755.3	1.92E-04	3.25E+03	1.47E+03	1.80E+04	5.1E-13	5.1E-09		
S014-16-T5-4	37200	04/12/2016 08:30:(	04/19/2016 08:40:02	366.62	284.11	196.79	1771.1	1.95E-04	3.35E+03	1.46E+03	1.80E+04	5.5E-13	5.5E-09	5.6E-09	7.1E-11
S014-16-T5-7	37200	04/12/2016 08:30:(	04/19/2016 08:40:03	365.76	283.44	197.96	1781.6	1.97E-04	3.35E+03	1.44E+03	1.80E+04	5.7E-13	5.7E-09		

T6

Name	NO2 (µg/L	Interval Begin	Sampling Date	Monlith mass (g)	Monlith Dry Mass (g)	Surface Area (cm^2)	Solution Volume (mL)	Monolith Volume (m^3)	M_{ti} (mg/m^2)	ρ (kg/m^3)	Co (mgNO2/kg mono)	D_e (m^2/s)	D_e (cm^2/s)	Average D_e (cm^2/s)	Standard Deviation of Average De
S014-16-T6-2	34700	04/12/2016 08:30:(	04/19/2016 08:40:00	363.78	284.09	196.70	1770.3	1.95E-04	3.12E+03	1.45E+03	1.78E+04	4.9E-13	4.9E-09	4.7E-09	2.7E-10
S014-16-T6-3	32700	04/12/2016 08:30:(	04/19/2016 08:40:01	364.78	284.87	197.29	1775.6	1.96E-04	2.94E+03	1.45E+03	1.78E+04	4.4E-13	4.4E-09		
S014-16-T6-5	36000	04/12/2016 08:30:(	04/19/2016 08:40:02	362.95	283.44	196.39	1767.5	1.95E-04	3.24E+03	1.45E+03	1.78E+04	5.3E-13	5.3E-09	5.2E-09	1.2E-10
S014-16-T6-6	35700	04/12/2016 08:30:(	04/19/2016 08:40:03	360.98	281.90	193.67	1743.0	1.91E-04	3.21E+03	1.48E+03	1.78E+04	5.0E-13	5.0E-09		

NO2 Sampling 63 d

Experiment Start 3/1/16 8:30:00

T1

Name	NO2 (µg/L	Interval Begin	Sampling Date	Monlith mass (g)	Monlith Dry Mass (g)	Surface Area (cm^2)	Solution Volume (mL)	Monolith Volume (m^3)	M_{ti} (mg/m^2)	ρ (kg/m^3)	Co (mgNO2/kg mono)	D_e (m^2/s)	D_e (cm^2/s)	Average D_e (cm^2/s)	Standard Deviation of Average De
S014-16-T1-1	67600	04/19/2016 08:40:0	05/3/2016 09:00:00	359.63	277.23	192.53	1732.8	1.89E-04	6.08E+03	1.46E+03	1.80E+04	5.5E-13	5.5E-09	5.3E-09	2.6E-10
S014-16-T1-2	62200	04/19/2016 08:40:01	05/3/2016 09:00:00	365.20	281.52	199.18	1792.6	1.99E-04	5.60E+03	1.41E+03	1.80E+04	5.0E-13	5.0E-09		
S014-16-T1-4	59900	04/19/2016 08:40:02	05/3/2016 09:00:00	360.86	278.18	195.83	1762.5	1.95E-04	5.39E+03	1.43E+03	1.80E+04	4.6E-13	4.6E-09	4.3E-09	2.4E-10
S014-16-T1-7	57500	04/19/2016 08:40:0	05/3/2016 09:00:00	361.60	278.75	194.35	1749.2	1.92E-04	5.18E+03	1.45E+03	1.80E+04	4.1E-13	4.1E-09		

T2

Name	NO2 (µg/L	Interval Begin	Sampling Date	Monlith mass (g)	Monlith Dry Mass (g)	Surface Area (cm^2)	Solution Volume (mL)	Monolith Volume (m^3)	M_{ti} (mg/m^2)	ρ (kg/m^3)	Co (mgNO2/kg mono)	D_e (m^2/s)	D_e (cm^2/s)	Average D_e (cm^2/s)	Standard Deviation of Average De
S014-16-T2-3	71800	04/19/2016 08:40:0	05/3/2016 09:00:00	364.71	283.41	195.83	1749.7	1.92E-04	6.42E+03	1.48E+03	1.78E+04	6.1E-13	6.1E-09	5.9E-09	1.8E-10
S014-16-T2-6	67900	04/19/2016 08:40:01	05/3/2016 09:00:00	367.70	285.74	197.83	1780.5	1.97E-04	6.11E+03	1.45E+03	1.78E+04	5.8E-13	5.8E-09		
S014-16-T2-7	70200	04/19/2016 08:40:02	05/3/2016 09:00:00	366.00	284.41	196.77	1770.9	1.95E-04	6.32E+03	1.46E+03	1.78E+04	6.1E-13	6.1E-09	5.7E-09	4.2E-10
S014-16-T2-8	64100	04/19/2016 08:40:0	05/3/2016 09:00:00	363.14	282.19	197.90	1781.1	1.97E-04	5.77E+03	1.43E+03	1.78E+04	5.3E-13	5.3E-09		

T3

Name	NO2 (µg/L	Interval Begin	Sampling Date	Monlith mass (g)	Monlith Dry Mass (g)	Surface Area (cm^2)	Solution Volume (mL)	Monolith Volume (m^3)	M_{ti} (mg/m^2)	ρ (kg/m^3)	Co (mgNO2/kg mono)	D_e (m^2/s)	D_e (cm^2/s)	Average D_e (cm^2/s)	Standard Deviation of Average De
S014-16-T3-1	65900	04/19/2016 08:40:0	05/3/2016 09:00:00	366.62	285.46	195.87	1762.9	1.94E-04	5.93E+03	1.47E+03	1.78E+04	5.3E-13	5.3E-09	5.0E-09	3.0E-10
S014-16-T3-3	61600	04/19/2016 08:40:01	05/3/2016 09:00:00	364.46	283.78	195.53	1759.7	1.94E-04	5.54E+03	1.46E+03	1.78E+04	4.7E-13	4.7E-09		
S014-16-T3-4	55700	04/19/2016 08:40:02	05/3/2016 09:00:00	362.76	282.46	194.51	1750.6	1.93E-04	5.01E+03	1.47E+03	1.78E+04	3.8E-13	3.8E-09	3.8E-09	2.0E-11
S014-16-T3-8	55800	04/19/2016 08:40:0	05/3/2016 09:00:00	360.88	280.99	194.17	1747.5	1.92E-04	5.02E+03	1.46E+03	1.78E+04	3.9E-13	3.9E-09		

T4

Name	NO2 (µg/L	Interval Begin	Sampling Date	Monlith mass (g)	Monlith Dry Mass (g)	Surface Area (cm^2)	Solution Volume (mL)	Monolith Volume (m^3)	M_{ti} (mg/m^2)	ρ (kg/m^3)	Co (mgNO2/kg mono)	D_e (m^2/s)	D_e (cm^2/s)	Average D_e (cm^2/s)	Standard Deviation of Average De
S014-16-T4-1	65000	04/19/2016 08:40:0	05/3/2016 09:00:00	364.02	284.12	195.68	1761.2	1.94E-04	5.85E+03	1.46E+03	1.83E+04	4.9E-13	4.9E-09	4.5E-09	4.1E-10
S014-16-T4-2	58800	04/19/2016 08:40:01	05/3/2016 09:00:00	369.27	288.22	199.22	1793.0	1.99E-04	5.29E+03	1.45E+03	1.83E+04	4.1E-13	4.1E-09		
S014-16-T4-5	58100	04/19/2016 08:40:02	05/3/2016 09:00:00	365.37	285.18	195.92	1763.3	1.94E-04	5.23E+03	1.47E+03	1.83E+04	3.9E-13	3.9E-09	3.8E-09	8.1E-11
S014-16-T4-7	56200	04/19/2016 08:40:0	05/3/2016 09:00:00	363.93	284.05	196.69	1770.2	1.96E-04	5.06E+03	1.45E+03	1.83E+04	3.8E-13	3.8E-09		

T5

Name	NO2 (µg/L	Interval Begin	Sampling Date	Monlith mass (g)	Monlith Dry Mass (g)	Surface Area (cm^2)	Solution Volume (mL)	Monolith Volume (m^3)	M_{ti} (mg/m^2)	ρ (kg/m^3)	Co (mgNO2/kg mono)	D_e (m^2/s)	D_e (cm^2/s)	Average D_e (cm^2/s)	Standard Deviation of Average De
S014-16-T5-2	64200	04/19/2016 08:40:0	05/3/2016 09:00:00	365.93	283.58	197.86	1780.7	1.97E-04	5.78E+03	1.44E+03	1.80E+04	5.2E-13	5.2E-09	4.8E-09	4.0E-10
S014-16-T5-3	60200	04/19/2016 08:40:01	05/3/2016 09:00:00	364.75	282.66	195.03	1755.3	1.92E-04	5.42E+03	1.47E+03	1.80E+04	4.4E-13	4.4E-09		
S014-16-T5-4	58600	04/19/2016 08:40:02	05/3/2016 09:00:00	366.62	284.11	196.79	1771.1	1.95E-04	5.27E+03	1.46E+03	1.80E+04	4.2E-13	4.2E-09	4.0E-09	1.7E-10
S014-16-T5-7	55500	04/19/2016 08:40:0	05/3/2016 09:00:00	365.76	283.44	197.96	1781.6	1.97E-04	5.00E+03	1.44E+03	1.80E+04	3.9E-13	3.9E-09		

T6

Name	NO2 (µg/L	Interval Begin	Sampling Date	Monlith mass (g)	Monlith Dry Mass (g)	Surface Area (cm^2)	Solution Volume (mL)	Monolith Volume (m^3)	M_{ti} (mg/m^2)	ρ (kg/m^3)	Co (mgNO2/kg mono)	D_e (m^2/s)	D_e (cm^2/s)	Average D_e (cm^2/s)	Standard Deviation of Average De
S014-16-T6-2	64200	04/19/2016 08:40:0	05/3/2016 09:00:00	363.78	284.09	196.70	1770.3	1.95E-04	5.78E+03	1.45E+03	1.78E+04	5.2E-13	5.2E-09	4.7E-09	4.4E-10
S014-16-T6-3	58400	04/19/2016 08:40:01	05/3/2016 09:00:00	364.78	284.87	197.29	1775.6	1.96E-04	5.26E+03	1.45E+03	1.78E+04	4.3E-13	4.3E-09		
S014-16-T6-5	57800	04/19/2016 08:40:02	05/3/2016 09:00:00	362.95	283.44	196.39	1767.5	1.95E-04	5.20E+03	1.45E+03	1.78E+04	4.2E-13	4.2E-09	4.0E-09	2.2E-10
S014-16-T6-6	55600	04/19/2016 08:40:0	05/3/2016 09:00:00	360.98	281.90	193.67	1743.0	1.91E-04	5.00E+03	1.48E+03	1.78E+04	3.8E-13	3.8E-09		

NO2 CO Calculation

LIMS Data

LIMS data on NO2 concentration measurement from the spiked 6.5 M Na simulants

These values show the initial NO2 content of the simulant prior to any getter addition

Test	LabNumber	SampleName	Result	Units	EQL
T1	1601042-01	T1 Initial	38200000	ug/L	5000
T2	1601042-03	T2 Initial	38300000	ug/L	5000
T3	1601042-05	T3 Initial	38200000	ug/L	5000
T4	1601042-08	T4 Initial	39300000	ug/L	5000
T5	1601042-11	T5 Initial	38400000	ug/L	5000
T6	1601042-13	T6 Initial	38200000	ug/L	5000
			3		

Simulant Volume

Density of the 6.5 M Na Average simulant [g/mL] 1.31

Test	Simulant Bottle Tare (g)	Bottle + Simulant (g)	Simulant Mass	Simulant Volume- (mL)	Simulant Volume after sampling (mL)	Dry Blend (g)	Total Weight of Slurry [g]
T1	100.1	1407.8	1307.7	998.2	994.2	1750.0	2744.2
T2	100.3	1408.1	1307.8	998.3	994.3	1757.3	2751.6
T3	100.1	1407.9	1307.8	998.3	994.3	1750.0	2744.3
T4	100	1408	1308	998.5	994.5	1745.0	2739.4
T5	99.8	1408	1308.2	998.6	994.6	1750.0	2744.6
T6	99.9	1410.2	1310.3	1000.2	996.2	1747.6	2743.8

Co

Calculation on NO2 C_0 in dry Cast Stone (mg/kg) monolith

		T1	T2	T3	T4	T5	T6
Dry solid fraction in Cast Stone Monolith		0.771	0.78	0.78	0.78	0.77	0.78

Test	NO2 (ug/g wet Cast Stone)- analytical	C_0 (mg/kg) in dry Cast Stone - analytical
T1	13839.92	**17953.68**
T2	13840.27	**17810.41**
T3	13840.60	**17775.59**
T4	14266.80	**18278.80**
T5	13915.79	**17957.12**
T6	13869.90	**17760.74**

Appendix D
Sn(II) Reduction of Tc Previous Work

Sn(II) apatite (Sn-A) was used in this study as a reductant for Tc, and our recent work has covered its capability in LAW. A comparison can be made to a similar scope of work performed in separate simulants. Taylor-Pashow et al. (2014) used Sn(II)Cl_2 coupled with hydroxyapatite sorbent in a reductive-sorbent precipitation process to remove Tc from an off-gas liquid waste simulants. Later, Taylor-Pashow and McCabe (2015) studied the use of just the reductant $SnCl_2$ as the Tc sequestering agent. They created off-gas simulants that are projections of the waste from the WTP melters during full WTP operations. A summary of their work is provided below.

The off-gas waste stream during both full WTP operations and during direct feed is near neutral pH, and will likely contain some insoluble solids from melter carryover. Soluble components are expected to be mostly sodium and ammonium salts of nitrate, chloride, and fluoride. The halide concentrations can be so high that extra LAW glass needs to be made to accommodate the halides in the glass. Approximately 32% of the sodium in ILAW (glass product) comes from glass formers used to make the extra glass to dilute the halides to acceptable concentrations in the final LAW glass If some of the radionuclides are removed from the off-gas condensate and flush water waste stream in an alternate process and the decontaminated liquid was then sent to the ETF, the fluoride, sulfate, and chloride would be purged from the LAW system, yielding substantial benefits to the overall WTP mission.

Taylor-Pashow et al. (2014) generated a WTP off-gas simulant shown in Table D-1 and proceeded to study various methods to remove radionuclides (^{137}Cs, ^{90}Sr, ^{99}Tc, U, and Pu). The simulant was produced based on models, calculations, and comparison with pilot-scale melter tests. The projected solution chemistry and radionuclide content were based on HTWOS modeling of **full operation of all of the WTP facilities, including supplemental LAW melters** (in the assumed second LAW facility. These HTWOS predictions are shown in the right side of Table D-1.

Table D-1. Measured Concentrations of Constituents Present in the Off-gas Simulant Used in Testing (Taylor-Pashow et al. 2014a)

Constituent	Measured WTP PT off-gas		HTWOS Predicted Off-gas (McCabe et al., 2013, Appendix A-1)			
	ppm	M	Constituent	ppm	M	Charge a)
Tc	1.99		^{99}Tc	2.44	2.47E-05	-2.47E-05
Al	<0.1	<3.70E-05	AlO_4^-	101	1.51E-03	-1.51E-03
B^{3+}	253	2.34E-02	B^{3+}	0.0422	3.90E-06	1.17E-05
Ca^{2+}	<0.1	<2.50E-06	Ca^{2+}	0.128	3.19E-06	6.39E-06
Cr	91	1.75E-03	CrO_4^{2-}	204	1.76E-03	-0.00352
Fe^{3+}	<0.1	<1.79E-06	Fe^{3+}	0.147	2.63E-06	7.90E-06
K^+	150	3.84E-03	K^+	115	2.94E-03	2.94E-03
Li^+	80.3	1.16E-02	Li^+	0.0053	7.64E-07	7.64E-07
Mg^{2+}	<0.1	<4.11E-06	Mg^{2+}	0.000432	1.78E-08	3.55E-08
Na^+	2980	1.30E-01	Na^+	2290	9.96E-02	9.96E-02
NH_4^+	1773	1.04E-01	NH_4^+	1510	8.88E-02	8.88E-02
P	<10	<3.23E-04				
S	832	2.59E-02				
Si^{4+}	52.7	1.88E-03	Si^{4+}	1.03	3.67E-05	1.47E-04
Ti^{4+}	<0.1	<2.09E-06	Ti^{4+}	0.000961	2.01E-08	8.03E-08
Zn^{2+}	28.6	4.38E-04	Zn^{2+}	0.00306	4.68E-08	9.36E-08
Zr^{4+}	<0.1	<1.10E-06	Zr^{4+}	0.0057	6.25E-08	2.50E-07

Constituent	Measured WTP PT off-gas		HTWOS Predicted Off-gas (McCabe et al., 2013, Appendix A-1)			
	ppm	M	Constituent	ppm	M	Charge [a)]
F^-	1250	6.58E-02	F^-	1450	7.63E-02	-7.63E-02
Cl^-	934	2.63E-02	Cl^-	950	2.68E-02	-2.68E-02
NO_2^-	<10	<2.17E-04	NO_2^-	11	2.39E-04	-2.39E-04
NO_3^-	4900	7.90E-02	NO_3^-	5530	8.92E-02	-8.92E-02
SO_4^{2-}	2410	2.51E-02	SO_4^{2-}	2340	2.44E-02	-4.88E-02
PO_4^{3-}	<10	<1.05E-04	PO_4^{3-}	21.5	2.26E-04	-6.79E-04
CO_3^{2-}	NR	NR	CO_3^{2-}	0	0	
pH	7.9					
			H^+	30.4	3.04E-02	3.04E-02
			OH^-	0.00022	1.29E-08	-1.29E-08
Cats						2.22E-01
Anions						2.47E-01

a) Charge= electrical charge for cited constituent in equivalents per liter (N)
Yellow highlight = constituents added by dissolution of glass formers; blue highlight= major cations; green highlight = major anions NR= not reported (not analyzed).

The aqueous phase was prepared from dissolution of reagent-grade chemicals and glass forming solids were added to the dissolved chemical solution. The simulant containing the glass formers was stirred for several days at room temperature. The solids were then removed by filtration with a 0.45-µm filter. The filtrate pH was adjusted to 7.3 ± 0.3 with ~ 50 drops of concentrated nitric acid to be within the range measured in pilot-scale testing off-gas condensates. The presence of measurable boron, lithium, silicon, and zinc in the final simulant were due to dissolution of some of the glass former solids. Radionuclides were then added to the filtered off-gas simulant at predicted concentrations from the HTWOS predictions. Of interest to us is the predicted Tc concentration of 2.44 mg/L. This is the average Tc concentration from the HTWOS predictions (the low to max range for predicted Tc in this waste stream is 1.2 to 3.6 mg/L (see Appendix A-1 in (McCabe et al. 2013)). This amount of Tc (2.44 mg/L) was added as ammonium pertechnetate but after stirring for ~6 days, a 1-L batch of radionuclide spiked simulant was filtered with a 0.45-µm filter and the measured Tc was 1.99 mg/L.

The Table D-1 off-gas simulant was used in batch experiments where several sorbents were used to remove the radionuclides. In general, the radionuclide removal tests were performed by adding a small amount of each sorbent/reagent to separate poly bottles, followed by addition of 20 mL of the radioactive simulant solution to each. The bottles were then agitated in a shaker oven at ~25 °C for the specified time (the Tc reduction test samples were sampled at two time points; 2 hr and 18 hr). Each sample was then filtered through a 0.1-µm filter. The filtrate was then analyzed for the radionuclide of interest. Test results indicate that excellent removal of Tc was achieved using $Sn(II)Cl_2$ as a reductant, combined with sorption onto hydroxyapatite, even in the presence of air and at room temperature. The specific test conditions were to add equal masses of the $Sn(II)Cl_2$ and hydroxyapatite to the Tc-spiked simulant at a solution to solid ratio of 167g:1g (equivalent to 1 L simulant to 3 g $Sn(II)Cl_2$ plus 3 g hydroxyapatite).

This Sn(II) reducing agent coupled with hydroxyapatite sorbent process was very effective at neutral pH; removing essentially all of the Tc (to below a method detection limit of 5 µg/L) within 2 hrs. This was equivalent to a Tc Decontamination Factor (DF) >577. It was less effective when the off-gas simulant was adjusted to an alkaline pH = 12; where the DF for Tc was reduced to 3.4 to 3.6. It was also observed that the chromium co-precipitates with the Tc during the $SnCl_2$ reduction.

A recent report (Taylor-Pashow et al. 2015) focused on determining the minimum amount of $SnCl_2$ required to effectively remove the ^{99}Tc from a new batch of the WTP off-gas simulant (similar to Table D-1[1]). In this study they did not use the "carrier" hydroxyapatite. In addition they studied the use of an alternate reductant, Fe(II), and examined other variables that may impact the ^{99}Tc reductive precipitation. Chromium is present in the off-gas waste stream as Cr(VI), and will consume some of the $SnCl_2$ added to reduce the Tc(VII); therefore testing was performed to examine the impact of varying Cr concentrations (3 different Cr concentrations-→0, 30, and 140 ppm).

Testing results indicated that 1.5 equivalents of electrons from Sn(II) relative to those needed to reduce Cr(VI) and Tc(VII)a was effective at removing the ^{99}Tc---added as ammonium pertechnetate solution at ~2 mg/L --to below the ICP-MS method detection limit.

The Sn(II) was much more successful at removal of Tc than Fe(II). Only 1.5 eq of Sn(II), which corresponds to ~0.8 g/L $SnCl_2$ in the off-gas simulant, was necessary for good Tc removal. Although not measured directly, it is expected that the Tc will be in the form of pertechnetate in the WTP melter off-gas condensate recycle stream due to the highly oxidizing conditions. Addition of $SnCl_2$ causes reduction from soluble TcO_4^- to form TcO_2 solids, which can be removed by settling or filtration. The Sn(II) was much more successful at removal of Tc than Fe(II).

The 1.5 eq of Sn(II) relative to moles of electrons required to reduce the Cr(VI) and Tc(VII) was shown to be successful at removing Tc to below detection limit values at two different Cr concentrations (30 and 140 ppm). In the case of the simulant containing no Cr, 1.5 eq based only on Tc was an insufficient amount of Sn(II); however, when the amount of Sn(II) was increased, successful removal of Tc was observed. The increased amount was based upon 1.5 eq of Sn(II) relative to Tc and Zn, which had also been shown to be removed by the Sn(II) precipitation. That is, soluble Zn in the simulant appears to be consuming some of the Sn(II) reduction capacity.

The presence of solid glass formers in the simulant was shown to have no effect on the Sn(II) promoted reductive precipitation of the ^{99}Tc and Cr(VI). The digested and analyzed solids from the Sn(II) reductant process were found to be predominately Sn, as expected, making up 45 wt% of the solids. Cr was also present at appreciable concentrations, representing 8.32 wt% of the solids. The precipitated ^{99}Tc accounted for 0.17 wt% of the solids. The balance of the mass was presumably the oxygen from the oxides and hydroxides of these metals, plus residual water of hydration and trace simulant constituents that were either not washed away from the solids or that were co-precipitated during the Sn(II) reduction process.

---

[1] The new 2015 WTP off-gas simulant composition is found in Table 3.2 in Taylor-Pashow and McCabe (2015) but is very similar in composition to Table D-1.

Stability testing, placing the Sn(II) derived precipitates, in a fresh batch of the neutral pH off-gas simulant demonstrated that the precipitated solids are stable to re-oxidation and dissolution for up to 72 hours, which should provide sufficient time for a solid-liquid separation of the ^{99}Tc/Cr solids if this Sn(II) reduction process was to be used. However, the precipitated solids would not be stable if returned to Hanford double-shell tanks for storage, as demonstrated by rapid re-dissolution of the ^{99}Tc when the precipitated solids were mixed with a LAW simulant. Approximately 94 – 99% of the precipitated Tc re-dissolved within one hour after being placed in LAW simulant. The precipitated Sn also followed a similar re-dissolution trend. The Cr that had precipitated also quickly re-dissolved (~90% at 1 hour) in the LAW simulant; however, Cr then appeared to re-precipitate with time with only ~75% left in the LAW simulant after 72 hours of contact.

In summary, the key findings of the SRNL studies are that Sn(II)Cl_2 alone or in combination with hydroxyapatite can effectively remove Tc and Cr(VII) from off-gas waste streams via a simple reduction process. 1.5 eq of Sn(II) relative to moles of electrons present in the total Cr(VI) and Tc(VII) in the off-gas simulant was shown to be required for successful precipitation. The precipitated Cr(III) -Tc(IV)-Sn(IV) solid, assumed to be oxides/hydroxides, was stable for at least 72 hr in the treated off-gas simulant when exposed to air. However, when this solid was placed in highly caustic highly saline (7.8 M Na) LAW simulant and exposed to air, the solid quickly (within a few hours) re-dissolved apparently via re-oxidation processes. Thus the long-term stability of reduced Tc(IV)/Cr(III) solids created by simple reductive treatment by dissolved Sn(II) is questionable when the solids are re-exposed to air or placed in certain high pH-high saline aerated solutions.

When Sn(II)Cl_2 is used in conjunction with apatite or hydroxyapatite, the Sn-apatite is a high surface material that would require further treatment to consolidate it into a discrete Tc waste form. Further, it was found (Taylor-Pashow et al. 2014)that a mixture of $SnCl_2$ and hydroxyapatite removed TcO_4^- effectively from off-gas liquid secondary waste simulant only at neutral pH. This Sn(II) reducing agent coupled with hydroxyapatite sorbent process was very effective at neutral pH; removing essentially all of the Tc (to below a method detection limit of 5 µg/L) within 2 hours. This was equivalent to a Tc Decontamination Factor (DF) >577. It was less effective when the off-gas simulant was adjusted to an alkaline pH = 12; where the DF for Tc was reduced to 3.4 to 3.6. It was also observed that the chromium co-precipitates with the ^{99}Tc during the $SnCl_2$ reduction.

Appendix E
EPA 1315 Slope Checks

Table E-1 – Summary of the slopes of the plots of log cumulative release vs log time for each analyte and each Cast Stone set in the EPA Method 1315 Testing

	Sample	T1	T2	T3	T4	T5	T6	T7
Solution	Analyte							
DIW								
	Tc	0.75	0.62	0.70	0.65	0.75	0.71	N/A
	I	0.57	0.61	0.55	0.52	0.56	0.54	N/A
	Na	0.57	0.58	0.55	0.52	0.57	0.54	N/A
	NO3	0.52	0.59	0.56	0.52	0.57	0.55	N/A
	NO2	0.56	0.58	0.55	0.51	0.56	0.54	N/A
VZPW								
	Tc	0.70	0.55	0.40	0.43	0.48	0.48	N/A
	I	0.52	0.55	0.49	0.56	0.49	0.50	0.44
	Na	0.53	0.55	0.51	0.58	0.51	0.52	N/A
	NO3	0.41	0.43	0.40	0.42	0.40	0.41	N/A
	NO2	0.51	0.53	0.49	0.56	0.48	0.50	N/A

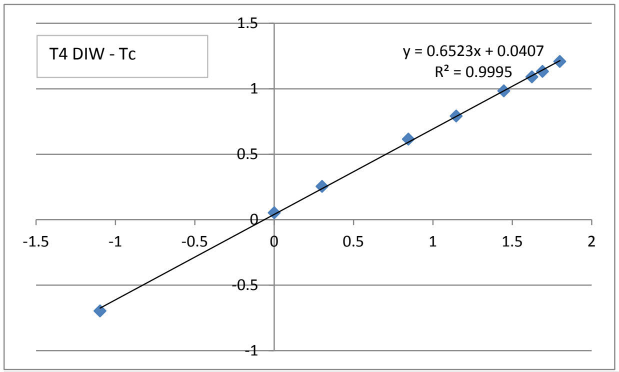

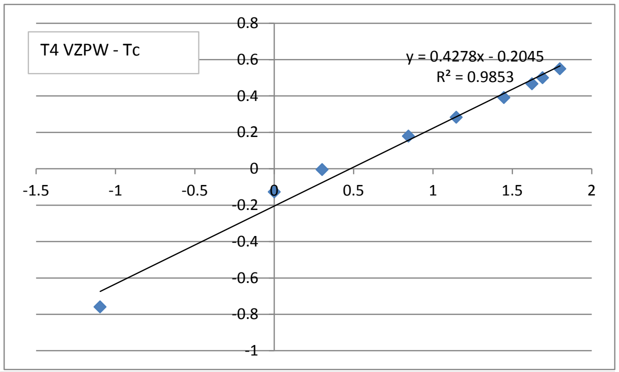

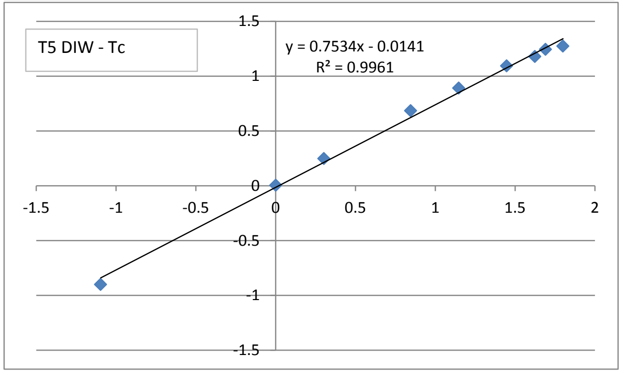

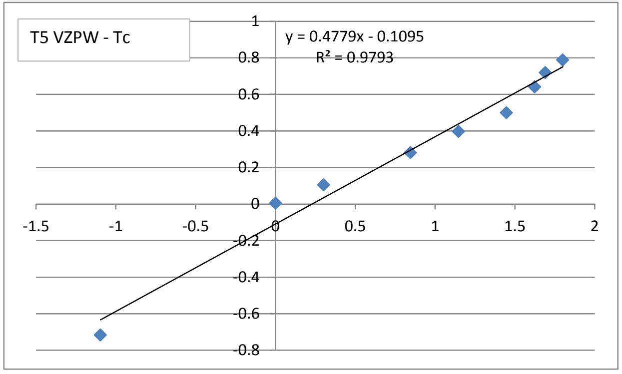

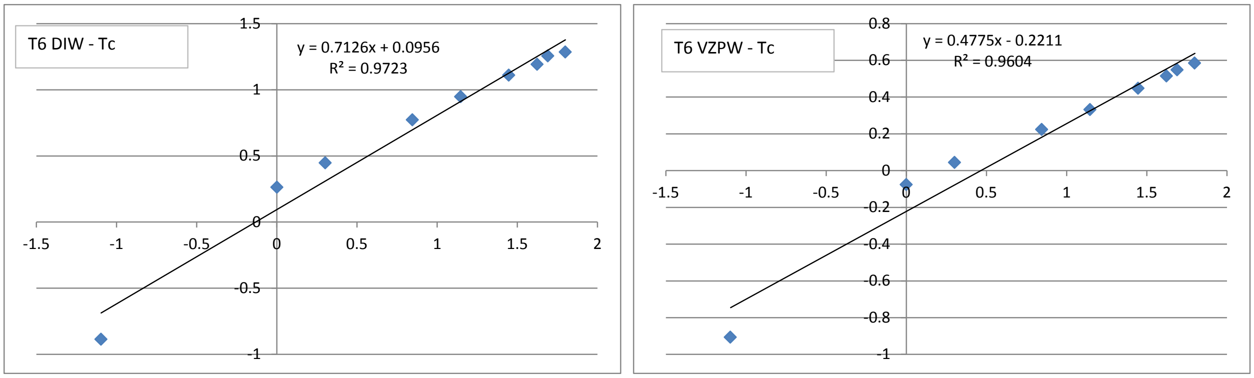

Figure E-1 : Additional plots of log cumulative Tc release vs log of leaching time for an individual monoliths in both DIW and VZPW. The equation of the trend line is shown in the upper left quadrant of the plots.

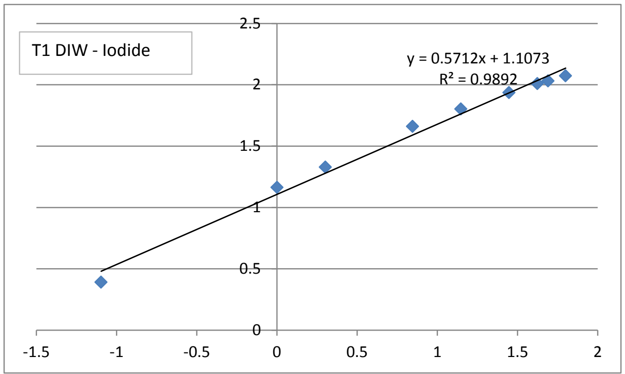

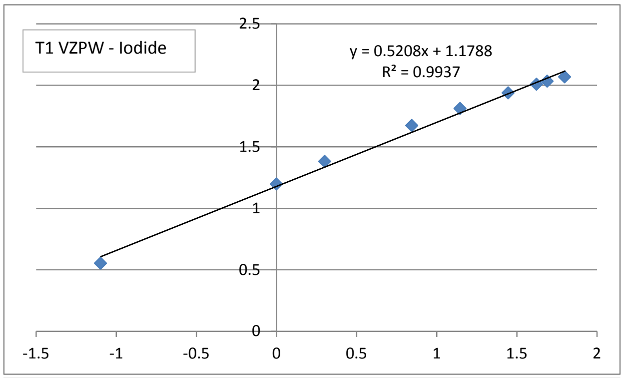

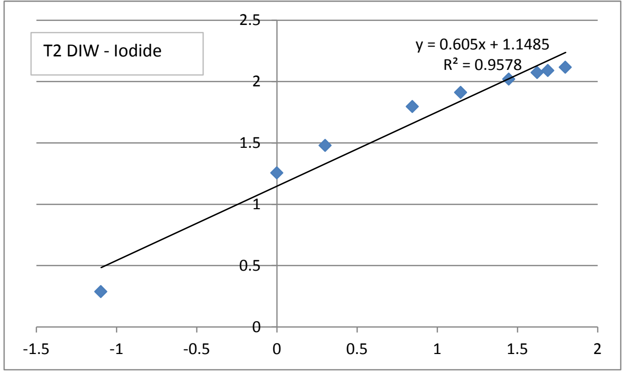

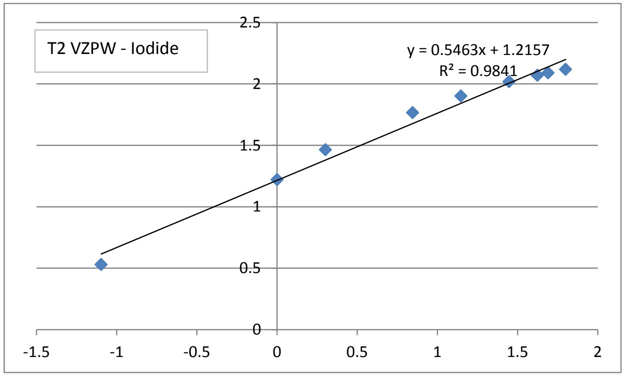

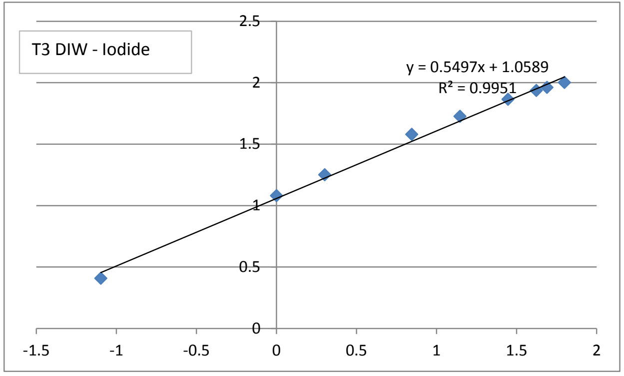

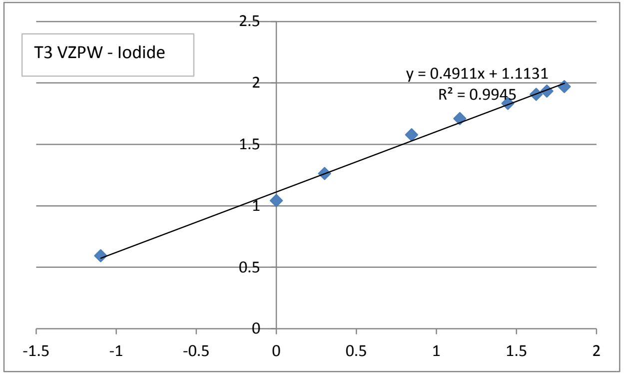

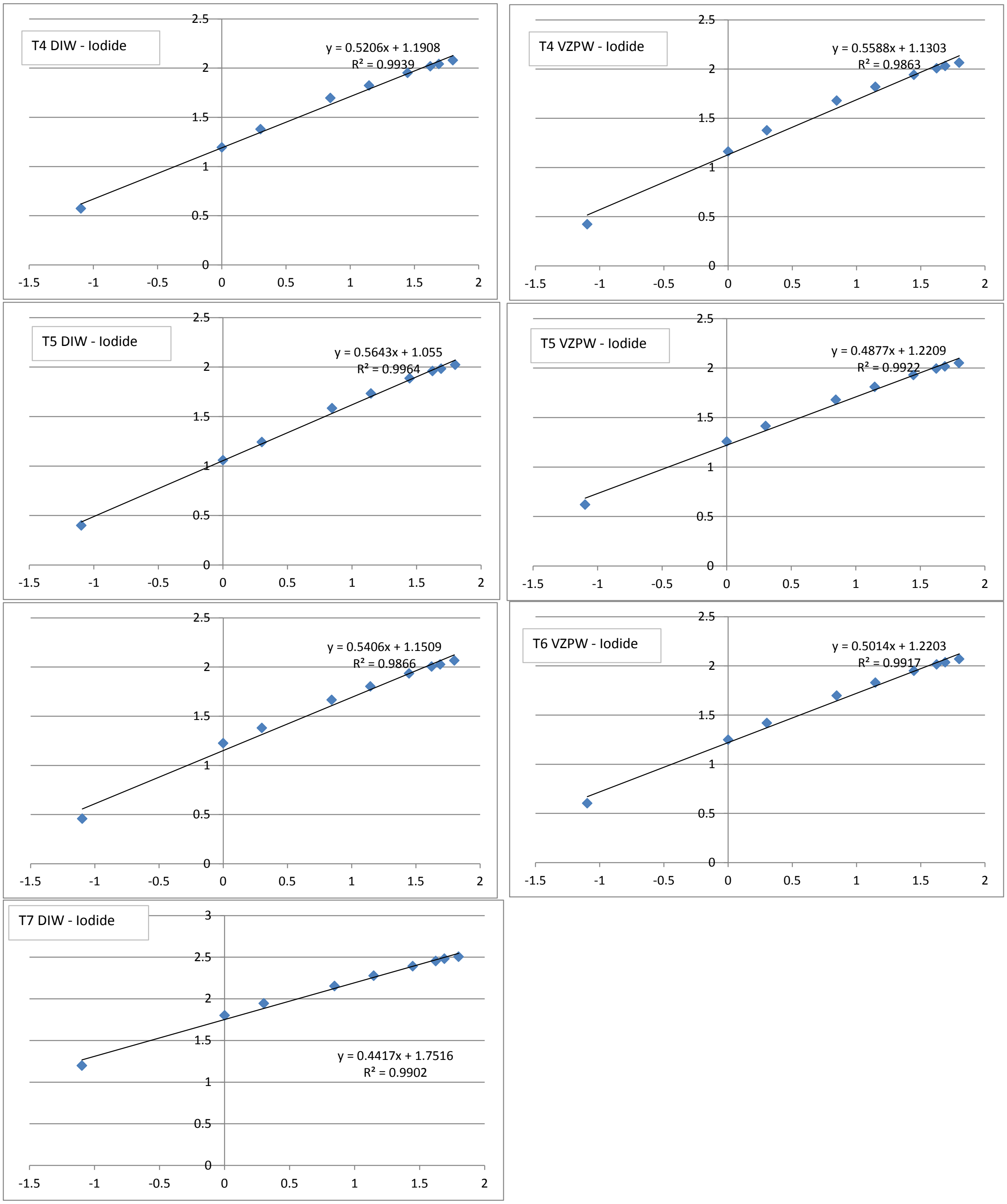

Figure E-2 : plots of log cumulative Iodide release vs log of leaching time for an individual monoliths in both DIW and VZPW. The equation of the trend line is shown in the upper left quadrant of the plots.

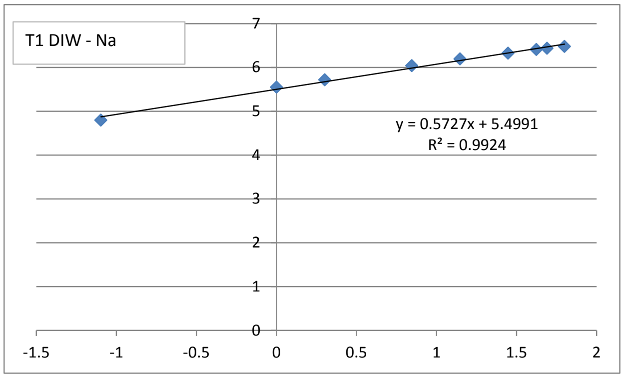
T1 DIW - Na
y = 0.5727x + 5.4991
R² = 0.9924
0
1
2
3
4
5
6
7
-1.5
-1
-0.5
0
0.5
1
1.5
2

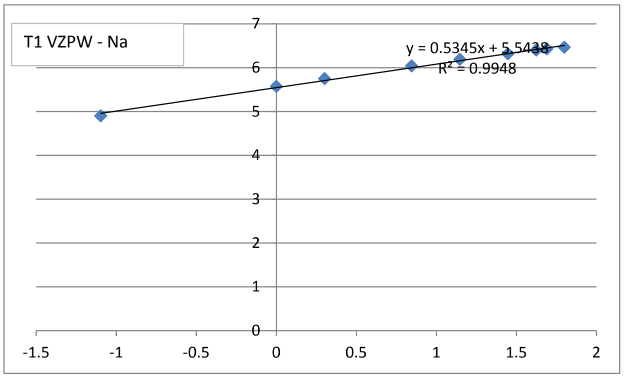
T1 VZPW - Na
y = 0.5345x + 5.5438
R² = 0.9948
0
1
2
3
4
5
6
7
-1.5
-1
-0.5
0
0.5
1
1.5
2

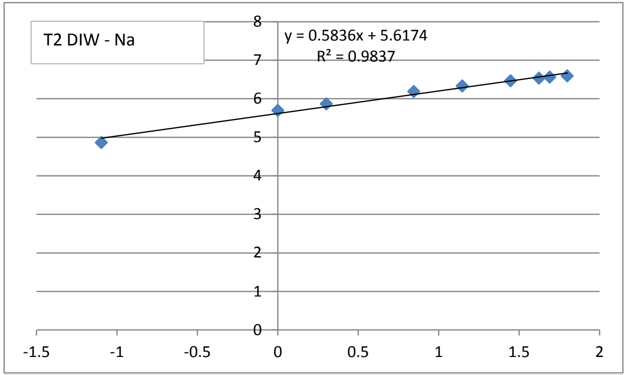
T2 DIW - Na
y = 0.5836x + 5.6174
R² = 0.9837
0
1
2
3
4
5
6
7
8
-1.5
-1
-0.5
0
0.5
1
1.5
2

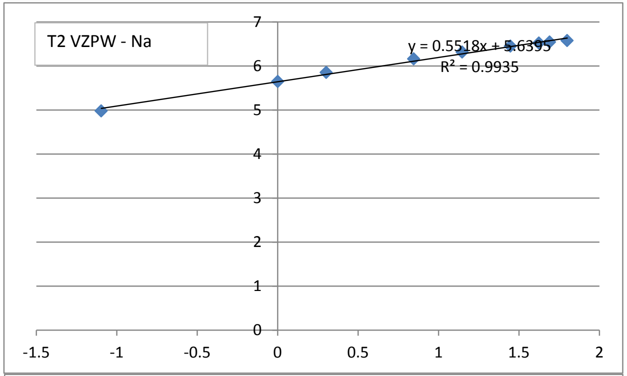
T2 VZPW - Na
y = 0.5518x + 5.6395
R² = 0.9935
0
1
2
3
4
5
6
7
-1.5
-1
-0.5
0
0.5
1
1.5
2

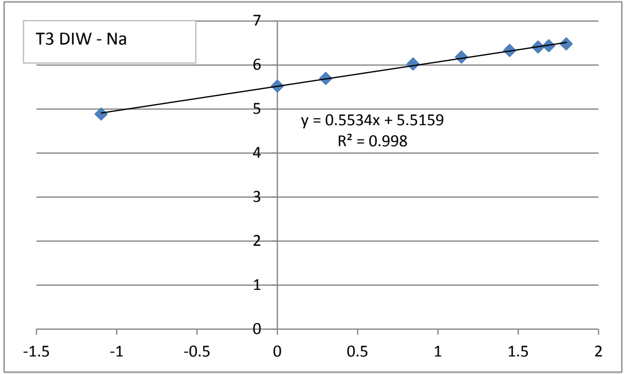
T3 DIW - Na
y = 0.5534x + 5.5159
R² = 0.998
0
1
2
3
4
5
6
7
-1.5
-1
-0.5
0
0.5
1
1.5
2

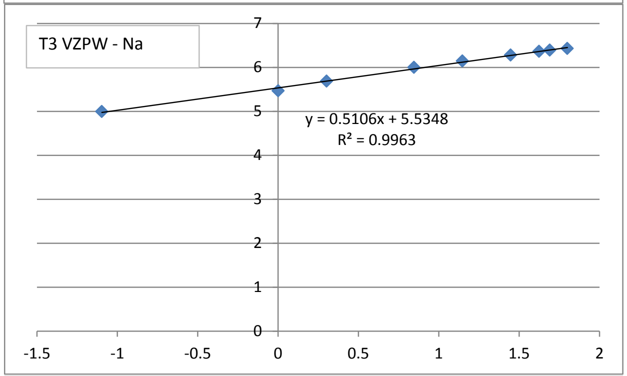
T3 VZPW - Na
y = 0.5106x + 5.5348
R² = 0.9963
0
1
2
3
4
5
6
7
-1.5
-1
-0.5
0
0.5
1
1.5
2

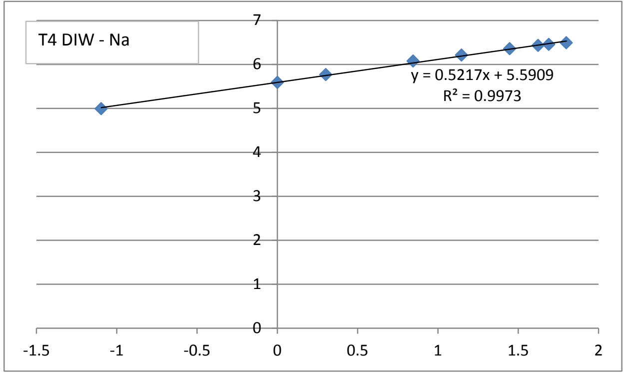
T4 DIW - Na
y = 0.5217x + 5.5909
R² = 0.9973
0
1
2
3
4
5
6
7
-1.5
-1
-0.5
0
0.5
1
1.5
2

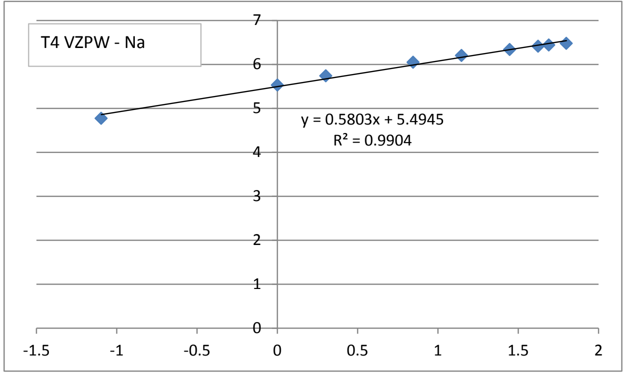
T4 VZPW - Na
y = 0.5803x + 5.4945
R² = 0.9904
0
1
2
3
4
5
6
7
-1.5
-1
-0.5
0
0.5
1
1.5
2

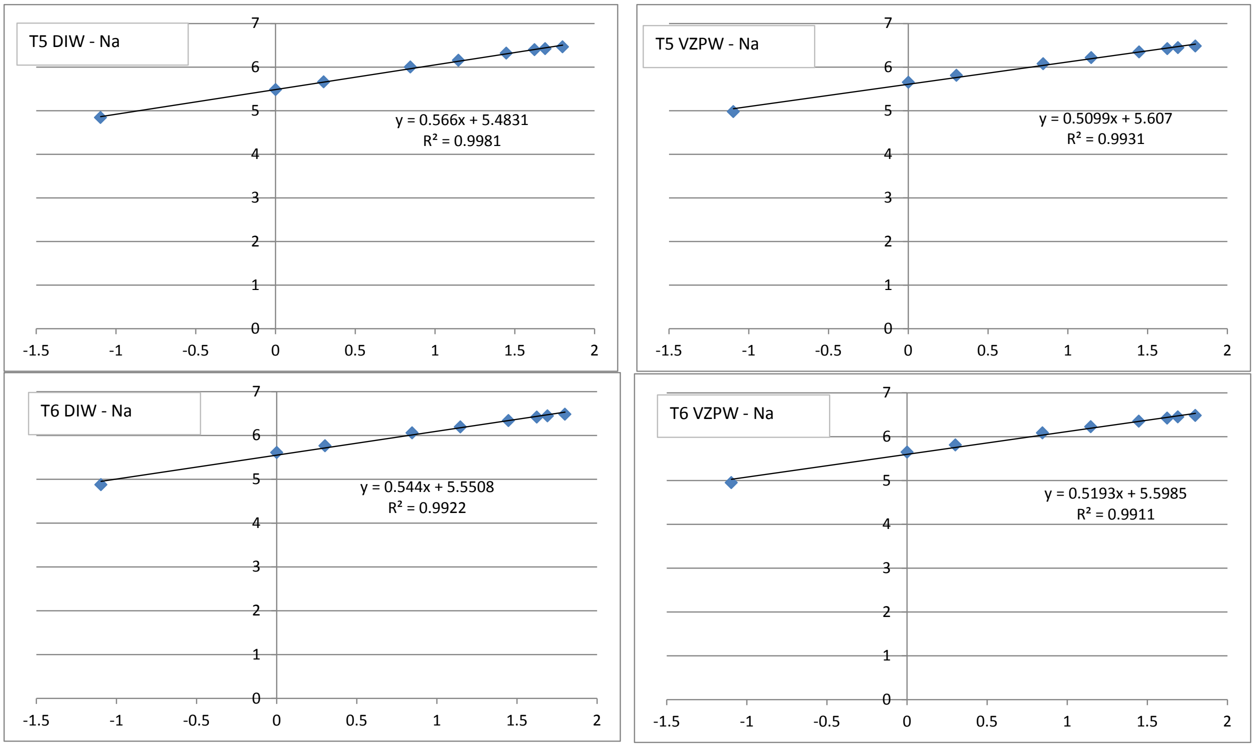

Figure E-3 : plots of log cumulative Na release vs log of leaching time for an individual monoliths in both DIW and VZPW. The equation of the trend line is shown in the upper left quadrant of the plots.

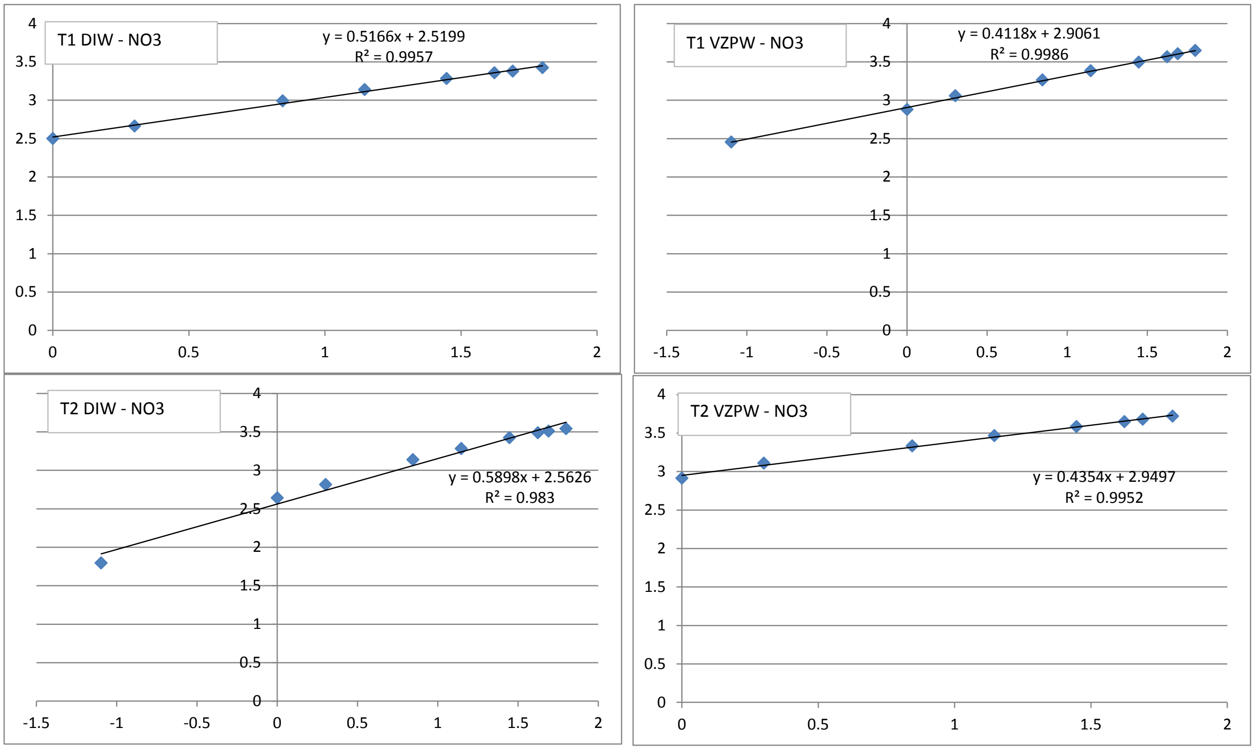

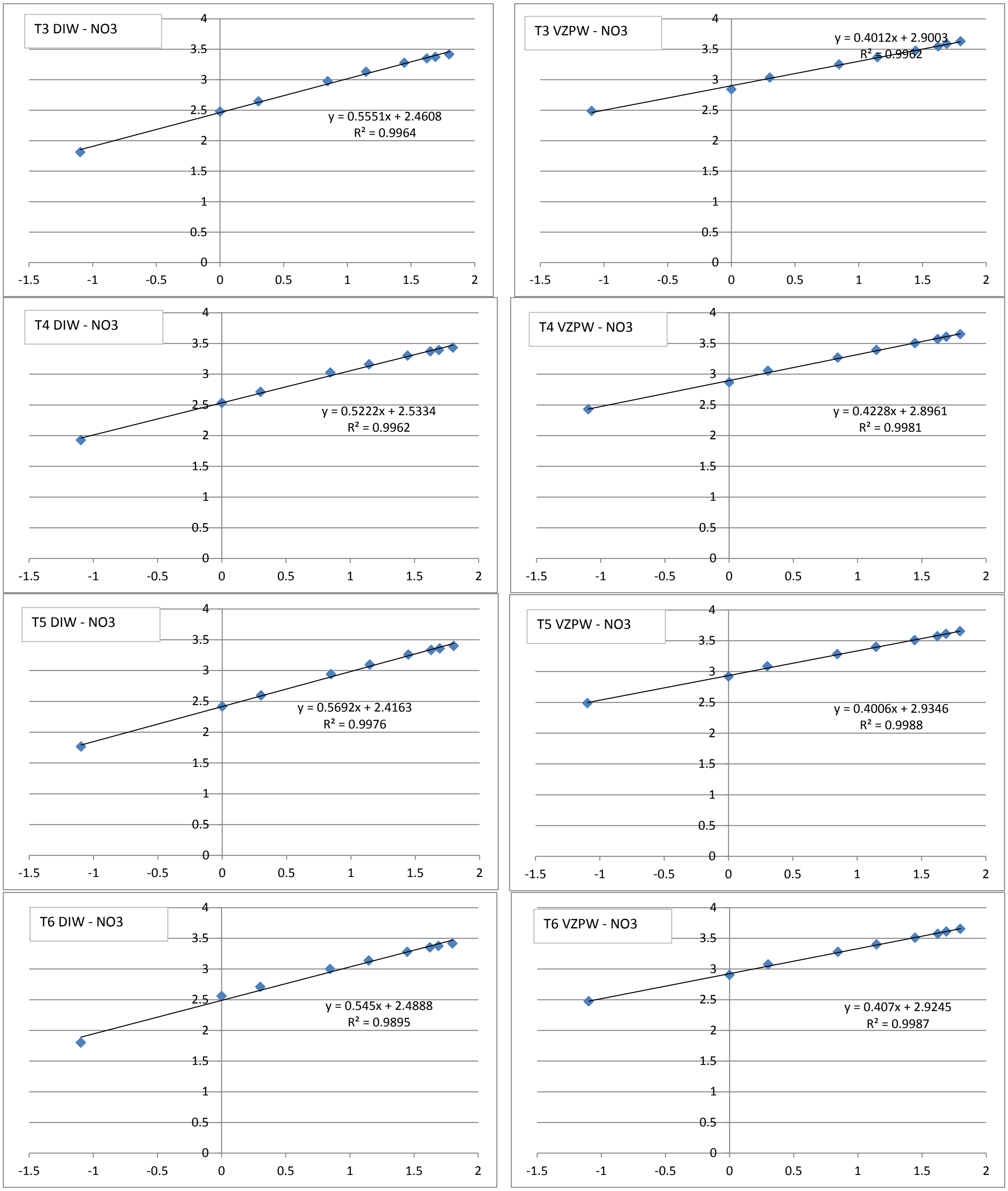

Figure E-4 : plots of log cumulative NO_3 release vs log of leaching time for an individual monoliths in both DIW and VZPW. The equation of the trend line is shown in the upper left quadrant of the plots.

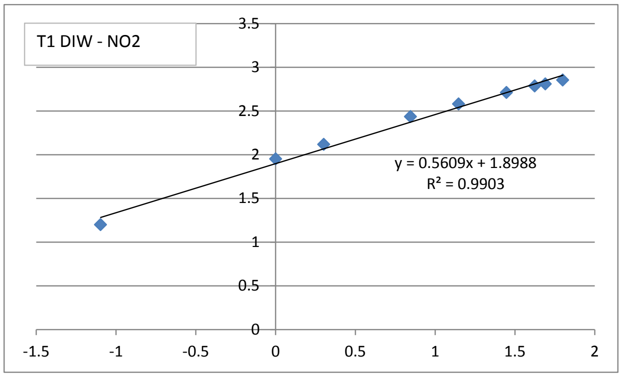
T1 DIW - NO2
y = 0.5609x + 1.8988
R² = 0.9903
0 0.5 1 1.5 2 2.5 3 3.5
-1.5 -1 -0.5 0 0.5 1 1.5 2

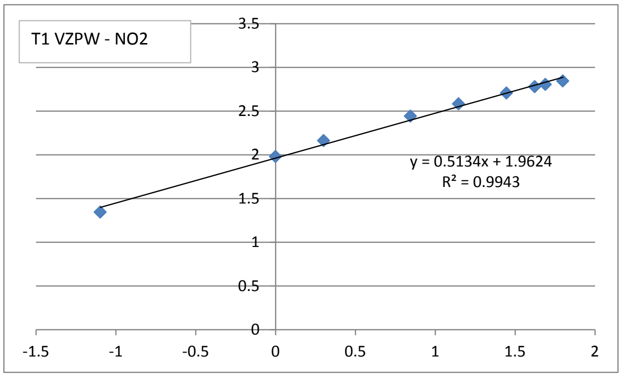
T1 VZPW - NO2
y = 0.5134x + 1.9624
R² = 0.9943
0 0.5 1 1.5 2 2.5 3 3.5
-1.5 -1 -0.5 0 0.5 1 1.5 2

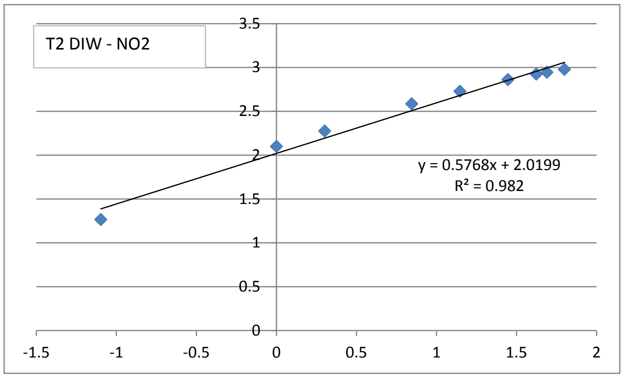
T2 DIW - NO2
y = 0.5768x + 2.0199
R² = 0.982
0 0.5 1 1.5 2 2.5 3 3.5
-1.5 -1 -0.5 0 0.5 1 1.5 2

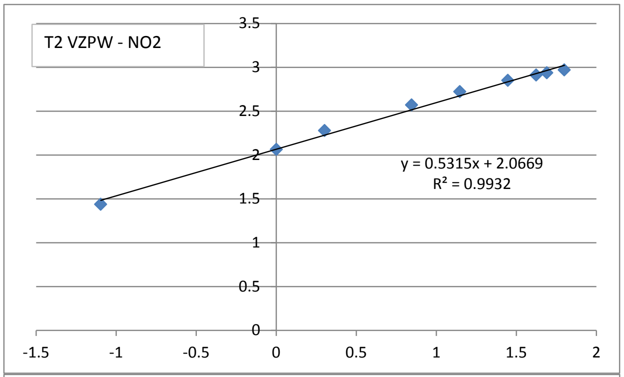
T2 VZPW - NO2
y = 0.5315x + 2.0669
R² = 0.9932
0 0.5 1 1.5 2 2.5 3 3.5
-1.5 -1 -0.5 0 0.5 1 1.5 2

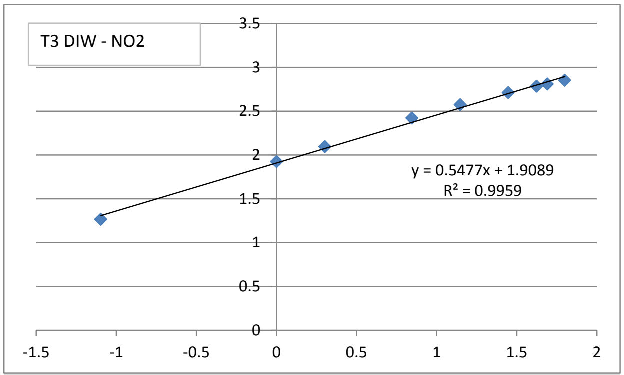
T3 DIW - NO2
y = 0.5477x + 1.9089
R² = 0.9959
0 0.5 1 1.5 2 2.5 3 3.5
-1.5 -1 -0.5 0 0.5 1 1.5 2

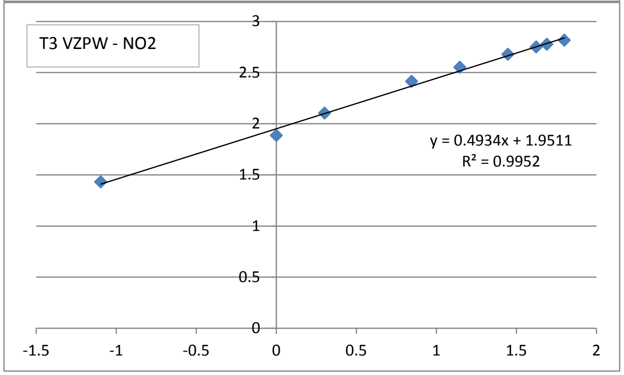
T3 VZPW - NO2
y = 0.4934x + 1.9511
R² = 0.9952
0 0.5 1 1.5 2 2.5 3
-1.5 -1 -0.5 0 0.5 1 1.5 2

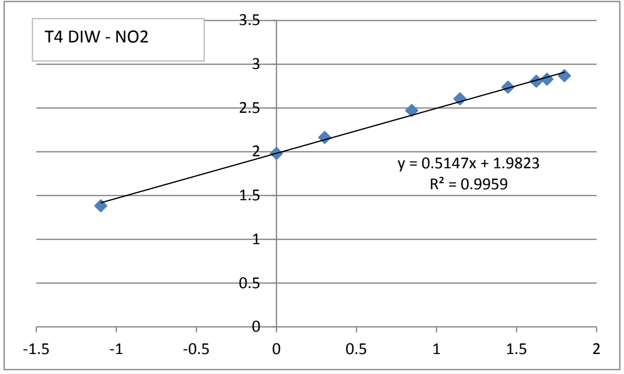
T4 DIW - NO2
y = 0.5147x + 1.9823
R² = 0.9959
0 0.5 1 1.5 2 2.5 3 3.5
-1.5 -1 -0.5 0 0.5 1 1.5 2

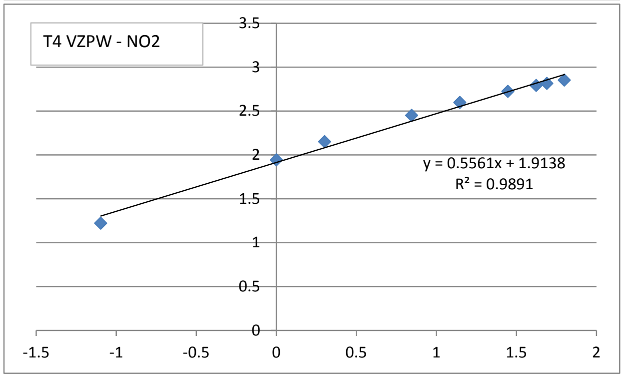
T4 VZPW - NO2
y = 0.5561x + 1.9138
R² = 0.9891
0 0.5 1 1.5 2 2.5 3 3.5
-1.5 -1 -0.5 0 0.5 1 1.5 2

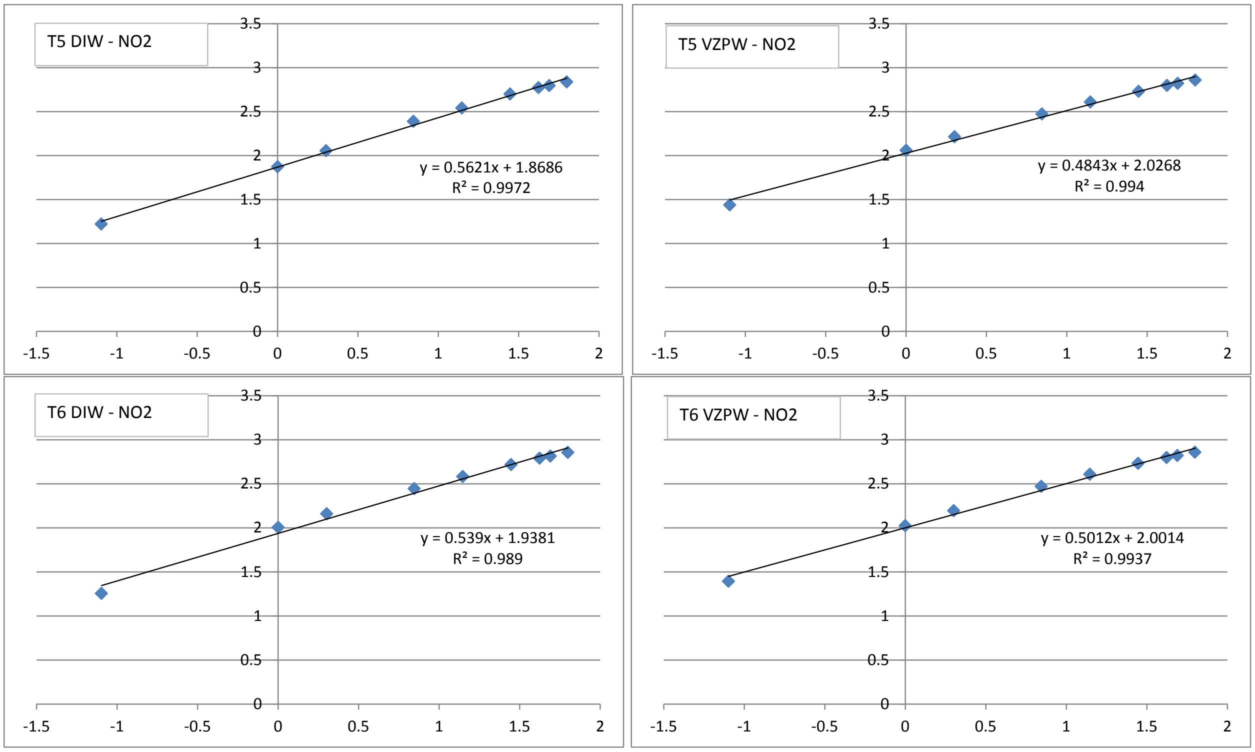

Figure E-5 : plots of log cumulative NO_2 release vs log of leaching time for an individual monoliths in both DIW and VZPW. The equation of the trend line is shown in the upper left quadrant of the plots.

Distribution

No. of
Copies

Washington River Protection Solutions &
Contractors

EE Brown
PA Cavanah
SE Kelly
KP Lee (AREVA)
RB Mabrouki
JL Mahoney (YAHSG)
WG Ramsey
PL Rutland
KH Subremanian
DJ Swanberg
WRPS Documents – TOCVND@rl.gov

Office of River Protection (ORP)
AA Kruger
GL Pyles

INTERA
R Andrews
M Apted
R Arthur
R Senger

Savannah River National Laboratory
AD Cozzi
G Flach
KM Fox
CC Herman
DI Kaplan
CA Langton
DJ McCabe
RR Seitz

No. of
Copies
Pacific Northwest National Laboratory
M Asmussen
M Bowden
E Buck
RE Clayton
E Cordova
VL Freedman
AR Lawter
TG Levitskaia
B Miller
JJ Neeway
CI Pearce
DK Peeler
N Qafoku
JV Ryan
RJ Serne
GL Smith
J Stephenson
W Um
JV Vienna
G Wang
N Washton
JH Westsik, Jr.
BD Williams
SB Yabusaki
Project File
Information Release (pdf)

* All distribution will be made electronically

Pacific Northwest
NATIONAL LABORATORY

U.S. DEPARTMENT OF
ENERGY

Proudly Operated by **Battelle** *Since 1965*

902 Battelle Boulevard
P.O. Box 999
Richland, WA 99352
1-888-375-PNNL (7665)

www.pnnl.gov